

# Marine microbial symbioses: Host-microbe interaction, holobiont's adaptation to niches and global climate change

**Edited by**

Zhiyong Li and Sen-Lin Tang

**Published in**

Frontiers in Microbiology

Frontiers in Marine Science



## FRONTIERS EBOOK COPYRIGHT STATEMENT

The copyright in the text of individual articles in this ebook is the property of their respective authors or their respective institutions or funders. The copyright in graphics and images within each article may be subject to copyright of other parties. In both cases this is subject to a license granted to Frontiers.

The compilation of articles constituting this ebook is the property of Frontiers.

Each article within this ebook, and the ebook itself, are published under the most recent version of the Creative Commons CC-BY licence. The version current at the date of publication of this ebook is CC-BY 4.0. If the CC-BY licence is updated, the licence granted by Frontiers is automatically updated to the new version.

When exercising any right under the CC-BY licence, Frontiers must be attributed as the original publisher of the article or ebook, as applicable.

Authors have the responsibility of ensuring that any graphics or other materials which are the property of others may be included in the CC-BY licence, but this should be checked before relying on the CC-BY licence to reproduce those materials. Any copyright notices relating to those materials must be complied with.

Copyright and source acknowledgement notices may not be removed and must be displayed in any copy, derivative work or partial copy which includes the elements in question.

All copyright, and all rights therein, are protected by national and international copyright laws. The above represents a summary only. For further information please read Frontiers' Conditions for Website Use and Copyright Statement, and the applicable CC-BY licence.

ISSN 1664-8714  
ISBN 978-2-8325-4902-5  
DOI 10.3389/978-2-8325-4902-5

## About Frontiers

Frontiers is more than just an open access publisher of scholarly articles: it is a pioneering approach to the world of academia, radically improving the way scholarly research is managed. The grand vision of Frontiers is a world where all people have an equal opportunity to seek, share and generate knowledge. Frontiers provides immediate and permanent online open access to all its publications, but this alone is not enough to realize our grand goals.

## Frontiers journal series

The Frontiers journal series is a multi-tier and interdisciplinary set of open-access, online journals, promising a paradigm shift from the current review, selection and dissemination processes in academic publishing. All Frontiers journals are driven by researchers for researchers; therefore, they constitute a service to the scholarly community. At the same time, the *Frontiers journal series* operates on a revolutionary invention, the tiered publishing system, initially addressing specific communities of scholars, and gradually climbing up to broader public understanding, thus serving the interests of the lay society, too.

## Dedication to quality

Each Frontiers article is a landmark of the highest quality, thanks to genuinely collaborative interactions between authors and review editors, who include some of the world's best academicians. Research must be certified by peers before entering a stream of knowledge that may eventually reach the public - and shape society; therefore, Frontiers only applies the most rigorous and unbiased reviews. Frontiers revolutionizes research publishing by freely delivering the most outstanding research, evaluated with no bias from both the academic and social point of view. By applying the most advanced information technologies, Frontiers is catapulting scholarly publishing into a new generation.

## What are Frontiers Research Topics?

Frontiers Research Topics are very popular trademarks of the *Frontiers journals series*: they are collections of at least ten articles, all centered on a particular subject. With their unique mix of varied contributions from Original Research to Review Articles, Frontiers Research Topics unify the most influential researchers, the latest key findings and historical advances in a hot research area.

Find out more on how to host your own Frontiers Research Topic or contribute to one as an author by contacting the Frontiers editorial office: [frontiersin.org/about/contact](https://frontiersin.org/about/contact)



# Marine microbial symbioses: Host-microbe interaction, holobiont's adaptation to niches and global climate change

## Topic editors

Zhiyong Li — Shanghai Jiao Tong University, China

Sen-Lin Tang — Biodiversity Research Center, Academia Sinica, Taiwan

## Citation

Li, Z., Tang, S.-L., eds. (2024). *Marine microbial symbioses: Host-microbe interaction, holobiont's adaptation to niches and global climate change*.

Lausanne: Frontiers Media SA. doi: 10.3389/978-2-8325-4902-5

# Table of contents

05	<b>Editorial: Marine microbial symbioses: host-microbe interaction, holobiont's adaptation to niches and global climate change</b> Zhiyong Li
08	<b>Identification of quorum sensing-regulated <i>Vibrio fortis</i> as potential pathogenic bacteria for coral bleaching and the effects on the microbial shift</b> Xiaohui Sun, Yan Li, Qian Yang, Han Zhang, Nuo Xu, Zheng Tang, Shishi Wu, Yusheng Jiang, Hala F. Mohamed, Danyun Ou and Xinqing Zheng
22	<b>Unraveling the metabolic effects of benzophenone-3 on the endosymbiotic dinoflagellate <i>Cladocopium goreau</i></b> Kaidian Zhang, Zhen Shen, Weilu Yang, Jianing Guo, Zhicong Yan, Jiashun Li, Jiamin Lin, Xiaocong Cao, Jia Tang, Zhaoqun Liu, Zhi Zhou and Senjie Lin
34	<b>Comparative genomic insights into habitat adaptation of coral-associated <i>Prosthecochloris</i></b> Zhaolong Nie, Kaihao Tang, Weiquan Wang, Pengxia Wang, Yunxue Guo, Yan Wang, Shuh-Ji Kao, Jianping Yin and Xiaoxue Wang
49	<b>A comparison of mesophotic and shallow sponge holobionts resilience to predicted future temperature elevation</b> Lilach Rajman-Nagar, Liron Goren, Sigal Shefer, Raz Moskovich, Zhiyong Li and Micha Ilan
65	<b>Genomic evidence for the first symbiotic Deferribacterota, a novel gut symbiont from the deep-sea hydrothermal vent shrimp <i>Rimicaris kairei</i></b> Li Qi, Mengke Shi, Fang-Chao Zhu, Chun-Ang Lian and Li-Sheng He
78	<b>The stability and composition of the gut and skin microbiota of Atlantic salmon throughout the yolk sac stage</b> Alexander W. Fiedler, Martha K. R. Drågen, Eirik D. Lorentsen, Olav Vadstein and Ingrid Bakke
94	<b>From friends to foes: fungi could be emerging marine sponge pathogens under global change scenarios</b> Yordanis Pérez-Llano, Luis Andrés Yarzabal Rodríguez, Esperanza Martínez-Romero, Alan D. W. Dobson, Nina Gunde-Cimerman, Vitor Vasconcelos and Ramón Alberto Batista-García
102	<b>Host habitat rather than evolutionary history explains gut microbiome diversity in sympatric stickleback species</b> Aruna M. Shankregowda, Prabhugouda Siriappagouda, Marijn Kuizenga, Thijs M. P. Bal, Yousri Abdelhafiz, Christophe Eizaguirre, Jorge M. O. Fernandes, Viswanath Kiron and Joost A. M. Raeymaekers

- 114 **First screening of bacteria assemblages associated with the marine polychaete *Melinna palmata* Grube, 1870 and adjacent sediments**  
Selma Menabit, Paris Lavin, Tatiana Begun, Mihaela Mureșan, Adrian Teacă and Cristina Purcarea
- 130 **Characterizing the bacterial communities associated with Mediterranean sponges: a metataxonomic analysis**  
Roberta Esposito, Serena Federico, Michele Sonnessa, Sofia Reddel, Marco Bertolino, Nadia Ruocco, Giacomo Zagami, Marco Giovine, Marina Pozzolini, Marco Guida, Valerio Zupo and Maria Costantini
- 140 **Consistent Symbiodiniaceae community assemblage in a mesophotic-specialist coral along the Saudi Arabian Red Sea**  
Silvia Vimercati, Tullia I. Terraneo, Carolina Bocanegra Castano, Federica Barreca, Benjamin C. C. Hume, Fabio Marchese, Mustapha Ouhssain, Alexandra Steckbauer, Giovanni Chimienti, Ameer A. Eweida, Christian R. Voolstra, Mattie Rodrigue, Vincent Pieribone, Sam J. Purkis, Mohammed Qurban, Burt H. Jones, Carlos M. Duarte and Francesca Benzoni



## OPEN ACCESS

EDITED AND REVIEWED BY  
Takema Fukatsu,  
National Institute of Advanced Industrial  
Science and Technology (AIST), Japan

\*CORRESPONDENCE  
Zhiyong Li  
✉ zyli@sjtu.edu.cn

RECEIVED 13 April 2024  
ACCEPTED 24 April 2024  
PUBLISHED 06 May 2024

CITATION  
Li Z (2024) Editorial: Marine microbial  
symbioses: host-microbe interaction,  
holobiont's adaptation to niches and global  
climate change. *Front. Microbiol.* 15:1416897.  
doi: 10.3389/fmicb.2024.1416897

COPYRIGHT  
© 2024 Li. This is an open-access article  
distributed under the terms of the [Creative  
Commons Attribution License \(CC BY\)](#). The  
use, distribution or reproduction in other  
forums is permitted, provided the original  
author(s) and the copyright owner(s) are  
credited and that the original publication in  
this journal is cited, in accordance with  
accepted academic practice. No use,  
distribution or reproduction is permitted  
which does not comply with these terms.

# Editorial: Marine microbial symbioses: host-microbe interaction, holobiont's adaptation to niches and global climate change

Zhiyong Li<sup>1,2\*</sup>

<sup>1</sup>State Key Laboratory of Microbial Metabolism and School of Life Sciences and Biotechnology, Shanghai Jiao Tong University, Shanghai, China, <sup>2</sup>SJTU Yezhou Bay Institute of Deepsea Sci-Tech, Shanghai Jiao Tong University, Sanya, China

## KEYWORDS

symbioses, microbiome, interaction, climate change, adaptation

## Editorial on the Research Topic

[Marine microbial symbioses: host-microbe interaction, holobiont's adaptation to niches and global climate change](#)

Symbiotic relationships between microbes and marine organisms have been found in a variety of marine ecosystems, ranging from shallow coral reefs to deep-sea hydrothermal vents. Marine microbial symbioses provide a way for holobiont's to survive in a very dynamic environment by changing metabolic pathways, and a possible selective force behind evolution (Li, 2019; Apprill, 2020). This Research Topic brings together 11 articles that highlight the association of microbial symbionts with marine sponges (Esposito et al.; Pérez-Llano et al.; Rajjman-Nagar et al.), corals (Nie et al.; Sun et al.; Vimercati et al.; Zhang et al.), polychaete (Menabit et al.), shrimps (Qi et al.) and fishes (Fiedler et al.; Shankregowda et al.), and their adaptation to environment changes, providing novel insights into the marine microbial symbioses in regard to host-microbe interaction, holobiont's adaptation to niches and global climate change. Meanwhile, the crucial need to elucidate the underlying mechanisms governing the interactions between the marine microbial symbionts and their hosts is suggested.

Global warming, ocean acidification and pollutants lead to increasingly serious problems of marine ecosystems (Gong et al., 2019; Li et al., 2023; Wu et al., 2023; Chai et al., 2024). Sponges are one of the major ecosystem engineers on the seafloor. Due to their critical roles in regulating marine element cycles, sponges are an essential model for studying and forecasting the impact of global change on marine organisms (Chai et al., 2024; Liu et al., 2024). The study by Rajjman-Nagar et al. compared the response of the sponge *Diacarnus erythraeanus*, a widespread Red Sea sponge, from the shallow and mesophotic reefs, to moderate and acute temperature elevation by measuring physiological parameters and the microbiome composition changes, and found that mesophotic and shallow populations of *D. erythraeanus* were highly tolerant to both moderate and acute heat stress. This study supports the hypothesis that mesophotic coral reefs could serve as thermal refugia for some sponge species.



Corals are important components of coral reef system and easily influenced by ocean warming (Gong et al., 2019; Li et al., 2023; Wu et al., 2023; Xiao et al., 2024). Coral bleaching is often accompanied by structural abnormalities of coral symbiotic microbiota, among which *Vibrio* is highly concerned. Sun et al. verified that *Vibrio fortis* was the primary pathogenic bacterium causing coral bleaching, revealed changes in the microbial community caused by *V. fortis* infection, and provided evidence for the “bacterial bleaching” hypothesis. As a well-known pseudo-persistent environmental pollutant, oxybenzone (BP-3) and its related organic ultraviolet filters have been verified to directly contribute to the increasing mortality rate of corals. Here, the impacts of BP-3 on the symbiotic Symbiodiniaceae *Cladocopium goreaui* were explored by Zhang et al.. Symbiodiniaceae could resist the toxicity of a range of BP-3 through promoting cell division, photosynthesis, and reprogramming amino acid metabolism.

Vimercati et al. characterized algal communities of a mesophotic specialist coral species, *Leptoseris cf. striatus*, along the Saudi Arabian Red Sea coast, and indicated that algal symbionts changed over time at the mesophotic depth. Compared to the knowledge of symbiotic Symbiodiniaceae in coral holobionts (Gong et al., 2019), little is known about bacteria in coral skeletons. *Prosthecochloris*, a marine representative genus of green sulfur bacteria, has been found to be dominant in some coral skeletons. *Prosthecochloris* genomes from the skeleton of the stony coral *Galaxea fascicularis* show specialized metabolic capacities to adapt to the microenvironments of coral skeletons, suggesting the adaptive strategy and population evolution of endolithic *Prosthecochloris* strains in coral skeletons (Nie et al.). A metataxonomic study by Esposito et al. revealed for the first time the presence of Rhizobiaceae bacteria in the sponge *Myxilla rosacea*. Global change scenarios could trigger the expression of fungal virulence genes and unearth new opportunistic pathogens, posing a risk to the health of sponges and severely damaging reef ecosystems. In contrast to sponge prokaryotic symbionts, the importance of fungi in sponge holobionts has been largely overlooked (He et al., 2014). Pérez-Llano et al. postulate that manipulating sponge-associated fungal community may be a new strategy to cope with the threats posed to sponge health by pathogens and pollutants, and anticipate that sponge-derived fungi might be used as novel sponge health promoters and beneficial members of the resident sponge microbiome in order to increase the sponge's resistance.

Host-associated microbiota can influence host phenotypic variation, fitness and potential to adapt to local environmental conditions. Both host evolutionary history and the abiotic/biotic environment can influence the diversity of microbiota. However, our understanding of host-microbiome interactions in natural populations is limited since environmental and host-specific factors remain largely unknown. Here, the results from Shankregowda et al. based on the bacterial diversity analysis of three-spined stickleback (*Gasterosteus aculeatus*) and nine-spined stickleback (*Pungitius pungitius*) suggested that host habitat rather than evolutionary history could explain gut microbiome diversity in sympatric stickleback species. The bacterial colonization of newly hatched fish is important for the larval development and health.

To date, little is known about the ontogeny of the early microbiota of fishes. According to Fiedler et al., the skin and gut microbiota of Atlantic salmon are similar, but start diverging during the yolk sac stage. Both the skin and gut microbiota are highly dynamic and underwent major changes throughout the yolk sac stage.

Although many studies have been focused on the microbial populations of benthic and pelagic habitats, little is known about bacteria colonizing tube-dwelling polychaetes. Menabit et al. found that polychaete *Melinna palmata* Grube harbored a distinct bacterial assemblage as compared to their sediments. The deduced functional profiles suggested the prevalence of the amino acid and carbohydrate metabolisms, providing a glimpse on the putative role of bacterial community associated with the *Melinna palmata* Grube host. The genus *Rimicaris* is the dominant organism living in hydrothermal vents, however, little is known about the functions of its intestinal microbes. Qi et al. provided genomic evidence for the first symbiotic *Deferribacterota*, a novel gut symbiont from the deep-sea hydrothermal vent shrimp *Rimicaris kairei*. Cofactors such as biotin, riboflavin, flavin mononucleotide, and flavin adenine dinucleotide synthesized by *R. kairei* gut *Deferribacterota* may assist their host in surviving under extreme conditions, suggesting its long-term coevolution with the host.

## Author contributions

ZL: Writing – original draft, Writing – review & editing.

## Funding

The author(s) declare that financial support was received for the research, authorship, and/or publication of this article. This work was supported by National Natural Science Foundation of China (NSFC, 42176146, 31861143020, 41776138) and the Oceanic Interdisciplinary Program of Shanghai Jiao Tong University (SL2021PT202) awarded to ZL.

## Conflict of interest

The author declares that the research was conducted in the absence of any commercial or financial relationships that could be construed as a potential conflict of interest.

The author(s) declared that they were an editorial board member of Frontiers, at the time of submission. This had no impact on the peer review process and the final decision.

## Publisher's note

All claims expressed in this article are solely those of the authors and do not necessarily represent those of their affiliated organizations, or those of the publisher, the editors and the reviewers. Any product that may be evaluated in this article, or claim that may be made by its manufacturer, is not guaranteed or endorsed by the publisher.

## References

- Apprill, A. (2020). The role of symbioses in the adaptation and stress responses of marine organisms. *Ann. Rev. Mar. Sci.* 12, 291–314. doi: 10.1146/annurev-marine-010419-010641
- Chai, G., Li, J., and Li, Z. (2024). The interactive effects of ocean acidification and warming on bioeroding sponge *Spherospongia vesparium* microbiome indicated by metatranscriptomics. *Microbiol. Res.* (2024) 278:127542. doi: 10.1016/j.micres.2023.127542
- Gong, S., Xu, L., Yu, K., Zhang, F., and Li, Z. (2019). Differences in Symbiodiniaceae communities and photosynthesis following thermal bleaching of massive corals in the northern part of the South China Sea. *Mar. Pollut. Bull.* 144, 196–204. doi: 10.1016/j.marpolbul.2019.04.069
- He, L., Liu, F., Karuppiah, V., Ren, Y., and Li, Z. (2014). Comparisons of the fungal and protistan communities among different marine sponge holobionts by pyrosequencing. *Microb. Ecol.* 67, 951–961. doi: 10.1007/s00248-014-0393-6
- Li, J., Chai, G., Xiao, Y., and Li, Z. (2023). The impacts of ocean acidification, warming and their interactive effects on coral prokaryotic symbionts. *Environm. Microb.* 18:49. doi: 10.1186/s40793-023-00505-w
- Li, Z. (2019). *Symbiotic Microbiomes of Coral Reefs Sponges and Corals*. New York: Springer Nature.
- Liu, F., Ryu, T., Ravasi, T., Wang, X., Wang, G., and Li, Z. (2024). Niche-dependent sponge hologenome expression profiles and the host-microbes interplay: a case of Hawaiian demosponge *Mycale grandis*. *Environm. Microb.* 19:22. doi: 10.1186/s40793-024-00563-8
- Wu, H., Li, J., Song, Q., Chai, G., Xiao, Y., and Li, Z. (2023). The synergistic negative effects of combined acidification and warming on the coral host and its symbiotic association with Symbiodiniaceae indicated by RNA-Seq differential expression analysis. *Coral Reefs*. 42, 1187–1201. doi: 10.1007/s00338-023-02425-0
- Xiao, Y., Gao, L., and Li, Z. (2024). Unique high-temperature tolerance mechanisms of zoochlorellae *Symbiolum hainanensis* derived from scleractinian coral *Porites lutea*. *MBio*. 15:e0278023. doi: 10.1128/mbio.02780-23



## OPEN ACCESS

EDITED BY  
Zhiyong Li,  
Shanghai Jiao Tong University, China

REVIEWED BY  
Zhi Zhou,  
Hainan University, China  
Jiayuan Liang,  
Guangxi University, China

\*CORRESPONDENCE  
Xiaohui Sun  
✉ sunxiaohui@hqu.edu.cn  
Danyun Ou  
✉ oudanyun@tio.org.cn  
Xinqing Zheng  
✉ zhengxinqing@tio.org.cn

SPECIALTY SECTION  
This article was submitted to  
Microbial Symbioses,  
a section of the journal  
Frontiers in Microbiology

RECEIVED 05 December 2022

ACCEPTED 09 January 2023

PUBLISHED 03 February 2023

## CITATION

Sun X, Li Y, Yang Q, Zhang H, Xu N, Tang Z,  
Wu S, Jiang Y, Mohamed HF, Ou D and  
Zheng X (2023) Identification of quorum  
sensing-regulated *Vibrio fortis* as potential  
pathogenic bacteria for coral bleaching  
and the effects on the microbial shift.  
*Front. Microbiol.* 14:1116737.  
doi: 10.3389/fmicb.2023.1116737

## COPYRIGHT

© 2023 Sun, Li, Yang, Zhang, Xu, Tang, Wu,  
Jiang, Mohamed, Ou and Zheng. This is an  
open-access article distributed under the terms  
of the [Creative Commons Attribution License](https://creativecommons.org/licenses/by/4.0/)  
(CC BY). The use, distribution or reproduction in  
other forums is permitted, provided the original  
author(s) and the copyright owner(s) are  
credited and that the original publication in this  
journal is cited, in accordance with accepted  
academic practice. No use, distribution or  
reproduction is permitted which does not  
comply with these terms.

# Identification of quorum sensing-regulated *Vibrio fortis* as potential pathogenic bacteria for coral bleaching and the effects on the microbial shift

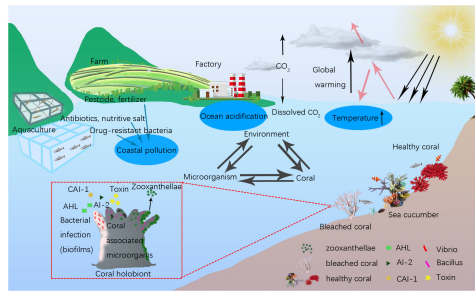
Xiaohui Sun<sup>1\*</sup>, Yan Li<sup>2</sup>, Qian Yang<sup>1</sup>, Han Zhang<sup>2</sup>, Nuo Xu<sup>1</sup>,  
Zheng Tang<sup>1</sup>, Shishi Wu<sup>1</sup>, Yusheng Jiang<sup>1</sup>, Hala F. Mohamed<sup>2,3</sup>,  
Danyun Ou<sup>2,4\*</sup> and Xinqing Zheng<sup>2,4,5\*</sup>

<sup>1</sup>College of Chemical Engineering, Huaqiao University, Xiamen, China, <sup>2</sup>Third Institute of Oceanography, Ministry of Natural Resources, Xiamen, China, <sup>3</sup>Botany and Microbiology Department (Girls Branch), Faculty of Science, Al-Azhar University, Cairo, Egypt, <sup>4</sup>Key Laboratory of Marine Ecological Conservation and Restoration, Ministry of Natural Resources, Xiamen, China, <sup>5</sup>Observation and Research Station of Coastal Wetland Ecosystem in Beibu Gulf, Ministry of Natural Resources, Xiamen, China

Coastal pollution, global warming, ocean acidification, and other reasons lead to the imbalance of the coral reef ecosystem, resulting in the increasingly serious problem of coral degradation. Coral bleaching is often accompanied by structural abnormalities of coral symbiotic microbiota, among which *Vibrio* is highly concerned. In this study, *Vibrio fortis* S10-1 (MCCC 1H00104), isolated from sea cucumber, was used for the bacterial infection on coral *Seriatopora guttatus* and *Pocillopora damicornis*. The infection of S10-1 led to coral bleaching and a significant reduction of photosynthetic function in coral holobiont, and the pathogenicity of *V. fortis* was regulated by quorum sensing. Meanwhile, *Vibrio* infection also caused a shift of coral symbiotic microbial community, with significantly increased abundant Proteobacteria and Actinobacteria and significantly reduced abundant Firmicutes; on genus level, the abundance of *Bacillus* decreased significantly and the abundance of *Rhodococcus*, *Ralstonia*, and *Burkholderia*–*Caballeronia*–*Paraburkholderia* increased significantly; S10-1 infection also significantly impacted the water quality in the micro-ecosystem. In contrast, S10-1 infection showed less effect on the microbial community of the live stone, which reflected that the microbes in the epiphytic environment of the live stone might have a stronger ability of self-regulation; the algal symbionts mainly consisted of *Cladocopium* sp. and showed no significant effect by the *Vibrio* infection. This study verified that *V. fortis* is the primary pathogenic bacterium causing coral bleaching, revealed changes in the microbial community caused by its infection, provided strong evidence for the “bacterial bleaching” hypothesis, and provided an experimental experience for the exploration of the interaction mechanism among microbial communities, especially coral-associated *Vibrio* in the coral ecosystem, and potential probiotic strategy or QS regulation on further coral disease control.

## KEYWORDS

coral bleaching, *Vibrio fortis*, symbiotic microbes, bacterial infection, microbial shift



#### GRAPHICAL ABSTRACT

Ecological balance among coral, microorganism and environment. Coral health was affected by the environmental changes of temperature raising, ocean acidification and coastal pollution, and microbial interaction in coral holobiont.

## 1. Introduction

Coral reef ecosystems possess the highest productivity and biodiversity among marine ecosystems; however, due to changes in environmental conditions, such as climate change and ocean acidification, the ecological balance among coral, microorganisms, and the environment has been affected (Stuart-Smith et al., 2018). In addition, the coastal pollution caused by human activities also led to ecological imbalance, especially the microorganism shift, resulting in the increasingly serious problems of coral degradation (Putnam and Gates, 2015) and arousing the wide attention of researchers.

The coral-associated microorganisms play important roles to maintain the health of coral holobiont (Rosenberg et al., 2009; Kang et al., 2022), which assists the coral host to adapt to the environmental changes by a shift of the symbiotic microorganism community. However, the changes in environmental conditions might lead to the disorder of the microorganism community, including the dissociation of algal symbionts from the coral symbiotic micro-ecosystem, which normally causes coral bleaching, or a shift in the bacterial community, which results in unbalanced nutrition metabolism, which causes coral disease, or the increasing richness of opportunistic pathogens, which causes bacterial infection (Mao-Jones et al., 2010). Although the proposed “bacterial bleaching” hypothesis (Kushmaro et al., 1996) is still controversial (Ainsworth et al., 2008), there have been continuous reports in recent years to prove the correlation between bacterial infection and coral disease (Ziegler et al., 2019), which highlighted the hypothesis that coral disease might be caused by the synergistic effects from one or more pathogenic bacteria. Moreover, marine animals such as fish, shrimp, sea cucumbers, and even starfish in coral reefs play the role of intermediate hosts of pathogens, increasing the probability of bacterial infection during their movement.

Coral bleaching is often accompanied by the abnormal structure of symbiotic microorganisms (Mhuantong et al., 2019; Mohamed et al., 2022). Almost all bacterial pathogens causing coral diseases are opportunistic pathogens, which produce virulence factors as a response to the changes in environmental conditions such as temperature and pH, or the interaction among bacteria during colonization competition, resulting in coral diseases (Kimes et al., 2012). Although *Vibrios* had been reported as the main kind of opportunistic pathogens to cause coral diseases, including *V. coralliilyticus*, *V. natriegens*, *V. parahaemolyticus*, and *V. shilonii* (Ushijima et al., 2014; Li et al., 2017; Ahmed et al., 2022),

the relationships between other *Vibrio* sp. and coral health remained unknown, and their infection pathway and the pathogenic mechanism remained unknown.

In the previous study, a significantly increased abundance of *V. fortis* had been found in the microbial symbionts in *Porites lutea* with pigment abnormalities in Lembeh Strait, North Sulawesi, Indonesia, which indicated that *V. fortis* may be involved in the bacterial infection and caused the coral inflammatory reaction (Ou et al., 2018). To verify this inference, and also to study the potential interaction of microorganism community caused by the *V. fortis* colonization, in this study, we carried out the *Vibrio* infection experiments on the laboratory-based model of *Seriatopora guttatus* and *Pocillopora damicornis*, both of which are fast-growing and easy-reproducing coral species, using a *V. fortis* strain from sea cucumber from coral reef area and a marine-source quorum quenching (QQ) enzyme, YtnP, with positive AHL degradation activity (Sun et al., 2021) to inhibit the pathogenicity of *V. fortis*, to investigate the relationship between extrinsic *V. fortis* and coral health and to reveal its effects on coral-associated microorganism community by bacterial interaction.

## 2. Materials and methods

### 2.1. Bacteria, coral, and QQ enzyme reagent

The *Vibrio fortis* strain S10-1 (MCCC 1H00104) was isolated from sea cucumber from the coral reef of Lembeh Strait, North Sulawesi, Indonesia, and kindly provided by the Third Institute of Oceanography, MNR (Xiamen, China). The corals *S. guttatus* and *P. damicornis* were artificially bred and kindly provided by the coral conservation laboratory of the Third Institute of Oceanography. The YtnP enzyme was prepared by this lab in a previous study (Sun et al., 2021).

### 2.2. Bacterial culture

The S10-1 strain was inoculated in a 100-ml of Marine Broth 2216 (BD, USA) media and incubated at 30°C with shaking at 180 rpm to obtain the bacterial growth curve. The overnight culture of S10-1 at exponential growth phase, with an absorbance of about 0.50 at the optical density (OD) at 595 nm (approximate  $1.0 \times 10^8$  CFU/ml), was resuspended using the same volume of seawater to prepare a bacterial solution for the further experiment of bacterial infection.

### 2.3. Coral culture and bacterial infection

The aquaria with the size of  $60 \times 45 \times 45$  cm (length  $\times$  wide  $\times$  high) were prepared for coral culture, with 20 L pump-recycling seawater at a salinity of 33.3‰, a protein skimmer to remove dissolved organic compounds, and a dimmable LED light to simulate the diurnal rhythm (light on between 6 a.m. and 6 p.m.). The live stone was moved from the coral conservation laboratory, randomly separated into pieces, and pre-cultured individually in the aquaria for 7 days at 25°C to maintain clean and stable water quality for coral growth. The corals were cut into branches with a length of about 80 mm, randomly separated, and placed in the aquaria for the



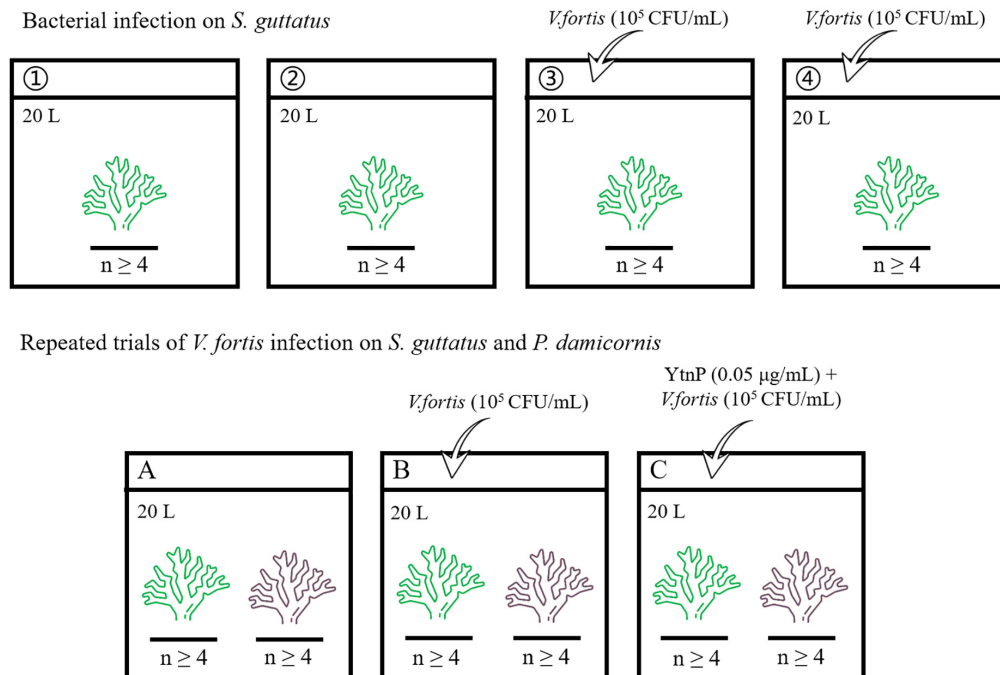


FIGURE 1  
Flowchart showing the experiment overview.

subsequent experiment, where each aquarium contains at least four coral branches for biological repetition. The overview of the bacterial infection experiment is shown in [Figure 1](#) and described later.

### 2.3.1. Bacterial infection on *S. guttatus*

The coral branches of *S. guttatus* in each aquarium were immersed in 20 ml of the above prepared *Vibrio* solution for 10 min for bacterial infection (first diluted with 180 mL of seawater in a beaker to ensure that all of the coral branches could be immersed, then poured into the aquarium to make the inoculation with a final concentration of about  $10^5$  CFU/mL), with the same volume of seawater as a negative control in blank groups. The treated coral branches were continuously cultured at 25°C. Each treatment was performed in duplicate.

### 2.3.2. Repeated trials of *V. fortis* infection on *S. guttatus* and *P. damicornis* with QQ treatment

The coral branches of *S. guttatus* and *P. damicornis* were placed in the same aquarium and performed the earlier *V. fortis* inoculation with a final concentration of  $10^5$  CFU/mL, using the control groups treated with *V. fortis* and an additional 2 mL of purified YtnP enzyme (working concentration at 0.05  $\mu$ g/mL) to inhibit the *V. fortis* pathogenicity as a control, and the same volume of seawater as a negative control in the blank. The treated coral branches were continually cultured at 25°C.

## 2.4. Data collection and sample preparation

The condition of coral health was recorded by a digital camera and judged by the marking of the color scale ([Rosado et al., 2019](#)),

according to the PANTONE Color Manager software V2.2.0. The images of corals in each group were taken using a digital camera (Canon EOS 600D with 50 mm lens, Japan), using the parameter of aperture at F/3.5, the exposure time for 1/50 s, and the sensitivity at ISO 200.

The Chlorophyll Fluorescence Quantum Yield ( $Q_y$ ,  $F_v'/F_m$ ) of coral was determined by the mean value of the measurement in light at the tip and middle of coral branches, using pulse amplitude modulated (PAM) fluorimetry (FluorPen FP100, Czech) in triplicate. The measurement was taken at a fixed time every day before light off for the first *Vibrio* infection and performed every 4 h during the experiment in repeated trials. Statistical differences of  $Q_y$  analyses were determined using one-way ANOVA.

The coral branches, about 5 g of live stone, and 500 ml of water from each group were sampled after bacterial infection. The sampled coral branches and live stones were immediately frozen by liquid nitrogen and crushed into powder using a pre-sterilized mortar and pestle, and the water was filtered by the 0.22  $\mu$ m membrane (Millipore, USA) to collect the microorganisms on the filter membrane. The treated coral, stone, and water samples containing the symbiotic microorganism were then stocked at  $-80^\circ\text{C}$  for further analysis.

## 2.5. DNA extraction and amplification

Total genomic DNA was extracted from samples using the MP FastDNA Spin kit for Soil (MP Biomedicals, USA). The DNA extract was checked on 1% agarose gel, and DNA concentration and purity were determined with NanoDrop 2000 UV-vis spectrophotometer (Thermo Scientific, USA) and used as a template DNA to amplify the hypervariable region V3–V4 of the bacterial 16S rRNA and Symbiodiniaceae ITS2 sequence with the primer pairs (listed in

**Table 1**) by PCR using Phusion® High-Fidelity PCR Master Mix kit (NEB, UK). The PCR amplification of 16S rRNA was performed as follows: initial denaturation at 95°C for 3 min, followed by 30 cycles of denaturing at 98°C for 30 s, annealing at 55°C for 30 s, and extension at 72°C for 15 s, and single extension at 72°C for 5 min, and end at 4°C. The PCR products containing bands of 400–450 bp were operated using electrophoresis on 2% agarose gel for detection, and the samples were extracted from the 2% agarose gel and purified using the DNA Gel Extraction Kit (Omega, China) according to the manufacturer’s instructions and quantified using a NanoDrop 2000 spectrophotometer (Thermo Scientific, USA).

2.6. High-throughput sequencing and microbial diversity analysis

The purified amplicons were pooled in equimolar and paired-end sequenced on an Illumina MiSeq PE300 platform/NovaSeqPE250 platform (Illumina, San Diego, USA) according to the standard protocols by Majorbio Bio-Pharm Technology Co., Ltd. (Shanghai, China).

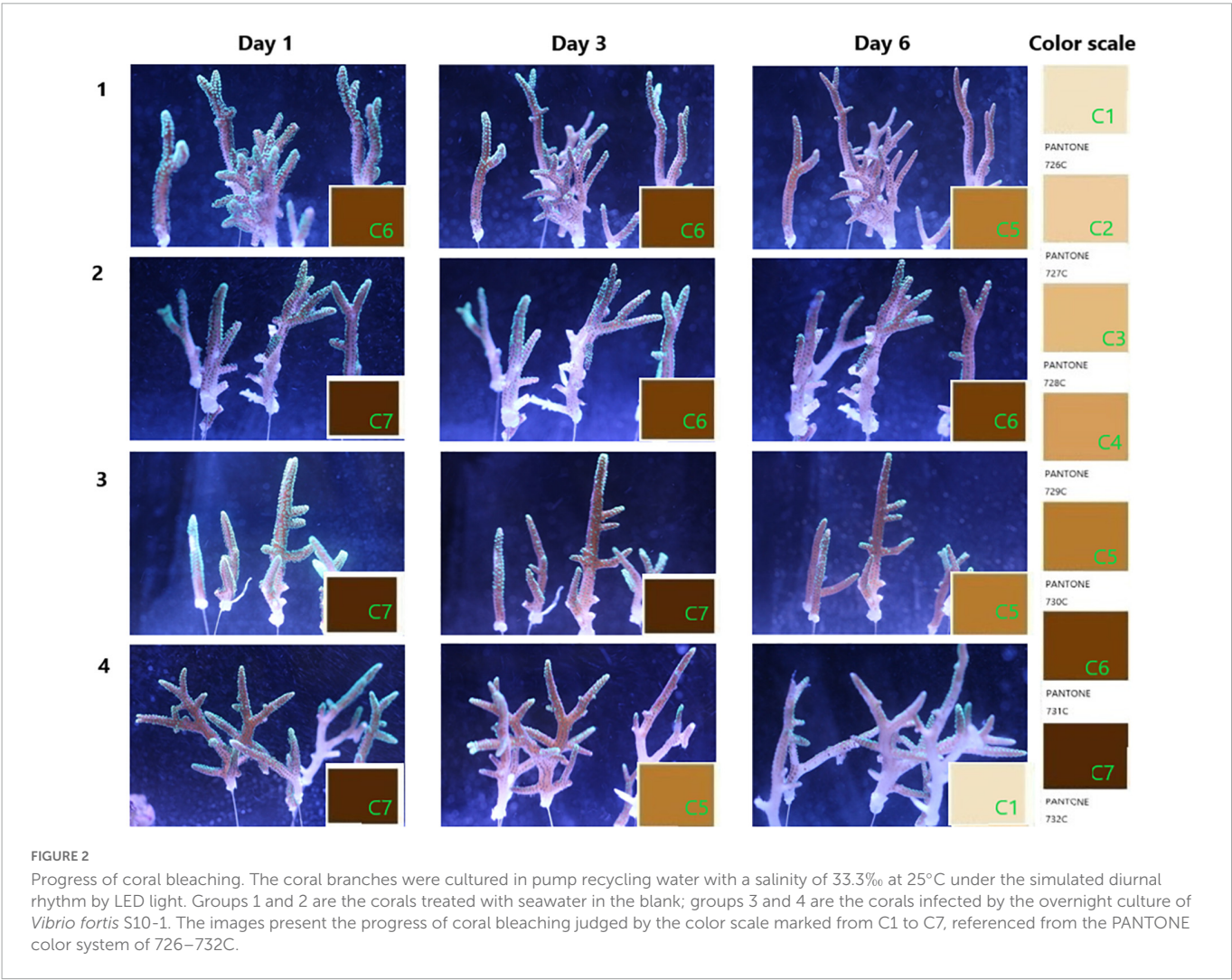
The raw bacterial 16S rRNA and Symbiodiniaceae ITS2 sequencing reads were demultiplexed, quality filtered by fastp version 0.20.0 (Chen et al., 2018), and merged by FLASH version 1.2.7

TABLE 1 Primer pairs tested.

Primer	Sequence	References
338F	5'-ACTCCTACGGGAGGCAGCAG-3'	Feng et al., 2020
806R	5'-GGACTACHVGGGTWTCTAAT-3'	Feng et al., 2020
ITS-DINO	5'-GTGAATTGCAGAACTCCGTG-3'	Hume et al., 2018
ITS2Rev2	5'-CCTCCGCTTACTTATATGCTT-3'	Hume et al., 2018

(Magoë and Salzberg, 2011) with the following criteria: (i) the 300 bp reads were truncated at any site receiving an average quality score of <20 over a 50 bp sliding window, and the truncated reads shorter than 50 bp and reads containing ambiguous characters were discarded; (ii) only overlapping sequences longer than 10 bp were assembled according to their overlapped sequence. The maximum mismatch ratio of the overlap region is 0.2. The reads that could not be assembled were discarded; (iii) samples were distinguished according to the barcode and primers, and the sequence direction was adjusted with exact barcode matching or a maximum of two nucleotide mismatch in primer matching.

Operational taxonomic units (OTUs) with a 97% similarity cutoff were clustered using the UPARSE version 7.1 (Edgar, 2013), and the chimeric sequences were identified and removed. The taxonomy of



each OTU representative sequence was analyzed by RDP Classifier version 2.2 (Wang et al., 2007) according to the SILVA ribosomal RNA database and algal symbionts Genomic resource database (Shi et al., 2021), using a confidence threshold of 0.7. Alpha diversity index, including observed OTUs, and richness estimators, such as Ace, Chao, Shannon, and Simpson indices, were calculated based on the frequency of OTUs and genera in the assigned sequence collections after rare sequences were removed. The OTUs were analyzed by Student's *t*-test to compare the difference of the abundance on the genus level.

### 3. Results

#### 3.1. Effect of *V. fortis* on the coral health

The condition of coral health is shown in Figure 2. After the inoculation of S10-1 for about 30 h, the corals in blank groups as the control were still observed in good condition, while the infected ones repeated in Groups 3 and 4 were observed with less tentacles extending for predation (Day 3). The second inoculation of *Vibrio* on Day 5 caused the symptoms to be more obvious on the second day (Day 6), and the images showed that Group 3 infected with *Vibrio* was observed with bleaching from C7 to C5, and Group 4 observed more serious bleaching from C5 to C1, accompanied with peeling of coral tissue. The damages mainly occurred starting from the middle of coral branches to the tip ends, while the coral polyps still seemed to be in good condition at the tip ends.

#### 3.2. Photosynthetic function of coral holobiont under *V. fortis* infection

The results from the visual response of the coral holobiont health in each treatment were confirmed by the chlorophyll fluorescence quantum yield (Fv'/Fm) measured by PAM fluorometry to indicate the algal symbionts' photosynthetic function. As shown in Figure 3, the Qy values from duplicated blank groups were similar, ranging between 0.50 and 0.40 in the first 6 days and remaining above 0.35 on Day 7 (*P*-value was 0.96857), while the Qy values from duplicated *Vibrio* infection groups also did not present a significant difference (*P*-value was 0.37669), with coral 3 being observed with a decreasing ratio of 13.17% after 6 days and further decreasing to about 0.21 on Day 7, while coral 4 present more sensitive to the *Vibrio* infection, decreased rapidly from healthy status at about 0.45 to an obvious bleaching status at Qy value of 0.208 on Day 6 than 0.014 on Day 7. According to the results of statistical analysis, the *Vibrio* infection significantly affected the photosynthetic function of coral holobiont with a *P*-value of 0.00491.

#### 3.3. Verification of *V. fortis* as a potential pathogen to coral disease

Later on, the S10-1 strain was isolated from the infected *S. guttatus* branches. According to Koch's rule, to verify the actual causative agent of *V. fortis*, subsequent infection experiments were carried out and inoculated the isolated S10-1 on both *S. guttatus*

and *P. damicornis*; in addition, the QQ enzyme was used to inhibit the pathogenicity of S10-1 as control. As shown in Figure 4, the two species of coral were observed with a significant decrease in Qy value accompanied by obvious bleaching, after the inoculation of re-isolated S10-1 for 30 h. Interestingly, the corals in QQ-treated groups were observed with a reduction tendency but far better than that of infected groups, while the corals in blank groups remained in good condition. The results demonstrated that the infection of *V. fortis* again caused coral bleaching after bacterial inoculation, confirming the hypothesis that *V. fortis* was highly responsive to coral bleaching and was a potential pathogen related to coral health. In addition, the positive effects of QQ also indicated the probability of quorum sensing (QS) inhibition as a potential strategy for coral disease control.

#### 3.4. Diversity and richness of total symbiotic bacteria

The diversity and richness of symbiotic bacteria from *S. guttatus* were further analyzed by the Alpha index, as shown in Table 2. The coverage of OTU from each sample was in the range of 98.79 to 99.95%, which indicated good recovery and reliable reflection of the symbiotic bacterial community of the tested samples.

The community of coral symbiotic bacteria was observed with a remarkable difference between the healthy corals and the *Vibrio*-infected ones; the infection of *V. fortis* increased the richness as indicated by the higher indices of Ace and Chao and enriched the diversity as indicated by the higher Shannon index and lower Simpson index. In contrast, the planktonic bacteria in the water sample of healthy corals present higher richness than that of diseased corals and showed similar diversity between groups. In addition, the richness and diversity of the bacterial community in live stones were rarely affected by the additional *V. fortis* and showed no significant difference.

#### 3.5. Structure of microbial community in the coral culture system

The microbial diversity in *S. guttatus* of each treatment group was analyzed. As shown in the community species abundance clustering in Figure 5, the upper clustering tree analyzed using the Bray–Curtis algorithm demonstrated a similarity and consistent tendency on the species abundance of the bacterial community in the duplicates, which indicated good reliability of the experiments. The results also indicated the relevance of bacterial community in the coral culture system, indicating that the *Vibrio* infection changed the abundance of the bacterial community in the symbiotic status of coral holobiont and planktonic status in seawater and that there was no significant difference among stones exposed under immersion of *Vibrio*, indicating the ability of self-regulation and stronger colonization resistance, which was probably acted by the abundant microorganisms adhered on the stones.

##### 3.5.1. Community of coral symbiotic microorganisms

The structure of the microbial community in corals is shown in Figure 6. The results of OTU analysis showed that the microbial

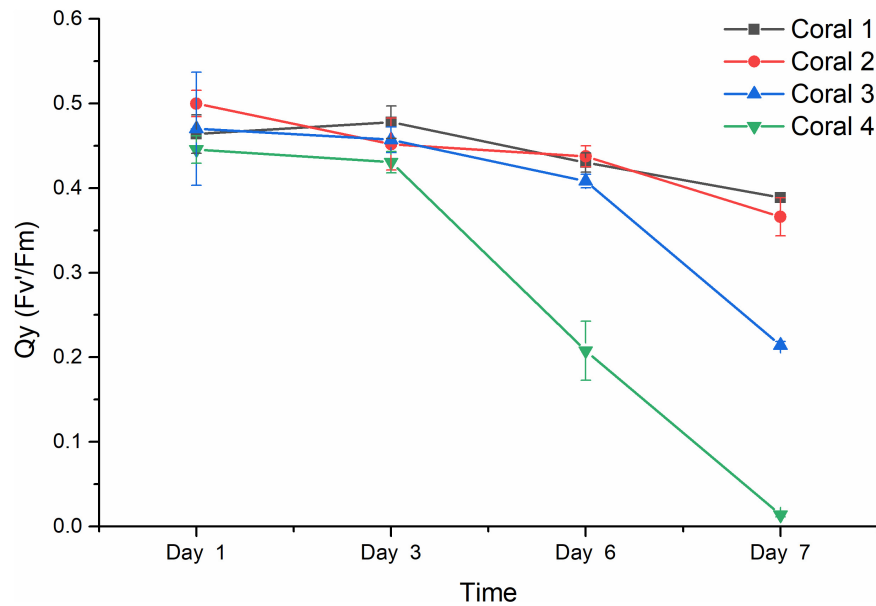


FIGURE 3

Chlorophyll fluorescence quantum yield ( $F_v'/F_m$ ) of coral holobiont. The  $Q_y$  ( $F_v'/F_m$ ) was measured using PAM fluorimetry at 3 points of coral middle parts and 3 points of coral tip ends, to obtain the average value and standard deviation of each coral branch. Corals 1 and 2 represented the corals treated with seawater in the blank; corals 3 and 4 represented the corals infected by *V. fortis* S10-1. The  $Q_y$  of coral 1 is presented by ■ in black line, coral 2 by ● in red line, coral 3 by ▲ in blue line, and coral 4 by ▼ in green line.

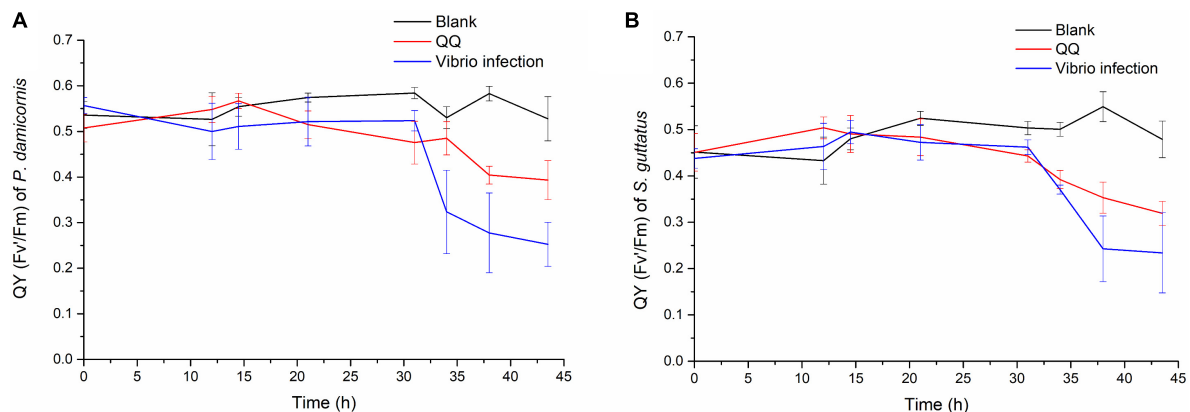


FIGURE 4

Photosynthetic function of coral holobiont under bacterial infection and QQ treatment. The  $Q_y$  ( $F_v'/F_m$ ) of *P. damicornis* (A) and *S. guttatus* (B) was measured using PAM fluorimetry at 3 points of coral middle parts and 3 points of coral tip ends, to obtain the average value and standard deviation of each coral branch. The  $Q_y$  from the *V. fortis* infected groups are presented in blue line, those infected groups with additional treatment of QQ enzyme are presented in red line, and the blank groups in black line.

community composition was significantly different between the groups with different treatments. On the phylum level, the microbial community of corals suffered from exogenous *V. fortis* infection which led to a significant decrease in Firmicutes from 93.14 to 6.624% ( $P$ -value lower than 0.001) but an increase in the abundance of Actinobacteriota from 1.085 to 49.26% ( $P$ -value was 0.002405), Proteobacteria from 4.68 to 33.19% ( $P$ -value was 0.001759), and Acidobacteriota from 0.08413 to 2.653% ( $P$ -value was 0.03163).

On the genus level, after infection with *V. fortis*, the abundance of *Bacillus* in the symbiotic microorganisms of bleaching coral decreased significantly from 87.57% in the blank group to only 2.273% in bleaching corals ( $P$ -value was 0.0009638), mostly contributed by more abundant *B. circulans* and *B. aryabhatai* and less

abundant *B. subtilis*, *B. anthracis*, and *B. infernus*, and the abundance of *Rhodococcus* with a  $P$ -value of 0.006542 (44.26% in bleaching coral and 0.2874% in the blank group, mostly identified as *R. erythropolis*), *Ralstonia* with a  $P$ -value of 0.0009664 (11.35% in bleaching corals and 0.3126% in the blank group, affected by *R. pickettii* and *R. insidiosa*), and *Burkholderia*–*Caballeronia*–*Paraburkholderia* with a  $P$ -value of 0.02048 (5.606% in bleaching corals and 0.4076% in the blank group, mostly constituted by *Paraburkholderia fungorum*) increased significantly.

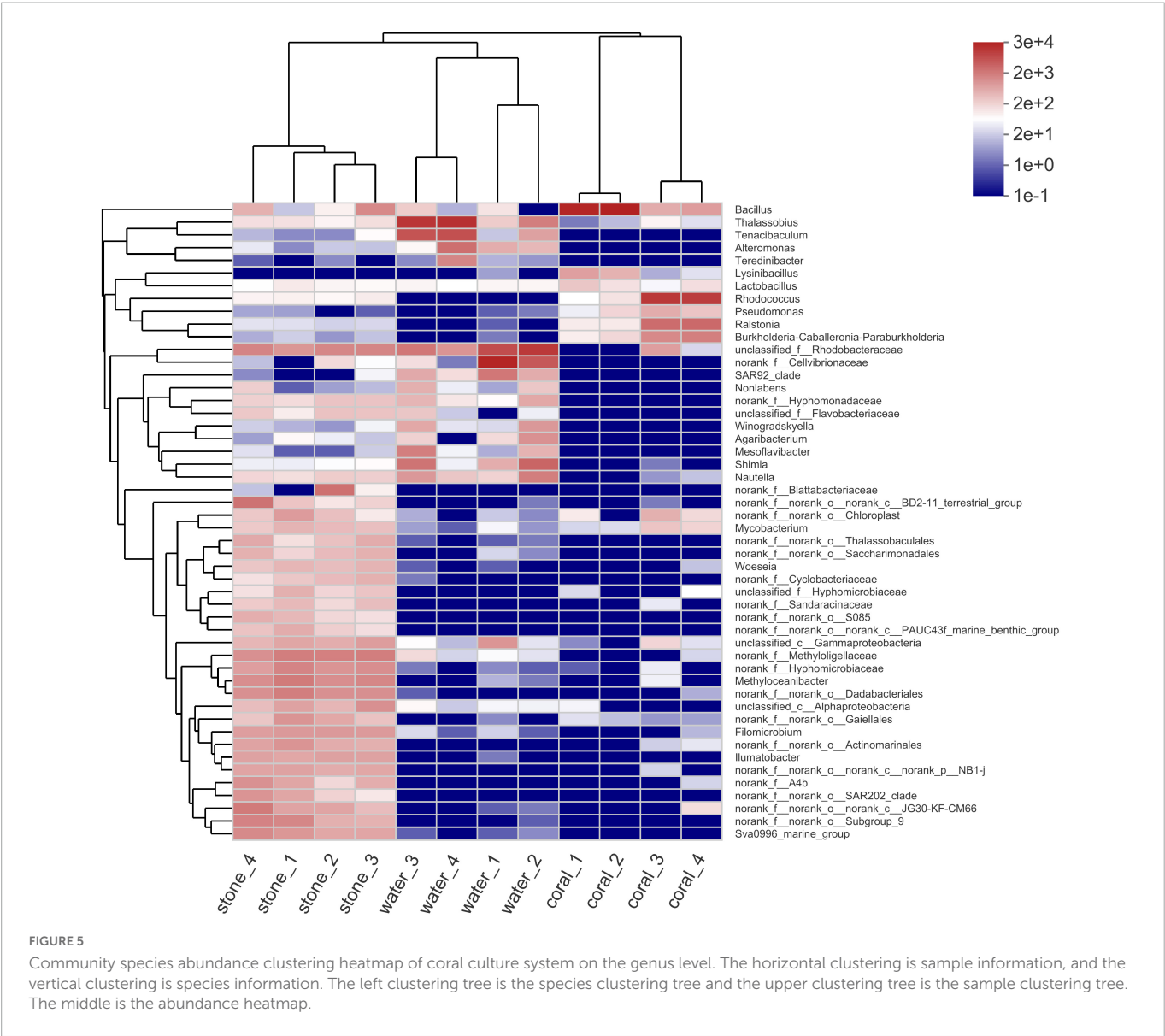
### 3.5.2. Community of planktonic bacteria in water

The planktonic bacteria in the culture water were also analyzed as shown in Figure 7. On the phylum level, Proteobacteria took



TABLE 2 Alpha diversity index analysis of symbiotic bacteria in the coral culture system.

Sample	OTU number	Ace	Chao	Shannon	Simpson	Coverage
coral_1	30855	249.1679	256.5556	1.3627	0.6033	99.91%
coral_2	31511	127.4174	157.7500	0.8403	0.7541	99.94%
coral_3	31731	407.2778	409.1579	2.9992	0.2437	99.95%
coral_4	32228	411.5785	414.5000	3.3771	0.1833	99.95%
water_1	42886	533.0147	499.2113	1.5774	0.4193	99.68%
water_2	37960	467.1878	463.1000	2.6786	0.1588	99.70%
water_3	36706	531.7272	488.5789	2.2264	0.2431	99.68%
water_4	33842	246.4882	238.0000	1.4988	0.3575	99.84%
stone_1	37081	1856.7257	1824.1246	5.7499	0.0103	99.24%
stone_2	30049	1738.6738	1704.2672	5.4152	0.0190	98.84%
stone_3	31703	1867.3839	1844.3333	5.5812	0.0118	98.79%
stone_4	38012	1601.2413	1580.1416	5.5155	0.0104	99.27%



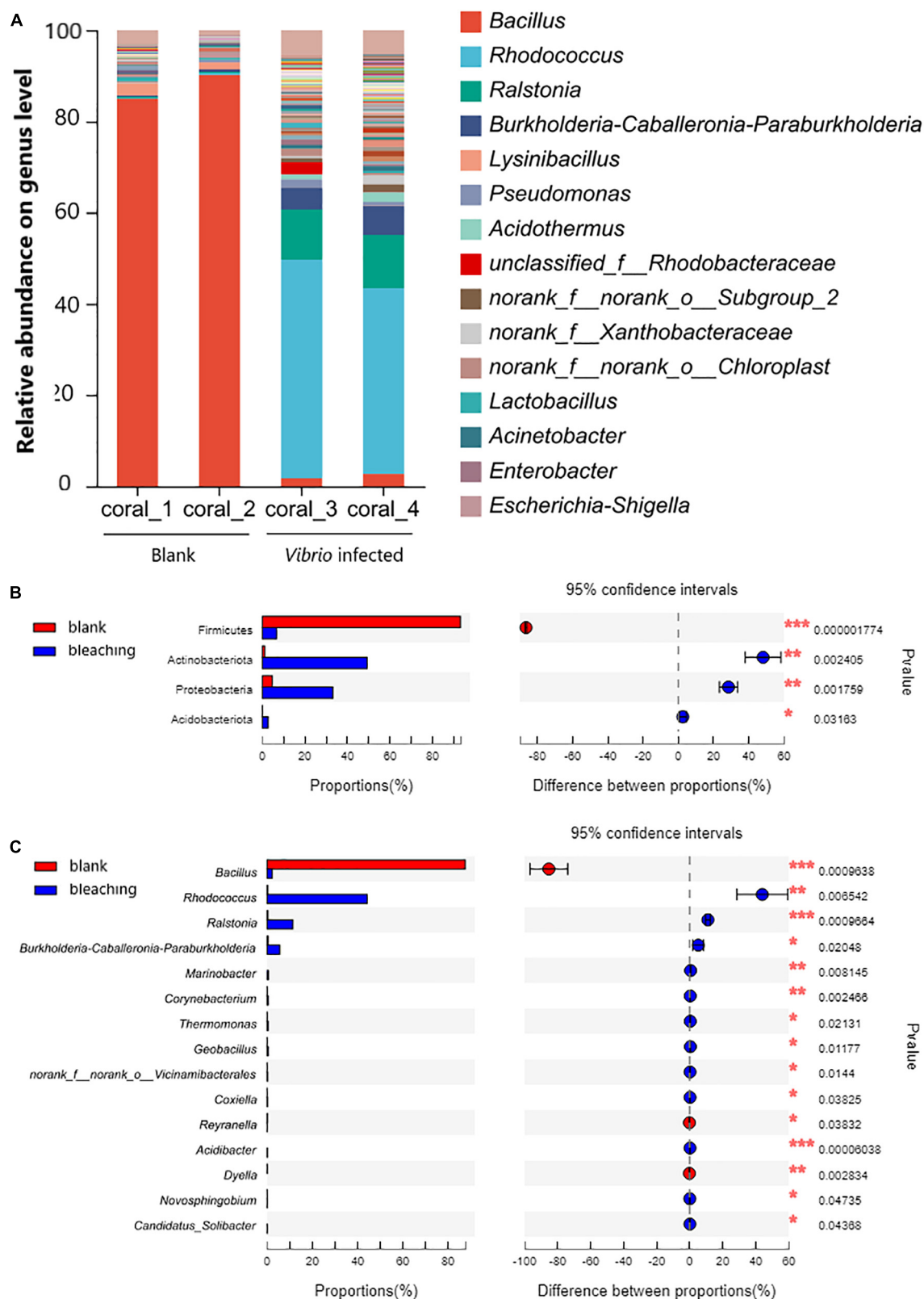


FIGURE 6

Community composition of coral symbiotic bacteria on the genus level. The total genomic DNA of coral symbiotic microorganisms from each group performed high-throughput sequencing on the 16S rRNA. The taxonomy of each OTU representative sequence was analyzed by RDP classifier version 2.2 and classified on the genus level. The OTUs were analyzed by student's *t*-test to compare the difference in abundance between groups: (A) is the microbial structure presented by relative community abundance; (B) is the phyla with a significant difference in abundance; and (C) is the top 15 genera with a significant difference in abundance were listed from higher abundance to low. Results of statistical analysis are presented by the significant difference indicated by \* where  $0.01 \leq P \leq 0.05$ , \*\* where  $0.001 \leq P \leq 0.01$ , and \*\*\* where  $P \leq 0.001$ .

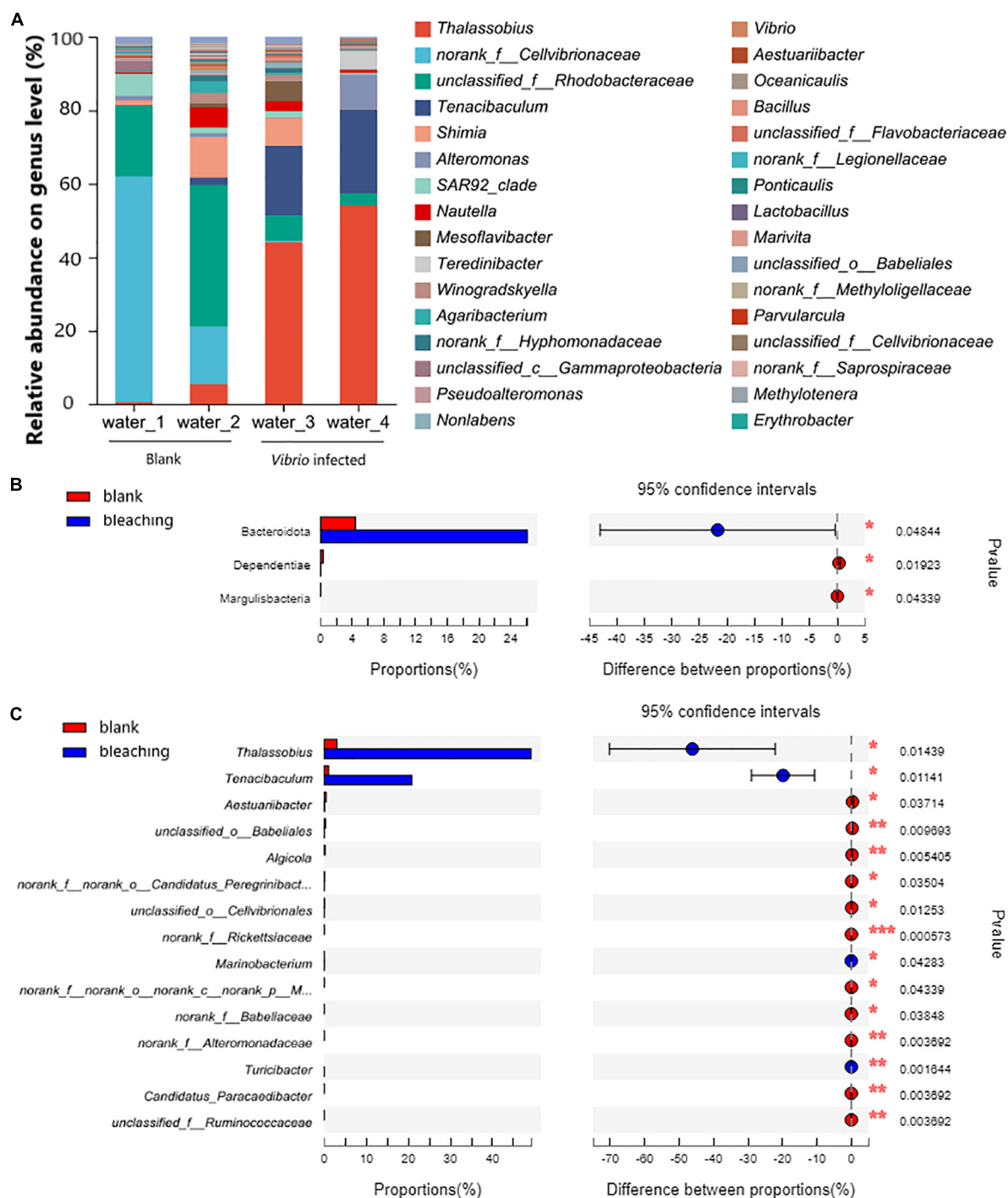


FIGURE 7

Community composition of planktonic bacteria in water on genus level. The total genomic DNA of planktonic bacteria in water from each group performed high-throughput sequencing on the 16S rRNA. The taxonomy of each OTU representative sequence was analyzed by RDP Classifier version 2.2 and classified on the genus level. The OTUs were analyzed by student's *t*-test to compare the difference in abundance between groups: (A) is the microbial structure presented by relative community abundance; (B) is the phyla with a significant difference in abundance; and (C) is the top 15 genera with a significant difference in abundance which were listed from higher abundance to low. Results of statistical analysis are presented by the significant difference indicated by \* where  $0.01 \leq P \leq 0.05$ , \*\* where  $0.001 \leq P \leq 0.01$ , and \*\*\* where  $P \leq 0.001$ .

the highest proportion in the community and showed no significant difference after infection (94.21% in blank and 73.1% after infection, the *P*-value was 0.05276); the *Vibrio* infection caused significantly increasing abundant Bacteroidota from 4.402 to 26.09% (*P*-value was 0.04844); decreasing abundant Dependitiae from 0.3424 to 0.01805% (*P*-value was 0.01923) and Margulisbacteria with 0.02686%

in the blank group and non-detected in *Vibrio*-infected groups (*P*-value was 0.04339).

On the genus level, the results of OTU analysis demonstrated a significantly increased abundance of *Thalassobius* and *Tenacibaculum*, and took as much as 49.15 and 20.83% in the *Vibrio*-infected culture water, while there were only 2.995 and 1.039%

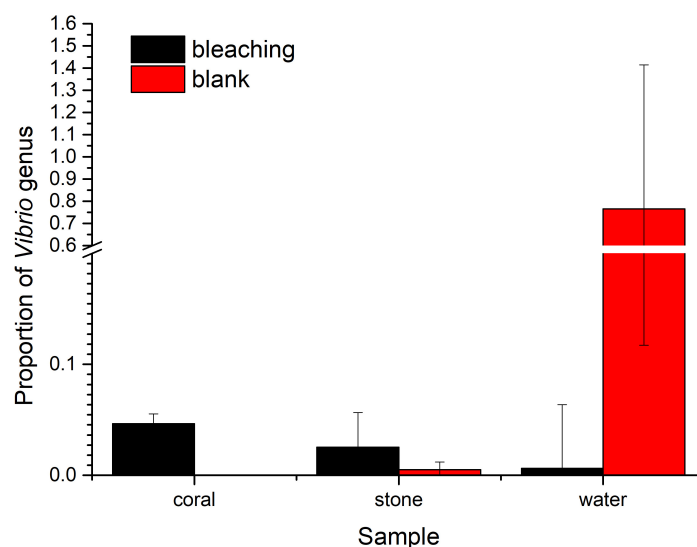


FIGURE 8

Proportion of *Vibrios* in each fraction of coral culture system. The taxonomy of each OTU representative sequence from the high-throughput sequencing result was analyzed by RDP classifier version 2.2 and classified on genus level. The proportion of the OTUs representing the *Vibrio* genus is presented in bar charts, where the samples in the blank group are presented in red, and those in S10-1-infected groups are presented in black. The error bars indicate the value of standard deviations.

in the blank group ( $P$ -values were 0.01439 and 0.01141, respectively). It was also observed that with abundant unclassified genera from the Rhodobacteraceae family (5.083% in the *Vibrio*-infected group and 28.91% in the blank group) and *Shimia* (3.862% in the *Vibrio*-infected group and 6.152% in the blank group) present in the culture water, there was no significant difference between groups ( $P$ -values were 0.1342 and 0.7453, respectively).

### 3.5.3. Proportion of *Vibrios* in the coral culture system

As for the *Vibrio* sp., the proportion of *Vibrios* in each fraction is shown in Figure 8. The abundance of *Vibrio* was 0.006206% in bleaching corals, while that was non-detected in the blank group, including OTU3764 whose sequence was 100% matched to the 16S rRNA sequence of S10-1 (which is consistent with the result of isolation of S10-1 from infected *S. guttatus*) and other four unidentified *Vibrio* sp. represented by OTU3690, OTU3768, OTU3779, and OTU38. A higher proportion of *Vibrios* was also observed in the stones under *Vibrio* infection; however, the *Vibrio* abundance of water in the S10-1 infected group was significantly lower than that of the blank group, indicating that the change in the bacterial community and coral health was not directly caused by the *Vibrios* under planktonic status, and probably affected by the symbiotic status in corals.

### 3.6. Effect of *Vibrio* infection on the algal symbionts

The community of algal symbionts was also analyzed to assess the effects of *Vibrio* infection as shown in Figure 9. The community of algal symbionts was observed with the most components of *Cladocopium* sp. in coral holobionts and very few *Breviolum* sp. and *Fugacium* sp. in live stone and seawater. No significant difference in community abundance and diversity was observed among the

groups in coral holobiont, which indicated the rare effect of *Vibrio* on the algal symbionts, and therefore verified that the phenomenon of bleaching might be caused by the bacterial infection reasoned by *Vibrio* and secondary disorder of bacterial community.

## 4. Discussion

### 4.1. Potential pathogenicity of *Vibrio* to coral health

The role of *Vibrios* in coral diseases was still limitedly known (Munn, 2015), though there are some *Vibrio* species had been identified as opportunistic pathogens to cause coral disease, there is disagreement about whether they should be regarded as primary causing agents, as some *Vibrios* appeared to contribute to nitrification (Thurber et al., 2009) or involved in defense against pathogens (Ritchie, 2006).

Unlike the better-studied species, such as *V. parahaemolyticus* and *V. coralliformis*, *V. fortis* is still rarely reported. To the best of our knowledge, it was reported for its pathogenicity to marine animals such as shrimps (Thompson et al., 2003), sea horses (Wang et al., 2016), and sea urchins (Ding et al., 2014), as well as one of the lists of abnormal abundant coral symbiotic microbes (Ou et al., 2018). Predictably, the activity of sea cucumber carrying *V. fortis* in coral reefs area would increase the risk of bacterial infection to the coral holobiont. However, the disease development and pathogenicity mechanism of coral bleaching caused by *V. fortis* are not yet clear.

It is currently known that the pathogenicity of *Vibrio* sp. is parallelly regulated by at least three QS pathways, LuxM/LuxN-related AHLs, CqsA/CqsS-related CAI-1, and LuxS/LuxP-related AI-2; all lead to the regulation of core regulatory protein LuxO (Herzog et al., 2019) and then to the synergistic action of key regulatory proteins AphA (Lu et al., 2018) and OpaR (Zhang et al., 2016), which

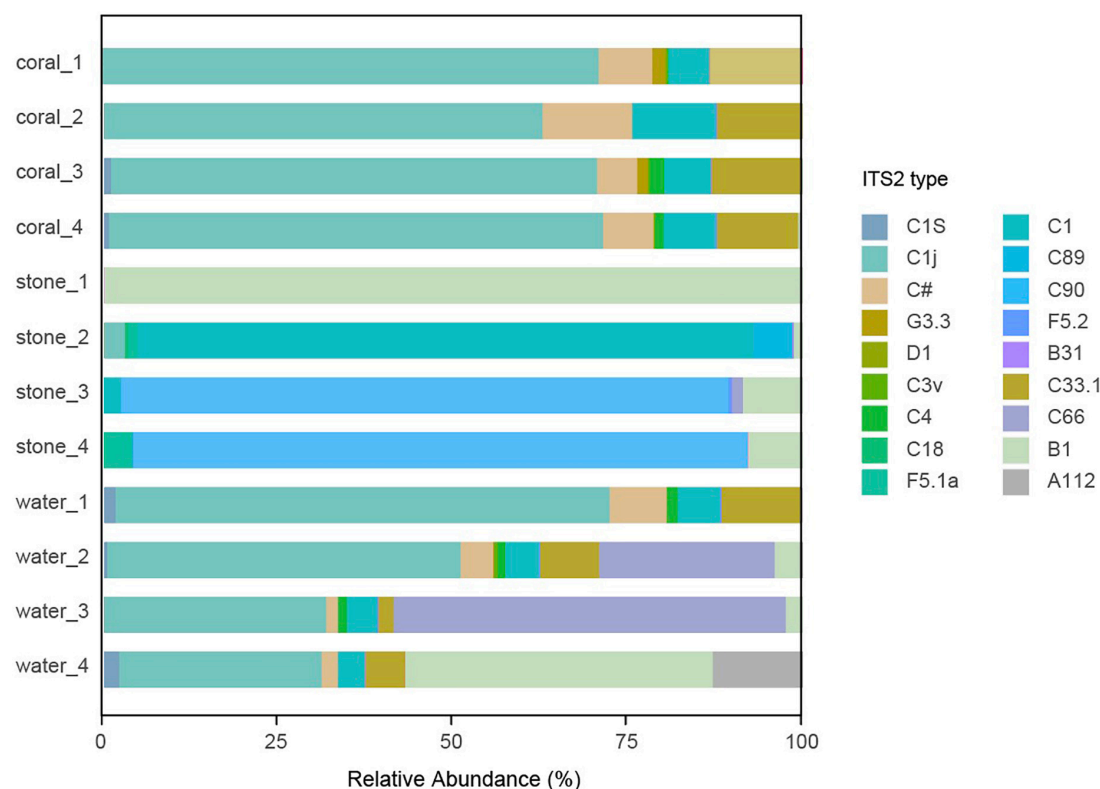


FIGURE 9

Community component of algal symbionts in the coral culture system. The total genomic DNA from each group performed high-throughput sequencing using the primer pair of ITS-DINO and ITS2Rev2. The taxonomy of each OTU representative sequence was analyzed according to the algal symbionts' genomic resource database and classified by ITS2 type.

regulate downstream exopolysaccharide synthesis genes to affect biofilm formation and virulence relative genes to release virulence factors including hemolysin. The findings of QS signals produced by bacteria in the coral mucus layer (Li et al., 2017), the signaling molecules and active hydrolytic enzymes released by *V. shilonii* AK1 in outer membrane vesicles (Li et al., 2016), and the interference of QS regulation against the AHL-mediated opportunistic bacteria of resident microbes in bleaching's initiation and progression (Zhou et al., 2020), in recent years, all supported the hypothesis of bacterial infection under QS regulation, which is consistent with the positive inhibition of *V. fortis* pathogenicity under QQ enzyme treatment in this study (Figure 4), and this phenomenon indicates the potential strategy of QQ on coral disease control.

## 4.2. Microbial shift and bacterial interaction behind *Vibrio* infection

In this article, the infection of *V. fortis* was designed as the only variable factor in coral health. The symptom development of coral bleaching and tissue lysis verified and strongly supported the hypothesis of "bacterial bleaching." The findings in this study demonstrated that its infection also caused significant changes in the coral-associated microsystem, especially the increased abundance of opportunistic pathogenic bacteria, which might synergistically affect coral health.

Among the microbial community, the decreasing abundance of *Bacillus* belonging to phylum Firmicutes seems to be the most

serious side effect caused by *Vibrio* infection (Figure 5). *Bacillus* had been widely accepted as the main antagonistic bacteria and used for biological control in agriculture (Jiang et al., 2018) and aquaculture (Wang et al., 2019), and recently reported as marine probiotics to increase coral resistance to bleaching (Rosado et al., 2019). *Bacillus* can produce secondary metabolites, including lipopeptides and polyketones with antibacterial, antiviral, or antitumor activities (Wu et al., 2019), and the quorum quenching (QQ) enzymes, such as AiiA (Dong et al., 2000) and YtnP (Sun et al., 2021), to degrade AHLs, inhibiting the biofilm formation and toxin release of AHLs/Lux-mediated pathogens including *V. fortis* that was known to contain an AHLs intermediated LuxM/LuxN QS pathway (Ding et al., 2014). The subsequent abnormal abundant *Bacillus*, *B. circulans* for instance, resulted from the simulated outbreaking of *V. fortis* when the inoculation of  $10^5$  CFU/ml was far beyond the threshold of QS; therefore, it might further weaken the resistance of coral holobiont to the stress from pathogens (Satpute et al., 2010; Niu et al., 2014).

The increased abundance of *Rhodococcus* in phylum Actinobacteria might also be related to the decreasing abundance of *Bacillus*, because *Rhodococcus* sp. was reported with antibacterial activity against *Bacillus subtilis* (Mahmoud and Kalendar, 2016). Among these, the most composition species, *R. erythropolis*, produces different types of QQ enzymes (Ryu et al., 2020) to recognize and degrade AHLs and could be used for biofouling control (Ergön-Can et al., 2017). The increasing abundance might be speculated to result from the self-regulation of the coral symbiotic microbiota after the sense of abnormally increased concentration of AHLs generated by the inoculated *V. fortis*.



The increasing abundance of the genera *Ralstonia* and *Burkholderia*–*Caballeronia*–*Paraburkholderia* in phylum Proteobacteria was probably eligible for the causal relationship of the declined abundance of *Bacillus* because of the less inhibition from the *Bacillus*-produced surfactin (Grady et al., 2019). However, the correlation between *Ralstonia* and *Burkholderia*–*Caballeronia*–*Paraburkholderia* of coral health is still unclear (Bernasconi et al., 2019). Reports are claiming that *Ralstonia* sp. is a known gram-negative phytopathogenic bacteria (Hayashi et al., 2019) and dental opportunistic pathogen (Tuttlebee et al., 2002), while the *Burkholderia*–*Caballeronia*–*Paraburkholderia*, which is mostly constituted by *Paraburkholderia fungorum*, is reported as a plant probiotic bacteria (Rahman et al., 2018) but still risky to human health (Tan et al., 2020).

In addition, considering that the planktonic bacteria in the water could flow into the gastrovascular cavity of coral along with the filter feeding, the significantly increased abundance of *Thalassobius* (also detected with higher abundance in bleaching coral but with no significant difference) and *Tenacibaculum* in water might also affect the coral health (Figure 7). *Thalassobius* belonging to the family Rhodobacteraceae has been reported as a microbial bioindicator enriched in the Stony Coral Tissue Loss Disease accompanied by *Vibrio* (Becker et al., 2021), and has been associated with invertebrate diseases (Roder et al., 2014), while the increased abundance of *Tenacibaculum* was also consistent with the findings from microbial community shift in the White syndrome-affected *Echinopora lamellosa* in aquaria (Smith et al., 2015).

Another unclassified genus belonging to the family Rhodobacteraceae and the genus *Shimia* was also detected in the planktonic bacterial community in water, though there was no significant difference observed yet. The indicator species in the coral hosts, family Rhodobacteraceae and genus *Shimia*, were observed to increase their relative abundance when corals are under stress (Casey et al., 2015; Pootakham et al., 2019) or with the emergence of *Porites* white patch syndrome accompanied with *Vibrio* (Séré et al., 2013). This phenomenon was verified in the later coral bleaching in the blank group caused by the deterioration of water quality 2 days after the experiments stopped (data not shown).

The virulence from the shift bacterial community of abundant opportunistic pathogens might not be the only reason for coral bleaching. The nutrients sources and waste products for coral holobiont are also a concern, which mainly come from the metabolism of symbiotic microbes such as carbon and nitrogen fixation (Gibbin et al., 2019) and the metabolic integration from algal symbionts (Sun et al., 2020), in such closed aquaria without extra exogenous nutrient sources. The shift in the bacterial community no doubt leads to an imbalance in the nutrient food chain in the coral holobiont (Raina et al., 2009); however, in this study, there is no direct relevance between the infection of *V. fortis* and the status of algal symbionts. The dominant population in the tested *S. guttatus* was *Cladocopium* sp., though with few relative abundances of other Symbiodiniaceae according to the reported ITS2 type (Yu et al., 2020), and no observation of *Durisdinium* sp., which was reported with stronger stress resistance (Sun et al., 2020); therefore, the findings indicated that the bleaching in this study was caused by *Vibrio* infection and the following shift of bacterial community, but not by the dissociation of algal symbionts.

To sum up, this study expands the cognition of the correlation between coral symbiotic *Vibrio* and coral health. According to the experience of other reported *Vibrio* pathogens, the outbreak

and pathogenicity enhancement of *Vibrio* may be related to environmental changes (Kimes et al., 2012). The symbiotic changes caused by the outbreak of *V. fortis*, especially the increased abundance of other pathogenic bacteria, may also cause more serious damage to the coral holobiont. In addition, the reduced abundance of potential probiotics *Bacillus* under the competition of microbiota might also provide an experimental experience for probiotic strategy (Zhao et al., 2019) or QS regulation (Zhou et al., 2020) on pathogen control or resistance enhancement (Rosado et al., 2019).

## 5. Conclusion

To identify the relationship between *V. fortis* and coral health and to understand its role in bacterial infection, *V. fortis* S10-1 was designed as the only variable factor to infect the coral *Seriatopora guttatus* and *Pocillopora damicornis*. The results of color scale analysis of S10-1-infected coral branches in aquaria indicated that *V. fortis* was responsible for coral bleaching, which leads to the high probability of pathogenicity of *V. fortis* in coral. The significant reduction of photosynthetic function in coral holobiont and shift of coral symbiotic microbial community upon the infection of S10-1 provided strong evidence for the "bacterial bleaching" hypothesis. The positive effect of quorum quenching indicated the potential strategy of bacterial disease control. The infection of S10-1 led to the imbalance in the coral-associated bacterial community but had no significant effect on the algal symbionts, and this was accompanied by a significant decrease in the abundance of probiotic *Bacillus* and an increase in the abundance of *Rhodococcus erythropolis* and other opportunistic pathogens including *Ralstonia* and *Burkholderia*–*Caballeronia*–*Paraburkholderia* in the coral-associated community, as well as increased abundance of *Shimia* and other unclassified genus in family Rhodobacteraceae in the planktonic bacterial community in water. The study provided experimental experience on corals in aquaria for the exploration of the interaction among coral-associated microbial communities in coral relative micro-ecosystem and revealed the potential probiotic strategy or QS regulation on pathogen control for coral health.

## Data availability statement

The datasets presented in this study can be found in online repositories. The names of the repository/repositories and accession number(s) can be found below: <https://doi.org/10.6084/m9.figshare.21707861.v1>.

## Author contributions

XS contributed to the conception of the study and drafted the manuscript. YL and XZ contributed to the design of the experiment of bacterial challenge and culture of corals. QY, NX, ZT, SW, and YJ performed the experiments. HZ helped the analysis of the ITS2 type of Symbiodiniaceae. XZ, HM, and DO helped the analysis with constructive discussions. XS and DO offered the funding acquisition. All authors reviewed the results and approved the final version of the manuscript.

## Funding

This project was sponsored by the National Key Research and Development Program of China (2022YFC3102003), the Fujian Provincial Department of Science and Technology (2021N0012), the Fundamental Research Funds for the Central Universities (ZQN-1018), and the Scientific Research Foundation of Third Institute of Oceanography, MNR (2020017).

## Acknowledgments

We thank MCCC from TIO, MNR for providing the bacterial isolates of *Vibrio fortis* S10-1 for this study.

## References

- Ahmed, N., Mohamed, H. F., Xu, C., Sun, X., and Huang, L. (2022). Novel antibacterial activity of *Sargassum fusiforme* extract against coral white band disease. *Electronic J. Biotechnol.* 57, 12–23. doi: 10.1016/j.ejbt.2022.03.002
- Ainsworth, T. D., Fine, M., Roff, G., and Hoegh-Guldberg, O. (2008). Bacteria are not the primary cause of bleaching in the mediterranean coral *Oculina patagonica*. *ISME J.* 2, 67–73. doi: 10.1038/ismej.2007.88
- Becker, C. C., Brandt, M., Miller, C. A., and Apprill, A. (2021). Microbial bioindicators of stony coral tissue loss disease identified in corals and overlying waters using a rapid field-based sequencing approach. *Environ. Microbiol.* 24, 1166–1182. doi: 10.1111/1462-2920.15718
- Bernasconi, R., Stat, M., Koenders, A., Paparini, A., Bunce, M., and Huggett, M. J. (2019). Establishment of coral-bacteria symbioses reveal changes in the core bacterial community with host ontogeny. *Front. Microbiol.* 10, 1529. doi: 10.3389/fmicb.2019.01529
- Casey, J. M., Connolly, S. R., and Ainsworth, T. D. (2015). Coral transplantation triggers shift in microbiome and promotion of coral disease associated potential pathogens. *Sci. Rep.* 5, 1–11. doi: 10.1038/srep11903
- Chen, S., Zhou, Y., Chen, Y., and Gu, J. (2018). Fastp: An ultra-fast all-in-one FASTQ preprocessor. *Bioinformatics* 34, i884–i890. doi: 10.1093/bioinformatics/bty560
- Ding, J., Dou, Y., Wang, Y., and Chang, Y. (2014). Draft genome sequence of *Vibrio fortis* Dalian14 isolated from diseased sea urchin (*Strongylocentrotus intermedius*). *Genome Announc.* 2, 14–15. doi: 10.1128/genomeA.00409-14
- Dong, Y., Xu, J., Li, X., and Zhang, L. (2000). AiiA, an enzyme that inactivates the acylhomoserine lactone quorum-sensing signal and attenuates the virulence of *Erwinia carotovora*. *Proc. Natl. Acad. Sci. U.S.A.* 97, 3526–3531. doi: 10.1073/pnas.97.7.3526
- Edgar, R. C. (2013). UPARSE: Highly accurate OTU sequences from microbial amplicon reads. *Nat. Methods* 10, 996–998. doi: 10.1038/nmeth.2604
- Ergön-Can, T., Köse-Mutlu, B., Koyuncu, İ., and Lee, C. H. (2017). Biofouling control based on bacterial quorum quenching with a new application: Rotary microbial carrier frame. *J. Membr. Sci.* 525, 116–124. doi: 10.1016/j.memsci.2016.10.036
- Feng, L., He, L., Jiang, S., Chen, J., Zhou, C., Qian, Z. J., et al. (2020). Investigating the composition and distribution of microplastics surface biofilms in coral areas. *Chemosphere* 252:126565. doi: 10.1016/j.chemosphere.2020.126565
- Gibbin, E., Gavish, A., Krueger, T., Kramarsky-Winter, E., Shapiro, O., Guet, R., et al. (2019). *Vibrio coralliilyticus* infection triggers a behavioural response and perturbs nutritional exchange and tissue integrity in a symbiotic coral. *ISME J.* 13, 989–1003. doi: 10.1038/s41396-018-0327-2
- Grady, E. N., MacDonald, J., Ho, M. T., Weselowski, B., McDowell, T., Solomon, O., et al. (2019). Characterization and complete genome analysis of the surfactin-producing, plant-protecting bacterium *Bacillus velezensis* 9D-6. *BMC Microbiol.* 19:5. doi: 10.1186/s12866-018-1380-8
- Hayashi, K., Senuma, W., Kai, K., Kiba, A., Ohnishi, K., and Hikichi, Y. (2019). Major exopolysaccharide, EPS I, is associated with the feedback loop in the quorum sensing of *Ralstonia solanacearum* strain OE1-1. *Mol. Plant Pathol.* 20, 1740–1747. doi: 10.1111/mp.12870
- Herzog, R., Peschek, N., Fröhlich, K. S., Schumacher, K., and Papenfort, K. (2019). Three autoinducer molecules act in concert to control virulence gene expression in *Vibrio cholerae*. *Nucleic Acids Res.* 47, 3171–3183. doi: 10.1093/nar/gky1320
- Hume, B. C. C., Ziegler, M., Poulain, J., Pochon, X., Romac, S., Boissin, E., et al. (2018). An improved primer set and amplification protocol with increased specificity and sensitivity targeting the Symbiodinium ITS2 region. *PeerJ* 6:e4816. doi: 10.7717/peerj.4816
- Jiang, C., Liao, M., Wang, H., Zheng, M., and Xu, J. (2018). *Bacillus velezensis*, a potential and efficient biocontrol agent in control of pepper gray mold caused by *Botrytis cinerea*. *Biol. Control* 126, 147–157. doi: 10.1016/j.biocontrol.2018.07.017
- Kang, J., Mohamed, H. F., Liu, X., Pei, L., Huang, S., Lin, X., et al. (2022). Combined culture and DNA metabarcoding analysis of cyanobacterial community structure in response to coral reef health status in the South China sea. *J. Mar. Sci. Eng.* 10:1984. doi: 10.3390/jmse10121984
- Kimes, N. E., Grim, C. J., Johnson, W. R., Hasan, N. A., Tall, B. D., Kothary, M. H., et al. (2012). Temperature regulation of virulence factors in the pathogen *Vibrio coralliilyticus*. *ISME J.* 6, 835–846. doi: 10.1038/ismej.2011.154
- Kushmaro, A., Loya, Y., Fine, M., and Rosenberg, E. (1996). Bacterial infection and coral bleaching. *Nature* 380, 396–396. doi: 10.1038/380396a0
- Li, J., Azam, F., and Zhang, S. (2016). Outer membrane vesicles containing signalling molecules and active hydrolytic enzymes released by a coral pathogen *Vibrio shilonii* AK1. *Environ. Microbiol.* 18, 3850–3866. doi: 10.1111/1462-2920.13344
- Li, J., Kuang, W., Long, L., and Zhang, S. (2017). Production of quorum-sensing signals by bacteria in the coral mucus layer. *Coral Reefs* 36, 1235–1241. doi: 10.1007/s00338-017-1616-3
- Lu, R., Osei-Adjei, G., Huang, X., and Zhang, Y. (2018). Role and regulation of the orphan AphA protein of quorum sensing in pathogenic vibrios. *Fut. Microbiol.* 13, 383–391. doi: 10.2217/fmb-2017-0165
- Magoč, T., and Salzberg, S. L. (2011). FLASH: Fast length adjustment of short reads to improve genome assemblies. *Bioinformatics* 27, 2957–2963. doi: 10.1093/bioinformatics/btr507
- Mahmoud, H. M., and Kalendar, A. A. (2016). Coral-associated actinobacteria: Diversity, abundance, and biotechnological potentials. *Front. Microbiol.* 7:204. doi: 10.3389/fmicb.2016.00204
- Mao-Jones, J., Ritchie, K. B., Jones, L. E., and Ellner, S. P. (2010). How microbial community composition regulates coral disease development. *PLoS Biol.* 8:e1000345. doi: 10.1371/journal.pbio.1000345
- Mhuantong, W., Nuryadi, H., Trianto, A., Sabdono, A., Tangphatsornruang, S., Eurwilachit, L., et al. (2019). Comparative analysis of bacterial communities associated with healthy and diseased corals in the Indonesian sea. *PeerJ* 2019, 1–20. doi: 10.7717/peerj.8137
- Mohamed, H. F., Abd-Elgawad, A., Cai, R., Luo, Z., and Xu, C. (2022). The bacterial signature offers vision into the machinery of coral fitness across high-latitude coral reef in the South China Sea. *Environ. Microbiol. Rep.* 15, 13–30. doi: 10.1111/1758-2229.13119
- Munn, C. B. (2015). The role of vibrios in diseases of corals. *Microbiol. Spectr.* 3, 1–12. doi: 10.1128/microbiolspec.VE-0006-2014
- Niu, Y., Defoirdt, T., Baruah, K., Van De Wiele, T., Dong, S., and Bossier, P. (2014). *Bacillus* sp. LT3 improves the survival of gnotobiotic brine shrimp (*Artemia franciscana*) larvae challenged with *Vibrio campbellii* by enhancing the innate immune response and by decreasing the activity of shrimp-associated vibrios. *Vet. Microbiol.* 173, 279–288. doi: 10.1016/j.vetmic.2014.08.007
- Ou, D., Chen, B., Hadi, T. A., Suharsono, Niu, W., and Alfiansah, Y. R. (2018). Next-generation sequencing revealed specific microbial symbionts in *Porites lutea* with pigment abnormalities in North Sulawesi, Indonesia. *Acta Oceanol. Sin.* 37, 78–84. doi: 10.1007/s13131-018-1291-4

## Conflict of interest

The authors declare that the research was conducted in the absence of any commercial or financial relationships that could be construed as a potential conflict of interest.

## Publisher's note

All claims expressed in this article are solely those of the authors and do not necessarily represent those of their affiliated organizations, or those of the publisher, the editors and the reviewers. Any product that may be evaluated in this article, or claim that may be made by its manufacturer, is not guaranteed or endorsed by the publisher.

- Pootakham, W., Mhuanong, W., Yoocha, T., Puchim, L., Jomchai, N., Sonthirod, C., et al. (2019). Heat-induced shift in coral microbiome reveals several members of the Rhodobacteraceae family as indicator species for thermal stress in *Porites lutea*. *Microbiol. Open* 8, 1–20. doi: 10.1002/mbo3.935
- Putnam, H. M., and Gates, R. D. (2015). Preconditioning in the reef-building coral *Pocillopora damicornis* and the potential for trans-generational acclimatization in coral larvae under future climate change conditions. *J. Exp. Biol.* 218, 2365–2372. doi: 10.1242/jeb.123018
- Rahman, M., Sabir, A. A., Mukta, J. A., Khan, M. M. A., Mohi-Ud-Din, M., Miah, M. G., et al. (2018). Plant probiotic bacteria *Bacillus* and *Paraburkholderia* improve growth, yield and content of antioxidants in strawberry fruit. *Sci. Rep.* 8:2504. doi: 10.1038/s41598-018-20235-1
- Raina, J. B., Tapiolas, D., Willis, B. L., and Bourne, D. G. (2009). Coral-associated bacteria and their role in the biogeochemical cycling of sulfur. *Appl. Environ. Microbiol.* 75, 3492–3501. doi: 10.1128/AEM.02567-08
- Ritchie, K. B. (2006). Regulation of microbial populations by coral surface mucus and mucus-associated bacteria. *Mar. Ecol. Prog. Ser.* 322, 1–14. doi: 10.3354/meps322001
- Roder, C., Arif, C., Bayer, T., Aranda, M., Daniels, C., Shibl, A., et al. (2014). Bacterial profiling of white plague disease in a comparative coral species framework. *ISME J.* 8, 31–39. doi: 10.1038/ismej.2013.127
- Rosado, P. M., Leite, D. C. A., Duarte, G. A. S., Chaloub, R. M., Jospin, G., and Nunes da Rocha, U. (2019). Marine probiotics: Increasing coral resistance to bleaching through microbiome manipulation. *ISME J.* 13, 921–936. doi: 10.1038/s41396-018-0323-6
- Rosenberg, E., Kushmaro, A., Kramarsky-Winter, E., Banin, E., and Yossi, L. (2009). The role of microorganisms in coral bleaching. *ISME J.* 3, 139–146. doi: 10.1038/ismej.2008.104
- Ryu, D. H., Lee, S. W., Mikolaityte, V., Kim, Y. W., Jeong, H., Lee, S. J., et al. (2020). Identification of a second type of ahllactonase from *Rhodococcus* sp. BH4, belonging to the  $\alpha/\beta$  hydrolase superfamily. *J. Microbiol. Biotechnol.* 30, 937–945. doi: 10.4014/jmb.2001.01006
- Satpute, S. K., Banat, I. M., Dhakephalkar, P. K., Banpurkar, A. G., and Chopade, B. A. (2010). Biosurfactants, bioemulsifiers and exopolysaccharides from marine microorganisms. *Biotechnol. Adv.* 28, 436–450. doi: 10.1016/j.biotechadv.2010.02.006
- Séré, M. G., Tortosa, P., Chabanet, P., Turquet, J., Quod, J. P., and Schleyer, M. H. (2013). Bacterial communities associated with *Porites* white patch syndrome (PWPS) on three western Indian Ocean (WIO) coral reefs. *PLoS One* 8:e83746. doi: 10.1371/journal.pone.0083746
- Shi, T., Niu, G., Kvitt, H., Zheng, X., Qin, Q., Sun, D., et al. (2021). Untangling ITS2 genotypes of algal symbionts in zooxanthellate corals. *Mol. Ecol. Resour.* 21, 137–152. doi: 10.1111/1755-0998.13250
- Smith, D., Leary, P., Craggs, J., Bythell, J., and Sweet, M. (2015). Microbial communities associated with healthy and white syndrome-affected *Echinopora lamellosa* in aquaria and experimental treatment with the antibiotic ampicillin. *PLoS One* 10:e0121780. doi: 10.1371/journal.pone.0121780
- Stuart-Smith, R. D., Brown, C. J., Ceccarelli, D. M., and Edgar, G. J. (2018). Ecosystem restructuring along the great barrier reef following mass coral bleaching. *Nature* 560, 92–96. doi: 10.1038/s41586-018-0359-9
- Sun, X., Hill, P., Liu, J., Qian, J., Ma, Y., and Zhou, S. (2021). Marine-source quorum quenching enzyme YtnP to improve hygiene quality in dental units. *Mar. Drugs* 19:225. doi: 10.3390/md19040225
- Sun, Y., Jiang, L., Gong, S., Guo, M., Yuan, X., Zhou, G., et al. (2020). Impact of ocean warming and acidification on symbiosis establishment and gene expression profiles in recruits of reef coral acropora intermedia. *Front. Microbiol.* 11:532447. doi: 10.3389/fmicb.2020.532447
- Tan, K. Y., Dutta, A., Tan, T. K., Hari, R., Othman, R. Y., and Choo, S. W. (2020). Comprehensive genome analysis of a pangolin-associated *Paraburkholderia fungorum* provides new insights into its secretion systems and virulence. *PeerJ* 8, 1–24. doi: 10.7717/peerj.9733
- Thompson, F. L., Thompson, C. C., Hoste, B., Vandemeulebroecke, K., Gullian, M., and Swings, J. (2003). *Vibrio fortis* sp. nov. and *Vibrio hepatarius* sp. nov., isolated from aquatic animals and the marine environment. *Int. J. Syst. Evol. Microbiol.* 53, 1495–1501. doi: 10.1099/ijs.0.02658-0
- Thurber, R. V., Willner-Hall, D., Rodriguez-Mueller, B., Desnues, C., Edwards, R. A., Angly, F., et al. (2009). Metagenomic analysis of stressed coral holobionts. *Environ. Microbiol.* 11, 2148–2163. doi: 10.1111/j.1462-2920.2009.01935.x
- Tuttlebee, C. M., Donnell, M. J. O., Keaney, C. T., Russell, R. J., Sullivan, D. J., Falkner, F., et al. (2002). Effective control of dental chair unit waterline biofilm and marked reduction of bacterial contamination of output water using two peroxide-based disinfectants. *J. Hosp. Infect.* 52, 192–205. doi: 10.1053/jhin.2002.1282
- Ushijima, B., Videau, P., Burger, A. H., Shore-Maggio, A., Runyon, C. M., Sudek, M., et al. (2014). *Vibrio coralliilyticus* strain OCN008 is an etiological agent of acute montipora white syndrome. *Appl. Environ. Microbiol.* 80, 2102–2109. doi: 10.1128/AEM.03463-13
- Wang, C., Liu, Y., Sun, G., Li, X., and Liu, Z. (2019). Growth, immune response, antioxidant capability, and disease resistance of juvenile *Atlantic salmon* (*Salmo salar* L.) fed *Bacillus velezensis* V4 and *Rhodotorula mucilaginosa* compound. *Aquaculture* 500, 65–74. doi: 10.1016/j.aquaculture.2018.09.052
- Wang, Q., Garrity, G. M., Tiedje, J. M., and Cole, J. R. (2007). Naïve Bayesian classifier for rapid assignment of rRNA sequences into the new bacterial taxonomy. *Appl. Environ. Microbiol.* 73, 5261–5267. doi: 10.1128/AEM.00062-07
- Wang, X., Zhang, Y., Qin, G., Luo, W., and Lin, Q. (2016). A novel pathogenic bacteria (*Vibrio fortis*) causing enteritis in cultured seahorses. *Hippoc. Erectus Perry* 39, 765–769. doi: 10.1111/jfd.12411
- Wu, Q., Zhi, Y., and Xu, Y. (2019). Systematically engineering the biosynthesis of a green biosurfactant surfactin by *Bacillus subtilis* 168. *Metab. Eng.* 52, 87–97. doi: 10.1016/j.ymben.2018.11.004
- Yu, L., Li, T., Li, L., Lin, X., Li, H., Liu, C., et al. (2020). SAGER: A database of symbiodiniaceae and algal genomic resource. *Database* 2020, 1–8. doi: 10.1093/database/baaa051
- Zhang, Y., Zhang, L., Hou, S., Huang, X., Sun, F., and Gao, H. (2016). The master quorum-sensing regulator OpaR is activated indirectly by H-NS in *Vibrio parahaemolyticus*. *Curr. Microbiol.* 73, 71–76. doi: 10.1007/s00284-016-1018-8
- Zhao, W., Yuan, T., Piva, C., Spinard, E. J., Schuttert, C. W., Rowley, D. C., et al. (2019). The probiotic bacterium *Phaeobacter inhibens* downregulates virulence factor transcription in the shellfish pathogen *Vibrio coralliilyticus* by N-Acyl homoserine lactone production. *Appl. Environ. Microbiol.* 85, e1545–e1518. doi: 10.1128/AEM.01545-18
- Zhou, J., Lin, Z. J., Cai, Z. H., Zeng, Y. H., Zhu, J. M., and Du, X. P. (2020). Opportunistic bacteria use quorum sensing to disturb coral symbiotic communities and mediate the occurrence of coral bleaching. *Environ. Microbiol.* 22, 1944–1962. doi: 10.1111/1462-2920.15009
- Ziegler, M., Grupstra, C. G. B., Barreto, M. M., Eaton, M., BaOmar, J., Zubier, K., et al. (2019). Coral bacterial community structure responds to environmental change in a host-specific manner. *Nat. Commun.* 10:3092. doi: 10.1038/s41467-019-10969-5



## OPEN ACCESS

## EDITED BY

Zhiyong Li,  
Shanghai Jiao Tong University, China

## REVIEWED BY

Xinqing Zheng,  
State Oceanic Administration, China  
Ke Pan,  
Shenzhen University, China

## \*CORRESPONDENCE

Zhi Zhou  
✉ zhouzhi@hainanu.edu.cn

## SPECIALTY SECTION

This article was submitted to  
Microbial Symbioses,  
a section of the journal  
Frontiers in Microbiology

RECEIVED 06 December 2022

ACCEPTED 28 December 2022

PUBLISHED 01 March 2023

## CITATION

Zhang K, Shen Z, Yang W, Guo J, Yan Z, Li J,  
Lin J, Cao X, Tang J, Liu Z, Zhou Z and Lin S  
(2023) Unraveling the metabolic effects  
of benzophenone-3 on the endosymbiotic  
dinoflagellate *Cladocopium goreau*.  
*Front. Microbiol.* 13:1116975.  
doi: 10.3389/fmicb.2022.1116975

## COPYRIGHT

© 2023 Zhang, Shen, Yang, Guo, Yan, Li, Lin,  
Cao, Tang, Liu, Zhou and Lin. This is an  
open-access article distributed under the terms  
of the [Creative Commons Attribution License  
\(CC BY\)](https://creativecommons.org/licenses/by/4.0/). The use, distribution or reproduction in  
other forums is permitted, provided the original  
author(s) and the copyright owner(s) are  
credited and that the original publication in this  
journal is cited, in accordance with accepted  
academic practice. No use, distribution or  
reproduction is permitted which does not  
comply with these terms.

# Unraveling the metabolic effects of benzophenone-3 on the endosymbiotic dinoflagellate *Cladocopium goreau*

Kaidian Zhang<sup>1,2</sup>, Zhen Shen<sup>1,2</sup>, Weilu Yang<sup>1,2</sup>, Jianing Guo<sup>1,2</sup>,  
Zhicong Yan<sup>1,2</sup>, Jiashun Li<sup>3</sup>, Jiamin Lin<sup>1,2</sup>, Xiaocong Cao<sup>1,2</sup>,  
Jia Tang<sup>1,2</sup>, Zhaoqun Liu<sup>1,2</sup>, Zhi Zhou<sup>1,2\*</sup> and Senjie Lin<sup>1,2,3,4</sup>

<sup>1</sup>State Key Laboratory of Marine Resource Utilization in South China Sea, Hainan University, Haikou, China,

<sup>2</sup>Key Laboratory of Tropical Hydrobiology and Biotechnology of Hainan, Hainan University, Haikou, China,

<sup>3</sup>State Key Laboratory of Marine Environmental Science, College of Ocean and Earth Sciences, Xiamen

University, Xiamen, Fujian, China, <sup>4</sup>Department of Marine Sciences, University of Connecticut, Groton, CT, United States

As a well-known pseudo-persistent environmental pollutant, oxybenzone (BP-3) and its related organic ultraviolet (UV) filters have been verified to directly contribute to the increasing mortality rate of coral reefs. Previous studies have revealed the potential role of symbiotic Symbiodiniaceae in protecting corals from the toxic effects of UV filters. However, the detailed protection mechanism(s) have not been explained. Here, the impacts of BP-3 on the symbiotic Symbiodiniaceae *Cladocopium goreau* were explored. *C. goreau* cells exhibited distinct cell growth at different BP-3 doses, with increasing growth at the lower concentration (2 mg L<sup>-1</sup>) and rapid death at a higher concentration (20 mg L<sup>-1</sup>). Furthermore, *C. goreau* cells showed a significant BP-3 uptake at the lower BP-3 concentration. BP-3 absorbing cells exhibited elevated photosynthetic efficiency, and decreased cellular carbon and nitrogen contents. Besides, the derivatives of BP-3 and aromatic amino acid metabolism highly responded to BP-3 absorption and biodegradation. Our physiological and metabolic results reveal that the symbiotic Symbiodiniaceae could resist the toxicity of a range of BP-3 through promoting cell division, photosynthesis, and reprogramming amino acid metabolism. This study provides novel insights into the influences of organic UV filters to coral reef ecosystems, which urgently needs increasing attention and management.

## KEYWORDS

oxybenzone, UV filters, toxic effects, *Cladocopium goreau*, amino acid metabolism, coral reef ecosystems

## Introduction

As a common ultraviolet absorbent, oxybenzone (benzophenone-3, hereafter BP-3) has been an ingredient in sunscreens and other personal care products including skin creams, cosmetics, shower gels, and shampoos, for over 40 years (Balmer et al., 2005; Mao et al., 2017). However, recently a mass of BP-3 residues have been detected in various environments including water bodies, sediment, and soil (Teoh et al., 2020). It has been estimated that thousands of tons of BP-3 are imported into the marine environment annually due to sewage discharge and recreational activities (e.g., swimming or diving) (Balmer et al., 2005; Goksøyr et al., 2009; Pintado-Herrera et al., 2017; Mitchelmore et al., 2019). Studies have identified that worldwide



BP-3 concentrations in seawater range from nanogram to milligram per liter (Kim and Choi, 2014; Tsui et al., 2014; O'Donovan et al., 2020). Due to the increasing recreational tourisms in the reef zone, the coral reef ecosystem is undoubtedly a high-risk area for BP-3 pollution (Mitchellmore et al., 2021). However, BP-3 has clear toxicity to aquatic biota in both freshwater and other marine organisms (Paredes et al., 2014; Campos et al., 2017; Mao et al., 2017; Seoane et al., 2017; He et al., 2019; Lozano et al., 2020). Therefore, the potential threat of BP-3 to coral health has received wide attention worldwide (Moeller et al., 2021).

Coral reefs provide habitats of about one third of marine species and become one of the most biodiverse and economically valuable ecosystems on the planet (Plaisance et al., 2011; Pendleton et al., 2019). In past decades, global coral reefs experienced massive mortality due to an array of climate change impacts and anthropogenic-derived stressors, including sustained global warming, coastal eutrophication, overfishing, and chemical industrial pollution (Hoegh-Guldberg et al., 2007; Hughes et al., 2018; Sully et al., 2019). In particular, there have been growing concerns about the effects of UV screens on corals since 2008 (Danovaro et al., 2008). Downs et al. (2016) observed coral bleaching and death after acute BP-3 exposure ( $\leq 24$  h) in *Stylophora pistillata*. So far, increasing laboratory studies have investigated the impact of BP-3 on the physiologies of corals, including photosynthetic yield, growth, bleaching, mortality, and the toxicity of BP-3 on larval and adult life stages of intact corals (Stien et al., 2018, 2020; Fel et al., 2019; He et al., 2019; Wijgerde et al., 2020). However, the toxicological mechanisms of BP-3 on corals have been contended. Recent researches implicated the metabolic products of BP-3, phototoxic oxybenzone-glucoside conjugates, can be considered as a culprit of the increasing bleaching rate of corals (Hansel, 2022; Vuckovic et al., 2022). On the contrary, it also has been revealed that Symbiodiniaceae could protect the coral host from the toxic effects of BP-3 metabolites by sequestering the phototoxins (Vuckovic et al., 2022). However, the protection mechanism by which Symbiodiniaceae protects the host remains unclear.

The endosymbiotic dinoflagellates Symbiodiniaceae are essential photosynthetic symbionts to the tropical and subtropical coral reef ecosystems. In oligotrophic tropical-subtropical shallow waters, algal symbionts absorb metabolic waste from the coral host and supply photosynthetically fixed carbon to coral hosts in return (Baker, 2003; Ceh et al., 2013). Until recently, seven Symbiodiniaceae lineages, from Clade A to G, are formally described according to systematic genetics and ecology analysis (LaJeunesse et al., 2018). Of these, *Cladocopium goreaui*, a type species of Symbiodiniaceae Clade C with physiological diversity, most species-specificity, and broad distribution, forms mutualistic associations with a broad diversity of hosts and is an important contributor to coral's adaption in a wide range of irradiances and temperatures (LaJeunesse et al., 2018; González-Pech et al., 2019). Therefore, it is an excellent model for studying the responses of *C. goreaui* to UV screens and understanding symbiont's protection mechanism against the toxicity of the UV screens in coral-Symbiodiniaceae holobionts.

In the present study, we investigated the metabolic and physiological responses of the symbiotic dinoflagellate *C. goreaui* to BP-3. Untargeted metabolomics in combination with physiological measurements were used to decipher the survival and molecular adaptive mechanisms of *C. goreaui* to BP-3 exposure. Our results provide a new perspective for furthering the understanding of detoxification mechanisms of coral-Symbiodiniaceae symbionts to environmental pollutants.

## Materials and methods

### Algal culture and experimental setup

The *C. goreaui* strain CCMP 2,466 was obtained from National Center for Marine Algae and Microbiota (NCMA). Prior to experiments, cells were cultured in L1 medium (Guillard, 1975) prepared with sterile-filtered (0.22  $\mu\text{m}$ ) seawater (30 PSU). Cultures were incubated at 25°C with a photon flux of 120  $\mu\text{E m}^{-2} \text{S}^{-1}$  under a 12: 12 h light: dark cycle.

For the BP-3 treatments, the *C. goreaui* cells in the logarithmic growth phase were transferred into three experimental groups with different concentrations of BP-3 added: LBP-3 group (2 mg L<sup>-1</sup> BP-3), HBP-3 group (20 mg L<sup>-1</sup> BP-3), and control group (no BP-3), each in triplicate and at a volume of 300 mL in conical flasks. The stock solution of BP-3 (CAS. No. 131-57-7) was prepared in methanol (HPLC grade) at the concentration of 5,000 mg L<sup>-1</sup> and stored at -20°C in the dark. For LBP-3 and HBP-3 treatments, 0.12 and 1.20 mL of the stock was added to each of the 300 mL cultures, respectively.

### Cell growth and cell size measurement

The cell concentrations were determined daily using a Sedgewick-Rafter counting chamber (Phycotech, St. Joseph, MI, USA). Growth rate ( $\mu$ ) was calculated using  $\mu = (\ln N_1 - \ln N_0) / (t_1 - t_0)$ , where  $N_1$  and  $N_0$  represent the cell concentrations at  $t_1$  and  $t_0$ , respectively (Zhang et al., 2021a). The average cell sizes were measured for each culture as the equivalent spherical diameter of over 500 cells using a Zeiss microscopy Axio Imager A2 (Carl Zeiss, Oberkochen, Germany) on the eighth day after incubation.

### Measurements of chlorophyll contents and photosynthetic rate

Chlorophyll contents were determined on the eighth day. Ten mL cultures of each group were collected by centrifugation at 5,000 g, 4°C for 10 min, and the cell pellets were immediately suspended in 4 mL pure acetone and kept in darkness at 4°C for 48 h to complete chlorophyll extraction. After centrifugation at 5,000 g for 10 min, the supernatants were separated to measure the chlorophyll contents using a UV-1100 Spectrophotometer (Mapada, Shanghai, China). The calculation of chlorophyll *a* (Chl *a*) and chlorophyll *c* (Chl *c*) contents was based on the equations from Jeffrey and Humphrey (1975) and Ritchie (2006). For the maximum photosystem II (PSII) quantum yield ( $F_v/F_m$ ), two mL cultures were sampled daily, acclimated in darkness for 30 min, and used for the quantification of  $F_v/F_m$  using a Dual-PAM-100 Fluorometer (Walz, Effeltrich, Germany).

### Measurement of BP-3 concentration in the medium

To assess the potential of BP-3 degradation by abiotic factors (e.g., photolysis, volatilization) during the experiment, BP-3 added



(2 mg L<sup>-1</sup>) cultures without algae were carried out and the BP-3 concentration in the medium was measured over time. Five mL cultures were collected at the start and end of the experiment, and centrifuged at 5,000 g for 10 min. Then the supernatant was subjected to the solid phase extraction (SPE) clean-up. Briefly, 20 ng isotopically-labeled standard was added in the supernatant and the mixture was passed through a hydrophilic-lipophilic balance (HLB) C18 SPE cartridge (200 mg, 6 mL) at a velocity of about 1 mL min<sup>-1</sup>. The cartridge was washed with 5 mL Milli-Q water after loading, followed by vacuum drying for 30 min. The target chemical was eluted with 5 mL of methanol and another 5 mL of methanol/acetone (1/1, v/v). The extract was concentrated under a gentle stream of high-purity nitrogen to less than 0.5 mL, and then reconstituted to 1 mL.

Subsequently, the concentration of BP-3 in each sample was quantified using high-performance liquid chromatography–tandem mass spectrometry (HPLC–MS/MS; TQ-S Micro, Waters, Milford, MA, USA) coupled with electro-spray ionization (ESI) tandem mass spectrometry (TQ-S Micro, Waters, Milford, MA, USA). The system was equipped with a reverse phase column (Acquity UPLC BEH C<sub>18</sub>, 50 mm length × 2.1 mm internal diameter; 1.7 μm particle size, Waters, Milford, MA, USA) connected with a guard column (Acquity UPLC BEH C<sub>18</sub>, 100 mm length × 2.1 mm internal diameter; 1.7 μm particle size, Waters, Milford, MA, USA), at a flow rate of 0.4 mL min<sup>-1</sup>. The mobile phases were 0.1% formic acid in Milli-Q water (mobile phase A) and acetonitrile/methanol (1/1, V/V) (mobile phase B). The gradient elution started with 10% B at 0 min, held for 1 min; linearly increased to 50% B at 1–2 min, then linearly increased to 75% B at 2–5 min, held for 5–10 min, then linearly increased to 100% B at 10–10.5 min, held for 10.5–14 min, and then the column was re-equilibrated to initial conditions at 14.1 min and stabilized for 2 min. The overall running time was 17 min. The injection volume was 2 μL and the column temperature was 40°C. Analytes were determined by ESI-MS/MS either in positive mode by multiple reaction monitoring (MRM). Turbo V ion source and MS/MS parameters were as follows: curtain gas (CUR), 10 psi; collision gas (CAD), medium; ion spray voltage, 4,000 V; temperature, 500°C; ion source gas 1 (GS1), 50 psi.

## Measurements of cellular carbon and nitrogen contents

About 2 × 10<sup>6</sup> cells from each culture were filtered onto a pre-combusted (combusted in a Muffle Furnace at 450°C for 5 h) 25 mm GF/F membrane on the eighth day and stored at -80°C for subsequent elemental analysis. The cellular carbon (C) and nitrogen (N) contents were measured using a PE2400 SERIESII CHNS/O Elemental Analyzer (Perkin Elmer, Norwalk, CT, USA) as previously reported (Li et al., 2022). The weight of each element was divided by the cell number in the sample to obtain per cell content.

## Activity assay of T-AOC, GST, and caspase-3

Fifty mL cultures were harvested on the eighth day by centrifugation at 5,000 g, 4°C for 10 min, then the cell pellets were resuspended in 1 mL PBS (pH 7.4) and homogenized using a bead homogenizer (Bioprep-24, Allsheng Instruments Co. Ltd., China).

After centrifugation at 14,000 g, 4°C for 10 min, the supernatant was used to detect various relevant activities. Total antioxidant capacity (T-AOC) and glutathione S-transferase (GST) detection kits (A015-1 and A004; Nanjing Jiancheng, China) were used for the measurements of T-AOC and GST activity, respectively. The caspase-3 activation level in different groups was determined with a Caspase-3 Colorimetric Assay Kit (KGA204; KeyGEN, China).

## Metabolite extraction and UPLC-MS analysis

About 1 × 10<sup>7</sup> cells from each culture were collected on the eighth day by centrifugation at 5,000 g, 4°C for 10 min. The cell pellets were suspended with PBS (pH 7.4) and washed twice. Subsequently, metabolites in each sample were extracted. Firstly, two magnetic beads and 10 μL of the prepared internal standard (d3-Leucine, 13C9-Phenylalanine, d5-Tryptophan, and 13C3-Progesterone) were added to each sample. Then, 800 μL of precooled extraction reagent [methanol: acetonitrile: water (2:2:1, v/v/v)] was added into each sample and grind at 50 Hz for 5 min. After keeping at -20°C for 2 h, the ground samples were centrifuged at 25,000 g, 4°C for 15 min. Then 600 μL of each sample was transferred in split-new EP tubes and frozen dry. After that, 120 μL of 50% methanol was added to the dried sample and completely dissolved. After centrifugation at 25,000 g, 4°C for 15 min, the supernatant was used for further analysis.

The separation and detection of metabolites were analyzed using Waters UPLC I-Class Plus (Waters, Milford, MA, USA) tandem Q Exactive high resolution mass spectrometry (Thermo Fisher Scientific, USA). The chromatographic separation was performed on a Waters ACQUITY UPLC BEH C<sub>18</sub> column (1.7 μm, 2.1 × 100 mm, Waters, Milford, MA, USA), and the column temperature was maintained at 45°C. The mobile phase consisted of 0.1% formic acid (A) and acetonitrile (B) in the positive mode. In the negative mode, the mobile phase consisted of 10 mM ammonium formate (A) and acetonitrile (B). The column was eluted with gradient conditions as follows: 0–1 min, 2% B; 1–9 min, 2–98% B; 9–12 min, 98% B; 12–12.1 min, 98% B–2% B; and 12.1–15 min, 2% B (Flow rate 0.35 mL min<sup>-1</sup>, injection volume 5 μL).

The primary and secondary MS data acquisition were performed using Q Exactive (Thermo Fisher Scientific, Waltham, MA, USA). The full scan range was 70–1,050 m/z with a resolution of 70,000, and the automatic gain control (AGC) target for MS acquisitions was set to 3e6 with a maximum ion injection time of 100 ms. The top three precursors were selected for subsequent MS fragmentation with a maximum ion injection time of 50 ms and AGC of 1e5 under the resolution of 17,500. In this time, the stepped normalized collision energy was set as 20, 40, and 60 eV. ESI was set to the following parameters: flow rates of sheath gas and aux gas were 40 and 10, respectively; Spray voltage (|KV|) of positive-ion mode and negative-ion mode were 3.80 and 3.20, respectively; Capillary temperature and aux gas heater temperature was 320 and 350°C, respectively.

## Differential metabolites identification

The collected raw data were imported into a Compound Discoverer 3.3 software (Thermo Fisher Scientific, USA) to identify

metabolites based on BMDB (BGI metabolome database), mzCloud database, and ChemSpider online database. The metaX software was used for further quality control (Wen et al., 2017). The screening of differentially changed metabolites between the control and LBP-3 groups [(LBP-3)/control comparison] was based on multivariate statistical analysis and univariate analysis. Firstly, the overall differences between the two groups were analyzed by principal component analysis (PCA) and partial least squares discriminant analysis (PLS-DA) (Barker and Rayens, 2003; Westerhuis et al., 2008). The variable importance in projection (VIP) value of metabolites in Orthogonal partial least squares discriminant analysis (OPLS-DA) (if OPLS-DA is over fitted, the VIP value of PLS-DA is used), fold change (FC), and  $q$ -value were used to filter differential metabolites. FC was obtained by FC analysis,  $p$ -value was obtained by  $T$ -test, and  $Q$ -value was obtained by Benjamini-Hochberg (BH) correction on  $p$ -value. In this study, the differential metabolites were identified according to the following criteria: (1) VIP of OPLS-DA model  $\geq 1$ ; (2) FC  $\geq 1.2$  or  $\leq 0.83$ ; (3)  $q$ -value  $< 0.05$ . And the metabolic pathway enrichment analysis was performed based on the KEGG database with a rigorous threshold ( $q$ -value  $< 0.05$ ).

## Data analysis and statistical evaluation

All experiments were performed in triplicate ( $n = 6$ ), and the data were processed to obtain means with standard deviations

(Mean  $\pm$  SD). Statistical analyses were performed using the software SPSS (version 16.0; IBM, US). In order to evaluate the statistical significance of the differences between control and BP-3 groups, we performed the normal distribution test and homogeneity of variances test, and then one-way analysis of variance (ANOVA) was carried out to evaluate the significant differences in physiological parameters. Statistical significance (\*) was determined at the level of  $p < 0.05$ .

## Results

### Algal growth under different BP-3 conditions

With the same initial cell concentration ( $1.1 \times 10^5$  cells  $\text{mL}^{-1}$ ), the growth of *C. goreau* under different BP-3 conditions started to diverge as soon as the first day (Figure 1A). A high concentration of BP-3 (20  $\text{mg L}^{-1}$ ) addition strongly suppressed algal growth (Figure 1A), with the cell concentration declining rapidly and reaching zero on the fourth day (Figure 1A). Therefore, for the HBP-3 group, no more measurements were carried out after day four. In contrast, rapid cell growth occurred in the LBP-3 group (2  $\text{mg L}^{-1}$ ) from the first day. Surprisingly, the LBP group exhibited even higher growth than the control group, with an average growth rate (from day 1 to day 8) of  $0.16 \pm 0.02$  day $^{-1}$ , which was significantly higher

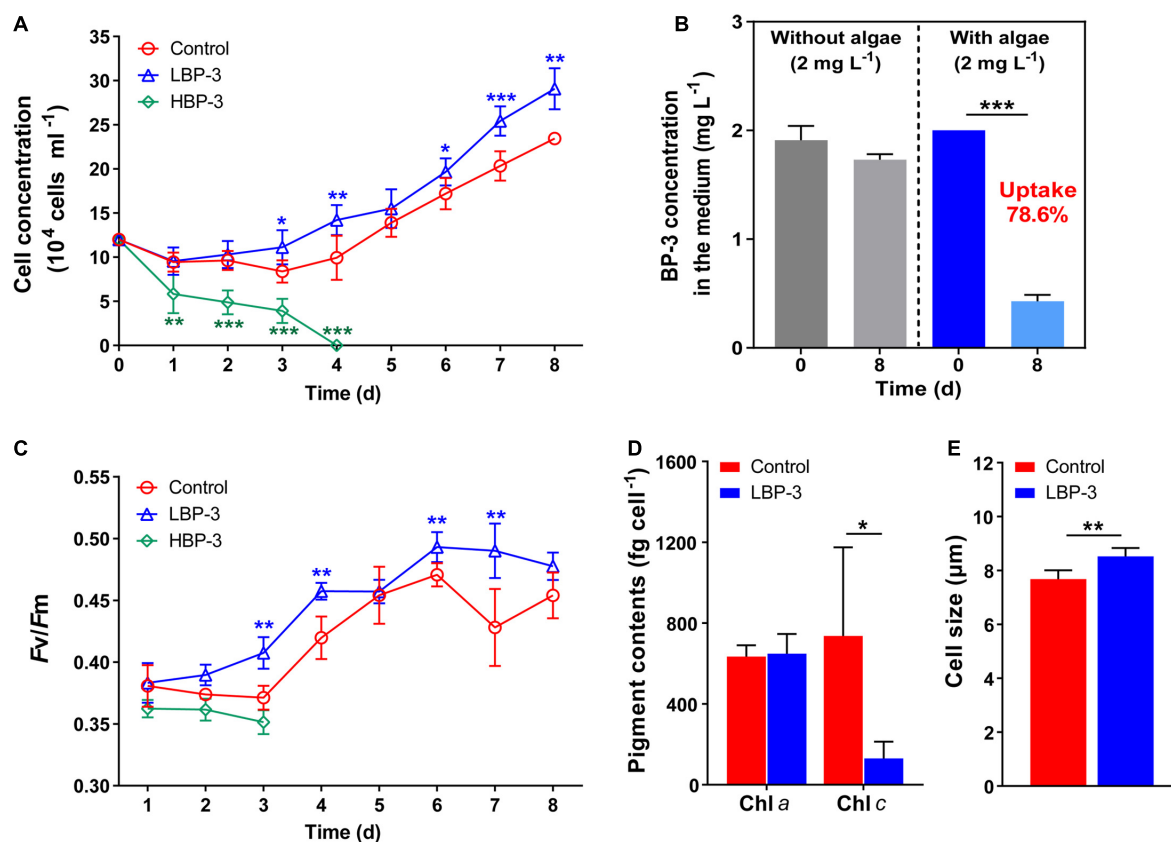


FIGURE 1

Physiological responses of *C. goreau* to benzophenone-3 (BP-3). (A) Cell concentration. (B) Photodegradation of BP-3 under abiotic conditions (left) and BP-3 uptake by *C. goreau* under the LBP-3 condition (right) over 8 days. (C) Photosystem II (PS II) maximum photochemical yield ( $F_v/F_m$ ). (D) Pigment contents. (E) Cell size. Each data point is the mean from six replicates with the error bar indicating standard deviation (mean  $\pm$  SD,  $n = 6$ ). Asterisks (\* $p < 0.05$ ; \*\* $p < 0.01$ ; \*\*\* $p < 0.001$ ) indicate significant differences between different groups.

than that in the control group ( $0.13 \pm 0.02 \text{ day}^{-1}$ ) ( $T$ -test,  $p < 0.05$ ) (Supplementary Figure 1).

## Uptake of BP-3 by the *C. goreau* cells

There was no significant difference in the BP-3 concentration in the medium without algae between day 1 and day 8 (Figure 1B), indicating the negligible degradation of BP-3 by abiotic factors during the experiment. In the LBP-3 group, the BP-3 concentration in the medium on the eighth day decreased from 2 to  $0.43 \pm 0.06 \text{ mg L}^{-1}$  (Figure 1B). Therefore, 78.59% of added BP-3 in the medium was absorbed by *C. goreau* cells after 8 days of cultivation (Figure 1B).

## Photosynthetic efficiency, chlorophyll contents, and cell size under BP-3 conditions

The  $F_v/F_m$  in the HBP-3 group was the lowest among the three groups of cultures. In contrast, the  $F_v/F_m$  of *C. goreau* increased in the LBP-3 group and remained significantly higher than that in control from day 2 on ( $T$ -test,  $p < 0.05$ ) (Figure 1C). Some fluctuations were observed in chlorophyll contents in the LBP-3 group compared to the control group (Figure 1D). Though no significant change was noted in the Chl *a* content after BP-3 addition

( $2 \text{ mg L}^{-1}$ ), the Chl *c* content in the LBP-3 group was 82% lower than that in control ( $T$ -test,  $p < 0.05$ ) (Figure 1D). In addition, the cell size in the LBP-3 group was 11% larger than that in control on the eighth day ( $T$ -test,  $p < 0.05$ ) (Figure 1E).

## Decreased cellular carbon, nitrogen contents under the LBP-3 condition

The cellular C content in the LBP-3 group decreased by 23% than that in the control group ( $T$ -test,  $p < 0.05$ ) (Figure 2A). Similarly, cellular N content in the LBP-3 group was 25% lower than that in control ( $T$ -test,  $p < 0.05$ ) (Figure 2B). Interestingly, the C: N ratio in *C. goreau* cells seemed to be unaffected by BP-3 addition and remained relatively similar between the LBP-3 and control groups (Figure 2C).

## Response of T-AOC, GST activities, and caspase-3 level under the LBP-3 condition

Total antioxidant capacity and GST activities in *C. goreau* cells were measured after BP-3 addition ( $2 \text{ mg L}^{-1}$ ). Overall, no significant changes in T-AOC and GST activities were observed in the LBP-3 group compared with the control group (Figures 2D, E). The caspase-3 level in the LBP-3 group was 14.71% lower than that in the control group, but without statistical significance (Figure 2F).

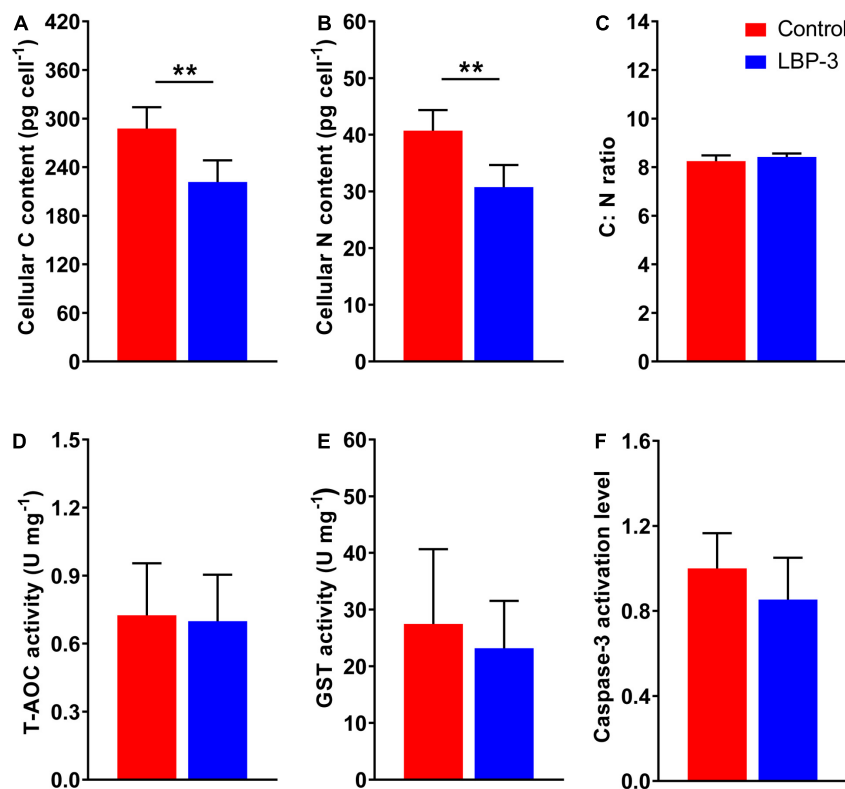


FIGURE 2

Cellular responses of *C. goreau* in response to  $2 \text{ mg L}^{-1}$  benzophenone-3 (BP-3) addition. (A) Cellular C content; (B) cellular N content; (C) C:N ratio; (D) total antioxidant capacity (T-AOC) activity; (E) glutathione S-transferase (GST) activity; (F) caspase-3 activation level. Data were collected from control and LBP-3 cultures ( $n = 6$ ) after 8 days incubation. Each data point is the mean from six replicates with the error bar indicating standard deviation (mean  $\pm$  SD,  $n = 6$ ). \*\* $p < 0.01$  indicate significant differences between different groups.

## Metabolic alteration induced by BP-3

A total of 12 metabolome libraries were constructed from both the LBP-3 and control groups, and the metabolome of the LBP-3 group was compared with that of the control group. After data preprocessing and quality control, 11,047 metabolic compounds were identified in both positive and negative ion mode, and among them 2,874 was identified ([Supplementary Table 1](#)). The obvious separation of the metabolite profiles was observed by PCA analysis ([Supplementary Figure 2](#)). Furthermore, 318 upregulated and 396 downregulated differential metabolites were detected in the (LBP-3)/control comparison ([Supplementary Figure 3](#) and [Supplementary Table 2](#)), revealing a dramatic response of *C. goreau*'s metabolomic landscape to BP-3 addition.

## Functional distribution of the differentially expressed metabolites in the LBP-3 versus control comparison

Among the total 714 differential metabolites in the (LBP-3)/control comparison, the 318 upregulated metabolites were mainly related to amino acid (AA) metabolism, biosynthesis of secondary metabolites, synthesis and degradation of ketone bodies, and citrate cycle ([Figure 3A](#) and [Supplementary Table 3](#)). Similarly, the 396 downregulated metabolites were enriched to AA metabolism, ubiquinone and other terpenoid-quinone biosynthesis, biosynthesis of secondary metabolites, biotin metabolism, and porphyrin and chlorophyll metabolism ([Figure 3B](#) and [Supplementary Table 4](#)). For aromatic AA metabolism pathways, six metabolites in the tyrosine (Tyr) metabolism, five metabolites in the phenylalanine

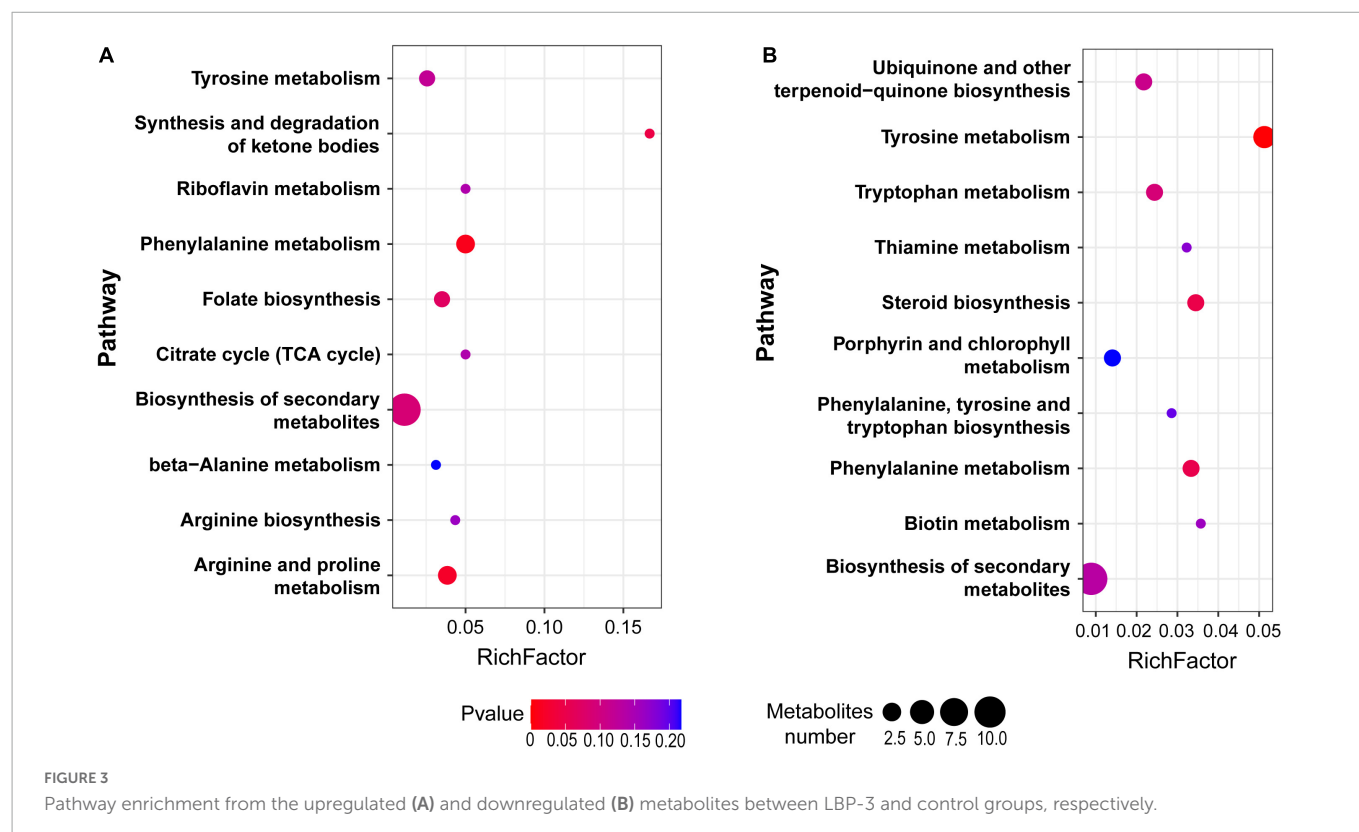
(Phe) metabolism (including a staggering 261-fold increase of benzoate), and three metabolites in the tryptophan (Trp) metabolism showed differential abundances in the (LBP-3)/control comparison ([Figure 4](#)). Another important AA metabolism affected by BP-3 addition was arginine (Arg) and proline (Pro) metabolism. Three metabolites in Arg and Pro metabolism, including L-arginine, 5-guanidino-2-oxopentanoic acid, and N2-succinyl-L-glutamic acid 5-semialdehyde, were significantly elevated in the LBP-3 group ([Figure 4](#) and [Supplementary Table 3](#)).

## Differential concentration of benzene and substituted derivatives under the LBP-3 condition

To explore the potential biodegradation mode of BP-3 in *C. goreau*, the significantly responded benzene and substituted derivatives were screened in the (LBP-3)/control comparison. Thirty-nine benzene and substituted derivatives were differentially changed, including 22 upregulated and 17 downregulated. The most dramatically changed were 2,3-dihydroxypropyl 3,4,5-trihydroxybenzoate, 3-phenoxybenzoic acid (3-PBA), benzoyl peroxide, and benzoate, which showed as high as 664-fold, 648-fold, 419-fold, and 261-fold increases in LBP-3 relative to control, respectively ([Table 1](#)).

## Discussion

It has been reported that the metabolites of BP-3 can increase the mortality rate of scleractinian corals, especially when the presence of





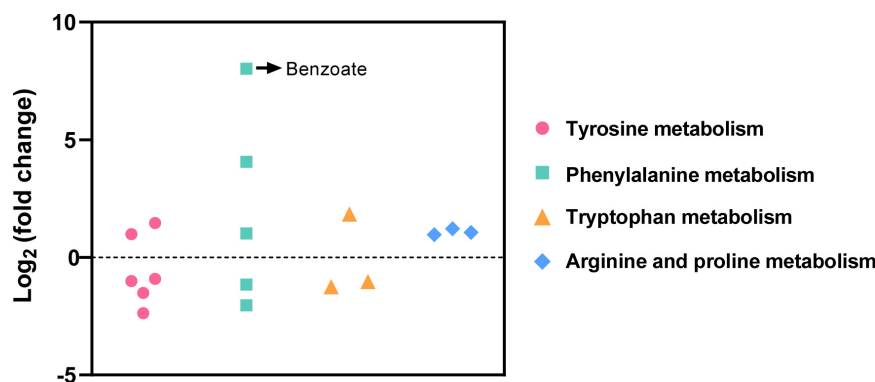


FIGURE 4

Differential metabolites related to amino acid metabolism in the (LBP-3)/control comparison.

BP-3 was combined with other stresses (Hansel, 2022). Meanwhile, symbiotic Symbiodiniaceae perform a potential role in the removal of BP-3 metabolites from the coral host (Vuckovic et al., 2022), but the protective mechanism has been poorly explored. In this study, using the *in vitro* batch culture of the type species of Symbiodiniaceae clade C, *C. goreau*, we found that the exposure on low BP-3 resulted in increased photosynthetic efficiency, larger cell size, quicker growth rate, and decreased cellular C and N contents in *C. goreau* cells. These responses manifested both at physiological and metabolomic levels. Our results demonstrated that *C. goreau*, and possibly other symbiotic Symbiodiniaceae, are able to effectively metabolize BP-3 at low concentrations and gain growth advantages through a series of metabolic reprogramming.

## BP-3 uptake and biodegradation in *C. goreau* cells

In this study, we monitored the BP-3 concentration in the medium of LBP-3 *C. goreau* cultures and observed a significant decrease on BP-3 concentration after an 8 days incubation (Figure 1C). This result indicated that *C. goreau* cells were able to take up BP-3 from the medium, which is in accordance with previous observations on other phytoplankton (Mao et al., 2017).

After BP-3 absorption, benzene and substituted derivatives in *C. goreau* showed significant increases (Table 1). Similarly, in the freshwater chlorophyte *Scenedesmus obliquus*, BP-3 could be degraded into benzene-containing intermediates, which are less toxic, after exposure to 3 mg L<sup>-1</sup> BP-3 (Lee et al., 2020). In the BP-3-grown *C. goreau*, 3-PBA, an important intermediate metabolite of pyrethroid (Zhao et al., 2020), showed an astounding 648-fold increase (Table 1). Due to a high solubility, strong mobility, and long half-life (Topp and Akhtar, 1990; Yuan et al., 2010), 3-PBA is able to harm the reproductive function, immune system, and endocrine system of animals (Sun et al., 2007; Han et al., 2008; Zhang et al., 2010). The high rate of mortality in *C. goreau* with high BP-3 exposure probably mirrors the negative effects of this degradation product (Figure 5). In addition, as the key intermediate for Phe metabolism (Wildermuth, 2006; Gonda et al., 2018), benzoate also showed a staggering 261-fold increase in the LBP-3 group (Figure 4 and Supplementary Table 2). These results indicate that the biodegradation of BP-3 by *C. goreau* cells could remodel the

benzene-containing secondary metabolites, thereby affecting cellular metabolic regulation (Figure 5).

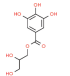
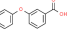
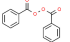
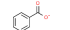
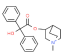
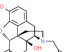
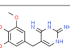
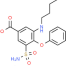
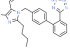
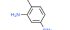
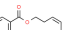
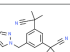
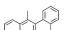
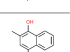

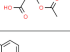

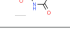
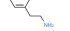
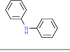
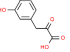
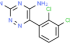
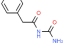
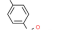
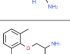
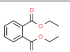
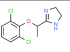
## BP-3 could affect symbiodiniaceae growth

At low BP-3 exposure level (2 mg L<sup>-1</sup>), *C. goreau* cells exhibited increased growth (Figure 1A), agreeing with recent observations on the freshwater chlorophyte *Scenedesmus quadricauda* (Teoh et al., 2020). Wijgerde et al. (2020) also found that the Symbiodiniaceae density in the coral *Stylophora pistillata* increased slightly (although not statistically significant) when exposed to BP-3. Recently, increasing studies demonstrated that the intracellular contaminants could be diluted by quick cell division, and phytoplankton can reduce the negative effects of toxic substance through faster proliferation (Skoglund and Swackhamer, 1994; Tikoo et al., 1997; Mao et al., 2017). Hence, the elevated growth of BP-3-grown *C. goreau* might be a mitigation mechanism for toxicity mitigation. Meanwhile, the cell size of *C. goreau* increased when exposed to 2 mg·L<sup>-1</sup> BP-3 (Figure 1F). Changes in cell size is a typical stress response (particularly nutrient deficiencies) in phytoplankton due to the inhibition of cell division (Li et al., 2016; Teoh et al., 2020; Wang et al., 2022). However, the LBP-3 treated cultures actually exhibited a higher cell division rate than the control. The cell size enlargement might result from a different reason. For instance, bigger cells can lead to slower uptake and alleviative propensity to biotoxicity (Duan et al., 2017), potentially another toxicity mitigation mechanism.

Benzophenone-3 exposure also induced a significant decrease in the Chl *c* content (Figure 1D). Correspondingly, there was a downregulation in porphyrin and chlorophyll metabolism in *C. goreau*, as shown in the metabolomic data (Figure 3B). This result indicates that BP-3 may disrupt the pigment synthesis in *C. goreau* cells. Interestingly, increased photosynthetic efficiency was also observed in *C. goreau* growth in the LBP-3 cultures (Figure 1C). The disparate effects of BP-3 on Chl *a*, photosynthetic efficiency, and growth rate versus Chl *c* is quite strikingly and might reflect the fact that Chl *a* is the major pigment that executes photosynthesis (Suggett et al., 2003). The enhanced photosynthetic efficiency in BP-3-grown *C. goreau* cells can potentially meet the elevated energy demand imposed for the biodegradation of BP-3 and its derivatives, and the faster cell division for the toxicity dilution.

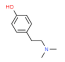
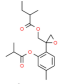
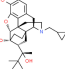
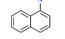
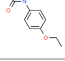
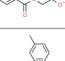
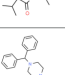
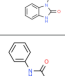
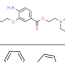
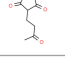
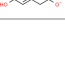



TABLE 1 The information of benzene and substituted derivatives in the (LBP-3)/control comparison of *C. goreau*.

Metabolite ID	Formula	Chemical structure	Name	MW <sup>a</sup>	FC <sup>b</sup>	q-value	VIP	Up/Down
6.626_244.05836	C <sub>10</sub> H <sub>12</sub> O <sub>7</sub>		2,3-dihydroxypropyl 3,4,5-trihydroxybenzoate	244.06	664.44	6.14E-10	3.53	Up
7.185_214.06272	C <sub>13</sub> H <sub>10</sub> O <sub>3</sub>		3-phenoxybenzoic acid	214.06	647.80	3.91E-08	3.52	Up
7.027_242.05802	C <sub>14</sub> H <sub>10</sub> O <sub>4</sub>		Benzoyl peroxide	242.06	418.53	6.19E-15	3.40	Up
6.046_104.02634	C <sub>7</sub> H <sub>5</sub> O <sub>2</sub>		Benzoate	104.03	260.74	1.61E-08	3.27	Up
7.691_352.19167	C <sub>22</sub> H <sub>26</sub> NO <sub>3</sub>		Clidinium	352.19	13.42	4.83E-06	2.23	Up
7.739_341.16268	C <sub>20</sub> H <sub>23</sub> NO <sub>4</sub>		Naltrexone	341.16	11.98	3.08E-05	2.15	Up
4.102_290.13789	C <sub>14</sub> H <sub>18</sub> N <sub>4</sub> O <sub>3</sub>		Trimethoprim	290.14	9.12	3.48E-04	2.01	Up
4.189_364.10906	C <sub>17</sub> H <sub>20</sub> N <sub>2</sub> O <sub>5</sub> S		Bumetanide	364.11	6.79	4.38E-06	1.87	Up
6.567_420.14830	C <sub>22</sub> H <sub>21</sub> ClN <sub>6</sub> O		Losartan carboxaldehyde	420.15	4.28	7.20E-07	1.65	Up
4.317_122.08464	C <sub>7</sub> H <sub>10</sub> N <sub>2</sub>		2,4-diaminotoluene	122.08	3.92	1.40E-03	1.59	Up
7.195_204.11535	C <sub>13</sub> H <sub>16</sub> O <sub>2</sub>		(z)-hex-3-enyl benzoate	204.12	3.75	4.47E-03	1.42	Up
4.032_293.16265	C <sub>17</sub> H <sub>19</sub> N <sub>5</sub>		Anastrozole	293.16	3.49	8.02E-03	1.36	Up
3.78_256.12486	C <sub>20</sub> H <sub>16</sub>		DMBA	256.12	2.46	3.40E-04	1.25	Up
4.532_215.09486	C <sub>13</sub> H <sub>13</sub> NO <sub>2</sub>		N-acetyl vitamin k5	215.09	2.44	8.13E-04	1.24	Up
4.236_180.04264	C <sub>9</sub> H <sub>8</sub> O <sub>4</sub>		Aspirin	180.04	2.31	2.62E-05	1.26	Up
4.013_236.15255	C <sub>13</sub> H <sub>20</sub> N <sub>2</sub> O <sub>2</sub>		Procaine	236.15	2.21	1.94E-03	1.18	Up
3.65_270.10384	C <sub>12</sub> H <sub>18</sub> N <sub>2</sub> O <sub>3</sub> S		Tolbutamide	270.10	2.15	8.56E-03	1.14	Up
3.362_121.08943	C <sub>8</sub> H <sub>11</sub> N		Phenethylamine	121.09	2.03	3.54E-03	1.06	Up
7.642_169.08946	C <sub>12</sub> H <sub>11</sub> N		Diphenylamine	169.09	2.02	8.70E-03	1.02	Up
5.102_196.03700	C <sub>9</sub> H <sub>8</sub> O <sub>5</sub>		3,4-dihydroxyphenylpyruvic acid	196.04	1.99	1.35E-02	1.09	Up
0.567_255.00807	C <sub>9</sub> H <sub>7</sub> Cl <sub>2</sub> N <sub>5</sub>		Lamotrigine	255.01	1.98	1.38E-04	1.11	Up
4.817_178.07450	C <sub>9</sub> H <sub>10</sub> N <sub>2</sub> O <sub>2</sub>		Phenacetamide	178.07	1.86	9.00E-04	1.04	Up
3.258_233.98766	C <sub>7</sub> H <sub>7</sub> ClN <sub>2</sub> O <sub>3</sub> S		4-chlorobenzenesulfonylurea	233.99	0.28	3.30E-02	1.24	Down
7.986_179.13134	C <sub>11</sub> H <sub>17</sub> NO		Mexiletine	179.13	0.31	9.92E-06	1.47	Down
3.977_222.08891	C <sub>12</sub> H <sub>14</sub> O <sub>4</sub>		Diethyl phthalate	222.09	0.32	2.67E-05	1.45	Down
4.204_258.03184	C <sub>11</sub> H <sub>12</sub> Cl <sub>2</sub> N <sub>2</sub> O		Lofexidine	258.03	0.34	7.58E-05	1.43	Down
4.073_223.04829	C <sub>10</sub> H <sub>9</sub> NO <sub>5</sub>		2-(carboxyacetamido)benzoic acid	223.05	0.35	1.97E-03	1.34	Down

(Continued)

TABLE 1 (Continued)

Metabolite ID	Formula	Chemical structure	Name	MW <sup>a</sup>	FC <sup>b</sup>	q-value	VIP	Up/Down
7.156_165.11568	C <sub>10</sub> H <sub>15</sub> NO		Hordenine	165.12	0.35	1.55E-04	1.36	Down
6.749_334.17766	C <sub>19</sub> H <sub>26</sub> O <sub>5</sub>		{2-[2-(isobutyryloxy)-4-methylphenyl]-2-oxiranylmethyl 2-methylbutanoate	334.18	0.36	1.25E-03	1.30	Down
8.445_467.30392	C <sub>29</sub> H <sub>41</sub> NO <sub>4</sub>		Buprenorphine	467.30	0.38	6.32E-05	1.33	Down
4.203_157.05308	C <sub>10</sub> H <sub>7</sub> NO		1-nitrosonaphthalene	157.05	0.42	5.09E-05	1.27	Down
4.423_180.09020	C <sub>9</sub> H <sub>12</sub> N <sub>2</sub> O <sub>2</sub>		(4-ethoxyphenyl)urea	180.09	0.42	6.81E-04	1.20	Down
4.964_161.04797	C <sub>9</sub> H <sub>9</sub> NO <sub>3</sub>		Hippurate	179.05	0.45	9.28E-04	1.17	Down
5.535_288.14739	C <sub>16</sub> H <sub>20</sub> N <sub>2</sub> O <sub>3</sub>		Imazamethabenz-methyl	288.15	0.47	1.62E-04	1.16	Down
9.927_426.24407	C <sub>27</sub> H <sub>30</sub> N <sub>4</sub> O		Oxatimide	426.24	0.48	4.71E-04	1.13	Down
1.516_136.06385	C <sub>7</sub> H <sub>8</sub> N <sub>2</sub> O		Yu0650000	136.06	0.51	4.67E-03	1.04	Down
9.453_308.21140	C <sub>17</sub> H <sub>28</sub> N <sub>2</sub> O <sub>3</sub>		Oxybuprocaine	308.21	0.53	1.09E-03	1.04	Down
5.756_322.13170	C <sub>19</sub> H <sub>18</sub> N <sub>2</sub> O <sub>3</sub>		Kebuzone	322.13	0.53	6.10E-03	1.05	Down
1.29_185.06915	C <sub>8</sub> H <sub>7</sub> O <sub>4</sub>		Homogentisate	185.07	0.53	1.38E-04	1.06	Down

<sup>a</sup>MW, molecular weight.<sup>b</sup>FC, fold change.

After 2 mg L<sup>-1</sup> BP-3 exposure, *C. goreau* showed no significant changes in T-AOC and GST activities (Figures 2D, E), indicating that cells did not experience significant toxic (oxidative stress) effects at this dosage. With all results taken together, it is rather clear that *C. goreau* can carry out a series of toxicity mitigation strategies, including rapid growth, expanded cell size, and elevated photosynthesis, to minimize the cytotoxicity of low concentration BP-3. However, based on the lethal effects of the high concentration we used (20 mg L<sup>-1</sup>), there seems to be a threshold concentration, beyond which BP-3 could damage the photosynthesis system and cause rapid death of *C. goreau* cells (Figure 5).

## Effects of BP-3 on cellular nutrition regulation

Besides algal growth, BP-3 exposure also highly impacted the cellular metabolisms in *C. goreau*. In marine bacterium *Epibacterium mobile*, BP-3 exposure has been found to result in perturbation of AA metabolism (Lozano et al., 2021). Similarly, significant changes in metabolites were noted in our present study, which impacted major AA metabolism pathways in BP-3 exposed *C. goreau* (Figure 4). The BP-3 biodegradation in microalgae can produce a series of aromatic

compounds, which are important precursor species for AA synthesis, especially Phe, Tyr, and Trp (Pérez et al., 2002; Gosset, 2009). Here, these three aromatic AA metabolites were all significantly affected in BP-3 exposed *C. goreau* cells (Figure 4), implying the potential interference of intracellular BP-3 metabolites with AA metabolism (Figure 5). In addition, Arg and Pro metabolism was significantly enriched by upregulated metabolites in BP-3 absorbed *C. goreau* cells (Figure 4). Arg and Pro are the proteinogenic AA which are essential for cellular primary metabolism (Szabados and Savouré, 2010; Trovato et al., 2019). Increasing Arg and Pro accumulation could confer biotic and abiotic stress tolerance, such as UV irradiation (Park et al., 2020), heavy metals (Seneviratne et al., 2019), and oxidative stress (Momose et al., 2010; Nishimura et al., 2010; Forlani et al., 2019). Therefore, at low BP-3 exposure, *C. goreau* cells may also resist the BP-3 stress via modulating Arg and Pro metabolism (Figure 5).

Besides AA metabolism, cellular element in *C. goreau* was also affected by BP-3 exposure. The cellular N and C content in *C. goreau* were significantly decreased under the LBP-3 condition (Figures 2A, B), indicating that cellular regulation of AA metabolism at low BP-3 exposure also affects N and C metabolism. As photosynthetic efficiency was elevated in cells exposed to a low dose of LBP-3 (Figure 1C), the depressed cellular C content might be due to a

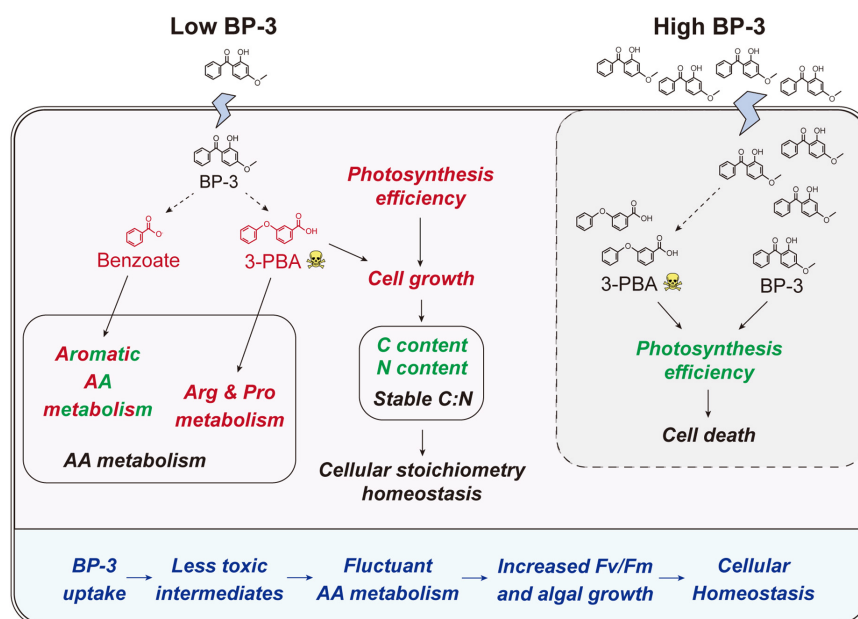


FIGURE 5

Schematic of the physiological and metabolic response in *C. goreau* cells to BP-3 addition. Red and green fonts indicate upregulated and downregulated metabolites or related metabolic activities after BP-3 addition, respectively. Dotted arrows represent the potential metabolic pathways for BP-3. BP-3, oxybenzone; 3-PBA, 3-phenoxybenzoic acid; AA, amino acid.

greater increase in cell division rate than in photosynthesis or that the apparently increased ATP production might be used for the BP-3 biodegradation than to fuel C fixation. Meanwhile, we also noticed that *C. goreau* cells in the LBP-3 cultures showed significantly decreased stearate content (Supplementary Table 3). Stearic acid is a long-chain saturated fatty acid functions as a crucial storage form of cellular C (Du et al., 2016). This might be another reason for the reduction in C content in LBP-3-grown cultures. Given the changes in C and N induced by BP-3 exposure, it is interesting to note that the C:N ratio of *C. goreau* cells exhibited no statistical changes (Figure 2C). As we all know, elemental stoichiometry is crucial to map the cellular nutrient status in phytoplankton (Zhang et al., 2021b; Li et al., 2022). Our results indicate that the low BP-3 dose used in our study did not disrupt cellular stoichiometric homeostasis in *C. goreau* cells (Figure 5).

## Conclusion

In coral reef ecosystems, endosymbiotic dinoflagellates are believed to be responsible for the detoxification of BP-3 and related UV filters in their coral hosts. In this study, we investigated the physiological and metabolic responses of symbiotic Symbiodiniaceae *C. goreau* after BP-3 exposure. Overall, *C. goreau* cells exhibited increased algal growth, elevated photosynthetic efficiency, decreased cellular C and N contents, and remodeled AA metabolism, potentially as multi-faceted means to cope with the toxic effects of absorbed BP-3. These findings shed light on how Symbiodiniaceae respond to BP-3 stress at low doses. However, the rapid algal death at high BP-3 concentration calls for further exploration to pinpoint the BP-3 tolerance threshold of Symbiodiniaceae. Information on the threshold will be crucial for assessing the environmental risk

of organic UV filters to coral reef ecosystems and informing the formulation of coral reef reserve management regulation.

## Data availability statement

The data presented in this study are deposited in the MetaboLights repository, accession number MTBLS6890.

## Author contributions

KZ and ZZ conceived and designed the study. KZ, ZS, WY, JG, ZY, JLi, JT, and ZL performed the experiments, with the help of JLin and XC for BP-3 measurement. KZ, SL, and ZZ interpreted the data and wrote the manuscript. All authors read and approved the final version of the manuscript.

## Funding

This research was supported by the National Key Research and Development Program of China (2022YFC3102003) and the Hainan Provincial Natural Science Foundation of China (422QN265 and 420CXTD432).

## Acknowledgments

The authors were grateful to all members of the Coral Reef Conservation Laboratory for their continuous technical advices and helpful suggestions.

## Conflict of interest

The authors declare that the research was conducted in the absence of any commercial or financial relationships that could be construed as a potential conflict of interest.

## Publisher's note

All claims expressed in this article are solely those of the authors and do not necessarily represent those of their affiliated

organizations, or those of the publisher, the editors and the reviewers. Any product that may be evaluated in this article, or claim that may be made by its manufacturer, is not guaranteed or endorsed by the publisher.

## Supplementary material

The Supplementary Material for this article can be found online at: <https://www.frontiersin.org/articles/10.3389/fmicb.2022.1116975/full#supplementary-material>

## References

- Baker, A. C. (2003). Flexibility and specificity in coral-algal symbiosis: Diversity, ecology, and biogeography of symbiodinium. *Annu. Rev. Ecol. Syst.* 34, 661–689. doi: 10.1146/annurev.ecolsys.34.011802.132417
- Balmer, M. E., Buser, H.-R., Müller, M. D., and Poiger, T. (2005). Occurrence of some organic UV filters in wastewater, in surface waters, and in fish from Swiss lakes. *Environ. Sci. Technol.* 39, 953–962. doi: 10.1021/es040055r
- Barker, M., and Rayens, W. (2003). Partial least squares for discrimination. *J. Chemom.* 17, 166–173. doi: 10.1002/cem.785
- Campos, D., Gravato, C., Fedorova, G., Burkina, V., Soares, A. M. V. M., and Pestana, J. L. T. (2017). Ecotoxicity of two organic UV-filters to the freshwater caddisfly *Sericostoma vittatum*. *Environ. Pollut.* 228, 370–377. doi: 10.1016/j.envpol.2017.05.021
- Ceh, J., Kilburn, M. R., Cliff, J. B., Raina, J. B., van Keulen, M., and Bourne, D. G. (2013). Nutrient cycling in early coral life stages: *Pocillopora damicornis* larvae provide their algal symbiont (Symbiodinium) with nitrogen acquired from bacterial associates. *Ecol. Evol.* 3, 2393–2400. doi: 10.1002/ece3.642
- Danovaro, R., Bongiorno, L., Corinaldesi, C., Giovannelli, D., Damiani, E., Astolfi, P., et al. (2008). Sunscreens cause coral bleaching by promoting viral infections. *Environ. Health Perspect.* 116, 441–447. doi: 10.2307/40040094
- Downs, C., Kramarsky-Winter, E., Segal, R., Fauth, J., Knutson, S., Bronstein, O., et al. (2016). Toxicopathological effects of the sunscreen UV filter, oxybenzone (benzophenone-3), on coral planulae and cultured primary cells and its environmental contamination in Hawaii and the US Virgin Islands. *Arch. Environ. Contam. Toxicol.* 70, 265–288. doi: 10.1007/s00244-015-0227-7
- Du, H., Huang, M., Hu, J., and Li, J. (2016). Modification of the fatty acid composition in *Arabidopsis* and maize seeds using a stearyl-acyl carrier protein desaturase-1 (ZmSAD1) gene. *BMC Plant Biol.* 16:137. doi: 10.1186/s12870-016-0827-z
- Duan, W., Meng, F., Lin, Y., and Wang, G. (2017). Toxicological effects of phenol on four marine microalgae. *Environ. Toxicol. Pharmacol.* 52, 170–176. doi: 10.1016/j.etap.2017.04.006
- Fel, J.-P., Lacherez, C., Bensetra, A., Mezzache, S., Béraud, E., Léonard, M., et al. (2019). Photochemical response of the scleractinian coral *Stylophora pistillata* to some sunscreen ingredients. *Coral Reefs* 38, 109–122. doi: 10.1007/s00338-018-01759-4
- Forlani, G., Trovato, M., Funck, D., and Signorelli, S. (2019). “Regulation of proline accumulation and its molecular and physiological functions in stress defence,” in *Osmoprotectant-mediated abiotic stress tolerance in plants*, eds M. A. Hossain, V. Kumar, D. J. Burritt, M. Fujita, and P. S. A. Mäkelä (Boston, MA: Springer), 73–97. doi: 10.1007/978-3-030-27423-8\_3
- Goksoyr, A., Tollefsen, K. E., Grung, M., Løken, K., Lie, E., Zenker, A., et al. (2009). Balsa raft crossing the pacific finds low contaminant levels. *Environ. Sci. Technol.* 43, 4783–4790. doi: 10.1021/es900154h
- Gonda, I., Davidovich-Rikanati, R., Bar, E., Lev, S., Jhirad, P., Meshulam, Y., et al. (2018). Differential metabolism of L-phenylalanine in the formation of aromatic volatiles in melon (*Cucumis melo* L.) fruit. *Phytochemistry* 148, 122–131. doi: 10.1016/j.phytochem.2017.12.018
- González-Pech, R. A., Bhattacharya, D., Ragan, M. A., and Chan, C. X. (2019). Genome evolution of coral reef symbionts as intracellular residents. *Trends Ecol. Evol.* 34, 799–806. doi: 10.1016/j.tree.2019.04.010
- Gosset, G. (2009). Production of aromatic compounds in bacteria. *Curr. Opin. Biotechnol.* 20, 651–658. doi: 10.1016/j.copbio.2009.09.012
- Guillard, R. R. L. (1975). “Culture of phytoplankton for feeding marine invertebrates,” in *Culture of marine invertebrate animals*, eds W. L. Smith and M. H. Chanley (Boston, MA: Springer), 29–60. doi: 10.1007/978-1-4615-8714-9\_3
- Han, Y., Xia, Y., Han, J., Zhou, J., Wang, S., Zhu, P., et al. (2008). The relationship of 3-PBA pyrethroids metabolite and male reproductive hormones among non-occupational exposure males. *Chemosphere* 72, 785–790. doi: 10.1016/j.chemosphere.2008.03.058
- Hansel, C. M. (2022). Sunscreens threaten coral survival. *Science* 376, 578–579. doi: 10.1126/science.abo4627
- He, T., Tsui, M. M. P., Tan, C. J., Ng, K. Y., Guo, F. W., Wang, L. H., et al. (2019). Comparative toxicities of four benzophenone ultraviolet filters to two life stages of two coral species. *Sci. Total Environ.* 651, 2391–2399. doi: 10.1016/j.scitotenv.2018.10.148
- Hoegh-Guldberg, O., Mumby, P. J., Hooten, A. J., Steneck, R. S., Greenfield, P., Gomez, E., et al. (2007). Coral reefs under rapid climate change and ocean acidification. *Science* 318, 1737–1742. doi: 10.1126/science.1152509
- Hughes, T. P., Kerry, J. T., Baird, A. H., Connolly, S. R., Dietzel, A., Eakin, C. M., et al. (2018). Global warming transforms coral reef assemblages. *Nature* 556, 492–496. doi: 10.1038/s41586-018-0041-2
- Jeffrey, S. W., and Humphrey, G. F. (1975). New spectrophotometric equations for determining chlorophylls a, b, c1 and c2 in higher plants, algae and natural phytoplankton. *Biochem. Physiol. Pflanz.* 167, 191–194. doi: 10.1016/S0015-3796(17)30778-3
- Kim, S., and Choi, K. (2014). Occurrences, toxicities, and ecological risks of benzophenone-3, a common component of organic sunscreen products: A mini-review. *Environ. Int.* 70, 143–157. doi: 10.1016/j.envint.2014.05.015
- LaJeunesse, T. C., Parkinson, J. E., Gabrielson, P. W., Jeong, H. J., Reimer, J. D., Voolstra, C. R., et al. (2018). Systematic revision of Symbiodiniaceae highlights the antiquity and diversity of coral endosymbionts. *Curr. Biol.* 28, 2570–2580.e6. doi: 10.1016/j.cub.2018.07.008
- Lee, S.-H., Xiong, J.-Q., Ru, S., Patil, S. M., Kurade, M. B., Govindwar, S. P., et al. (2020). Toxicity of benzophenone-3 and its biodegradation in a freshwater microalga *Scenedesmus obliquus*. *J. Hazard. Mater.* 389:122149. doi: 10.1016/j.jhazmat.2020.122149
- Li, J., Zhang, K., Lin, X., Li, L., and Lin, S. (2022). Phytate as a phosphorus nutrient with impacts on iron stress-related gene expression for phytoplankton: Insights from the diatom *Phaeodactylum tricornutum*. *Appl. Environ. Microbiol.* 88, e2097–e2021. doi: 10.1128/AEM.02097-21
- Li, M., Shi, X., Guo, C., and Lin, S. (2016). Phosphorus deficiency inhibits cell division but not growth in the dinoflagellate *Amphidinium carterae*. *Front. Microbiol.* 7:826. doi: 10.3389/fmicb.2016.00826
- Lozano, C., Givens, J., Stien, D., Matallana-Surget, S., and Lebaron, P. (2020). “Bioaccumulation and toxicological effects of UV-filters on marine species,” in *Sunscreens in coastal ecosystems*, eds A. Tovar-Sánchez, D. Sánchez-Quiles, and J. Blasco (Boston, MA: Springer), 85–130. doi: 10.1007/978-2019\_442
- Lozano, C., Lee, C., Wattiez, R., Lebaron, P., and Matallana-Surget, S. (2021). Unraveling the molecular effects of oxybenzone on the proteome of an environmentally relevant marine bacterium. *Sci. Total Environ.* 793:148431. doi: 10.1016/j.scitotenv.2021.148431
- Mao, F., He, Y., Kushmaro, A., and Gin, K. Y.-H. (2017). Effects of benzophenone-3 on the green alga *Chlamydomonas reinhardtii* and the cyanobacterium *Microcystis aeruginosa*. *Aquat. Toxicol.* 193, 1–8. doi: 10.1016/j.aquatox.2017.09.029
- Mitchellmore, C. L., Burns, E. E., Conway, A., Heyes, A., and Davies, I. A. (2021). A critical review of organic ultraviolet filter exposure, hazard, and risk to corals. *Environ. Toxicol. Chem.* 40, 967–988. doi: 10.1002/etc.4948
- Mitchellmore, C. L., He, K., Gonsior, M., Hain, E., Heyes, A., Clark, C., et al. (2019). Occurrence and distribution of UV-filters and other anthropogenic contaminants in coastal surface water, sediment, and coral tissue from Hawaii. *Sci. Total Environ.* 670, 398–410. doi: 10.1016/j.scitotenv.2019.03.034
- Moeller, M., Pawlowski, S., Petersen-Thiery, M., Miller, I. B., Nietzer, S., Heisel-Sure, Y., et al. (2021). Challenges in current coral reef protection—possible impacts of UV filters used in sunscreens, a critical review. *Front. Mar. Sci.* 8:665548. doi: 10.3389/fmars.2021.665548
- Momose, Y., Matsumoto, R., Maruyama, A., and Yamaoka, M. (2010). Comparative analysis of transcriptional responses to the cryoprotectants, dimethyl sulfoxide and

- trehalose, which confer tolerance to freeze-thaw stress in *Saccharomyces cerevisiae*. *Cryobiology* 60, 245–261. doi: 10.1016/j.cryobiol.2010.01.001
- Nishimura, A., Kotani, T., Sasano, Y., and Takagi, H. (2010). An antioxidative mechanism mediated by the yeast N-acetyltransferase Mpr1: Oxidative stress-induced arginine synthesis and its physiological role. *FEMS Yeast Res.* 10, 687–698. doi: 10.1111/j.1567-1364.2010.00650.x
- O'Donovan, S., Mestre, N. C., Abel, S., Fonseca, T. G., Carteny, C. C., Willems, T., et al. (2020). Effects of the UV filter, oxybenzone, adsorbed to microplastics in the clam *Scrobicularia plana*. *Sci. Total Environ.* 733:139102. doi: 10.1016/j.scitotenv.2020.139102
- Paredes, E., Pérez, S., Rodil, R., Quintana, J. B., and Beiras, R. (2014). Ecotoxicological evaluation of four UV filters using marine organisms from different trophic levels *Isochrysis galbana*, *Mytilus galloprovincialis*, *Paracentrotus lividus*, and *Siriella armata*. *Chemosphere* 104, 44–50. doi: 10.1016/j.chemosphere.2013.10.053
- Park, M.-H., Park, C.-H., Sim, Y. B., and Hwang, S.-J. (2020). Response of *Scenedesmus quadricauda* (Chlorophyceae) to salt stress considering nutrient enrichment and intracellular proline accumulation. *Int. J. Environ. Res. Public Health* 17:3624. doi: 10.3390/ijerph17103624
- Pendleton, L., Hoegh-Guldberg, O., Albright, R., Kaup, A., Marshall, P., Marshall, N., et al. (2019). The great barrier reef: Vulnerabilities and solutions in the face of ocean acidification. *Reg. Stud. Mar. Sci.* 31:100729. doi: 10.1016/j.rsma.2019.100729
- Pérez, A. G., Olías, R., Luaces, P., and Sanz, C. (2002). Biosynthesis of strawberry aroma compounds through amino acid metabolism. *J. Agric. Food Chem.* 50, 4037–4042. doi: 10.1021/jf011465r
- Pintado-Herrera, M. G., Wang, C., Lu, J., Chang, Y.-P., Chen, W., Li, X., et al. (2017). Distribution, mass inventories, and ecological risk assessment of legacy and emerging contaminants in sediments from the Pearl River Estuary in China. *J. Hazard. Mater.* 323, 128–138. doi: 10.1016/j.jhazmat.2016.02.046
- Plaisance, L., Caley, M. J., Brainard, R. E., and Knowlton, N. (2011). The diversity of coral reefs: What are we missing? *PLoS One* 6:e25026. doi: 10.1371/journal.pone.0025026
- Ritchie, R. J. (2006). Consistent sets of spectrophotometric chlorophyll equations for acetone, methanol and ethanol solvents. *Photosynth. Res.* 89, 27–41. doi: 10.1007/s11120-006-9065-9
- Seneviratne, M., Rajakaruna, N., Rizwan, M., Madawala, H., Ok, Y. S., and Vithanage, M. (2019). Heavy metal-induced oxidative stress on seed germination and seedling development: A critical review. *Environ. Geochem. Health* 41, 1813–1831. doi: 10.1007/s10653-017-0005-8
- Seoane, M., Esperanza, M., Rioboo, C., Herrero, C., and Cid, Á. (2017). Flow cytometric assay to assess short-term effects of personal care products on the marine microalga *Tetraselmis suecica*. *Chemosphere* 171, 339–347. doi: 10.1016/j.chemosphere.2016.12.097
- Skoglund, R. S., and Swackhamer, D. L. (1994). "Fate of hydrophobic organic contaminants: Processes affecting uptake by phytoplankton," in *Environmental chemistry of lakes and reservoirs*, (Washington, DC: ACS Publications), 559–573. \*ed name doi: 10.1021/ba-1994-0237.ch018
- Stien, D., Clergeaud, F., Rodrigues, A. M., Lebaron, K., Pillot, R., Romans, P., et al. (2018). Metabolomics reveal that octocrylene accumulates in *Pocillopora damicornis* tissues as fatty acid conjugates and triggers coral cell mitochondrial dysfunction. *Anal. Chem.* 91, 990–995. doi: 10.1021/acs.analchem.8b04187
- Stien, D., Suzuki, M., Rodrigues, A., Yvin, M., Clergeaud, F., Thorel, E., et al. (2020). A unique approach to monitor stress in coral exposed to emerging pollutants. *Sci. Rep.* 10, 1–11. doi: 10.1038/s41598-020-66117-3
- Suggett, D. J., Oxenburgh, K., Baker, N. R., MacIntyre, H. L., Kana, T. M., and Geider, R. J. (2003). Fast repetition rate and pulse amplitude modulation chlorophyll a fluorescence measurements for assessment of photosynthetic electron transport in marine phytoplankton. *Eur. J. Phycol.* 38, 371–384. doi: 10.1080/09670260310001612655
- Sully, S., Burkepille, D. E., Donovan, M. K., Hodgson, G., and van Woessik, R. (2019). A global analysis of coral bleaching over the past two decades. *Nat. Commun.* 10:1264. doi: 10.1038/s41467-019-09238-2
- Sun, H., Xu, X.-L., Xu, L.-C., Song, L., Hong, X., Chen, J.-F., et al. (2007). Antiandrogenic activity of pyrethroid pesticides and their metabolite in reporter gene assay. *Chemosphere* 66, 474–479. doi: 10.1016/j.chemosphere.2006.05.059
- Szabados, L., and Savouré, A. (2010). Proline: A multifunctional amino acid. *Trends Plant Sci.* 15, 89–97. doi: 10.1016/j.tplants.2009.11.009
- Teoh, M.-L., Sanusi, N. S., Wong, C.-Y., and Beardall, J. (2020). Effects of the sunscreen ultraviolet filter, oxybenzone, on green microalgae. *Adv. Polar Sci.* 31, 112–123. doi: 10.13679/j.advps
- Tikoo, V., Scragg, A. H., and Shales, S. W. (1997). Degradation of pentachlorophenol by microalgae. *J. Chem. Technol. Biotechnol.* 68, 425–431.
- Topp, E., and Akhtar, M. H. (1990). Mineralization of 3-phenoxybenzoate by a two-membered bacterial co-culture. *Can. J. Microbiol.* 36, 495–499. doi: 10.1139/m90-086
- Trovato, M., Forlani, G., Signorelli, S., and Funck, D. (2019). "Proline metabolism and its functions in development and stress tolerance," in *Osmoprotectant-mediated abiotic stress tolerance in plants*, eds M. A. Hossain, V. Kumar, D. Burritt, M. Fujita, and P. Mäkelä (Boston, MA: Springer), 41–72. doi: 10.1007/978-3-030-27423-8\_2
- Tsui, M. M. P., Leung, H. W., Wai, T.-C., Yamashita, N., Taniyasu, S., Liu, W., et al. (2014). Occurrence, distribution and ecological risk assessment of multiple classes of UV filters in surface waters from different countries. *Water Res.* 67, 55–65. doi: 10.1016/j.watres.2014.09.013
- Vuckovic, D., Tinoco, A. I., Ling, L., Renicke, C., Pringle, J. R., and Mitch, W. A. (2022). Conversion of oxybenzone sunscreen to phototoxic glucoside conjugates by sea anemones and corals. *Science* 376, 644–648. doi: 10.1126/science.abn2600
- Wang, C., Sun, X., Wang, J., Tang, J.-M., Gu, Y., and Lin, S. (2022). Physiological and metabolic effects of glyphosate as the sole P source on a cosmopolitan phytoplankton and biogeochemical implications. *Sci. Total Environ.* 832:155094. doi: 10.1016/j.scitotenv.2022.155094
- Wen, B., Mei, Z., Zeng, C., and Liu, S. (2017). MetaX: A flexible and comprehensive software for processing metabolomics data. *BMC Bioinform.* 18:183. doi: 10.1186/s12859-017-1579-y
- Westerhuis, J. A., Hoefsloot, H. C. J., Smit, S., Vis, D. J., Smilde, A. K., van Velzen, E. J. J., et al. (2008). Assessment of PLS-DA cross validation. *Metabolomics* 4, 81–89. doi: 10.1007/s11306-007-0099-6
- Wijgerde, T., Van Ballegoijen, M., Nijland, R., Van Der Loos, L., Kwadijk, C., Osinga, R., et al. (2020). Adding insult to injury: Effects of chronic oxybenzone exposure and elevated temperature on two reef-building corals. *Sci. Total Environ.* 733:139030. doi: 10.1016/j.scitotenv.2020.139030
- Wildermuth, M. C. (2006). Variations on a theme: Synthesis and modification of plant benzoic acids. *Curr. Opin. Plant Biol.* 9, 288–296. doi: 10.1016/j.pbi.2006.03.006
- Yuan, C., Wang, C., Gao, S.-Q., Kong, T.-T., Chen, L., Li, X.-F., et al. (2010). Effects of permethrin, cypermethrin and 3-phenoxybenzoic acid on rat sperm motility in vitro evaluated with computer-assisted sperm analysis. *Toxicol. In Vitro* 24, 382–386. doi: 10.1016/j.tiv.2009.11.001
- Zhang, K., Li, J., Zhou, Z., Huang, R., and Lin, S. (2021a). Roles of alkaline phosphatase PhoA in algal metabolic regulation under phosphorus-replete conditions. *J. Phycol.* 57, 703–707. doi: 10.1111/jpy.13151
- Zhang, K., Zhou, Z., Li, J., Wang, J., Yu, L., and Lin, S. (2021b). SPX-related genes regulate phosphorus homeostasis in the marine phytoplankton, *Phaeodactylum tricornutum*. *Commun. Biol.* 14:797. doi: 10.1038/s42003-021-02284-x
- Zhang, Y., Zhao, M., Jin, M., Xu, C., Wang, C., and Liu, W. (2010). Immunotoxicity of pyrethroid metabolites in an in vitro model. *Environ. Toxicol. Chem.* 29, 2505–2510. doi: 10.1002/etc.208
- Zhao, J., Jia, D., Chi, Y., and Yao, K. (2020). Co-metabolic enzymes and pathways of 3-phenoxybenzoic acid degradation by *Aspergillus oryzae* M-4. *Ecotoxicol. Environ. Saf.* 189:109953. doi: 10.1016/j.ecoenv.2019.109953





## OPEN ACCESS

## EDITED BY

Zhiyong Li,  
Shanghai Jiao Tong University, China

## REVIEWED BY

Guanghua Wang,  
Guangxi University, China  
Denis Grouzdev,  
SciBear OU, Estonia

## \*CORRESPONDENCE

Kaihao Tang  
✉ khtang@scsio.ac.cn

RECEIVED 06 January 2023

ACCEPTED 03 April 2023

PUBLISHED 20 April 2023

## CITATION

Nie Z, Tang K, Wang W, Wang P, Guo Y, Wang Y,  
Kao S-J, Yin J and Wang X (2023) Comparative  
genomic insights into habitat adaptation of  
coral-associated *Prosthecochloris*.  
*Front. Microbiol.* 14:1138751.  
doi: 10.3389/fmicb.2023.1138751

## COPYRIGHT

© 2023 Nie, Tang, Wang, Wang, Guo, Wang,  
Kao, Yin and Wang. This is an open-access  
article distributed under the terms of the  
[Creative Commons Attribution License \(CC BY\)](https://creativecommons.org/licenses/by/4.0/).  
The use, distribution or reproduction in other  
forums is permitted, provided the original  
author(s) and the copyright owner(s) are  
credited and that the original publication in this  
journal is cited, in accordance with accepted  
academic practice. No use, distribution or  
reproduction is permitted which does not  
comply with these terms.

# Comparative genomic insights into habitat adaptation of coral-associated *Prosthecochloris*

Zhaolong Nie<sup>1,2</sup>, Kaihao Tang<sup>1,2,3\*</sup>, Weiquan Wang<sup>2</sup>,  
Pengxia Wang<sup>2,3,4</sup>, Yunxue Guo<sup>2,3,4</sup>, Yan Wang<sup>1</sup>, Shuh-Ji Kao<sup>1</sup>,  
Jianping Yin<sup>2</sup> and Xiaoxue Wang<sup>2,3,4</sup>

<sup>1</sup>State Key Laboratory of Marine Resource Utilization in South China Sea, Hainan University, Haikou, China, <sup>2</sup>Key Laboratory of Tropical Marine Bio-resources and Ecology, Guangdong Key Laboratory of Marine Materia Medica, Innovation Academy of South China Sea Ecology and Environmental Engineering, South China Sea Institute of Oceanology, Chinese Academy of Sciences, Guangzhou, China, <sup>3</sup>Southern Marine Science and Engineering Guangdong Laboratory (Guangzhou), Guangzhou, China, <sup>4</sup>University of Chinese Academy of Sciences, Beijing, China

Green sulfur bacteria (GSB) are a distinct group of anoxygenic phototrophic bacteria that are found in many ecological niches. *Prosthecochloris*, a marine representative genus of GSB, was found to be dominant in some coral skeletons. However, how coral-associated *Prosthecochloris* (CAP) adapts to diurnal changing microenvironments in coral skeletons is still poorly understood. In this study, three *Prosthecochloris* genomes were obtained through enrichment culture from the skeleton of the stony coral *Galaxea fascicularis*. These divergent three genomes belonged to *Prosthecochloris marina* and two genomes were circular. Comparative genomic analysis showed that between the CAP and non-CAP clades, CAP genomes possess specialized metabolic capacities (CO oxidation, CO<sub>2</sub> hydration and sulfur oxidation), gas vesicles (vertical migration in coral skeletons), and *cbb*<sub>3</sub>-type cytochrome c oxidases (oxygen tolerance and gene regulation) to adapt to the microenvironments of coral skeletons. Within the CAP clade, variable polysaccharide synthesis gene clusters and phage defense systems may endow bacteria with differential cell surface structures and phage susceptibility, driving strain-level evolution. Furthermore, mobile genetic elements (MGEs) or evidence of horizontal gene transfer (HGT) were found in most of the genomic loci containing the above genes, suggesting that MGEs play an important role in the evolutionary diversification between CAP and non-CAP strains and within CAP clade strains. Our results provide insight into the adaptive strategy and population evolution of endolithic *Prosthecochloris* strains in coral skeletons.

## KEYWORDS

*Prosthecochloris*, coral skeleton, endolithic bacteria, adaptive strategy, mobile genetic elements

## 1. Introduction

The coral animal and its associated zooxanthella, bacteria, archaea, fungi, and viruses, collectively constitute the coral holobiont (Rosenberg et al., 2007; Bourne et al., 2016). Microorganisms inhabiting coral surface mucus, tissue and gastric cavity play different roles in coral health, including nutrient cycling, and antimicrobial and antioxidant activities (Morris et al., 2019; Peixoto et al., 2021; Cardenas et al., 2022). Similarly, a variety of algae, fungi, bacteria

and microeukaryotes inhabit coral skeletons (Li et al., 2014; Yang et al., 2016; Marcelino et al., 2018; Cardenas et al., 2022), and some groups of endolithic microorganisms are also involved in the nutrient cycling and metabolite transfer of coral holobionts (Pernice et al., 2020). *Prosthecochloris*, green sulfur bacteria (GSB) capable of anoxygenic photosynthesis and nitrogen fixation, was dominant in some layers of coral skeletons or whole coral samples in different corals (Yang et al., 2016, 2019; Cai et al., 2017; Yu et al., 2021; Chen et al., 2021b).

*Prosthecochloris* are regarded as typical marine representatives of GSB, which represent one phylum Chlorobiota, with one family Chlorobiaceae, including the genera *Chlorobium*, *Chlorobaculum*, *Prosthecochloris* and *Chloroherpeton* (Imhoff, 2014; Oren and Garrity, 2021). GSB are a distinct group of strictly anaerobic and anoxygenic phototrophic bacteria with specialized photosynthetic reactions and metabolic properties of carbon fixation and nitrogen fixation (Imhoff, 2014). GSB possess light-harvesting complexes called chlorosomes which contain a large number of special bacteriochlorophylls. Chlorosomes are highly efficient and can capture minute amounts of light, which enables bacteria to adapt to low-light conditions (Imhoff, 2014). GSB have been in many marine ecological niches with variable light availability (Imhoff, 2014) including special photosynthetic habitats such as coral skeletons (Li et al., 2014; Yang et al., 2016) and deep-sea hydrothermal vents (Beatty et al., 2005). GSB are obligately phototrophic and strictly dependent on photosynthesis under anoxic conditions, using inorganic electron donors and fixing carbon dioxide through reductive citrate cycle. Sulfide is an important photosynthetic electron donor in GSB and the oxidation of sulfide usually deposits elemental sulfur globules outside the cells. This process enables syntrophic associations between GSB and sulfur- and sulfate-reducing bacteria (Imhoff, 2014). Species of *Prosthecochloris* possess all the above features of GSB and are nonmotile (Gorlenko, 2015). *Prosthecochloris* spp. differ in cell shapes, spherical or ovoid, and have different requirements for vitamin B<sub>12</sub> as a growth factor (Anil Kumar et al., 2009; Gorlenko, 2015; Bryantseva et al., 2019). *Prosthecochloris* spp. were found in diverse environments including hydrogen sulfide-rich mud, hot spring sediment and coral skeletons (Gorlenko, 1970; Imhoff, 2003; Beatty et al., 2005; Nabhan et al., 2016; Cai et al., 2017; Thiel et al., 2017; Grouzdev et al., 2018; Bryantseva et al., 2019; Yang et al., 2019; Kyndt et al., 2020; Athen et al., 2021; Chen et al., 2021a,b). The major difference between coral-associated and other non-coral-associated *Prosthecochloris* remains poorly understood, although preliminary analysis of coral-associated *Prosthecochloris* was performed previously (Chen et al., 2021b).

The microniches within the skeleton can be shaped by physico-chemical gradients and diurnal rhythms (Shashar and Stambler, 1992; Ricci et al., 2019). In the daytime, sunlight is mostly depleted by coral, and only small amounts of light reach the skeleton (Ricci et al., 2019). Meanwhile, the O<sub>2</sub> concentration is gradually decreased from the vicinity of tissue to the inside of skeleton but with a high O<sub>2</sub> concentration in the endolithic algal zone due to photosynthesis (Ricci et al., 2019). At night, the O<sub>2</sub> concentration in the skeleton is greatly decreased because of the dominance of heterotrophic metabolism during the night (Ricci et al., 2019). Accordingly, the pH is high up to 8.5 in the daytime and low at night (Shashar and Stambler, 1992). How endolithic *Prosthecochloris* adapts to these changing microenvironments in coral skeletons is not well understood.

*Galaxea fascicularis* is a massive stony coral belonging to the family Oculinidae, having large connected coenosteum with

skeletal vesicles varying from 0.2 to 0.5 mm (Wewengkang et al., 2007; Hou et al., 2018). In this study, *Prosthecochloris* was found in the skeleton of *G. fascicularis*, and three *Prosthecochloris* genomes were obtained through enrichment culture. Two *Prosthecochloris* genomes were circular. Comprehensive comparative genomic analysis was performed and the genomic features of CAP genomes were revealed. Between CAP and non-CAP genomes, CAP genomes possess specialized metabolic capacities and genes coding gas vesicle proteins and *cbb*<sub>3</sub>-type cytochrome *c* oxidases. Within CAP clade genomes, polysaccharide synthesis gene clusters and phage defense systems may endow bacteria with differential cell surface structures and phage susceptibility, driving strain-level evolution. Our results provide insight into the adaptive strategy of *Prosthecochloris* strains to thrive in ecological niches such as coral skeletons.

## 2. Materials and methods

### 2.1. Sample collection and enrichment culture

Skeleton samples were obtained from *G. fascicularis* fragments used in our previous study (Wang et al., 2022). Medium for enrichment culture was prepared according to previous studies (Zyakun et al., 2009; Yang et al., 2019), with additional glucose (0.05%) and resazurin (1 µg L<sup>-1</sup>) as a redox indicator. Skeleton samples were rapidly added to filter sterilized medium in Hungate anaerobic tubes and cultured at room temperature (~25–28°C) under natural sunlight. After approximately 2 weeks, green colors were visible in the two enrichment cultures (with or without resazurin) and cells were examined by microscopy and collected by centrifugation for DNA extraction.

### 2.2. DNA extraction, genome sequencing, and assembly

Total DNA of collected cells was isolated using the TIANamp Bacteria DNA kit (Tiangen Biotech Co. Ltd., Beijing, China) and sequenced using PacBio and Illumina platforms. Metagenome assembly and binning were performed using MetaWRAP pipeline v1.3.2 (Uritskiy et al., 2018) with wrapped tools of SPAdes 3.13.0 (Bankevich et al., 2012), MaxBin2 v2.2.7 (Wu et al., 2016), CONCOCT v1.0.0 (Alneberg et al., 2014) and metaBAT2 v2.12.1 (Kang et al., 2019). The qualities of metagenomic bins were accessed by CheckM v1.2.1 (Parks et al., 2015). The percentage of reads mapped to each bin and proportion of a bin relative to all recovered bins were evaluated by CheckM. Classification of metagenomic bins was performed by GTDB-TK v2.1.1 (Chaumeil et al., 2022). In order to obtain complete genomes belonging to *Prosthecochloris*, long reads were used to assemble genomes by HGAP v4 within SMRT Link, and polished by pilon (Walker et al., 2014) and homopolish (Huang et al., 2021). Pairwise ANI between genomes calculations were performed using FastANI (Jain et al., 2018). Phylogenetic analysis of 16S rRNA genes was performed using MEGA (Kumar et al., 2016) and phylogenetic analysis of whole genomes based on core gene was performed using FastTree (Price et al., 2009).

## 2.3. 16S rRNA gene amplicon sequencing

The barcoded primers 515 (Parada) (5'-GTGYCAGCMGCCG CGGTAA-3')/806 (Apprill) (5'-GGACTACNVG GGTWTCTAAT-3') were used to amplify the V4 region of microbial 16S rRNA (Apprill et al., 2015; Parada et al., 2016). The purified PCR products were sequenced on the Illumina platform. Quality-filtered reads were submitted to the MicrobiomeAnalyst platform (Chong et al., 2020) using DADA2 pipeline (Callahan et al., 2016) against taxonomy reference database of Silva (version 138.1; Yilmaz et al., 2014). A total of 129,228 sequences from two samples corresponding to 55 unique ASVs were recovered. Taxa abundance profiling was performed on the MicrobiomeAnalyst platform with default parameters (Chong et al., 2020).

## 2.4. Comparative genomic analysis

All available *Prosthecochloris* genomes (Table 1) and two *Chlorobium* genomes were downloaded from NCBI and reannotated by Prokka (Seemann, 2014). The highly divergent rates among different protein families may affect the accuracies of protein homolog detection methods, therefore, it is more reliable to combine different methods to identify protein homologs for comparative genomic analysis. Briefly, KEGG orthologs in genomes were identified by BlastKOALA (Kanehisa et al., 2016) and KofamKOALA (Aramaki et al., 2020) online.<sup>1</sup> Pathway comparisons were performed by KEMET with default parameters (Palu et al., 2022). Pfam domains (Mistry et al., 2021) of proteins were further analyzed by Interproscan (v5.54–87.0) (Jones et al., 2014) with in a local searching mode. Pangenome analysis was performed using Roary (Page et al., 2015) with the following parameter: -I 70. Core gene alignment generated by Roary was used for phylogenetic analysis by FastTree (Price et al., 2009). Furthermore, Scoary (Brynildsrud et al., 2016) was used to explore potential specific genes that were missed in the KEGG pathway comparison. The protein homologs identified by all the above methods were used as a cross validation to obtain a reliable gene presence and absence analysis. Meanwhile, visualization of multiple genome alignments was performed by Mauve (Darling et al., 2004, 2010) and Proksee with its built-in tools (Vernikos and Parkhill, 2006; Couvin et al., 2018; Guo et al., 2021; Brown et al., 2022). A Venn diagram was drawn by jvenn (Bardou et al., 2014). GO enrichment of genes was performed by TBtools (Chen et al., 2020).

## 3. Results and discussion

### 3.1. *Prosthecochloris* cells in enrichment cultures from the skeleton of *Galaxea fascicularis*

During our previous study of the microbiome of the reef-building coral *Galaxea fascicularis* (Wang et al., 2022), a light green layer in the

skeleton directly under the coenosarc was observed (Figure 1A left panel), similar to the *Prosthecochloris* formed green layer in the skeleton of *Isopora palifera* (Yang et al., 2019; Chen et al., 2021b). Occasionally, this green layer could cover the corallites after polyp bleaching (Figure 1A right panel). *Prosthecochloris* was found in our previous 16S rRNA gene amplicon sequencing data of *G. fascicularis* polyp samples (Supplementary Figure S1), therefore, we tended to culture *Prosthecochloris* from the skeleton of *G. fascicularis*. We finally obtained two enrichment cultures (with or without the redox indicator resazurin in the medium) from the same skeleton sample (Figure 1A left panel). 16S rRNA gene amplicon sequencing showed that the relative abundance of Chlorobia and Gammaproteobacteria accounted for ~90% of total reads at class level (Figure 1B). Accordingly, two species of *Prosthecochloris* accounted for the majority of Chlorobia, while *Marinobacter*, *Vibrio* and *Halomonas* accounted for the majority of Gammaproteobacteria (Figure 1C). Furthermore, *Halodesulfobivrio* sp., belonging to sulfate-reducing bacteria, was also found in the enrichment cultures (Figure 1C). *Candidatus* *Halodesulfobivrio* lyudaonia was previously recovered along with *Prosthecochloris* spp. from the same enrichment culture and proposed having a syntrophic relationship with coral-associated *Prosthecochloris* (Chen et al., 2021b). Amplification and sequencing 16S rRNA gene sequences using the 27F/1492R primer pair from total DNA of these two cultures showed both ~99% to *Prosthecochloris marina* V1 (abbreviated as PmV1; Bryantseva et al., 2019). Observation of cells by microscopy revealed many cells with gas vesicles (Figure 1D), a typical feature of *Prosthecochloris* (Bryantseva et al., 2019). Bright granules were observed in enrichment culture 2, highly similar to the extracellular sulfur granules previously observed in *Prosthecochloris indica* (Anil Kumar et al., 2009). Furthermore, some cells were connected in a chain, similar with that cells of *Prosthecochloris aestuarii* were often connected by one or two filaments (Gorlenko, 1970; Gorlenko, 2015). These results indicate that *Prosthecochloris* with other potentially syntrophic bacteria were cultured from the skeleton of *G. fascicularis*.

### 3.2. Complete *Prosthecochloris* genomes recovered from *Galaxea fascicularis* endolithic cultures

In order to obtain the genomes in the enrichment cultures, total DNA of each culture was extracted and sequenced using PacBio and Illumina sequencing platforms. Analysis of metagenome-assembled genomes (MAGs) using short reads revealed that bacterial genomes belonging to *Prosthecochloris*, *Marinobacter*, *Vibrio*, *Halomonas* and *Halodesulfobivrio* were obtained (Supplementary Table S1), consistent with the 16S rRNA gene amplicon sequencing data. *Prosthecochloris*-derived bins accounted for 81 and 58% of total communities of enrichment culture 1 and 2. In order to obtain the complete genomes of *Prosthecochloris*, genomes were reassembled using long and short reads. Finally, one circular genome with 3.02 Mbp (SCSIO W1101) and one circular genome with 2.79 Mbp (SCSIO W1103) were recovered from enrichment cultures 1 and 2, respectively (Table 1). A partial genome with 1.32 Mbp (SCSIO W1102) was also recovered from enrichment culture 1. Analysis using GTDB-Tk (Chaumeil et al., 2022) confirmed that these three genomes belong to the *Prosthecochloris* genus. The 16S rRNA gene sequences in these genomes are nearly identical to the extracted full-length 16S rRNA

<sup>1</sup> <https://www.kegg.jp/blastkoala/> and <https://www.genome.jp/tools/kofamkoala/>

TABLE 1 Information of *Prosthecochloris* genomes assembled from pure cultures, enrichment cultures or metagenomes.

Strain	Contig	CDS	Size (Mb)	GC%	Source <sup>b</sup>	Isolation	Reference <sup>c</sup>
<i>Prosthecochloris</i> sp. Ty-1 (=TY Vent = GSB1)	1	2,270	2.47	56	PC	Deep-sea hydrothermal vent	Beatty et al. (2005)
<i>Candidatus Prosthecochloris</i> sp. C10	41	1,953	2.13	49.1	MAG	Seawater lake chemocline	GCA_010912745.1
<i>Candidatus Prosthecochloris</i> sp. A305	75	1,999 <sup>a</sup>	2.09	47.8	MAG	Skeleton of coral <i>Isopora palifera</i>	Yang et al. (2019)
<i>Candidatus Prosthecochloris</i> sp. N2	46	2,534 <sup>a</sup>	2.65	47.4	EC	Skeleton of coral <i>Isopora palifera</i>	Chen et al. (2021b)
<i>Candidatus Prosthecochloris korallensis</i>	68	2,485 <sup>a</sup>	2.58	48.3	MAG	Skeleton of coral	Cai et al. (2017)
<i>Candidatus Prosthecochloris</i> sp. SCSIO W1101	1	2,918 <sup>a</sup>	3.02	47.2	EC	Skeleton of coral <i>Galaxea fascicularis</i>	This study
<i>Candidatus Prosthecochloris</i> sp. N1	24	2,630 <sup>a</sup>	2.79	47	EC	Skeleton of coral <i>Isopora palifera</i>	Chen et al. (2021b)
<i>Prosthecochloris marina</i> V1	19	2,474	2.72	47	PC	South China Sea coastal zone	Bryantseva et al. (2019)
<i>Candidatus Prosthecochloris</i> sp. SCSIO W1102	1	1,270 <sup>a</sup>	1.32	47.1	EC	Skeleton of coral <i>Galaxea fascicularis</i>	This study
<i>Candidatus Prosthecochloris</i> sp. SCSIO W1103	1	2,627 <sup>a</sup>	2.79	47.1	EC	Skeleton of coral <i>Galaxea fascicularis</i>	This study
<i>Candidatus Prosthecochloris</i> sp. B10	32	2,007	2.26	50.1	MAG	Seawater lake chemocline	GCA_010912735.1
<i>Prosthecochloris</i> sp. ZM	40	2,416	2.66	50	PC	Meromictic lakes Green cape	Grouzdev et al. (2018)
<i>Prosthecochloris aestuarii</i> DSM 271	2	2,308	2.58	50.1	PC	Hydrogen sulfide-rich mud	Gorlenko (1970)
<i>Prosthecochloris vibrioformis</i> DSM 260	75	2,103	2.31	52.1	PC	Rivermouth	Imhoff (2003)
<i>Prosthecochloris</i> sp. CIB 2401	1	2,166	2.40	52.1	PC	Coastal brackish lagoon	Nabhan et al. (2016)
<i>Candidatus Prosthecochloris vibrioformis</i> M55B161	8	1,959	2.13	52.4	MAG	Saline lake water	Chen et al. (2021a)
<i>Candidatus Prosthecochloris vibrioformis</i> M50B85	18	2,031	2.23	52.2	MAG	Saline lake water	Chen et al. (2021a)
<i>Prosthecochloris</i> sp. HL-130-GSB	1	2,152	2.41	52	PC	Microbial mat in Hot Lake	Thiel et al. (2017)
<i>Prosthecochloris</i> sp. SM2_Orange-Green1	112	2,245	2.43	51.8	EC	Inland salt marsh	Athen et al. (2021)
<i>Candidatus Prosthecochloris aestuarii</i> SpSt-1,181	228	1,908	2.03	52.2	MAG	Hot spring sediment	GCA_011054385.1
<i>Prosthecochloris</i> sp. ZM_2	117	2,203	2.40	55.5	PC	Meromictic lakes Green cape	Grouzdev et al. (2018)
<i>Prosthecochloris ethylica</i> DSM 1685	66	2,179	2.44	55.1	PC	Mud sample from estuary	Kyndt et al. (2020)
<i>Candidatus Prosthecochloris ethylica</i> N2	60	2,181	2.44	55.1	EC	Lake mud	Kyndt et al. (2020)
<i>Candidatus Prosthecochloris ethylica</i> N3	72	2,189	2.45	55.1	EC	Mud sample from estuary	Kyndt et al. (2020)

<sup>a</sup>Counts of coding sequences (CDS) are from Prokka annotation.

<sup>b</sup>PC, pure culture; EC, metagenomic assembly of enrichment culture; MAG, metagenome-assembled genomes.

<sup>c</sup>If no publication was found, genome assembly accessions were provided instead.

gene amplicon sequence variants (ASVs) of *G. fascicularis*, suggesting that cultured *Prosthecochloris* cells are indeed from the skeleton of *G. fascicularis* (Supplementary Figure S2). Along with four previous metagenome-assembled *Prosthecochloris* genomes (Table 1), pairwise

comparison of 16S rRNA gene sequences showed that the 16S rRNA genes shared high identity (98.5–100%) with each other (Supplementary Figure S2), and they fell into one clade in the phylogenetic tree (Figure 2A), consistent with the previous report



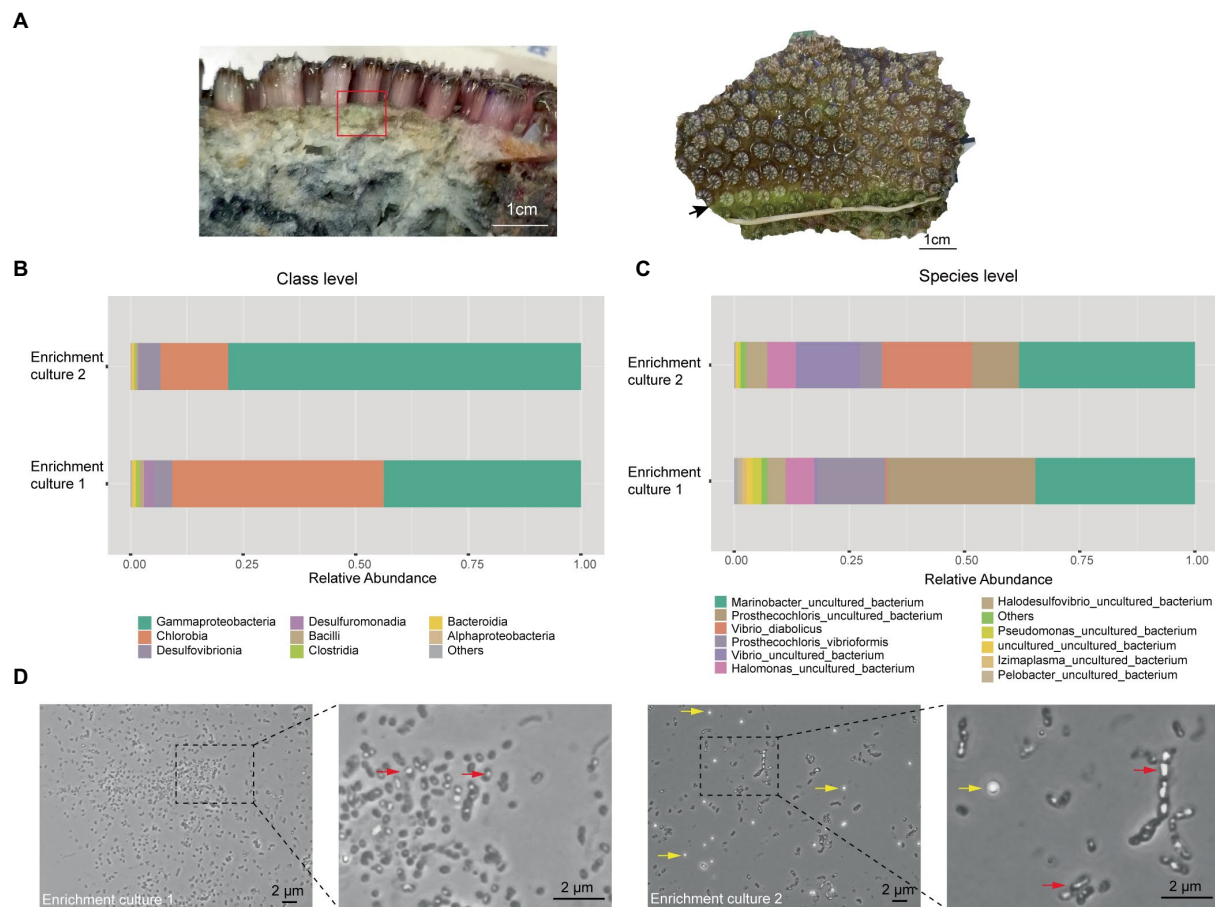


FIGURE 1

*Prosthecochloris* cells were enriched from the skeleton of *Galaxea fascicularis*. (A) Lateral and frontal views of the *Galaxea fascicularis* skeleton. The red rectangle indicates the region of the skeleton sampled for enrichment culture. The black arrow indicates a green layer in the corallites after polyp bleaching. Relative abundance of major microbial taxa in enrichment cultures at class level (B) and at species level (C). (D) Cell morphology of *Prosthecochloris* cells. Red arrows indicate gas vesicles in cells and yellow arrows indicate sulfur granules outside cells.

(Chen et al., 2021b). Further analysis based on average nucleotide identity (ANI) across whole genome sequences indicated that strains SCSIO W1101, SCSIO W1102, SCSIO W1103, N1 and V1 belong to the same species, namely *Prosthecochloris marina* and SCSIO W1101 is divergent to the other four strains (ANI 95.3–96.1%; Figure 2B). Constantly, this relationship was confirmed by the phylogenetic analysis using concatenated DNA sequence of core genes (Figure 3). Therefore, this clade was designated the coral-associated *Prosthecochloris* (CAP) clade as previously proposed (Chen et al., 2021b). Accordingly, this relationship indicates that individual and chain-like cells in enrichment cultures may be derived from SCSIO W1101 and SCSIO W1103, respectively (Figure 1). Taken together, these results suggest that the *G. fascicularis* endolithic *Prosthecochloris* population is not a monolithic group that may have high genetic diversity, which is consistent with the *Prosthecochloris* population in the skeleton of coral *I. palifera* (Yang et al., 2019; Chen et al., 2021b).

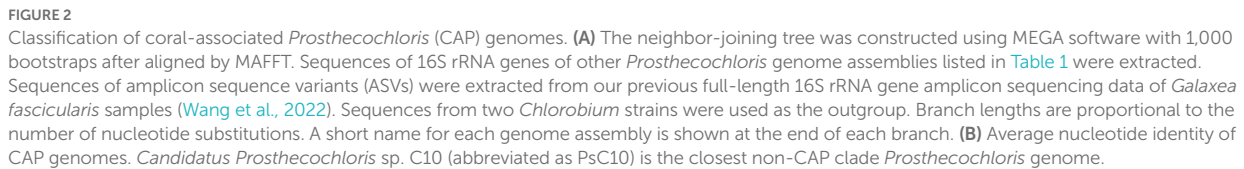
Among these CAP clade genomes, SCSIO W1101 and SCSIO W1103 are the only two complete genome assemblies, and SCSIO W1101 has the largest genome size among all of these *Prosthecochloris* genomes (Table 1; Supplementary Figure S3A). Moreover, these CAP clade genomes have significantly lower G + C content than non-CAP genomes (Supplementary Figure S3B). A trend toward high G + C

content in free-living organisms and low G + C content in bacteria living in nutrient-limiting and nutrient-poor environments (e.g., some symbiotic bacteria) was found previously (Mann and Chen, 2010). Therefore, the low G + C content may be an indicator to differentiate CAP and non-CAP genomes.

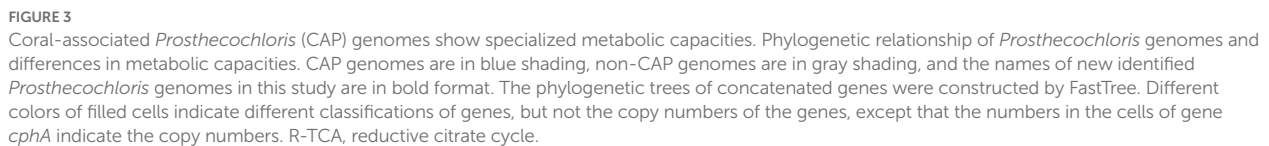
### 3.3. Coral-associated *Prosthecochloris* genomes show specialized metabolic capacities

In order to determine metabolic capacity differences between CAP genomes and non-CAP genomes, comprehensive comparative genomic analysis combining KEGG pathway reconstitution and genome-wide analysis of protein homolog presence or absence was used (see Methods). Phylogenetic analysis using concatenated core genes showed that CAP genomes and non-CAP genomes were separated into different clades (Figure 3). The CAP clade contains 8 genomes belonging to at least 4 species. The non-CAP clade contains 14 genomes belonging to 4 species, i.e., *P. aestuarii*, *P. vibrioformis*, *Prosthecochloris* sp. HL-130-GSB and *P. ethylica*. Generally, the pattern of the presence or absence of several pathways is mostly conserved within the CAP or





Bacteriochlorophyll is important for phototrophic bacteria and different bacteriochlorophylls may enable bacteria to adapt to variable light intensity for photosynthesis. GSB synthesize bacteriochlorophylls (BChls) *a*, *b*, *c*, *d*, or *e* to assemble chlorosomes for light harvesting (Imhoff, 2014). In BChl *c*- and *d*-containing *Chlorobium vibrioforme* strain NCIB 8327 (Huster and Smith, 1990), the ratio of BChl *c*/BChl *d* could increase at low-light intensities (Saga et al., 2003). Green and brown color are two major morphotypes of GSB, and it was found that compared with green-colored BChl *c*-containing *Chlorobium* spp., only brown-colored BChl *e*-containing *Chlorobium* spp. were able to grow at low-light intensities (Borrego and Garcigil, 1995). Another



**FIGURE 3**  
Coral-associated *Prosthecochloris* (CAP) genomes show specialized metabolic capacities. Phylogenetic relationship of *Prosthecochloris* genomes and differences in metabolic capacities. CAP genomes are in blue shading, non-CAP genomes are in gray shading, and the names of new identified *Prosthecochloris* genomes in this study are in bold format. The phylogenetic trees of concatenated genes were constructed by FastTree. Different colors of filled cells indicate different classifications of genes, but not the copy numbers of the genes, except that the numbers in the cells of gene *cphA* indicate the copy numbers. R-TCA, reductive citrate cycle.

### 3.3.2. Carbon metabolism

a single genomic locus, a putative operon between the *Prosthecochloris* conserved genes *pckG* (phosphoenolpyruvate carboxykinase) and *mnpA* (Na<sup>+</sup>/H<sup>+</sup> antiporter subunit A; Figure 4A). This operon also encodes an additional C-type cytochrome and NifT/TauT family transport system including substrate-binding protein, permease protein and ATP-binding protein. Furthermore, many mobile genetic elements (MGEs) such as restriction modification (RM) systems, toxin-antitoxin (TA) systems and recombination-related gene *recQ*, are located directly downstream of this operon, suggesting that this genomic locus undergoes active genome recombination. This genome recombination may also cause the loss of the *cooS* operon in non-CAP genomes, leading to the differentiation of CO metabolic capacities.

### 3.3.3. Nitrogen metabolism

For nitrogen metabolism, all *Prosthecochloris* genomes encode nitrogenase NifDKH for nitrogen fixation, generating ammonia (Figure 3). The major difference between CAP and non-CAP genomes in nitrogen metabolism based on KEGG orthology is the distinct

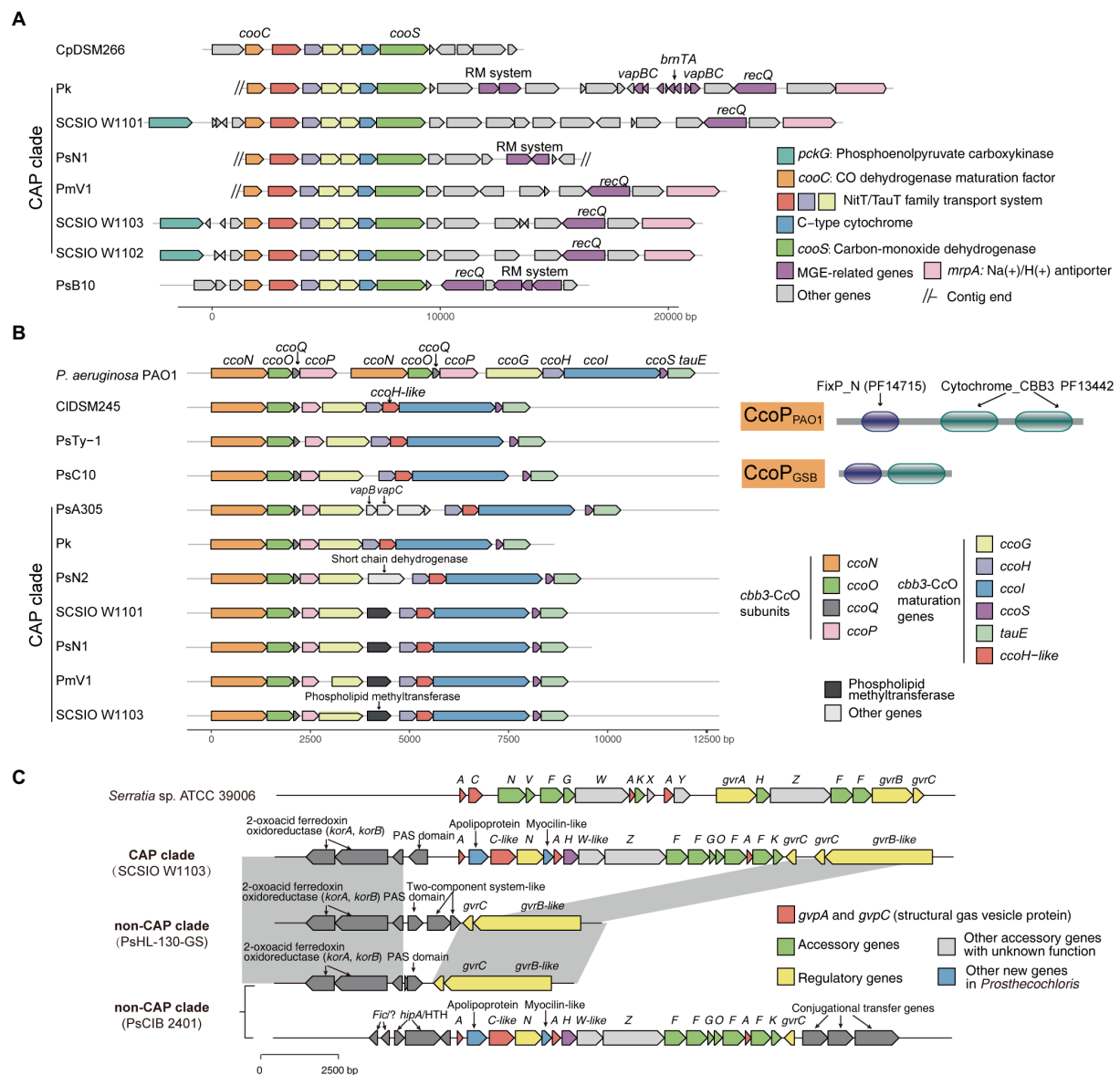


FIGURE 4

Mobile genetic elements and related genome rearrangements reshape gene clusters involved in the metabolic capacity divergence between coral-associated *Prothoeochloris* (CAP) and non-CAP genomes. (A) gene clusters of carbon monoxide dehydrogenase. (B) Gene clusters of *cbb3*-type cytochrome c oxidases (*cbb3*-CcOs). The domain architectures of different CcoP proteins are shown. PF14715: FixP\_N (N-terminal domain of cytochrome oxidase-*cbb3*; FixP). PF13442: Cytochrome\_CBB3 (Cytochrome C oxidase, *cbb3*-type, subunit III). (C) Gene clusters of gas vesicle proteins (*gvp*). Gray shading indicates conserved genomic regions.

distribution of carbonic anhydrase, which is involved in the transformation of two important nitrogen-containing compounds, carbamate and cyanate. Specifically, *Prothoeochloris* genomes encode three carbonic anhydrases (CAs) with different distribution patterns.  $\gamma$ -CA-1 is conserved in all *Prothoeochloris* genomes, while  $\gamma$ -CA-2 and  $\beta$ -CA are exclusively present in CAP genomes. CA catalyzes the interconversion of carbonic acid and carbon dioxide ( $\text{HCO}_3^- + \text{H}^+ \rightleftharpoons \text{CO}_2 + \text{H}_2\text{O}$ ). This capacity is critical for aquatic photoautotrophs to maintain productivity at ambient concentrations of  $\text{CO}_2$  by concentrating  $\text{CO}_2$  (Kaplan and Reinhold, 1999). At present, three classes of CAs ( $\alpha$ ,  $\beta$  and  $\gamma$ ) were found in bacteria and they share low sequence similarities (Capasso and Supuran, 2015; Supuran and Capasso, 2017). Bacterial  $\alpha$ -CAs usually contain an N-terminal signal

sequence and possess a periplasmic or extracellular localization and  $\beta$ -CAs and  $\gamma$ -CAs were mostly found in cytoplasm (Marcus et al., 2005; Dobrinski et al., 2010; Gai et al., 2014; Capasso and Supuran, 2015). Bacterial CAs also differs in the catalytic efficiency and the equilibrium toward the formation of  $\text{CO}_2$  or  $\text{HCO}_3^-$  (Gai et al., 2014; Capasso and Supuran, 2015). In general, bacterial  $\alpha$ -CAs have higher catalytic efficiency than that of  $\beta$ -CAs which in turn are more efficient than  $\gamma$ -CAs (Capasso and Supuran, 2015). In *Ralstonia eutropha*, it was proposed that the periplasmic  $\alpha$ -CA converts diffused  $\text{CO}_2$  to  $\text{HCO}_3^-$  and may be responsible for supplementation of cellular bicarbonate, while one cytoplasmic  $\gamma$ -CA converts  $\text{HCO}_3^-$  to  $\text{CO}_2$  and may be responsible for the supplementation of  $\text{CO}_2$  to RuBisCO, and one  $\beta$ -CA may function in pH homeostasis (Gai et al., 2014).

Furthermore, different types of CAs were found in photosynthetic purple bacteria, that were able to synthesize CAs under both photoautotrophic and photoheterotrophic conditions (Ivanovsky et al., 2020). The diurnal rhythm of coral endosymbiont photosynthesis may lead to different availability of CO<sub>2</sub> in skeletons for endolithic *Prosthecochloris*. During the day, dominant by photosynthesis of coral, the pH inside of coral skeletons reached over 8.5 and the major form of inorganic carbon is HCO<sub>3</sub><sup>-</sup> but not CO<sub>2</sub> (Shashar and Stambler, 1992). During the night, dominant by respiration of coral, pH decreased to approximately 7.7 (Shashar and Stambler, 1992). Therefore, the availability of HCO<sub>3</sub><sup>-</sup> or CO<sub>2</sub> in coral skeletons for coral endolithic *Prosthecochloris* at night may differ with that in the daytime. It is proposed that different CAs in *Prosthecochloris* genomes may play different roles in the utilization of CO<sub>2</sub>. Furthermore, considering that many pumps can deliver HCO<sub>3</sub><sup>-</sup>, which is also important for coral calcification, it is a straightforward speculation that CAs in CAP genomes may facilitate coral calcification.

### 3.3.4. Sulfur metabolism

Comparing all the known KEGG pathways of *Prosthecochloris* genomes, the numbers of modules (≥80% completeness) in sulfur metabolism were higher in CAP genomes (Supplementary Figure S7). Further analysis showed that the numbers of genes involved in assimilatory sulfate reduction (ASR), dissimilatory sulfate reduction (DSR) and thiosulfate oxidation by SOX complex were significantly higher in CAP genomes than that in non-CAP genomes (Supplementary Figure S8). ASR and DSR are the classical sulfate-reducing pathways that are involved in converting between sulfate and sulfide, with cysteine and sulfide as end products, respectively. For the ASR, *sat*, *cysND* and *cysC* are present in CAP genomes, while these genes are only present in a few non-CAP genomes (Figure 3). For DSR, *dsrAB* (dissimilatory sulfite reductase), *sat* (sulfate adenylyltransferase) and *aprAB* (adenylylsulfate reductase) are present in CAP genomes, while *sat* and *aprAB* are absent in non-CAP genomes. The DSR pathway can convert sulfide to sulfate (Grein et al., 2013), and the lack of *sat* and *aprAB* genes suggests that non-CAP genomes can only convert the sulfide to sulfite (Supplementary Figure S9A). Analysis of the genomic loci of these genes revealed that the genes involved in DSR are located in a single genomic locus, while genomic regions containing *sat* and *aprAB* undergo genome rearrangement, which may lead to the loss of *sat* and *aprAB* genes (Supplementary Figure S9B).

Similarly, for thiosulfate oxidation by SOX complex, *soxYZ* *soxAX* and *soxB* are present in CAP genomes, while *soxAX* and *soxB* are absent in non-CAP genomes (Figure 3). In SOX complex, SoxYZ is responsible for substrate binding, the manganese-containing SoxB is responsible for hydrolyzing cysteinyl S-thiosulfonate to cysteinyl persulfide and sulfate, and SoxAX is a heterodimeric c-type cytochrome mediating electron transfer (Sakurai et al., 2010). Although SoxYZ homologs are present in both CAP and non-CAP genomes, they shared low amino acid sequence identity (~30%), suggesting different evolutionary sources of SoxYZ in *Prosthecochloris*. In CAP genomes, the SOX complex related genes *soxXYZABW*, along with a porin-encoding gene and *dsbD* (cytochrome c-type biogenesis protein), apparently consist of an operon that was inserted in a genomic region conserved in all *Prosthecochloris* genomes (Supplementary Figure S9C). In non-CAP genomes, *soxYZ* are located adjacent to *fccAB* (sulfide dehydrogenase) forming the *soxYZ-fccAB*

cluster. The gene cluster *soxYZ-fccAB* is conserved in other GSB (Gregersen et al., 2011). However, this *soxYZ* are absent in CAP genomes, leaving only *fccAB* genes (Supplementary Figure S9C). Furthermore, although the non-CAP genome *Prosthecochloris* sp. CIB 2401 (abbreviated PsCIB2401) has the *soxXYZABW* gene cluster, it is located at a different genomic locus. BlastP searching using these two SoxF homologs found hits mostly from Gammaproteobacteria or sulfur-oxidizing bacteria (e.g., *Thiothrix*), consistent with the analysis of the *sox* gene cluster in another GSB *Chlorobium phaeovibrioides* DSM 265 (Gregersen et al., 2011). These results indicate that SOX complex related genes in *Prosthecochloris* genomes may be acquired by horizontal gene transfer (HGT) with subsequent gene loss events.

GSB typically oxidize sulfide and thiosulfate to sulfate, with extracellular sulfur globules as an intermediate, formed by incomplete oxidation of sulfide (Frigaard and Dahl, 2009; Holkenbrink et al., 2011). Oxidizing sulfide can provide GSB electrons for carbon fixation. It was found that the DSR system is required for sulfur globule oxidation in GSB, but is dispensable in environments with sufficiently high sulfide concentrations (Holkenbrink et al., 2011). Extracellular sulfur globules were observed in enrichment culture 2 dominated by SCSIO W1103 (Figure 1B), confirming that genes involved in sulfur metabolism are active in SCSIO W1103. PsC10, which shared the last common ancestor with the CAP clade, has the DSR pathway (Figure 3). Therefore, it is proposed that the last ancestor of *Prosthecochloris* can metabolize sulfur through assimilatory sulfate reduction, dissimilatory sulfate reduction and thiosulfate oxidation. However, genomic loci involved in sulfur metabolism undergo genome rearrangement leading to the evolutionary divergence of different sulfur metabolic capacities between CAP and non-CAP strains to adapt to sulfide-limiting habitats.

### 3.3.5. *cbb*<sub>3</sub>-type cytochrome c oxidases and gas vesicles

Further analysis of modules in KEGG pathways revealed that genes encoding *cbb*<sub>3</sub>-type cytochrome c oxidases (*cbb*<sub>3</sub>-CcoOs) are present in CAP genomes but not in non-CAP genomes (Figure 3; Supplementary Figure S8). Similar to the well-studied *cbb*<sub>3</sub>-CcoOs in *Pseudomonas aeruginosa* PAO1, which contains two independent *ccoNOQP* operons, *cbb*<sub>3</sub>-CcoO operons in CAP genomes have all the *cbb*<sub>3</sub>-CcoO subunit genes *ccoNOQP* and *cbb*<sub>3</sub>-CcoO maturation genes *ccoGHIS* with an additional conserved gene encoding putative sulfite exporter *tauE*. Unlike the *cbb*<sub>3</sub>-CcoOs in strain PAO1, this *cbb*<sub>3</sub>-CcoO operon contains an additional gene encoding a remote homolog of CcoH, and the CcoP protein (138 aa) in GSB is only half the length of that in strain PAO1 (319 aa). Further analysis of domain architectures showed that CcoP<sub>GSB</sub> has only one Cyochrome\_CBB3 domain (PF13442), while CcoP<sub>PAO1</sub> has two Cyochrome\_CBB3 domains (Figure 4B). CcoH is essential for *cbb*<sub>3</sub>-CcoO assembly and interacts with CcoP primarily via interactions with the single transmembrane span of CcoH (Pawlik et al., 2010). Therefore, the GSB-derived *cbb*<sub>3</sub>-CcoO may be different from classical *cbb*<sub>3</sub>-CcoO in assembled enzymes. Similar to the *ccoS* operon, *cbb*<sub>3</sub>-CcoO operons are located in the conserved genomic loci of *Prosthecochloris* and were inserted with variable MGEs including TA systems (Figure 4B), suggesting that MGEs may be involved in the evolution of the *cbb*<sub>3</sub>-CcoO operon. Furthermore, according to the phylogenetic tree and distribution of *cbb*<sub>3</sub>-CcoO operon, it is proposed that *cbb*<sub>3</sub>-CcoO operon was lost in non-CAP genomes due to environments diversification.



Different multiple terminal oxidases in bacterial respiratory chains can help bacteria to adapt to different environmental O<sub>2</sub> concentrations. The *cbb<sub>3</sub>*-CcOs are important for microaerobic respiration, being essential for important nitrogen-fixing endosymbionts and for some human pathogens (Kulajta et al., 2006; Xie et al., 2014). In pathogens, *cbb<sub>3</sub>*-CcOs support aerobic respiration, and are also involved in denitrification of *P. aeruginosa* PAO1 and nitrite reduction of *Neisseria gonorrhoeae* under oxygen-limited conditions (Hopper et al., 2009; Hamada et al., 2014), as a strategy for pathogens to adapt to hypoxia during infection. In *Rhodobacter* group bacteria, photosynthetic bacteria that can grow under both anaerobic and aerobic conditions, *cbb<sub>3</sub>*-CcO can repress photosynthesis gene expression, as a regulator under different oxygen conditions (Kim et al., 2007; Ekici et al., 2012; Wang et al., 2014). In *Bradyrhizobium japonicum*, a nitrogen fixing bacterium, *cbb<sub>3</sub>*-CcO can protect nitrogenase from oxygen inactivation (Page and Guerinot, 1995). Oxygen levels in coral skeletons showed a diurnal rhythm (Kuhl et al., 2008). O<sub>2</sub> concentrations increased in the daytime due to photosynthesis of endolithic algae, while greatly reduced at night. Although GSB are thought to be strictly anaerobic photoautotrophs, the presence of the *cbb<sub>3</sub>*-CcO in CAP genomes may enable CAP strains to detoxify oxygen and adapt to dynamic conditions to regulate photosynthesis and nitrogen fixing processes.

Further analysis of genes that were not included in the KEGG pathways revealed that gene clusters of gas vesicle proteins (*gvp*) were found in CAP genomes, which is consistent with our observation of gas vesicles in cells (Figure 1). Similar to the *gvp* gene cluster in *Serratia* sp. ATCC 39006, the *gvp* gene cluster in CAP genomes contains structural genes *gvpA* and *gvpC*, accessory genes and regulatory genes (Figure 4C). Additionally, this gene cluster contains genes encoding an apolipoprotein and a myocilin-like protein, a component of a membrane-associated protein complex. Comparing the upstream and downstream genes of the *gvp* gene cluster revealed that genome rearrangement may cause the loss of *gvp* gene cluster in non-CAP genomes, with one exception that the *gvp* gene cluster was rearranged to another genomic locus in PsCIB2401 (Figure 4C).

Many bacteria and archaea can produce gas vesicles, providing cells with buoyancy to maintain a suitable depth in the aqueous environment (Pfeifer, 2012; Tashiro et al., 2016). In cyanobacteria, the gas vesicles and the carbohydrates produced by photosynthesis serve as buoyancy and ballast to enable diurnal vertical migrations. This can help cells maintain photosynthesis and avoid floating to the ocean surface, where ultraviolet light may have a strong DNA-damaging effect on cells (Walsby, 1994). Similarly, the green sulfur bacterium *Pelodictyon phaeoclathratiforme* (now recognized as *Chlorobium clathratiforme*) also uses such a strategy when the light intensities are too high (Overmann et al., 1991). Although it is thought that gas vesicles are not used for gas storage, gas vesicles are permeable to oxygen, nitrogen, hydrogen, carbon dioxide, carbon monoxide and methane (Walsby et al., 1992). It was reported that different *Prosthecochloris* strains can form separated layers at different depths of the coral skeleton (Chen et al., 2021b). Additionally, the diurnal changing of CO<sub>2</sub> and O<sub>2</sub> concentration in coral skeletons may alter the positions of optimal micro-niches for *Prosthecochloris*. Considering that flagellar or gliding related genes were not present in CAP genomes, the presence of the *gvp* gene cluster in CAP genomes may enable cells to position inside the coral skeleton.

Moreover, CAP genomes encode 2–5 homologs of CphA (cyanophycin synthetases), while most non-CAP genomes lack CphA (Figure 3). Cyanophycin is a proteinogenic biopolymer that is composed of mainly arginine-aspartate dipeptides and is naturally produced by cyanobacteria. Cyanophycin serves as transient storage for extra nitrogen, carbon and energy (Ziegler et al., 1998), suggesting that CAP strains may store extra nutrients for survival in changing niches.

### 3.4. Differentiation of cell surface polysaccharides and phage susceptibility may drive the evolution and divergence within CAP clade genomes

We observed different cell morphologies between SCSIO W1101 and SCSIO W1103, although we have shown that CAP specific features are conserved within CAP genomes. Therefore, we questioned what is the difference between these highly similar genomes. Pangenome analysis showed that these five CAP genomes have 2033 conserved genes, and there were more specific genes in PsN2 or SCSIO W1101 than in *Candidatus Prosthecochloris* sp. N1 (abbreviated as PsN1), PmV1 or SCSIO W1103 (Figures 5A,B), consistent with the pairwise ANI among these genomes (Figure 2B). GO enrichment analysis of 429 specific genes of SCSIO W1101 showed that the functions of these genes are related to processes of DNA binding, transposase activity, nucleotide metabolism and transporters (Figure 5C; Supplementary Figure S10). Comparing these genomes using each genome as the reference, these variable genomic loci showed a mosaic pattern and were conserved in only one or a few genomes, and most of these were derived from MGEs, such as RM systems, CRISPR–Cas systems and prophages (Figure 5D). The SCSIO W1101 genome contains a P22-like prophage that is absent in other genomes and specifically contains genes encoding an energy-coupling factor transport system consisting of conserved modules (EcfA: ATP-binding protein; EcfT: permease protein; HtsT: substrate-specific component; Figure 5D), which is involved in the uptake of vitamins in prokaryotes (Rodionov et al., 2009). Additionally, polysaccharide synthesis gene clusters are the major specific genes in SCSIO W1101, which was predicted as HGT from other bacteria by Alien Hunter (Vernikos and Parkhill, 2006). Some of the genes in the polysaccharide synthesis gene clusters were also found in other CAP genomes, suggesting that these partially conserved polysaccharide synthesis gene clusters may undergo rapid evolution. These results suggest that these CAP strains may have variable cell surface structures, consistent with our observed different cell morphologies.

Further analysis revealed a genomic hotspot in CAP genomes inserted by variable phage defense systems. This genomic locus is located between conserved genes encoding acetyltransferase and erythromycin 3'-O-methyltransferase (Figure 5E). Compressive annotation of these genes found that most of these genes encode MGEs including TA systems and nucleases. Among them, the gene in SCSIO W1102 encodes an antiviral STAND (Asv4)-like protein, a recently identified phage defense system that belongs to nucleotide-binding oligomerization domain-like receptors (Gao et al., 2022). Similarly, the gene in SCSIO W1103 encodes a short



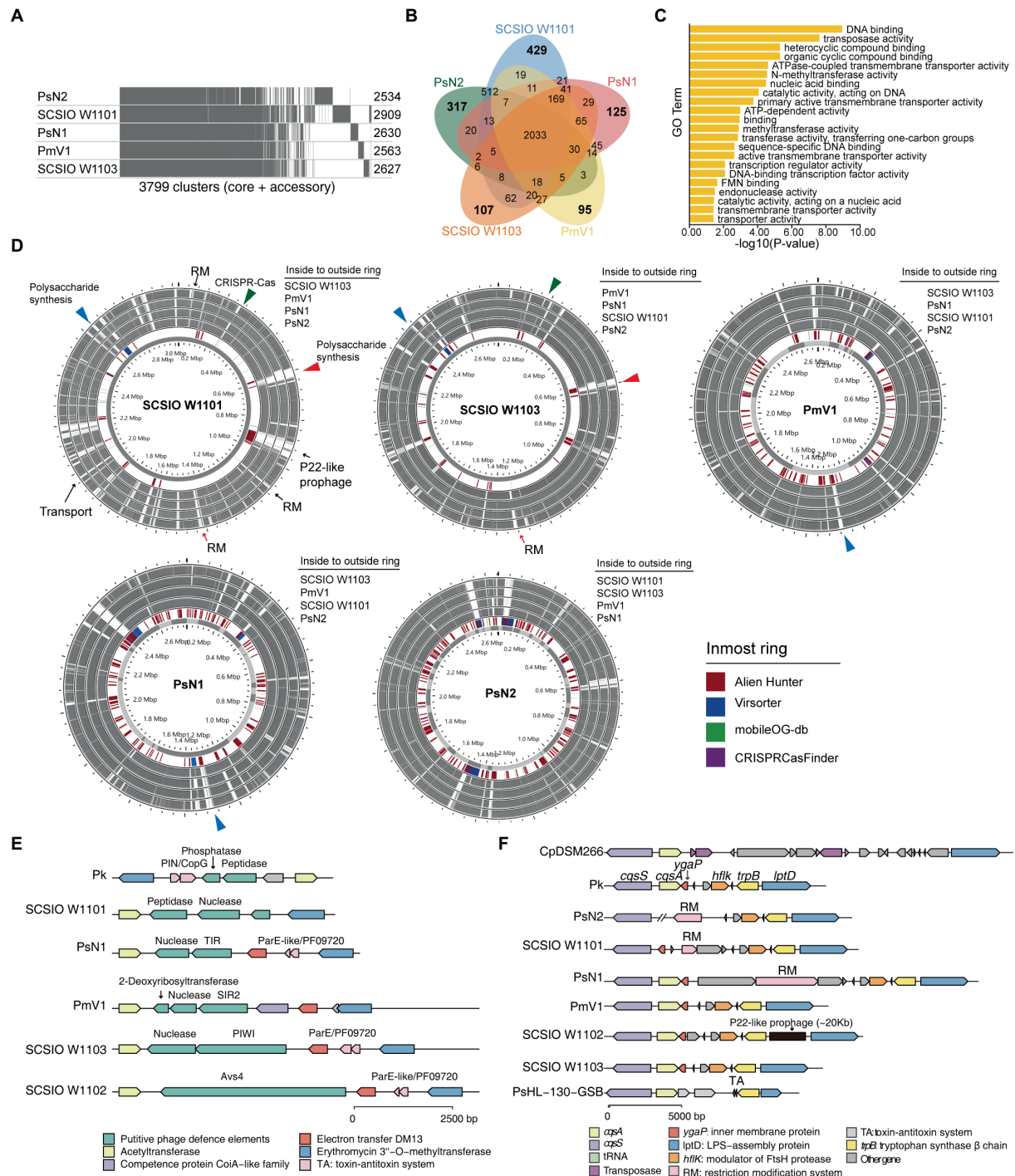


FIGURE 5

Polysaccharide synthesis gene cluster and phage defense systems drive the divergence and evolution within coral-associated *Prosthecochloris* (CAP) genomes. (A) Pangenome analysis of five CAP genomes. Considering the genome quality of MAGs, *Candidatus Prosthecochloris korallensis* and *Candidatus Prosthecochloris* sp. A305 and *Candidatus Prosthecochloris* sp. SCSIO W1102 were not included. Numbers at each line indicate the CDS numbers of each genome. A total of 3,799 gene clusters were found. (B) Venn diagrams of shared and specific genes among five CAP genomes. (C) Enrichment of *Candidatus Prosthecochloris* sp. SCSIO W1101 specific genes based on GO annotation of molecular functions (MF). (D) Genome alignment of these five genomes. Each genome was used as the reference, and MGE related regions predicted by different tools are indicated in the inmost ring. The same colored arrows or triangles indicate aligned variable genomic regions in different genomes. (E) Different phage defense systems are inserted in the conserved genomic regions in different genomes. (F) The absence of *cqsA* in the SCSIO W1101 genome may be caused by the integration or excision of MGEs.

prokaryotic Argonaute system (containing a PIWI domain) with a nuclease as the effector, which was also a phage defense system identified recently (Koopal et al., 2022). Furthermore, genes

encoding the SIR2 or TIR domain were identified in PmV1 and PsN1. SIR2 and TIR domains were demonstrated as part of phage defense systems (Ofir et al., 2021; Garb et al., 2022; Millman et al.,

2022), which can both generate the signal molecule cyclic ADP-ribose analog once infected by phages, activating their associated effectors and leading to an abortive infection (Abi). Therefore, the TIR associated nuclease and SIR2 associated 2-deoxyribosyltransferase and nuclease may be putative effectors of phage defense systems in PmV1 and PsN1. Furthermore, the genes encoding putative phosphatase and peptidase were identified in SCSIO W1101 and *Candidatus Prosthecochloris korallensis* (abbreviated as Pk). Variable phage defense systems were previously found to be inserted in the same genomic locus among highly similar genomes (Rousset et al., 2022). Therefore, phosphatase and peptidase in SCSIO W1101 and Pk may represent novel phage defense systems. These results suggest that the interaction of the *Prosthecochloris* population with phages occurs in the coral skeleton, which also drives the evolution of the *Prosthecochloris* population. These results also indicate that rapid evolutionary turnover of phage defense systems by MGEs may endow anti-phage activity against different phages among clonal CAP strains, similar to a previous finding that MGEs drive *Vibrio* resistance to phages in the wild (Hussain et al., 2021).

In addition to polysaccharide synthesis gene clusters and phage defense systems, quorum sensing (QS) system may be another potential factor that can drive the evolution within CAP genomes. QS system is a process of bacterial cell- to-cell communication based on small signaling molecules to coordinate social behavior including bioluminescence, virulence factor production, CRISPR-Cas system activity and biofilm formation (Pawlik et al., 2010; Hoyland-Kroghsbo et al., 2017; Mukherjee and Bassler, 2019). Acyl-homoserine lactone, AI-2, CAI-1 and diffusible signal factor (DSF) based QS systems in Gram-negative bacteria have been extensively studied (Papenfort and Bassler, 2016). Only the CAI-1 QS system was found in GSB genomes (Figures 3, 5F). The *cqsA/cqsS* gene pair is always located adjacent to each other. CqsA is the CAI-1 autoinducer synthase, and CqsS is the CAI-1 autoinducer sensor kinase/phosphatase. Alignment of all the genomes revealed that the *cqsA/cqsS* gene pair was located in a conserved genomic locus, while the *cqsA* gene was lost in PsN2 and SCSIO W1101. We further confirmed that the loss of *cqsA* in SCSIO W1101 is real and that the loss of *cqsA* in PsN2 is caused by incomplete genome assembly (Figure 5F). Moreover, genes encoding transposases, tRNA, RM systems, TA systems and prophages were inserted in this genomic locus, indicating this genomic locus is a hotspot for MGE integration and recombination, which may also lead to the loss of *cqsA* in SCSIO W1101. Synthesis of autoinducers is an energy-consuming process, and loss of *cqsA* and maintenance of *cqsS* can enable bacteria to sense signals in a population without consuming energy to produce signals. Signaling-deficient mutant strains were prevalent in the QS system harboring bacteria (Keller and Surette, 2006), which is an evolutionary consequence in clonal bacterial populations. Taken together, differentiated QS systems may also drive the strain-level evolution of CAP strains.

## 4. Conclusion

In this study, complete circular genomes in the CAP clade from *G. fascicularis* were obtained. Comparative genomic analysis revealed the difference between CAP and non-CAP genomes, including genes

involved the specialized metabolic capacities (CO oxidation, CO<sub>2</sub> hydration and sulfur oxidation), gas vesicles (vertical migration in coral skeleton), and *cbb<sub>3</sub>*-type cytochrome *c* oxidases (oxygen tolerance and regulation). Within the CAP genomes, variable polysaccharide synthesis gene clusters and phage defense systems may endow bacteria with differential cell surface structures and phage susceptibility. Furthermore, MGEs or evidence of MGE-related HGT were found in most of the genomic loci containing the above genes, suggesting that MGEs play an important role in the evolutionary diversification between CAP and non-CAP strains and within CAP clade strains. These findings are similar to a previous report that the endolithic *Ruegeria* population may adapt to skeletons through sulfur oxidation and swimming motility (Luo et al., 2021), suggesting that the capacities of sulfur oxidation and motility may be important for bacterial adaptation in coral skeletons. Nonetheless, how these different capacities are involved in the symbiotic relationship with corals still needs further study.

## Data availability statement

The datasets presented in this study can be found in online repositories. The names of the repository/repositories and accession number(s) can be found at: <https://www.ncbi.nlm.nih.gov/>, PRJNA668462.

## Ethics statement

The animal study was reviewed and approved by the Management Office of the Sanya National Coral Reef Nature Reserve (China) and the Department of Ocean and Fisheries of Hainan Province.

## Author contributions

KT and XW contributed to conception and design of the study. ZN, KT, and WW collected and analyzed the data. PW and YG contributed to the statistical analysis. YW provided the samples. KT wrote the first draft of the manuscript. XW, S-JK, and JY revised the manuscript. All authors contributed approved the submitted version.

## Funding

This work was supported by the National Science Foundation of China (91951203 and 42188102), National Key R&D Program of China (2022YFC3103600), Foundation Incubation Fund of Chinese Academy of Sciences (JCPYJJ-22025), Guangdong Basic and Applied Basic Research Foundation (2022A1515010702), the Open Project of State Key Laboratory of Marine Resource Utilization in South China Sea of Hainan University (MRUKF2021004), Science & Technology Fundamental Resources Investigation Program (2022FY100600), Local Innovative and Research Teams Project of Guangdong Pearl River Talents Program (2019BT02Y262), Guangdong Major Project of Basic and Applied Basic Research (2019B030302004) and the Youth Innovation Promotion Association CAS (2021345 to PW).

## Conflict of interest

The authors declare that the research was conducted in the absence of any commercial or financial relationships that could be construed as a potential conflict of interest.

## Publisher's note

All claims expressed in this article are solely those of the authors and do not necessarily represent those of their affiliated

organizations, or those of the publisher, the editors and the reviewers. Any product that may be evaluated in this article, or claim that may be made by its manufacturer, is not guaranteed or endorsed by the publisher.

## Supplementary material

The Supplementary material for this article can be found online at: <https://www.frontiersin.org/articles/10.3389/fmicb.2023.1138751/full#supplementary-material>

## References

- Agostini, S., Suzuki, Y., Higuchi, T., Casareto, B. E., Yoshinaga, K., Nakano, Y., et al. (2012). Biological and chemical characteristics of the coral gastric cavity. *Coral Reefs* 31, 147–156. doi: 10.1007/s00338-011-0831-6
- Alneberg, J., Bjarnason, B. S., De Bruijn, I., Schirmer, M., Quick, J., Ijaz, U. Z., et al. (2014). Binning metagenomic contigs by coverage and composition. *Nat. Methods* 11, 1144–1146. doi: 10.1038/nmeth.3103
- Anil Kumar, P., Naga Radha Srinivas, T., Sasikala, C., Venkata Ramana, C., Suling, J., and Imhoff, J. (2009). *Prosthecochloris indica* sp. nov., a novel green sulfur bacterium from a marine aquaculture pond, Kakinada. *India. J. Gen. Appl. Microbiol.* 55, 163–169. doi: 10.2323/jgam.55.163
- Apprill, A., McNally, S., Parsons, R., and Weber, L. (2015). Minor revision to V4 region SSU rRNA 806R gene primer greatly increases detection of SAR11 bacterioplankton. *Aquat. Microb. Ecol.* 75, 129–137. doi: 10.3354/ame01753
- Aramaki, T., Blanc-Mathieu, R., Endo, H., Ohkubo, K., Kanehisa, M., Goto, S., et al. (2020). Kofam KOALA: KEGG Ortholog assignment based on profile HMM and adaptive score threshold. *Bioinformatics* 36, 2251–2252. doi: 10.1093/bioinformatics/btz859
- Athen, S. R., Dubey, S., and Kyndt, J. A. (2021). The eastern Nebraska salt marsh microbiome is well adapted to an alkaline and extreme saline environment. *Life* 11:446. doi: 10.3390/life11050446
- Bankevich, A., Nurk, S., Antipov, D., Gurevich, A. A., Dvorkin, M., Kulikov, A. S., et al. (2012). SPAdes: a new genome assembly algorithm and its applications to single-cell sequencing. *J. Comput. Biol.* 19, 455–477. doi: 10.1089/cmb.2012.0021
- Bardou, P., Mariette, J., Escudie, F., Djemiel, C., and Klopp, C. (2014). Jvarkit: an interactive Venn diagram viewer. *BMC Bioinformatics* 15:293. doi: 10.1186/1471-2105-15-293
- Beatty, J. T., Overmann, J., Lince, M. T., Manske, A. K., Lang, A. S., Blankenship, R. E., et al. (2005). An obligately photosynthetic bacterial anaerobe from a deep-sea hydrothermal vent. *Proc. Natl. Acad. Sci. U. S. A.* 102, 9306–9310. doi: 10.1073/pnas.0503674102
- Borrego, C. M., and Garciagil, L. J. (1995). Rearrangement of light-harvesting bacteriochlorophyll homologs as a response of green sulfur bacteria to low-light intensities. *Photosynth. Res.* 45, 21–30. doi: 10.1007/Bf00032232
- Bourne, D. G., Morrow, K. M., and Webster, N. S. (2016). Insights into the coral microbiome: underpinning the health and resilience of reef ecosystems. *Annu. Rev. Microbiol.* 70, 317–340. doi: 10.1146/annurev-micro-102215-095440
- Brown, C. L., Mullet, J., Hindi, F., Stoll, J. E., Gupta, S., Choi, M., et al. (2022). Mobile OG-db: a manually curated database of protein families mediating the life cycle of bacterial mobile genetic elements. *Appl. Environ. Microbiol.* 88:e0099122. doi: 10.1128/aem.00991-22
- Bryantseva, I. A., Tarasov, A. L., Kostrikina, N. A., Gaisin, V. A., Grouzdev, D. S., and Gorlenko, V. M. (2019). *Prosthecochloris marina* sp. nov., a new green sulfur bacterium from the coastal zone of the South China Sea. *Arch. Microbiol.* 201, 1399–1404. doi: 10.1007/s00203-019-01707-y
- Brnyldsrud, O., Bohlin, J., Scheffer, L., and Eldholm, V. (2016). Rapid scoring of genes in microbial pan-genome-wide association studies with Scoary. *Genome Biol.* 17:238. doi: 10.1186/s13059-016-1108-8
- Cai, L., Zhou, G., Tian, R.-M., Tong, H., Zhang, W., Sun, J., et al. (2017). Metagenomic analysis reveals a green sulfur bacterium as a potential coral symbiont. *Sci. Rep.* 7:9320. doi: 10.1038/s41598-017-09032-4
- Callahan, B. J., McMurdie, P. J., Rosen, M. J., Han, A. W., Johnson, A. J., and Holmes, S. P. (2016). DADA2: high-resolution sample inference from Illumina amplicon data. *Nat. Methods* 13, 581–583. doi: 10.1038/nmeth.3869
- Capasso, C., and Supuran, C. T. (2015). An overview of the alpha-, beta- and gamma-carbonic anhydrases from bacteria: can bacterial carbonic anhydrases shed new light on evolution of bacteria? *J. Enzyme Inhib. Med. Chem.* 30, 325–332. doi: 10.3109/14756366.2014.910202
- Cardenas, A., Raina, J. B., Pogoreutz, C., Radecker, N., Bougoure, J., Guagliardo, P., et al. (2022). Greater functional diversity and redundancy of coral endolithic microbiomes align with lower coral bleaching susceptibility. *ISME J.* 16, 2406–2420. doi: 10.1038/s41396-022-01283-y
- Chaumeil, P. A., Mussig, A. J., Hugenholtz, P., and Parks, D. H. (2022). GTDB-Tk v2: memory friendly classification with the genome taxonomy database. *Bioinformatics* 38, 5315–5316. doi: 10.1093/bioinformatics/btac672
- Chen, C., Chen, H., Zhang, Y., Thomas, H. R., Frank, M. H., He, Y., et al. (2020). TBtools: An integrative toolkit developed for interactive analyses of big biological data. *Mol. Plant* 13, 1194–1202. doi: 10.1016/j.molp.2020.06.009
- Chen, Y. H., Chiang, P. W., Rogozin, D. Y., Degermendzh, A. G., Chiu, H. H., and Tang, S. L. (2021a). Salvaging high-quality genomes of microbial species from a meromictic lake using a hybrid sequencing approach. *Commun. Biol.* 4:996. doi: 10.1038/s42003-021-02510-6
- Chen, Y. H., Yang, S. H., Tandon, K., Lu, C. Y., Chen, H. J., Shih, C. J., et al. (2021b). Potential syntrophic relationship between coral-associated *Prosthecochloris* and its companion sulfate-reducing bacterium unveiled by genomic analysis. *Microb. Genom.* 7:000574. doi: 10.1099/mgen.0.000574
- Chong, J., Liu, P., Zhou, G., and Xia, J. (2020). Using microbiome analyst for comprehensive statistical, functional, and meta-analysis of microbiome data. *Nat. Protoc.* 15, 799–821. doi: 10.1038/s41596-019-0264-1
- Conrad, R., Seiler, W., Bunse, G., and Giehl, H. (1982). Carbon monoxide in seawater (Atlantic Ocean). *J. Geophys. Res.* 87:8839. doi: 10.1029/JC087iC11p08839
- Couvin, D., Bernheim, A., Toffano-Nioche, C., Touchon, M., Michalik, J., Neron, B., et al. (2018). CRISPRCasFinder, an update of CRISPRFinder, includes a portable version, enhanced performance and integrates search for Cas proteins. *Nucleic Acids Res.* 46, W246–W251. doi: 10.1093/nar/gky425
- Croft, M. T., Lawrence, A. D., Raux-Deery, E., Warren, M. J., and Smith, A. G. (2005). Algae acquire vitamin B12 through a symbiotic relationship with bacteria. *Nature* 438, 90–93. doi: 10.1038/nature04056
- Darling, A. C., Mau, B., Blattner, F. R., and Perna, N. T. (2004). Mauve: multiple alignment of conserved genomic sequence with rearrangements. *Genome Res.* 14, 1394–1403. doi: 10.1101/gr.2289704
- Darling, A. E., Mau, B., and Perna, N. T. (2010). Progressive mauve: multiple genome alignment with gene gain, loss and rearrangement. *PLoS One* 5:e11147. doi: 10.1371/journal.pone.0011147
- Dobrynski, K. P., Boller, A. J., and Scott, K. M. (2010). Expression and function of four carbonic anhydrase homologs in the deep-sea chemolithoautotroph *Thiomicrospira crunogena*. *Appl. Environ. Microbiol.* 76, 3561–3567. doi: 10.1128/AEM.00064-10
- Ekici, S., Pawlik, G., Lohmeyer, E., Koch, H. G., and Daldal, F. (2012). Biogenesis of cbb 3-type cytochrome c oxidase in *Rhodobacter capsulatus*. *Biochim. Biophys. Acta* 1817, 898–910. doi: 10.1016/j.bbabo.2011.10.011
- Frigaard, N. U., and Dahl, C. (2009). Sulfur metabolism in phototrophic sulfur bacteria. *Adv. Microb. Physiol.* 54, 103–200. doi: 10.1016/S0065-2911(08)00002-7
- Gai, C. S., Lu, J., Brigham, C. J., Bernardi, A. C., and Sinskey, A. J. (2014). Insights into bacterial CO<sub>2</sub> metabolism revealed by the characterization of four carbonic anhydrases in *Ralstonia eutropha* H16. *AMB Express* 4:2. doi: 10.1186/2191-0855-4-2
- Gao, L. A., Wilkinson, M. E., Strecker, J., Makarova, K. S., Macrae, R. K., Koonin, E. V., et al. (2022). Prokaryotic innate immunity through pattern recognition of conserved viral proteins. *Science* 377:eabm4096. doi: 10.1126/science.abm4096
- Garb, J., Lopatina, A., Bernheim, A., Zaremba, M., Siksnys, V., Melamed, S., et al. (2022). Multiple phage resistance systems inhibit infection via SIR2-dependent NAD<sup>+</sup> depletion. *Nat. Microbiol.* 7, 1849–1856. doi: 10.1038/s41564-022-01207-8
- Gorlenko, V. M. (1970). A new phototrophic green Sulphur bacterium. *Prosthecochloris aestuarii* nov. gen. Nov. spec. *Z. Allg. Mikrobiol.* 10, 147–149. doi: 10.1002/jobm.19700100207



- Gorlenko, V. M. (2015). "Prosthecochloris," in *Bergey's Manual of Systematics of Archaea and Bacteria*, eds. M. E. Trujillo, S. Dedysh, P. De Vos, B. Hedlund, P. Kämpfer, F. A. Rainey and W. B. Whitman (John Wiley & Sons and Bergey's Manual Trust), 1–6.
- Gregersen, L. H., Bryant, D. A., and Frigaard, N. U. (2011). Mechanisms and evolution of oxidative sulfur metabolism in green sulfur bacteria. *Front. Microbiol.* 2:116. doi: 10.3389/fmicb.2011.00116
- Grein, F., Ramos, A. R., Venceslau, S. S., and Pereira, I. A. (2013). Unifying concepts in anaerobic respiration: insights from dissimilatory sulfur metabolism. *Biochim. Biophys. Acta* 1827, 145–160. doi: 10.1016/j.bbabo.2012.09.001
- Grouzdev, D. S., Gaisin, V. A., Krutkina, M. S., Bryantseva, I. A., Lunina, O. N., Savvichev, A. S., et al. (2018). Genome sequence of *Prosthecochloris* sp. strain ZM and *Prosthecochloris* sp. strain ZM-2, isolated from an Arctic meromictic lake. *Microbiol. Resour. Announc.* 7, 7:e01415-18. doi: 10.1128/MRA.01415-18
- Grouzdev, D., Gaisin, V., Lunina, O., Krutkina, M., Krasnova, E., Voronov, D., et al. (2022). Microbial communities of stratified aquatic ecosystems of Kandalaksha Bay (White Sea) shed light on the evolutionary history of green and brown morphotypes of Chlorobiota. *FEMS Microbiol. Ecol.* 98:103. doi: 10.1093/femsec/fiac103
- Guo, J., Bolduc, B., Zayed, A. A., Varsani, A., Dominguez-Huerta, G., Delmont, T. O., et al. (2021). Vir sorter 2: a multi-classifier, expert-guided approach to detect diverse DNA and RNA viruses. *Microbiome* 9:37. doi: 10.1186/s40168-020-00990-y
- Hamada, M., Toyofuku, M., Miyano, T., and Nomura, N. (2014). Cbb 3-type cytochrome c oxidases, aerobic respiratory enzymes, impact the anaerobic life of *Pseudomonas aeruginosa* PAO1. *J. Bacteriol.* 196, 3881–3889. doi: 10.1128/JB.01978-14
- Holkenbrink, C., Barbas, S. O., Møllerup, A., Otaki, H., and Frigaard, N. U. (2011). Sulfur globule oxidation in green sulfur bacteria is dependent on the dissimilatory sulfite reductase system. *Microbiol. SGM* 157, 1229–1239. doi: 10.1099/mic.0.044669-0
- Hopper, A., Tovell, N., and Cole, J. (2009). A physiologically significant role in nitrite reduction of the Cco P subunit of the cytochrome oxidase cbb 3 from *Neisseria gonorrhoeae*. *FEMS Microbiol. Lett.* 301, 232–240. doi: 10.1111/j.1574-6968.2009.01824.x
- Hou, J., Xu, T., Su, D., Wu, Y., Cheng, L., Wang, J., et al. (2018). RNA-seq reveals extensive transcriptional response to heat stress in the stony coral *Galaxea fascicularis*. *Front. Genet.* 9:37. doi: 10.3389/fgene.2018.00037
- Hoyland-Kroghsbo, N. M., Paczkowski, J., Mukherjee, S., Broniewski, J., Westra, E., Bondy-Denomy, J., et al. (2017). Quorum sensing controls the *Pseudomonas aeruginosa* CRISPR-Cas adaptive immune system. *Proc. Natl. Acad. Sci. U. S. A.* 114, 131–135. doi: 10.1073/pnas.1617415113
- Huang, Y. T., Liu, P. Y., and Shih, P. W. (2021). Homopolish: a method for the removal of systematic errors in nanopore sequencing by homologous polishing. *Genome Biol.* 22:95. doi: 10.1186/s13059-021-02282-6
- Hussain, F. A., Dubert, J., Elsherbini, J., Murphy, M., Vaninsberghe, D., Arevalo, P., et al. (2021). Rapid evolutionary turnover of mobile genetic elements drives bacterial resistance to phages. *Science* 374, 488–492. doi: 10.1126/science.abb1083
- Huster, M. S., and Smith, K. M. (1990). Biosynthetic studies of substituent homology in bacteriochlorophylls c and d. *Biochemistry (Mosc)* 29, 4348–4355. doi: 10.1021/bi00470a013
- Imhoff, J. F. (2003). Phylogenetic taxonomy of the family Chlorobiaceae on the basis of 16S rRNA and fmo (Fenna-Matthews-Olson protein) gene sequences. *Int. J. Syst. Evol. Microbiol.* 53, 941–951. doi: 10.1099/ijs.0.02403-0
- Imhoff, J. F. (2014). "Biology of Green Sulfur Bacteria" in *eLS*, eds. M. Maccarrone, A. Clarke, Y. Zheng, H. Kehrer-Sawatzki, D. N. Cooper, G. Pettis, M. Victoria Niklison Chirou, D. J. Perkel, A. M. Hetherington, W. F. Bynum and J. M. Valpuesta (Chichester: John Wiley & Sons, Ltd)
- Ivanovsky, R. N., Keppen, I., Lebedeva, N. V., and Gruzdev, D. S. (2020). Carbonic anhydrase in anoxygenic phototrophic bacteria. *Microbiology* 89, 266–272. doi: 10.1134/S0026261720020058
- Jain, C., Rodriguez, R. L., Phillippy, A. M., Konstantinidis, K. T., and Aluru, S. (2018). High throughput ANI analysis of 90K prokaryotic genomes reveals clear species boundaries. *Nat. Commun.* 9:5114. doi: 10.1038/s41467-018-07641-9
- Jones, P., Binns, D., Chang, H. Y., Fraser, M., Li, W., Mcanulla, C., et al. (2014). Interpro scan 5: genome-scale protein function classification. *Bioinformatics* 30, 1236–1240. doi: 10.1093/bioinformatics/btu031
- Kanehisa, M., Sato, Y., and Morishima, K. (2016). Blast KOALA and ghost KOALA: KEGG tools for functional characterization of genome and metagenome sequences. *J. Mol. Biol.* 428, 726–731. doi: 10.1016/j.jmb.2015.11.006
- Kang, D. D., Li, F., Kirton, E., Thomas, A., Egan, R., An, H., et al. (2019). Meta BAT 2: an adaptive binning algorithm for robust and efficient genome reconstruction from metagenome assemblies. *PeerJ* 7:e7359. doi: 10.7717/peerj.7359
- Kaplan, A., and Reinhold, L. (1999). CO<sub>2</sub> concentrating mechanisms in photosynthetic microorganisms. *Annu. Rev. Plant Physiol. Plant Mol. Biol.* 50, 539–570. doi: 10.1146/annurev.arplant.50.1.539
- Keller, L., and Surette, M. G. (2006). Communication in bacteria: an ecological and evolutionary perspective. *Nat. Rev. Microbiol.* 4, 249–258. doi: 10.1038/nrmicro1383
- Kim, Y. J., Ko, I. J., Lee, J. M., Kang, H. Y., Kim, Y. M., Kaplan, S., et al. (2007). Dominant role of the cbb3 oxidase in regulation of photosynthesis gene expression through the PrrBA system in *Rhodobacter sphaeroides* 2.4.1. *J. Bacteriol.* 189, 5617–5625. doi: 10.1128/JB.00443-07
- Koopal, B., Potocnik, A., Mutte, S. K., Aparicio-Maldonado, C., Lindhoud, S., Vervoort, J. J. M., et al. (2022). Short prokaryotic Argonaute systems trigger cell death upon detection of invading DNA. *Cells* 185:e1419, 1471–1486.e19. doi: 10.1016/j.cell.2022.03.012
- Kuhl, M., Holst, G., Larkum, A. W. D., and Ralph, P. J. (2008). Imaging of oxygen dynamics within the endolithic algal community of the massive coral *Porites lobata*. *J. Phycol.* 44, 541–550. doi: 10.1111/j.1529-8817.2008.00506.x
- Kulajta, C., Thumfart, J. O., Haid, S., Daldal, F., and Koch, H. G. (2006). Multi-step assembly pathway of the cbb3-type cytochrome c oxidase complex. *J. Mol. Biol.* 355, 989–1004. doi: 10.1016/j.jmb.2005.11.039
- Kumar, S., Stecher, G., and Tamura, K. (2016). MEGA7: molecular evolutionary genetics analysis version 7.0 for bigger datasets. *Mol. Biol. Evol.* 33, 1870–1874. doi: 10.1093/molbev/msw054
- Kyndt, J. A., Van Beeumen, J. J., and Meyer, T. E. (2020). Simultaneous genome sequencing of *Prosthecochloris ethylica* and *Desulfuromonas acetoxidans* within a syntrophic mixture reveals unique pili and protein interactions. *Microorganisms* 8:1939. doi: 10.3390/microorganisms8121939
- Li, J., Chen, Q., Long, L. J., Dong, J. D., Yang, J., and Zhang, S. (2014). Bacterial dynamics within the mucus, tissue and skeleton of the coral *Porites lutea* during different seasons. *Sci. Rep.* 4:7320. doi: 10.1038/srep07320
- Luo, D., Wang, X., Feng, X., Tian, M., Wang, S., Tang, S. L., et al. (2021). Population differentiation of Rhodobacteraceae along with coral compartments. *ISME J.* 15, 3286–3302. doi: 10.1038/s41396-021-01009-6
- Mann, S., and Chen, Y.-P. P. (2010). Bacterial genomic G+C composition-eliciting environmental adaptation. *Genomics* 95, 7–15. doi: 10.1016/j.ygeno.2009.09.002
- Marcelino, V. R., Van Oppen, M. J., and Verbruggen, H. (2018). Highly structured prokaryote communities exist within the skeleton of coral colonies. *ISME J.* 12, 300–303. doi: 10.1038/ismej.2017.164
- Marcus, E. A., Moshfegh, A. P., Sachs, G., and Scott, D. R. (2005). The periplasmic alpha-carbonic anhydrase activity of *Helicobacter pylori* is essential for acid acclimation. *J. Bacteriol.* 187, 729–738. doi: 10.1128/Jb.187.2.729-738.2005
- Maresca, J. A., Graham, J. E., Wu, M., Eisen, J. A., and Bryant, D. A. (2007). Identification of a fourth family of lycopene cyclases in photosynthetic bacteria. *Proc. Natl. Acad. Sci. U. S. A.* 104, 11784–11789. doi: 10.1073/pnas.0702984104
- Maresca, J. A., Romberger, S. P., and Bryant, D. A. (2008). Isorenieratene biosynthesis in green sulfur bacteria requires the cooperative actions of two carotenoid cyclases. *J. Bacteriol.* 190, 6384–6391. doi: 10.1128/JB.00758-08
- Millman, A., Melamed, S., Leavitt, A., Doron, S., Bernheim, A., Hor, J., et al. (2022). An expanded arsenal of immune systems that protect bacteria from phages. *Cell Host Microbe* 30:e1555, 1556–1569.e5. doi: 10.1016/j.chom.2022.09.017
- Mistry, J., Chuguransky, S., Williams, L., Qureshi, M., Salazar, G. A., Sonnhammer, E. L. L., et al. (2021). Pfam: the protein families database in 2021. *Nucleic Acids Res.* 49, D412–D419. doi: 10.1093/nar/gkaa913
- Morris, L. A., Voolstra, C. R., Quigley, K. M., Bourne, D. G., and Bay, L. K. (2019). Nutrient availability and metabolism affect the stability of coral–Symbiodiniaceae symbioses. *Trends Microbiol.* 27, 678–689. doi: 10.1016/j.tim.2019.03.004
- Mukherjee, S., and Bassler, B. L. (2019). Bacterial quorum sensing in complex and dynamically changing environments. *Nat. Rev. Microbiol.* 17, 371–382. doi: 10.1038/s41579-019-0186-5
- Nabhan, S., Bunk, B., Sproer, C., Liu, Z., Bryant, D. A., and Overmann, J. (2016). Genome sequence of *Prosthecochloris* sp. strain CIB 2401 of the phylum Chlorobi. *Genome Announc.* 4, e01222–e01216. doi: 10.1128/genomeA.01222-16
- Ofir, G., Herbst, E., Baroz, M., Cohen, D., Millman, A., Doron, S., et al. (2021). Antiviral activity of bacterial TIR domains via immune signalling molecules. *Nature* 600, 116–120. doi: 10.1038/s41586-021-04098-7
- Oren, A., and Garrity, G. M. (2021). Valid publication of the names of forty-two phyla of prokaryotes. *Int. J. Syst. Evol. Microbiol.* 71:5056. doi: 10.1099/ijsem.0.005056
- Overmann, J., Lehmann, S., and Pfennig, N. (1991). Gas vesicle formation and buoyancy regulation in *Pelodictyon phaeoclathratiforme* (green sulfur bacteria). *Arch. Microbiol.* 157, 29–37. doi: 10.1007/BF00245331
- Page, A. J., Cummins, C. A., Hunt, M., Wong, V. K., Reuter, S., Holden, M. T., et al. (2015). Roary: rapid large-scale prokaryote pan genome analysis. *Bioinformatics* 31, 3691–3693. doi: 10.1093/bioinformatics/btv421
- Page, K. M., and Gueriot, M. L. (1995). Oxygen control of the Bradyrhizobium japonicum hemA gene. *J. Bacteriol.* 177, 3979–3984. doi: 10.1128/jb.177.14.3979-3984.1995
- Palu, M., Basile, A., Zampieri, G., Treu, L., Rossi, A., Morlino, M. S., et al. (2022). KEMET-A python tool for KEGG module evaluation and microbial genome annotation expansion. *Comput. Struct. Biotechnol. J.* 20, 1481–1486. doi: 10.1016/j.csbj.2022.03.015
- Papenfert, K., and Bassler, B. L. (2016). Quorum sensing signal-response systems in gram-negative bacteria. *Nat. Rev. Microbiol.* 14, 576–588. doi: 10.1038/nrmicro.2016.89
- Parada, A. E., Needham, D. M., and Fuhrman, J. A. (2016). Every base matters: assessing small subunit rRNA primers for marine microbiomes with mock communities, time series and global field samples. *Environ. Microbiol.* 18, 1403–1414. doi: 10.1111/1462-2920.13023
- Parks, D. H., Imelfort, M., Skennerton, C. T., Hugenholtz, P., and Tyson, G. W. (2015). CheckM: assessing the quality of microbial genomes recovered from

- isolates, single cells, and metagenomes. *Genome Res.* 25, 1043–1055. doi: 10.1101/gr.186072.114
- Pawlik, G., Kulajta, C., Sachelar, I., Schroder, S., Waidner, B., Hellwig, P., et al. (2010). The putative assembly factor CcoH is stably associated with the cbb3-type cytochrome oxidase. *J. Bacteriol.* 192, 6378–6389. doi: 10.1128/JB.00988-10
- Peixoto, R. S., Sweet, M., Villela, H. D. M., Cardoso, P., Thomas, T., Voolstra, C. R., et al. (2021). Coral probiotics: premise, promise, prospects. *Annu. Rev. Anim. Biosci.* 9, 265–288. doi: 10.1146/annurev-animal-090120-115444
- Pernice, M., Raina, J. B., Radecker, N., Cardenas, A., Pogoreutz, C., and Voolstra, C. R. (2020). Down to the bone: the role of overlooked endolithic microbiomes in reef coral health. *ISME J.* 14, 325–334. doi: 10.1038/s41396-019-0548-z
- Pfeifer, F. (2012). Distribution, formation and regulation of gas vesicles. *Nat. Rev. Microbiol.* 10, 705–715. doi: 10.1038/nrmicro2834
- Price, M. N., Dehal, P. S., and Arkin, A. P. (2009). FastTree: computing large minimum evolution trees with profiles instead of a distance matrix. *Mol. Biol. Evol.* 26, 1641–1650. doi: 10.1093/molbev/msp077
- Ricci, F., Rossetto Marcelino, V., Blackall, L. L., Kuhl, M., Medina, M., and Verbruggen, H. (2019). Beneath the surface: community assembly and functions of the coral skeleton microbiome. *Microbiome* 7:159. doi: 10.1186/s40168-019-0762-y
- Robbins, S. J., Singleton, C. M., Chan, C. X., Messer, L. F., Geers, A. U., Ying, H., et al. (2019). A genomic view of the reef-building coral *Porites lutea* and its microbial symbionts. *Nat. Microbiol.* 4, 2090–2100. doi: 10.1038/s41564-019-0532-4
- Rodionov, D. A., Hebbeln, P., Eudes, A., Ter Beek, J., Rodionova, I. A., Erkens, G. B., et al. (2009). A novel class of modular transporters for vitamins in prokaryotes. *J. Bacteriol.* 191, 42–51. doi: 10.1128/jb.01208-08
- Rosenberg, E., Koren, O., Reshef, L., Efrony, R., and Zilber-Rosenberg, I. (2007). The role of microorganisms in coral health, disease and evolution. *Nat. Rev. Microbiol.* 5, 355–362. doi: 10.1038/nrmicro1635
- Rousset, F., Depardieu, F., Miele, S., Dowding, J., Laval, A. L., Lieberman, E., et al. (2022). Phages and their satellites encode hotspots of antiviral systems. *Cell Host Microbe* 30:e745, 740–753.e5. doi: 10.1016/j.chom.2022.02.018
- Saga, Y., Oh-Oka, H., Hayashi, T., and Tamiaki, H. (2003). Presence of exclusively bacteriochlorophyll-*c* containing substrain in the culture of green sulfur photosynthetic bacterium *Chlorobium vibrioforme* strain NCIB 8327 producing bacteriochlorophyll-*d*. *Anal. Sci.* 19, 1575–1579. doi: 10.2116/analsci.19.1575
- Sakurai, H., Ogawa, T., Shiga, M., and Inoue, K. (2010). Inorganic sulfur oxidizing system in green sulfur bacteria. *Photosynth. Res.* 104, 163–176. doi: 10.1007/s1120-010-9531-2
- Salem, H., Bauer, E., Strauss, A. S., Vogel, H., Marz, M., and Kaltenpoth, M. (2014). Vitamin supplementation by gut symbionts ensures metabolic homeostasis in an insect host. *Proc. Biol. Sci.* 281:20141838. doi: 10.1098/rspb.2014.1838
- Schultz, J. E., and Weaver, P. F. (1982). Fermentation and anaerobic respiration by *Rhodospirillum rubrum* and *Rhodopseudomonas capsulata*. *J. Bacteriol.* 149, 181–190. doi: 10.1128/jb.149.1.181-190.1982
- Seemann, T. (2014). Prokka: rapid prokaryotic genome annotation. *Bioinformatics* 30, 2068–2069. doi: 10.1093/bioinformatics/btu153
- Shashar, N., and Stambler, N. (1992). Endolithic algae within corals - life in an extreme environment. *J. Exp. Mar. Biol. Ecol.* 163, 277–286. doi: 10.1016/0022-0981(92)90055-F
- Sorokin, D. Y., Merkel, A. Y., Messina, E., Tugui, C., Pabst, M., Golyshin, P. N., et al. (2022). Anaerobic carboxydrotrophy in sulfur-respiring haloarchaea from hypersaline lakes. *ISME J.* 16, 1534–1546. doi: 10.1038/s41396-022-01206-x
- Supuran, C. T., and Capasso, C. (2017). An overview of the bacterial carbonic anhydrases. *Meta* 7:56. doi: 10.3390/metabo7040056
- Tashiro, Y., Monson, R. E., Ramsay, J. P., and Salmond, G. P. (2016). Molecular genetic and physical analysis of gas vesicles in buoyant enterobacteria. *Environ. Microbiol.* 18, 1264–1276. doi: 10.1111/1462-2920.13203
- Thiel, V., Drautz-Moses, D. I., Purbojati, R. W., Schuster, S. C., Lindemann, S., and Bryant, D. A. (2017). Genome sequence of *Prosthecochloris* sp. strain HL-130-GSB from the phylum Chlorobi. *Genome Announc.* 5:17. doi: 10.1128/genomeA.00538-17
- Uritskiy, G. V., DiRuggiero, J., and Taylor, J. (2018). MetaWRAP-a flexible pipeline for genome-resolved metagenomic data analysis. *Microbiome* 6:158. doi: 10.1186/s40168-018-0541-1
- Vernikos, G. S., and Parkhill, J. (2006). Interpolated variable order motifs for identification of horizontally acquired DNA: revisiting the salmonella pathogenicity islands. *Bioinformatics* 22, 2196–2203. doi: 10.1093/bioinformatics/btl369
- Walker, B. J., Abeel, T., Shea, T., Priest, M., Abouelliel, A., Sakthikumar, S., et al. (2014). Pilon: an integrated tool for comprehensive microbial variant detection and genome assembly improvement. *PLoS One* 9:e112963. doi: 10.1371/journal.pone.0112963
- Walsby, A. E. (1994). Gas vesicles. *Microbiol. Rev.* 58, 94–144. doi: 10.1128/mr.58.1.94-144.1994
- Walsby, A. E., Revsbech, N. P., and Griffel, D. H. (1992). The gas permeability coefficient of the cyanobacterial gas vesicle wall. *J. Gen. Microbiol.* 138, 837–845. doi: 10.1099/00221287-138-4-837
- Wang, W., Tang, K., Wang, P., Zeng, Z., Xu, T., Zhan, W., et al. (2022). The coral pathogen *Vibrio coralliilyticus* kills non-pathogenic holobiont competitors by triggering prophage induction. *Nat. Ecol. Evol.* 6, 1132–1144. doi: 10.1038/s41559-022-01795-y
- Wang, X., Yang, H., Ma, C., and Guo, L. (2014). Enhanced photosynthetic hydrogen production performance of *Rhodobacter capsulatus* by deactivating CBB cycle and cytochrome *c* oxidase. *Int. J. Hydrog. Energy* 39, 3176–3184. doi: 10.1016/j.ijhydene.2013.12.098
- Wewengkang, D. S., Watanabe, T., and Hidaka, M. (2007). Studies on morphotypes of the coral *Galaxea fascicularis* from Okinawa: polyp color, nematocyst shape, and coenosteum density. *J. Japanese Coral Reef Soc.* 9, 49–59. doi: 10.3755/jcrs.9.49
- Wu, Y. W., Simmons, B. A., and Singer, S. W. (2016). MaxBin 2.0: an automated binning algorithm to recover genomes from multiple metagenomic datasets. *Bioinformatics* 32, 605–607. doi: 10.1093/bioinformatics/btv638
- Xie, H., Buschmann, S., Langer, J. D., Ludwig, B., and Michel, H. (2014). Biochemical and biophysical characterization of the two isoforms of cbb3-type cytochrome *c* oxidase from *Pseudomonas stutzeri*. *J. Bacteriol.* 196, 472–482. doi: 10.1128/JB.01072-13
- Yang, S.-H., Lee, S. T. M., Huang, C.-R., Tseng, C.-H., Chiang, P.-W., Chen, C.-P., et al. (2016). Prevalence of potential nitrogen-fixing, green sulfur bacteria in the skeleton of reef-building coral *Isopora palifera*. *Limnol. Oceanogr.* 61, 1078–1086. doi: 10.1002/lno.10277
- Yang, S.-H., Tandon, K., Lu, C.-Y., Wada, N., Shih, C.-J., Hsiao, S. S.-Y., et al. (2019). Metagenomic, phylogenetic, and functional characterization of predominant endolithic green sulfur bacteria in the coral *Isopora palifera*. *Microbiome* 7:3. doi: 10.1186/s40168-018-0616-z
- Yilmaz, P., Parfrey, L. W., Yarza, P., Gerken, J., Priesse, E., Quast, C., et al. (2014). The SILVA and all-species living tree project (LTP) taxonomic frameworks. *Nucleic Acids Res.* 42, D643–D648. doi: 10.1093/nar/gkt1209
- Yu, X., Yu, K., Liao, Z., Chen, B., Deng, C., Yu, J., et al. (2021). Seasonal fluctuations in symbiotic bacteria and their role in environmental adaptation of the scleractinian coral *Acropora pruinosa* in high-latitude coral reef area of the South China Sea. *Sci. Total Environ.* 792:148438. doi: 10.1016/j.scitotenv.2021.148438
- Ziegler, K., Diener, A., Herpin, C., Richter, R., Deutzmann, R., and Lockau, W. (1998). Molecular characterization of cyanophycin synthetase, the enzyme catalyzing the biosynthesis of the cyanobacterial reserve material multi-L-argininyl-poly-L-aspartate (cyanophycin). *Eur. J. Biochem.* 254, 154–159. doi: 10.1046/j.1432-1327.1998.2540154.x
- Zygun, A. M., Lunina, O. N., Prusakova, T. S., Pimenov, N. V., and Ivanov, M. V. (2009). Fractionation of stable carbon isotopes by photoautotrophically growing anoxygenic purple and green sulfur bacteria. *Microbiology* 78, 757–768. doi: 10.1134/s0026261709060137





## OPEN ACCESS

## EDITED BY

Manuel Maldonado,  
Center for Advanced Studies of Blanes  
(CSIC), Spain

## REVIEWED BY

Cristiane Cassiolato Pires Hardoim,  
São Paulo State University, Brazil  
Lucia Pita,  
Institute of Marine Sciences (CSIC), Spain

## \*CORRESPONDENCE

Lilach Rajjman-Nagar  
✉ [ralilah2@gmail.com](mailto:ralilah2@gmail.com)

RECEIVED 08 February 2023

ACCEPTED 18 May 2023

PUBLISHED 05 June 2023

## CITATION

Rajjman-Nagar L, Goren L, Shefer S,  
Moskovich R, Li Z and Ilan M (2023) A  
comparison of mesophotic and shallow  
sponge holobionts resilience to predicted  
future temperature elevation.  
*Front. Mar. Sci.* 10:1161648.  
doi: 10.3389/fmars.2023.1161648

## COPYRIGHT

© 2023 Rajjman-Nagar, Goren, Shefer,  
Moskovich, Li and Ilan. This is an open-  
access article distributed under the terms of  
the [Creative Commons Attribution License](https://creativecommons.org/licenses/by/4.0/)  
(CC BY). The use, distribution or  
reproduction in other forums is permitted,  
provided the original author(s) and the  
copyright owner(s) are credited and that  
the original publication in this journal is  
cited, in accordance with accepted  
academic practice. No use, distribution or  
reproduction is permitted which does not  
comply with these terms.

# A comparison of mesophotic and shallow sponge holobionts resilience to predicted future temperature elevation

Lilach Rajjman-Nagar<sup>1\*</sup>, Liron Goren<sup>1,2</sup>, Sigal Shefer<sup>1,2</sup>,  
Raz Moskovich<sup>1,3</sup>, Zhiyong Li<sup>4</sup> and Micha Ilan<sup>1</sup>

<sup>1</sup>School of Zoology, Faculty of Life Sciences, Tel- Aviv University, Tel-Aviv, Israel, <sup>2</sup>The Steinhardt Museum of Natural History, Tel- Aviv University, Tel-Aviv, Israel, <sup>3</sup>Ruppin Academic Center, Faculty of Marine Sciences, Michmoret, Israel, <sup>4</sup>School of Life Sciences and Biotechnology, Shanghai Jiao Tong University, Shanghai, China

Climate change is predicted to have detrimental impacts on sessile invertebrates, including sponges. Mesophotic ecosystems have been suggested to play a major role as refugia for coral reef sponge species, however knowledge regarding the ability of mesophotic sponges to cope with thermal stress is scarce. In this study we compared the response of the sponge *Diacarnus erythraeanus*, a widespread Red Sea sponge, from the shallow and mesophotic reef, to moderate and acute temperature elevation (2°C and 6°C, respectively) for short and long term periods (two and 35 days, respectively) by measuring physiological parameters (respiration, oxygen removal, pumping rates, and photosynthetic efficiency), and the microbiome composition change. The results indicated that mesophotic and shallow populations of *D. erythraeanus* are highly tolerant to both moderate and acute heat stress, demonstrating a high survival rate (100%) across the experimental treatments, with no visible signs of bleaching or necrosis. Exposure to heat stress resulted in significant alterations in the physiological parameters of sponges, including higher respiration rate and lower photosynthetic efficiency. These alterations were accompanied by correspondingly significant microbial adjustments, thus emphasizing the essential role of the microbiome in the host's ability to persist when facing essential environmental stress. Moreover, while shallow and mesophotic sponges showed similar physiological tolerance to heat stress, their microbial response differed: while the microbiome diversity of the mesophotic sponges remained stable throughout the experiment, the shallow one significantly changed. This result suggests that their underlying coping mechanisms might differ between mesophotic and shallow populations. Since the associated-microbiome is largely regulated by the sponge-host genetics, difference in microbial adjustments to stress between populations, could indicate genetic variability between hosts. Therefore, while the results of this study support the hypothesis that mesophotic coral reefs could serve as thermal refugia for some

sponge species, it raises the question regarding the validity of MCEs as a refuge for shallow populations. Finally, it emphasizes the crucial need to elucidate the underlying mechanisms governing the sponge-microbiome interactions, specifically in the context of the anticipated climate change scenarios.

#### KEYWORDS

bacteria, climate change, *Diacarnus erythraeanus*, holobiont, mesophotic, microbiome, ocean warming, sponges

## 1 Introduction

Global climate changes have already been shown to have detrimental effects on marine coastal ecosystems (Hughes et al., 2018a; Forster et al., 2021). These effects are predicted to worsen as the intensity, frequency, and duration of marine heatwave events are expected to increase in the future (Frölicher et al., 2018; Oliver et al., 2018; Muñoz-Castillo et al., 2019; IPCC, 2023). The magnitude of the climate change effects varies among the different habitats. Mesophotic coral ecosystems (MCEs), considered as those between 30–150 m depth (Lesser et al., 2009; Kahng et al., 2010), are less affected compared to their adjacent shallower reefs (Hoegh-Guldberg et al., 2007; Kahng et al., 2017). Due to their distance from the sea surface, MCEs are considered to be more stable and environmentally predictable than shallow reefs (Baker et al., 2016). Accordingly, thermal anomalies are reduced in MCEs and the water temperature is cooler compared to that of the shallow depths (Lesser et al., 2009; Shlesinger et al., 2018; Turner et al., 2019). Since the former are genetically and physically associated with their shallow reefs counterparts, they have been suggested to play a major role as refugia and as a larval source for species unable to tolerate the current changing conditions in the shallow waters (Bongaerts et al., 2010; Weiss, 2017). A recent example of the mesophotic depth serving as a thermal refugium is the case of the Mediterranean sponge *Agelas oroides*. This sponge vanished from the shallow habitats along the Israeli coast in the 1970s, but was recently re-discovered in the mesophotic sponge grounds (100–120 m) in the same area. An experiment transplanting mesophotic individuals to the shallow waters, revealed that the sponges survived well until the temperature exceeded 28°C, when they rapidly perished, suggesting that this sponge's disappearance from the Israeli shallow waters might have occurred following prolonged periods of elevated temperature (Idan et al., 2020). Another example is that of coral bleaching after a heatwave event in French Polynesia. The bleaching significantly decreased with depth, with minor to no bleaching observed at the mesophotic depths (Pérez-Rosales et al., 2021). Such examples emphasize the potential of mesophotic depths to serve as a thermal shelters for various benthic organisms.

Among the variety of organisms affected by these environmental changes, sessile organisms, such as sponges and corals, are presumably the most sensitive, since they are unable to relocate (Hughes et al., 2018b). Sponges (Phylum Porifera) are widespread benthic organisms, fulfilling fundamental roles in

ecosystem functioning (Bell, 2008; Rix et al., 2018). In some coral reefs, sponges are considered the second most abundant component in the benthic assemblage after corals (Diaz and Rützler, 2001). Accumulating evidence from recent years suggests that sponges' responses to thermal stress vary, with some species more tolerant to a rise in temperature (Luter et al., 2020; Ribeiro et al., 2021; Vargas et al., 2021; Posadas et al., 2022), while others are more sensitive, manifesting bleaching, necrosis, and death (Cebrian et al., 2011; Ramsby et al., 2018; Beepat et al., 2020; Rubio-Portillo et al., 2021). How a sponge responds to environmental stress, however, might be largely a function of its specific associated microbial community (Marangon et al., 2021). The sponge's microbiome benefits the host by providing key functions that support the sponge-host's health and fitness (Hentschel et al., 2012; Webster and Thomas, 2016; Zhang et al., 2019; Engelberts et al., 2020; Marangon et al., 2021; Taylor et al., 2021), particularly when subjected to environmental stress (Webster and Reusch, 2017; Pita et al., 2018; Marangon et al., 2021; Posadas et al., 2022).

The diverse associations and dependence between the sponge-host and its microbiome have led to the consortium of microorganisms and their host being regarded as a “meta-organism” or holobiont (Bosch and McFall-Ngai, 2011; Webster and Thomas, 2016), rather than as autonomous components. Upon experiencing environmental stress, the sponge-microbiome might respond in several ways, such as dysbiosis (a break-down of the association), which mostly results in host health decline, disease, and possible mortality. Once dysbiosis occurs, it is characterized by a sharp increase (usually of opportunistic bacteria) or decrease of the natural microbial community (Fan et al., 2013; Lesser et al., 2016; Rondon et al., 2020). For example, the microbiome of the barrel sponge, *Xestospongia muta*, was destabilized following exposure to low pH and thermal stress conditions, leading to a decline in the host's nutrient budget (e.g., carbohydrates) (Lesser et al., 2016). In the Great Barrier Reef (GBR) sponge, *Rhopaloeide odorabile*, various symbiotic functions were lost due to interruption of the host-symbiotic interactions following thermal stress, while pathogenic functions or virulent protein-associated functions were enriched (Fan et al., 2013). However, the microbiome can also be reconstructed, either by changes in the bacterial abundance or by acquiring new bacteria (Ribes et al., 2016; Vargas et al., 2021), leading to a more suitable and beneficial composition that might enhance the host's resilience under stress (Reshef et al., 2006; Webster and Reusch, 2017). For example, a sponge's ability to

restructure its microbial assemblage was identified as a major factor contributing to its tolerance following exposure to acidification conditions (Ribes et al., 2016). Similarly, in the common aquarium sponge *Lendenfeldia chondroides*, re-accommodation of bacterial members was associated with the sponge's acclimation to heat stress (Vargas et al., 2021). Alternatively, resilience might be an outcome of a microbial stable state, in which no change occurs in the bacterial diversity and composition up to a certain temperature (Webster et al., 2008; Simister et al., 2012). These various interactions suggest that the sponge host's stability is largely attributed to its dynamic equilibrium with its associated microbiome (Fan et al., 2013; Glasl et al., 2018).

While there are accumulating experimental data regarding the microbial response of sponges to thermal stress (Luter et al., 2020; Moreno-Pino et al., 2020; Ribeiro et al., 2021; Vargas et al., 2021), studies on the combined response of the holobiont (both host and microbiome) are sparse (reviewed in Pita et al., 2018). Moreover, although MCEs are being considered as potential thermal refugia, the research to date has been mainly focused on the response of sponges from shallow sites to thermal stress and not that of mesophotic sponges (Simister et al., 2012; Fan et al., 2013; Guzman and Conaco, 2016; Rubio-Portillo et al., 2021). The latter are not exposed to extreme temperature fluctuations and, therefore, may not be adapted to thermal stress, unlike their shallow counterparts. Since MCEs are not immune to the predicted climate change effects (Neal et al., 2014; Nir et al., 2014), it is of importance to determine the ability of sponges from MCEs to tolerate thermal stress (Morrow et al., 2016; Gould et al., 2021), as well as that of the adjacent shallow sponges. Finally, in the face of an increase in global warming, understanding the spatial dynamics (shallow vs. mesophotic) of the holobiont is crucial in order to obtain new insights into the resilience of already degraded coral reefs (Birkeland, 2019).

The coral reefs of Eilat, located at the northern tip of the Gulf of Aqaba, are among the most diverse coral reefs worldwide (Loya, 2004). They are characterized by a steep depth gradient, with only a very short distance (~50–250 m) separating the shallow from the mesophotic reefs (Kramer et al., 2019). Additionally, fauna in the Gulf of Eilat/Aqaba are characterized by their heat tolerance and resilience to thermal stress, so much that the shallow corals in Eilat, were described as 'super-corals' (Fine et al., 2013; Grottoli et al., 2017). Despite the study of coral resilience, the heat tolerance of sponges in the Gulf of Eilat/Aqaba has yet to be evaluated. Moreover, while various studies examined the role of MCEs to serve as coral refugia in the Gulf of Eilat/Aqaba, they have neither been evaluated for sponges, nor in other coral reefs worldwide. The endemic Red Sea sponge *Diacarnus erythraeanus* (Kelly-Borges and Vacelet, 1995; Demospongiae, Poecilosclerida) is widespread in the benthic communities from shallow to mesophotic depths, and hosts a diverse microbial community, including cyanobacteria (Oren et al., 2005). Hence it offers a unique opportunity to examine possible differences in resilience to heat stress, of shallow vs. mesophotic individuals. It also allows for the first time to evaluate the role of MCEs as thermal sponge refugia at the Gulf of Eilat/Aqaba. In this study, we compared the response of *D. erythraeanus* individuals from both shallow (5–10 m) and mesophotic reefs (45–

55 m) to thermal stress *in vitro*. The response of both the sponge host and its microbiome were assessed for short- and long-term periods (two and after 35 days of heat stress exposure), using physiological measurements and meta-barcoding sequencing of the bacterial assemblage (16S rRNA gene).

We hypothesized that, in response to elevated temperature scenarios, the mesophotic sponges would: a) exhibit higher stress and lower survival compared to shallow sponges, expressed in terms of physiological performance (lower survival, higher respiration rates, lower photosynthetic activity, etc.); and b) exhibit extreme shifts in their microbial composition compared to the shallow sponges.

## 2 Materials and methods

### 2.1 Sponge sampling

*Diacarnus erythraeanus* specimens were collected from the northern Gulf of Aqaba (Eilat) (29°31'19.0"N 34°56'09.3"E) in July 2019. Six individuals were sampled using SCUBA diving from shallow reefs (5–10 m) and six from mesophotic reefs (40–50 m) using a Remotely Operated Vehicle (ROV, ECA-Robotics H800) onboard the R/V Sam Rothberg (Permit no. 2018/42031 and 2019/42248). Immediately after collection each sponge was cut into 15–17 clones (~18 cm<sup>3</sup>). One clone from each original specimen was flash-frozen in liquid nitrogen and stored (-80°C) to await further characterization of the sponges' wild-type bacterial composition. All the other clones were tagged to enable identification of the individual sponge, and secured to underwater nursery structures *in situ* (~10 m depth), for ~5 months of regeneration and acclimation, before being translocated to the experimental system (Supplementary Figures 1A, B).

### 2.2 Experimental design

The experiment was conducted in 40 L aquaria in a flow-through mesocosm system, Red Sea Simulator, located at the Interuniversity Institute for Marine Sciences (IUI) in Eilat, Israel (for technical details see Bellworthy and Fine (2018)). Temperature treatments comprised of the current ambient temperature (~24°C), the predicted local temperature for 2100, as calculated by IPCC RCP8.5 of 2°C (~26°C, 'Moderate' treatment) (Hoegh-Guldberg et al., 2014) and an acute increase of 6°C above ambient (~30°C, 'Acute' treatment). The clones were distributed across the three treatments to ensure that each sponge-individual had clones in each of the treatments and at each sampling point. Moderate and acute treatments were each incorporated in four aquaria replicates, together containing a total of 48 clones (24 per treatment), six per aquarium. Each aquarium contained sponge clones from both mesophotic and shallow habitats (Figure 1A), randomly assigned to the different aquaria. Following an acclimation period of five days at ambient temperature (24°C), temperature in the aquarium was then increased by 1°C/day until the desired treatment temperatures were reached (Figure 1B). Since each thermal treatment reached the

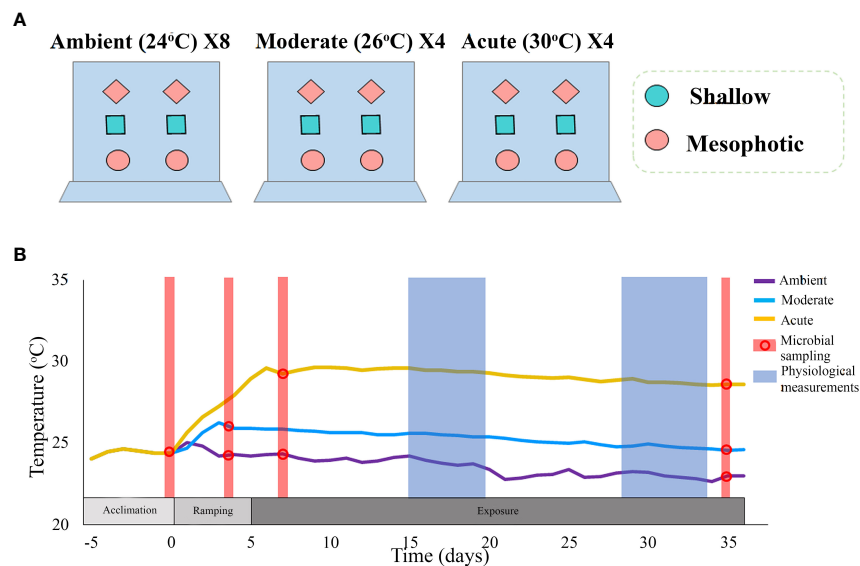


FIGURE 1

(A) An illustrated description of the experimental set-up. The experiment comprised two thermal treatments: moderate (~26°C) and acute (~30°C), each with four aquaria replicates; and a control ambient temperature (~24°C), with eight replicates. Each thermal treatment comprised 24 clones (six clones per aquarium), originating from 12 different sponge individuals: six from a shallow reef and six from a mesophotic reef. The sponge clones were randomly assigned to the aquaria with each aquarium containing sponges from both mesophotic and shallow habitats, and with each type of individual-clone present in every treatment. (B) Timeline and temperature throughout the duration of the experiment. Different colors represent the various treatments. Dots represent the time-points at which microbial sampling was performed. Physiological measurements comprised respiration rate, oxygen removal, pumping rate, buoyant weight, and photosynthetic efficiency (measured only at  $T_H$ ).

target temperature at a different time, two groups of control ambient temperature were assigned, one group to each thermal treatment, each comprising of 24 sponge clones which were placed in eight aquaria replicates. The experiment lasted 35 days.

## 2.3 Physiological measurements

*Sponge pumping activity* [ $L_{\text{pumped}} \text{ hr}^{-1} \text{ ind}^{-1}$ ] was evaluated using a modification of the Dye Front Speed method (DFS) as described by (Yahel et al., 2005; Morganti et al., 2019). Each DFS measurement was calculated as the average of repeated measurements (4–6 times) per sponge.

*Dissolved oxygen (DO) removal* [ $\mu\text{mol O}_2 \text{ L}^{-1}$ ], was measured using GO2 FireSting (PyroScience, German, hereafter “optodes”). Each measurement lasted for 10 min at 10 s intervals. Optodes were located in the sponge excurrent water ( $DO_{\text{EX},t}$ ), near the osculum, using custom-made manipulators that minimized interruption of the sponge clone during the measurement and stabilized the sensor (Supplementary Figure 1C). Oxygen concentration measurement in the aquarium surrounding water ( $DO_{\text{Surr},t}$ ) took place before each measurement of the sponge-oxygen removal. Oxygen concentration median values (for 10 min measurement) were then calculated for both,  $DO_{\text{Surr},t}$  and  $DO_{\text{EX},t}$ , and the DO removal per liter ( $\Delta\text{O}_2$ ,  $\mu\text{mol L}^{-1}$ ) was calculated as follows (Moskovish et al., 2022):

$$\text{Eq. 1. } \Delta\text{O}_{2,t} = DO_{\text{Surr},t} - DO_{\text{EX},t}$$

*Respiration rate* [ $\mu\text{mol O}_2 L_{\text{pumped}}^{-1} \text{ hr}^{-1} \text{ ind}^{-1}$ ] was calculated by multiplying the sponge’s pumping rate by its DO removal for consecutive measurements.

*Changes in buoyant weight* were measured using a digital scale (ViBRA AJ-320CE) following Osinga (1999).

Sponge physiological measurements were conducted in the middle (days 15–20) and at the end (days 28–35) of the experiment (Figure 1B).

*Changes in photosynthetic efficiency* of the sponge-associated cyanobacteria under the different thermal treatments were thus assessed by determining the changes in maximal quantum yields ( $F_v/F_m$ ) of Photosystem II in dark-adapted samples. For this, we used a Diving-Pulse Amplitude Modulation fluorometer (Diving-PAM; Walz, Germany), in which the ground fluorescence in the dark-adapted state signal ( $F_0$ ) was detected by emitting red modulated measuring light (a weak pulsed light;  $< 1 \mu\text{mol photons m}^{-2} \text{ s}^{-1}$ ), followed by a short saturating pulse, to estimate the maximal fluorescence level ( $F_m$ ). The maximal quantum yield was obtained from the ratio of  $F_v/F_m$ , where the variable fluorescence of dark-adapted samples ( $F_v$ ) was calculated as the subtraction of ( $F_0 - F_m$ ). The measurement was repeated 3–5 times for each sponge clone, at different locations on the clone surface. Measurements took place on day 34 of the experiment, two hours after sunset, to ensure dark acclimation of the PSII.

## 2.4 Statistical analyses of the physiological measurements

Differences in the physiological measurements were evaluated using a permuted ANOVA test ( $n=5000$  permutations) followed by pairwise comparisons with FDR correction for multiple



comparisons, where  $p$  value < 0.05 was defined as the significant threshold in all analyses. A mixed model was designed to examine the interaction of treatment and depth as fixed factors, and, when relevant, sponge-individual was considered as a random effect within treatment or sampling time. The respiration and pumping rates from the middle and end of the experiment did not diverge in their variance of medians. This, and since only a small number of consecutive measurements (of sponge pumping rate and oxygen removal) were made, their values were pooled to increase power analysis.

Statistical analyses were carried out using the *permuco* (Frossard and Renaud, 2021), *rcompanion* (Mangiafico and Mangiafico, 2017), and *ggplot2* (Wickham, 2016) packages within RStudio environment (V. 2021.09.0 + 351) (Allaire, 2012).

## 2.5 Microbial sampling, gene sequencing, and bioinformatic processing

All sponges were sampled for microbiome analysis at four sampling points: on the day of sponge collection from their natural habitat (“wild-type”, as noted in section 2.1); after the five-day acclimation period at an ambient temperature of 24°C, prior to temperature raising (“pre-experiment”); and on 2 days after the aquarium water had reached the desired temperatures (“T2”) and at the last day of the experiment (“T<sub>f</sub>”, Figure 1B). At each sampling point, one clone from the shallow waters and one from the mesophotic waters were randomly selected from each aquarium and immediately flash-frozen in liquid nitrogen and stored at –80°C for later DNA extraction.

Genomic DNA was extracted from the sponges using the DNeasy Blood & Tissue Kit (Qiagen) following the manufacturer’s protocol. DNA quantity and purity were assessed using Qubit 3.0 (ThermoFisher, USA) and gel electrophoresis (respectively). The 16S V4 rRNA gene region was amplified using modified 515f forward and 806r reverse primers (Apprill et al., 2015; Parada et al., 2016), and sequencing of 2X250 bp paired-end reads was performed on the Illumina NovaSeq 6000 platform (San Diego, CA, USA) at Magigene Biotechnology Co., Ltd. (Guangdong, China). Error sequencing correction, chimeric removal and denoising of the paired reads into contigs were applied on the resulting FASTQ files using DADA2 package (Callahan et al., 2016) and grouped into Amplicon Sequence Variants (ASVs) based in the naive Bayesian classifier method (Wang et al., 2007) against the SILVA v138.1 database (Quast et al., 2012). Sequences originating from Archaea, chloroplasts, mitochondria, and eukaryotes were removed. Raw sequences were deposited in the NCBI BioProject database under the accession number PRJNA931995.

## 2.6 Microbiome composition and diversity analyses

The sponges’ microbial community composition and diversity indices (richness and Shannon) were calculated at each sampling point for all the sampled clones (see section 2.5). A *Phyloseq* object was constructed to import sample data (metadata, abundance, and

taxonomy tables) and to calculate microbiome dissimilarities between treatments and sampling points using the RStudio environment (V. 2021.09.0 + 351). Microbial dissimilarities were calculated with weighted-Unifrac distance matrix based on the samples’ relative abundance. In addition, to examine the effect of treatments and depths on microbial diversity, while considering sponge-individual origin, a mixed model was designed, with treatment and depth as fixed effects and sponge-individual as a random effect (nested within treatment). When examining the effect of time on the microbial diversity indices, time was defined as a fixed effect and sponge-individual as a random effect nested within time. Statistical differences were examined using permuted ANOVA ( $n=999$ ), followed by *post-hoc* testing for pairwise comparisons, using the Friedman-Nemenyi test. Differences in microbial composition of the samples among treatments and depths were visualized using non-metric multidimensional distance analysis (nMDS) 3D ordinations, based on weighted UniFrac distance matrix. Statistical differences in the microbial communities’ composition among treatments, depths, and sampling points were examined using permutational MANOVA and pairwise comparisons with 999 permutations, where treatment, depth, and sponge-individual were set as the main factors and the interactions of treatment\*depth and treatment\*sponge-individual were also assessed. In addition, the 20 most abundant ASVs for each sampling point\*treatment were calculated and then visualized using bar plots displaying the bacterial relative abundance on the order level. To further investigate which ASVs contributed to the difference across treatments and depths, differentially abundant ASV changes ( $\log$  fold change  $\geq |2|$ , Wald test, adjusted  $p$  value  $\leq 0.01$ ) were identified using *Phyloseq-DESeq* and *DESeq* function.

Microbial diversity calculations and visualizations were carried out using the following packages: *phyloseq* (McMurdie and Holmes, 2013), *microbiome* (Lahti and Shetty, 2018), *ggpubr* (Kassambara and Kassambara, 2020), *ggplot2* (Wickham, 2016), *vegan* (Oksanen et al., 2013), *Tidverse* (Wickham et al., 2019), *DESeq2* (Love et al., 2014), *permuco* (Frossard and Renaud, 2021) and *PMCMRplus* (Pohlert and Pohlert, 2018).

## 3 Results

### 3.1 Sponge physiological responses to elevated temperature

All *Diacarnus erythraeanus* clones appeared to be intact and healthy throughout the 35 days of the experiment, with no signs of bleaching or necrosis, and without mortality under both the ambient and thermal treatments. However, temperature had a significant effect on the sponges’ respiration rate, with those exposed to acute temperature exhibiting a significantly higher rate ( $14.5 \pm 1 \mu\text{mol O}_2\text{L}_p\text{H}^{-1}\text{Ind}^{-1}$ ) compared to both ambient ( $4.9 \pm 0.8 \mu\text{mol O}_2\text{L}_p\text{H}^{-1}\text{Ind}^{-1}$ ) and moderate treatments ( $4.5 \pm 1.6 \mu\text{mol O}_2\text{L}_p\text{H}^{-1}\text{Ind}^{-1}$ ,  $p < 0.005$ , Figure 2A, Table 1; Supplementary Table 1). Neither depth nor the interaction of temperature\*depth had a significant effect on the sponges’ respiration rate ( $p > 0.05$ , Table 1). Similarly, the sponges’ oxygen removal was significantly



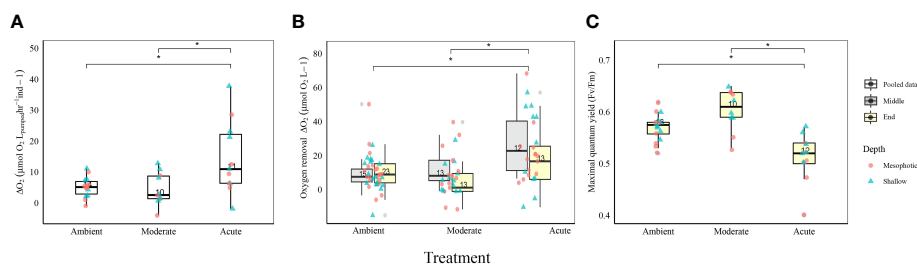


FIGURE 2

Physiological measurements of *D. erythraeanus* shallow (triangle) and mesophotic (circle) sponges exposed to ambient, moderate, or acute temperature. **(A)** Respiration rates ( $\mu\text{mol } \Delta\text{O}_2 \text{ L}^{-1} \text{ h}^{-1}$ ), pooled data. **(B)** Oxygen removal ( $\mu\text{mol O}_2 \text{ L}^{-1}$ ) in the middle (gray) and at the end (yellow) of the experiment. Significant difference refers to the oxygen removal measurements in the middle of the experiment **(C)** Photosynthetic efficiency (maximal quantum yield  $F_v/F_m$ ), pooled data. Median and 25–75 percent quartiles are indicated by the box. Dots are measurement values. The number of measurements is indicated within each box. Significant difference between treatments indicated by an asterisk. See Table 1 for detailed statistical information.

higher in those under acute heat treatment ( $29.6 \pm 5.3 \mu\text{mol O}_2 \text{ L}^{-1}$ ) compared to both ambient ( $13.3 \pm 3.1 \mu\text{mol O}_2 \text{ L}^{-1}$ ) and moderate treatments ( $14.7 \pm 2.9 \mu\text{mol O}_2 \text{ L}^{-1}$ ), which did not differ from one another (Figure 2B, Table 1; Supplementary Table 1). Interestingly, the oxygen removal rate in both thermal treatments significantly decreased over the course of the experiment, while the ambient treatment oxygen removal remained stable. Consequently, at the end of the experiment the oxygen removal of the acute treatment sponges was similar to that of the other treatments (acute:  $12 \pm 3.6 \mu\text{mol O}_2 \text{ L}^{-1}$ , moderate:  $5.0 \pm 2.3 \mu\text{mol O}_2 \text{ L}^{-1}$ , ambient:  $13.2 \pm 1.7 \mu\text{mol O}_2 \text{ L}^{-1}$ , Figure 2B, Table 1; Supplementary Table 1). In addition, while no differences in the sponge's oxygen removal were attributed to the sponge's depth-origin, at the end of the experiment, the oxygen removal was significantly affected by the treatment\*depth interaction (Table 1).

The sponges' pumping rates remained stable throughout the experiment, with no significant effect of temperature, depth, or temperature\*depth interaction. Likewise, the sponges' buoyant weight remained stable throughout the course of the experiment, and was similar for both the ambient and the thermal treatments, with no effect of treatment\*depth (Table 1).

## 3.2 Sponge microbiome response to elevated temperature

### 3.2.1 Photosymbionts function decrease

Photosymbionts exposed to the acute treatment exhibited a significantly lower photosynthetic efficiency ( $0.51 \pm 0.01$ ) compared to the moderate ( $0.6 \pm 0.01$ ) and the ambient treatment sponges ( $0.57 \pm 0.00$ , Figure 2C, Table 1; Supplementary Table 1). The results also indicated that a sponge's depth-origin had a significant effect on its photosynthetic efficiency, with a generally lower photosynthetic efficiency of the mesophotic sponges ( $0.55 \pm 0.0$ ) compared to the shallow ones ( $0.57 \pm 0.0$ ). However, no significant effect on the photosymbionts' photosynthetic efficiency was found for the interaction between depth and temperature (Table 1).

### 3.2.2 16S rRNA bioinformatics analysis

A total of 110 samples were successfully sequenced, achieving 24,228,075 16S V4 rRNA raw sequences. After quality filtering, 18,317,714 reads remained, with an average of  $166,524.6 \pm 2631.3$  reads per sample, which were classified into 7305 ASVs. Rarefaction curves indicated a sufficient bacterial diversity coverage, with curves reaching asymptotes in all samples (Supplementary Figure 2). The obtained ASVs affiliated with 37 bacterial phyla and 74 classes. In addition, 12 samples of the wild-type sponges were successfully sequenced, achieving 608,078 16S V4 rRNA raw sequences. After quality filtering, 278,840 reads remained, with an average of  $23,236.6 \pm 2485.1$  reads per sample, which were classified into a sum of 1387 ASVs.

### 3.2.3 Microbial diversity and species composition change across time, temperature, and depth

Microbial diversity indices (richness, Shannon) of the wild-type sponges were similar for both shallow and mesophotic sponges (Table 2; Supplementary Table 3A). In addition, the microbial communities were mostly composed of similar orders. They differed, however, in their relative abundance (Figure 3A), and significantly differed in their microbial composition (weighted UniFrac,  $R^2 = 0.21$ ,  $p = 0.009$ , Figure 4A, Table 2). The wild-type shallow samples were primarily composed of the orders HOC36 (Proteobacteria, 38.5%), Caldilineales (15%) and JTB23 (Proteobacteria, 7.5%), while in the mesophotic samples the orders HOC36 (21%), KI89A\_clade (Proteobacteria, 21%) and Nitrospirales (20.1%) were the most dominant. Moreover, Rhodobacterales and Puniceispirillales appeared only in the mesophotic samples, while SBR1031 (Chloroflexi) and Dadabacteriales were present only in the shallow ones (Figure 3A). Likewise, several bacterial members significantly changed in abundance between depths. For example, a significant change in ASV abundance (log-fold change,  $p < 0.01$ ) was affiliated with the families Flavobacteriaceae (ASV592), Caldilineaceae (ASV1), Rhodobacteraceae (ASV42), SAR11\_clade\_lb (ASV769), Bdellovibrionaceae (ASV 392), Prevotellaceae (ASV181), and Kiloniellaceae (ASV135, Figure 5).

TABLE 1 Physiological measurements', mean values + SE for each treatment (right) and summary statistics of temperature, depth-origin and their combined effect on the sponge respiration, oxygen removal rate, pumping rate, buoyant weight, and photosynthetic efficiency (Fv/Fm).

	df	F	p	Ambient	Moderate	Acute
Respiration $\mu\text{mol O}_2\text{LpH}^{-1}\text{Ind}^{-1}$						
Temp	2, 29	5.808	0.007	4.9±0.8	4.5±1.6	14.5±1
Depth	1, 29	1.296	0.264			
Temp*Depth	2, 29	0.123	0.884			
Oxygen removal/Middle $\mu\text{mol O}_2\text{L}^{-1}$						
Temp	2, 18	5.981	0.01	13.3±3.1	14.7±2.9	29.6±5.3
Depth	1, 18	0.35	0.569			
Temp*Depth	2,18	0.787	0.797			
Oxygen removal/End $\mu\text{mol O}_2\text{L}^{-1}$						
Temp	2, 35	4.777	0.010	13.3±1.7	5.0±2.3	12±3.6
Depth	1, 35	0.251	0.252			
Temp*Depth	2, 35	6.619	0.004			
Pumping rate/Middle $\text{L}_{\text{pumped}} \text{hr}^{-1}\text{ind}^{-1}$						
Temp	2, 9	0.575	0.575	2.4±0.5	1.6±2.8	2.6±0.5
Depth	1, 9	1.681	0.218			
Temp*Depth	2, 9	0.723	0.517			
Pumping rate/End $\text{L}_{\text{pumped}} \text{hr}^{-1}\text{ind}^{-1}$						
Temp	2, 31	1.24	0.291	2.2±0.2	1.9±0.2	2.8±0.4
Depth	1, 31	7.60E-05	0.992			
Temp*Depth	2, 31	7.20E-01	0.456			
Buoyant weight (g')						
Temp	2, 19	0.008	0.451	1.4±1.5	3.1±1.6	0.8±1.5
Depth	1, 20	0.849	0.932			
Temp*Depth	2, 19	2.077	0.155			
Maximum quantum yield (Fv/Fm)						
Temp	1, 20	15.71	2.00E-04	0.57±0.0	0.6±0.0	0.51±0.0
Depth	1, 10	5.713	0.038			
Temp*Depth	2, 20	0.870	0.442			

Significant values are indicated in bold. The table presents the following statistical estimates: degrees of freedom (df), F ratio (F), and P value (P). *Post-hoc* analysis included in [Supplementary Table 1](#).

Following the 5-month regeneration period and five-day acclimation at ambient temperature (24°C), and before any temperature increase in the aquaria (pre-experiment sampling point), the microbial communities of the shallow and mesophotic sponges did not differ substantially from each other. No significant differences were detected in diversity indices and microbial composition as a function of their depth origin (weighted UniFrac,  $R^2 = 0.03$ ,  $p=0.23$ , [Table 2](#)). Similarly, at T2, that is, two days after temperature in the aquaria had reached the target temperature values (26° vs 30 °C), the microbial diversity indices remained similar across temperature treatments and depth origin ([Table 2](#); [Supplementary Table 3A](#)).

These results suggest that a 5-month regeneration period under identical field conditions caused the original microbiomes of mesophotic and shallow-water individuals, which differed initially ([Figures 3A](#), [4A](#), weighted UniFrac,  $R^2 = 0.21$ ,  $p=0.009$ , [Table 2](#)) to shift and largely converge in composition and abundance.

Moreover, samples from the pre-experiment sampling-point and at T2 shared similar orders, primarily composed of SAR202 clade (27 vs. 30%, respectively), Caldilineales (15 vs. 14%), and Thermoanaerobaculales (10.7 vs. 10.2%, respectively). No unique pattern emerged in the bacterial orders' identity or in their abundance between depths for the pre-experiment sampling-point, or in treatments between depths for the T2 samples, except

**TABLE 2** Summary statistics for the effects of temperature, depth-origin, sponge-individual and their interaction at each time point on microbial diversity indices (richness and Shannon) and on the microbiome community composition at each time point (PERMANOVA results using weighted -unifrac distance).

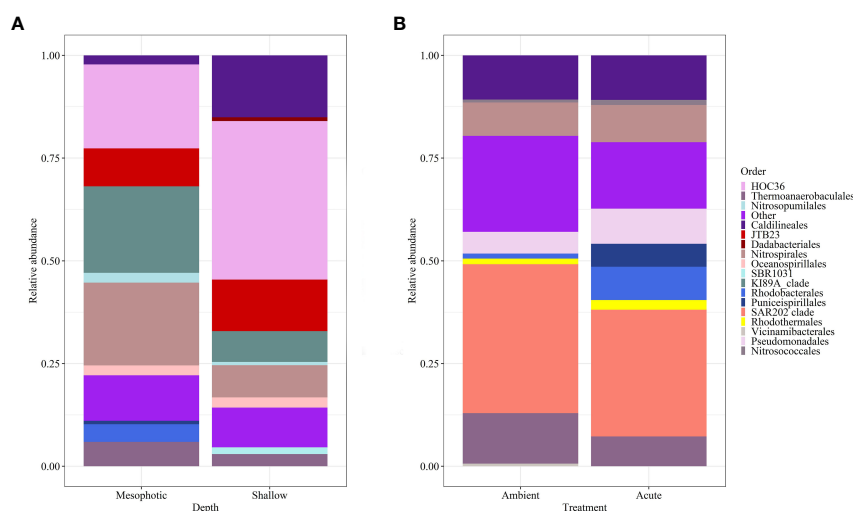
Time point	Factor	Richness			Shannon			Weighted UniFrac		
		df	F	p	df	F	p	pseudo F	R <sup>2</sup>	p
Wild-type	Depth	1,10	0.34	0.16	1,10	2.84	0.12	2.81	0.21	<b>0.009</b>
Pre-experiment	Depth	1,12	1.5	0.2	1, 12	0.1	0.8	1.6	0.1	0.2
	Individual	–	–	–	–	–	–	1.3	0.8	0.4
T <sub>2</sub>	Temperature	2,20	0.4	0.7	2, 20	2.1	0.2	2.3	0.0	<b>0.005</b>
	Depth	1,10	0.5	0.5	1, 10	1.5	0.3	23.3	0.2	<b>&lt;0.001</b>
	Individual							6.7	0.5	<b>&lt;0.001</b>
	Temp*Depth	2,20	0.0	1.0	2, 20	0.3	0.7	2.1	0.0	<b>0.01</b>
	Temp*Individual							1.7	0.2	<b>0.006</b>
T <sub>f</sub>	Temperature	2,20	3.4	<b>0.01</b>	2, 20	5.9	0.07	11.3	0.2	<b>&lt;0.001</b>
	Depth	1,10	9.3	<b>0.04</b>	1, 10	4.4	<b>0.01</b>	15.5	0.1	<b>&lt;0.001</b>
	Individual	–	–	–	–	–	–	6.0	0.4	<b>&lt;0.001</b>
	Temp*Depth	2,20	1.7	0.2	2, 20	4.5	<b>0.02</b>	1.1	0.0	<b>0.07</b>
	Temp*Individual	–	–	–	–	–	–	1.1	0.2	0.3
T <sub>2</sub> vs. T <sub>f</sub>	Shallow	1,5	51.3	<b>0.022</b>	1,5	11.6	<b>0.02</b>	–	–	–
	Mesophotic	1,5	0.5	0.5	1,5	0.7	0.4	–	–	–

The table presents the following statistical estimates: degrees of freedom (df), F ratio (F), and P value (p), proportion of variance explained (R<sup>2</sup>). Significant values are indicated in bold. Diversity indices *post-hoc* analysis and mean values are presented in [Supplementary Tables 3A, B](#). PERMANOVA *post-hoc* analysis is provided in [Supplementary Table 4](#).

for the order Thermoanaerobaculales, which was higher in the shallow samples, and Vicinamibacteriales, which was unique to the shallow pre-experiment samples ([Supplementary Figure 3](#)).

At the end of the experiment, however, after 35 days, changes in the microbial diversity indices and community composition could be observed, mostly in sponges exposed to the acute temperature

stress. Thus, at T<sub>f</sub>, the richness and Shannon indices of the acute samples were significantly lower ( $142 \pm 8.1$  and  $3.74 \pm 0.03$ , respectively) compared to the moderate ( $162 \pm 4.3$ ,  $3.78 \pm 0.03$ ) and ambient samples ( $162 \pm 4.9$ ,  $3.8 \pm 0.02$ ), which were similar to one another ([Figure 6](#), [Table 2](#); [Supplementary Tables 3A, B](#)). Moreover, while the diversity indices of the mesophotic samples



**FIGURE 3**

Relative abundance of *D. erythraeanus* microbial ASVs at the order level of (A) wild-type shallow vs. mesophotic sponges; and (B) sponges exposed to ambient and acute temperature treatment at the end of the experiment - T<sub>f</sub>.

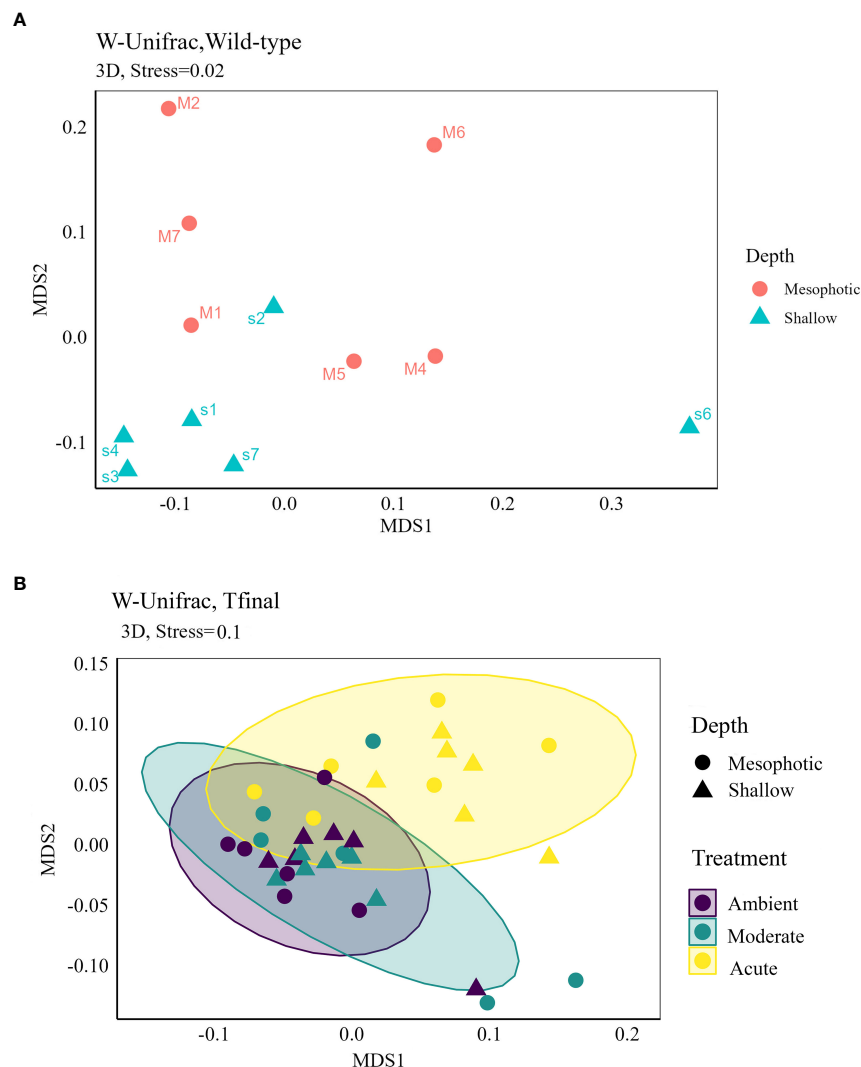


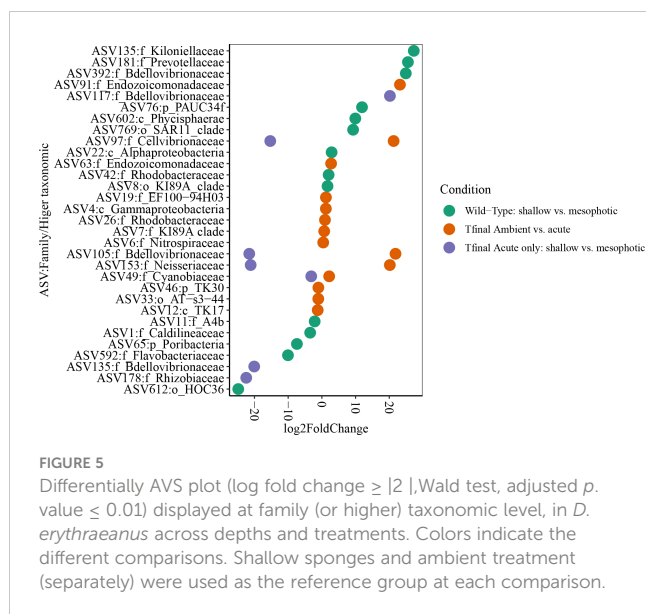
FIGURE 4

Non-metric multidimensional scaling (NMDS) 3D ordinations based on weighted UniFrac distance matrix of *D. erythraeanus* microbial community for (A) wild-type samples of shallow and mesophotic sponges; and (B) ambient, moderate and acute treatments of shallow and mesophotic sponges at T<sub>f</sub>. Each dot represents one sponge sample (mesophotic=circle, shallow=triangle). See also Table 2 and Supplementary Table 4.

remained stable throughout the experiment under the acute treatment, those of the shallow samples significantly decreased (Table 2; Supplementary Table 3A). In addition, the microbial community composition of the acute treatment sponges significantly differed from the moderate treatment and ambient samples, which were similar to one another (Weighted UniFrac, Figure 4B, Table 2; Supplementary Table 4). For example, a significant increase in ASV abundance in the acute treatment sponges (compared to the ambient treatment) at T<sub>f</sub> was associated with members of the families Endozoicomonadaceae (ASV63, ASV91), Nitrospiraceae (ASV6), Neisseriaceae (ASV153), Bdellovibrionaceae (ASV105), Cyanobiaceae (ASV49), Cellvibrionaceae (ASV97), and Rhodobacteraceae (ASV 26, Figure 5). A change in microbial composition of the acute vs. ambient sponge treatments at T<sub>f</sub> was also observed in the bacterial orders. For example, the relative abundance of the orders Pseudomonadales and Rhodobacterales was higher in the acute

treatment sponges (8.5%; 8% respectively) compared to the ambient samples (5.3%; 1% respectively). In contrast, the SAR202 clade was less abundant in the acute treatment samples (30%) compared to the ambient treatment ones (36%), as were the Thermoanaerobacterales (acute: 7%, ambient: 12%). In addition, at T<sub>f</sub> only the acute samples possessed members of the order Puniceispirillales (5%), while Vicinamibacterales were present only in the ambient samples, although at low abundance (0.6%) (Figure 3B).

At T<sub>f</sub> differences in the microbial composition were also associated with the sponge's depth-origin (Weighted UniFrac R<sup>2</sup> = 0.11,  $p < 0.01$ , Figure 4B, Table 2; Supplementary Table 3A). Numerous bacterial members were found to significantly change in abundance between the shallow and mesophotic samples under the acute treatment. For example, the mesophotic samples were associated with a decreased abundance of members of the families Rhizobiaceae (ASV178), Neisseriaceae (ASV153), Bdellovibrionaceae



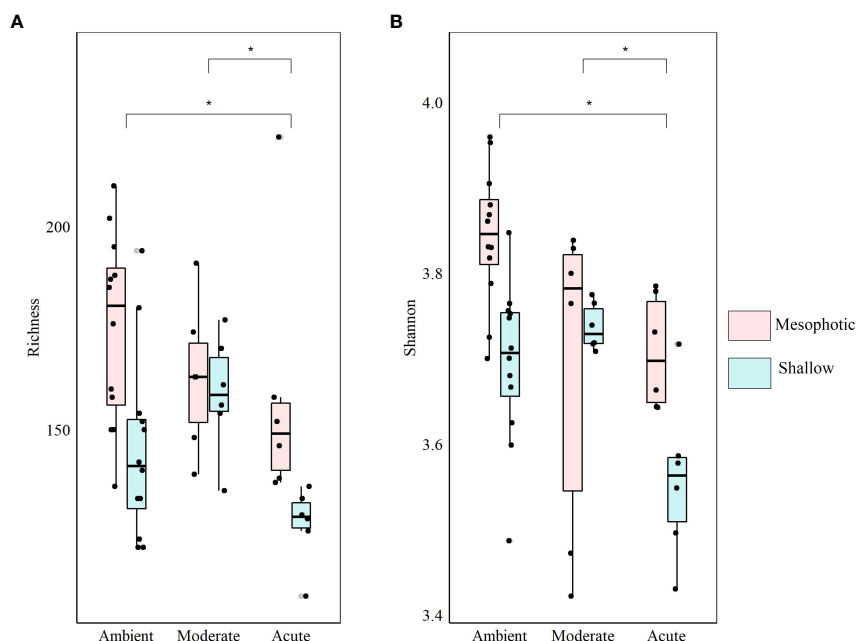
(ASV105, 135), Cyanobiaceae (ASV49), and Cellvibrionaceae (ASV97), and an increased abundance of members of the family Bdellovibrionaceae (ASV117) (log-fold change,  $p < 0.01$ , Figure 5). In addition, as previously described for the wild-type samples, also at  $T_f$ , the shallow and mesophotic samples in the acute treatment generally shared similar bacterial orders, with a few exceptions, and with differences in the orders' relative abundance (Supplementary Figure 3). For example, Pseudomonadales and Puniceispirillales abundance was higher in the shallow samples (11%, 7% respectively) compared to the mesophotic ones (5%, 3%,

respectively). In addition, Nitrosococcales were unique to the shallow samples and Caldilineales were generally higher in the mesophotic samples.

Finally, the sponge-host individual was found to be the most meaningful factor in shaping the microbial composition, both at  $T_2$  and  $T_f$  (Weighted UniFrac,  $R^2 = 0.5$ ,  $p < 0.001$ ;  $R^2 = 0.4$ ,  $p < 0.001$ , respectively, Table 2). Nevertheless, for the pre-experiment sponges, the effect of sponge individual origin was not significant. It was, however, the only factor meaningfully contributing to the explained variance in microbial composition ( $R^2 = 0.78$ ,  $p = 0.37$ , Table 2).

## 4 Discussion

We characterized the effects of temperature elevation on the common Red Sea sponge *Diacarnus erythraeanus*, as a holobiont, while comparing the responses of shallow vs. mesophotic populations. The results indicate that a temperature rise of up to  $2^\circ\text{C}$  ("moderate"), as predicted for the Gulf of Eilat/Aqaba in 2100 (Fine et al., 2013; Hoegh-Guldberg et al., 2014), will probably not have a detrimental effect on the *D. erythraeanus* holobiont. In addition, this sponge exhibited a high stress tolerance under the acute treatment as well, suggesting its survival even under the extremest climate scenarios for 2100 in this region. Moreover, while no difference in sponge survival or any external noticeable effect was detected, irrespective of collection depth, the microbiome of shallow vs. their mesophotic counterparts, responded differently. Although, during the 5-month regeneration period, the microbiomes of mesophotic and shallow-water individuals largely converged in diversity and composition, it is likely that





characteristic members of each persisted in low abundance, proliferating differentially during the long-term acute temperature treatment to produce differential responses depending on depth origin.

## 4.1 Sponge physiological responses imply a tolerance to elevated temperatures

Our results suggest that a temperature increase of up to 6°C for 35 days might not affect the survival of *D. erythraeanus*, which survived throughout the experiment under the different thermal treatments. However, the experiment was conducted during the autumn, when the ambient temperature was generally lower (mean 5 m: 23.4°C, 45 m: 23.2°C) than the maximum temperature that these sponges experience seasonally during the summer (max temp 5 m: 28.9°C, 45 m: 27.1°C, Shlesinger et al., 2018; Liberman et al., 2022). Therefore, although the moderate temperature treatment (~26°C) exceeded the typical autumn temperatures that these sponges encounter, it was not beyond the temperature range they are exposed to throughout the year. Thus, it is not surprising that the moderate treatment had only a minor effect on the sponge physiology. In contrast, the acute treatment (~30°C) reached above the maximum temperature in present-day to which these sponges are exposed locally during the summer (see above). Although all the clones survived the experimental increased temperatures, changes were observed in their respiration and in their microbial composition. The respiration rate of *D. erythraeanus* clones in the acute treatment was significantly higher than those in the ambient and moderate treatments (Figure 2A, Table 1). Congruent with our findings, increased respiration rates have previously been reported for several sponge species exposed *in situ* to thermal stress (Coma, 2002), as well as in aquaria experimental systems (Strand et al., 2017; Beepat et al., 2020). It has been suggested that increased respiration in sponges acts as a coping mechanism under elevated temperature in order to maintain cellular homeostasis through the activation of intra-cellular repair and protection processes (Guzman and Conaco, 2016). This could also be the result of an increased carbon fixation rate by the sponge microsymbionts (Fang et al., 2014). Congruent with the respiration rate, in the middle of the experiment (days 15–20), the oxygen removal was significantly higher in the acute treatment compared to the ambient and moderate treatments. However, by the end of the experiment (days 28–35), the oxygen removal of sponges in the acute treatment had decreased and was similar to that of the ambient treatment sponges (Figure 2B, Table 1). This could imply, on the one hand, that *D. erythraeanus* might have become adapted to the high temperature stress; or, on the other hand, that the prolonged exposure to an elevated temperature might have resulted in a cumulative thermal stress, followed by physiological dysfunctioning (Rodolfo-Metalpa et al., 2014), with no external signs. Similarly, the respiration rate of the sponge *Cliona orientalis* was shown to be generally higher under an intermediate temperature stress (compared to the control), while sponges that were exposed to the high temperature treatment (32°C) and were bleached, presented a respiration rate similar to that of the control

(Ramsby et al., 2018). Conversely, our *D. erythraeanus* specimens revealed no external signs of stress and their buoyant weight did not change during the experiment (Table 1), supporting the assumption that an adaptation mechanism, rather than sensitivity, underlay the decrease in the sponge's oxygen removal consumption under the acute temperature treatment. It is possible, however, that the high spicule and collagen content of this species (Kelly and Samaai, 2002) might have obscured possible changes in tissue weight. Another possibility is that under a longer stress period (over 35 days), this sponge would eventually succumb to disease and possibly mortality. Further focused metabolic analysis, such as examination of the tissue metabolic profile (Strand et al., 2017; Ramsby et al., 2018) or gene expression analysis (Fan et al., 2013; Guzman and Conaco, 2016), could shed additional light on the sponge's physiological condition following heat stress.

In addition, our findings indicate that the respiration rate of shallow and mesophotic sponges were similarly affected by the rise in temperature (Figure 2A, Table 1). A similar phenomenon was reported from four coral species in Bermuda, which demonstrated a similar thermal tolerance (including respiration rate) by both mesophotic and shallow individuals (Gould et al., 2021). The respiration rate of the Mediterranean sponge *Chondrosia reniformis* was also found to be depth-independent (Gökalp et al., 2020). Since both shallow and mesophotic individuals of *D. erythraeanus* exhibited similar rates of respiration under elevated temperature, it is plausible to assume that, in the case of *D. erythraeanus*, local adaptation toward thermal stress did not take place, at least at the sponge-host level. The latter conclusion is reinforced when considering the potential for vertical connectivity between the shallow and mesophotic populations in the Gulf of Aqaba (Berenshtein, 2018).

## 4.2 Sponge microbiome response to elevated temperature

### 4.2.1 Reduction in photo-symbiont functioning

Although none of the *D. Erythraeanus* clones bleached, a significant decline in photosynthetic efficiency ( $\Delta F/FM$ ) was observed in the sponges under acute temperature treatment (Figure 2C, Table 1). A decrease in photosynthesis in organisms experiencing heat stress has been documented in multiple studies on sponges (Cebrian et al., 2011; Bennett et al., 2017; Ramsby et al., 2018; Beepat et al., 2020). The reduced functioning of photosymbionts could further result in a potential reduction in the translocation of photosynthesis-derived products from the photosymbionts to the sponge-host (Wilkinson and Fay, 1979). This might severely affect the sponge's energetic budget and threaten its continued survival. Various mechanisms have been suggested to compensate the host's nutritional loss following a decline in photosymbiont functioning. For example, the high survivorship of the bleached sponge *Xestospongia muta* was attributed to its low nutritional dependence on photosymbionts, and greater reliance on heterotrophic sources (McMurray et al., 2011). Another mechanism was demonstrated in bleached individuals of the sponge *Cliona orientalis*, which used its lipid

stores to overcome periods of low or no photoautotrophic-derived food-sources (Fang et al., 2014). Thus, it can be assumed that similar mechanisms are also involved in the case of *D. Erythraeanus*, enabling its high survival rate during a reduction in photosynthetic-derived nutrition sources.

#### 4.2.2 Mesophotic and shallow microbial communities: general description

The bacterial community composition of the wild-type mesophotic sponges differed significantly from that of the shallow-reef sponges (Figure 4A, Table 2). These differences were mainly attributed to the relative abundance of the bacterial orders rather than their identity, which was similar at all depths (Figure 3A). These findings are in line with previous studies that compared microbial assemblages in relation to depth, and revealed similar patterns (Morrow et al., 2016; Indraningrat et al., 2022). Along the shallow to mesophotic depths the physical, biochemical, and biotic factors undergo change (Lesser et al., 2018). Some of those factors have been identified as meaningful drivers in shaping microbial communities (Busch et al., 2022). For example, temperature and light intensity decrease along shallow to mesophotic depths, while nutrient concentration is usually higher (Kahng et al., 2017; Lesser et al., 2018). All of those factors were previously indicated to drive changes in microbial communities composition (Olson and Gao, 2013; Morrow et al., 2016; Steffen et al., 2022). The shift in the bacterial composition with depth could therefore indicate the holobiont's functional adjustment to the changing ecological conditions along this depth range (shallow and mesophotic). In the Gulf of Aqaba, light availability, temperature, sedimentation rate, and the hydrodynamic regimes differ between shallow and mesophotic habitats (Eyal et al., 2019). These environmental variations could significantly affect the microbial community of *D. erythraeanus* populations from different depths. Many bacterial members have been found to change in abundance between the wild-type shallow and mesophotic sponges. For example, ASV members of the order Caldilineales (Chloroflexi) were enriched in the wild-shallow samples, as found for the sponges *X. muta* and *Agelas sventres* (Indraningrat et al., 2022). In the mesophotic sponges, a higher abundance of Nitrospirota bacteria was found (Figure 3A). Considering the reduced light availability at the mesophotic depths (Kahng et al., 2019), it is plausible that the increased abundance of Nitrospirota could constitute a sort of "metabolic compensation", whereby the photoautotrophy efficiency is reduced. In addition, sponges from the shallow and the mesophotic waters in the pre-experiment (post-acclimation) sampling possessed similar bacterial communities, as opposed to the distinct bacterial communities found in the wild-type shallow and mesophotic sponges, sampled immediately after collection (Figure 4A, Table 2). However, because the pre-experiment sampling occurred after a recovery (acclimation) period (~5 months) of the sponges at 10 m depth, it is possible that the transplantation of both the mesophotic and the shallow samples to the (shallow) recovery site, induced a microbiome transitioning towards microbial communities resembling those of the transplanted site. These

results emphasize the flexibility of microorganisms in rapidly adapting to environmental changes (Reshef et al., 2006; Lesser et al., 2020; Voolstra and Ziegler, 2020; Maldonado et al., 2021; Vargas et al., 2021), while facilitating their sponge-host's adjustment to the new conditions.

#### 4.2.3 Microbiome adjustments under elevated temperature

Sponges rely on intimate associations with diverse microorganisms (Thomas et al., 2016; Webster and Thomas, 2016), which fulfill various crucial roles in the host's functioning and stability (Pita et al., 2018; Engelberts et al., 2020; Moreno-Pino et al., 2020; Posadas et al., 2022; Schmittmann et al., 2022). In the present study, a meaningful change in the microbial community was observed only at the end of the experiment ( $T_f$ ), and mainly under the acute temperature treatment (Figures 3-6, Tables 1, 2). Changes in microbial community diversity and composition under heat stress often result in deterioration of the holobiont's physical condition, as previously documented in numerous sponge species (Fan et al., 2013; Lesser et al., 2016; Ramsby et al., 2018; Rubio-Portillo et al., 2021). In the current study, however, the external appearance of *D. erythraeanus* remained stable throughout the experiment, with no visible signs of bleaching or necrosis. It is thus plausible that the changes in the microbial community were part of a resilience process rather than a collapse (Pita et al., 2018; Vargas et al., 2021).

Our results indicate that under acute thermal stress the microbial community of *D. erythraeanus* undergoes restructuring, mostly through a change in the relative abundance of the ASVs (Figures 3B, 4B, 5). We found that while the increased abundance of some bacterial members might reflect sponge-host stress, other bacteria were found to potentially possess essential functions that could support sponge-host resilience under the acute elevated temperature. For example, the SAR202 clade (Chloroflexi) in sponges was suggested to have a potential for DOM recalcitrant degradation. In addition, this clade possesses biosynthetic pathways for cofactor biosynthesis (Thiamine) (Bayer et al., 2018), possibly supporting the host's metabolism. SAR202 significantly decreased in abundance in the acute heat treatment sponges at the end of the experiment (LFC,  $p < 0.01$ , Figure 5), possibly reflecting a nutritional impediment to the sponge-host. Other bacteria that might have negative effects on their sponge-host are the Neisseria (ASV153), which significantly increased in abundance under the acute heat treatment (LFC,  $p < 0.01$ , Figure 5). Neisseria are recognized as pathogenic bacteria (Tinsley and Nassif, 1996; Livorsi et al., 2011) and were found to be predominant in coral tissue invaded by sponges (Thinesh et al., 2020). Nevertheless, except of Neisseria, no other pathogenic bacteria were detected in the microbiome of the acute or moderate temperature treatment sponges. As opposed to that, the members of the families Cyanobiaceae (ASV49), Endozoicomonadaceae and Nitrospira significantly increased in abundance in the acute-stressed sponges (ASV91, ASV63 and ASV6, LFC,  $p < 0.01$ ), possibly possessing key functions for the sponge-host's stability under stress, such as increased carbon supply and nutrient cycling functions (Raina et al., 2009; Fiore

et al., 2013; Morrow et al., 2015; Neave et al., 2016; Moitinho-Silva et al., 2017; Zhang et al., 2019).

Similarly, a dynamic relationship between the host and its associated microbiome under environmental stress, known as the “Coral probiotic hypothesis” (Reshef et al., 2006), was suggested to promote the coral holobiont’s resilience. In sponges, several studies reported a microbial shift following environmental stress, suggesting that these changes are involved in the host resilience (Morrow et al., 2015; Ribes et al., 2016; Webster and Reusch, 2017; Ribeiro et al., 2021; Vargas et al., 2021).

#### 4.2.4 Possible different coping mechanisms underly the shallow and mesophotic sponges’ responses to elevated temperature

The microbial response of shallow sponges significantly differed from that of their mesophotic counterparts under elevated temperature stress. While the microbial diversity indices of the shallow sponges decreased throughout the experiment under the acute temperature treatment, those of the mesophotic sponges remained stable and similar to those of the ambient treatment sponges (Table 2; Supplementary Table 3A). The flexibility in microbial community response of the shallow and mesophotic sponges to elevated temperatures, suggests the existence of different underlying coping mechanisms for each sponge population (Guzman and Conaco, 2016). Whereas at the mesophotic depths the environmental conditions are relatively stable, shallow sponges (and hence their microbiome) often encounter environmental disturbances, such as increased temperature fluctuations (Lesser et al., 2009; Bongaerts et al., 2010; Kahng et al., 2010). A prior exposure to environmental stress (e.g., elevated temperatures) could improve the organism’s response to subsequent and more extreme exposures (Guzman and Conaco, 2016; Hilker et al., 2016; Hackerott et al., 2021). For example, in the sponge *Haliclona tubifera*, heat stress induced gene activation related to innate immunity and various processes such as initiation of cellular damage repair and heat shock proteins pathways (Guzman and Conaco, 2016). Likewise, the survivorship of the sponge *Neopetrosia compacta* to acidification and warming stress was related to changes in the sponge-host immune functions, microbiome stability and increased abundance of beneficial microbial groups (Posadas et al., 2022). Therefore, under chronic or sequentially occurring environmental stresses, microbial adjustments might act as a key feature in a sponge acclimation (Ribes et al., 2016; Pita et al., 2018; Turon et al., 2018; Voolstra and Ziegler, 2020; Marangon et al., 2021; Ribeiro et al., 2021; Vargas et al., 2021; Posadas et al., 2022; Schmittmann et al., 2022) and possibly even lead to population adaptation (Webster and Reusch, 2017). Thus, the observed shift in the microbial diversity indices of the shallow sponges in the present study, could be an expression of acclimatization or adaptation, following previous events of exposure to elevated temperatures in the shallow waters. In contrast, the stability of the microbial diversity indices in the mesophotic sponges, might suggest that their healthy condition was maintained by means of resistance mechanisms. Microbial

resistance is considered to occur when a microbial community remains unchanged following perturbation (Moya and Ferrer, 2016; Zaneveld et al., 2017). Nevertheless, changes in the relative abundance of the microbial community were observed for both, the shallow and mesophotic sponges under elevated temperatures (Figures 4–6), indicating that both are resilient to such increases (Allison and Martiny, 2008; Comte et al., 2013).

Finally, our results indicate that the sponge-host individual (the original clonal individual sponge) was the most meaningful factor in shaping the microbial community’s structure, irrespective of the other factors examined in the current study (temperature, time, depth). Correspondingly, host genotype was previously suggested to act as a main factor in shaping the microbial assemblage of a sponge’s microbiome (Easson and Thacker, 2014; Reveillaud et al., 2014; Chaib De Mares et al., 2017; Glasl et al., 2018).

## 5 Conclusion

We examined the holobiont sponge *D. erythraeanus*’s response to elevated temperature. The findings indicate that both shallow and mesophotic individuals of *D. erythraeanus* are highly tolerant to moderate temperature elevation of 2°C, as predicted for 2100 in the Red Sea (Hoegh-Guldberg et al., 2014), and acute heat stress of 6°C above the ambient. Furthermore, we posit that its high survival rate coincides with microbial adjustments, suggesting the essential role of the microbiome to the host’s adaptation and stability when facing significant environmental stressors. We found that both shallow and mesophotic sponges are tolerant to heat stress, hence, our hypothesis that mesophotic sponges will be less resilient to elevated temperature was not supported. However, our results suggest that their underlying coping mechanisms might differ. We argue that while *D. erythraeanus* mesophotic sponges are resistant to heat stress, their shallow water counterparts might have become adapted to elevated temperatures, following previous exposure to increased heat events in the shallow waters. Therefore, these results cast doubt on the potential function of mesophotic coral ecosystems (MCEs) as thermal refugia for some sponge species. While both shallow and mesophotic sponge individuals demonstrated high levels of heat tolerance, their variability in the microbial response to heat stress might reflect local ecological adaptation and questions the validity of MCEs as a refuge for shallow populations. The variability in the responses of these populations further highlights the importance of uncovering the mechanisms that structure the sponge-microbiome interactions, particularly in regard to the predicted climate change scenarios.

## Data availability statement

The datasets presented in this study can be found in online repositories. The names of the repository/repositories and accession number(s) can be found below: <https://www.ncbi.nlm.nih.gov/bioproject>, PRJNA931995.

## Author contributions

LR-N, LG, SS and MI conceived the idea. LR wrote the manuscript. All authors read, critically reviewed, and edited the manuscript. RM assisted with the physiological measurements and analysis. ZL conducted the samples sequencing. All authors contributed to the article and approved the submitted version.

## Funding

This research was supported by the ISF-NSFC joint research program (Grant No. 2577/18 to MI & 31861143020 to ZL). LR was supported by the *Lev Tzion* scholarship from the Israeli council for higher education.

## Acknowledgments

We acknowledge the invaluable support from the M. Fine Lab in providing access to the experimental system. Our special thanks go to Komet and T. Yamin for their assistance in maintaining the experiment. We would also like to express our sincere gratitude to the editor and reviewers for their major contributions in improving this manuscript. We appreciate N. Paz for the scientific editorial support and the lab members of Ilan's lab for their support in both laboratory and fieldwork. Our gratitude also extends to the staff of the R/V Sam Rothberg and the Interuniversity Institute for Marine

Sciences in Eilat (IUI) for their ongoing support and access to facilities. Finally, we would like to thank Dr. M. Lalar and Prof. L. Steindler for their inspiring guidance in the result interpretation and microbiome analysis and Dr. T. Shlesinger for generously sharing the temperature measurements with us.

## Conflict of interest

The authors declare that the research was conducted in the absence of any commercial or financial relationships that could be construed as a potential conflict of interest.

## Publisher's note

All claims expressed in this article are solely those of the authors and do not necessarily represent those of their affiliated organizations, or those of the publisher, the editors and the reviewers. Any product that may be evaluated in this article, or claim that may be made by its manufacturer, is not guaranteed or endorsed by the publisher.

## Supplementary material

The Supplementary Material for this article can be found online at: <https://www.frontiersin.org/articles/10.3389/fmars.2023.1161648/full#supplementary-material>

## References

- Allaire, J. (2012). *RStudio: integrated development environment for r*. (Boston, MA: RStudio Inc) 537, 538.
- Allison, S. D., and Martiny, J. B. (2008). Resistance, resilience, and redundancy in microbial communities. *Proc. Natl. Acad. Sci.* 105 (supplement\_1), 11512–11519. doi: 10.1073/pnas.0801925105
- Apprill, A., McNally, S., Parsons, R., and Weber, L. (2015). Minor revision to V4 region SSU rRNA 806R gene primer greatly increases detection of SAR11 bacterioplankton. *Aquat. Microbial Ecol.* 75 (2), 129–137. doi: 10.3354/ame01753
- Baker, E., Thygesen, K., Harris, P., Andradi-Brown, D., Appeldoorn, R. S., Ballantine, D., et al. (2016). Mesophotic coral ecosystems: a lifeboat for coral reefs? *The United Nations Environment Programme (UNEP) and GRID-Arendal, Nairobi and Arendal*, 98.
- Bayer, K., Jahn, M. T., Slaby, B. M., Moitinho-Silva, L., and Hentschel, U. (2018). Marine sponges as chloroflexi hot spots: genomic insights and high-resolution visualization of an abundant and diverse symbiotic clade. *MSystems* 3 (6), e00150–e00118. doi: 10.1128/mSystems.00150-18
- Beepat, S. S., Davy, S. K., Woods, L., and Bell, J. J. (2020). Short-term responses of tropical lagoon sponges to elevated temperature and nitrate. *Mar. Environ. Res.* 157, 104922. doi: 10.1016/j.marenvres.2020.104922
- Bell, J. J. (2008). The functional roles of marine sponges. *Estuarine Coast. Shelf Sci.* 79 (3), 341–353. doi: 10.1016/j.ecss.2008.05.002
- Bellworthy, J., and Fine, M. (2018). The red Sea simulator: a high-precision climate change mesocosm with automated monitoring for the long-term study of coral reef organisms. *Limnology Oceanography: Methods* 16 (6), 367–375. doi: 10.1002/lom3.10250
- Bennett, H. M., Altenrath, C., Woods, L., Davy, S. K., Webster, N. S., and Bell, J. J. (2017). Interactive effects of temperature and pCO<sub>2</sub> on sponges: from the cradle to the grave. *Global Change Biol.* 23 (5), 2031–2046. doi: 10.1111/gcb.13474
- Berenshtein, I. (2018). "Connectivity in the gulf of Aqaba/Eilat," in *Israel Nature and parks authority report*, 27. doi: 10.13140/rg.2.2.17500.64643
- Birkeland, C. (2019). "Global status of coral reefs: in combination, disturbances and stressors become ratchets," in *World seas: an environmental evaluation* (Amsterdam: Elsevier), 35–56.
- Bongaerts, P., Ridgway, T., Sampayo, E., and Hoegh-Guldberg, O. (2010). Assessing the 'deep reef refugia' hypothesis: focus on Caribbean reefs. *Coral Reefs* 29 (2), 309–327. doi: 10.1007/s00338-009-0581-x
- Bosch, T. C., and McFall-Ngai, M. J. (2011). Metaorganisms as the new frontier. *Zoology* 114 (4), 185–190. doi: 10.1016/j.zool.2011.04.001
- Busch, K., Slaby, B. M., Bach, W., Boetius, A., Clefsen, I., Colaço, A., et al. (2022). Biodiversity, environmental drivers, and sustainability of the global deep-sea sponge microbiome. *Nat. Commun.* 13 (1), 1–16. doi: 10.1038/s41467-022-32684-4
- Callahan, B. J., McMurdie, P. J., Rosen, M. J., Han, A. W., Johnson, A. J. A., and Holmes, S. P. (2016). DADA2: high-resolution sample inference from illumina amplicon data. *Nat. Methods* 13 (7), 581–583. doi: 10.1038/nmeth.3869
- Cebrian, E., Uriz, M. J., Garrabou, J., and Ballesteros, E. (2011). Sponge mass mortalities in a warming Mediterranean Sea: are cyanobacteria-harboring species worse off? *PloS One* 6 (6), e20211. doi: 10.1371/journal.pone.0020211
- Chaib De Mares, M., Sipkema, D., Huang, S., Bunk, B., Overmann, J., and Van Elsas, J. D. (2017). Host specificity for bacterial, archaeal and fungal communities determined for high- and low-microbial abundance sponge species in two genera. *Front. Microbiol.* 8, 2560. doi: 10.3389/fmicb.2017.02560
- Coma, R. (2002). Seasonality of *in situ* respiration rate in three temperate benthic suspension feeders. *Limnology oceanography* 47 (1), 324–331. doi: 10.4319/lo.2002.47.1.0324
- Comte, J., Fautoux, L., and Giorgio, P. (2013). Links between metabolic plasticity and functional redundancy in freshwater bacterioplankton communities. *Front. Microbiol.* 4, 112. doi: 10.3389/fmicb.2013.00112
- Diaz, M. C., and Rützler, K. (2001). Sponges: an essential component of Caribbean coral reefs. *Bull. Mar. Sci.* 69 (2), 535–546.



- Easson, C. G., and Thacker, R. W. (2014). Phylogenetic signal in the community structure of host-specific microbiomes of tropical marine sponges. *Front. Microbiol.* 5, 532. doi: 10.3389/fmicb.2014.00532
- Engelberts, J. P., Robbins, S. J., de Goeij, J. M., Aranda, M., Bell, S. C., and Webster, N. S. (2020). Characterization of a sponge microbiome using an integrative genome-centric approach. *ISME J.* 14 (5), 1100–1110. doi: 10.1038/s41396-020-0591-9
- Eyal, G., Tamir, R., Kramer, N., Eyal-Shaham, L., and Loya, Y. (2019). “The red sea: Israel,” in *Mesophotic coral ecosystems*. Eds. Y. Loya, K. A. Puglise and T. C. L. Bridge (New York: Springer), 199–214.
- Fan, L., Liu, M., Simister, R., Webster, N. S., and Thomas, T. (2013). Marine microbial symbiosis heats up: the phylogenetic and functional response of a sponge holobiont to thermal stress. *ISME J.* 7 (5), 991. doi: 10.1038/ismej.2012.165
- Fang, J. K., Schönberg, C. H., Mello-Athayde, M. A., Hoegh-Guldberg, O., and Dove, S. (2014). Effects of ocean warming and acidification on the energy budget of an excavating sponge. *Global Change Biol.* 20 (4), 1043–1054. doi: 10.1111/gcb.12369
- Fine, M., Gildor, H., and Genin, A. (2013). A coral reef refuge in the red Sea. *Global Change Biol.* 19 (12), 3640–3647. doi: 10.1111/gcb.12356
- Fiore, C. L., Jarett, J. K., and Lesser, M. P. (2013). Symbiotic prokaryotic communities from different populations of the giant barrel sponge, *Xestospongia muta*. *Microbiologyopen* 2 (6), 938–952. doi: 10.1002/mbo3.135
- Forster, P., Storelvmo, T., Armour, K., Collins, W., Dufresne, J. L., Frame, D., et al. (2021). “Earth’s energy budget, climate feedbacks, and climate sensitivity,” in *Climate change 2021: the physical science basis. contribution of working group I to the sixth assessment report of the intergovernmental panel on climate change*. Eds. V. Masson-Delmotte, et al (Cambridge Univ. Press), 923–1054.
- Frölicher, T. L., Fischer, E. M., and Gruber, N. (2018). Marine heatwaves under global warming. *Nature* 560 (7718), 360–364. doi: 10.1038/s41586-018-0383-9
- Frossard, J., and Renaud, O. (2021). Permutation tests for regression, ANOVA, and comparison of signals: the permuco package. *J. Stat. Software* 99, 1–32. doi: 10.18637/jss.v099.i15
- Glas, B., Smith, C. E., Bourne, D. G., and Webster, N. S. (2018). Exploring the diversity-stability paradigm using sponge microbial communities. *Sci. Rep.* 8 (1), 1–9. doi: 10.1038/s41598-018-26641-9
- Gökulp, M., Kooistra, T., Rocha, M. S., Silva, T. H., Osinga, R., Murk, A. J., et al. (2020). The effect of depth on the morphology, bacterial clearance, and respiration of the mediterranean sponge *chondrosia reniformis* (Nardo 1847). *Mar. Drugs* 18 (7), 358. doi: 10.3390/md18070358
- Gould, K., Bruno, J. F., Ju, R., and Goodbody-Gringley, G. (2021). Upper-mesophotic and shallow reef corals exhibit similar thermal tolerance, sensitivity and optima. *Coral Reefs* 40 (3), 907–920. doi: 10.1007/s00338-021-02095-w
- Grottoli, A. G., Tchernov, D., and Winters, G. (2017). Physiological and biogeochemical responses of super-corals to thermal stress from the northern gulf of aqaba, red Sea. *Front. Mar. Sci.* 215. doi: 10.3389/fmars.2017.00215
- Guzman, C., and Conaco, C. (2016). Gene expression dynamics accompanying the sponge thermal stress response. *PLoS One* 11 (10), e0165368. doi: 10.1371/journal.pone.0165368
- Hackerott, S., Martell, H. A., and Eirin-Lopez, J. M. (2021). Coral environmental memory: causes, mechanisms, and consequences for future reefs. *Trends Ecol. Evol.* 36 (11), 1011–1023. doi: 10.1016/j.tree.2021.06.014
- Hentschel, U., Piel, J., Degnan, S. M., and Taylor, M. W. (2012). Genomic insights into the marine sponge microbiome. *Nat. Rev. Microbiol.* 10 (9), 641–654. doi: 10.1038/nrmicro2839
- Hilker, M., Schwachtje, J., Baier, M., Balazadeh, S., Bäurle, I., Geiselhardt, S., et al. (2016). Priming and memory of stress responses in organisms lacking a nervous system. *Biol. Rev.* 91 (4), 1118–1133. doi: 10.1111/brv.12215
- Hoegh-Guldberg, O., Cai, R., Poloczanska, E. S., Brewer, P. G., Sundby, S., Hilmi, K., et al. (2014). “The ocean,” in *Climate change 2014: impacts, adaptation, and vulnerability. part b: regional aspects. contribution of working group II to the fifth assessment report of the intergovernmental panel on climate change*. Eds. V. R. Barros, C. B. Field, D. J. Dokken, M. D. Mastrandrea, K. J. Mach, T. E. Bilir, M. Chatterjee, K. L. Ebi, Y. O. Estrada, R. C. Genova, B. Girma, E. S. Kissel, A. N. Levy, S. MacCracken, P. R. Mastrandrea and L. L. White (Cambridge, United Kingdom and New York, NY, USA: Cambridge University Press), 1655–1731.
- Hoegh-Guldberg, O., Mumby, P. J., Hooten, A. J., Steneck, R. S., Greenfield, P., Gomez, E., et al. (2007). Coral reefs under rapid climate change and ocean acidification. *science* 318 (5857), 1737–1742. doi: 10.1126/science.1152509
- Hughes, T. P., Anderson, K. D., Connolly, S. R., Heron, S. F., Kerry, J. T., Lough, J. M., et al. (2018a). Spatial and temporal patterns of mass bleaching of corals in the anthropocene. *Science* 359 (6371), 80–83. doi: 10.1126/science.aan8048
- Hughes, T. P., Kerry, J. T., Baird, A. H., Connolly, S. R., Dietzel, A., Eakin, C. M., et al. (2018b). Global warming transforms coral reef assemblages. *Nature* 556 (7702), 492–496. doi: 10.1038/s41586-018-0041-2
- Idan, T., Goren, L., Shefer, S., and Ilan, M. (2020). Sponges in a changing climate: survival of *Agelas oroides* in a warming Mediterranean Sea. *Front. Mar. Science*. 7. doi: 10.3389/fmars.2020.603593
- Indraningrat, A. A. G., Steinert, G., Becking, L. E., Mueller, B., de Goeij, J. M., Smidt, H., et al. (2022). Sponge holobionts shift their prokaryotic communities and antimicrobial activity from shallow to lower mesophotic depths. *Antonie van Leeuwenhoek* 115, 1265–1283. doi: 10.1007/s10482-022-01770-4
- IPCC (2023). Summary for policymakers. In *limte change 2023: synthesis report. A report of the intergovernmental panel on climate change. Contribution of working groups I, II and III to the sixth assessment report of the intergovernmental panel on climate change* Core Writing Team, H. Lee, J. Romero eds. (Geneva, Switzerland: IPCC), 36. (in press).
- Kahng, S. E., Akkaynak, D., Shlesinger, T., Hochberg, E. J., Wiedenmann, J., Tamir, R., et al. (2019). “Light, temperature, photosynthesis, heterotrophy, and the lower depth limits of mesophotic coral ecosystems,” in *Mesophotic Coral Ecosystems. Coral Reefs of the World*. Eds. Y. Loya, K. Puglise and T. Bridge (Cham: Springer) 12, 801–828.
- Kahng, S., Copus, J. M., and Wagner, D. (2017). Mesophotic coral ecosystems. *Mar. Anim. forests* 10, 978–973. doi: 10.1007/978-3-319-21012-4\_4
- Kahng, S., Garcia-Sais, J., Spalding, H., Brokovich, E., Wagner, D., Weil, E., et al. (2010). Community ecology of mesophotic coral reef ecosystems. *Coral Reefs* 29 (2), 255–275. doi: 10.1007/s00338-010-0593-6
- Kassambara, A., and Kassambara, M. A. (2020). “Package ‘ggpubr,’” in *R package version 0.1.6*.
- Kelly, M., and Samaai, T. (2002). “Family podospongiidae de laubenfel,” in *Systema Porifera* (New York: Springer), 694–702. doi: 10.1007/978-1-4615-0747-5\_75
- Kelly-Borges, M., and Vacelet, J. (1995). A revision of *Diacamus* Burton and *Negombata* de laubenfels (Demospongiae: Iatrunculiidae) with descriptions of new species from the west central pacific and the red Sea. *Memoirs-Queensland Museum* 38, 477–504.
- Kramer, N., Eyal, G., Tamir, R., and Loya, Y. (2019). Upper mesophotic depths in the coral reefs of elat, red Sea, offer suitable refuge grounds for coral settlement. *Sci. Rep.* 9 (1), 1–12. doi: 10.1038/s41598-019-38795-1
- Lahti, L., and Shetty, S. (2018). *Introduction to the microbiome r package*.
- Lesser, M. P., Fiore, C., Slattery, M., and Zaneveld, J. (2016). Climate change stressors destabilize the microbiome of the Caribbean barrel sponge, *Xestospongia muta*. *J. Exp. Mar. Biol. Ecol.* 475, 11–18. doi: 10.1016/j.jembe.2015.11.004
- Lesser, M. P., Mueller, B., Pankey, M. S., Macartney, K. J., Slattery, M., and de Goeij, J. M. (2020). Depth-dependent detritus production in the sponge, *Halysarca caerulea*. *Limnology Oceanography* 65 (6), 1200–1216. doi: 10.1002/lno.11384
- Lesser, M. P., Slattery, M., and Leichter, J. J. (2009). Ecology of mesophotic coral reefs. *J. Exp. Mar. Biol. Ecol.* 375 (1–2), 1–8. doi: 10.1016/j.jembe.2009.05.009
- Lesser, M. P., Slattery, M., and Mobley, C. D. (2018). Biodiversity and functional ecology of mesophotic coral reefs. *Annu. Rev. Ecology Systematics* 49 (1), 49–71. doi: 10.1146/annurev-ecolsys-110617-062423
- Liberman, R., Shlesinger, T., Loya, Y., and Benayahu, Y. (2022). Soft coral reproductive phenology along a depth gradient: can “going deeper” provide a viable refuge? *Ecology* 103 (9), e3760. doi: 10.1002/ecy.3760
- Livorsi, D. J., Stenehjem, E., and Stephens, D. S. (2011). Virulence factors of gram-negative bacteria in sepsis with a focus on *Neisseria meningitidis*. *Sepsis-Pro-Inflammatory Anti-Inflammatory Responses* 17, 31–47. doi: 10.1159/000324008
- Love, M. I., Huber, W., and Anders, S. (2014). Moderated estimation of fold change and dispersion for RNA-seq data with DESeq2. *Genome Biol.* 15 (12), 1–21. doi: 10.1186/s13059-014-0550-8
- Loya, Y. (2004). “The coral reefs of elat—past, present and future: three decades of coral community structure studies,” in (Eds.) E. Rosenberg and Y. Loya *Coral Reef Health and Disease* (Berlin: Springer), 1–34.
- Luter, H. M., Andersen, M., Versteegen, E., Laffy, P., Uthicke, S., Bell, J. J., et al. (2020). Cross-generational effects of climate change on the microbiome of a photosynthetic sponge. *Environ. Microbiol.* 22 (11), 4732–4744. doi: 10.1111/1462-2920.15222
- Maldonado, M., López-Acosta, M., Busch, K., Slaby, B. M., Bayer, K., Beazley, L., et al. (2021). A microbial nitrogen engine modulated by bacteriosyncytia in hexactinellid sponges: ecological implications for deep-sea communities. *Front. Mar. Sci.* 8, 638505. doi: 10.3389/fmars.2021.638505
- Mangiafico, S., and Mangiafico, M. S. (2017). Package ‘rcompanion’. *Cran Repos* 20, 1–71. Available at: <https://CRAN.R-project.org/package=rcompanion>.
- Marangon, E., Laffy, P. W., Bourne, D. G., and Webster, N. S. (2021). Microbiome-mediated mechanisms contributing to the environmental tolerance of reef invertebrate species. *Mar. Biol.* 168 (6), 1–18. doi: 10.1007/s00227-021-03893-0
- McMurdie, P. J., and Holmes, S. (2013). Phyloseq: an R package for reproducible interactive analysis and graphics of microbiome census data. *PLoS One* 8 (4), e61217. doi: 10.1371/journal.pone.0061217
- McMurray, S. E., Blum, J. E., Leichter, J. J., and Pawlik, J. R. (2011). Bleaching of the giant barrel sponge *Xestospongia muta* in the Florida keys. *Limnology Oceanography* 56 (6), 2243–2250. doi: 10.4319/lo.2011.56.6.2243
- Moitinho-Silva, L., Diez-Vives, C., Batani, G., Esteves, A. I., Jahn, M. T., and Thomas, T. (2017). Integrated metabolism in sponge-microbe symbiosis revealed by genome-centered metatranscriptomics. *ISME J.* 11 (7), 1651–1666. doi: 10.1038/ismej.2017.25
- Moreno-Pino, M., Cristi, A., Gillooly, J. F., and Trefault, N. (2020). Characterizing the microbiomes of Antarctic sponges: a functional metagenomic approach. *Sci. Rep.* 10 (1), 1–12. doi: 10.1038/s41598-020-57464-2
- Morganti, T. M., Ribes, M., Yahel, G., and Coma, R. (2019). Size is the major determinant of pumping rates in marine sponges. *Front. Physiol.* 10. doi: 10.3389/fphys.2019.01474
- Morrow, K. M., Bourne, D. G., Humphrey, C., Botté, E. S., Laffy, P., Zaneveld, J., et al. (2015). Natural volcanic CO<sub>2</sub> seeps reveal future trajectories for host-microbial associations in corals and sponges. *ISME J.* 9 (4), 894–908. doi: 10.1038/ismej.2014.188

- Morrow, K. M., Fiore, C. L., and Lesser, M. P. (2016). Environmental drivers of microbial community shifts in the giant barrel sponge, *Xestospongia muta*, over a shallow to mesophotic depth gradient. *Environ. Microbiol.* 18 (6), 2025–2038. doi: 10.1111/1462-2920.13226
- Moskovish, R., Diga, R., Ilan, M., and Yahel, G. (2022). High variability and enhanced nocturnal oxygen uptake in coral-reef sponges. *Limnol. Oceanogr.* doi: 10.1002/lno.12361
- Moya, A., and Ferrer, M. (2016). Functional redundancy-induced stability of gut microbiota subjected to disturbance. *Trends Microbiol.* 24 (5), 402–413. doi: 10.1016/j.tim.2016.02.002
- Muñiz-Castillo, A. L., Rivera-Sosa, A., Chollett, I., Eakin, C. M., Andrade-Gómez, L., McField, M., et al. (2019). Three decades of heat stress exposure in Caribbean coral reefs: a new regional delineation to enhance conservation. *Sci. Rep.* 9 (1), 1–14. doi: 10.1038/s41598-019-47307-0
- Neal, B., Condit, C., Liu, G., dos Santos, S., Kahru, M., Mitchell, B., et al. (2014). When depth is no refuge: cumulative thermal stress increases with depth in bocas del toro, Panama. *Coral Reefs* 33, 193–205. doi: 10.1007/s00338-013-1081-6
- Neave, M. J., Apprill, A., Ferrier-Pagès, C., and Voolstra, C. R. (2016). Diversity and function of prevalent symbiotic marine bacteria in the genus *endozoonas*. *Appl. Microbiol. Biotechnol.* 100 (19), 8315–8324. doi: 10.1007/s00253-016-7777-0
- Nir, O., Gruber, D. F., Shemesh, E., Glasser, E., and Tchernov, D. (2014). Seasonal mesophotic coral bleaching of *Stylophora pistillata* in the northern red Sea. *PLoS One* 9 (1), e84968. doi: 10.1371/journal.pone.0084968
- Oksanen, J., Blanchet, F. G., Kindt, R., Legendre, P., Minchin, P. R., O'hara, R., et al. (2013). Package 'vegan'. *Community Ecol. package version 2* (9). Available at: <https://github.com/vegandevs/vegan>.
- Oliver, E. C., Donat, M. G., Burrows, M. T., Moore, P. J., Smale, D. A., Alexander, L. V., et al. (2018). Longer and more frequent marine heatwaves over the past century. *Nat. Commun.* 9 (1), 1–12. doi: 10.1038/s41467-018-03732-9
- Olson, J. B., and Gao, X. (2013). Characterizing the bacterial associates of three Caribbean sponges along a gradient from shallow to mesophotic depths. *FEMS Microbiol. Ecol.* 85 (1), 74–84. doi: 10.1111/1574-6941.12099
- Oren, M., Steindler, L., and Ilan, M. (2005). Transmission, plasticity and the molecular identification of cyanobacterial symbionts in the red Sea sponge *Diaccarnus erythraeus*. *Mar. Biol.* 148 (1), 35–41. doi: 10.1007/s00227-005-0064-8
- Osinga, R. (1999). Measurement of sponge growth by projected body area and underwater weight. *Mem. Queensl. Mus.* 44, 419–426.
- Parada, A. E., Needham, D. M., and Fuhrman, J. A. (2016). Every base matters: assessing small subunit rRNA primers for marine microbiomes with mock communities, time series and global field samples. *Environ. Microbiol.* 18 (5), 1403–1414. doi: 10.1111/1462-2920.13023
- Pérez-Rosales, G., Rouzé, H., Torda, G., Bongaerts, P., Pichon, M., Consortium, U. T. P., et al. (2021). Mesophotic coral communities escape thermal coral bleaching in French Polynesia. *R. Soc. Open Sci.* 8 (11), 210139. doi: 10.1098/rsos.210139
- Pita, L., Rix, L., Slaby, B. M., Franke, A., and Hentschel, U. (2018). The sponge holobiont in a changing ocean: from microbes to ecosystems. *Microbiome* 6 (1), 1–18. doi: 10.1186/s40168-018-0428-1
- Pohlert, T., and Pohlert, M. T. (2018). Package 'PMCMRplus' (Vienna, Austria: R Foundation for Statistical Computing). Available at: <https://cran.r-project.org/package=PMCMRplus>.
- Posadas, N., Baquiran, J. I. P., Nada, M. A. L., Kelly, M., and Conaco, C. (2022). Microbiome diversity and host immune functions influence survivorship of sponge holobionts under future ocean conditions. *ISME J.* 16 (1), 58–67. doi: 10.1038/s41396-021-01050-5
- Quast, C., Pruesse, E., Yilmaz, P., Gerken, J., Schweer, T., Yarza, P., et al. (2012). The SILVA ribosomal RNA gene database project: improved data processing and web-based tools. *Nucleic Acids Res.* 41 (D1), D590–D596. doi: 10.1093/nar/gks1219
- Raina, J.-B., Tapiolas, D., Willis, B. L., and Bourne, D. G. (2009). Coral-associated bacteria and their role in the biogeochemical cycling of sulfur. *Appl. Environ. Microbiol.* 75 (11), 3492–3501. doi: 10.1128/AEM.02567-08
- Ramsby, B. D., Hoogenboom, M. O., Smith, H. A., Whalan, S., and Webster, N. S. (2018). The bioeroding sponge *Cliona orientalis* will not tolerate future projected ocean warming. *Sci. Rep.* 8 (1), 1–13. doi: 10.1038/s41598-018-26535-w
- Reshef, L., Koren, O., Loya, Y., Zilber-Rosenberg, I., and Rosenberg, E. (2006). The coral probiotic hypothesis. *Environ. Microbiol.* 8 (12), 2068–2073. doi: 10.1111/j.1462-2920.2006.01148.x
- Reveillaud, J., Maignien, L., Eren, A. M., Huber, J. A., Apprill, A., Sogin, M. L., et al. (2014). Host-specificity among abundant and rare taxa in the sponge microbiome. *ISME J.* 8 (6), 1198–1209. doi: 10.1038/ismej.2013.227
- Ribeiro, B., Padua, A., Barno, A., Villela, H., Duarte, G., Rossi, A., et al. (2021). Assessing skeleton and microbiome responses of a calcareous sponge under thermal and pH stresses. *ICES J. Mar. Sci.* 78 (3), 855–866. doi: 10.1093/icesjms/fsaa231
- Ribes, M., Calvo, E., Movilla, J., Logares, R., Coma, R., and Pelejero, C. (2016). Restructuring of the sponge microbiome favors tolerance to ocean acidification. *Environ. Microbiol. Rep.* 8 (4), 536–544. doi: 10.1111/1758-2229.12430
- Rix, L., de Goeij, J. M., van Oevelen, D., Struck, U., Al-Horani, F. A., Wild, C., et al. (2018). Reef sponges facilitate the transfer of coral-derived organic matter to their associated fauna via the sponge loop. *Mar. Ecol. Prog. Ser.* 589, 85–96. doi: 10.3354/meps12443
- Rodolfo-Metalpa, R., Hoogenboom, M. O., Rottier, C., Ramos-Esplá, A., Baker, A. C., Fine, M., et al. (2014). Thermally tolerant corals have limited capacity to acclimatize to future warming. *Global Change Biol.* 20 (10), 3036–3049. doi: 10.1111/gcb.12571
- Rondon, R., González-Aravena, M., Font, A., Osorio, M., and Cárdenas, C. A. (2020). Effects of climate change stressors on the prokaryotic communities of the Antarctic sponge *Isodictya kerguelensis*. *Front. Ecol. Evol.* 262. doi: 10.3389/fevo.2020.00262
- Rubio-Portillo, E., Ramos-Esplá, A. A., and Antón, J. (2021). Shifts in marine invertebrate bacterial assemblages associated with tissue necrosis during a heat wave. *Coral Reefs* 40 (2), 395–404. doi: 10.1007/s00338-021-02075-0
- Schmittmann, L., Rahn, T., Busch, K., Fraune, S., Pita, L., and Hentschel, U. (2022). Stability of a dominant sponge-symbiont in spite of antibiotic-induced microbiome disturbance. *Environ. Microbiol.* 24 (12), 6392–6410. doi: 10.1111/1462-2920.16249
- Shlesinger, T., Grinblat, M., Rapuano, H., Amit, T., and Loya, Y. (2018). Can mesophotic reefs replenish shallow reefs? reduced coral reproductive performance casts a doubt. *Ecology* 99 (2), 421–437. doi: 10.1002/ecy.2098
- Simister, R., Taylor, M. W., Tsai, P., Fan, L., Bruxner, T. J., Crowe, M. L., et al. (2012). Thermal stress responses in the bacterial biosphere of the great barrier reef sponge, *Rhopaloeides odorabile*. *Environ. Microbiol.* 14 (12), 3232–3246. doi: 10.1111/1462-2920.12010
- Steffen, K., Indraningrat, A. A. G., Emgren, I., Haglöf, J., Becking, L. E., Smidt, H., et al. (2022). Oceanographic setting influences the prokaryotic community and metabolome in deep-sea sponges. *Sci. Rep.* 12 (1), 1–16. doi: 10.1038/s41598-022-07292-3
- Strand, R., Whalan, S., Webster, N. S., Kutti, T., Fang, J. K.-H., Luter, H. M., et al. (2017). The response of a boreal deep-sea sponge holobiont to acute thermal stress. *Sci. Rep.* 7 (1), 1–12. doi: 10.1038/s41598-017-01091-x
- Taylor, J. A., Palladino, G., Wemheuer, B., Steinert, G., Sipkema, D., Williams, T. J., et al. (2021). Phylogeny resolved, metabolism revealed: functional radiation within a widespread and divergent clade of sponge symbionts. *ISME J.* 15 (2), 503–519. doi: 10.1038/s41396-020-00791-z
- Thinesh, T., Meenatchi, R., Lipton, A. N., Anandham, R., Jose, P. A., Tang, S.-L., et al. (2020). Metagenomic sequencing reveals altered bacterial abundance during coral-sponge interaction: insights into the invasive process of coral-killing sponge *Terpios hoshinota*. *Microbiological Res.* 240, 126553. doi: 10.1016/j.micres.2020.126553
- Thomas, T., Moitinho-Silva, L., Lurgi, M., Björk, J. R., Easson, C., Astudillo-García, C., et al. (2016). Diversity, structure and convergent evolution of the global sponge microbiome. *Nat. Commun.* 7, 11870. doi: 10.1038/ncomms11870
- Tinsley, C., and Nassif, X. (1996). Analysis of the genetic differences between *Neisseria meningitidis* and *Neisseria gonorrhoeae*: two closely related bacteria expressing two different pathogenicities. *Proc. Natl. Acad. Sci.* 93 (20), 11109–11114. doi: 10.1073/pnas.93.20.11109
- Turner, J. A., Andradi-Brown, D. A., Gori, A., Bongaerts, P., Burdett, H. L., Ferrier-Pagès, C., et al. (2019). "Key questions for research and conservation of mesophotic coral ecosystems and temperate mesophotic ecosystems," in *Mesophotic coral ecosystems: Coral reefs of the world*. Eds. Y. Loya, K. Puglise and T. Bridge (Cham: Springer) 12, 989–1003.
- Turon, M., Cáliz, J., Garate, L., Casamayor, E. O., and Uriz, M. J. (2018). Showcasing the role of seawater in bacteria recruitment and microbiome stability in sponges. *Sci. Rep.* 8 (1), 1–10. doi: 10.1038/s41598-018-33545-1
- Vargas, S., Leiva, L., and Wörheide, G. (2021). Short-term exposure to high-temperature water causes a shift in the microbiome of the common aquarium sponge *Lendenfeldia chondrodes*. *Microbial Ecol.* 81 (1), 213–222. doi: 10.1007/s00248-020-01556-z
- Voolstra, C. R., and Ziegler, M. (2020). Adapting with microbial help: microbiome flexibility facilitates rapid responses to environmental change. *BioEssays* 42 (7), 2000004. doi: 10.1002/bies.202000004
- Wang, Q., Garrity, G. M., Tiedje, J. M., and Cole, J. R. (2007). Naive Bayesian classifier for rapid assignment of rRNA sequences into the new bacterial taxonomy. *Appl. Environ. Microbiol.* 73 (16), 5261–5267. doi: 10.1128/AEM.00062-07
- Webster, N. S., Cobb, R. E., and Negri, A. P. (2008). Temperature thresholds for bacterial symbiosis with a sponge. *ISME J.* 2 (8), 830–842. doi: 10.1038/ismej.2008.42
- Webster, N. S., and Reusch, T. B. (2017). Microbial contributions to the persistence of coral reefs. *ISME J.* 11 (10), 2167–2174. doi: 10.1038/ismej.2017.66
- Webster, N. S., and Thomas, T. (2016). The sponge hologenome. *MBio* 7 (2), e00135–e00116. doi: 10.1128/mBio.00135-16
- Weiss, K. R. (2017). Can deep reefs rescue shallow ones? *Science* 355 (6328), 903–903. doi: 10.1126/science.355.6328.903
- Wickham, H. (2016). "Data analysis," in *ggplot2* (Houston, TX: Springer), 189–201.
- Wickham, H., Averick, M., Bryan, J., Chang, W., McGowan, L. D. A., François, R., et al. (2019). Welcome to the tidyverse. *J. Open Source software* 4 (43), 1686. doi: 10.21105/joss.01686
- Wilkinson, C., and Fay, P. (1979). Nitrogen fixation in coral reef sponges with symbiotic cyanobacteria. *Nature* 279 (5713), 527–529. doi: 10.1038/279527a0
- Yahel, G., Marie, D., and Genin, A. (2005). InEx—a direct *in situ* method to measure filtration rates, nutrition, and metabolism of active suspension feeders. *Limnology Oceanography: Methods* 3 (2), 46–58. doi: 10.4319/lom.2005.3.46
- Zaneveld, J. R., McMinds, R., and Vega Thurber, R. (2017). Stress and stability: applying the Anna Karenina principle to animal microbiomes. *Nat. Microbiol.* 2 (9), 1–8. doi: 10.1038/nmicrobiol.2017.121
- Zhang, S., Song, W., Wemheuer, B., Reveillaud, J., Webster, N., and Thomas, T. (2019). Comparative genomics reveals ecological and evolutionary insights into sponge-associated thaumarchaeota. *Msystems* 4 (4), e00288–e00219. doi: 10.1128/mSystems.00288-19



## OPEN ACCESS

## EDITED BY

Zhiyong Li,  
Shanghai Jiao Tong University, China

## REVIEWED BY

Ida Helene Steen,  
University of Bergen, Norway  
Heng-Lin Cui,  
Jiangsu University, China

## \*CORRESPONDENCE

Li-Sheng He  
✉ he-lisheng@idsse.ac.cn

RECEIVED 05 March 2023

ACCEPTED 08 June 2023

PUBLISHED 29 June 2023

## CITATION

Qi L, Shi M, Zhu F-C, Lian C-A and He L-S  
(2023) Genomic evidence for the first  
symbiotic Deferribacterota, a novel gut  
symbiont from the deep-sea hydrothermal  
vent shrimp *Rimicaris kairei*.  
*Front. Microbiol.* 14:1179935.  
doi: 10.3389/fmicb.2023.1179935

## COPYRIGHT

© 2023 Qi, Shi, Zhu, Lian and He. This is an  
open-access article distributed under the terms  
of the [Creative Commons Attribution License  
\(CC BY\)](https://creativecommons.org/licenses/by/4.0/). The use, distribution or reproduction  
in other forums is permitted, provided the  
original author(s) and the copyright owner(s)  
are credited and that the original publication in  
this journal is cited, in accordance with  
accepted academic practice. No use,  
distribution or reproduction is permitted which  
does not comply with these terms.

# Genomic evidence for the first symbiotic Deferribacterota, a novel gut symbiont from the deep-sea hydrothermal vent shrimp *Rimicaris kairei*

Li Qi<sup>1,2</sup>, Mengke Shi<sup>1,2</sup>, Fang-Chao Zhu<sup>3</sup>, Chun-Ang Lian<sup>1</sup> and Li-Sheng He<sup>1\*</sup>

<sup>1</sup>Institute of Deep-Sea Science and Engineering, Chinese Academy of Sciences, Sanya, China,

<sup>2</sup>University of Chinese Academy of Sciences, Beijing, China, <sup>3</sup>Key Laboratory of Tropical Marine Ecosystem and Bioresource, Fourth Institute of Oceanography, Ministry of Natural Resources, Beihai, China

The genus *Rimicaris* is the dominant organism living in hydrothermal vents. However, little research has been done on the functions of their intestinal flora. Here, we investigated the potential functions of Deferribacterota, which is dominant in the intestine of *Rimicaris kairei* from the Central Indian Ridge. In total, six metagenome-assembled genomes (MAGs) of Deferribacterota were obtained using the metagenomic approach. The six Deferribacterota MAGs (Def-MAGs) were clustered into a new branch in the phylogenetic tree. The six Def-MAGs were further classified into three species, including one new order and two new genera, based on the results of phylogenetic analysis, relative evolutionary divergence (RED), average nucleotide identity (ANI), average amino acid identity (AAI) and DNA–DNA hybridization (DDH) values. The results of the energy metabolism study showed that these bacteria can use a variety of carbon sources, such as glycogen, sucrose, salicin, arbutin, glucose, cellobiose, and maltose. These bacteria have a type II secretion system and effector proteins that can transport some intracellular toxins to the extracellular compartment and a type V CRISPR–Cas system that can defend against various invasions. In addition, cofactors such as biotin, riboflavin, flavin mononucleotide (FMN), and flavin adenine dinucleotide (FAD) synthesized by *R. kairei* gut Deferribacterota may also assist their host in surviving under extreme conditions. Taken together, the potential function of Deferribacterota in the hydrothermal *R. kairei* gut suggests its long-term coevolution with the host.

## KEYWORDS

Deferribacterota, gut microbiota, *Rimicaris kairei*, metagenomic, hydrothermal vent

## 1. Introduction

The *Rimicaris* shrimp is dominant in many hydrothermal vents. There are at least ten species in this genus, including *R. chacei*, *R. paulexa*, *R. parva*, *R. susannae*, *R. exoculata*, *R. falkorae*, *R. hybisae*, *R. kairei*, *R. vandoverae*, and *R. variabilis*. They mainly live in the hydrothermal fields with some difference in distribution among these species. For examples, *R. exoculata* is mainly living at the hydrothermal vent of the Mid-Atlantic Ridge (MAR), *R. kairei* is mainly resident at



the Central Indian Ridge (Watabe and Hashimoto, 2002), and *R. chacei* also lives in the Atlantic Ridge, but most at the periphery of *R. exoculata* aggregates (Apremont et al., 2018). Within the *Rimicaris* genus, *R. exoculata*, *R. kairei*, and *R. hybisae* have an enlarged branchial chamber with a highly dense population of epibiotic bacteria (Zbinden and Cambon-Bonavita, 2020). *R. exoculata* is reported to house a density of epibiotic bacteria in cephalothoracic chamber and modified mouthparts (Gebruk et al., 2000). Due to that, a body of studies has focused on the epibionts and their benefits to *Rimicaris* species. The main epibiotic communities in *R. exoculata* are *Gamma*-, *Alpha*-, *Beta*-, *Delta*-, *Zetaproteobacteria*, *Campylobacteria*, and *Bacteroidetes* (Zbinden et al., 2008; Petersen et al., 2010; Hügler et al., 2011; Guri et al., 2012; Jan et al., 2014; Jiang et al., 2020). A few studies have also reported the gut microbial composition of *R. exoculata*. Three major groups, *Deferribacteres*, *Mollicutes*, and *Campylobacteria*, were found in the midgut, along with small amounts of *Gammaproteobacteria* (Zbinden and Cambon-Bonavita, 2003; Durand et al., 2010; Cowart et al., 2017). Additionally, the three main lineages were still present after 72 h of starvation, so they have designated resident epibionts rather than transient microflora (Durand et al., 2010). Besides, Apremont et al. showed that *Deferribacteres*, *Mollicutes*, and *Epsilon*- and *Gammaproteobacteria* were the main microbes existed in the digestive tract of *R. chacei* (Apremont et al., 2018). The difference between the intestinal microbial composition of *R. exoculata* and *R. chacei* may be due to the different living environments. In our previous studies, we showed that the intestinal microbiota of *R. kairei*, which was from the Central Indian Ridge, was dominant by *Deferribacterota*, *Campylobacter*, *Bacteroidetes*, *Firmicutes*, and *Proteobacteria*, although there is a significant difference in the composition between different developing stages (Qi et al., 2021). To date, some studies have been reported on the intestinal microbial community of *Rimicaris* species, but there are few studies on their functions, even though the functions of the gill symbiotic microbiota have been extensively investigated. Therefore, we will further investigate the functions of the gut microbiota and present the relationship with their host *Rimicaris* species.

*Deferribacteres*, a new phylum recorded in 2001 (Garrity et al., 2001), was emended in 2009 to represent only the family *Deferribacteriaceae* (Jumas-Bilak et al., 2009). In 2011, the phylogeny of the phylum was repositioned (Kunisawa, 2011), and the new name *Deferribacterota* was given in 2018 (Whitman et al., 2018). At present, there are few reports on the genomic function of *Deferribacterota*. Members of the phylum *Deferribacterota* are organized into a single order and six families. A deep lineage is the *Deferribacteraceae* family, whose genus *Deferribacter* includes four species, *D. thermophilus*, *D. desulfuricans*, *D. abyssii*, and *D. autotrophicus*. *D. thermophilus* was isolated from a high-temperature around 60°C, seawater-flooded oil reservoir in the North Sea (Greene et al., 1997), while the other three species were all isolated from deep-sea hydrothermal vents (Miroshnichenko et al., 2003; Takaki et al., 2010; Slobodkin et al., 2019). *D. desulfuricans* was obtained from the Suiyo Seamount hydrothermal chimney (Takaki et al., 2010), *D. abyssii* was isolated from the Rainbow hydrothermal vent field of the Mid-Atlantic Ridge (Miroshnichenko et al., 2003), and *D. autotrophicus* was isolated from Ashadze hydrothermal chimney on the Mid-Atlantic Ridge at a depth of 4,100 m (Slobodkin et al., 2019). All recognized *Deferribacter* species are strictly anaerobic and thermophilic organisms, which can oxidize various complex organic compounds and organic acids in the presence of diverse electron acceptors. *D. desulfuricans* can use formate, acetate, and pyruvate as substrates; *D. abyssii* is capable of using molecular hydrogen,

acetate, succinate, pyruvate, and proteinaceous compounds as electron donors and elemental sulfur, nitrate, or Fe (III) as electron acceptors; *D. autotrophicus* used molecular hydrogen, acetate, lactate, succinate, pyruvate and complex proteinaceous compounds as electron donors, and Fe (III), Mn (IV), nitrate or elemental sulfur as electron acceptors; *D. thermophilus* obtained energy from the reduction of manganese (IV), iron (III), and nitrate in the presence of yeast extract, peptone, casamino acid, tryptone, hydrogen, malate, acetate, citrate, pyruvate, lactate, succinate, and valerate. *D. desulfuricans* is a heterotrophic bacterium, while all of the other three species are chemolithoautotrophic bacteria. In addition, *Flexistipes sinuansarabici*, which was most closely related to *Deferribacter* and isolated from the Atlantis Deep brines of the Red Sea, is tolerant to high temperature, high salt concentration and heavy metals, and strictly anaerobic. This organism prefers complex growth substrates such as yeast extract, meat extract, peptone, and trypsin, while formate, lactate, citrate, malate, carbohydrate, amino acid, and alcohol do not support cell growth (Lapidus et al., 2011). Up to now, only one species of *Mucispirillum schaedleri* in the phylum of *Deferribacterota* has been isolated from the intestine. *M. schaedleri* inhabits the intestinal mucus layer of rodents and other animals in abundance and are considered pathogenic. *M. schaedleri* harbors a complete Embden-Meyerhof-Parnas (EMP) pathway and a nonoxidative pentose phosphate pathway as well as a complete tricarboxylic acid cycle. *M. schaedleri* can also alter gene expression in mucosal tissues, suggesting an intimate interaction with the host (Loy et al., 2017).

Different from the reported *Deferribacterota* in the hydrothermal zone, the six *Deferribacterota* from *R. kairei* guts are heterotrophic according to the MAG analysis. Def-MAGs do not have genes related to carbon, nitrogen, and sulfur utilization. Instead, they have a complete glycolysis pathway and genes for transporting and degrading polysaccharides. Although slight differences among the six Def-MAGs, the main functions of carbohydrate metabolism, polysaccharide degradation, vitamin synthesis and so on were similar. This study further elucidated the diversity of *Deferribacterota* and their host interaction relationships, supplementing the understanding of existing *Deferribacterota*.

## 2. Materials and methods

### 2.1. Sample collection

The shrimp were collected from two sites in the Central Indian Ridge by the manned submersible *Deep-Sea Yongshi* during R/V *Tansuoyihao* research cruise TS10 (February 2019). Sampling sites were located in Edmond (69.59667°E, 23.87782°S) and Kairei (70.04010°E, 25.32048°S) at depths of 3,281 m and 2,421 m, respectively (Supplementary Figure S1). All shrimp were obtained using the suction sampler. Once onboard, individuals were immediately frozen at −80°C or stored in 75% ethanol at −20°C.

### 2.2. DNA extraction and metagenome sequencing

The samples were identified as *R. kairei* in our previous article (Qi et al., 2021). The intestinal anatomy of *R. kairei* was performed in a



sterile environment, and the total DNA of the gut was extracted using a PowerSoil DNA isolation kit (Qiagen, Germany) following the manufacturer's procedures. The quality and quantity of genomic DNA were checked by gel electrophoresis. The DNA concentration was determined by using a Qubit dsDNA HS assay kit with a Qubit 2.0 fluorometer (Invitrogen, Carlsbad, CA). A total of 100 ng DNA was used for library preparation. High-throughput sequencing was performed with the Novaseq 6000 platform to produce 2 × 150 bp paired-end reads (Illumina).

## 2.3. Metagenomic assembly and genome binning

Metagenomic DNA sequencing produced a total of 154,387,934 reads, with a total length of 45 Gbp. Trimmomatic v0.36 was used for trimming with parameters (LEADING: 3; The TRAILING: 3; HEADCROP: 4; SLIDINGWINDOW: 4:15; MINLEN: 80) (Bolger et al., 2014), and FastQC v0.11.9 was used to evaluate the quality of data before and after filtering (Brown et al., 2017). The qualified reads were further assembled into contigs by SPAdes-3.11 (Bankevich et al., 2012) software with a k-mer range of 21 to 127. MetaWRAP v1.2.1 (Uritskiy et al., 2018) was used for genome binning and subsequent refinement with parameters (three different algorithms MaxBin2, metaBAT2, and CONCOCT for metagenomic binning; contig length: >2000 bp; completeness: >50%; and contamination: <10%). The MAGs (metagenome assembled genomes) were checked by CheckM v1.1.3 (Parks et al., 2015) to filter those with low completeness (<50%) and high contamination (>10%). Taxonomic annotation of the MAGs was performed using GTDB-tk v1.4.0 software (Chaumeil et al., 2019). The whole-genome average nucleotide identity (ANI) between genomes was calculated by fastANI v1.33 software (Jain et al., 2018). Average Amino acid Identity (AAI) was calculated by AAI calculator online tool (Rodríguez-R and Konstantinidis, 2014). DNA–DNA hybridization (DDH) was calculated by Genome-to-Genome Distance Calculator 3.0 online tool (Meier-Kolthoff et al., 2021). GTDB-tk software was used to calculate the relative evolutionary divergence (RED) values when a query genome could not be classified based on the ANI values. Then, the MAGs belonging to Deferribacterota bacteria were retrieved for downstream analyses.

## 2.4. Phylogenetic analyses

There were 79 genomes in total for phylogenetic analyses, including 57 genomes from Tenericutes, Firmicutes, Acidobacteria, Chrysiogenetes, and Proteobacteria, and the others were from the phylum Deferribacterota. Firstly, 43 ribosome proteins were obtained by CheckM analysis from all of these genomes and then aligned by MAFFT v7.487 (Katoh et al., 2002) with the default settings, and poorly aligned regions were removed by trimAI v1.4 (Capella-Gutiérrez et al., 2009). The maximum likelihood (ML) phylogenomic tree was constructed using the concatenated aligned protein sequences with the IQ-TREE tool (Nguyen et al., 2015) and the best-fit substitution model (LG + R10 model) for 1,000 replicates. In addition, all phylogenetic trees were visualized using the interactive Tree of Life (iTOL) online tool (Letunic and Bork, 2019).

## 2.5. Genome annotation

Reference genomes included *D. autotrophicus*, *D. desulfuricans* SSM1, *F. sinuarabici* DSM4947, and *M. schaedleri* ASF457, of which *D. autotrophicus*, *D. desulfuricans* SSM1 and *F. sinuarabici* DSM4947 were free-living bacteria from hydrothermal environments, and *M. schaedleri* ASF457 was from the mouse intestine. The studied MAGs and reference genomes were annotated using Prokka v1.14.6, and the parameters were set to metagenome and kingdom bacteria (Seemann, 2014). This annotation pipeline relied on several external prediction tools, including Prodigal for coding sequences, Aragorn for transfer RNA genes, RNAmmer for ribosomal RNA genes, and Infernal for noncoding RNAs. Kofamscan v1.3.0 (Aramaki et al., 2020) was used for functional annotations of the predicted genes, and the amino acid sequences of each genome were inputted and then compared with the KEGG database using the mapper model. KEGG-Decoder was performed to determine the completeness of various metabolic pathways by Kofamscan results (Graham et al., 2018). GO annotation was analysed using eggNOG-mapper v2.1.3 software (Huerta-Cepas et al., 2017), and the parameters were set as follows: -seed\_ortholog\_value, 0.00001; -m, hmmer; and -d, bact. Carbohydrate enzyme annotation was performed by searching the CAZyme database using dbCAN2 software, which used default settings (Zhang et al., 2018). Annotation of the deduced proteins was also performed using BLASTP against the NCBI Nr, KEGG (Kanehisa et al., 2016), Pfam (El-Gebali et al., 2019) and COG (Tatusov et al., 2000; Galperin et al., 2021) databases, with a maximum e-value cut-off of 1e-05. The CRISPR region was identified using CRISPRCasTyper v1.6.1 (Russel et al., 2020) and the CRISPRCasFinder online tool (Grissa et al., 2007).

## Data availability

The MAGs obtained from the samples of Gut of *Rimicaris kairei* in this study have been submitted to the NCBI database under BioProject ID PRJNA931729.

## 3. Results

### 3.1. Metagenome assembly and characteristics

Deferribacterota was the dominant phylum in both microbial communities of the juvenile and adult *R. kairei* intestinal tracts in our previous study (Qi et al., 2021). To further investigate the potential functions of the intestinal Deferribacterota, metagenomes were assembled and analysed. A total of 45 Gbps of raw data were obtained by high-throughput sequencing, and 42.4 Gbps of clean data were retained. After *de novo* assembly based on three different algorithms (MaxBin2, metaBAT2, and CONCOCT), genomic bins with each longer than 2 kbp, completeness >50%, and contamination <10% were selected. There were 18 MAGs obtained in total, including Firmicutes, Bacteroidetes, Spirochaetota, Campylobacterota and Deferribacterota, based on the analysis by GTDB-tk (Supplementary Table S1). The six Def-MAGs (Deferribacterota MAGs, defined as Def\_J1, Def\_J3, Def\_J5, Def\_J6, Def\_A4, and Def\_A7, respectively) with four related reference genomes, including *D. autotrophicus*, *D. desulfuricans* SSM1, *F. sinuarabici* DSM4947, and *M. schaedleri* ASF457, are shown in

**Table 1.** Among the six Def-MAGs, the completeness of *Def\_J6* is close to 90%, and its genome size is 2.5 Mb, similar to the four reference MAGs with a genome size of 2.2–2.5 Mb. The completeness of other Def-MAGs ranged from 55.33 to 88.76%, with genome sizes ranging from 0.9 to 1.8 Mb. Notably, the average G + C content of the six Def-MAGs ranged from 46.4 to 50.7%, much higher than that of the reference genomes, in which the G + C content ranged from 30 to 38%. We also listed the number of tRNAs and rRNAs and the number and percentage of genes annotated by each genome in the KEGG and COG databases (Table 1).

## 3.2. Phylogenetic analysis of Deferribacterota

To further investigate the taxonomic status of the six species from the *R. kairei* intestine, phylogenetic analysis was performed using 43 conserved proteins with five phyla adjacent to the phylum Deferribacterota: Tenericutes, Firmicutes, Acidobacteria, Chrysiogenetes, and Proteobacteria. In addition to the six studied species from Deferribacterota, 16 other genome sequences in the phylum Deferribacterota, including 8 identified and 8 unidentified species, were selected from the RefSeq database, and a total of 79 genomes were constructed for phylogenetic analyses (Figure 1). The results showed that the six Def-MAGs were clustered into a single branch and separated from other strains in the phylum Deferribacterota. We also tested the average nucleotide identity (ANI) value (Table 2). The results, consistent with the phylogenetic tree, were that the six Def-MAGs clustered together (Supplementary Figure S2). The Average Amino acid Identity (AAI) and DNA–DNA hybridization (DDH) values are similar to the ANI values, and the six Def-MAGs are classified into three species (Table 2). According to the classification analysis by GTDB-tk software, *Def\_J3*, *Def\_J5*, *Def\_J6*, and *Def\_A7* are classified as the *Deferribacteres* class but could not be further classified into any known order. The relative evolutionary divergence (RED) values are 0.467, 0.460, 0.467, and 0.455 for *Def\_J3*, *Def\_J5*, *Def\_J6*, and *Def\_A7*, respectively. *Def\_J1* and *Def\_A4* are classified as the *Mucispirillaceae* family but could not be further classified into any known genus. The RED values were 0.747 and 0.749 for *Def\_J1* and *Def\_A4*, respectively (Table 2). Therefore, *Def\_J3*, *Def\_J5*, *Def\_J6*, and *Def\_A7* could be in new orders, while *Def\_J1* and *Def\_A4* could be in new genera. Together with the phylogenetic results and ANI values, the six Def-MAGs were classified into three species, with *Def\_J1* representing a new genus, *Def\_J3*, *Def\_J6*, and *Def\_A7* representing a new order, and *Def\_J5* and *Def\_A4* representing another new genus. Here, the classification of *Def\_J5* is slightly confused, which is probably due to its genome with only 50% integrity and needs to be further clarified by obtaining a longer length.

## 3.3. Metabolic features

### 3.3.1. Energy metabolism

Six Def-MAGs and four reference MAGs were used to comparatively analyse the metabolic pathways by KEGG decoding. Based on the heatmap, both groups have a similar integrity of metabolism for the glycolysis and gluconeogenesis pathways, but the gluconeogenesis pathway was almost absent in the genome of

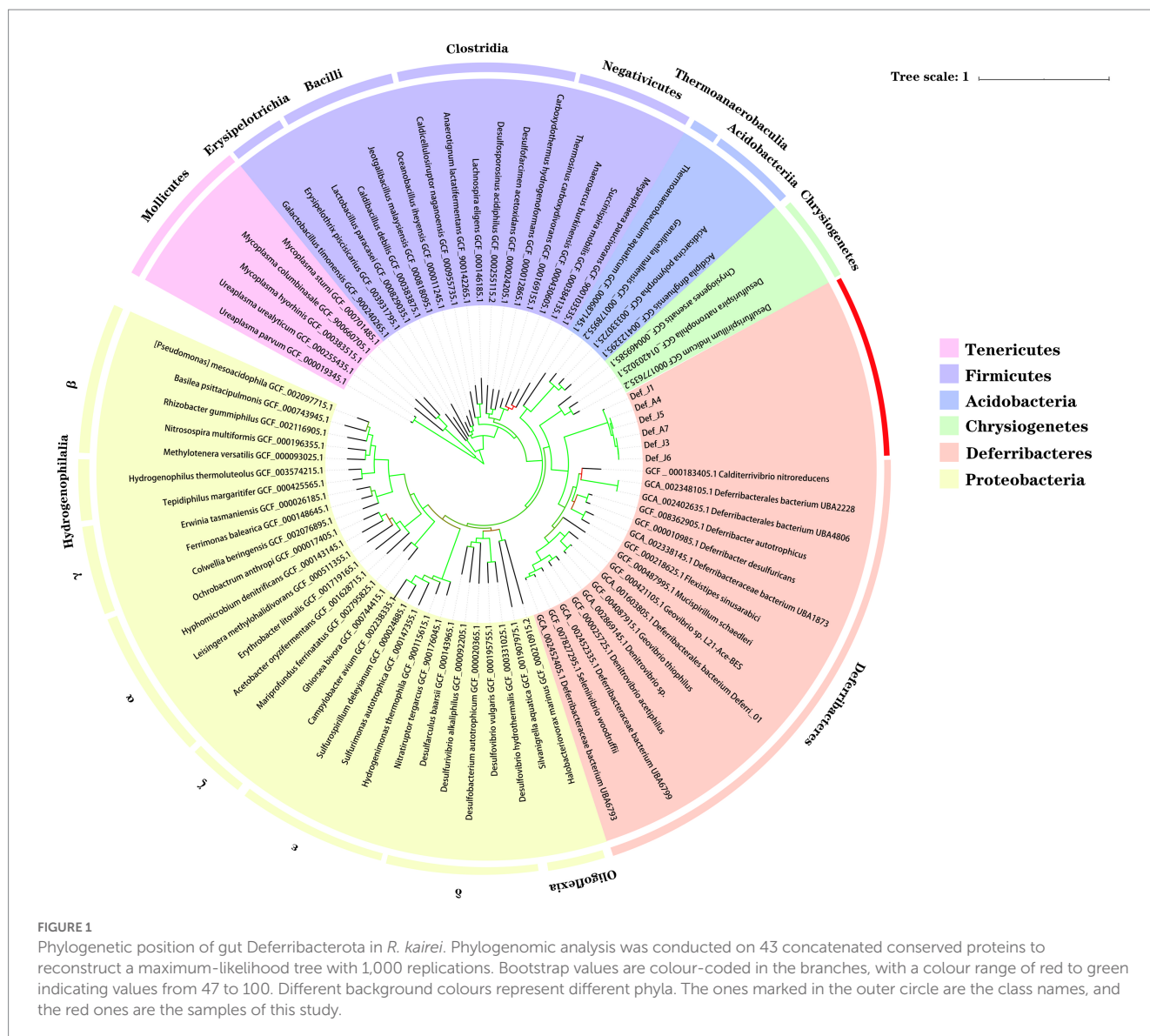
*M. schaedleri* ASF457 (Figure 2). Genes related to the tricarboxylic acid cycle were severely absent in Def-MAG compared to the reference MAGs (Figure 2). Taking *Def\_J6*-MAG, with the highest completeness, as an example, only malate dehydrogenase (EC1.1.1.37), fumarate hydratase (EC4.2.1.2), and succinate dehydrogenase (ubiquinone) flavoprotein subunit (EC1.3.5.1) were found, and most of the enzymes, including key enzymes such as citrate synthase (EC2.3.3.1) and ATP citrate lyase (EC2.3.3.8), were absent. In Def-MAG and *M. schaedleri* ASF457, starch or glycogen has 33–66% integrity for the synthesis pathway and 100% integrity for the degradation pathway. However, both pathways were absent in the three environmental reference genomes (Supplementary Table S2). We found that all six Def-MAGs have the key enzyme glycogen phosphorylase (EC2.4.1.1.1), which is involved in glycogen degradation, while 1,4- $\alpha$ -glucan branching enzyme (EC2.4.1.18), which is essential for increasing the solubility of glycogen molecules and reducing the osmotic pressure within cells, is only present in *Def\_J1*, *Def\_J3*, *Def\_J6* and *Def\_A4* (Figure 3). Notably, the carbon degradation of the six Def-MAGs was mainly via  $\beta$ -N-acetylhexosaminidase and  $\beta$ -glucosidase, while the three environmental reference genomes were mainly via D-galacturonate epimerase, and the carbon degradation process was not present in the *M. schaedleri* ASF457 MAG from the mouse intestine (Figure 2).  $\beta$ -N-acetylhexosaminidase and  $\beta$ -glucosidase are key enzymes for the degradation of chitin and cellulose, respectively, while D-galacturonate epimerase is able to convert UDP-d-glucuronide into D-galacturonide, a monosaccharide that is one of the activating precursors necessary for the synthesis of pectinas, indicating that the six Def-MAGs from the *R. kairei* intestine are able to degrade cellulose and chitin, while the reference genomes have the potential to degrade pectin. Def-MAGs contain many phosphotransferases, which transport extracellular glucose (EC2.7.1.199), salicin (EC2.7.1.-), arbutin (EC2.7.1.-), cellobiose (EC2.7.1.205), maltose (EC2.7.12.08), and other carbon sources into cells (Figure 3). The large number of PTSs identified in the Def-MAG genomes suggests that Def-MAG may utilize multiple carbon sources. In addition, we found that Def-MAG has carbamate kinase (EC2.7.2.2) and ornithine carbamoyltransferase (EC2.1.3.3) (Figure 3), both of which convert  $\text{NH}_3$  to citrulline and over the process reversibly. Although no nitric oxide synthase (EC1.14.14.17) was found for the conversion from citrulline to arginine, arginine deiminase (EC3.5.3.6), which catabolizes arginine to citrulline, is present and can irreversibly hydrolyse L-arginine to L-citrulline and ammonia, suggesting that Def-MAGs could provide energy by arginine metabolism generating ATP.

### 3.3.2. Carbohydrate enzymes

In the six Def-MAGs and four reference genomes, a total of 33 carbohydrate-active enzymes were identified, which were classified into 5 types: AA (auxiliary activities), CBM (carbohydrate-binding modules), CE (carbohydrate esterases), GH (glycoside hydrolases) and GT (glycosyltransferases). Among them, a total of 21 carbohydrate enzymes were in six Def-MAGs, nine of which were specific in the six Def-MAGs, including one CBM, CBM67; one CE, CE9; and 7 GHs, GH1, GH133, GH19, GH3, GH4, GH42, and GH78 (Figure 4). A total of 18 carbohydrate enzymes were identified in the genome of *M. schaedleri*, among which CBM13 and GH57 were specific (Figure 4). A total of 20 carbohydrate enzymes were identified in the genomes of the three environmental Deferribacterota isolates, five of which were specific to these genomes, namely, AA4, CE4, GH109,

TABLE 1 Genomic features of gut Deferribacterota in *R. kairei* and reference genomes.

Genome features	<i>Def_J1</i>	<i>Def_J3</i>	<i>Def_J5</i>	<i>Def_J6</i>	<i>Def_A4</i>	<i>Def_A7</i>	<i>Mucispirillum schaedleri</i> ASF457	<i>Deferribacter autotrophicus</i>	<i>Deferribacter desulfuricans</i> SSM1	<i>Flexistipes sinuarabici</i> DSM4947
Habitat	<i>R. kairei</i> intestine	<i>R. kairei</i> intestine	<i>R. kairei</i> intestine	<i>R. kairei</i> intestine	<i>R. kairei</i> intestine	<i>R. kairei</i> intestine	Mouse caecal mucus	Hydrothermal vent	Hydrothermal vent	Brine water (Atlantis II Deep, Red Sea)
Genome size (bp)	1,364,439	1,821,084	927,196	2,565,562	1,567,595	1,248,453	2,332,248	2,542,980	2,234,389	2,526,590
G + C content (%)	49.6	50.2	49	46.4	49.3	50.7	31	32.6	30.3	38.3
CheckM Completeness (%)	78.19	88.76	55.33	90.05	75.13	71.92	98.28	96.55	96.55	99.14
CheckM Contamination (%)	0	0.143	0	0	0	1.754	2.59	2.59	1.72	0.86
Coding density (%)	83.4	82.2	86.6	71.6	83.5	81.9	87.3	90.8	93	88.4
Contig number (≥50,000 bp)	6	8	0	10	2	7	22	10	2	1
N50 (scaffolds)	39,456	43,507	5,119	22,155	10,807	38,451	530,101	319,692	2,234,389	2,526,590
CDS number	1,119	1,382	824	1743	1,309	935	2,162	2,488	2,470	2,356
tRNA genes	32	17	29	39	11	31	41	43	44	44
No.(%) of KEGG genes	685 (61.22)	896 (64.833)	413 (50.12)	725 (41.59)	710 (54.24)	539 (57.65)	1,319 (61.01)	1,521 (61.13)	1,540 (62.35)	1,518 (64.43)
No.(%) of COG genes	827 (73.91)	1,091 (78.94)	503 (61.04)	939 (53.87)	872 (66.62)	664 (71.02)	1719 (79.51)	2,121 (85.25)	2070 (83.81)	2,136 (90.66)



GH114, and GH130 (Figure 4). In addition, the six Def-MAGs were predominantly rich in glycoside hydrolases compared to the mouse intestine, where the main type of carbohydrase was glycosyltransferase. Compared with the environmental Deferribacterota genomes, the six Def-MAGs have specific GT35 and GT5 glycosyltransferases (Figure 4). These two glycosyltransferases can phosphorylate or synthesize glycogen, suggesting that Deferribacterota in the gut may provide a carbon source for the host.

### 3.3.3. Amino acids, vitamins, and cofactors

Compared to the three environmental reference genomes, the six Def-MAGs lost most amino acid synthesis genes except serine, glycine, and alanine; however, for the genome of *M. schaedleri* ASF457, the Deferribacterota from the mouse intestine, only the alanine and tryptophan synthesis pathways were absent (Figure 2). This result suggests the interdependent relationship between Def-MAGs and their host *R. kaiei*. Except for Def\_J5, the integrity of the pathways involved in riboflavin synthesis was 100% in the remaining five Def-MAGs and four reference genomes

(Supplementary Table S2), and the flavin-like compound biosynthesis-related genes *ribA*, *ribAB*, *ribD*, *ribB*, *ribH*, *ribE*, and *ribF* were identified in the six Def-MAG genomic metabolic pathway reconstructions (Figure 3). In addition, Def-MAGs also have biotin, flavin mononucleotide (FMN), flavin adenine dinucleotide (FAD) and other cofactor synthesis pathways (Figure 3).

### 3.3.4. Secretome and immune protection

The secretory system is essential for prokaryotic cell growth and other physiological processes (Green and Mecsas, 2016). Compared with the reference genomes, the six Def-MAGs contained only a type II secretion system (T2SS), but the reference genomes also have type I, type IV, and type VI secretion systems (Figure 2). T2SS effectors are transferred from the cytoplasm to the outer membrane or into the extracellular environment in two steps. First, Protein translocation across the inner membrane *via* the general secretion (Sec) pathway or twin arginine translocation (Tat) pathway (Pugsley et al., 1991; Voulhoux et al., 2001). Second, protein folded in the periplasm crosses the outer membrane by transport of T2SS (Johnson et al., 2006; Douzi



TABLE 2 Average nucleotide identity, average amino acid identity, DNA–DNA hybridization and relative evolutionary branching values of gut Deferribacterota in *R. kairei*.

ANI	Def_J1	Def_J3	Def_J5	Def_J6	Def_A4	Def_A7
Def_J1	100%	81.22%	81.73%	81.16%	83.62%	80.99%
Def_J3	80.91%	100%	79.80%	98.79%	80.92%	98.33%
Def_J5	81.96%	79.72%	100%	80.51%	98.26%	79.54%
Def_J6	81.01%	98.91%	80.49%	100%	80.48%	98.53%
Def_A4	83.54%	80.74%	97.65%	80.70%	100%	80.03%
Def_A7	81.11%	98.66%	79.62%	98.58%	80.25%	100%
AAI	Def_J1	Def_J3	Def_J5	Def_J6	Def_A4	Def_A7
Def_J1	100%	78.37%	77.33%	78.48%	81.26%	78.23%
Def_J3	78.37%	100%	74.49%	97.69%	78.22%	96.92%
Def_J5	77.33%	74.49%	100%	73.49%	95.38%	73.61%
Def_J6	78.48%	97.69%	73.49%	100%	76.93%	96.60%
Def_A4	81.26%	78.22%	95.38%	76.93%	100%	75.91%
Def_A7	78.23%	96.92%	73.61%	96.60%	75.91%	100%
DDH	Def_J1	Def_J3	Def_J5	Def_J6	Def_A4	Def_A7
Def_J1	100%	23.60%	23.50%	23.10%	25.90%	24.40%
Def_J3	23.60%	100%	21.90%	76.30%	25.80%	69.70%
Def_J5	23.50%	21.90%	100%	23.30%	74.20%	22.00%
Def_J6	23.10%	76.30%	23.30%	100%	24.30%	70.90%
Def_A4	25.90%	25.80%	74.20%	24.30%	100%	22.80%
Def_A7	24.40%	69.70%	22.00%	70.90%	22.80%	100%
RED	0.7469	0.4667	0.4596	0.467	0.749	0.455
(GTDB)	Family	Class	Class	Class	Family	Class

ANI and AAI >95%, and DDH >70% are considered one species, both of them are marked in red.

et al., 2011; Nivaskumar and Francetic, 2014). Key proteins of the Sec pathway and the signal recognition particle (SRP) pathway were blasted and found in six Def-MAGs, including SecA, SecYEG, SecDE, YajC, YidC, FtsY, and Ffh, but the Secret monitor (SecM) protein was absent. In Def-MAGs, six of different general secretory pathway (Gsp) protein of T2SS were also found, namely, GspC, GspD, GspE, GspG, GspJ, and GspK (Figure 3). These results indicate that the protein secretion of Deferribacterota in the *R. kairei* intestine mainly transfers the protein to the periplasmic space through the Sec pathway, and then the protein folds, while the Tat pathway existing in reference genomes transfers the folded protein to the periplasmic space.

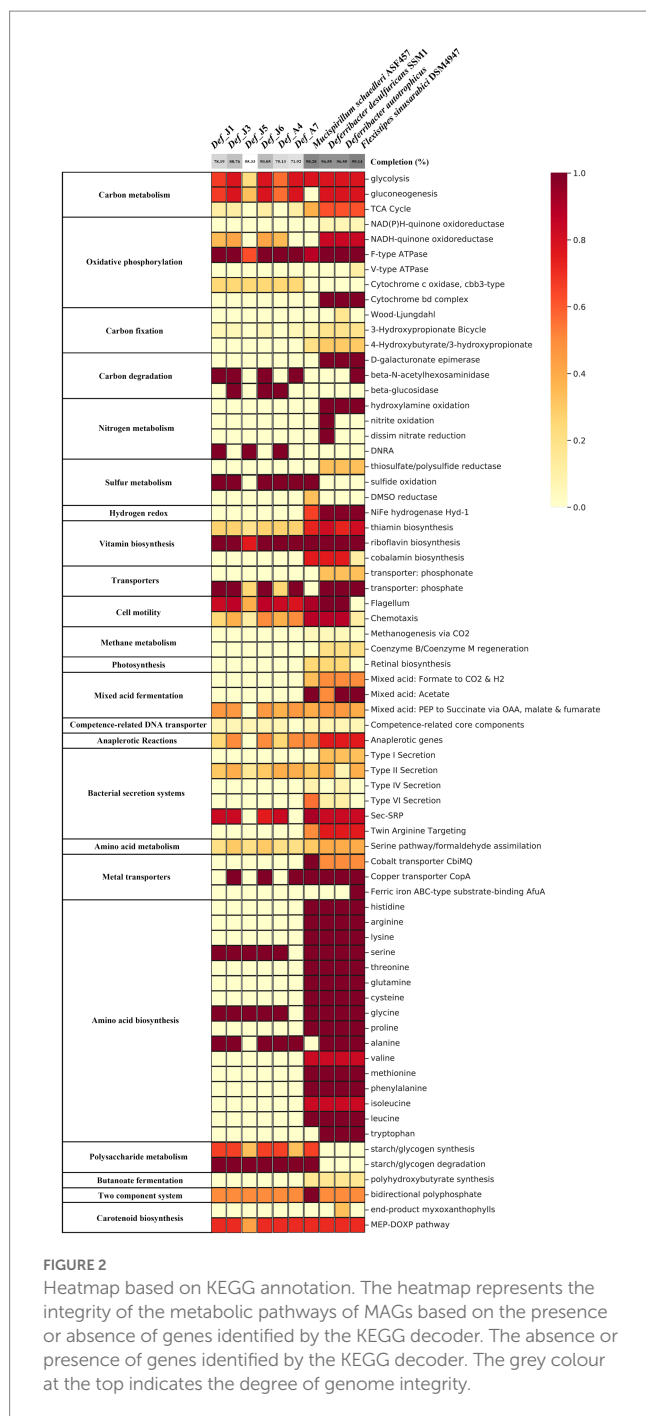
The CRISPR-cas system was investigated in six Def-MAGs, and which in Def\_J1, Def\_J3, Def\_J6, and Def\_A7 consisted of three cas genes, *cas1*, *cas2*, and *cas12b*, and 70–190 spacers (Figure 5). These Def-MAGs were dominated by the type V CRISPR-cas system, belonging to the class II CRISPR-cas system due to the *cas12b* gene, the key enzyme for type V CRISPR-cas. In contrast, in the reference genomes, only *D. desulfuricans* SSM1 and *F. sinusarabici* DSM4947 have a complete CRISPR–Cas system and belong to types I and III of class I, respectively. Furthermore, by blasting the spacer sequences of the Def-MAGs in the CRISPRCasdb database, most of them are unknown spacer sequences. A total of 17 spacer sequences were matched with identities of 92–100%, and most of them were pathogenic bacteria (Supplementary Table S4). These results suggest that the CRISPR system of hydrothermal *R. kairei* intestinal

Deferribacterota genomes is likely to provide immune protection to the host against invasion by other pathogenic bacteria.

## 4. Discussion

In this study, functional annotation analysis was comparably performed between the six Def-MAGs and three free-living bacteria in the phylum Deferribacterota from the environment and one Deferribacterota from the intestinal tract of mice. Based on the features of the six Def-MAGs, Deferribacterota from the intestinal tract of *R. kairei* can utilize various carbon sources, including glycogen, sucrose, salicin, arbutin, glucose, cellobiose, and maltose.

Glycogen in bacteria plays a significant role in carbon and energy storage. It presently has been found in species such as archaea, bacteria, and heterotrophic eukaryotes (Ball et al., 2015). Glycogen is a highly soluble homogeneous polysaccharide and contains hundreds of thousands of glucose units. Glycogen can accumulate in bacteria when the carbon content exceeds that of another nutrient and limits growth (Wilson et al., 2010). During disadvantageous periods, glycogen is decomposed as a carbon and energy reserve to support the long-term survival of bacteria (Wang and Wise, 2011). Glycogen plays a central role in the widespread connectivity of various cellular pathways and can be involved in bacterial energy metabolism, environmental durability, dormancy, and virulence (McMeechan

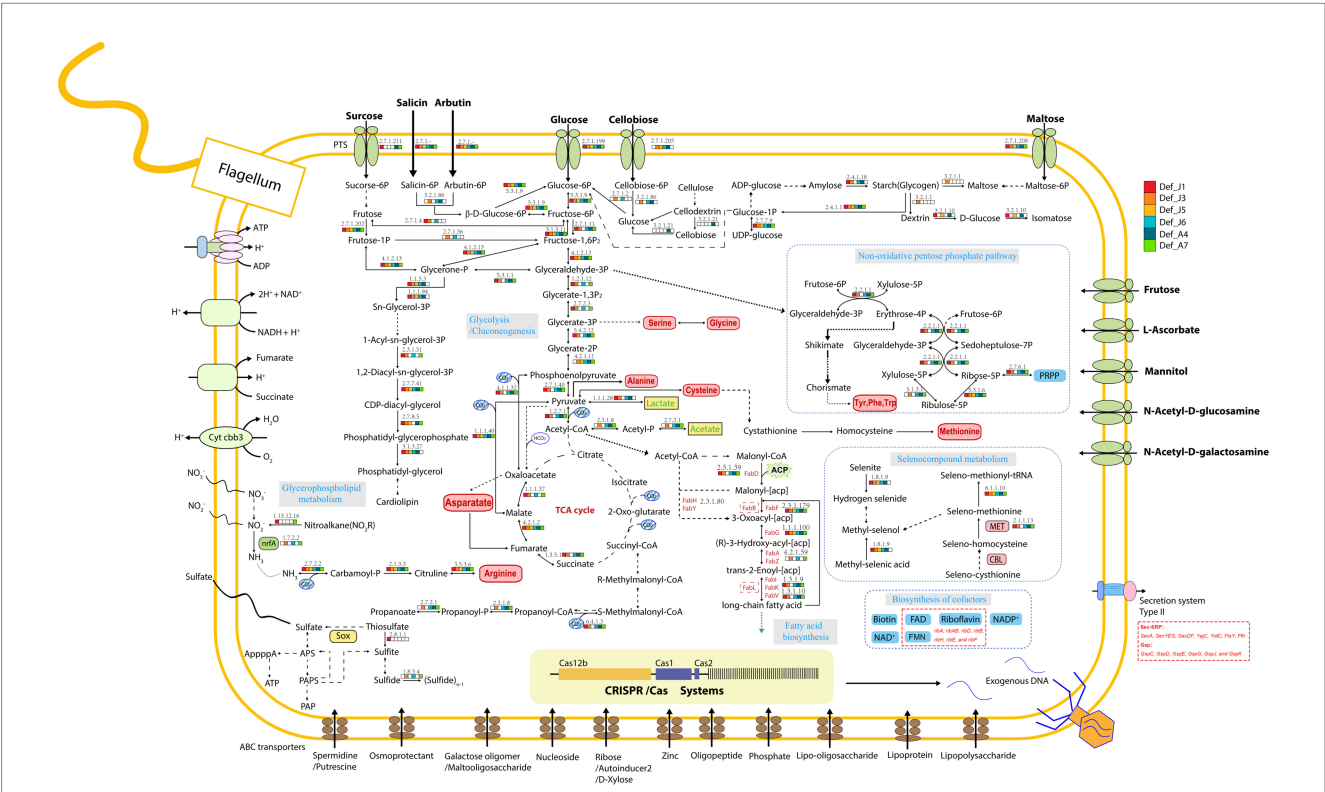


et al., 2005; Jones et al., 2008; Chandra et al., 2011; Sawers, 2016; Gupta et al., 2017; Klotz and Forchhammer, 2017). The classical pathway for glycogen synthesis is the GlgC-GlgA pathway, which generates activated glucose nucleotide diphosphate from glucose 1-phosphate *via* nucleotide diphosphate glucose pyrophosphorylase (GlgC), which then polymerizes by glycogen synthase (GlgA) to produce linear glucans. Finally, a non-reducing-end oligoglucan transfer mediated by branching enzymes (GlgB or GBE) to the 6-position of residues within a chain generates side branches that convert it to glycogen (Preiss, 2006). GBE (EC 2.4.1.18) is a determinant of glycogen structure and highly conserved (Zmasek and Godzik,

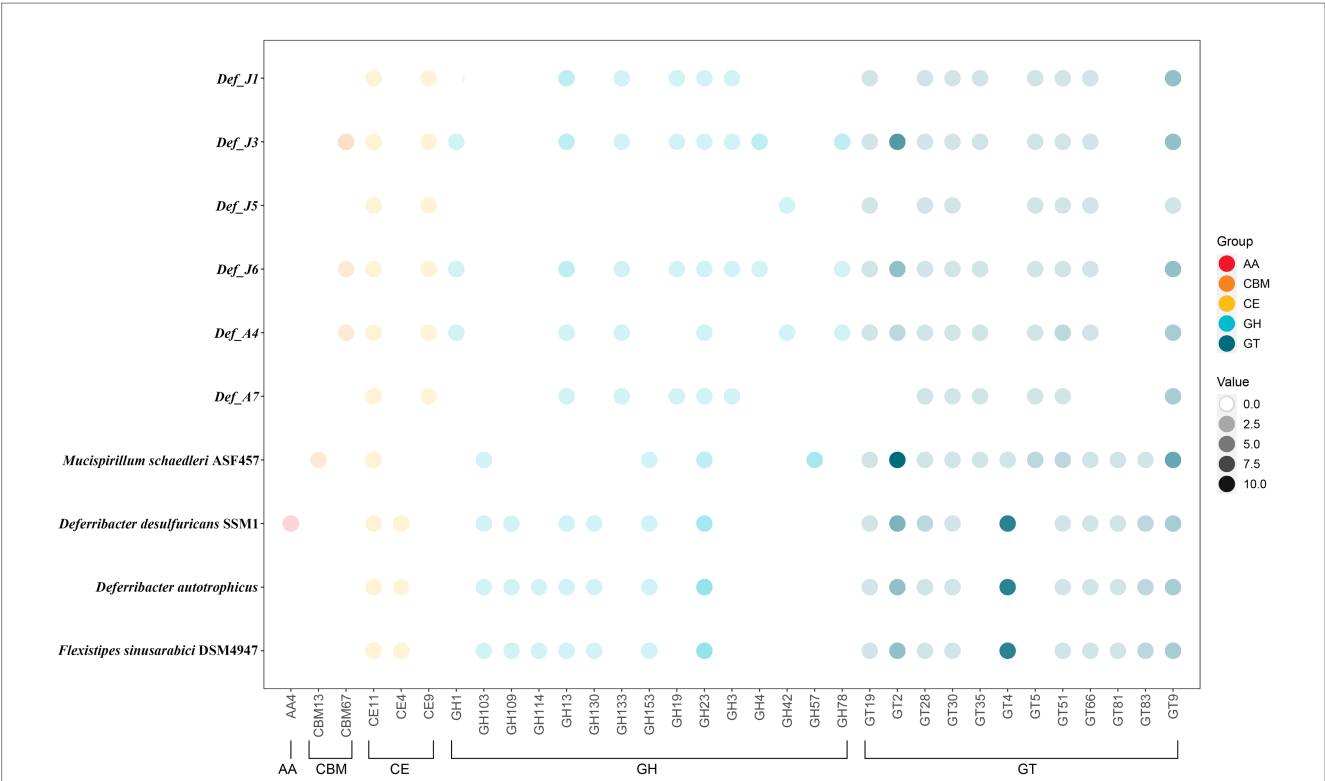
2014). Bacterial GBE belongs to the GH13 family of glucose hydrolases ( $\alpha$ -amylase family; Feng et al., 2015). In prokaryotes, glycogen has been considered to be degraded by highly conserved glycogen phosphorylases (GlgP) and debranching enzymes (GlgX; Wilson et al., 2010; Wang and Wise, 2011). GlgP can remove non-reducing terminal glycosyl residues until four glycosyl residues remain at the branching point, then GlgX acts on the short chain by truncating the  $\alpha$ -1,6-glycosidic bond (Dauvillée et al., 2005; Alonso-Casajús et al., 2006). The glucose 1-phosphate generated by glycogen degradation readily enters the primary generation. We found GlgP in six of the Def-MAGs, and GBE was in *Def\_J1*, *Def\_J3*, *Def\_J6*, and *Def\_A4*, indicating that Def-MAGs can participate in glycogen degradation and synthesis.

Based on the carbohydrate enzyme annotation, we found that there were nine specific enzymes in the six Def-MAGs of *R. kairei*, namely, CBM67, CE9, GH1, GH133, GH19, GH3, GH4, GH42, and GH78, compared with the four reference genomes of *Deferribacterota*. Of these, CBM67 is mainly able to bind L-rhamnose. CE9 esterases catalyse the deacetylation of N-acetylglucosamine-6-phosphate to glucosamine-6-phosphate. This reaction has been demonstrated to be important for bacterial amino sugar metabolism and peptidoglycan cell wall recycling (Park, 2001; Ahangar et al., 2018). GH1 mainly includes  $\beta$ -glucosidases and  $\beta$ -galactosidases but also includes 6-phosphate- $\beta$ -glucosidase and 6-phosphate- $\beta$ -galactosidases,  $\beta$ -mannosidase,  $\beta$ -D-fucosidase, and  $\beta$ -glucuronidase (Michalska et al., 2013). Def-MAGs mainly have  $\beta$ -glucosidases and  $\beta$ -galactosidases. GH133 is mainly amylo- $\alpha$  1,6-glucosidase (Stam et al., 2006). GH19 is an endo-acting enzyme that hydrolyses glycosidic bonds within chitin, a partially deacetylated chitin, with high degrees of acetylation, even though it lacks a CBM (Kawase et al., 2006). GH3 is widely distributed in bacteria, fungi, and plants and has a variety of functions, including cellulose biomass degradation, plant and bacterial cell wall remodelling, energy metabolism, and pathogen defence. It has been reported that GH3 can hydrolyse cellulose disaccharides and hydrolyse the nonreducing end  $\beta$ -1,4 bond of cellulose dextrans *via*  $\beta$ -glucosidase (Karkehabadi et al., 2018). GH4 differs from the other glycoside hydrolases in the family with different substrate specificities from each other. This family contains  $\alpha$ -glucosidases,  $\alpha$ -galactosidases,  $\alpha$ -glucosidase, 6-phospho- $\alpha$ -glucosidases and 6-phospho- $\beta$ -glucosidases. Similar to GH1, some enzymes prefer phosphorylated substrates to nonphosphorylated substrates (Henrissat and Bairoch, 1996; Henrissat and Davies, 1997). GH42 is active against lactose (Yuan et al., 2008). The only activity identified for GH78 was the hydrolysis of  $\alpha$ -L-rhamnosides (Mutter et al., 1994). These results indicate that the intestinal Def-MAGs can hydrolyse a variety of polysaccharides and can hydrolyse and utilize residues such as cellulose and chitin that are ingested by the hydrothermal shrimp *R. kairei* as an energy source.

In this study, we found that the six Def-MAGs have a type II secretory system for transferring endotoxin and exotoxin to the extracellular system. Many gram-negative bacteria secrete toxic factors and effectors for molecular communication with their hosts through the bacterial secretory system. There are six types of protein-secreting systems in gram-negative bacteria (Costa et al., 2015). Among them, the type II secretion system is mainly centred on the general secretory pathway (GSP) gene cluster. The other reference genomes mainly contain the bacterial type VI secretory



**FIGURE 3** Diagram of the major predicted metabolic pathways. Metabolites are shown in black, amino acids in red, cofactors in blue, and the enzymes predicted for each MAG in each process are shown in different small blocks of colour in the diagram, with white indicating that the enzyme is not present. PTS, ABC transporters, CRISPR–Cas systems, etc., are indicated in the diagram.



**FIGURE 4** Relative abundance of carbohydrate-active enzyme genes. The different coloured circles represent the different types of enzymes, auxiliary activity (AA), carbohydrate-binding module (CBM), carbohydrate esterase (CE), glycoside hydrolase (GH), and glycosyltransferase (GT). The darkness of the circles indicates the number of each carbohydrate-active enzyme gene in different MAGs. Gene distribution, classification, and functions are reported in [Supplementary Table S3](#).

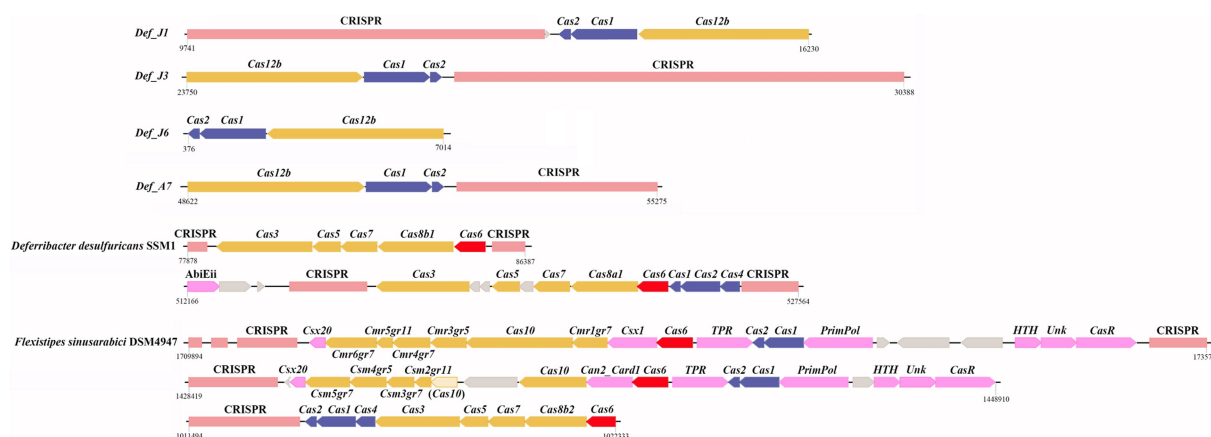


FIGURE 5

Structures of CRISPR–Cas systems. Structures of CRISPR–Cas systems in *Deferribacterota* and reference genomes. The CRISPR sequence is in pink. The interference module is in yellow. The adaptation module is in blue. *Cas6* is in red. Accessory genes are in purple. Genes with alignment scores below the thresholds are lighter and with parentheses around names. Unknown genes are in gray. The number represents the starting and ending positions on the contig. The arrow indicates the direction of the gene. The spacer BLAST results for spacers in the database of CRISPR/Casdb database are shown in [Supplementary Table S4](#).

system (T6SS), which is widely found in gram-negative bacteria and is an important “weapon” of bacterial competition. Its structure is similar to that of a phage’s caudal tube, which is inverted on the inside of the bacterial cell membrane (Cianfanelli et al., 2016). T6SS is commonly produced in multiple processes associated with bacterial virulence and had shown to attack bacterial competitors or defeat host defense mechanisms to survive in competition or colonized host ecological niches (Russell et al., 2011; Basler et al., 2013). The presence of a type VI secretion system and a putative effector protein in the mouse gut of *M. schaedleri* has been reported to alter gene expression in mucosal tissue, suggesting a close interaction with the host and a possible role in inflammation (Loy et al., 2017). The type II secretory system is widely found in animal and plant pathogens and can secrete various proteins for exocytosis, which is very common in gram-negative bacteria. We also identified a type V CRISPR–Cas immune protection system in the intestinal Def-MAGs of the hydrothermal shrimp *R. kairei*, which is capable of providing immune protection to the host against multiple pathogen invasions. In conclusion, intestinal Def-MAGs of the hydrothermal shrimp *R. kairei* may enhance its viability and competitiveness in the host intestinal environment through interaction with the host and provide immune protection to the host.

Only serine, glycine, and alanine synthesis pathways are present in Def-MAGs, but other amino acid synthesis pathways are missing, suggesting that these bacteria may acquire some amino acids from the host. However, synthetic pathways of riboflavin, biotin, FMN, and FAD are found in Def-MAGs, and these cofactors can provide nutritional help for the host under extreme environments. Although it has been reported in terrestrial animals that the *Deferribacterota* bacterium may be a pathogen causing some diseases, we found that the intestinal *Deferribacterota* of the hydrothermal shrimp *R. kairei* may provide a variety of nutritional and immune protection to the

host. Perhaps due to long-term coevolution, the intestinal *Deferribacterota* bacterium of the hydrothermal shrimp *R. kairei* has formed a mutualistic relationship with the host.

## 5. Conclusion and outlook

There is an interdependent relationship between the *Deferribacterota* bacterium and its host *R. kairei* in terms of material and energy, suggesting that *Deferribacterota* is a symbiont in the gut of *R. kairei*. The predominant occupation of *Deferribacterota* in the intestine of *R. kairei* plays an important role in survival. The study of the functions of *Deferribacterota* not only further explains the survival strategy and mechanism of blind shrimp in extreme environments but also deepens the understanding of the viability and living conditions of microorganisms.

## Data availability statement

The datasets presented in this study can be found in online repositories. The names of the repository/repositories and accession number(s) can be found in the article/[Supplementary material](#).

## Author contributions

QL and L-SH conceived and designed the experiments. QL performed the experiments. QL, MS, F-CZ, and C-AL analysed the data. QL and L-SH wrote the manuscript with input from all other authors. L-SH directed and supervised all of the research. All authors contributed to the article and approved the submitted version.



## Funding

This study was supported by the general projects of National Natural Science Foundation of China (42176125); the Scientific research and manufacture projects of Sanya City, Grant (NO. 2020KS01); Hainan Provincial Natural Science Foundation of China, grant (322CXTD531); the major scientific and technological projects of Hainan Province (ZDKJ2019011); and the major scientific and technological projects of Hainan Province (ZDKJ2021028).

## Conflict of interest

The authors declare that the research was conducted in the absence of any commercial or financial relationships that could be construed as a potential conflict of interest.

## References

- Ahangar, M. S., Furze, C. M., Guy, C. S., Cooper, C., Maskew, K. S., Graham, B., et al. (2018). Structural and functional determination of homologs of the *Mycobacterium tuberculosis* N-acetylglucosamine-6-phosphate deacetylase (NagA). *J. Biol. Chem.* 293, 9770–9783. doi: 10.1074/jbc.RA118.002597
- Alonso-Casajús, N., Dauvillée, D., Viale, A. M., Muñoz, F. J., Baroja-Fernández, E., Morán-Zorzano, M. T., et al. (2006). Glycogen phosphorylase, the product of the *glgP* gene, catalyzes glycogen breakdown by removing glucose units from the nonreducing ends in *Escherichia coli*. *J. Bacteriol.* 188, 5266–5272. doi: 10.1128/jb.01566-05
- Apremont, V., Cambon-Bonavita, M. A., Cuff-Gauchard, V., François, D., Pradillon, F., Corbari, L., et al. (2018). Gill chamber and gut microbial communities of the hydrothermal shrimp *Rimicaris chacei* Williams and Rona 1986: a possible symbiosis. *PLoS One* 13:e0206084. doi: 10.1371/journal.pone.0206084
- Aramaki, T., Blanc-Mathieu, R., Endo, H., Ohkubo, K., Kanehisa, M., Goto, S., et al. (2020). KofamKOALA: KEGG Ortholog assignment based on profile HMM and adaptive score threshold. *Bioinformatics* 36, 2251–2252. doi: 10.1093/bioinformatics/btz859
- Ball, S., Colleoni, C., and Arias, M. C. (2015). “The transition from glycogen to starch metabolism in Cyanobacteria and eukaryotes” in *Starch: Metabolism and Structure*. ed. Y. Nakamura (Tokyo: Springer Japan), 93–158.
- Bankovich, A., Nurk, S., Antipov, D., Gurevich, A. A., Dvorkin, M., Kulikov, A. S., et al. (2012). SPAdes: a new genome assembly algorithm and its applications to single-cell sequencing. *J. Comput. Biol.* 19, 455–477. doi: 10.1089/cmb.2012.0021
- Basler, M., Ho, B. T., and Mekalanos, J. J. (2013). Tit-for-tat: type VI secretion system counterattack during bacterial cell-cell interactions. *Cells* 152, 884–894. doi: 10.1016/j.cell.2013.01.042
- Bolger, A. M., Lohse, M., and Usadel, B. (2014). Trimmomatic: a flexible trimmer for Illumina sequence data. *Bioinformatics* 30, 2114–2120. doi: 10.1093/bioinformatics/btu170
- Brown, J., Pirrung, M., and McCue, L. A. (2017). FQC dashboard: integrates FastQC results into a web-based, interactive, and extensible FASTQ quality control tool. *Bioinformatics* 33, 3137–3139. doi: 10.1093/bioinformatics/btx373
- Capella-Gutiérrez, S., Silla-Martínez, J. M., and Gabaldón, T. (2009). trimAl: a tool for automated alignment trimming in large-scale phylogenetic analyses. *Bioinformatics* 25, 1972–1973. doi: 10.1093/bioinformatics/btp348
- Chandra, G., Chater, K. F., and Bornemann, S. (2011). Unexpected and widespread connections between bacterial glycogen and trehalose metabolism. *Microbiology (Reading)* 157, 1565–1572. doi: 10.1099/mic.0.044263-0
- Chaumeil, P. A., Mussig, A. J., Hugenholtz, P., and Parks, D. H. (2019). GTDB-Tk: a toolkit to classify genomes with the genome taxonomy database. *Bioinformatics* 36, 1925–1927. doi: 10.1093/bioinformatics/btz848
- Cianfanelli, F. R., Monlezun, L., and Coulthurst, S. J. (2016). Aim, load, fire: the type VI secretion system, a bacterial Nanoweapon. *Trends Microbiol.* 24, 51–62. doi: 10.1016/j.tim.2015.10.005
- Costa, T. R. D., Felisberto-Rodrigues, C., Meir, A., Prevost, M. S., Redzej, A., Trokter, M., et al. (2015). Secretion systems in gram-negative bacteria: structural and mechanistic insights. *Nat. Rev. Microbiol.* 13, 343–359. doi: 10.1038/nrmicro3456
- Cowart, D. A., Durand, L., Cambon-Bonavita, M. A., and Arnaud-Haond, S. (2017). Investigation of bacterial communities within the digestive organs of the hydrothermal vent shrimp *Rimicaris exoculata* provide insights into holobiont geographic clustering. *PLoS One* 12:e0172543. doi: 10.1371/journal.pone.0172543
- Dauvillée, D., Kinderf, I. S., Li, Z., Kosar-Hashemi, B., Samuel, M. S., Rampling, L., et al. (2005). Role of the *Escherichia coli* *glgX* gene in glycogen metabolism. *J. Bacteriol.* 187, 1465–1473. doi: 10.1128/jb.187.4.1465-1473.2005
- Douzi, B., Ball, G., Cambillau, C., Tegoni, M., and Voulhoux, R. (2011). Deciphering the Xcp *Pseudomonas aeruginosa* type II secretion machinery through multiple interactions with substrates. *J. Biol. Chem.* 286, 40792–40801. doi: 10.1074/jbc.M111.294843
- Durand, L., Zbinden, M., Cuff-Gauchard, V., Duperron, S., Roussel, E. G., Shillito, B., et al. (2010). Microbial diversity associated with the hydrothermal shrimp *Rimicaris exoculata* gut and occurrence of a resident microbial community. *FEMS Microbiol. Ecol.* 71, 291–303. doi: 10.1111/j.1574-6941.2009.00806.x
- El-Gebali, S., Mistry, J., Bateman, A., Eddy, S. R., Luciani, A., Potter, S. C., et al. (2019). The Pfam protein families database in 2019. *Nucleic Acids Res.* 47, D427–D432. doi: 10.1093/nar/gky995
- Feng, L., Fawaz, R., Hovde, S. L., Gilbert, L., Chiou, J., and Geiger, J. H. (2015). Crystal structures of *Escherichia coli* branching enzyme in complex with linear oligosaccharides. *Biochemistry* 54, 6207–6218. doi: 10.1021/acs.biochem.5b00228
- Galperin, M. Y., Wolf, Y. I., Makarova, K. S., Vera Alvarez, R., Landsman, D., and Koonin, E. V. (2021). COG database update: focus on microbial diversity, model organisms, and widespread pathogens. *Nucleic Acids Res.* 49, D274–D281. doi: 10.1093/nar/gkaa1018
- Garrity, G. M., Holt, J. M., Huber, H., Stetter, K. O., Greene, A. C., Patel, B. K. C., et al. (2001). “Phylum BIX. Deferribacteres phyl. nov.” in *Bergey's Manual® of Systematic Bacteriology: Volume One: The Archaea and the Deeply Branching and Phototrophic Bacteria*. eds. D. R. Boone, R. W. Castenholz and G. M. Garrity (New York, NY: Springer New York), 465–471.
- Gebruk, A., Southward, E., Kennedy, H., and Southward, A. (2000). Food sources, behaviour, and distribution of hydrothermal vent shrimps at the mid-Atlantic ridge. *J. Mar. Biol. Assoc. U K* 80, 485–499. doi: 10.1017/S0025315400002186
- Graham, E. D., Heidelberg, J. F., and Tully, B. J. (2018). Potential for primary productivity in a globally-distributed bacterial phototroph. *ISME J.* 12, 1861–1866. doi: 10.1038/s41396-018-0091-3
- Green, E. R., and Mecsas, J. (2016). Bacterial secretion systems: an overview. *Microbiol. Spectr.* 4:VMBF-0012-2015. doi: 10.1128/microbiolspec.VMBF-0012-2015
- Greene, T., Patel, B., and Sheehy, A. J. (1997). *Deferribacter thermophilus* gen. nov., sp. nov., a novel thermophilic manganese- and iron-reducing bacterium isolated from a petroleum reservoir. *Int. J. Syst. Bacteriol.* 47, 505–509. doi: 10.1099/00207713-47-2-505
- Grissa, I., Vergnaud, G., and Pourcel, C. (2007). CRISPRFinder: a web tool to identify clustered regularly interspaced short palindromic repeats. *Nucleic Acids Res.* 35, W52–W57. doi: 10.1093/nar/gkm360
- Gupta, A. K., Singh, A., and Singh, S. (2017). “Glycogen as key energy storehouse and possibly responsible for multidrug resistance in mycobacterium tuberculosis,” in *Drug Resistance in Bacteria, Fungi, Malaria, and Cancer*. eds. G. Arora, A. Sajid and V. C. Kalia (Cham: Springer International Publishing), 263–285.
- Guri, M., Durand, L., Cuff-Gauchard, V., Zbinden, M., Crassous, P., Shillito, B., et al. (2012). Acquisition of epibiotic bacteria along the life cycle of the hydrothermal shrimp *Rimicaris exoculata*. *ISME J.* 6, 597–609. doi: 10.1038/ismej.2011.133
- Henrissat, B., and Bairoch, A. (1996). Updating the sequence-based classification of glycosyl hydrolases. *Biochem. J.* 316, 695–696. doi: 10.1042/bj3160695

## Publisher's note

All claims expressed in this article are solely those of the authors and do not necessarily represent those of their affiliated organizations, or those of the publisher, the editors and the reviewers. Any product that may be evaluated in this article, or claim that may be made by its manufacturer, is not guaranteed or endorsed by the publisher.

## Supplementary material

The Supplementary material for this article can be found online at: <https://www.frontiersin.org/articles/10.3389/fmicb.2023.1179935/full#supplementary-material>

- Henrissat, B., and Davies, G. (1997). Structural and sequence-based classification of glycoside hydrolases. *Curr. Opin. Struct. Biol.* 7, 637–644. doi: 10.1016/s0959-440x(97)80072-3
- Huerta-Cepas, J., Forslund, K., Coelho, L. P., Szklarczyk, D., Jensen, L. J., von Mering, C., et al. (2017). Fast genome-wide functional annotation through Orthology assignment by eggNOG-mapper. *Mol. Biol. Evol.* 34, 2115–2122. doi: 10.1093/molbev/msx148
- Hügler, M., Petersen, J., Dubilier, N., Imhoff, J., and Sievert, S. (2011). Pathways of carbon and energy metabolism of the Epibiotic community associated with the Deep-Sea hydrothermal vent shrimp *Rimicaris exoculata*. *PLoS One* 6:e16018. doi: 10.1371/journal.pone.0016018
- Jain, C., Rodriguez, R. L., Phillippy, A. M., Konstantinidis, K. T., and Aluru, S. (2018). High throughput ANI analysis of 90K prokaryotic genomes reveals clear species boundaries. *Nat. Commun.* 9:5114. doi: 10.1038/s41467-018-07641-9
- Jan, C., Petersen, J. M., Werner, J., Teeling, H., Huang, S., Glöckner, F. O., et al. (2014). The gill chamber epibiosis of deep-sea shrimp *Rimicaris exoculata*: an in-depth metagenomic investigation and discovery of Zetaproteobacteria. *Environ. Microbiol.* 16, 2723–2738. doi: 10.1111/1462-2920.12406
- Jiang, L., Liu, X., Dong, C., Huang, Z., Cambon-Bonavita, M. A., Alain, K., et al. (2020). "Candidatus Desulfobulbus rimicariensis," an uncultivated Deltaproteobacterial Epibiont from the Deep-Sea hydrothermal vent shrimp *Rimicaris exoculata*. *Appl. Environ. Microbiol.* 86:e02549-19. doi: 10.1128/aem.02549-19
- Johnson, T. L., Abendroth, J., Hol, W. G., and Sandkvist, M. (2006). Type II secretion: from structure to function. *FEMS Microbiol. Lett.* 255, 175–186. doi: 10.1111/j.1574-6968.2006.00102.x
- Jones, S. A., Jorgensen, M., Chowdhury, F. Z., Rodgers, R., Hartline, J., Leatham, M. P., et al. (2008). Glycogen and maltose utilization by *Escherichia coli* O157:H7 in the mouse intestine. *Infect. Immun.* 76, 2531–2540. doi: 10.1128/iai.00096-08
- Jumas-Bilak, E., Roudière, L., and Marchandin, H. (2009). Description of 'Synergistetes' phyl. Nov. and emended description of the phylum 'Deferribacteres' and of the family Syntrophomonadaceae, phylum 'Firmicutes'. *Int. J. Syst. Evol. Microbiol.* 59, 1028–1035. doi: 10.1099/ijs.0.006718-0
- Kanehisa, M., Sato, Y., and Morishima, K. (2016). BlastKOALA and GhostKOALA: KEGG tools for functional characterization of genome and metagenome sequences. *J. Mol. Biol.* 428, 726–731. doi: 10.1016/j.jmb.2015.11.006
- Karkehabadi, S., Hansson, H., Mikkelsen, N. E., Kim, S., Kaper, T., Sandgren, M., et al. (2018). Structural studies of a glycoside hydrolase family 3  $\beta$ -glucosidase from the model fungus *Neurospora crassa*. *Acta Crystallogr. F Struct. Biol. Commun.* 74, 787–796. doi: 10.1107/s2053230x18015662
- Katoh, K., Misawa, K., Kuma, K., and Miyata, T. (2002). MAFFT: a novel method for rapid multiple sequence alignment based on fast Fourier transform. *Nucleic Acids Res.* 30, 3059–3066. doi: 10.1093/nar/gkf436
- Kawase, T., Yokokawa, S., Saito, A., Fujii, T., Nikaidou, N., Miyashita, K., et al. (2006). Comparison of enzymatic and antifungal properties between family 18 and 19 chitinases from *S. coelicolor* A3(2). *Biosci. Biotechnol. Biochem.* 70, 988–998. doi: 10.1271/bbb.70.988
- Klotz, A., and Forchhammer, K. (2017). Glycogen, a major player for bacterial survival and awakening from dormancy. *Future Microbiol.* 12, 101–104. doi: 10.2217/fmb-2016-0218
- Kunisawa, T. (2011). Inference of the phylogenetic position of the phylum Deferribacteres from gene order comparison. *Antonie Van Leeuwenhoek* 99, 417–422. doi: 10.1007/s10482-010-9492-7
- Lapidus, A., Chertkov, O., Nolan, M., Lucas, S., Hammon, N., Deshpande, S., et al. (2011). Genome sequence of the moderately thermophilic halophile *Flexistipes sinusarabici* strain (MAS10T). *Stand. Genomic Sci.* 5, 86–96. doi: 10.4056/sigs.2235024
- Leticia, I., and Bork, P. (2019). Interactive Tree Of Life (iTOL) v4: recent updates and new developments. *Nucleic Acids Res.* 47, W256–W259. doi: 10.1093/nar/gkz239
- Loy, A., Pfann, C., Steinberger, M., Hanson, B., Herp, S., Brugiroux, S., et al. (2017). Lifestyle and horizontal gene transfer-mediated evolution of *Mucispirillum schaedleri*, a Core member of the murine gut microbiota. *mSystems* 2:e00171-16. doi: 10.1128/mSystems.00171-16
- McMeechan, A., Lovell, M. A., Cogan, T. A., Marston, K. L., Humphrey, T. J., and Barrow, P. A. (2005). Glycogen production by different *Salmonella enterica* serotypes: contribution of functional glgC to virulence, intestinal colonization and environmental survival. *Microbiology (Reading)* 151, 3969–3977. doi: 10.1099/mic.0.28292-0
- Meier-Kolthoff, J. P., Carbasse, J. S., Peinado-Olarte, R. L., and Göker, M. (2021). TYGS and LPSN: a database tandem for fast and reliable genome-based classification and nomenclature of prokaryotes. *Nucleic Acids Res.* 50, D801–D807. doi: 10.1093/nar/gkab902
- Michalska, K., Tan, K., Li, H., Hatzos-Skintges, C., Bearden, J., Babnigg, G., et al. (2013). GH1-family 6-P- $\beta$ -glucosidases from human microbiome lactic acid bacteria. *Acta Crystallogr. D Biol. Crystallogr.* 69, 451–463. doi: 10.1107/s0907444912049608
- Miroshnichenko, M. L., Slobodkin, A. I., Kostrikina, N. A., L'Haridon, S., Nercessian, O., Spring, S., et al. (2003). *Deferribacter abyssi* sp. nov., an anaerobic thermophile from deep-sea hydrothermal vents of the mid-Atlantic ridge. *Int. J. Syst. Evol. Microbiol.* 53, 1637–1641. doi: 10.1099/ijs.0.02673-0
- Mutter, M., Beldman, G., Schols, H. A., and Voragen, A. G. (1994). Rhamnogalacturonan alpha-L-rhamnopyranohydrolase. A novel enzyme specific for the terminal nonreducing rhamnosyl unit in rhamnogalacturonan regions of pectin. *Plant Physiol.* 106, 241–250. doi: 10.1104/pp.106.1.241
- Nguyen, L. T., Schmidt, H. A., von Haeseler, A., and Minh, B. Q. (2015). IQ-TREE: a fast and effective stochastic algorithm for estimating maximum-likelihood phylogenies. *Mol. Biol. Evol.* 32, 268–274. doi: 10.1093/molbev/msu300
- Nivaskumar, M., and Francetic, O. (2014). Type II secretion system: a magic beanstalk or a protein escalator. *Biochim. Biophys. Acta* 1843, 1568–1577. doi: 10.1016/j.bbamcr.2013.12.020
- Park, J. T. (2001). Identification of a dedicated recycling pathway for anhydro-N-acetylmuramic acid and N-acetylglucosamine derived from *Escherichia coli* cell wall murein. *J. Bacteriol.* 183, 3842–3847. doi: 10.1128/jb.183.13.3842-3847.2001
- Parks, D. H., Imelfort, M., Skennerton, C. T., Hugenholtz, P., and Tyson, G. W. (2015). CheckM: assessing the quality of microbial genomes recovered from isolates, single cells, and metagenomes. *Genome Res.* 25, 1043–1055. doi: 10.1101/gr.186072.114
- Petersen, J. M., Ramette, A., Lott, C., Cambon-Bonavita, M.-A., Zbinden, M., and Dubilier, N. (2010). Dual symbiosis of the vent shrimp *Rimicaris exoculata* with filamentous gamma- and epsilonproteobacteria at four mid-Atlantic ridge hydrothermal vent fields. *Environ. Microbiol.* 12, 2204–2218. doi: 10.1111/j.1462-2920.2009.02129.x
- Preiss, J. (2006). "Bacterial glycogen inclusions: enzymology and regulation of synthesis," in *Inclusions in Prokaryotes*. ed. J. M. Shively (Berlin, Heidelberg: Springer Berlin Heidelberg), 71–108.
- Pugsley, A. P., Kornacker, M. G., and Poquet, I. (1991). The general protein-export pathway is directly required for extracellular pullulanase secretion in *Escherichia coli* K12. *Mol. Microbiol.* 5, 343–352. doi: 10.1111/j.1365-2958.1991.tb02115.x
- Qi, L., Lian, C. A., Zhu, F. C., Shi, M., and He, L. S. (2021). Comparative analysis of intestinal microflora between two developmental stages of *Rimicaris kairei*, a hydrothermal shrimp from the central Indian ridge. *Front. Microbiol.* 12:802888. doi: 10.3389/fmicb.2021.802888
- Rodriguez-R, L., and Konstantinidis, K. (2014). Bypassing cultivation to identify bacterial species: culture-independent genomic approaches identify credibly distinct clusters, avoid cultivation bias, and provide true insights into microbial species. *Microbe Magazine* 9, 111–118. doi: 10.1128/microbe.9.111.1
- Russel, J., Pinilla-Redondo, R., Mayo-Muñoz, D., Shah, S. A., and Sørensen, S. J. (2020). CRISPR-CasTyper: automated identification, annotation, and classification of CRISPR-Cas loci. *Crispr J* 3, 462–469. doi: 10.1089/crispr.2020.0059
- Russell, A. B., Hood, R. D., Bui, N. K., LeRoux, M., Vollmer, W., and Mougous, J. D. (2011). Type VI secretion delivers bacteriolytic effectors to target cells. *Nature* 475, 343–347. doi: 10.1038/nature10244
- Sawers, R. G. (2016). Dormancy: illuminating how a microbial sleeping beauty awakens. *Curr. Biol.* 26, R1139–r1141. doi: 10.1016/j.cub.2016.08.039
- Seemann, T. (2014). Prokka: rapid prokaryotic genome annotation. *Bioinformatics* 30, 2068–2069. doi: 10.1093/bioinformatics/btu153
- Slobodkin, A., Slobodkina, G., Allieux, M., Alain, K., Jebbar, M., Shadrin, V., et al. (2019). Genomic insights into the carbon and energy metabolism of a thermophilic Deep-Sea bacterium *Deferribacter autotrophicus* revealed new metabolic traits in the phylum Deferribacteres. *Genes (Basel)* 10:849. doi: 10.3390/genes10110849
- Stam, M. R., Danchin, E. G., Rancurel, C., Coutinho, P. M., and Henrissat, B. (2006). Dividing the large glycoside hydrolase family 13 into subfamilies: towards improved functional annotations of alpha-amylase-related proteins. *Protein Eng. Des. Sel.* 19, 555–562. doi: 10.1093/protein/gz1044
- Takaki, Y., Shimamura, S., Nakagawa, S., Fukuhara, Y., Horikawa, H., Ankai, A., et al. (2010). Bacterial lifestyle in a deep-sea hydrothermal vent chimney revealed by the genome sequence of the thermophilic bacterium *Deferribacter desulfuricans* SSM1. *DNA Res.* 17, 123–137. doi: 10.1093/dnares/dsq005
- Tatusov, R. L., Galperin, M. Y., Natale, D. A., and Koonin, E. V. (2000). The COG database: a tool for genome-scale analysis of protein functions and evolution. *Nucleic Acids Res.* 28, 33–36. doi: 10.1093/nar/28.1.33
- Uritskiy, G. V., DiRuggiero, J., and Taylor, J. (2018). MetaWRAP-a flexible pipeline for genome-resolved metagenomic data analysis. *Microbiome* 6:158. doi: 10.1186/s40168-018-0541-1
- Voulhoux, R., Ball, G., Ize, B., Vasil, M. L., Lazdunski, A., Wu, L. F., et al. (2001). Involvement of the twin-arginine translocation system in protein secretion via the type II pathway. *EMBO J.* 20, 6735–6741. doi: 10.1093/emboj/20.23.6735
- Wang, L., and Wise, M. J. (2011). Glycogen with short average chain length enhances bacterial durability. *Naturwissenschaften* 98, 719–729. doi: 10.1007/s00114-011-0832-x
- Watabe, H., and Hashimoto, J. (2002). A new species of the genus *Rimicaris* (Alvinocarididae: Caridea: Decapoda) from the active hydrothermal vent field, "Kairei field," on the central Indian ridge, the Indian Ocean. *Zool. Sci.* 19, 1167–1174. doi: 10.2108/zsj.19.1167
- Whitman, W. B., Oren, A., Chuvochina, M., da Costa, M. S., Garrity, G. M., Rainey, F. A., et al. (2018). Proposal of the suffix -ota to denote phyla. Addendum to 'Proposal to include the rank of phylum in the international code of nomenclature of Prokaryotes'. *Int. J. Syst. Evol. Microbiol.* 68, 967–969. doi: 10.1099/ijsem.0.002593
- Wilson, W. A., Roach, P. J., Montero, M., Baroja-Fernández, E., Muñoz, F. J., Eydollin, G., et al. (2010). Regulation of glycogen metabolism in yeast and bacteria. *FEMS Microbiol. Rev.* 34, 952–985. doi: 10.1111/j.1574-6976.2010.00220.x

- Yuan, T., Yang, P., Wang, Y., Meng, K., Luo, H., Zhang, W., et al. (2008). Heterologous expression of a gene encoding a thermostable beta-galactosidase from *Alicyclobacillus acidocaldarius*. *Biotechnol. Lett.* 30, 343–348. doi: 10.1007/s10529-007-9551-y
- Zbinden, M., and Cambon-Bonavita, M.-A. (2003). Occurrence of Deferribacterales and Entomoplasmatales in the deep-sea Alvinocarid shrimp *Rimicaris exoculata* gut. *FEMS Microbiol. Ecol.* 46, 23–30. doi: 10.1016/S0168-6496(03)00176-4
- Zbinden, M., and Cambon-Bonavita, M. A. (2020). *Rimicaris exoculata*: biology and ecology of a shrimp from deep-sea hydrothermal vents associated with ectosymbiotic bacteria. *Mar. Ecol. Prog. Ser.* 652, 187–222. doi: 10.3354/meps13467
- Zbinden, M., Shillito, B., le Bris, N., de Villardi de Montlaur, C., Roussel, E., Guyot, F., et al. (2008). New insights on the metabolic diversity among the epibiotic microbial community of the hydrothermal shrimp *Rimicaris exoculata*. *J. Exp. Mar. Biol. Ecol.* 359, 131–140. doi: 10.1016/j.jembe.2008.03.009
- Zhang, H., Yohe, T., Huang, L., Entwistle, S., Wu, P., Yang, Z., et al. (2018). dbCAN2: a meta server for automated carbohydrate-active enzyme annotation. *Nucleic Acids Res.* 46, W95–w101. doi: 10.1093/nar/gky418
- Zmasek, C. M., and Godzik, A. (2014). Phylogenomic analysis of glycogen branching and debranching enzymatic duo. *BMC Evol. Biol.* 14:183. doi: 10.1186/s12862-014-0183-2



## OPEN ACCESS

## EDITED BY

Zhiyong Li,  
Shanghai Jiao Tong University, China

## REVIEWED BY

Jaime Romero,  
University of Chile, Chile  
David Pérez-Pascual,  
Institut Pasteur, France

## \*CORRESPONDENCE

Ingrid Bakke  
✉ Ingrid.bakke@ntnu.no

RECEIVED 02 March 2023

ACCEPTED 19 June 2023

PUBLISHED 06 July 2023

## CITATION

Fiedler AW, Drågen MKR, Lorentsen ED,  
Vadstein O and Bakke I (2023) The stability and  
composition of the gut and skin microbiota of  
Atlantic salmon throughout the yolk sac stage.  
*Front. Microbiol.* 14:1177972.  
doi: 10.3389/fmicb.2023.1177972

## COPYRIGHT

© 2023 Fiedler, Drågen, Lorentsen, Vadstein  
and Bakke. This is an open-access article  
distributed under the terms of the [Creative  
Commons Attribution License \(CC BY\)](#). The  
use, distribution or reproduction in other  
forums is permitted, provided the original  
author(s) and the copyright owner(s) are  
credited and that the original publication in this  
journal is cited, in accordance with accepted  
academic practice. No use, distribution or  
reproduction is permitted which does not  
comply with these terms.

# The stability and composition of the gut and skin microbiota of Atlantic salmon throughout the yolk sac stage

Alexander W. Fiedler, Martha K. R. Drågen, Eirik D. Lorentsen,  
Olav Vadstein and Ingrid Bakke\*

Department of Biotechnology and Food Science, Norwegian University of Science and Technology,  
Trondheim, Norway

The bacterial colonization of newly hatched fish is important for the larval development and health. Still, little is known about the ontogeny of the early microbiota of fish. Here, we conducted two independent experiments with yolk sac fry of Atlantic salmon that were (1) either reared conventionally, with the eggs as the only source for bacteria (egg-derived microbiota; EDM) or (2) hatched germ-free and re-colonized using lake water (lake-derived microbiota; LDM). First, we characterized the gut and skin microbiota at 6, 9, and 13 weeks post hatching based on extracted RNA. In the second experiment, we exposed fry to high doses of either a fish pathogen or a commensal bacterial isolate and sampled the microbiota based on extracted DNA. The fish microbiota differed strongly between EDM and LDM treatments. The phyla Proteobacteria, Bacteroidetes, and Actinobacteria dominated the fry microbiota, which was found temporarily dynamic. Interestingly, the microbiota of EDM fry was more stable, both between replicate rearing flasks, and over time. Although similar, the skin and gut microbiota started to differentiate during the yolk sac stage, several weeks before the yolk was consumed. Addition of high doses of bacterial isolates to fish flasks had only minor effects on the microbiota.

## KEYWORDS

Atlantic salmon, initial colonization, microbiota, yolk sac fry, 16s sequencing

## 1. Introduction

All naturally living animals harbor a complex community of microorganisms, termed the animal's microbiota. The microbiota as assemblages of commensal and pathogenic bacteria have mainly been studied in mammalian species like mice and humans, and it has been shown that the microbiota serves its host in a multitude of ways, e.g., by providing nutrients, protecting against pathogens and enabling a proper development (Lynch and Hsiao, 2019; Zheng et al., 2020). The early bacterial colonization is crucial for the host's later development, influencing all aspects of adult life, like immune responses (Sevelsted et al., 2015), cognitive functions (Carlson et al., 2021), and nutrition (Huh et al., 2012).

These mechanisms are conserved between fish and mammals (Rawls et al., 2004; Phelps et al., 2017; Legrand et al., 2020; Borges et al., 2021). Fish live in close contact with bacteria in the surrounding water, which leads to an intimate relationship between fish and their surrounding bacteria. Fish therefore need strong barriers to protect themselves against unwanted microbes. The mucosal surfaces that cover the fish act as a selective barrier with antagonistic



properties against pathogens by providing nutrients and colonization space for the surrounding bacteria (Merrifield and Rodiles, 2015; Gomez and Primm, 2021). These mucosal surfaces on both skin and digestive tract are therefore the primary interaction site between the fish, its microbiota, and the microbes of the surrounding water (Li et al., 2019).

Generally, fish are microbe-free when they are in their eggs and immediately get colonized by the water microbes after hatching, making bacteria in the water an important source of the fish's microbiome at this stage (Llewellyn et al., 2014). This contrasts with mammals, where the initial microbiota mainly originates from the mother's microbiome (Ferretti et al., 2018). Generally, the skin of fish is colonized by bacteria immediately after hatching, and consensus is that the gut is colonized after the opening of the mouth (Reitan et al., 1998; Lokesh et al., 2019; Nikouli et al., 2019). Detailed studies of the early fish microbiota have been conducted in only a few species, and with a focus on the gut (reviewed by Borges et al., 2021). These few studies indicate that the initial fish gut bacterial community is dominated by Proteobacteria, Bacteroidetes, Firmicutes, and Actinomycetes and is increasing in diversity from early larval stages until the juvenile stage (Borges et al., 2021). Lokesh et al. (2019) investigated the ontogeny of the microbiota of Atlantic salmon and found that Proteobacteria were dominating the gut microbiota during the weeks before feeding. The onset of feeding seems to have a great influence on the composition of the gut microbiota (Ingerslev et al., 2014a,b; Michl et al., 2019). However, a well-established gut microbial community is probably already present before the fish start exogenous feeding (Ingerslev et al., 2014a,b; Sun et al., 2015; Stephens et al., 2016; Califano et al., 2017; Nikouli et al., 2019; Wilkes Walburn et al., 2019). Which factors influence these early microbial communities is, however, not thoroughly examined.

Further, not much research has been done on comparing the larval gut and skin microbiota and how they are assembled and interact (Dodd et al., 2020; Gomez and Primm, 2021). For adult fish, both the skin and gut microbiota are influenced by both abiotic factors (e.g., water temperature, salinity and diet) and biotic factors (e.g., sex, genetic background, and developmental stage) (Bakke et al., 2015; Dehler et al., 2017; Legrand et al., 2020). Viral and bacterial infections also influence the microbial community structures in the fish (Ingerslev et al., 2014a,b; Reid et al., 2017; Bozzi et al., 2021). It is further assumed that certain bacterial groups are selected for at the mucosal surfaces of the fish (Reitan et al., 1998; Lokesh et al., 2019).

Understanding the factors that affect the community assembly in developing fish is important as it could be used to steer against the presence of pathogenic and opportunistic bacteria in aquaculture systems, and thereby counteract negative fish-microbe interactions (Verschuere et al., 2000; Vadstein et al., 2018). This is especially important in the early life stages, when the immune system is not fully developed (Zapata et al., 2006) and the fish are explicitly vulnerable (Vadstein et al., 2013). The early life stages therefore generally represent a bottleneck in aquaculture (Sifa and Mathias, 1987). It has further been suggested that the fish microbiota plays a crucial role in protecting especially fish in their early life stages against pathogens (Liu et al., 2014; Pérez-Pascual et al., 2021; Stressmann et al., 2021). The early life stages of fish are therefore especially interesting for treatments to promote positive host-microbe interactions to reduce mortality and sickness. However, this requires more fundamental

knowledge of mechanisms involved in community assembly of early life stages.

Atlantic salmon (*Salmo salar*) is an important aquaculture species, with more than 2.4 million tonnes being produced per year (FAO, 2020). This species has a long yolk sac stage of around 500 day-degrees, and recently a protocol for raising germ-free salmon has been developed (Gomez de la Torre Canny et al., 2022). Thus, germ-free or gnotobiotic Atlantic salmon can be kept in their yolk sac stage for as long as 13 weeks at 6°C without feeding. This system is therefore an ideal model system for studying the initial colonization of a host and allows for complete manipulation of the colonizing bacterial communities. By using this experimental design, we recently showed that colonizing newly hatched salmon with fish distinct aquatic microbial communities resulted in distinct fish microbiota, which again influenced the skin mucosa, the somatic growth, and the utilization of the yolk (Gomez de la Torre Canny et al., 2022).

In this study, we used the gnotobiotic Atlantic salmon model system to investigate the initial bacterial colonization and the development of the gut and skin microbiota of Atlantic salmon throughout the yolk sac stage. We aimed to assess the influence of the composition of the bacterial source community present at hatching on the development of both the gut and skin microbiota. We hatched fish under germ-free conditions and exposed them to either their egg microbiota or to a lake water microbiota. Furthermore, we examined the potential for manipulating the early larval bacterial communities by exposing the fish to high concentrations of both a presumptive pathogenic (*Yersinia ruckeri* 06059) and a putative commensal bacterial strain (*Janthinobacterium* sp. 3.108). Finally, we compared skin and gut microbiota to the microbiota of the rearing water. Characterization of the host microbiota was done by extracting RNA (Exp.1) or DNA (Exp.2) from gut and skin samples (and water samples for Exp.2) and sequencing the v3 + v4 hypervariable region of the 16S rRNA (gene) using the Illumina platform. The microbiota analysis of Exp.1 was based on extracted RNA instead of DNA as the original intent with these samples was to investigate gene expression in the fish. Here, we used the extracted RNA to characterize the microbiota of the yolk sac fry.

## 2. Materials and methods

### 2.1. Experimental design

Two independent fish experiments were conducted from October 2019 to January 2020 (Exp.1) and from February to April 2020 (Exp.2).

For both experiments, Atlantic salmon yolk sac fry were raised under two microbial conditions: (1) Fish were raised under conventional microbial conditions, i.e., the eggs were not sterilized after arrival to the laboratory. However, they were hatched and reared in a sterile freshwater medium so that the only source of bacteria for colonization after hatching was bacteria originating from their eggs (egg-derived microbiota, EDM). (2) Alternatively, eggs were hatched under germ-free conditions and then exposed to bacteria by adding untreated lake water to the sterile rearing flasks (lake-derived microbiota, LDM). In the following, the terms “EDM flasks” and “LDM flasks” are used to refer to these two experimental groups, and

the terms “EDM samples” and “LDM samples” are used to refer to samples taken from EDM and LDM rearing flasks, respectively.

For Exp.1, samples were collected during the experiment described in Figure 4A in [Gomez de la Torre Canny et al. \(2022\)](#) from conventionally raised fish (corresponding to the EDM experimental group in the present study) and conventionalized fish (corresponding to the LDM experimental group in the present study). [Gomez de la Torre Canny et al. \(2022\)](#) included the analysis of the skin and gut at 13 weeks post hatching (wph). Here, we extended the analyses of the gut and skin microbiota at 13 wph and also included samples taken at 6 and 9 wph from two replicate flasks per sampling time. Characterization of microbial communities was performed by Illumina sequencing of the v3 + v4 16S rRNA amplicons, based on RNA extracts from gut and skin samples (for details, see below). Total RNA was extracted from fish samples in Exp.1 instead of DNA, because the samples were originally planned to be used to study gene expression in the fish by qPCR. Here, we used the extracted RNA to analyze the microbial communities.

Exp.2 was originally designed as a challenge experiment, with *Y. ruckeri* as the pathogen, and the commensal *Janthinobacterium* sp. 3.108 as a control, representing a non-pathogenic bacterium. The design originally included both germ-free fish, and colonized fish (EDM and LDM). However, the *Y. ruckeri* strain did not induce mortality in the fish, and we were therefore not able to investigate the potential protective role of the fish microbiota in pathogenic infection. Here, we used the fish and water samples that were collected to examine the effect on the fish and water microbiota of the exposure to high doses of *Y. ruckeri* and *J. sp. 3.108*. The experiment had a factorial design, with source bacterial community (EDM vs. LDM) and addition of high quantities of two bacterial isolates (added vs. not added) as the two factors. Exp.2 included nine EDM and nine LDM flasks. At 6 wph, either the fish pathogen *Yersinia ruckeri* 06059 or the fish commensal *Janthinobacterium* sp. 3.108 was added to three replicate flasks for both EDM and LDM, whereas three flasks were left untreated. This resulted in six experimental groups. Characterization of bacterial communities by 16S rRNA gene amplicon sequencing was based on total DNA extracts from gut, skin and water samples taken at 8 wph.

## 2.2. Fish husbandry

In general, the derivation of Atlantic salmon eggs and their husbandry as described in [Gomez de la Torre Canny et al. \(2022\)](#) was followed for Atlantic salmon husbandry. Briefly, salmon eggs were obtained at around 80% developmental status from AquaGen AS (Hemne, Norway), transferred to a dark room, and kept at a constant water temperature of  $5.8 \pm 0.3^\circ\text{C}$ . The eggs were placed in petri dishes (13.5 cm Ø) at a density of 100 eggs/dish and covered with Salmon Gnotobiotic Medium (SGM). SGM contained 0.5 mM  $\text{MgSO}_4$ , 0.054 mM KCl, 0.349 mM  $\text{CaSO}_4$  and 1.143 mM  $\text{NaHCO}_3$  dissolved in MilliQ water and was sterilized by autoclaving prior to use ( $121^\circ\text{C}$  for 20 min). One day after arrival, the fish eggs were split into two groups. One group was surface-sterilized to obtain germ-free fish [for generating conventionalized fry; LDM group, corresponding to CVZ in the study by [Gomez de la Torre Canny et al. \(2022\)](#)], whereas the other group was not treated [for generating conventionally reared fry; EDM group, corresponding to CVR in the study by [Gomez de la Torre](#)

[Canny et al. \(2022\)](#)]. Two days after arrival, all eggs were distributed into 250 ml cell culture flasks with vented caps and covered with 100 ml sterile SGM (17 eggs per flask). The eggs, and, after hatching, the fish, were reared in these flasks for the rest of the experiment. To maintain good water quality, 60% of the SGM in the fish flasks was exchanged three times a week and replaced with sterile SGM. Fish mortality was checked regularly, and dead fish were removed. For sampling and at the end of the experiment, fish were euthanized by a lethal dose of tricaine [5.2 g tricaine (20 mM final concentration) in 27.3 ml 1 M Tris buffer (pH 9), ad 1 L with SGM, sterilized by filtration through a 0.2 µm filter].

## 2.3. Sterilization of fish eggs and reintroduction of bacteria (conventionalization)

The sterilization procedure described by [Gomez de la Torre Canny et al. \(2022\)](#) was followed. Eggs were surface-sterilized 24 h after arrival at our laboratory. The eggs were submerged in an antibiotic cocktail (10 mg l<sup>-1</sup> Rifampicin, 10 mg l<sup>-1</sup> Erythromycin, 10 mg l<sup>-1</sup> Kanamycin, 100 mg l<sup>-1</sup> Ampicillin, 250 µg l<sup>-1</sup> Amphotericin B, 150 mg l<sup>-1</sup> Penicillin, and 75 mg l<sup>-1</sup> Oxolinic acid) and incubated at  $6^\circ\text{C}$  for 24 h. Afterwards, groups of 17 eggs were incubated in a Buffodine® solution (FishTech AS) containing 50 mg l<sup>-1</sup> available iodine for 30 min, washed four times in 50 ml SGM and were then transferred into 250 ml cell-culture flasks with vented caps containing 100 ml SGM. A sterility check was performed on the hatching day (hatching day defined as the day when 80% of all eggs have hatched) and regularly throughout the experiment by inoculating four different liquid media (Brain Heart Infusion, Glucose Yeast Broth, Sabourad-Dextrose Broth and Nutrient Broth) and Tryptic Soy Agar plates with 100 µl rearing water. The liquid media and TSA plates were incubated at room temperature for up to 3 weeks. If bacterial growth was observed in one of the media, the fish flask was considered contaminated and was removed from the experiment. One week after hatching, the axenic fish were conventionalized by removing 60 ml rearing water and adding 60 ml water from the lake Jonsvatnet (Trondheim, Norway). The water from lake Jonsvatnet was untreated and taken from a depth of 50 m in October 2019 (Exp.1) and March 2020 (Exp.2), respectively.

## 2.4. Isolation of *Janthinobacterium* sp. 3.108

*Janthinobacterium* sp. strain 3.108 was isolated from the skin of healthy Atlantic salmon fry in a commercial flow-through-system as follows: skin was scraped off both sides of an individual under aseptic conditions. The skin mucus was collected in a cryotube, added 500 µl glycerol (50%), snap-frozen on dry ice, and transported back to the laboratory. The sample was added Maximum Recovery Diluent (MRD), thawed and homogenized using a glass rod (MRD added step-wise to a total of 1 ml) and finally vortexed. The homogenate was serially diluted (1:10) in MRD and streaked on Plate Count Agar plates (PCA; 5 g tryptone, 2.5 g yeast extract, 1 g glucose and 12 g bacteriological agar per l). Single colonies were picked and resuspended in 50 µl MRD, serially diluted in MRD and streaked again on PCA plates. This was repeated two more times to ensure that the picked colony represented a single

bacterial isolate. The isolate was taxonomically assigned by PCR amplification of the 16S rRNA gene, followed by Sanger sequencing. PCR was performed using the primers Eub8F (5'-AGAGTTTGATCMTGGCTCAG-3') and 1492R (5'-TACGGYTACCTTGTACGACTT-3'). The PCR reactions were run for 35 cycles (98°C 15 s, 55°C 20 s, and 72°C 20 s) with 0.2 mM of each dNTP, 0.3 µM of each primer, and Phusion Hot Start II DNA polymerase and reaction buffer (Thermo Scientific). As template, we used 1 µl of a lysate generated by boiling a colony of the relevant isolate for 10 min. The resulting PCR product was purified using the QIAquick® PCR Purification Kit (Qiagen) as described by the manufacturers. The purified PCR product (5 µl) were mixed with 5 µl sequencing primer (5 mM) and sent to Eurofins Genomics for Sanger sequencing. Three sequencing primers were applied: Eub8F, 1492R, and 805R (5'-ATTACCGCGGCTGCTGG-3'). For the resulting sequences, regions of poor quality in the 5'- and 3'-ends, as well as primer sequences, were trimmed off, and the sequences were assembled. The resulting sequence is provided in [Supplementary Figure S7](#).

## 2.5. Bacterial exposure in Exp.2

At 5 wph, the number of fish was adjusted to 10 individuals per flask and the water temperature was gradually increased to  $14.0 \pm 0.1^\circ\text{C}$  over the course of 7 days. Two bacterial isolates were used in this experiment: *Y. ruckeri* 06059 and *Janthinobacterium* sp. 3.108 (described above). A virulent strain of *Yersinia ruckeri* (strain 06059; Serotype O1) that was isolated from Atlantic salmon in the UK in 2006 was kindly provided by Tim Wallis (Ridgeway Biologicals Ltd., UK; [Haig et al., 2011](#)). At 6 wph, three EDM and LDM flasks were added *Y. ruckeri* and three *J. sp.* 3.108. Three EDM and three LDM flasks served as untreated control. *Y. ruckeri* and *J. sp.* 3.108 were grown in liquid TSB medium overnight at room temperature in an orbital shaker at 120 rpm under aerobic conditions and harvested at an  $\text{OD}_{600}$  of app. 1. One ml culture was centrifuged at 13,000xg for 1 min to obtain a bacterial pellet. The pellet was washed with SGM once, before it was resuspended in 1 ml of SGM and added to the fish flasks. This resulted in a theoretical final concentration of app.  $10^7$  CFUml<sup>-1</sup> of the respective strains in the fish flasks. After addition of bacteria, the fish were reared at 14°C for 2 weeks (until 8 wph) and then sampled.

## 2.6. Sampling

For Exp.1, three fish were sampled from each of two replicate flasks for both EDM and LDM fish per timepoint (12 fish sampled at 6, 9, and 13 wph), resulting in a total of 36 fish sampled. The flasks were removed from the experiment after sampling. Sampling of gut and skin at 13 wph in Exp.1 is described by [Gomez de la Torre Canny et al. \(2022\)](#) and samples from 6 and 9 wph of Exp.1 were prepared the same way. In brief, individual fish were transferred to individual wells of a 12-well plate prefilled with sterile SGM. The SGM was replaced with sterile tricaine solution for euthanization and each fry was rinsed three times with sterile SGM. Excess SGM was removed and fish were individually dissected in sterile petri dishes. Using sterile forceps, the yolk sac was removed and discarded. The gut was dissected out of the fish by pulling it out from esophagus to anus and was placed in screw-cap centrifuge tubes prefilled with 200 µl 1.4 mm zirconium

beads and TRIzol (0.5 ml TRIzol for gut samples, 0.75 ml for skin samples from 6 and 9 wph and 1 ml TRIzol for skin samples from 13 wph). For samples from 6 and 9 wph, the remainder of the fish was used as an approximation for a skin sample, since the skin mucosa could not be dissected off the fish at these early stages, while for samples taken at 13 wph the skin was dissected off the fish.

In Exp.2, three fish were sampled at 8 wph from three flasks each of both EDM and LDM flasks for the two bacteria-treated groups and the untreated control. In addition, a water sample was taken from each flask, resulting in a total of 54 fish samples and 18 water samples. Fish samples were prepared by replacing the rearing water of the sampled fish flasks with sterile tricaine solution. After euthanisation of the fish, individual fish were transferred to individual wells of a 6-well petri dish prefilled with sterile SGM. For rinsing, each individual was transferred to a new well prefilled with sterile SGM. The fish were removed from the wells using sterile forceps and excessive SGM was removed using Kimtech-Wipes, without the fish touching the wipes. Each fish was transferred to a sterile petri dish and was dissected under a stereoscope. Using sterile forceps, the yolk sac was removed and discarded and the gut was dissected from the fish by pulling it from anus to esophagus. The rest of the fish was used as skin sample. Gut and skin samples were each transferred into separate 2-ml empty sterile screw-cap centrifuge tubes. Water samples were taken by filtrating 45 ml of fish rearing water through a 0.2 µm filter (STERIVEX™, Millipore) and placing the filter in an empty sterile 2 ml screw-cap tube. All samples from both experiments were snap frozen in liquid nitrogen and stored at  $-80^\circ\text{C}$  until DNA/RNA extraction.

## 2.7. DNA and RNA extraction and cDNA synthesis

For Exp.1, total RNA was extracted and cDNA synthesized as previously described ([Gomez de la Torre Canny et al., 2022](#)). In brief, gut and skin samples were homogenized and total RNA was extracted using the Purelink™ RNA Mini Kit (Invitrogen™), then treated with DNase (On-Column Purelink DNase Treatment; Invitrogen), and immediately frozen at  $-80^\circ\text{C}$ . The iScript™ cDNA Synthesis kit (Bio-Rad) was used for cDNA synthesis with 800 ng DNase treated RNA as template, following the manufacturer's instructions.

For samples collected in Exp.2, DNA was extracted from skin, gut and water samples using a KingFisher Flex instrument with the ZymoBIOMICS™ 96 MagBead DNA kit. First, all samples were homogenized and lysed in 750 µl lysis buffer from the kit by vortexing them horizontally in 2 ml screwcap tubes with 1.4 mm Zirconium beads for 45 min. DNA was extracted from 300 µl lysate following the kit's protocol for the KingFisher Flex (50 µl DNase-free water was used for elution) and samples were frozen at  $-20^\circ\text{C}$  until examination. For a few samples we could not generate 16S rRNA gene amplicons, here, the DNA extraction was repeated using the remaining 400 µl of the lysate.

## 2.8. Amplification of the v3-v4 region of the 16S rRNA gene

Two amplicon libraries were prepared, one for samples from Exp.1 and one for samples from Exp.2. For DNA extracts from Exp.2, the v3 + v4 region of the 16S rRNA gene was amplified using the primers



III-338F (5'-TCGTCGGCAGCGTCAGATGTGTATAAGAGACAG NNNN**ACTCCTACGGGWWGCAGCAG**-3') and III-805R (5'-GTCTCGTGGGCTCGGAGATGTGTATAAGAGACAGNNNN**GACTACNVGGGTATCTAAKCC**-3'), with the target sequences shown in bold (Nordgard et al., 2017). For the cDNA representing total RNA from the samples from Exp.1, we had problems with co-amplification of host DNA, and therefore designed a new forward primer that had lower similarity to the *Salmo salar* 18S rRNA gene (III-329F: 5'-TCGTCGGCAGCGTCAGATGTGTATAAGAGACAGNNNN**CKGNCCWDACWCCTACGGG**-3'; Gomez de la Torre Canny et al., 2022). The same reverse primer as for Exp.2 was used for Exp.1.

The PCRs were performed in 25 µl total reaction volume with either 1 µl cDNA extracts (Exp.1) or 2 µl of 1:10 diluted DNA extracts (Exp.2) as templates. Each PCR reaction contained 0.3 µM of each primer (0.15 µM for Exp.2) and 0.25 µM of each dNTP as well as 0.4 U Phusion hot start polymerase and the respective buffer from Thermo Scientific. The PCRs were run with the following temperature cycling conditions: an initial denaturation step at 98°C for 60 s followed by 38–40 cycles (33 cycles for water samples) of 98°C for 15 s, 58°C for 20 s (55°C for the second experiment) and 72°C for 20 s. The final elongation step was 72°C for 5 min before the samples were cooled to 10°C. PCR products were evaluated by electrophoresis on 1.5% agarose gels containing 50 µM GelRed (Biotium) for 1 h at 110 V.

## 2.9. Amplicon library preparation and Illumina sequencing

PCR products of expected size and quantity were normalized using Sequal Prep™ Normalization plates (96 wells, Invitrogen) before they were indexed using the Nextera® XT Index Kit v2 Set A in a second round of PCR. Indexing PCR consisted of 2.5 µl normalized and purified PCR product as template, 2.5 µl of both indexing primers, 0.25 µM of each dNTP, 0.5 mM MgCl<sub>2</sub> (in addition to MgCl<sub>2</sub> contained in the buffer) as well as 0.4 U Phusion hot start polymerase and the respective buffer from Thermo Scientific in a total reaction volume of 25 µl. The indexing PCR was run with an annealing temperature of 58°C and 10 cycles, the other cycling conditions were as described above. The indexed PCR products were normalized using the Sequal Prep Normalization kit and then pooled and up-concentrated using an Amicon® Ultra 0.5 ml centrifugal filter (30 K membrane, Merck Millipore). The quality of the DNA of the amplicon libraries was determined using a NanoDrop™ One Microvolume Spectrophotometer (Thermo Scientific™). For Exp.1, the amplicon library included 93 samples, whereas for Exp.2 the amplicon library included 96 samples (both libraries included few samples not relevant for this study). The samples were sent to the Norwegian Sequencing Center using one run on a MiSeq v3 instrument for each amplicon library with 300 paired ends. The sequencing data was deposited at the European Nucleotide Archive (ERS14440101-ERS14440192).

## 2.10. Analysis of the Illumina sequencing data

The USEARCH pipeline (v.11) (Edgar, 2010) was used to process the data obtained from Illumina sequencing. For Exp.1, all data were

processed together as described in Gomez de la Torre Canny et al. (2022), while the data obtained from Exp.2 were processed together using the same pipeline. In brief, the paired reads were merged, and primer sequences trimmed off using the Fastq\_mergepairs command with a minimal length of 390 bp. The merged sequences were quality-filtered using the Fastq-filter function with the default error threshold value of 1. The reads were pooled, dereplicated and singleton reads removed. Zero-range OTUs (zOTUs, synonymous to amplicon sequence variants, ASVs) were generated using the Unoise3 command (Edgar, 2016b) with the default minimum abundance threshold of 8 reads in the total dataset. Taxonomical assignment of the ASVs was achieved using the SINTAX command (Edgar, 2016a) with a confidence threshold of 0.8 and the ribosomal database project (RDP) reference dataset. RDP training set v16 was used for the data obtained from Exp.2 and training set v18 for the data obtained from Exp.1. A minor fraction of the reads was classified as eukaryotes and chloroplasts and were removed from the data set. A few ASVs that were highly abundant in negative controls for the DNA extraction, but less abundant in the samples, were considered to represent contaminating DNA associated with the DNA extraction kit and/or PCR reagents and were removed from the data sets. For Exp.2, ASV3 and ASV15 were combined to ASV3-15, since both ASVs corresponded to *Janthinobacterium* sp. 3.108, which has two highly similar 16S rRNA gene sequences, differing in only one base pair that corresponded to an ambiguous nucleotide position in the 16S rDNA sequence of *J.* sp. 3.108 (Supplementary Figure S7). After quality filtering, the 70 samples of Exp.1 contained a total of 1,562 ASVs and 4,777,641 reads (68,252 reads per sample on average). For Exp.2, the 91 samples consisted of 598 ASVs and 9,583,497 reads (105,312 reads per sample on average). The mean sequencing depth, as indicated by Chao-1 was 83.8% for Exp.1 and 83.4% for Exp.2 (Supplementary Tables S1, S2). The final ASV tables were normalized by scaling to 26,000 reads per sample (Exp.1) and 43,347 reads per sample (Exp.2), respectively. All statistical analyses were performed using the normalized ASV tables.

## 2.11. Statistical analysis

All statistical analyses were performed in R (v. 4.0.4)<sup>1</sup> using the packages Phyloseq (v. 1.34.0) and Vegan (v. 2.5.7). α-diversities were calculated as Hill's diversity numbers (Hill, 1973; Lucas et al., 2017) using the *renyi* function of vegan. The evenness was calculated by dividing Hill's diversity of order 1 (exponential Shannon index) by Hill's diversity of order 0 (richness). Ordination by principal coordinate analyses (PCoAs) were performed using the *ordinate* function from phyloseq for Bray–Curtis similarities, if not stated otherwise. For PCoAs based on weighted Unifrac analysis, phylogenetic trees were generated using the MEGA-X software. The trees were generated employing the maximum likelihood method using a Tamura–Nei model with 1,000 bootstrap replications. The trees were rooted by using the longest branch as root. To compare similarity in community composition between groups of samples, PERMANOVA analyses (Anderson, 2001) based on Bray–Curtis similarities (if not stated otherwise) were done using the *adonis2*

<sup>1</sup> <https://cran.rstudio.com/>



function from *vegan* by running it in 100 iterations with 999 permutations each and the mean value of  $p$  of the 100 iterations was reported (mathematically lowest possible value of  $p=0.001$ ). Whenever the sample size allowed it, PERMANOVAs were run as nested PERMANOVAs with “replicate flask” as sublevel. For statistical univariate data (e.g.,  $\alpha$ -diversity indices or abundance of certain ASVs), the data was checked for normality using the Shapiro–Wilk test (*shapiro.test* function). Generally, the data were not normally distributed and therefore a Mann–Whitney  $U$  test was used for data with two groups (*wilcox.test* function) and a Kruskal–Wallis test (*Kruskal.test* function) was used when more than two groups were compared. A significant Kruskal–Wallis test was followed by a Bonferroni-corrected Dunn test (*dunnTest* function).

### 3. Results

#### 3.1. Hatching rate and survival of the fish

The hatchability of eggs in Exp.1 was very high and has already been reported in [Gomez de la Torre Canny et al. \(2022\)](#). The hatchability of Exp.2 was equally high, being >90% in both LDM and EDM flasks. For Exp.2, none of the fish died after addition of *Y. ruckeri* and two fish died after *J. sp. 3.108* was added to their replicate flasks. One fish died in the untreated control group. The bacterial fish pathogen *Y. ruckeri* did therefore not induce mortality in the 6-week-old Atlantic salmon under the experimental conditions applied in this study.

#### 3.2. The influence of the source microbiota on the gut and skin microbiota of Atlantic salmon larvae

The fish in both experiments included in this study derived their bacterial communities from one of two source microbiota, either from their eggs (egg-derived microbiota, EDM, i.e., the eggs were not hatched germ-free, but in the presence of the microbiota associated with the eggs) or from lake water (lake-derived microbiota, LDM, lake water added to germ-free fry soon after hatching). All the bacteria in EDM flasks therefore originated from the fish eggs (EDM source microbiota) and all bacteria in the LDM flasks originated from the freshwater lake water (LDM source microbiota). Principal coordinate analysis (PCoA) based on the Bray–Curtis similarities for samples from Exp.1 showed that the fish microbiota differed considerably between EDM and LDM samples ([Figure 1A](#)). A nested PERMANOVA test with “replicate flask” as sublevel showed that the fish microbiota differed significantly between EDM and LDM samples at all sampling times (6, 9 and 13 wph; PERMANOVA, value of  $p$ s = 0.002,  $\leq 0.001$  and  $\leq 0.001$ , respectively; gut and skin samples combined). Average Bray–Curtis similarities showed that the microbiota of the EDM and LDM became increasingly different with increasing age ([Supplementary Figure S1](#)).

Also for Exp.2, a PCoA corroborated this finding, and showed a clear separation of the fish microbiota between the EDM and LDM samples ([Figure 1B](#)). A nested PERMANOVA test with “replicate flask” as sublevel showed again that the fish microbiota differed significantly between LDM and EDM samples (value of

$p \leq 0.001$ ). Interestingly, the separation between the microbiota of the EDM and LDM fish was less prominent in a PCoA based on weighted UniFrac distances ([Supplementary Figure S2](#)). However, for Exp.1 the differences were still significant for samples from week 9 and 13 (nested PERMANOVA,  $p \leq 0.001$ ; gut and skin combined) but not for week 6 samples ( $p = 0.464$ ). Also for Exp.2, the nested PERMANOVA showed that the difference between EDM and LDM microbiota was significantly different when UniFrac distances were used ( $p = 0.019$ ). Altogether, these results show that the source microbiota had a major impact on the bacterial communities associated with the fish.

Pseudomonadales, Burkholderiales, Propionibacteriales, and Flavobacteriales were the dominant bacterial orders for all fish samples in both experiments ([Figure 2](#)). Interestingly, the order Pseudomonadales had a significantly higher relative abundance in the fish microbiota in LDM flasks, both in Exp.1 and Exp.2 ( $t$ -test,  $p < 0.001$  and  $p = 0.013$  for Exp.1 and Exp.2, respectively), and accounted on average for as much as 20–60% of the reads in the samples. Furthermore, Flavobacteriales was more abundant in the fish microbiota of EDM than the LDM samples in both experiments.

At ASV level, most of the abundant ASVs were exclusively present in either EDM or LDM samples ([Figure 3](#) and [Supplementary Figures S3, S4](#)). Most samples, especially of the LDM group, were dominated by only a few ASVs that accounted for the majority of the reads ([Supplementary Figures S3, S4](#)). Accordingly, the evenness was significantly lower in LDM samples compared to EDM samples at 9 and 13 wph in Exp.1 (Mann–Whitney  $U$  test,  $p = 0.022$  and  $0.006$  for 9 and 13 wph, respectively). There was however no significant difference in the evenness between EDM and LDM samples at 6 wph in Exp.1 and not in Exp.2.

We examined the  $\alpha$ -diversity by determining the ASV richness (Hill's diversity of order 0) and Hill's diversity of order 1. The  $\alpha$ -diversity between EDM and LDM samples was similar in both gut and skin microbiota ([Figure 4](#)). There was no significant difference in Hill's diversity of the order 0 (ASV richness) between the EDM and LDM microbiota in Exp.1 (Mann–Whitney  $U$  test,  $p > 0.05$ ), except for samples taken at 9 wph (Mann–Whitney  $U$  test,  $p < 0.001$ ), where LDM samples had a higher richness ([Figure 4A](#)). Further, the  $\alpha$ -diversity measured as Hill's diversity of order 1 was very similar between the EDM and LDM gut and skin microbiota (Mann–Whitney  $U$  test,  $p = 0.889$ ; [Figure 4A](#)). In Exp.2, this was the case for both order 0 (Mann–Whitney  $U$  test,  $p = 0.610$ ) and 1 (Mann–Whitney  $U$  test,  $p = 0.682$ ; [Figure 4B](#)). These results show that even though the source microbiota strongly influenced the bacterial composition of the early Atlantic salmon gut and skin microbiota, it had little influence on the  $\alpha$ -diversity.

#### 3.3. Temporal development of the gut and skin microbiota throughout the yolk sac stage

We used the samples collected in Exp.1 to examine the temporal development of the skin and gut microbiota of the fish. A PCoA indicated that the microbiota was dynamic throughout the yolk sac stage, especially for samples from the LDM flasks ([Figure 1A](#)). A nested PERMANOVA test with flasks as sublevels showed that for both EDM and LDM samples (gut and skin samples analyzed

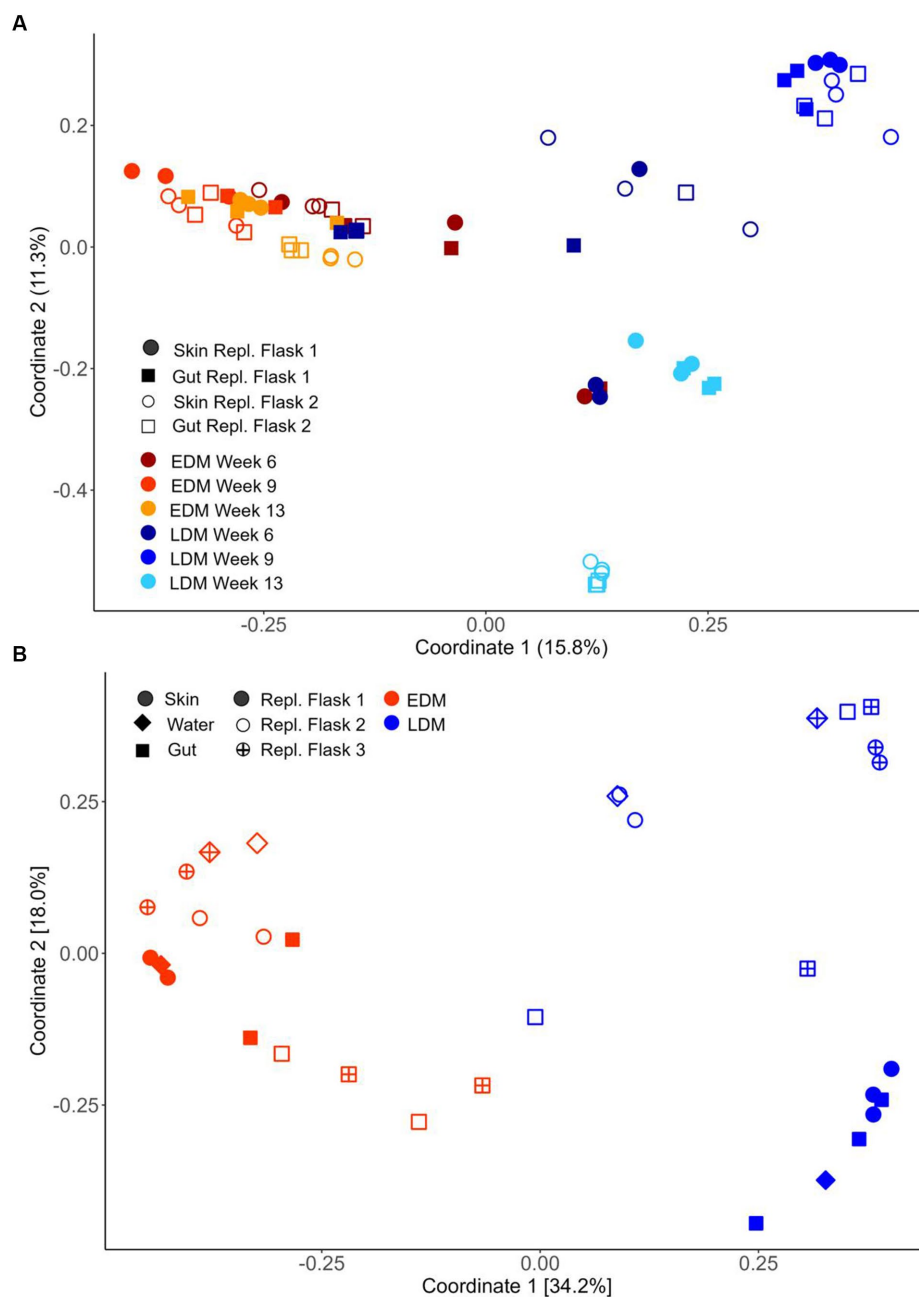


FIGURE 1

Ordination by PCoA based on Bray–Curtis similarities for skin, water (only Exp.2) and gut samples for groups receiving egg-derived (EDM) or lake-derived (LDM) microbiota. (A) Samples from Exp.1 based on 16S rRNA and (B) untreated samples from Exp.2 based on the 16S rRNA gene. For all samples of Exp.2, see Figure 6.

together), the microbiota changed significantly both from 6 to 9 wph and from 9 to 13 wph (value of  $p \leq 0.001$ ).

From 9 to 13 wph, the microbiota of the LDM flasks changed to a significantly larger extent than the EDM microbiota (Mann–Whitney  $U$  test,  $p < 0.001$ ), as indicated by lower Bray–Curtis similarities between the samples (Supplementary Figure S1). Thus, the microbiota of fish that had been colonized by the lake water was less stable over time than that of the fish that had been colonized by their egg microbiota. This temporal development is reflected in the community composition at the order level: for the EDM samples, the relative

abundance of Pseudomonadales decreased, while that of Flavobacteriales and Burkholderiales increased with increasing age (Figure 2A). For the LDM samples, Pseudomonadales remained the dominant order for most samples, even at the end of the yolk sac stage (Figure 2A). The microbiota of the fish also underwent major changes at the ASV level (Supplementary Figure S3B). This was particularly profound for the microbiota of the LDM samples. For example, even though the genus *Pseudomonas* was highly abundant at all sampling times for the LDM samples, different ASVs (classified as *Pseudomonas*) accounted for this high relative abundance at different age (e.g., ASV7

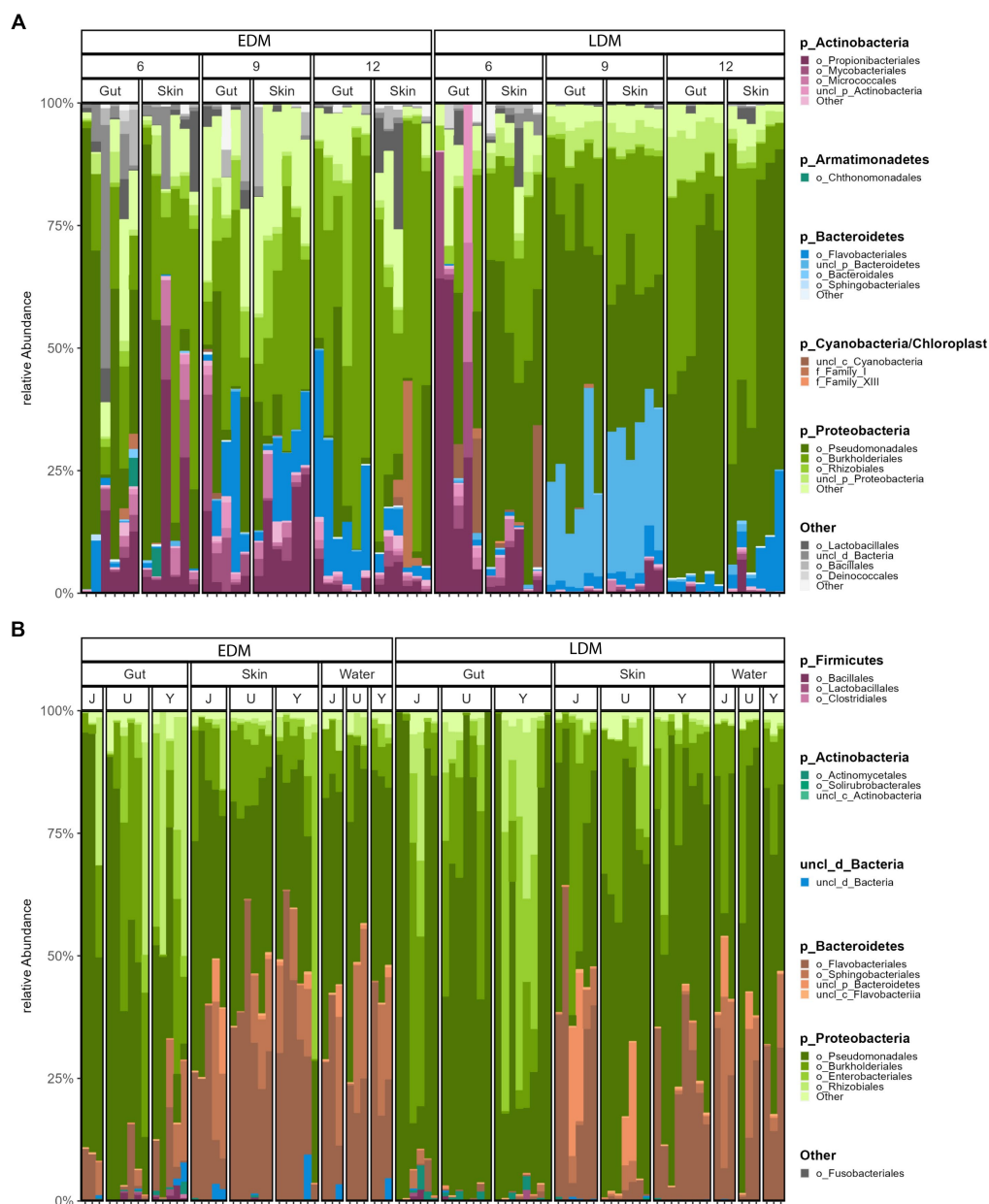


FIGURE 2

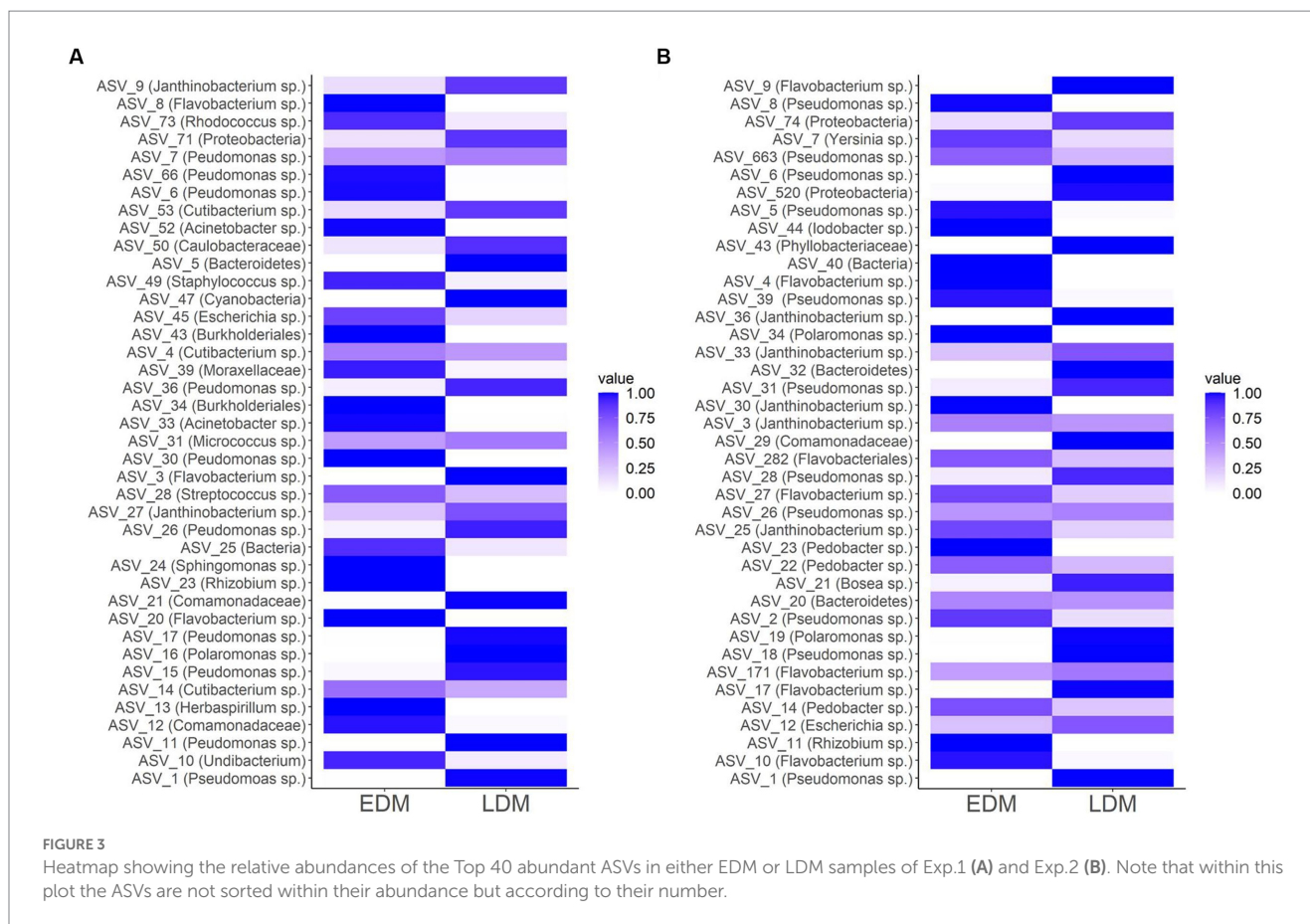
The relative bacterial community composition at the order level for all samples of Exp.1 (A) and Exp.2 (B). For each phylum, the four most abundant orders are shown, others are summarized as "others." ASVs not classified at order level are shown at the highest taxonomic level.

and 15 on 6wph, ASV11, and 26 on 9wph, and ASV1 and 17 on 13wph; [Supplementary Figure S3B](#)). The ASV richness increased significantly for both the EDM and LDM samples over time (Kruskal–Wallis test, value of  $p=0.019$  and  $0.001$  for EDM and LDM, respectively), while Hill's diversity of order 1 increased significantly only for the LDM samples (Kruskal–Wallis test, value of  $p=0.169$  and  $0.008$  for EDM and LDM, respectively; [Figure 4A](#)).

### 3.4. The effect of rearing flask on the larval microbiota

The PCoA for the fish samples from Exp.1 ([Figure 1A](#)) indicated that the skin and gut microbiota differed between replicate rearing

flasks. This was particularly clear for the LDM flasks at 13 wph. A PERMANOVA test revealed that the fish microbiota differed significantly between the two replicate flasks for each timepoint for both EDM and LDM samples (value of  $ps < 0.05$ ), except for LDM samples from 6 wph ( $p=0.171$ ). Interestingly, average Bray–Curtis similarities suggested that the fish microbiota both differed more between replicate LDM flasks and was more alike within replicate flasks ([Figure 5](#)). This was more pronounced at the last sampling time at 13 wph ([Figure 5](#) and [Supplementary Figure S5A](#)). Also in Exp.2, the fish microbiota differed between replicate flasks, and again, this was especially profound for the LDM samples ([Figure 1B](#) and [Supplementary Figure S5B](#)). A PERMANOVA tests confirmed a significant difference in the fish microbiota between the three LDM replicate flasks ( $p \leq 0.001$ ), but not the EDM flasks ( $p=0.109$ ). Thus,



the microbiota of fish colonized by their egg bacteria was more stable between replicate rearing flasks than that of fish colonized by the lake microbiota.

### 3.5. Comparison of skin, gut, and rearing water microbiota

For Exp.1, we collected skin and gut samples, but did not sample the rearing water. The PCoA (Figure 1A) and the community composition at the order level (Figure 2A) indicated that the microbiota of gut and skin samples were relatively similar and PERMANOVA tests did not show significant differences ( $p$ -values  $>0.05$ ) between the gut and skin microbiota at any of the sampling times for neither the EDM nor the LDM samples. To avoid potential biases due to the effect of the replicate flask on the microbiota, we compared the Bray–Curtis similarities of gut and skin samples within replicate flasks. This indicated that the gut and skin microbiota differed for fish in the LDM flasks, and in the EDM flasks at 13 wph (Supplementary Figure S6). A Mann–Whitney  $U$  test showed that for the LDM flasks at 9 and 13 wph, the Bray–Curtis similarities were significantly lower for gut–skin comparisons than for skin–skin and gut–gut comparisons ( $p=0.003$  and  $0.002$  for 9 and 13 wph, respectively). The microbiota of gut and skin samples did not significantly differ in Hill's diversity of order 0, 1 or evenness for any of the timepoints (Mann–Whitney  $U$  test,  $p$ -value  $>0.05$ ; Figure 4A).

In Exp.2, we characterized the rearing water microbiota in addition to the gut and skin microbiota at 8 wph. Interestingly, the PCoA indicated that for the EDM rearing flasks, the skin and water microbiota seemed to be more alike to each other than to the gut microbiota (Figure 1B). For the LDM flasks, the samples clustered according to the replicate flask, and a potential higher similarity between skin and water samples was not obvious. Accordingly, a PERMANOVA test for the EDM samples showed that the gut microbiota differed significantly from both the skin and water ( $p=0.013$  and  $0.003$ , respectively), whereas the microbiota of EDM skin and water samples did not differ significantly (PERMANOVA,  $p=0.261$ ). For the LDM samples, no significant difference was found between the microbiota of the different sample types (PERMANOVA,  $p>0.05$ ). However, the microbiota of both skin and water appeared to be characterized by a higher abundance of Flavobacteriales and Sphingobacteriales compared to the gut samples (Figure 2B). This might indicate differences in bacterial community compositions between gut and skin/water samples also for the LDM samples, even though this was not statistically significant in a PERMANOVA test. The  $\alpha$ -diversity was highest for the water samples and lowest for the gut microbiota samples, both in terms of Hill's diversity of order 0 and 1 (Figure 4B). The differences in  $\alpha$ -diversity between the gut and skin samples were however only significant for the EDM samples (Kruskal–Wallis test,  $p=0.020$  and  $0.038$  for order 0 and 1, respectively) but not for LDM samples (Kruskal–Wallis test,  $p=0.084$  and  $0.202$  for order 0 and 1, respectively).



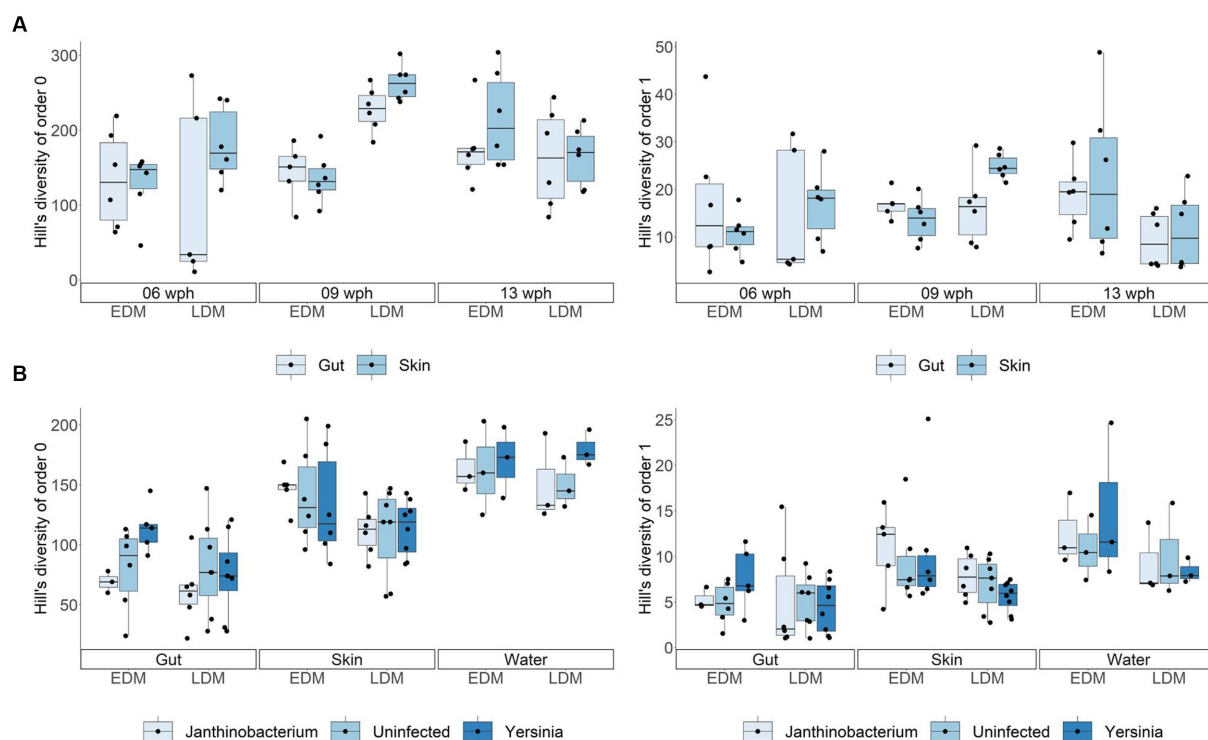


FIGURE 4

Hill's diversity of order 0 (ASV richness) and order 1 (exponential Shannon index) for all samples from Exp.1 (A) and Exp.2 (B). The box in the boxplots represent the median of all samples as well as the upper and lower quartiles. Whiskers include all samples except for outliers.

These results indicate that while the skin microbiota was similar to the water microbiota, a distinctive gut bacterial community was developing already in the yolk sac stage, prior to the onset of external feeding. Still, the differences between the gut and skin microbiota were small compared to the differences we observed in the fry microbiota between replicate flasks and between LDM and EDM samples (Figure 1).

### 3.6. Potential for manipulating the larval microbiota through exposure to bacterial isolates

In Exp.2, we further examined the potential for manipulating the microbiota of the fish by adding high concentrations of either the fish pathogen *Yersinia ruckeri* 06059 or the fish commensal *Janthinobacterium* sp. 3.108 to the rearing water of both EDM and LDM flask at 6 wph (2 weeks prior to bacterial sampling). By comparing the 16S rRNA gene sequences of these two strains (Supplementary Figure S7) with the ASV sequences, we identified ASV7 as *Y. ruckeri* 06059 and ASV3 and ASV15 (combined to ASV3-15; see Methods, "Analysis of the Illumina sequencing data") as *J. sp. 3.108*.

Both strains successfully colonized the gut and skin of the salmon yolk sac fry (Supplementary Figure S8). As expected, ASV7 was generally not present in samples from flasks to which *Y. ruckeri* was not added and the relative abundance of ASV7 was significantly higher in samples taken from flasks to which *Y. ruckeri* 06059 was added (in both the EDM and LDM group; Mann-Whitney *U* test  $p = 0.012$  and  $< 0.001$ , respectively). However, it varied strongly

between individuals, from not observed for some samples and up to 50% in relative abundance for other samples, indicating that the colonization success for the *Y. ruckeri* isolate varied. Generally, the relative abundance of ASV7 was higher in gut samples than in skin or water samples (Supplementary Figure S8), however this was not significant (Kruskal-Wallis test  $p = 0.944$  and  $p = 0.969$  for EDM and LDM, respectively). Surprisingly, and in contrast to what we found for ASV7/*Y. ruckeri*, ASV3-15, representing *J. sp. 3.108*, was detected in considerable quantities in water, gut, and skin samples (on average around 5% in relative abundance), even for samples from flasks to which *J. sp. 3.108* had not been added (Supplementary Figure S8). This was the case for samples from both EDM and LDM flasks, even though EDM and LDM samples were highly dissimilar in community composition at ASV level, with few highly abundant shared ASVs (Supplementary Figure S4). Furthermore, there was no significant difference in the relative abundance of ASV3-15 between samples from flasks that had been added *J. sp. 3.108* and samples from flasks that had not been added this bacterial isolate (Mann-Whitney *U* test  $p = 0.305$  and  $p = 0.682$  for EDM and LDM, respectively). This means that the addition of *J. sp. 3.108* to the fish flasks did not result in increased relative abundance of this strain in the gut and skin microbiota. Apart from ASV3, as many as 19 more ASVs were classified to the genus *Janthinobacterium* and these ASVs together had an average relative abundance of  $10.3 \pm 11.0\%$  of all reads per sample. This, together with the fact that strain *J. sp. 3.108* was originally isolated from the skin of salmon fry, might indicate a role of *Janthinobacterium* as a part of the commensal Atlantic salmon microbiota (see Discussion).

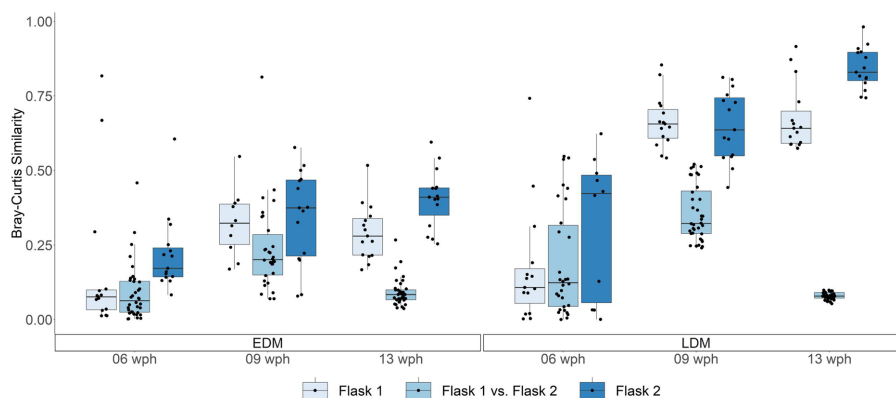


FIGURE 5

Boxplot showing Bray–Curtis similarities for comparisons of fish microbiota (both gut and skin) within and between replicate flasks for Exp.1. Each point represents a single comparison of two samples. The box in the boxplots represent the median of all samples as well as the upper and lower quartiles. Whiskers include all samples except for outliers.

A PCoA suggested that for EDM samples, there were no major differences in the fish's microbiota between flasks that had been added *Y. ruckeri* or *J. sp. 3.108* and flasks that had not been added bacterial isolates (Figure 6). A PERMANOVA confirmed that there was no significant difference in neither the gut nor the skin microbiota between EDM flasks added bacterial isolates and control flasks, not added bacterial isolates ( $p=0.098$  and  $p=0.348$ , for gut and skin samples of the *Yersinia*-treatment and  $p=0.468$  and  $p=0.225$  for gut and skin samples of *Janthinobacterium*-treated samples, respectively). For the LDM samples however, the PCoA plot indicated that the fish's microbiota was influenced by addition of *Y. ruckeri* and *J. sp. 3.108* (Figure 6). A PERMANOVA test demonstrated that the skin microbiota, but not the gut microbiota, differed significantly between non-treated flasks and flasks that had been added bacterial isolates ( $p=0.007$  and  $0.030$  for *Y. ruckeri*-treated and *Janthinobacterium*-treated samples, respectively). However, a potential explanation for this observation could be the general difference in fish microbiota between replicate rearing flasks rather than the treatment with bacterial isolates *per se*. A nested PERMANOVA was performed to clarify this, however, due to the limited sample size, no conclusions could be drawn. Additionally, neither the richness, nor the exponential Shannon index were significantly affected by addition of *J. sp. 3.108* or *Y. ruckeri* (Figure 4B).

Taken together, these findings suggest that neither addition of high loads of the fish pathogen *Y. ruckeri* nor of the presumed fish commensal *J. sp. 3.108* to the rearing flasks lead to any major changes in the gut and skin microbiota of the Atlantic salmon yolk sac fry.

## 4. Discussion

The microbiota of fish is crucial for host health and development (Rawls et al., 2004), but little is known about the assembly of the fish microbiota just after hatching. In this study, we investigated the microbiota of the developing fish larvae that had been exposed to two different sources of microbiota present at hatching: either from the eggs of the fish (EDM; fish hatched under conventional, i.e., non-germ-free conditions) or from a freshwater lake (LDM; fish

hatched under germ-free conditions and re-colonized). We found that the source microbiota had a strong influence on the skin and gut microbiota of the fish, as the microbiota differed significantly between the EDM and LDM group at all sampling timepoints. Interestingly, the microbiota of fish for which the source of bacteria was the egg (EDM) were more stable, both over time and between replicate rearing flasks, than fish colonized by lake water bacteria (LDM). A possible reason for this might be that egg-derived microbes were better adapted to colonizing the fish, whereas the bacterial populations in the lake water-microbiota were probably poorly adapted for colonization of the fish. This may have increased the significance of stochastic processes, such as ecological drift, that play an important role in the initial community assembly (Dini-Andreote et al., 2015; Gu et al., 2021). Vestrum et al. (2020) showed that drift was important for creating variation in the microbiota between individuals in rearing systems with Atlantic cod larvae. Thus, a stronger influence of drift on the community assembly could explain the divergence in the fish microbiota between replicate rearing flasks.

Previous studies of fish in larger rearing systems, for example for Atlantic cod larvae (Bakke et al., 2013) and Atlantic salmon (Schmidt et al., 2016; Minich et al., 2020), have also demonstrated that the fish microbiota differed between replicate rearing tanks. Interestingly, we observed that the effect was more prominent when comparisons were based on the abundance-based Bray–Curtis similarity than on the presence/absence-based Sørensen-Dice similarity (Supplementary Figure S9). This indicates that the effect arose rather due to differences in the relative abundances of ASVs than the presence of distinct ASVs. In Exp.2, we found that the water and fish microbiota was similar within each rearing flask, and that a distinctive system microbiota developed in each replicate rearing flasks, although the same lake water was used as source community, and that the same bacterial populations thus were present during the initial bacterial colonization of the fish. This indicates that the water microbiota has a stronger influence on the fish microbiota than the selection pressure in the gut and skin of the fry. Comparisons of water and fish microbiota throughout the yolk sac stage might bring new insight about the interrelationship between the water and fish microbiota during the establishment and development of the early fish microbiota.

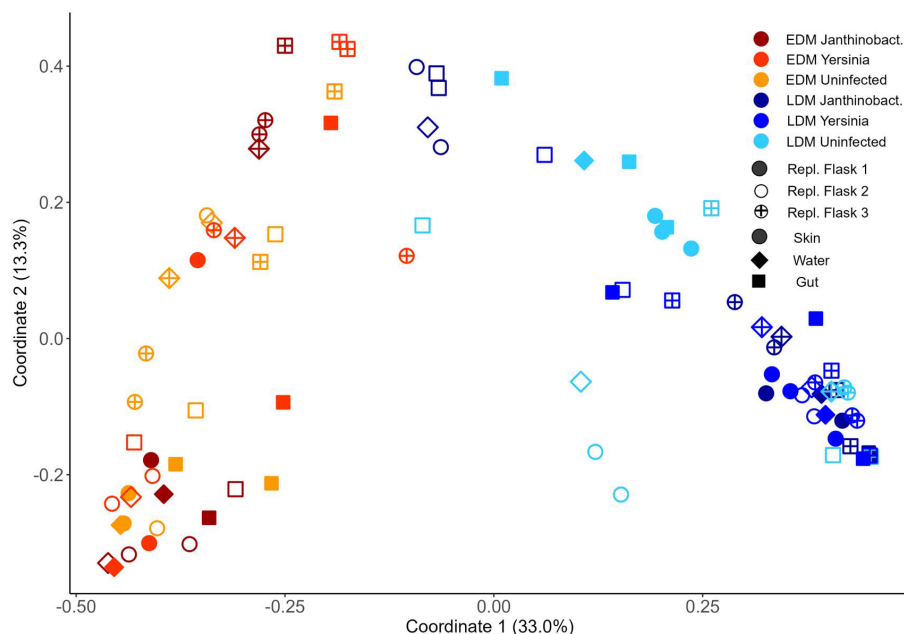


FIGURE 6

Ordination by PCoA based on the Bray–Curtis similarity of all samples from Exp.2, sampled 2 weeks after treatment.

However, unfortunately, we did not characterize the rearing water microbiota in Exp.1.

The finding that the source of bacteria present in the environment after hatching had a major impact on the composition and the stability of the fry's microbiota, points to the possibility for steering the microbiota of the yolk sac fry by manipulating the microbial environments upon hatching. This might have an applied potential in the aquaculture industry, where eggs are routinely disinfected prior to the distribution to hatcheries. In principal, this could be a strategy to counteract negative host – microbe interactions and to develop robust fry by, e.g., introducing probiotic strains. However, research is needed to identify strategies for obtaining this, and to investigate the consequences in terms of host responses.

The differences in the larval microbiota between the EDM and LDM flasks were more profound when PCoA was based on Bray–Curtis similarities than on the weighted UniFrac similarity, which also takes into account the phylogenetic distances between the ASVs. This indicates that the fish in EDM and LDM flasks were colonized by different bacterial populations, which represent related taxa, and thus, that certain phylogenetic groups were selected for on the mucosal surfaces of the fish. Proteobacteria, Bacteroidetes and Actinobacteria were the most abundant phyla of the yolk sac fry microbiota. These phyla were also found to be highly abundant in the microbiota of Atlantic salmon yolk sac fry in a study by Lokesh et al. (2019). They characterized the egg microbiota and followed the Atlantic salmon gut microbiota until the fish were fully developed but included only one sample between hatching and onset of active feeding. Both our and their study found that Proteobacteria was the dominating phylum in the yolk sac fry, and we further found that Actinobacteria were strongly present in the early timepoints and later decreased. These findings are in line with the conclusion of Borges et al. (2021), that summarized for different fish species that Proteobacteria, Bacteroidetes, Firmicutes and Actinomycetes are the dominant phyla

in the fish larvae gut (Borges et al., 2021). The main bacterial phyla of the skin microbiota in juvenile and adult Atlantic salmon have been found to be Proteobacteria, Bacteroidetes and Firmicutes (Lokesh and Kiron, 2016; Minniti et al., 2017; Wynne et al., 2020; Bugten et al., 2022) and our study shows that they were highly abundant already at the larval stage.

In Exp.1, we observed that the gut and skin microbiota underwent major changes throughout the yolk sac stage. This was particularly profound at the ASV level and for LDM samples, and very few ASVs were highly abundant at all sampling timepoints. Interestingly, even though *Pseudomonadales* dominated the fish microbiota in LDM flasks at all sampling times, this phylum was represented by distinct ASVs at the three sampling times, indicating that distinct *Pseudomonas* populations colonized the fish at different ages. Also in other vertebrates and fish species, it has been observed that the early microbiome is dynamic, and is only stabilizing later in life (Schloss et al., 2012; Chen and Garud, 2022; Woodruff et al., 2022; Xiao et al., 2022). We further observed large interindividual variation in the microbiota, an observation often made in other aquatic larvae (e.g., Verschuere et al., 1999; Stephens et al., 2016; Vestrum et al., 2020), which has been suggested to be a consequence of ecological drift (Vestrum et al., 2020).

For adult fish, several studies have shown that the skin and gut of fish harbors distinct microbial communities (e.g., Lowrey et al., 2015; Sylvain et al., 2020). However, few studies have focused on the skin microbiota of fish larvae (e.g., Dodd et al., 2020), and little is known about the diverging development of the gut and skin microbiota in the early developmental stages, especially prior to onset of active feeding. Already at 7 dph, long before the fish starts to feed, the anus and the mouth of Atlantic salmon is opened and therefore available for bacterial colonization (Sahlmann et al., 2015). Here, we dissected out the fish guts and studied the development of both the gut and skin microbiota prior to the onset of external feeding. Both in Exp.1 and 2

we found indications that the skin and gut microbiota started to differentiate already at 8–9 wph, several weeks before the yolk sac was consumed. We observed however, that the gut was filled with yolk material (not shown), which might provide nutrients to the gut microbiota. Sahlmann et al. (2015) further observed that distinct gut organs and structures formed already from 7 dph on. This structuring of the gut might already provide colonization space for bacterial populations filling different niches, resulting in a distinct gut microbiota.

Moreover, Exp.2 showed that the microbial skin communities resembled the water microbiota, whereas the gut microbiota differed from the water and skin microbiota. In studies of Gilthead Sea Bream and Atlantic cod larvae the microbiota of the whole fish (no differentiation between gut and skin) was found to differ from the water microbiota (Bakke et al., 2015; Nikouli et al., 2019; Vestrum et al., 2020), indicating that the selection of bacterial populations differed between the water and mucosal surfaces of the larvae. In our study we could now show that in the larval stage it indeed appears to be only the gut microbiota that is different from the water microbiota, not the skin microbiota. Studies in adult fish report that the skin microbiota is distinctive and differs from the surrounding water microbiota (Razak et al., 2019; Gomez and Primm, 2021). It would be interesting to further investigate to which extent the skin and water microbiota diverge throughout the yolk sac stage.

In Exp.2, we further investigated the potential of manipulating the fish's microbiota by addition of one of two bacterial isolates in high densities (a theoretical final concentration of  $10^7$  CFU ml<sup>-1</sup>) 6 weeks after the fish had hatched. Either the fish pathogen *Y. ruckeri* or the presumed non-pathogenic fish commensal *Janthinobacterium* sp. 3.108 was added to EDM and LDM flasks. Surprisingly, the ASV corresponding to the *J. sp. 3.108* isolate (or a strain with the same partial 16S rDNA gene sequence) was found in the microbiota of fish from all flasks, also those that had not been added the isolate. The relative abundances of that ASV varied extensively between individuals, but the average relative abundances did not increase in samples from flasks that had been added *J. sp. 3.108*. Accordingly, we found that addition of the commensal *J. sp. 3.108* did not significantly change the microbiota. The fish pathogen *Y. ruckeri* was not present in significant amounts in flasks to which we did not add it. In flasks to which we added it, its abundance among individuals was highly variable and mainly present in low relative abundances. It further did not have a large impact on the skin and gut microbiota. These results may indicate that the microbiota of the larval Atlantic salmon is resistant to invasion by introduced bacterial strains. Skjermo et al. (2015) showed that none of the four probiotic candidate bacterial strains originally isolated from cod larvae were able to establish themselves as part of the microbiota of Atlantic cod larvae. Further, Puvanendran et al. (2021) found that their probiotic *Carnobacterium* isolate could not establish itself in Atlantic cod larvae. This shows that manipulating the microbiota of fish with, e.g., probiotic strains might be difficult to achieve already in the larval stage, when the fish's microbiota is still unstable. As discussed above, manipulating the microbial environments at hatching might be a better strategy for influencing the early fish microbiota.

Apart from the *Janthinobacterium* strain we added (strain 3.108), we also found several other ASVs classified as "*Janthinobacterium*" in high relative abundances. Strain *J. sp. 3.108* was originally isolated from the skin of Atlantic salmon fry from a commercial RAS, and

its 16S rRNA gene sequence is highly similar to the *Janthinobacterium lividum* type strain (99% similarity over the whole 16S rRNA gene, data not shown). *J. lividum* commonly occurs in freshwater (Pantanello et al., 2007) and is a commensal of both the amphibian (Brucker et al., 2008; Becker et al., 2009) and human (Grice et al., 2008; Ramsey et al., 2015) skin microbiota, and it has antagonistic properties against fungi and bacteria (Munakata et al., 2021). *Janthinobacterium* spp. have also been found in tank biofilms of fish farms for rainbow trout (Nakamura et al., 2002; Testerman et al., 2021). A *J. lividum* strain was shown to be capnophilic (Valdes et al., 2015), meaning it thrives under high concentrations of CO<sub>2</sub>. The salmon larvae exchange gas mainly through the skin, and this could be an explanation for the presence of *Janthinobacterium* in the skin microbiota. As we also found high abundances of several ASVs classified as *Janthinobacterium* associated with the skin and gut samples in both experiments, we propose that strains from the genus *Janthinobacterium* are commensal bacteria for Atlantic salmon larvae. Members of *Janthinobacterium* have also been found in the intestine of adult Atlantic salmon (Wang et al., 2018).

In contrast to *Janthinobacterium*, *Y. ruckeri* is a well-known pathogen in later life stages of the salmon (e.g., Kumar et al., 2015). However, it appears as if no lethal disease was triggered by the addition of *Y. ruckeri*, even though the strain used in this study (*Y. ruckeri* 06059) has successfully been used to inflict mortality in Atlantic salmon fry (Haig et al., 2011). A possible reason for this might be that either the temperature used here was too low (14°C) or that the yolk sac fry was not developed enough for *Y. ruckeri* to induce mortality.

In this study, RNA extracts were available for characterization of the fish microbiota for the samples collected in Exp.1, while in Exp.2, the analyses of the microbiota were based on DNA. RNA-based microbiota analyses are assumed to reflect the actively growing populations in the microbial communities to a larger extent as compared to DNA-based analyses, which will also represent inactive bacterial cells. As these two experiments also differed in other parts of the methodology (e.g., in how the nucleic acids were extracted), it is not possible to compare these two datasets directly. We therefore analyzed the data from the two experiments separately and compared how they answered our research questions. We found that the key findings were shared for the two experiments, as for both experiments the fish microbiota varied between LDM and EDM flask and also between replicate rearing flasks. We further saw differences between gut and skin samples in both the RNA-based and DNA-based data. Therefore, even though different approaches were used in the two experiments, both answered our research questions in similar ways, which indicates that our findings are robust.

In conclusion, we showed that the skin and gut microbiota were similar, but started diverging during the yolk sac stage, several weeks before the yolk sac was consumed. The skin microbiota was more similar to the water microbiota than the gut microbiota. Furthermore, the microbiota differed profoundly between fish that had been conventionally reared, i.e., the egg microbiota was the only source of bacteria (EDM), and fish that had been made germ-free and were then colonized by using lake water as a source for bacteria (LDM). Proteobacteria, Bacteroidetes and Actinobacteria were the most abundant phyla in the fry microbiota. Both the skin and gut microbiota were highly dynamic and underwent major changes at



the ASV level throughout the yolk sac stage, and this was particularly evident for fry reared in LDM flasks. The fry microbiota differed profoundly between replicate rearing flasks, and again, this was particularly evident for the LDM flasks. Thus, the fry reared in EDM flasks had a more stable microbiota, both between rearing flasks and over time. Additions of high doses of the pathogen *Y. ruckeri* to fish flasks did not cause mortality. Addition of *Y. ruckeri* had only minor impact on the community composition. Finally, we exposed the fry to high doses of a *Janthinobacterium* sp. isolate and found no effects on the fry microbiota. An ASV sequence corresponding to the one for the added *J.* sp. isolate was abundant in most fry samples and indicated that this represented a commensal member of the early fry microbiota.

## Data availability statement

The datasets presented in this study can be found in online repositories. The names of the repository/repositories and accession number(s) can be found at: <https://www.ebi.ac.uk/ena/ERS14440101-ERS14440192>.

## Ethics statement

Ethical review and approval was not required for the animal study because the Atlantic salmon yolk sac fry are not defined as living animals according to Norwegian legislation, therefore no ethical review was required.

## Author contributions

MD and AF conducted the fish experiments. AF and EL prepared the 16S libraries and analyzed the resulting data. AF, OV, and IB conceived and designed the experiments. AF wrote the first draft of the manuscript. All authors contributed to the article and approved the submitted version.

## References

- Anderson, M. J. (2001). A new method for non-parametric multivariate analysis of variance. *Austral Ecol.* 26, 32–46. doi: 10.1111/j.1442-9993.2001.01070.pp.x
- Bakke, I., Coward, E., Andersen, T., and Vadstein, O. (2015). Selection in the host structures the microbiota associated with developing cod larvae (*Gadus morhua*). *Environ. Microbiol.* 17, 3914–3924. doi: 10.1111/1462-2920.12888
- Bakke, I., Skjermo, J., Vo, T. A., and Vadstein, O. (2013). Live feed is not a major determinant of the microbiota associated with cod larvae (*Gadus morhua*). *Environ. Microbiol. Rep.* 5, 537–548. doi: 10.1111/1758-2229.12042
- Becker, M. H., Brucker, R. M., Schwantes, C. R., Harris, R. N., and Minbiole, K. P. C. (2009). The bacterially produced metabolite violacein is associated with survival of amphibians infected with a lethal fungus. *Appl. Environ. Microbiol.* 75, 6635–6638. doi: 10.1128/AEM.01294-09
- Borges, N., Keller-Costa, T., Sanches-Fernandes, G. M. M., Louvado, A., Gomes, N. C. M., and Costa, R. (2021). Bacteriome structure, function, and probiotics in fish Larviculture: the good, the bad, and the gaps. *Ann Rev Anim Biosci* 9, 423–452. doi: 10.1146/annurev-animal-062920-113114
- Bozzi, D., Rasmussen, J. A., Caroe, C., Sveier, H., Nordoy, K., Gilbert, M. T. P., et al. (2021). Salmon gut microbiota correlates with disease infection status: potential for monitoring health in farmed animals. *Anim Microbiome* 3:30. doi: 10.1186/s42523-021-00096-2
- Brucker, R. M., Harris, R. N., Schwantes, C. R., Gallaher, T. N., Flaherty, D. C., Lam, B. A., et al. (2008). Amphibian chemical Defense: antifungal metabolites of the microsymiont *Janthinobacterium lividum* on the salamander *Plethodon cinereus*. *J. Chem. Ecol.* 34, 1422–1429. doi: 10.1007/s10886-008-9555-7
- Bugten, A. V., Attramadal, K. J. K., Fossmark, R. O., Rosten, T. W., Vadstein, O., and Bakke, I. (2022). Changes in rearing water microbiomes in RAS induced by membrane filtration alters the hindgut microbiomes of Atlantic salmon (*Salmo salar*) parr. *Aquaculture* 548:737661. doi: 10.1016/j.aquaculture.2021.737661
- Califano, G., Castanho, S., Soares, F., Ribeiro, L., Cox, C. J., Mata, L., et al. (2017). Molecular taxonomic profiling of bacterial communities in a gilthead seabream (*Sparus aurata*) hatchery. *Front. Microbiol.* 8. doi: 10.3389/fmicb.2017.00204
- Carlson, A. L., Xia, K., Azcarate-Peril, M. A., Rosin, S. P., Fine, J. P., Mu, W., et al. (2021). Infant gut microbiome composition is associated with non-social fear behavior in a pilot study. *Nat. Commun.* 12:3294. doi: 10.1038/s41467-021-23281-y
- Chen, D. W., and Garud, N. R. (2022). Rapid evolution and strain turnover in the infant gut microbiome. *Genome Res.* 32, 1124–1136. doi: 10.1101/gr.276306.121
- Dehler, C. E., Secombes, C. J., and Martin, S. A. M. (2017). Environmental and physiological factors shape the gut microbiota of Atlantic salmon parr (*Salmo salar* L.). *Aquaculture* 467, 149–157. doi: 10.1016/j.aquaculture.2016.07.017
- Dini-Andreote, F., Stegen, J. C., van Elsas, J. D., and Salles, J. F. (2015). Disentangling mechanisms that mediate the balance between stochastic and deterministic processes in microbial succession. *P Natl Acad Sci USA* 112, E1326–E1332. doi: 10.1073/pnas.1414261112

## Funding

This work was supported by the Department of Biotechnology and Food Science at NTNU, and by the Research Council of Norway (RCN) through their funding of the FRIPRO project number 262929.

## Acknowledgments

The authors would like to thank Madeleine Gundersen for help with the analysis of the data and Sol Gomez de la Torre Canny for help with conducting Exp.1. We thank Amalie Mathisen for assistance in conducting experimental works. Many thanks also to Rolf Myklebust from AquaGen AS for providing us with Atlantic salmon eggs.

## Conflict of interest

The authors declare that the research was conducted in the absence of any commercial or financial relationships that could be construed as a potential conflict of interest.

## Publisher's note

All claims expressed in this article are solely those of the authors and do not necessarily represent those of their affiliated organizations, or those of the publisher, the editors and the reviewers. Any product that may be evaluated in this article, or claim that may be made by its manufacturer, is not guaranteed or endorsed by the publisher.

## Supplementary material

The Supplementary material for this article can be found online at: <https://www.frontiersin.org/articles/10.3389/fmicb.2023.1177972/full#supplementary-material>

- Dodd, E. T., Pierce, M. L., Lee, J. S. F., and Poretsky, R. S. (2020). Influences of claywater and greenwater on the skin microbiome of cultured larval sablefish (*Anoplopoma fimbria*). *Anim Microbiome* 2:27. doi: 10.1186/s42523-020-00045-5
- Edgar, R. C. (2010). Search and clustering orders of magnitude faster than BLAST. *Bioinformatics* 26, 2460–2461. doi: 10.1093/bioinformatics/btq461
- Edgar, R. C. (2016a). SINTAX: a simple non-Bayesian taxonomy classifier for 16S and ITS sequences. *bioRxiv*:074161
- Edgar, R. C. (2016b). UNOISE2: improved error-correction for Illumina 16S and ITS amplicon sequencing. *bioRxiv*:081257
- FAO (2020) *The state of world fisheries and aquaculture 2020. Sustainability in action*. Rome: FAO.
- Ferretti, P., Pasolli, E., Tett, A., Asnicar, F., Gorfer, V., Fedi, S., et al. (2018). Mother-to-infant microbial transmission from different body sites shapes the developing infant gut microbiome. *Cell Host Microbe* 24, 133–145.e5. doi: 10.1016/j.chom.2018.06.005
- Gomez de la Torre Canny, S., Norgård, C. T., Mathisen, A. J., Lorentsen, E. D., Vadstein, O., and Bakke, I. (2022). A novel gnotobiotic experimental system for Atlantic salmon (*Salmo salar* L.) reveals a microbial influence on mucosal barrier function and adipose tissue accumulation during the yolk sac stage. *Front. Cell. Infect. Microbiol.* 12:1068302. doi: 10.3389/fcimb.2022.1068302
- Gomez, J. A., and Primm, T. P. (2021). A slimy business: the future of fish skin microbiome studies. *Microb. Ecol.* 82, 275–287. doi: 10.1007/s00248-020-01648-w
- Grice, E. A., Kong, H. H., Renaud, G., Young, A. C., Bouffard, G. G., Blakesley, R. W., et al. (2008). A diversity profile of the human skin microbiota. *Genome Res.* 18, 1043–1050. doi: 10.1101/gr.075549.107
- Gu, Z., Liu, K., Pedersen, M. W., Wang, F., Chen, Y., Zeng, C., et al. (2021). Community assembly processes underlying the temporal dynamics of glacial stream and lake bacterial communities. *Sci. Total Environ.* 761:143178. doi: 10.1016/j.scitotenv.2020.143178
- Haig, S. J., Davies, R. L., Welch, T. J., Reese, R. A., and Verner-Jeffreys, D. W. (2011). Comparative susceptibility of Atlantic salmon and rainbow trout to *Yersinia ruckeri*: relationship to O antigen serotype and resistance to serum killing. *Vet. Microbiol.* 147, 155–161. doi: 10.1016/j.vetmic.2010.06.022
- Hill, M. O. (1973). Diversity and evenness: a unifying notation and its consequences. *Ecology* 54, 427–432. doi: 10.2307/1934352
- Huh, S. Y., Rifas-Shiman, S. L., Zera, C. A., Edwards, J. W. R., Oken, E., Weiss, S. T., et al. (2012). Delivery by caesarean section and risk of obesity in preschool age children: a prospective cohort study. *Arch. Dis. Child.* 97, 610–616. doi: 10.1136/archdischild-2011-301141
- Ingerslev, H. C., Jorgensen, L. V., Strube, M. L., Larsen, N., Dalsgaard, I., Boye, M., et al. (2014a). The development of the gut microbiota in rainbow trout (*Oncorhynchus mykiss*) is affected by first feeding and diet type. *Aquaculture* 424–425, 24–34. doi: 10.1016/j.aquaculture.2013.12.032
- Ingerslev, H. C., Strube, M. L., Jorgensen, L. V., Dalsgaard, I., Boye, M., and Madsen, L. (2014b). Diet type dictates the gut microbiota and the immune response against *Yersinia ruckeri* in rainbow trout (*Oncorhynchus mykiss*). *Fish Shellfish Immunol.* 40, 624–633. doi: 10.1016/j.fsi.2014.08.021
- Kumar, G., Menanteau-Ledouble, S., Saleh, M., and El-Matbouli, M. (2015). *Yersinia ruckeri*, the causative agent of enteric redmouth disease in fish. *Vet. Res.* 46:103. doi: 10.1186/s13567-015-0238-4
- Legrand, T. P. R. A., Wynne, J. W., Weyrich, L. S., and Oxley, A. P. A. (2020). A microbial sea of possibilities: current knowledge and prospects for an improved understanding of the fish microbiome. *Rev. Aquac.* 12, 1101–1134. doi: 10.1111/raq.12375
- Li, X. M., Ringo, E., Hoseinifar, S. H., Lauzon, H. L., Birkbeck, H., and Yang, D. G. (2019). The adherence and colonization of microorganisms in fish gastrointestinal tract. *Rev. Aquac.* 11, 603–618. doi: 10.1111/raq.12248
- Liu, Y., de Bruijn, I., Jack, A. L. H., Drynan, K., van den Berg, A. H., Thoen, E., et al. (2014). Deciphering microbial landscapes of fish eggs to mitigate emerging diseases. *ISME J.* 8, 2002–2014. doi: 10.1038/ismej.2014.44
- Llewellyn, M. S., Boutin, S., Hoseinifar, S. H., and Derome, N. (2014). Teleost microbiomes: the state of the art in their characterization, manipulation and importance in aquaculture and fisheries. *Front. Microbiol.* 5. doi: 10.3389/fmicb.2014.00207
- Lokes, J., and Kiron, V. (2016). Transition from freshwater to seawater reshapes the skin-associated microbiota of Atlantic salmon. *Sci. Rep.* 6:19707. doi: 10.1038/srep19707
- Lokes, J., Kiron, V., Sipkema, D., Fernandes, J. M. O., and Moum, T. (2019). Succession of embryonic and the intestinal bacterial communities of Atlantic salmon (*Salmo salar*) reveals stage-specific microbial signatures. *Microbiology* 8:e00672. doi: 10.1002/mbo3.672
- Lowrey, L., Woodhams, D. C., Tacchi, L., and Salinas, I. (2015). Topographical mapping of the rainbow trout (*Oncorhynchus mykiss*) microbiome reveals a diverse bacterial community with antifungal properties in the skin. *Appl. Environ. Microbiol.* 81, 6915–6925. doi: 10.1128/AEM.01826-15
- Lucas, R., Groeneveld, J., Harms, H., Johst, K., Frank, K., and Kleinstaub, S. (2017). A critical evaluation of ecological indices for the comparative analysis of microbial communities based on molecular datasets. *FEMS Microbiol. Ecol.* 93. doi: 10.1093/femsec/fiw209
- Lynch, J. B., and Hsiao, E. Y. (2019). Microbiomes as sources of emergent host phenotypes. *Science* 365, 1405–1409. doi: 10.1126/science.aay0240
- Merrifield, D. L., and Rodiles, A. (2015). “10 – the fish microbiome and its interactions with mucosal tissues” in *Mucosal health in aquaculture*. eds. B. H. Beck and E. Peatman (San Diego: Academic Press), 273–295.
- Michl, S. C., Beyer, M., Ratten, J. M., Hasler, M., LaRoche, J., and Schulz, C. (2019). A diet-change modulates the previously established bacterial gut community in juvenile brown trout (*Salmo trutta*). *Sci Rep* 9. doi: 10.1038/s41598-019-38800-7
- Minich, J. J., Poore, G. D., Jantawong, K., Johnston, C., Bowie, K., Bowman, J., et al. (2020). Microbial ecology of Atlantic Salmon (*Salmo salar*) hatcheries: impacts of the built environment on fish mucosal microbiota. *Appl. Environ. Microbiol.* 86, 1–19. doi: 10.1128/AEM.00411-20
- Minniti, G., Hagen, L. H., Porcellato, D., Jørgensen, S. M., Pope, P. B., and Vaaje-Kolstad, G. (2017). The skin-mucus microbial Community of Farmed Atlantic Salmon (*Salmo salar*). *Front. Microbiol.* 8. doi: 10.3389/fmicb.2017.02043
- Munakata, Y., Gavira, C., Genestier, J., Bourgaud, F., Hehn, A., and Slezacek-Deschaumes, S. (2021). Composition and functional comparison of vetiver root endophytic microbiota originating from different geographic locations that show antagonistic activity towards *Fusarium graminearum*. *Microbiol. Res.* 243:126650. doi: 10.1016/j.micres.2020.126650
- Nakamura, Y., Sawada, T., Morita, Y., and Tamiya, E. (2002). Isolation of a psychrotrophic bacterium from the organic residue of a water tank keeping rainbow trout and antibacterial effect of violet pigment produced from the strain. *Biochem. Eng. J.* 12, 79–86. doi: 10.1016/S1369-703X(02)00079-7
- Nikouli, E., Meziti, A., Antonopoulou, E., Mente, E., and Kormas, K. A. (2019). Host-associated bacterial succession during the early embryonic stages and first feeding in farmed Gilthead Sea bream (*Sparus aurata*). *Genes* 10:483. doi: 10.3390/genes10070483
- Nordgard, A. S. R., Bergland, W. H., Vadstein, O., Mironov, V., Bakke, R., Ostgaard, K., et al. (2017). Anaerobic digestion of pig manure supernatant at high ammonia concentrations characterized by high abundances of Methanosaeta and non-euryarchaeotal archaea. *Sci. Rep.* 7:15077. doi: 10.1038/s41598-017-14527-1
- Pantarella, F., Berlutti, F., Passariello, C., Sarli, S., Morea, C., and Schippa, S. (2007). Violacein and biofilm production in *Janthinobacterium lividum*. *J. Appl. Microbiol.* 102, 992–999. doi: 10.1111/j.1365-2672.2006.03155.x
- Pérez-Pascual, D., Vendrell-Fernández, S., Audrain, B., Bernal-Bayard, J., Patiño-Navarrete, R., Petit, V., et al. (2021). Gnotobiotic rainbow trout (*Oncorhynchus mykiss*) model reveals endogenous bacteria that protect against *Flavobacterium columnare* infection. *PLoS Pathog.* 17:e1009302. doi: 10.1371/journal.ppat.1009302
- Phelps, D., Brinkman, N. E., Keely, S. P., Anneken, E. M., Catron, T. R., Betancourt, D., et al. (2017). Microbial colonization is required for normal neurobehavioral development in zebrafish. *Sci Rep* 7:12447. doi: 10.1038/s41598-017-10517-5
- Puvanendran, V., Rud, I., Msw, B., Arnesen, J. A., and Axelsson, L. (2021). Probiotic *Carnobacterium divergens* increase growth parameters and disease resistance in farmed Atlantic cod (*Gadus morhua*) larvae without influencing the microbiota. *Aquaculture* 532:736072. doi: 10.1016/j.aquaculture.2020.736072
- Ramsey, J. P., Mercurio, A., Holland, J. A., Harris, R. N., and Minbiole, K. P. C. (2015). The cutaneous bacterium *Janthinobacterium lividum* inhibits the growth of trichophyton rubrum in vitro. *Int. J. Dermatol.* 54, 156–159. doi: 10.1111/ijd.12217
- Rawls, J. F., Samuel, B. S., and Gordon, J. I. (2004). Gnotobiotic zebrafish reveal evolutionarily conserved responses to the gut microbiota. *Proc. Natl. Acad. Sci. U. S. A.* 101, 4596–4601. doi: 10.1073/pnas.0400706101
- Razak, S. A., Griffin, M. J., Mischke, C. C., Bosworth, B. G., Waldbieser, G. C., Wise, D. J., et al. (2019). Biotic and abiotic factors influencing channel catfish egg and gut microbiome dynamics during early life stages. *Aquaculture* 498, 556–567. doi: 10.1016/j.aquaculture.2018.08.073
- Reid, K. M., Patel, S., Robinson, A. J., Bu, L. J., Jarungsriapit, J., Moore, L. J., et al. (2017). Salmonid alphavirus infection causes skin dysbiosis in Atlantic salmon (*Salmo salar* L.) post-smolts. *PLoS One* 12:e0172856. doi: 10.1371/journal.pone.0172856
- Reitan, K. I., Natvik, C. M., and Vadstein, O. (1998). Drinking rate, uptake of bacteria and microalgae in turbot larvae. *J. Fish Biol.* 53, 1145–1154. doi: 10.1111/j.1095-8649.1998.tb00238.x
- Sahlmann, C., Gu, J., Kortner, T. M., Lein, I., Kroghdahl, A., and Bakke, A. M. (2015). Ontogeny of the digestive system of Atlantic Salmon (*Salmo salar* L.) and effects of soybean meal from start-feeding. *PLoS One* 10:e0124179. doi: 10.1371/journal.pone.0124179
- Schloss, P. D., Schubert, A. M., Zackular, J. P., Iverson, K. D., Young, V. B., and Petrosino, J. F. (2012). Stabilization of the murine gut microbiome following weaning. *Gut Microbes* 3, 383–393. doi: 10.4161/gmic.21008
- Schmidt, V., Amaral-Zettler, L., Davidson, J., Summerfelt, S., and Good, C. (2016). Influence of fishmeal-free diets on microbial communities in Atlantic Salmon (*Salmo salar*) recirculation aquaculture systems. *Appl. Environ. Microbiol.* 82, 4470–4481. doi: 10.1128/AEM.00902-16

- Sevelsted, A., Stokholm, J., Bønnelykke, K., and Bisgaard, H. (2015). Cesarean section and chronic immune disorders. *Pediatrics* 135, e92–e98. doi: 10.1542/peds.2014-0596
- Sifa, L., and Mathias, J. A. (1987). The critical period of high mortality of larvae fish — a discussion based on current research. *Chin. J. Oceanol. Limnol.* 5, 80–96. doi: 10.1007/BF02848526
- Skjermo, J., Bakke, I., Dahle, S. W., and Vadstein, O. (2015). Probiotic strains introduced through live feed and rearing water have low colonizing success in developing Atlantic cod larvae. *Aquaculture* 438, 17–23. doi: 10.1016/j.aquaculture.2014.12.027
- Stephens, W. Z., Burns, A. R., Stagaman, K., Wong, S., Rawls, J. F., Guillemin, K., et al. (2016). The composition of the zebrafish intestinal microbial community varies across development. *ISME J.* 10, 644–654. doi: 10.1038/ismej.2015.140
- Stressmann, F. A., Bernal-Bayard, J., Perez-Pascual, D., Audrain, B., Rendueles, O., Briolat, V., et al. (2021). Mining zebrafish microbiota reveals key community-level resistance against fish pathogen infection. *ISME J.* 15, 702–719. doi: 10.1038/s41396-020-00807-8
- Sun, Y. Z., Yang, H. L., Ling, Z. C., and Ye, J. D. (2015). Microbial communities associated with early stages of intensively reared orange-spotted grouper (*Epinephelus coioides*). *Aquac. Res.* 46, 131–140. doi: 10.1111/are.12167
- Sylvain, F. E., Holland, A., Bouslama, S., Audet-Gilbert, E., Lavoie, C., Val, A. L., et al. (2020). Fish skin and gut microbiomes show contrasting signatures of host species and habitat. *Appl. Environ. Microbiol.* 86, 1–15. doi: 10.1128/AEM.00789-20
- Testerman, T., Reichley, S. R., King, S., and Graf, J. (2021). Draft genome sequence of *Janthinobacterium lividum* ID1246, Isolated from a Rainbow Trout Hatchery Biofilm. *Microbiol. Resour. Ann* 10:10. doi: 10.1128/MRA.00444-21
- Vadstein, O., Attramadal, K. J. K., Bakke, I., and Olsen, Y. (2018). K-selection as microbial community management strategy: a method for improved viability of larvae in aquaculture. *Front. Microbiol.* 9:2730. doi: 10.3389/fmicb.2018.02730
- Vadstein, O., Bergh, O., Gatesoupe, F. J., Galindo-Villegas, J., Mulero, V., Picchietti, S., et al. (2013). Microbiology and immunology of fish larvae. *Rev. Aquac.* 5, S1–S25. doi: 10.1111/j.1753-5131.2012.01082.x
- Valdes, N., Soto, P., Cottet, L., Alarcon, P., Gonzalez, A., Castillo, A., et al. (2015). Draft genome sequence of *Janthinobacterium lividum* strain MTR reveals its mechanism of capnophilic behavior. *Stand. Genomic Sci.* 10. doi: 10.1186/s40793-015-0104-z
- Verschuere, L., Rombaut, G., Huys, G., Dhont, J., Sorgeloos, P., and Verstraete, W. (1999). Microbial control of the culture of *Artemia* juveniles through preemptive colonization by selected bacterial strains. *Appl. Environ. Microbiol.* 65, 2527–2533. doi: 10.1128/AEM.65.6.2527-2533.1999
- Verschuere, L., Rombaut, G., Sorgeloos, P., and Verstraete, W. (2000). Probiotic bacteria as biological control agents in aquaculture. *Microbiol. Mol. Biol. Rev.* 64, 655–671. doi: 10.1128/MMBR.64.4.655-671.2000
- Vestrum, R. I., Attramadal, K. J. K., Vadstein, O., Gundersen, M. S., and Bakke, I. (2020). Bacterial community assembly in Atlantic cod larvae (*Gadus morhua*): contributions of ecological processes and metacommunity structure. *FEMS Microbiol. Ecol.* 96. doi: 10.1093/femsec/fiaa163
- Wang, C., Sun, G. X., Li, S. S., Li, X., and Liu, Y. (2018). Intestinal microbiota of healthy and unhealthy Atlantic salmon *Salmo salar* L. in a recirculating aquaculture system. *J. Oceanol. Limnol.* 36, 414–426. doi: 10.1007/s00343-017-6203-5
- Wilkes Walburn, J., Wemheuer, B., Thomas, T., Copeland, E., O'Connor, W., Booth, M., et al. (2019). Diet and diet-associated bacteria shape early microbiome development in yellowtail kingfish (*Seriola lalandi*). *Microb. Biotechnol.* 12, 275–288. doi: 10.1111/1751-7915.13323
- Woodruff, K. L., Hummel, G. L., Austin, K. J., Lake, S. L., and Cunningham-Hollinger, H. C. (2022). Calf rumen microbiome from birth to weaning and shared microbial properties to the maternal rumen microbiome. *J. Anim. Sci.* 100. doi: 10.1093/jas/skac264
- Wynne, J. W., Thakur, K. K., Slinger, J., Samsing, F., Milligan, B., Powell, J. F. F., et al. (2020). Microbiome profiling reveals a microbial dysbiosis during a natural outbreak of Tenacibaculosis (yellow mouth) in Atlantic Salmon. *Front. Microbiol.* 11:586387. doi: 10.3389/fmicb.2020.586387
- Xiao, F., Zhu, W., Yu, Y., Huang, J., Li, J., He, Z., et al. (2022). Interactions and stability of gut microbiota in zebrafish increase with host development. *Microbiol. Spectr.* 10:e0169621. doi: 10.1128/spectrum.01696-21
- Zapata, A., Diez, B., Cejalvo, T., Frias, C. G., and Cortes, A. (2006). Ontogeny of the immune system of fish. *Fish Shellfish Immunol.* 20, 126–136. doi: 10.1016/j.fsi.2004.09.005
- Zheng, D., Liwinski, T., and Elinav, E. (2020). Interaction between microbiota and immunity in health and disease. *Cell Res.* 30, 492–506. doi: 10.1038/s41422-020-0332-7



## OPEN ACCESS

## EDITED BY

Zhiyong Li,  
Shanghai Jiao Tong University, China

## REVIEWED BY

Tina Keller-Costa,  
University of Lisbon, Portugal

## \*CORRESPONDENCE

Ramón Alberto Batista-García  
✉ rabg@uaem.mx;  
✉ rbatista25@yahoo.com

RECEIVED 27 April 2023

ACCEPTED 31 July 2023

PUBLISHED 15 August 2023

## CITATION

Pérez-Llano Y, Yarzabal Rodríguez LA,  
Martínez-Romero E, Dobson ADW,  
Gunde-Cimerman N, Vasconcelos V and  
Batista-García RA (2023) From friends to foes:  
fungi could be emerging marine sponge  
pathogens under global change scenarios.  
*Front. Microbiol.* 14:1213340.  
doi: 10.3389/fmicb.2023.1213340

## COPYRIGHT

© 2023 Pérez-Llano, Yarzabal Rodríguez,  
Martínez-Romero, Dobson, Gunde-Cimerman,  
Vasconcelos and Batista-García. This is an  
open-access article distributed under the terms  
of the [Creative Commons Attribution License](#)  
(CC BY). The use, distribution or reproduction  
in other forums is permitted, provided the  
original author(s) and the copyright owner(s)  
are credited and that the original publication in  
this journal is cited, in accordance with  
accepted academic practice. No use,  
distribution or reproduction is permitted which  
does not comply with these terms.

# From friends to foes: fungi could be emerging marine sponge pathogens under global change scenarios

Yordanis Pérez-Llano<sup>1,2</sup>, Luis Andrés Yarzabal Rodríguez<sup>3</sup>,  
Esperanza Martínez-Romero<sup>2</sup>, Alan D. W. Dobson<sup>4</sup>,  
Nina Gunde-Cimerman<sup>5</sup>, Vitor Vasconcelos<sup>6,7</sup> and  
Ramón Alberto Batista-García<sup>1,6\*</sup>

<sup>1</sup>Centro de Investigación en Dinámica Celular, Instituto de Investigación en Ciencias Básicas y Aplicadas, Universidad Autónoma del Estado de Morelos, Cuernavaca, Morelos, Mexico, <sup>2</sup>Center for Genomic Sciences, Autonomous National University of Mexico (UNAM), Cuernavaca, Morelos, Mexico, <sup>3</sup>Carrera de Bioquímica y Farmacia, Unidad de Salud y Bienestar, Universidad Católica de Cuenca, Cuenca, Ecuador, <sup>4</sup>School of Microbiology, University College Cork, Cork, Ireland, <sup>5</sup>Department of Biology, Biotechnical Faculty, University of Ljubljana, Ljubljana, Slovenia, <sup>6</sup>CIIMAR – Interdisciplinary Centre of Marine and Environmental Research, University of Porto, Matosinhos, Portugal, <sup>7</sup>Faculty of Sciences, University of Porto, Porto, Portugal

Global change, experienced in the form of ocean warming and pollution by man-made goods and xenobiotics, is rapidly affecting reef ecosystems and could have devastating consequences for marine ecology. Due to their critical role in regulating marine food webs and trophic connections, sponges are an essential model for studying and forecasting the impact of global change on reef ecosystems. Microbes are regarded as major contributors to the health and survival of sponges in marine environments. While most culture-independent studies on sponge microbiome composition to date have focused on prokaryotic diversity, the importance of fungi in holobiont behavior has been largely overlooked. Studies focusing on the biology of sponge fungi are uncommon. Thus, our current understanding is quite limited regarding the interactions and “crosstalk” between sponges and their associated fungi. Anthropogenic activities and climate change may reveal sponge-associated fungi as novel emerging pathogens. Global change scenarios could trigger the expression of fungal virulence genes and unearth new opportunistic pathogens, posing a risk to the health of sponges and severely damaging reef ecosystems. Although ambitious, this hypothesis has not yet been proven. Here we also postulate as a pioneering hypothesis that manipulating sponge-associated fungal communities may be a new strategy to cope with the threats posed to sponge health by pathogens and pollutants. Additionally, we anticipate that sponge-derived fungi might be used as novel sponge health promoters and beneficial members of the resident sponge microbiome in order to increase the sponge's resistance to opportunistic fungal infections under a scenario of global change.

## KEYWORDS

sponge microbiome, sponge holobiont, fungal-based probiotics, sponge-derived fungi, symbiosis continuum



## Introduction

Sponges are early-derived and simple metazoans that have significant functions in marine ecosystems, including sediment stabilization, nutrient cycling, and the provision of habitats for numerous species (van Soest et al., 2012; Zhang et al., 2019). The incredible global diversity of sponges, surpassing 18,000 recognized species, spans a vast range of environments. The presence of sponges in all types of waters, from fresh to saline, from intertidal to deep-sea, from tropical to occasionally frozen aquatic systems, clearly demonstrates their capacity to respond and adapt to a broad range of environmental conditions (van Soest et al., 2012). Nonetheless, sponges and coral reef systems are currently exposed to ocean warming, acidification, and pollution by xenobiotics, likely to have devastating consequences for marine ecosystems (Carballo and Bell, 2017). Recurrent epidemic disease outbreaks pose a significant challenge for sponge populations both for long-lived slow-growing species, and for biotechnologically important species farmed in aquaculture systems (Blanquer et al., 2016; Belikov et al., 2019). Thus, both local and global pressures on sponge ecosystems are leading to an increasingly deteriorating health of sponges across the world (Webster, 2007; Blanquer et al., 2016; Pita et al., 2018; Belikov et al., 2019; Taylor et al., 2021).

Microbes are regarded as major contributors to the health and survival of sponges (Carballo and Bell, 2017). The diversity of bacteria and to a lesser extent of archaea, associated with sponges has been extensively investigated (Alex et al., 2013; Alex and Antunes, 2015; Thomas et al., 2016; Glasl et al., 2018; Turon et al., 2019; Vargas et al., 2021). Strikingly, except for a few published studies (Nguyen and Thomas, 2018; Hardoim et al., 2021), the eukaryotic fraction of this sponge microbiome is almost unknown (Pita et al., 2018). This is surprising as fungi promote health, defense, nutrition, and survival in their ecological interaction with plant and animal hosts and might perform similar services for sponges. On the other hand, fungi might act as *bona fide* or opportunistic pathogens for sponges as they behave similarly with other animals, including corals (Pita et al., 2018; Jones et al., 2022). Hence, in this perspective article, we propose the hypothesis that sponge-associated fungi could act as potential indicators or “forecasters” of marine environmental perturbations and even become opportunistic pathogens of sponges upon global change.

## The holobiont concept is pivotal to understanding the future ecology of marine sponges

The microbiomes of sponges are both complex and diverse, as highlighted in several studies (Thomas et al., 2016; Glasl et al., 2018; Turon et al., 2019; Vargas et al., 2021). As much as 40–60 percent of the volume of certain sponge species corresponds to abundant and diverse microorganisms that are able to colonize their mesohyl matrix (Thomas et al., 2016; Yang et al., 2019; Díez-Vives et al., 2020). It has been widely hypothesized that the nutrient flux originating from sponges benefits their resident microbial communities (Zhang et al., 2019; Hudspeth et al., 2021). In turn, symbiotic microbes support their hosts by contributing to vitamin and natural product biosynthesis, promoting the production of chemical defenses, and facilitating the

biodegradation of xenobiotics that reach coral reef habitats as a result of global change (Pita et al., 2018; Hudspeth et al., 2021).

The collection of persistent (and usually abundant) microbial taxa that are found in all individuals of a species is regarded as the core microbiota (Astudillo-García et al., 2017). The ecological unit formed by the sponge and its core microbiota can be considered a holobiont, i.e., an entity formed by the intertwined evolution of the animal and microbial partners. The outcome of symbiosis within sponges depends, however, on the physiology of the host and individual microbes in specific environmental conditions. The lifestyles and strategies of microorganisms in their interaction with the host can fluctuate in a continuum from mutualism to parasitism as they adapt to the environmental constraints, making the holobiont and eco-evolutionary concept that is transient and plastic across spatial and temporal scales (Stengel et al., 2022).

Sponges control their microbial residents by distinguishing between foreign and symbiotic microorganisms most likely via immune-related responses (Wehrli et al., 2007). Although some progress has been made toward understanding how sponges differentiate between microbial “friends or foes” (Pita et al., 2018; Schmittmann et al., 2021), the field of sponge immunity remains at its infancy. For example, the sponge *Suberites domuncula* might recognize fungi via the  $\beta$ -glucans on their cell walls, but the specific effect of the cytokine produced by the activation of this signaling pathway has not been described (Perovic-Ottstadt et al., 2004). High-throughput sequencing data has revealed that sponges harbor a complex genomic repertoire of immune receptors, collectively called pattern recognition receptors (PRRs). Notably, these include Toll-like receptors (TLR), Nod-like receptors (NLR), and several members of the scavenger receptor cysteine-rich (SRCR) family; the functions of which are only beginning to be elucidated in response to microbes (Degnan, 2015).

There are conflicting reports in the literature regarding the stability and resilience of the sponge holobiont in response to global change conditions (Bell et al., 2018; Glasl et al., 2018; Posadas et al., 2022). While some studies report environmentally-induced shifts in the microbiome that precede sponge disease (Blanquer et al., 2016; Belikov et al., 2019; Turon et al., 2019; Taylor et al., 2021), others have found that sponge microbiomes can withstand sustained stress conditions (Glasl et al., 2018; Yang et al., 2019). This arises from observed changes in the species-specific dynamics of the sponge microbiomes (Yang et al., 2019), resulting in different adaptability profiles of the sponge holobionts to varying stressful conditions. Even though sponges have been predicted to potentially benefit from ocean warming and acidification (Bell et al., 2018), leading to a predominance of sponges in the benthic ecosystem in future global warming scenarios; this really only applies to a limited subset of species. The forecasted consequence is a reduction in sponge diversity in combination with an increase in microbiome diversity, resulting in reduced stability of the core microbiota (Turon et al., 2019).

In some cases, the dysbiosis of the sponge microbiome, rather than the presence of a single pathogen, has been identified as a key factor contributing to sponge disease (Glasl et al., 2018; Pita et al., 2018; Turon et al., 2019). Dysbiosis refers to the disruptions in the normal or healthy structure and function of the microbial community within the holobiont, which can have detrimental effects on the host's health and ecological interactions. These modifications in the sponge microbiome can occur even before the host exhibits any sign of stress (Taylor et al., 2021), and have been associated with environmental pressures such as ocean warming, acidification, and exposure to

pollution (Blanquer et al., 2016; Belikov et al., 2019; Botté et al., 2019; Turon et al., 2019; Taylor et al., 2021; Vargas et al., 2021). For example, after conducting electron microscopy, infection assays to propagate the syndrome in healthy sponges, and molecular community analyses, the presence of brown spot lesions and necrosis in *Ianthella basta* was attributed to environmental conditions, as these approaches failed to identify any microbial etiology. In addition, pollution affected the bacterial community of *Aplysina cauliformis* with red band syndrome (Gochfeld et al., 2012), with nutrient-enriched treatments exacerbating symptoms in this Caribbean sponge.

Abiotic factors influence not only the structure of sponge microbiomes but also their functions. For instance, CO<sub>2</sub> concentration affects microbial functions in *Coelocarteria singaporensis* and *Stylissa flabelliformis* (Botté et al., 2019), which changed drastically with ocean acidification. Temperature, depth, and geographic location all affect the sponge microbial composition globally (Lurgi et al., 2019). As a result, recent studies have suggested that microbial community composition could be a predictor of sponge disease risk (Taylor et al., 2021). For example, in the marine sponge *Scopalina* sp. bacterial signatures in healthy sponges could predict disease outcomes under an ocean warming scenario.

Thus, the holobiont concept has profound implications in helping to predict the effect of future environmental variations on sponge health and benthic ecology. There is an increasing interest to understand how microbiome diversity influences the sponge immune functions under future ocean conditions (Posadas et al., 2022). This could represent a starting point to design new strategies for the conservation of sponge diversity and mitigating the global change consequences.

## From friends to foes: fungi could be emerging pathogens under global change scenarios

While most culture-independent studies on sponge microbiome composition to date have focused on prokaryotic diversity, the importance of fungi in holobiont behavior has been largely overlooked. Studies focusing on the biology of sponge fungi are uncommon compared to reports on the chemistry of natural products derived from sponge fungi (de Oliveira et al., 2020; Zhang et al., 2020).

An increasing number of fungal species have been linked to marine sponges in the last decades (Höller et al., 2000; Morrison-Gardiner, 2000; Li and Wang, 2009). In one of the most comprehensive studies of sponge-associated fungal biodiversity, Höller et al. isolated a total of 681 fungal strains from 16 sponge species from temperate, subtropical, and tropical regions (Höller et al., 2000). The isolates were distributed among 37 genera of mitosporic fungi, 13 genera of Ascomycota, and 2 genera of Zygomycota. The number of isolates per sample and the diversity of genera varied significantly between the various sites. Almost all the locations yielded *Acremonium*, *Arthrium*, *Coniothyrium*, *Fusarium*, *Mucor*, *Penicillium*, *Phoma*, *Trichoderma*, and *Verticilum* strains, though different fungal genera predominated at each site. In addition, different fungal genera predominated in different sponges sampled from the same location (Höller et al., 2000). In a different study, Morrison-Gardiner isolated 617 fungi from sediments, algae, and vertebrates/invertebrates in Australian coral reefs that included 70 Porifera sample sources (Morrison-Gardiner, 2000). The findings suggest that some reef residents might act as a

natural reservoir for fungal genera that are typically connected to other organisms, whereas many of the fungi isolated from sponges were not present in other sources (Morrison-Gardiner, 2000). The main disadvantage of both studies was that the identification of fungi was achieved by morphological characterization.

A recent study based on culture-independent characterization of the sponge eukaryotic communities from seven sponge species of the Mediterranean Sea found that around 0.75% of the 18S rRNA gene reads had a fungal origin, and from these more than half could also be found in seawater (Naim et al., 2017). These led the authors to the conclusion that the presence of fungi in sponges is largely accidental and does not support the existence of a fungal community unique to sponges (Naim et al., 2017). This observation is also supported by metabarcoding studies from three co-occurring sponges from Australian benthic ecosystems that showed that, within any given sponge species, the fungal communities were found to be highly variable compared to bacterial communities (Nguyen and Thomas, 2018). In these sponges, only a few “core” fungal taxa could be identified as enriched when compared to surrounding seawater (Nguyen and Thomas, 2018). This suggests that only those fungi that can thrive in the sponge environment are selected and therefore horizontal transmission, although possible, may be uncommon in this scenario.

There is, however, observational evidence of interactions between sponges and fungi. Immunocytochemical and transmission electron microscopy evidence suggests that an endosymbiotic yeast is vertically transmitted in the marine sponge *Chondrilla* sp. (Maldonado et al., 2005). The putative horizontal gene transfer of a fungal mitochondrial intron into the genome of the sponge *Tetilla* sp. has also been considered as indirect evidence for a symbiotic relationship between fungi and a sponge (Rot et al., 2006). Koralionastes ascomycetes, found only in the ocean, are said to form their ascomata on or inside crustacean sponges (Kohlmeyer and Volkmann-Kohlmeyer, 1990). Therefore, the symbiotic relationship between fungi and sponges is still a relatively unexplored area of biology and evolution.

Sponge pathogenic fungi, on the other hand, are also largely unexplored. In 1884, a considerable number of sponges (*Ircinia* spp.) in the Indian Ocean were affected by an unknown disease that was most probably caused by a filamentous fungus. Later, mortality between 70 and 95% of the affected individuals was recorded in commercial sponges in the Florida Keys (1939), Bahamas (1938–1939), Cuba (1939), and British Honduras (1939) (Webster, 2007). Again, unidentified filamentous fungi were observed in the tissues of the diseased sponges, but no microbiological analyses were performed to identify the etiological agent(s) (Webster, 2007; Carballo and Bell, 2017). In 2015, Sweet and coworkers described a novel disease in *Callyspongia* (*Euplaccella*) aff. *Biru* sponges colonizing Maldivian ecosystems (Sweet et al., 2015). The individuals exhibited brown necrotic lesions caused by a microbial consortium, which included the fungus *Rhabdocline* sp.

While studies show that certain fungi (such as *Aspergillus sydowii*) may infect corals, there is, to the best of our knowledge, only one recent study demonstrating that a fungus (*Aspergillus tubingensis*) can cause a fatal infection in the marine sponge *Chondrosia reniformis* (Greco et al., 2019). The symptoms include loss in pigmentation, softening of the cortical portions, detachment of the outer portion of the ectosome, and, finally, death of the sponges (Greco et al., 2019). This finding takes on added significance when viewed within the framework of One Health, as *A. tubingensis* is already known to be a human pathogen

(Gautier et al., 2016), raising concerns about the potential emergence of marine zoonotic diseases that could pose threats to human health in the face of a changing environment. The possibility that sponges could serve as reservoirs or substrates for the spread of fungal infections adds another layer of complexity, potentially affecting not only marine ecosystems but also terrestrial animals. Interestingly, the marine sponge *Spongia obscura* has been found to harbor *A. sydowii* without exhibiting symptoms of infection, suggesting that it could be a reservoir of this coral pathogen (Ein-Gil et al., 2009).

Fungi are known for their extremotolerance, demonstrated as the ability to endure a wide range of harsh environmental conditions. Like sponges, certain fungal species might also benefit from climate change (Jones et al., 2022). For instance, the acidification of marine waters, salinization of estuaries, and slight increases in water temperature could benefit the proliferation of many species of fungi since, as in general, they are well adapted to these conditions (Krause et al., 2013a,b). Global change could trigger the expression of genes related to toxin production, cell wall properties, osmotolerance, unicellular and dimorphic growth, motility, attachment, chemotaxis, or quorum sensing. These genes are crucial for adapting to new environments and can also contribute to virulence in pathogenic fungal ecotypes (Roik et al., 2022). The mechanisms by which fungi become harmful to sponges and the causes and triggers of the switch from non-detrimental fungal colonizer to fungal pathogen have not been explored (Webster, 2007; Greco et al., 2019).

A major obstacle in studying the ecological interactions between marine sponges and their resident microbes is the current methodology used to identify pathogens. Existing aquarium systems used in laboratory settings to replicate natural sponge microbiomes are inadequate for the safe utilization of fungal inoculants, which can pose risks to human and environmental health. For instance, the presence of *A. tubingensis*, a pathogen of sponges and an opportunistic human pathogen (Gautier et al., 2016), highlights the need for caution. Moreover traditional approaches fail to anticipate the ecological context in which interactions between sponges, resident fungi, and the changing environment may trigger previously unrecognized—but potentially lethal—infections (Greco et al., 2019).

To advance our understanding of emerging fungal pathogens, it is crucial to implement novel experimental approaches (Figure 1). Until recently, the lack of sponge cell lines and cultures hindered our understanding of pathogenesis and sponge cellular response to infection. However, recent advancements have demonstrated the successful cultivation of sponge cells *in vitro* (Conkling et al., 2019; Hesp et al., 2023) and 3D cultures that mimic the architecture of sponge tissues (Urban-Gedamke et al., 2021), which should pave the way to more reproducible and mechanistic studies on host-pathogen interactions. The identification of fungi and other microbes that could shift away from mutualism/commensalism to pathogenicity requires the use of mesocosm experiments conducted under controlled conditions using marine simulator systems. These simulators will enable the emulation of different global change scenarios (e.g., light, temperature, CO<sub>2</sub>, salinity, pollutants) and facilitate long-term simulations, allowing for multi-generational studies. This approach would allow the identification of fungal taxa that could be harmful to marine sponges at different temporal scales. Moreover, it may also provide useful insights into fungal signatures, whether in the form of community structure or potential functionality, that could serve as predictors of sponge health within marine ecosystems.

## Fungal-based probiotics as sponge health promoters

In recent years, the potential use of microbial transplants and probiotics for treating a wide variety of human and animal disorders have emerged as novel paradigms (Peixoto et al., 2017, 2021; Rosado et al., 2019; Ushijima et al., 2023). Microbiome engineering offers a unique opportunity to improve not only human health but also agricultural productivity and climate management (Peixoto et al., 2017). However, environmental applications of microbiome engineering are progressing slowly because, even at a laboratory scale, they entail several logistical problems. Although some successful microbiome engineering applications have been reported (i.e., bioremediation, wastewater engineering, and biocontrol in agriculture), selecting appropriate strains, ensuring their sufficient abundance in the ecological unit to sustain a physiological benefit, and preventing contamination of non-target ecosystems, are still major concerns. For example, the deliberate release of inoculants, particularly in aquatic environments, could be detrimental to the resident microbial communities and to ecosystem functioning, as the dispersal of microbes is easier in aqueous media (Peixoto et al., 2017).

The use of microbial transplant and microbiome engineering in sponges has not been explored as in corals, the cnidarian animals that coincide with sponges in benthic ecosystems (Peixoto et al., 2017, 2021; Rosado et al., 2019). Although the use of probiotics in corals is in its infancy, several studies have been conducted to demonstrate the positive effect of bacterial inoculants on different coral species (Rosado et al., 2019). For example, some native bacterial populations enhance coral tolerance to a variety of pressures associated with global change (e.g., temperature stress or oil pollution) and are critical for nutrient cycling, coral defense responses, and coral health (Ziegler et al., 2019). Microbiota transplantation experiments, reported in the same study, have shown that these bacterial communities also promote the environmental plasticity of both coral and their associated microbiota when they are relocated to new habitats (Ziegler et al., 2019). In another example, Rosado et al. reported that manipulating a bacterial consortium of *Pseudoalteromonas* sp., *Holomonas taeanensis*, and *Cobetia marina*-related species, isolated from the coral *Pocillopora damicornis*, partially mitigated coral-bleaching and significantly improved the coral resistance to water warming. In addition, inoculation with this consortium controlled the development of the temperature-dependent pathogen *Vibrio coralliilyticus* (Rosado et al., 2019). However, the aforementioned development of coral probiotics has focused exclusively on bacteria, and no research has been conducted to date to investigate the use of fungi for enhancing health and stress tolerance in corals and sponges.

While fungi are not typically regarded as permanent members of the sponge holobiont, the use of fungal inoculants as probiotics presents an intriguing approach to transiently modulate microbial dynamics within the sponge, thereby aiding in the restoration of host physiology in the face of changing environmental conditions. In theory, by introducing fungal probiotics, the holobiont can undergo a transformative process, attaining a new stable configuration that is facilitated by the beneficial effects of these fungi. Once the desired recovery is achieved, and the use of the inoculant is discontinued, the holobiont would maintain this improved state.

Fungal probiotics have been used extensively as feed additive in fish, pigs, ruminants, poultry, and other animals. Yeasts, particularly those belonging to the *Saccharomyces* genus, have been studied for their ability



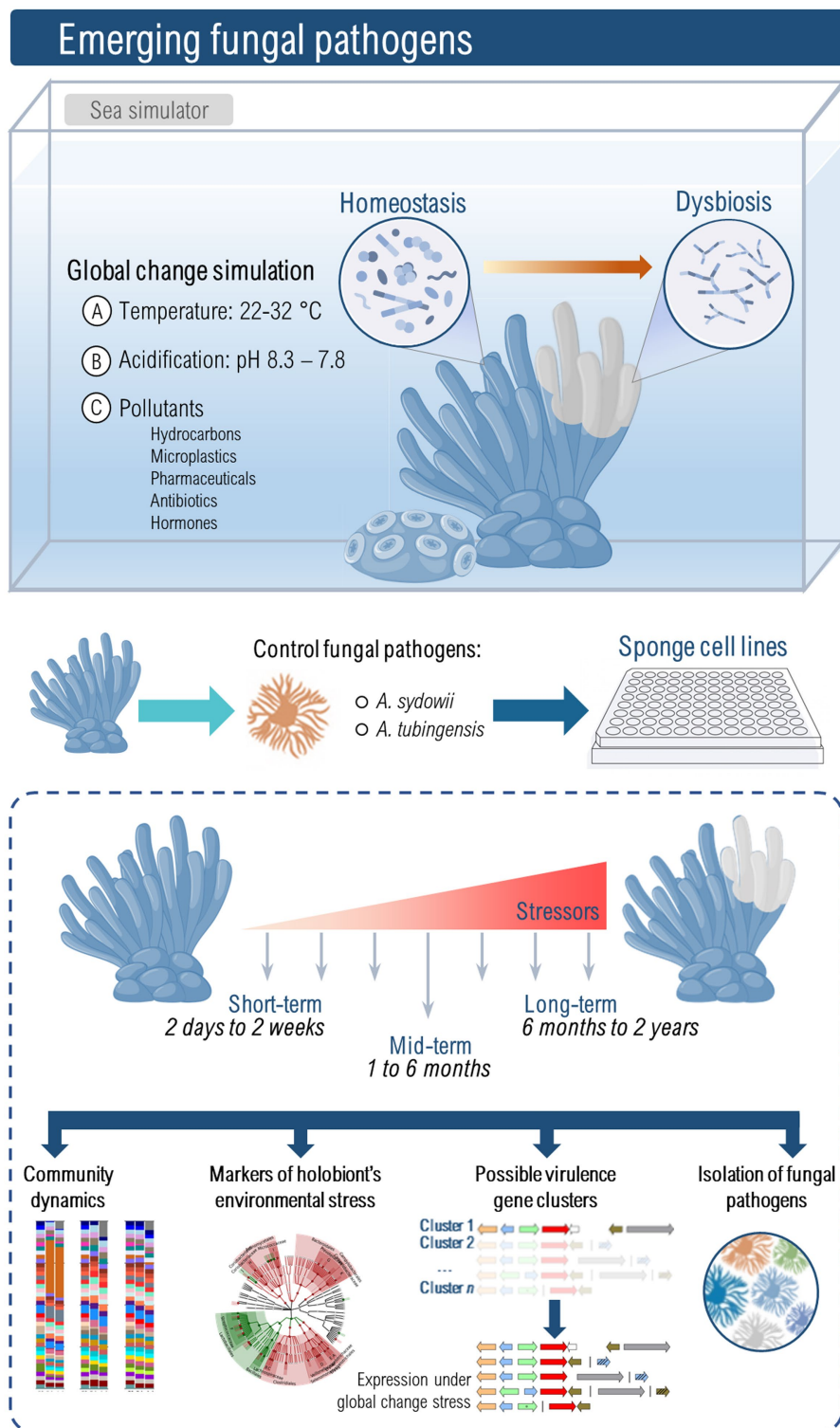


FIGURE 1

The study of emerging marine fungal pathogens due to global change requires dedicated facilities that perform mesocosm-style experiments, also known as sea simulators. Only a select few places worldwide have the characteristics of these kinds of laboratories, and therefore not many studies have been conducted in these settings (Krause et al., 2013b; Rosado et al., 2019; Luter et al., 2020). The variables controlled in these experiments include seawater temperature and pH, dissolved carbon dioxide, lighting, salinity, and the presence of pollutants such as hydrocarbons, microplastics, pharmaceuticals, hormones, or antibiotics. Mesocosm experiments allow an understanding of the multiscale temporal dynamics of gene expression, physiological traits, microbial community composition, and multispecies ecological interactions. These types of experiments are pivotal to identifying markers of holobiont stress or dysbiosis, changes in the immune status of the host in response to environmental conditions, activation of genes and clusters that promote fungal virulence, and the emergence of pathogens from previously innocuous strains. *Aspergillus tubingensis* or *A. sydowii* might become model fungal pathogens to understand fungal impact on resident microbial communities and immune responses of sponges. Naturally, this will require extreme measures of biosafety and containment since, in addition to infect —at least— one marine sponge species (Gautier et al., 2016), *A. tubingensis* is also a Risk Group 2 pathogen.



to positively influence the gut microbiota and overall digestive processes. In humans, *S. boulardii* has shown health-promoting effects and is commonly used to treat multiple gastrointestinal diseases (Pais et al., 2020; Abid et al., 2022). In fish, the yeasts *S. cerevisiae*, *Geotrichum candidum*, and *Yarrowia lipolytica* have been investigated for their probiotic potential, both alone and in combination with bacterial strains (Melo-Bolívar et al., 2021; Reyes-Becerril et al., 2021). Filamentous fungi, such as *Aspergillus niger* or *A. oryzae*, have also been used in fish to improve digestion, nutrient utilization, and immunity (Dawood et al., 2020; Shukry et al., 2021; Jasim et al., 2022). These findings suggest that both unicellular and filamentous fungi play significant roles in modulating host physiology and highlight their potential to perform similar functions in sponges.

The factors required in a workflow to isolate and characterize novel candidates for coral probiotics have been previously highlighted and seem to apply to sponges as well. Examples of desirable roles for these probiotic strains could be the supply of nutrients and their cycling, modulation of immune responses, UV protection, dissemination of beneficial genes/pathways, and the biological control of pathogen populations, among others (Peixoto et al., 2021).

Manipulating sponge-associated fungal communities may be an important new strategy to cope with the threats posed to sponge health by pathogens and pollutants (Figure 2). Additionally, we anticipate that sponge-derived fungi might be used as novel sponge health promoters, to increase the sponge's resistance to opportunistic infections under a scenario of global change. To develop

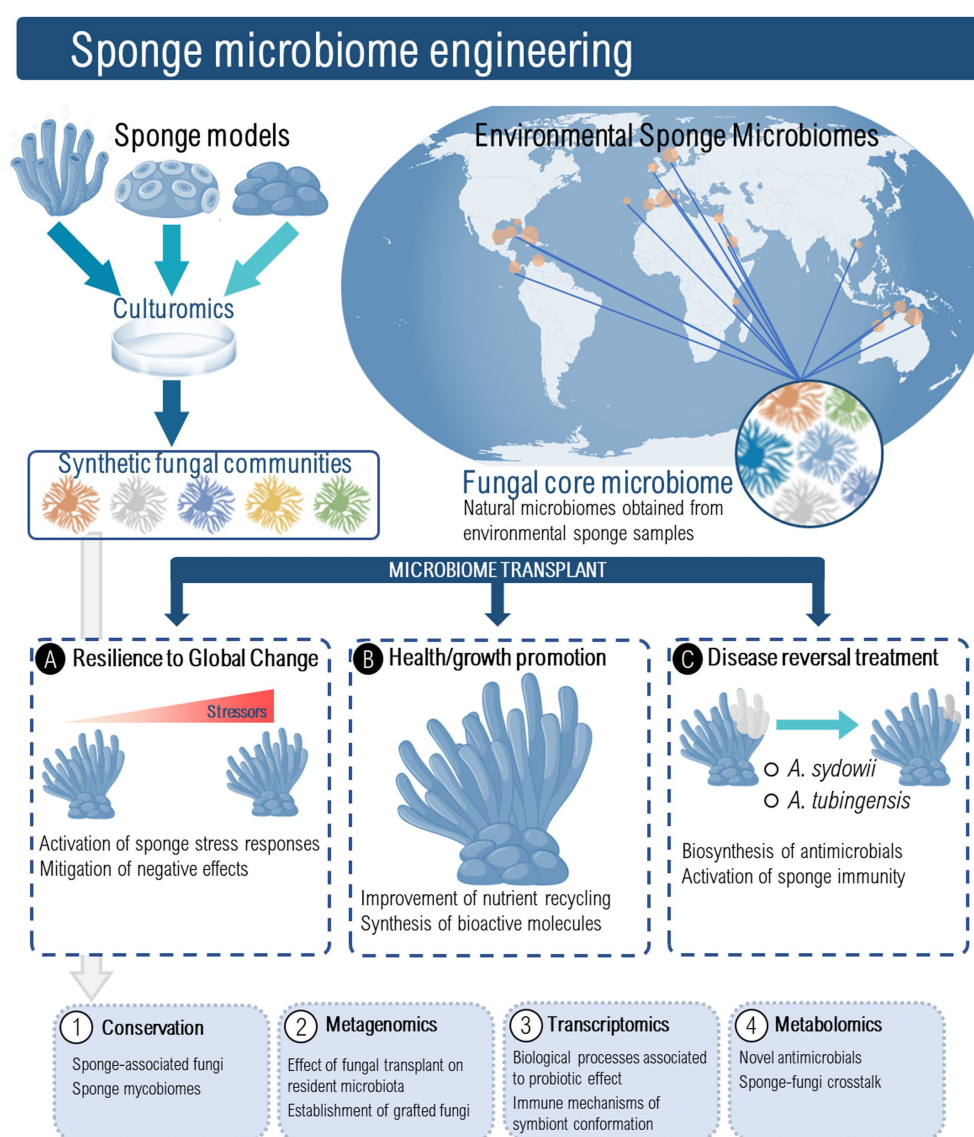


FIGURE 2

Sponge microbiome engineering using sponge associated fungi could serve as a novel strategy to induce resilience to global change, promote sponge health and growth, and as treatment for disease reversal. Fungal probiotics might be prospected from laboratory and aquaculture sponge models as well as from environmental sponge mycobiomes. The conservation and characterization of these fungal probiotics should encompass a multi-omics approach to understand the effect of fungal transplant on resident microbiota and its persistence, the immune mechanisms of holobiont conformation, and the molecular crosstalk between sponges and their resident microbes under global change stress conditions.

fungus-based probiotics for marine sponges several hurdles should be overcome, and crucial questions must be first elucidated. These include (but are not limited to): (1) What roles do fungi play in sponge ecosystems? (2) How can fungi influence sponge immune functions? (3) Which fungi are essential for sponge ecosystem functioning? (4) How do the fungal communities interact with other members of the sponge microbiome? (5) How do sponge-associated fungi respond to environmental perturbations? (6) What are the critical steps in isolating and selecting putative beneficial sponge microbes? and (7) What is the best way for inoculating fungi in sponge ecosystems? In addition, pilot-scale trials will need to be undertaken involving the use of fungus-based probiotics, under controlled aquarium conditions to prove that the overall concept of sponge probiotics is in fact viable (Figure 2).

## Concluding remarks

Fungi are thought to be relevant sponge pathogens but there is scarce knowledge regarding the potential role of fungi as opportunistic—even emergent—pathogens in the field of sponge biology, particularly in the context of stress due to global change scenarios. In this setting, global change might cause microbial partners, particularly fungi, to flip from symbiosis to pathogenicity. We hypothesize that anthropogenic activities and climate change may reveal sponge-associated fungi as novel emerging pathogens. Global change scenarios could trigger the expression of fungal virulence genes and unearth new opportunistic pathogens, posing a risk to the health of sponges thus severely damaging reef ecosystems. Although it is not yet clear that such a scenario could come to pass, this hypothesis should be investigated to enable timely bioprospection and interventions. This knowledge could lead to identifying sponge-associated fungi as potential indicators or “forecasters” of environmental perturbations or as tools to promote sponge health under stress.

## References

- Abid, R., Waseem, H., Ali, J., Ghazanfar, S., Ali, G. M., Elsbali, A. M., et al. (2022). Probiotic yeast *Saccharomyces*: Back to nature to improve human health. *J. Fungi*. 8, 1–12. doi: 10.3390/jof8050444
- Alex, A., and Antunes, A. (2015). Pyrosequencing characterization of the microbiota from Atlantic intertidal marine sponges reveals high microbial diversity and the lack of co-occurrence patterns. *PLoS One* 10, 1–17. doi: 10.1371/journal.pone.0127455
- Alex, A., Silva, V., Vasconcelos, V., and Antunes, A. (2013). Evidence of unique and generalist microbes in distantly related sympatric intertidal marine sponges (Porifera: Demospongiae). *PLoS One* 8:e80653. doi: 10.1371/journal.pone.0080653
- Astudillo-García, C., Bell, J. J., Webster, N. S., Glasl, B., Jompa, J., Montoya, J. M., et al. (2017). Evaluating the core microbiota in complex communities: a systematic investigation. *Environ. Microbiol.* 19, 1450–1462. doi: 10.1111/1462-2920.13647
- Belikov, S., Belkova, N., Butina, T., Chernogor, L., Van, K. A. M., Nalian, A., et al. (2019). Diversity and shifts of the bacterial community associated with Baikal sponge mass mortalities. *PLoS One* 14, 1–19. doi: 10.1371/journal.pone.0213926
- Bell, J. J., Bennett, H. M., Rovellini, A., and Webster, N. S. (2018). Sponges to be winners under near-future climate scenarios. *Bioscience* 68, 955–968. doi: 10.1093/biosci/biy142
- Blanquer, A., Uriz, M. J., Cebrian, E., and Galand, P. E. (2016). Snapshot of a bacterial microbiome shift during the early symptoms of a massive sponge die-off in the western Mediterranean. *Front. Microbiol.* 7, 1–10. doi: 10.3389/fmicb.2016.00752
- Botté, E. S., Nielsen, S., Abdul Wahab, M. A., Webster, J., Robbins, S., Thomas, T., et al. (2019). Changes in the metabolic potential of the sponge microbiome under ocean acidification. *Nat. Commun.* 10, 1–10. doi: 10.1038/s41467-019-12156-y
- Carballo, J. L., and Bell, J. J. *Climate change, ocean acidification and sponges: impacts across multiple levels of organization*. (2017). Singapore: Springer.
- Conkling, M., Hesp, K., Munroe, S., Sandoval, K., Martens, D. E., Sipkema, D., et al. (2019). Breakthrough in marine invertebrate cell culture: sponge cells divide rapidly in improved nutrient medium. *Sci. Rep.* 9, 1–10. doi: 10.1038/s41598-019-53643-y
- Dawood, M. A. O., Eweedah, N. M., Moustafa, E. M., and Farahat, E. M. (2020). Probiotic effects of *Aspergillus oryzae* on the oxidative status, heat shock protein, and immune related gene expression of Nile tilapia (*Oreochromis niloticus*) under hypoxia challenge. *Aquaculture* 520:734669. doi: 10.1016/j.aquaculture.2019.734669
- de Oliveira, B. F. R., Carr, C. M., Dobson, A. D. W., and Laport, M. S. (2020). Harnessing the sponge microbiome for industrial biocatalysts. *Appl. Microbiol. Biotechnol.* 104, 8131–8154. doi: 10.1007/s00253-020-10817-3
- Degnan, S. M. (2015). The surprisingly complex immune gene repertoire of a simple sponge, exemplified by the NLR genes: a capacity for specificity? *Dev. Comp. Immunol.* 48, 269–274. doi: 10.1016/j.dci.2014.07.012
- Díez-Vives, C., Taboada, S., Leiva, C., Busch, K., Hentschel, U., and Riesgo, A. (2020). On the way to specificity - microbiome reflects sponge genetic cluster primarily in highly structured populations. *Mol. Ecol.* 29, 4412–4427. doi: 10.1111/mec.15635
- Ein-Gil, N., Ilan, M., Carmeli, S., Smith, G. W., Pawlik, J. R., and Yarden, O. (2009). Presence of *Aspergillus sydowii*, a pathogen of gorgonian sea fans in the marine sponge *Spongia obscura*. *ISME J.* 3, 752–755. doi: 10.1038/ismej.2009.18
- Gautier, M., Normand, A. C., L’Ollivier, C., Cassagne, C., Reynaud-Gaubert, M., Dubus, J. C., et al. (2016). *Aspergillus tubingensis*: a major filamentous fungus found in the airways of patients with lung disease. *Med. Mycol.* 54, 459–470. doi: 10.1093/mmy/myv118

## Author contributions

The first draft of the manuscript was written by YP-L, LY, and RB-G. Figures were prepared by YP-L and RB-G. All authors commented on previous versions of the manuscript, read and approved the final manuscript.

## Funding

This project has received funding from the European Union’s Horizon 2020 research and innovation programme under Grant Agreement no. 101000392 (MARBLES). This output reflects only the author’s view, and the Research Executive Agency (REA) cannot be held responsible for any use that may be made of the information contained therein. YP-L received postdoctoral fellowships from UNAM-DGAPA and from CONACyT (CVU: 697462). RB-G received a Sabbatical fellowship (CVU: 389616) from the National Council of Science and Technology (CONACyT), Mexico.

## Conflict of interest

The authors declare that the research was conducted in the absence of any commercial or financial relationships that could be construed as a potential conflict of interest.

## Publisher’s note

All claims expressed in this article are solely those of the authors and do not necessarily represent those of their affiliated organizations, or those of the publisher, the editors and the reviewers. Any product that may be evaluated in this article, or claim that may be made by its manufacturer, is not guaranteed or endorsed by the publisher.

- Glasl, B., Smith, C. E., Bourne, D. G., and Webster, N. S. (2018). Exploring the diversity-stability paradigm using sponge microbial communities. *Sci. Rep.* 8, 1–9. doi: 10.1038/s41598-018-26641-9
- Gochfeld, D. J., Easson, C. G., Freeman, C. J., Thacker, R. W., and Olson, J. B. (2012). Disease and nutrient enrichment as potential stressors on the Caribbean sponge *Aplysina cauliformis* and its bacterial symbionts. *Mar. Ecol. Prog. Ser.* 456, 101–111. doi: 10.3354/meps09716
- Greco, G., Di Piazza, S., Gallus, L., Amaroli, A., Pozzolini, M., Ferrando, S., et al. (2019). First identification of a fatal fungal infection of the marine sponge *Chondrosia reniformis* by *aspergillus tubingensis*. *Dis. Aquat. Org.* 135, 227–239. doi: 10.3354/dao03397
- Hardoim, C. C. P., Lôbo-Hajdu, G., Custódio, M. R., and Hardoim, P. R. (2021). Prokaryotic, fungal, and unicellular eukaryotic core communities across three sympatric marine sponges from the southwestern Atlantic coast are dominated largely by deterministic assemblage processes. *Front. Microbiol.* 12. doi: 10.3389/fmicb.2021.674004
- Hesp, K., van der Heijden, J. M. E., Munroe, S., Sipkema, D., Martens, D. E., Wijffels, R. H., et al. (2023). First continuous marine sponge cell line established. *Sci. Rep.* 13:5766. doi: 10.1038/s41598-023-32394-x
- Höller, G., Wright, A. D., Matthée, G. F., König, G. M., Draeger, S., Aust, H. J., et al. (2000). Fungi from marine sponges: diversity, biological activity and secondary metabolites. *Mycol. Res.* 104, 1354–1365. doi: 10.1017/S0953756200003117
- Hudspeth, M., Rix, L., Achlatis, M., Bougoure, J., Guagliardo, P., Clode, P. L., et al. (2021). Subcellular view of host–microbiome nutrient exchange in sponges: insights into the ecological success of an early metazoan–microbe symbiosis. *Microbiome* 9, 1–15. doi: 10.1186/s40168-020-00984-w
- Jaśim, S. A., Abdelbasset, W. K., Shichiyakh, R. A., Al-Shawi, S. G., Yasin, G., Jalil, A. T., et al. (2022). Probiotic effects of the fungi, *aspergillus niger* on growth, immunity, haematology, intestine fungal load and digestive enzymes of the common carp, *Cyprinus carpio*. *Aquac. Res.* 53, 3828–3840. doi: 10.1111/are.15890
- Jones, E. B. G., Ramakrishna, S., Vikineswary, S., Das, D., Bahkali, A. H., Guo, S., et al. (2022). How do fungi survive in the sea and respond to climate change? *J. Fungi*. 8:291. doi: 10.3390/jof8030291
- Kohlmeyer, J., and Volkmann-Kohlmeyer, B. (1990). New species of Koralionastes (Ascomycotina) from the Caribbean and Australia. *Can. J. Bot.* 68, 1554–1559. doi: 10.1139/b90-199
- Krause, E., Wichels, A., Erler, R., and Gerdt, G. (2013a). Study on the effects of near-future ocean acidification on marine yeasts: a microcosm approach. *Helgol. Mar. Res.* 67, 607–621. doi: 10.1007/s10152-013-0348-1
- Krause, E., Wichels, A., Giménez, L., and Gerdt, G. (2013b). Marine fungi may benefit from ocean acidification. *Aquat. Microb. Ecol.* 69, 59–67. doi: 10.3354/ame01622
- Li, Q., and Wang, G. (2009). Diversity of fungal isolates from three Hawaiian marine sponges. *Microbiol. Res.* 164, 233–241. doi: 10.1016/j.micres.2007.07.002
- Lurgi, M., Thomas, T., Wemheuer, B., Webster, N. S., and Montoya, J. M. (2019). Modularity and predicted functions of the global sponge-microbiome network. *Nat. Commun.* 10:992. doi: 10.1038/s41467-019-08925-4
- Luter, H. M., Andersen, M., Versteegen, E., Laffy, P., Uthick, S., Bell, J. J., et al. (2020). Cross-generational effects of climate change on the microbiome of a photosynthetic sponge. *Environ. Microbiol.* 22, 4732–4744. doi: 10.1111/1462-2920.15222
- Maldonado, M., Cortadellas, N., Trillas, M. I., and Rützler, K. (2005). Endosymbiotic yeast maternally transmitted in a marine sponge. *Biol. Bull.* 209, 94–106. doi: 10.2307/3593127
- Melo-Bolívar, J. F., Ruiz Pardo, R. Y., Hume, M. E., and Villamil Díaz, L. M. (2021). Multistain probiotics use in main commercially cultured freshwater fish: a systematic review of evidence. *Rev. Aquac.* 13, 1758–1780. doi: 10.1111/raq.12543
- Morrison-Gardiner, S. (2000). Dominant fungi from Australian coral reefs. *Water Resour. Manag.* 14, 105–121.
- Naim, M. A., Smidt, H., and Sipkema, D. (2017). Fungi found in Mediterranean and North Sea sponges: how specific are they? *Peer J.* 5, e3722–e3719. doi: 10.7717/peerj.3722
- Nguyen, M. T. H. D., and Thomas, T. (2018). Diversity, host-specificity and stability of sponge-associated fungal communities of co-occurring sponges. *Peer J.* 2018, 1–26. doi: 10.7717/peerj.4965
- Pais, P., Almeida, V., Yilmaz, M., and Teixeira, M. C. (2020). *Saccharomyces boulardii*: what makes it tick as successful probiotic? *J. Fungi*. 6, 1–15. doi: 10.3390/jof6020078
- Peixoto, R. S., Rosado, P. M., de Leite, D. C. A., Rosado, A. S., and Bourne, D. G. (2017). Beneficial microorganisms for corals (BMC): proposed mechanisms for coral health and resilience. *Front. Microbiol.* 8, 1–16. doi: 10.3389/fmicb.2017.00341
- Peixoto, R. S., Sweet, M., Villela, H. D. M., Cardoso, P., Thomas, T., Voolstra, C. R., et al. (2021). Coral probiotics: premise, promise, prospects. *Annu. Rev. Anim. Biosci.* 9, 265–288. doi: 10.1146/annurev-animal-090120-115444
- Perovic-Ottstadt, S., Adell, T., Proksch, P., Wiens, M., Korzhnev, M., Gamulin, V., et al. (2004). A (13)-beta-D-glucan recognition protein from the sponge *Suberites domuncula*. Mediated activation of fibrinogen-like protein and epidermal growth factor gene expression. *Eur. J. Biochem.* 271, 1924–1937. doi: 10.1111/j.1432-1033.2004.04102.x
- Pita, L., Rix, L., Slaby, B. M., Franke, A., and Hentschel, U. (2018). The sponge holobiont in a changing ocean: from microbes to ecosystems. *Microbiome*. 6:46. doi: 10.1186/s40168-018-0428-1
- Posadas, N., Baquiran, J. I. P., Nada, M. A. L., Kelly, M., and Conaco, C. (2022). Microbiome diversity and host immune functions influence survivorship of sponge holobionts under future ocean conditions. *ISME J.* 16, 58–67. doi: 10.1038/s41396-021-01050-5
- Reyes-Becerril, M., Alamillo, E., and Angulo, C. (2021). Probiotic and immunomodulatory activity of marine yeast *Yarrowia lipolytica* strains and response against *Vibrio parahaemolyticus* in fish. *Probiot. Antimicrob. Proteins* 13, 1292–1305. doi: 10.1007/s12602-021-09769-5
- Roik, A., Reverter, M., and Pogoreutz, C. (2022). A roadmap to understanding diversity and function of coral reef-associated fungi. *FEMS Microbiol. Rev.* 46, 1–26. doi: 10.1093/femsre/fuac028
- Rosado, P. M., Leite, D. C. A., Duarte, G. A. S., Chaloub, R. M., Jospin, G., Nunes da Rocha, U., et al. (2019). Marine probiotics: increasing coral resistance to bleaching through microbiome manipulation. *ISME J.* 13, 921–936. doi: 10.1038/s41396-018-0323-6
- Rot, C., Goldfarb, I., Ilan, M., and Huchon, D. (2006). Putative cross-kingdom horizontal gene transfer in sponge (Porifera) mitochondria. *BMC Evol. Biol.* 6, 1–11. doi: 10.1186/1471-2148-6-71
- Schmittmann, L., Franzenburg, S., and Pita, L. (2021). Individuality in the immune repertoire and induced response of the sponge *Halichondria panicea*. *Front. Immunol.* 12, 1–13. doi: 10.3389/fimmu.2021.689051
- Shukry, M., Abd El-Kader, M. F., Hendam, B. M., Dawood, M. A. O., Farrag, F. A., Aboelenin, S. M., et al. (2021). Dietary *aspergillus oryzae* modulates serum biochemical indices, immune responses, oxidative stress, and transcription of hsp 70 and cytokine genes in Nile tilapia exposed to salinity stress. *Animals* 11, 1–14. doi: 10.3390/ani11061621
- Stengel, A., Drijber, R. A., Carr, E., Egreja, T., Hillman, E., Krause, T., et al. (2022). Rethinking the roles of pathogens and mutualists: exploring the continuum of symbiosis in the context of microbial ecology and evolution. *Phytobiomes J.* 6, 108–117. doi: 10.1094/PBIOMES-05-21-0031-P
- Sweet, M., Bulling, M., and Cerrano, C. (2015). A novel sponge disease caused by a consortium of micro-organisms. *Coral Reefs* 34, 871–883. doi: 10.1007/s00338-015-1284-0
- Taylor, J. A., Díez-Vives, C., Majzoub, M. E., Nielsen, S., and Thomas, T. (2021). Stress response of the marine sponge *Scopalina* sp. can microbial community composition predict sponge disease? *FEMS Microbiol. Ecol.* 97, 1–11. doi: 10.1093/femsec/fiab095
- Thomas, T., Moitinho-Silva, L., Lurgi, M., Björk, J. R., Easson, C., Astudillo-García, C., et al. (2016). Diversity, structure and convergent evolution of the global sponge microbiome. *Nat. Commun.* 7, 1–12. doi: 10.1038/ncomms11870
- Turon, M., Cáliz, J., Triadó-Margarit, X., Casamayor, E. O., and Uriz, M. J. (2019). Sponges and their microbiomes show similar community metrics across impacted and well-preserved reefs. *Front. Microbiol.* 10, 1–13. doi: 10.3389/fmicb.2019.01961
- Urban-Gedamke, E., Conkling, M., McCarthy, P. J., Wills, P. S., and Pomponi, S. A. (2021). 3-D culture of marine sponge cells for production of bioactive compounds. *Mar. Drugs* 19, 1–15. doi: 10.3390/md19100569
- Ushijima, B., Gunasekera, S. P., Meyer, J. L., Tittl, J., Pitts, K. A., Thompson, S., et al. (2023). Chemical and genomic characterization of a potential probiotic treatment for stony coral tissue loss disease. *Commun. Biol.* 6:248. doi: 10.1038/s42003-023-04590-y
- van Soest, R. W. M., Boury-Esnault, N., Vacelet, J., Dohrmann, M., Erpenbeck, D., de Voogd, N. J., et al. (2012). Global diversity of sponges (Porifera). *PLoS One* 7:e35105. doi: 10.1371/journal.pone.0035105
- Vargas, S., Leiva, L., and Wörheide, G. (2021). Short-term exposure to high-temperature water causes a shift in the microbiome of the common aquarium sponge *Lendenfeldia chondrodes*. *Microb. Ecol.* 81, 213–222. doi: 10.1007/s00248-020-01556-z
- Webster, N. S. (2007). Sponge disease: a global threat? *Environ. Microbiol.* 9, 1363–1375. doi: 10.1111/j.1462-2920.2007.01303.x
- Wehrli, M., Steinert, M., and Hentschel, U. (2007). Bacterial uptake by the marine sponge *Aplysina aerophoba*. *Microb. Ecol.* 53, 355–365. doi: 10.1007/s00248-006-9090-4
- Yang, Q., Franco, C. M. M., Lin, H. W., and Zhang, W. (2019). Untapped sponge microbiomes: structure specificity at host order and family levels. *FEMS Microbiol. Ecol.* 95, 1–16. doi: 10.1093/femsec/fiz136
- Zhang, F., Jonas, L., Lin, H., and Hill, R. T. (2019). Microbially mediated nutrient cycles in marine sponges. *FEMS Microbiol. Ecol.* 95, 1–14. doi: 10.1093/femsec/fiz155
- Zhang, B., Zhang, T., Xu, J., Lu, J., Qiu, P., Wang, T., et al. (2020). Marine sponge-associated fungi as potential novel bioactive natural product sources for drug discovery: a review. *Mini Rev. Med. Chem.* 20, 1966–2010. doi: 10.2174/1389557520066200826123248
- Ziegler, M., Grupstra, C. G. B., Barreto, M. M., Eaton, M., BaOmar, J., Zubier, K., et al. (2019). Coral bacterial community structure responds to environmental change in a host-specific manner. *Nat. Commun.* 10:3092. doi: 10.1038/s41467-019-10969-5





## OPEN ACCESS

## EDITED BY

Zhiyong Li,  
Shanghai Jiao Tong University, China

## REVIEWED BY

Jianping Jiang,  
Chinese Academy of Sciences (CAS), China  
Libby Wilson,  
Kansas State University, United States

## \*CORRESPONDENCE

Aruna M. Shankregowda  
✉ arungowda9738@gmail.com

RECEIVED 31 May 2023

ACCEPTED 18 September 2023

PUBLISHED 12 October 2023

## CITATION

Shankregowda AM, Siriappagoudar P,  
Kuizenga M, Bal TMP, Abdelhafiz Y, Eizaguirre C,  
Fernandes JMO, Kiron V and  
Raeymaekers JAM (2023) Host habitat rather  
than evolutionary history explains gut  
microbiome diversity in sympatric stickleback  
species.  
*Front. Microbiol.* 14:1232358.  
doi: 10.3389/fmicb.2023.1232358

## COPYRIGHT

© 2023 Shankregowda, Siriappagoudar,  
Kuizenga, Bal, Abdelhafiz, Eizaguirre,  
Fernandes, Kiron and Raeymaekers. This is an  
open-access article distributed under the terms  
of the [Creative Commons Attribution License  
\(CC BY\)](https://creativecommons.org/licenses/by/4.0/). The use, distribution or reproduction  
in other forums is permitted, provided the  
original author(s) and the copyright owner(s)  
are credited and that the original publication in  
this journal is cited, in accordance with  
accepted academic practice. No use,  
distribution or reproduction is permitted which  
does not comply with these terms.

# Host habitat rather than evolutionary history explains gut microbiome diversity in sympatric stickleback species

Aruna M. Shankregowda<sup>1\*</sup>, Prabhugouda Siriappagoudar<sup>1</sup>,  
Marijn Kuizenga<sup>1</sup>, Thijs M. P. Bal<sup>1</sup>, Yousri Abdelhafiz<sup>1</sup>,  
Christophe Eizaguirre<sup>2</sup>, Jorge M. O. Fernandes<sup>1</sup>, Viswanath Kiron<sup>1</sup>  
and Joost A. M. Raeymaekers<sup>1</sup>

<sup>1</sup>Faculty of Biosciences and Aquaculture, Nord University, Bodø, Norway, <sup>2</sup>School of Biological and Behavioural Sciences, Queen Mary University of London, London, United Kingdom

Host-associated microbiota can influence host phenotypic variation, fitness and potential to adapt to local environmental conditions. In turn, both host evolutionary history and the abiotic and biotic environment can influence the diversity and composition of microbiota. Yet, to what extent environmental and host-specific factors drive microbial diversity remains largely unknown, limiting our understanding of host-microbiome interactions in natural populations. Here, we compared the intestinal microbiota between two phylogenetically related fishes, the three-spined stickleback (*Gasterosteus aculeatus*) and the nine-spined stickleback (*Pungitius pungitius*) in a common landscape. Using amplicon sequencing of the V3-V4 region of the bacterial 16S rRNA gene, we characterised the  $\alpha$  and  $\beta$  diversity of the microbial communities in these two fish species from both brackish water and freshwater habitats. Across eight locations,  $\alpha$  diversity was higher in the nine-spined stickleback, suggesting a broader niche use in this host species. Habitat was a strong determinant of  $\beta$  diversity in both host species, while host species only explained a small fraction of the variation in gut microbial composition. Strong habitat-specific effects overruled effects of geographic distance and historical freshwater colonisation, suggesting that the gut microbiome correlates primarily with local environmental conditions. Interestingly, the effect of habitat divergence on gut microbial communities was stronger in three-spined stickleback than in nine-spined stickleback, possibly mirroring the stronger level of adaptive divergence in this host species. Overall, our results show that microbial communities reflect host habitat divergence rather than colonisation history or dispersal limitation of host species.

## KEYWORDS

host microbiota, sticklebacks, evolutionary history, host habitat, adaptation, symbiotic microbiota, adaptive divergence

## 1. Introduction

Host-associated microbiota play a key role in the biology, ecology and evolution of their hosts (Alberdi et al., 2016; Henry et al., 2021). In vertebrates, gut microbial symbionts support diverse functions such as host immunity, organ development, digestion, and physiology (Sommer and Bäckhed, 2013). There is growing evidence that symbiont metagenomes help their



hosts to adapt to new environmental conditions and expand their ecological niches, thus contributing to their broad ecological success (Jackson et al., 2022; Cornwallis et al., 2023). Thus, the responses of an organism to its environment are not only based on the interaction between the genotype and the environment (McFall-Ngai et al., 2013), but are also a function of its symbiotic microbiota (Bordenstein and Theis, 2015; Alberdi et al., 2016; Kolodny and Schulenburg, 2020).

In turn, microbiome composition is strongly influenced by both host characteristics as well as the environment (Sullam et al., 2012; Small et al., 2022). For instance, the composition of gut microbial communities may change with the age of the host (Lokesh et al., 2019), and is influenced by abiotic factors such as temperature and pollution (Claus et al., 2016; Sepulveda and Moeller, 2020), and by biotic factors including parasites and diet (Maslowski and Mackay, 2011; Leung et al., 2018; Hahn et al., 2022; Hodžić et al., 2023).

At the population level, both ecological and evolutionary processes such as selection, dispersal, and ecological drift shape the gut microbiome (Kohl, 2020). Previous studies mainly focused on how these various factors affect the microbiome, but did not explicitly investigate the relationship between host and microbiota in natural populations with known evolutionary history, and population characteristics under different environmental conditions. This limits our understanding of the larger evolutionary patterns that occur between hosts and their associated microbiota in natural populations. Furthermore, most studies focus on a single host species, and therefore cannot simultaneously characterise host-specific and environmental effects on microbiota.

Stickleback fishes (Gasterosteidae) are a group of small fishes that are found in both marine and freshwater habitats (Gibson, 2005). The three-spined stickleback (*Gasterosteus aculeatus* Linnaeus, 1758) and the nine-spined stickleback (*Pungitius pungitius* Linnaeus, 1758) are important model organisms for the study of natural selection and adaptive evolution (Gibson, 2005; Raeymaekers et al., 2005; DeFaveri et al., 2012; Feulner et al., 2013; Merilä, 2013; Fang et al., 2021). Both species diverged around 26 million years ago (Varadharajan et al., 2019), but have overlapping habitat requirements (Zander, 1990), diet preferences (Hart, 2003) and parasite communities (Raeymaekers et al., 2008; Thorburn et al., 2022). Studies in three-spined stickleback have identified several environmental and host-specific factors that correlate with the diversity and community structure of the gut microbiota. In a North American three-spined stickleback population, gut microbiota composition was associated with sex, diet, ecotype, and habitat (Bolnick et al., 2014b,c; Smith et al., 2015). In addition, there was a relationship between gut microbiota and the level of polymorphism at the major histocompatibility genes that play a key role at the onset of adaptive immune response (Bolnick et al., 2014a). Furthermore, across three Canadian benthic-limnetic stickleback pairs, microbial communities cluster more by ecotype than by lake, suggesting that host–microbe interactions play a potential role in host adaptation (Rennison et al., 2019). No studies have been performed thus far on the gut microbiome of the nine-spined stickleback.

Three-spined and nine-spined stickleback populations in Belgium and Netherlands co-occur in a wide range of habitats, including estuaries, creeks, rivers, ditches, and ponds (Raeymaekers et al., 2017; Bal et al., 2021; Thorburn et al., 2022). In this part of their distribution range, both species differ markedly in the strength and nature of local adaptation, where brackish water and freshwater populations show stronger morphological and genomic differentiation in the

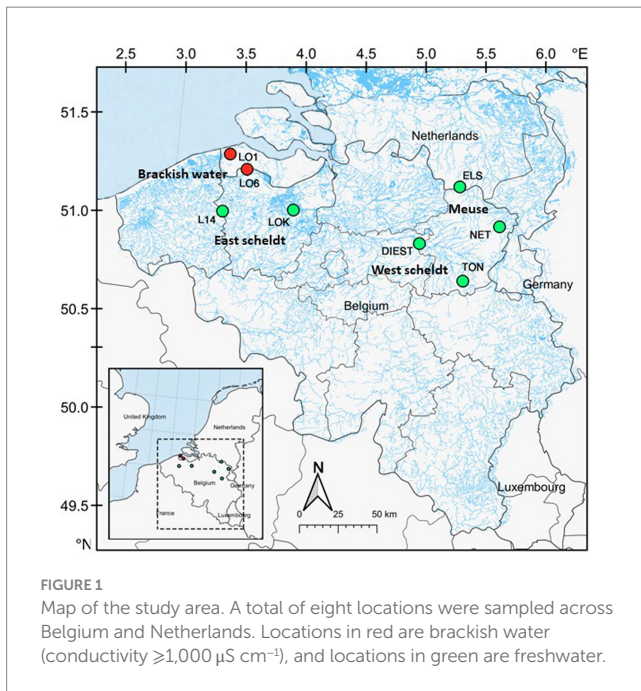
three-spined stickleback than in the nine-spined stickleback (Raeymaekers et al., 2017; Bal et al., 2021). This implies that the three-spined stickleback might be more sensitive to natural selection, and entails the possibility that the nine-spined stickleback relies more on non-genetic mechanisms for coping with varying environmental conditions. For instance, it could be that microbiome-mediated plasticity facilitates the freshwater-brackish water transition in nine-spined stickleback.

In this study, we investigate to what extent the gut microbiome of natural populations reflects these different evolutionary histories and putative underlying adaptive contexts of the two host species. To do so, we compare their microbial communities within and between the two main habitat types where they co-occur. Specifically, the study of the diversity of the gut microbial community (alpha diversity) at locations of sympatric host species, as well as the level of divergence in community composition (beta diversity) between freshwater and brackish water populations, allows us to test to what extent intestinal microbial communities are shaped by host characteristics, environmental factors, and their interaction. We hypothesised that if the composition of the gut microbiome is mostly driven by environmental characteristics, there should be substantial overlap in microbial composition between the two host species. Alternatively, if the composition of the gut microbiome mostly reflects the host's evolutionary history, we expect microbial compositions unique to each host species, with differentiation patterns that mirror population genomic differentiation. We thus characterised the shared and unique microbiota of the two stickleback species, and tested for species-specific and habitat-specific effects on the composition of the microbiota of the two host species.

## 2. Materials and methods

### 2.1. Sample collection

The study system is located in brackish and freshwater habitats of Belgium and Netherlands, including estuaries, creeks, rivers and ditches, where both three-spined stickleback and nine-spined stickleback co-exist. All the samples were collected across eight locations, including two brackish water and six freshwater locations (Figure 1; Supplementary Table S1). The two brackish water locations are located in the Belgian–Dutch coastal lowlands (LO1 and LO6). The freshwater locations were selected from the Meuse basin (ELS and NET), the Eastern Scheldt basin (DIEST and TON), and the Western Scheldt basin (L14 and LOK). Fish from these locations were sampled in the autumn of 2020. From each location, 16 individuals per species (256 individuals in total) were collected using a dip net. Sticklebacks were flash-frozen in dry ice after being killed with a lethal dose of buffered Tricaine methanesulfonate (MS-222, Syndel, United States) with procedural approval from the Ethical Commission Animal Experiments of KU Leuven Belgium. The samples were transferred to Nord University (Bodø, Norway) in dry ice. The fish were thawed on ice, and they were dissected to collect the posterior intestine. In contrast to the anterior intestine, the posterior intestine appears to have a more stable core microbial community during unperturbed conditions. Because of its stability, it is a good option for comparative studies across various populations and environments (Ray and Ringø, 2014). Any visible gut content in the posterior intestine was removed



and then intestine samples were transferred to cryotubes using sterile instruments. The samples were stored at  $-80^{\circ}\text{C}$  until further use.

## 2.2. DNA extraction and sequencing

Genomic DNA was extracted from individual posterior intestinal tissues using DNeasy Blood & Tissue Kit (Qiagen, Hilden, Germany) as per the manufacturer's instructions with slight modifications. The whole posterior intestinal tissue was incubated overnight ( $56^{\circ}\text{C}$ ) to allow the tissue lysis. The tissue lysate was eluted with  $25 \mu\text{L}$  pre-heated ( $50^{\circ}\text{C}$ ) elution buffer for 5 min before centrifugation to enhance the DNA yield. Then, the purity and concentration of extracted DNA was determined using NanoDrop OneC Microvolume UV-Vis Spectrophotometer (Thermo Fisher Scientific – Invitrogen, Waltham, MA, United States) and Qubit® dsDNA HS assay kit (Thermo Fisher Scientific), respectively.

The resulting DNA was amplified using the specific bacterial primers 341F (5'CCTACGGGNGGCWGCAG 3') and 805R (5'GACTACNVGGGTWTCTAATCC 3') flanked by overhang Illumina adapters targeting the hypervariable V3–V4 region (~460 bp). All PCR reactions were performed with  $25 \mu\text{L}$  reaction volume consisting of  $12.5 \mu\text{L}$  AmpliTaq gold 360 Master Mix (Thermo Fisher Scientific),  $1 \mu\text{L}$  ( $10 \mu\text{M}$ ) of each barcoded PCR primer pair and 2–20 ng of DNA template (Siriyyappagoudar et al., 2018). In case of the negative control,  $2 \mu\text{L}$  PCR grade  $\text{H}_2\text{O}$  was used instead of a DNA template. The PCR products were visualised on 1.5% (w/v) agarose gel, and positive bands (~550 bp) were excised from the gel and purified using the QIAquick Gel Extraction Kit (Qiagen) according to the manufacturer's instructions.

The first PCR product was used as template for a second PCR (8 cycles, 16S Metagenomic Sequencing Library Preparation, Illumina). This step was done to add dual indices and Illumina sequencing adapters (Nextera XT Index Primers, Illumina, San Diego, California, United States). Amplified PCR products were purified using Mag-Bind TotalPure NGS (Omega Bio-tek, United States) to

obtain the amplicon libraries (Sample/Beads ratio – 1/1.12). In the last step, all amplicon libraries were pooled in equimolar concentrations. Fragment size distribution, quality and quantity of pooled library were assessed using the TapeStation 2200 (Agilent Technologies, Santa Clara, CA, United States). Furthermore, the pooled libraries were quantified using the KAPA Library quantification kit (Roche, Basel, Switzerland) and the Qubit® dsDNA HS assay kit (Thermo Fisher Scientific). Finally, 300 bp paired-end sequencing was performed at the Norwegian Sequencing Centre on an Illumina MiSeq platform using the MiSeq® reagent kit (Illumina).

## 2.3. Bioinformatic analyses

The sequenced paired-end reads were processed with the Quantitative Insights Into Microbial Ecology 2 (QIIME 2–2022.8) tool (Bolyen et al., 2018, 2019). Paired-end sequences were imported, quality controlled and merged (see Supplementary Table S1) using the DADA2 algorithm in QIIME 2 ( $-p\text{-trim-left-f } 13 -p\text{-trim-left-r } 13 -p\text{-trunc-len-f } 240 -p\text{-trunc-len-r } 240$ ) (Callahan et al., 2016). The SILVA database (version 138) (Quast et al., 2012) trained with a naive Bayes machine-learning classifier (Robeson et al., 2021) was used to assign the taxonomy in QIIME 2. The generated Amplicon Sequence Variants (ASVs) table, taxonomy table, and phylogenetic tree were imported and merged into a phyloseq dataset object in R using qiime2R scripts (Bisanz, 2018) for further analysis. The resulting ASVs were subsequently filtered by removing singletons, unassigned ASVs, and ASVs assigned to Archaea, Euryarchaeota, or chloroplast DNA. Subsequently, only samples containing at least 5 distinct ASVs per sample were retained for further analyses.

## 2.4. Data analyses

All statistical analyses were carried out in the R v4.2.1 language in the Rstudio environment v2022.12.0 + 353 (R Core Team, 2021; RStudio Team, 2021). The data analysis was performed using the functions from the packages phyloseq (McMurdie and Holmes, 2013) and vegan (Oksanen et al., 2013). Data visualisation was done using ggplot2 (Wickham, 2016) and microViz (Barnett et al., 2021). In order to take into account the read variation across samples and prepare the data for further analysis, reads were rarefied to 9,000 reads per sample, except for the analysis of differential abundance of ASVs.

Our analyses aimed at (1) identifying the shared and unique microbial communities of the two species at the eight locations, and (2) testing for species-specific and habitat-specific effects on the composition of the microbiota in each host species. To do so, we first examined the overall taxon diversity, and then compared alpha and beta diversity across host species, habitats and locations.

### 2.4.1. Taxon composition

For an initial understanding of the composition of the microbial communities, a Venn diagram was constructed to visualise the percentage of shared and unique ASVs across host species and habitats. To identify key differences between host species and locations, we determined the top five phyla in the entire dataset, and assessed which of the commonly reported genera in other fish microbiome studies were present. For both the top phyla and these selected genera, two-way ANOVA was used to test for differences in

abundance between host species and locations. In addition, the *microbiome* package in R was used to calculate the core microbiota of each host species across eight locations. Here, core microbiota were defined as genera with a prevalence of at least 80%, and a detection level (relative abundance) of 0.10. Core genera were identified after comparing the core microbiota of each host species separately, across eight locations. Finally, to describe the difference in microbiome composition between species in each habitat, ASVs were pooled by freshwater and brackish water locations, for each host species separately. A Wald test implemented in the *DESeq2* package (Love et al., 2014) was then used to determine differential abundance based on non-rarified abundance data.

## 2.4.2. Alpha diversity

Differences in alpha diversity of gut microbial communities between host species and sampling locations were calculated using three ecological diversity measures: Simpson diversity (dominant species), Chao1 diversity (species richness) and Shannon diversity (evenness of the community). Two-way ANOVA was used to test for the effect of species, location and the species  $\times$  location interaction term on infracommunity alpha diversity. Finally, Pearson correlations were calculated to assess the association of alpha diversity with salinity and distance to the coast (km), and to test if alpha diversity in three-spined stickleback is correlated with alpha diversity in nine-spined stickleback.

## 2.4.3. Beta diversity

$\beta$ -diversity was estimated using weighted and unweighted UniFrac (phylogenetic) dissimilarity matrices (Lozupone and Knight, 2005; Lozupone et al., 2011). The use of unweighted UniFrac matrices increases the effect of rare ASVs by considering their presence or absence, while weighted UniFrac matrices take into consideration the abundance of the ASVs and, thus, can be strongly impacted by highly abundant ASVs, particularly if the bacterial phylogeny is separated by long branches (Lozupone and Knight, 2005; Lozupone et al., 2011). For comparison, we also added Bray–Curtis dissimilarity (non-phylogenetic) matrices. The differences between the bacterial communities in host species and populations were further visualised and compared with non-metric multidimensional scaling (NMDS) analysis. Using the same dissimilarity matrices, we then performed permutational multivariate ANOVAs using the *adonis2* function in *vegan* R package to quantify the effects of species, location, and the species  $\times$  location interaction term on the gut microbiota composition. Permutational multivariate ANOVAs were also conducted on each host species separately, this time to assess the effects of habitat and location (nested in habitat).

Furthermore, we tested for different spatial scenarios of microbiome differentiation, measured as Bray–Curtis distances (beta diversity). In scenario 1, we assessed whether more distant host populations harbour more dissimilar microbiome communities. This scenario was tested by correlating gut microbiome differentiation (Bray–Curtis dissimilarity matrix) with Euclidean distances among sampling locations. In scenario 2, we assessed whether host populations from different habitats (freshwater or brackish water) harbour more dissimilar microbiome communities. This scenario was tested by correlating gut microbiome differentiation with a theoretical matrix assigning value 0 to habitat similarity and value 1 to habitat dissimilarity. In scenario 3, we tested whether host populations with a different freshwater colonisation history harbour more dissimilar microbiome communities, assuming

that brackish water populations are ancestral and freshwater populations are derived [see raceme scenario in Raeymaekers et al. (2005)]. This scenario was tested by correlating gut microbiome differentiation with another theoretical matrix, assigning values 0 to brackish water population pairs (no freshwater colonisation history), values 0 to freshwater population pairs from the same watershed (same colonisation history), values 1 to brackish water–freshwater pairs (direct ancestry), and values 2 to freshwater populations from different watersheds (independent colonisation). The three scenarios were tested using Mantel tests. In addition, partial Mantel tests were used to test scenario 2 and 3 after accounting for scenario 1, i.e., the correlations between microbiome differentiation and the theoretical matrices of scenario 2 or scenario 3 were corrected for Euclidean distance.

# 3. Results

## 3.1. Taxon composition

A total of 5,987,681 high-quality reads were obtained from 253 samples with an average of 23,666 reads per sample (see [Supplementary Table S1](#) and [Supplementary methods](#)).

We observed a mix of shared and unique ASVs across host species and habitats. Nine-spined stickleback populations harboured 6,149 and 2,558 ASVs unique to freshwater and brackish water habitats, respectively ([Figure 2](#)). Three-spined stickleback populations harboured 5,214 and 1,092 ASVs unique to each habitat. Interestingly, the nine-spined stickleback shared more ASVs (5.9%) among both habitats than the three-spined stickleback (3.4%) ([Figure 2](#)). We found that populations of the two host species at the same locations share 7% to 21% ASVs ([Supplementary Figure S1](#)). The proportion of shared ranged from 11 to 19% in freshwater populations, and was both highest (LO1–21%) and lowest (LO6–7%) in brackish water populations ([Supplementary Figure S1](#)).

A total of 46 phyla were detected in both species, out of which 38 phyla were shared between two species. Eight phyla were unique to nine-spined stickleback, and two were unique to three-spined stickleback. We then identified the 15 most dominant microbial phyla and the 23 most dominant genera across host species and locations based on relative abundances ([Figures 3, 4](#)). Five phyla accounted for 80 to 90% of the community composition, irrespective of their host species. The most abundant phyla in the gut microbiota across the two host species and all locations were Proteobacteria, Actinobacteriota, Planctomycetota, Firmicutes, Chloroflexi and Verrucomicrobiota ([Figure 3](#)). The most abundant genera were *Rickettsiella*, *Aurantimicrobium*, *Candidatus bacilloplasma* and *PeM15* ([Figure 4](#)). Proteobacteria was the most abundant phylum in both brackish water and freshwater populations ([Figure 3](#)). The gut microbiota was highly location-specific, and was dominated by the *Rickettsiella* genus in both species.

Two-way ANOVA revealed variable effects of host species and location on the most abundant phyla and genera ([Supplementary Tables S2, S3](#)). For six out of ten taxa (five phyla and five genera), there was a significant location  $\times$  host species interaction effect, with higher abundances for some locations in the three-spined stickleback, and higher abundances for other locations in the nine-spined stickleback ([Supplementary Tables S2, S3](#)). For the remaining taxa, there was a main effect of location, but there was no systematic difference in abundance between the host species.



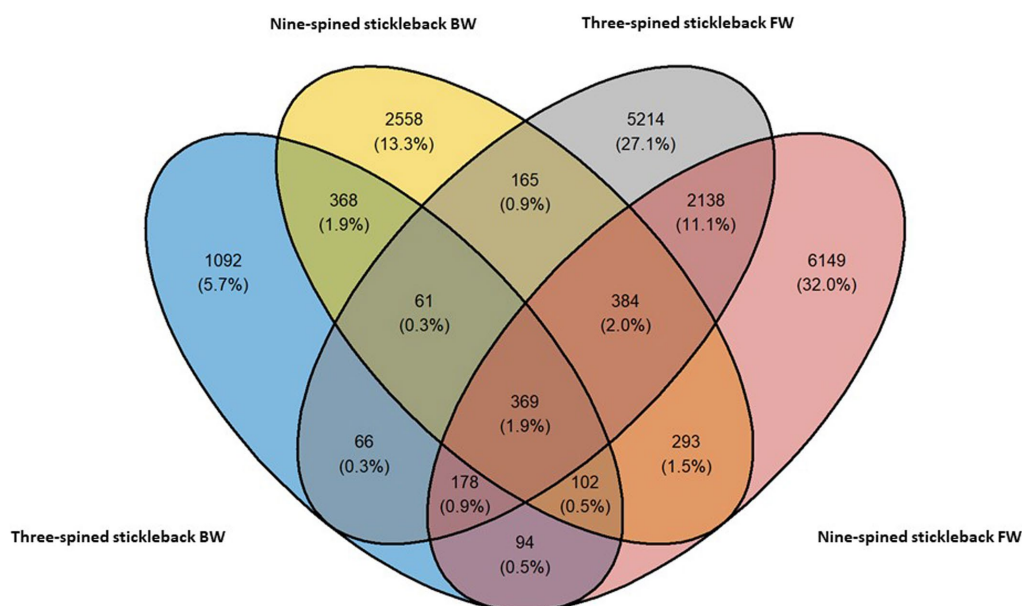


FIGURE 2  
Shared and distinct ASVs of the three-spined and nine-spined stickleback populations from freshwater (FW) and brackish water (BW) habitat.

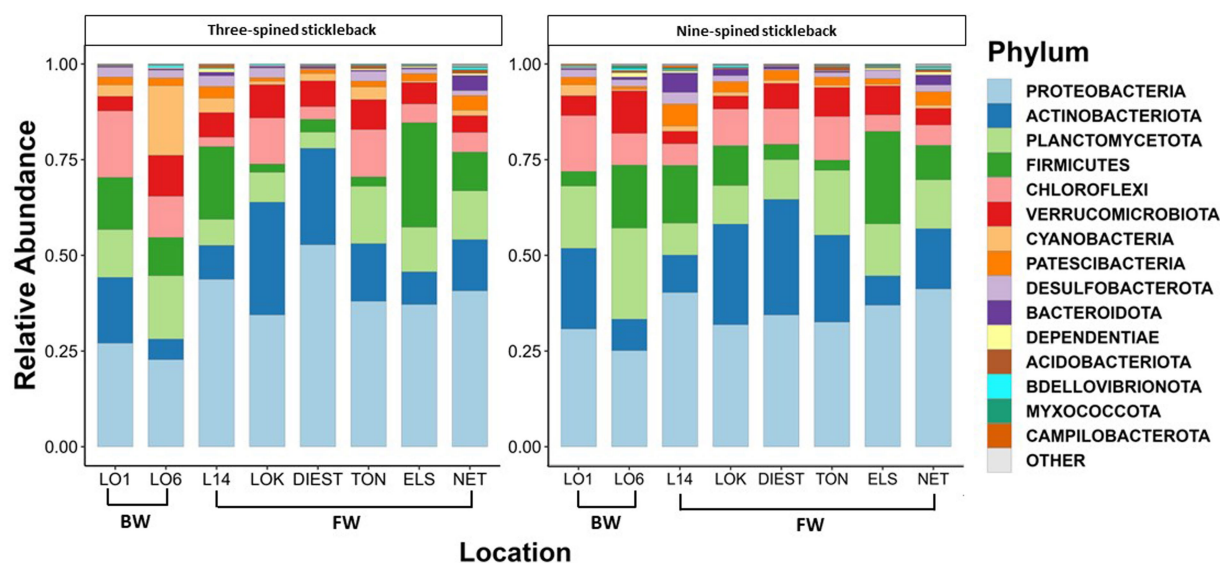


FIGURE 3  
Relative abundance of the 15 most represented bacterial phyla in three-spined and nine-spined stickleback populations from brackish water (BW) and freshwater (FW) habitat.

### 3.2. Alpha diversity

Overall, alpha diversity varied between host species and locations, and was on average higher in nine-spined stickleback (Table 1; Figure 5). There were significant differences in both Shannon and Simpson diversity between locations (Shannon diversity:  $F_{7,198} = 4.35$ ,  $p$ -value = 0.0001; Simpson diversity:  $F_{7,198} = 3.56$ ,  $p$ -value = 0.001, Table 1) and host species (Shannon diversity:  $F_{1,198} = 5.79$ ,  $p$ -value = 0.016; Simpson diversity:  $F_{1,198} = 5.94$ ,  $p$ -value = 0.015, Table 1). In case of Chao1 diversity, we observed significant differences among locations

( $F_{7,198} = 2.77$ ,  $p$ -value = 0.008), and a significant location  $\times$  host species interaction effect ( $F_{7,198} = 4.44$ ,  $p$ -value = 0.0001, Table 1). Interestingly, while there were no significant correlations between alpha diversity and salinity or distance to coast in either host species, Simpson diversity in nine-spined stickleback was positively correlated with Simpson diversity in three-spined stickleback (Pearson correlation:  $r = 0.74$ ,  $p$ -value = 0.03).

In brackish water, the abundance of 19 bacterial ASVs from six phyla differed significantly between three-spined and nine-spined stickleback (Figure 6). Thirteen of those ASVs belonged to phyla Proteobacteria (*Legionella* and *Amaricoccus*), Actinobacteriota



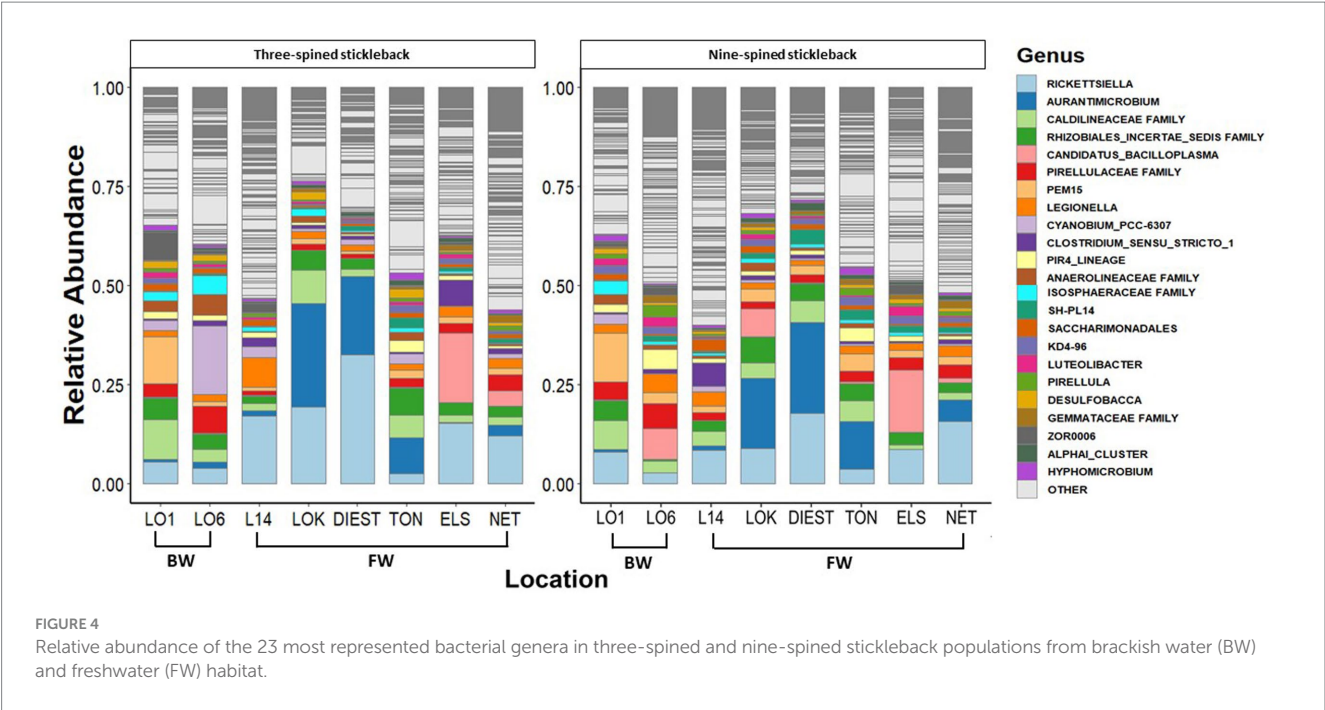
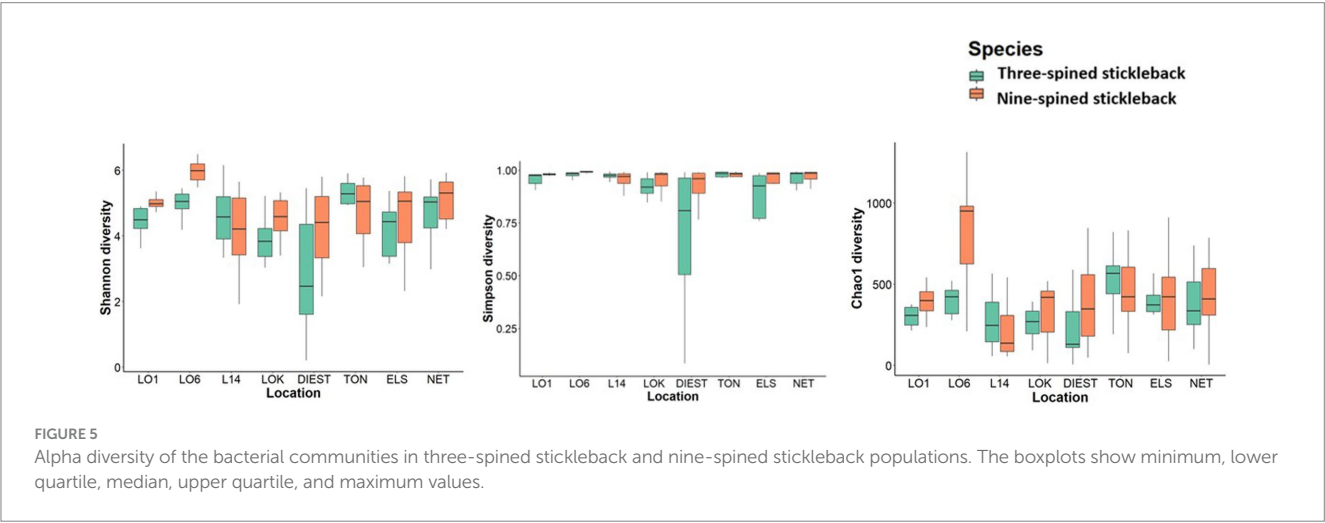


TABLE 1 Two-way ANOVA for the effect of location, host-species and the interaction between location, and host-species on alpha-diversity.

	Shannon diversity				Simpson diversity				Chao1 diversity			
	Df	Sum Sq	F	p-value	Df	Sum Sq	F	p-value	Df	Sum Sq	F	p-value
Location	7	44.48	4.35	<b>0.0001</b>	7	0.79	3.56	<b>0.001</b>	7	776,505	2.77	<b>0.008</b>
Host species	1	8.46	5.79	<b>0.016</b>	1	0.18	5.94	<b>0.015</b>	1	154,443	3.86	0.0505
Location: host species	7	12.28	1.20	0.30	7	0.22	0.99	0.43	7	1,240,889	4.44	<b>0.0001</b>
Residuals	198	288.9			198	6.28			198	7,904,347		

Df denotes degrees of freedom, F denotes F statistic, and Sum Sq denotes the variation attributed to the error. Significant results are shown in bold.



(IMCC26256), Firmicutes (*Candidatus\_Bacilloplasma* and *Paludicola*), and Chloroflexi (*A4b* and *KD4-96*), and were more abundant in nine-spined stickleback (Figure 6). The other 6 ASVs were more abundant in three-spined stickleback, and belonged to the phyla Actinobacteriota (*Aurantimicrobium* and *Kocuria*), Firmicutes (*Clostridium\_sensu\_stricto\_1* and *Gottschalkia*) and Cyanobacteria (*Cyanobium\_PCC-6307*). In contrast, within the freshwater habitat, there were no differences in abundance between the two host species for any ASVs.

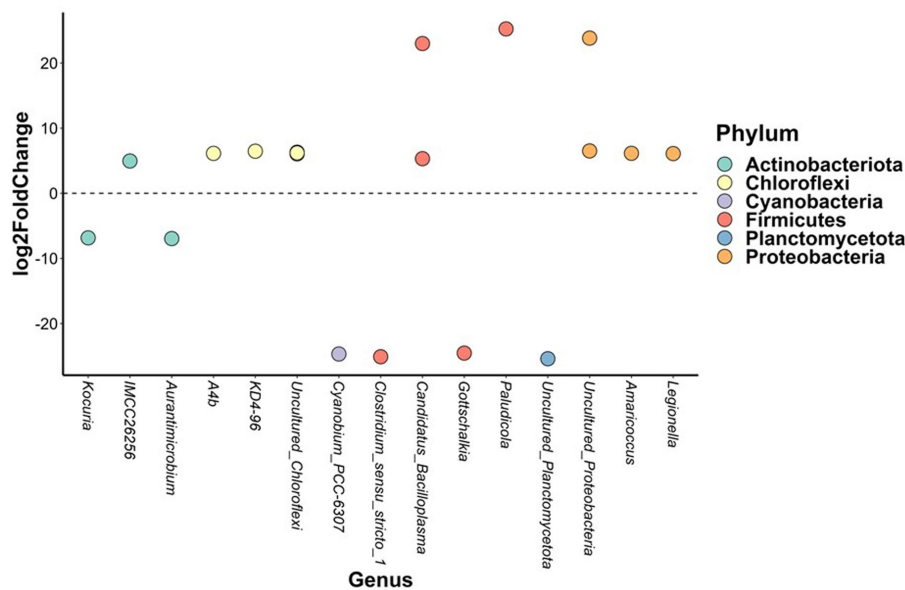


FIGURE 6

Differentially abundant amplicon sequence variants between brackish water populations from the three-spined stickleback and brackish water populations from the nine-spined stickleback. The X-axis labels are genus-level annotations of the microbes identified in the nine-spined stickleback.

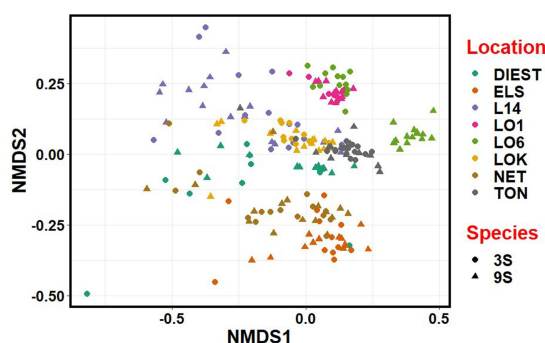


FIGURE 7

Non-metric multidimensional scaling (NMDS) plot based on Bray-Curtis distances between the microbiota communities from three-spined (3S) and nine-spined (9S) stickleback populations. Individual sticklebacks are labelled by location and species.

### 3.3. Beta diversity

NMDS revealed that the microbial communities clustered more by location, river basin and habitat than by species (Figure 7). Accordingly, there was considerable overlap between the two host species from each location, except for one brackish water population (LO6) of the nine-spined stickleback where the microbial community was clearly distinct from other brackish water populations (Figure 7).

PERMANOVA revealed that location explained most of the variation in microbial communities (weighted UniFrac;  $R^2 = 0.22$ , unweighted UniFrac;  $R^2 = 0.156$ , Bray-Curtis;  $R^2 = 0.22$ ,  $p$ -value  $\leq 0.0001$ ), followed by species (weighted UniFrac;  $R^2 = 0.015$ , unweighted UniFrac;  $R^2 = 0.009$ , Bray-Curtis;  $R^2 = 0.009$ ,  $p$ -value  $\leq 0.0001$ ) and the species  $\times$  location interaction term (weighted UniFrac;  $R^2 = 0.057$ ,

unweighted UniFrac;  $R^2 = 0.046$ , Bray-Curtis;  $R^2 = 0.051$ ,  $p$ -value  $\leq 0.0001$ ) (Table 2; Supplementary Figure S2). PERMANOVA in each species separately indicated that habitat and location explained more variation in gut microbial composition in three-spined stickleback than in nine-spined stickleback for weighted UniFrac and Bray-Curtis dissimilarity matrices, but we observed no such difference for unweighted UniFrac matrices (Table 2; Supplementary Figure S2).

Mantel tests revealed a positive relationship between microbial Bray-Curtis dissimilarities and habitat dissimilarities in both species, and this effect was strongest in three-spined stickleback (scenario 2, three-spined stickleback:  $r = 0.65$ ,  $p$ -value = 0.03; nine-spined stickleback:  $r = 0.54$ ,  $p$ -value = 0.02, Table 3; Figure 8). These results remained significant after accounting for Euclidean distance (three-spined stickleback:  $r = 0.67$ ,  $p$ -value = 0.01; nine-spined stickleback:  $r = 0.50$ ,  $p$ -value = 0.03, Table 3). In contrast, there was no significant relationship between Euclidean distance and microbial Bray-Curtis dissimilarities (scenario 1, three-spined stickleback:  $r = 0.08$ ,  $p$ -value = 0.26; nine-spined stickleback:  $r = 0.13$ ,  $p$ -value = 0.19, Table 3; Supplementary Figure S3) or between colonisation history and microbial Bray-Curtis dissimilarities (scenario 3, three-spined stickleback:  $r = -0.29$ ,  $p$ -value = 0.95; nine-spined stickleback:  $r = -0.22$ ,  $p$ -value = 0.88, Table 3; Supplementary Figure S4).

## 4. Discussion

Here, we characterised the gut microbiota of two co-existing and phylogenetically related stickleback species using bacterial 16S rRNA (V3-V4) gene sequencing. To understand how host habitat and host factors shape the sticklebacks' microbiota, we investigated the diversity of the gut microbiota in the two species across populations from freshwater and brackish water habitats. First, microbial communities were clustered by location and habitat, rather than by species, and

TABLE 2 PERMANOVA on distances (Weighted UniFrac, Unweighted UniFrac and Bray-Curtis) between microbial communities of individual three-spined and nine-spined sticklebacks from eight locations.

	Weighted UniFrac				Unweighted UniFrac				Bray-Curtis			
	Df	F	R <sup>2</sup>	p-value	Df	F	R <sup>2</sup>	p-value	Df	F	R <sup>2</sup>	p-value
Location	7	9.08	0.225	<b>0.0001</b>	7	5.62	0.156	<b>0.0001</b>	7	8.75	0.22	<b>&lt;0.0001</b>
Host species	1	4.36	0.015	<b>0.0001</b>	1	2.41	0.009	<b>0.0002</b>	1	2.63	0.009	<b>&lt;0.0001</b>
Location: Host species	7	2.32	0.057	<b>0.0001</b>	7	1.66	0.046	<b>0.0001</b>	7	2.05	0.051	<b>&lt;0.0001</b>
Residuals	198				198				198			
<b>Three-spined stickleback</b>												
Habitat	1	12.02	0.089	<b>0.0001</b>	1	4.18	0.035	<b>0.0001</b>	1	9.56	0.074	<b>&lt;0.0001</b>
Location	6	5.06	0.226	<b>0.0001</b>	6	3.37	0.173	<b>0.0001</b>	6	4.60	0.21	<b>&lt;0.0001</b>
Residuals	92				92				92			
<b>Nine-spined stickleback</b>												
Habitat	1	9.66	0.067	<b>0.0001</b>	1	5.83	0.043	<b>0.0001</b>	1	8.98	0.062	<b>&lt;0.0001</b>
Location	6	4.63	0.193	<b>0.0001</b>	6	3.55	0.160	<b>0.0001</b>	6	4.91	0.20	<b>&lt;0.0001</b>
Residuals	106				106				106			

Df denotes degrees of freedom and F denotes F statistic. Significant results are shown in bold.

TABLE 3 Mantel tests statistics for both host species.

Test	Matrices	Three-spined stickleback	Nine-spined stickleback
Simple Mantel test	X = Habitat; Y = Beta diversity	$R = 0.65$ ; $p$ -value = <b>0.03</b>	$R = 0.54$ ; $p$ -value = <b>0.02</b>
	X = Geographic distance; Y = Beta diversity	$R = 0.08$ ; $p$ -value = 0.26	$R = 0.13$ ; $p$ -value = 0.19
	X = Colonisation history; Y = Beta diversity	$R = -0.29$ ; $p$ -value = 0.95	$R = -0.22$ ; $p$ -value = 0.88
Partial Mantel test	X = Habitat; Y = Beta diversity; Z = Geographic distance	$R = 0.67$ ; $p$ -value = <b>0.01</b>	$R = 0.50$ ; $p$ -value = <b>0.03</b>
	X = Colonisation history; Y = Beta diversity; Z = Geographic distance	$R = -0.36$ ; $p$ -value = 0.96	$R = -0.35$ ; $p$ -value = 0.92
	X = Geographic distance; Y = Beta diversity; Z = Habitat	$R = -0.11$ ; $p$ -value = 0.71	$R = 0.005$ ; $p$ -value = 0.44
	X = Geographic distance; Y = Beta diversity; Z = Colonisation history	$R = 0.19$ ; $p$ -value = 0.12	$R = 0.23$ ; $p$ -value = 0.09

R denotes the Mantel test statistic. Beta diversity denotes Bray-Curtis distance based matrix generated from the ASV table. Significant results are shown in bold.

there was a substantial similarity between the microbial communities of the two host species from the same locations. Second,  $\alpha$  diversity was on average higher in nine-spined stickleback, while habitat was a stronger determinant of  $\beta$  diversity in three-spined stickleback.

#### 4.1. Microbial diversity shared between host species

The most dominant phyla found in our study populations included Proteobacteria, Actinobacteriota, Firmicutes, Planctomycetota, Chloroflexi and Cyanobacteria. Overall, the similarity between the three-spined and nine-spined stickleback gut microbiota at phylum level was strong. This comes as no surprise, since numerous studies, both on wild as well as lab-reared populations, detected the same dominant phyla in different fish species (Baldo et al., 2015; Estruch et al., 2015; Fietz et al., 2018; Kim et al., 2021; Abdelhafiz et al., 2022; Xu et al., 2022). The single phylum that dominates the gut microbiota of most fishes is the Proteobacteria (Roesslers et al., 2011; Sullam et al., 2015). The presence

of dominant phyla is thus conserved across many fish species, but their abundance is affected by different environmental and host-related factors (Kim et al., 2021). The bacterial phyla observed in stickleback guts are phyla that help in homeostasis and nutrient uptake. This includes Proteobacteria, which aid in digestion of complex sugars (Colston and Jackson, 2016) and Actinobacteriota, which help inhibit pathogens and lactic acid fermentation (Colston and Jackson, 2016). Both stickleback species also hosted Cyanobacteria in every single location. The presence of Cyanobacteria suggests that they are important food sources (Xu et al., 2022). Similar observations were made in Asian silver carp (*Hypophthalmichthys molitrix*) and gizzard shad (*Dorosoma cepedianum*) by Ye et al. (2014), who attribute the presence of Cyanobacteria to their role as the fish's primary food source.

At the genus level, *Rickettsiella*, *Clostridium sensu stricto* 1, *Aurantimicrobium*, *Candidatus bacilloplasm* and *PeM15* dominated the microbiome of both stickleback species. The genus *Clostridium* is widely distributed in the animal intestinal community, and many *Clostridium* species may function as mutualistic symbionts with their hosts (Lopetuso et al., 2013). *Clostridium sensu stricto* 1 is found in

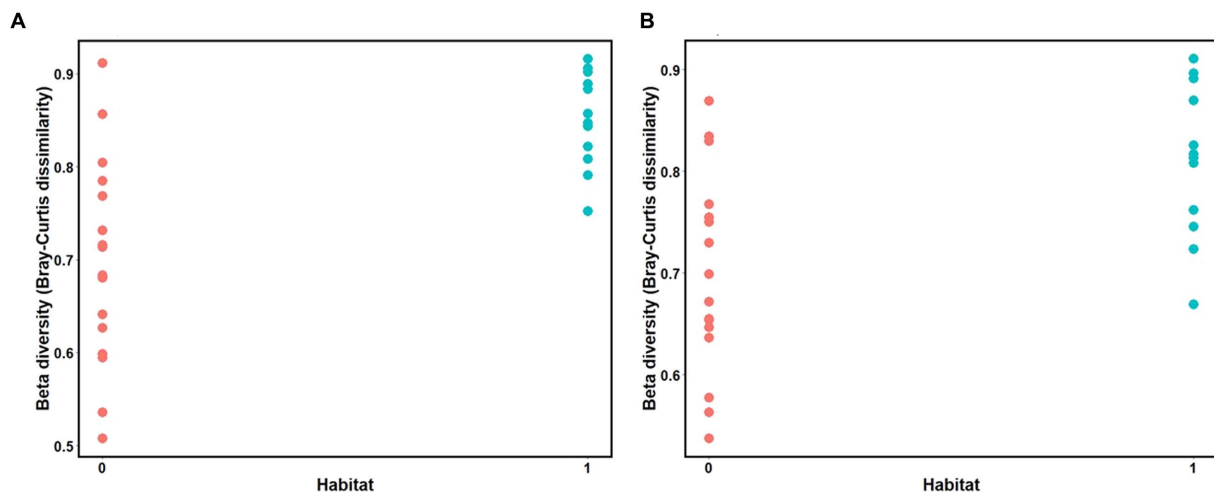


FIGURE 8

Mantel test for isolation by distance between the matrix of habitat dissimilarities and Bray Curtis dissimilarities. (A) Three-spined stickleback ( $R = 0.65$ ,  $p$ -value = 0.03). (B) Nine-spined stickleback ( $R = 0.54$ ,  $p$ -value = 0.02). Value 0 indicates habitat similarity and value 1 indicates habitat dissimilarity.

both species and has the ability to digest proteins. Thus, certain bacteria that produce proteases (like *C. sensu stricto 1*) may aid three-spined and nine-spined sticklebacks in using nutrients and obtaining energy from diets high in protein (e.g., aquatic insects and zooplankton) (Schwab et al., 2011). In the three-spined stickleback, a positive relationship has been reported between the abundance of *Clostridiaceae* taxa and the expression of immune genes (Fuess et al., 2021).

Few studies have tested or reported how much overlap there is between populations of coexisting species at the same locations. We found that 7% to 21% ASVs were shared between the populations of the two host species at the same locations. Likewise, in lake whitefish (*Coregonus clupeaformis*), between 22% and 65% (mean ~44%) of genera were shared between sympatric species within lakes (Sevellec et al., 2018). However, this study only considered the core ASVs to calculate the shared fraction of the microbiome, while here the total number of ASVs were taken into account. Other studies have reported the overlap among ecotypes within species (Sullam et al., 2015) or between conspecifics from multiple locations (Baldo et al., 2019).

## 4.2. Microbial diversity unique to each host species

Despite the strong similarities between three-spined and nine-spined stickleback populations from the same locations, alpha diversity was overall higher in nine-spined stickleback (Figure 5). This was also confirmed by the higher number of ASVs in the nine-spined stickleback (Figure 2). Higher microbial diversity suggests broader niche use in the nine-spined stickleback, which is consistent with the observation that nine-spined stickleback occupies a slightly higher trophic position (Thorburn et al., 2022). A comparable study by Fietz et al. (2018) observed a similar alpha diversity pattern in sand lance fishes (*Ammodytes tobianus* and *Hyperoplus lanceolatus*) from the Baltic Sea, with higher alpha diversity in *A. tobianus*. In case of sympatric salmonids, the pattern of microbial diversity was similar in brackish water and freshwater habitats, with lake whitefish (*Coregonus clupeaformis*) showing higher alpha diversity than Arctic char (*Salvelinus alpinus*) (Element et al., 2020). The authors reported that it is possible that the diet

of lake whitefish is more diverse than that of Arctic char, which in turn may influence microbial richness and diversity (Element et al., 2020). Interestingly, within a population of three-spined stickleback and Eurasian perch (*Perca fluviatilis*), an opposite pattern was observed at the individual level, as individuals with a high diet diversity had low microbial diversity and vice versa (Bolnick et al., 2014b). This result was confirmed with experimental diet manipulations in the three-spined stickleback, where a much lower variation in intestinal microbiota was observed in a mixed diet treatment than in a simple diet treatment (Bolnick et al., 2014b). Finally, Xu et al. (2022) reported highest alpha diversity in a herbivore fish, followed by a carnivore, and then an omnivore fish. Microbial alpha diversity is probably connected with diet (Bolnick et al., 2014b,c; Baldo et al., 2015; Element et al., 2020; Xu et al., 2022). Stomach content analyses may help us to better understand how local environmental conditions affect alpha diversity of the gut microbiome.

In both stickleback species, the alpha diversity of the gut microbial communities varied substantially between populations. Across all locations, Simpson diversity in nine-spined stickleback correlated with Simpson diversity in three-spined stickleback. However, alpha diversity did not correlate with salinity or distance to the coast in either species. Few studies have investigated the determinants of fish gut microbiota alpha diversity across populations and species, which includes habitat, pollution, and diet (Bolnick et al., 2014b; Solovyev et al., 2019; Degregori et al., 2021; Kim et al., 2021). For instance, the gut microbiota of Atlantic salmon (*Salmo salar*) kept in sea cages was more diverse than the gut microbiota of salmon in freshwater (Wang et al., 2021; Morales-Rivera et al., 2022). In two sand lance species of the Baltic Sea, it has been observed that brackish populations for *A. tobianus* had higher Shannon and Chao1 indices than marine populations, but no such difference was observed in *H. lanceolatus* (Fietz et al., 2018). In an experimental setting, Fuess et al. (2021) showed a positive association between microbial alpha diversity and the expression of host immune genes in the three-spined stickleback. Yet, it remains unclear to what extent immunological or any other biological responses affect alpha diversity in natural populations and how this might differ between species.

We observed a strong habitat effect on beta diversity in the two species, since the composition of the microbiome of freshwater



populations differed consistently from the composition of the microbiome in brackish water populations. Mantel tests indicated that habitat divergence rather than colonisation history correlated with beta diversity, and this effect remained significant even after correction for geographic distance. A meta-analysis across fish species and populations confirmed that freshwater and marine fish often differ in their gut microbiota communities (Sullam et al., 2012; Kim et al., 2021). The composition of microbiota communities are often shaped by environmental factors, and are also to some extent reflective of their environmental microbial communities (Smith et al., 2015; Dulski et al., 2020). In our study, the fact that the microbial communities of the two host species at a given location are rather similar underlines the importance of the environment in shaping the fish gut microbiota.

Our analysis of beta diversity based on both weighted UniFrac and Bray-Curtis matrices revealed that habitat and location explained a somewhat larger proportion of variation in gut microbiota communities in three-spined stickleback than in nine-spined stickleback. This result was also confirmed with partial Mantel tests with a stronger correlation between Bray-Curtis matrices and habitat dissimilarities. One potential explanation for this stronger effect of habitat divergence is the level of adaptive divergence among host populations. Adaptive divergence among populations and ecotypes of three-spined stickleback is common (McKinnon and Rundle, 2002; Raeymaekers et al., 2007; Hendry et al., 2009; Feulner et al., 2013; Guo et al., 2015), and in our study area, the level of adaptive divergence is markedly stronger in three-spined stickleback than in nine-spined stickleback (Raeymaekers et al., 2017; Bal et al., 2021). So, it could be that the populations of three-spined stickleback in our study area have experienced stronger selection pressures than the populations of nine-spined stickleback, and that this selection history has also led to stronger divergence at the microbiome level. Yet, the weaker effect of habitat divergence in nine-spined stickleback than in three-spined stickleback is not in line with our expectation that microbiome-mediated plasticity could facilitate the freshwater-brackish water transition in this species. Further studies are needed to better understand to what extent the microbiome can play a role in habitat transition.

## 5. Conclusion

Local environmental conditions were a major determinant of the composition of the microbial communities in both host species. Since we did not detect any effect of historical colonisation, we conclude that habitat use is the strongest determinant of microbial diversity. The effect of the local environment was especially pronounced in the three-spined stickleback, which might mirror its stronger propensity for local adaptation. These findings contribute to our understanding of the determinants of host-associated microbial diversity in nature, which will help us to further understand the larger evolutionary patterns that occur between hosts and their associated microbiota.

## Data availability statement

The data presented in the study are deposited in the Sequence Read Archive (SRA) repository, accession number PRJNA942318.

## Ethics statement

The animal study was approved by Ethical Commission Animal Experiments of KU Leuven Belgium. The study was conducted in accordance with the local legislation and institutional requirements.

## Author contributions

AS, JR, JE, and VK: conceptualization. JR: funding acquisition and supervision. AS, TB, and JR: fieldwork. JR and VK: chemicals and resources. AS, MK, and PS: molecular work. AS, CE, and JR: formal analysis. AS and JR: project administration and writing-original draft. AS, CE, JE, VK, TB, MK, PS, YA, and JR: review & editing. All authors contributed to the article and approved the submitted version.

## Acknowledgments

We thank Filip Volckaert and his team at the Laboratory of Biodiversity and Evolutionary Genomics (KU Leuven, Belgium) for field support, Benedikt Berger, Niklas H. Kohl and Ionatan Malmsten for help with the stickleback dissections, and Adrienne Kerley, Sudeep D. Ghatge and Kanchana Bandara for sharing their experience with DNA extraction, data analyses and figures. The sequencing service was provided by the Norwegian Sequencing Centre, a national technology platform hosted by the University of Oslo and supported by the “Functional Genomics” and “Infrastructure” programs of the Research Council of Norway and the Southeastern Regional Health Authorities.

## Conflict of interest

The authors declare that the research was conducted in the absence of any commercial or financial relationships that could be construed as a potential conflict of interest.

## Publisher's note

All claims expressed in this article are solely those of the authors and do not necessarily represent those of their affiliated organizations, or those of the publisher, the editors and the reviewers. Any product that may be evaluated in this article, or claim that may be made by its manufacturer, is not guaranteed or endorsed by the publisher.

## Supplementary material

The Supplementary material for this article can be found online at: <https://www.frontiersin.org/articles/10.3389/fmicb.2023.1232358/full#supplementary-material>

## References

- Abdelhafiz, Y., Fernandes, J. M., Donati, C., Pindo, M., and Kiron, V. (2022). Intergenerational transfer of persistent bacterial communities in female Nile Tilapia. *Front. Microbiol.* 13:879990. doi: 10.3389/fmicb.2022.879990
- Alberdi, A., Aizpurua, O., Bohmann, K., Zepeda-Mendoza, M. L., and Gilbert, M. T. P. (2016). Do vertebrate gut metagenomes confer rapid ecological adaptation? *Trends Ecol. Evol.* 31, 689–699. doi: 10.1016/j.tree.2016.06.008
- Bal, T. M., Llanos-Garrido, A., Chaturvedi, A., Verdonck, I., Hellema, B., and Raeymaekers, J. A. (2021). Adaptive divergence under gene flow along an environmental gradient in two coexisting stickleback species. *Genes* 12:435. doi: 10.3390/genes12030435
- Baldo, L., Riera, J. L., Salzburger, W., and Barluenga, M. (2019). Phylogeography and ecological niche shape the cichlid fish gut microbiota in central American and African lakes. *Front. Microbiol.* 10:2372. doi: 10.3389/fmicb.2019.02372
- Baldo, L., Riera, J. L., Tooming-Klunderud, A., Albà, M. M., and Salzburger, W. (2015). Gut microbiota dynamics during dietary shift in eastern African cichlid fishes. *PLoS One* 10:e0127462. doi: 10.1371/journal.pone.0127462
- Barnett, D. J., Arts, I. C., and Penders, J. (2021). microViz: an R package for microbiome data visualization and statistics. *J. Open Source Softw.* 6:3201. doi: 10.21105/joss.03201
- Bisanz, J. E. (2018). qiime2R: Importing QIIME2 artifacts and associated data into R sessions. Version 0.99.13.
- Bolnick, D. I., Snowberg, L. K., Caporaso, J. G., Lauber, C., Knight, R., and Stutz, W. E. (2014a). Major histocompatibility complex class II b polymorphism influences gut microbiota composition and diversity. *Mol. Ecol.* 23, 4831–4845. doi: 10.1111/mec.12846
- Bolnick, D. I., Snowberg, L. K., Hirsch, P. E., Lauber, C. L., Knight, R., Caporaso, J. G., et al. (2014b). Individuals' diet diversity influences gut microbial diversity in two freshwater fish (threespine stickleback and Eurasian perch). *Ecol. Lett.* 17, 979–987. doi: 10.1111/ele.12301
- Bolnick, D. I., Snowberg, L. K., Hirsch, P. E., Lauber, C. L., Org, E., Parks, B., et al. (2014c). Individual diet has sex-dependent effects on vertebrate gut microbiota. *Nat. Commun.* 5, 1–13. doi: 10.1038/ncomms5500
- Bolyen, E., Rideout, J. R., Dillon, M. R., Bokulich, N. A., Abnet, C., Al-Ghalith, G. A., et al. (2018). QIIME 2: reproducible, interactive, scalable, and extensible microbiome data science. *PeerJ Preprints*
- Bolyen, E., Rideout, J. R., Dillon, M. R., Bokulich, N. A., Abnet, C. C., Al-Ghalith, G. A., et al. (2019). Reproducible, interactive, scalable and extensible microbiome data science using QIIME 2. *Nat. Biotechnol.* 37, 852–857. doi: 10.1038/s41587-019-0209-9
- Bordenstein, S. R., and Theis, K. R. (2015). Host biology in light of the microbiome: ten principles of holobionts and hologenomes. *PLoS Biol.* 13:e1002226. doi: 10.1371/journal.pbio.1002226
- Callahan, B. J., McMurdie, P. J., Rosen, M. J., Han, A. W., Johnson, A. J. A., and Holmes, S. P. (2016). DADA2: high-resolution sample inference from Illumina amplicon data. *Nat. Methods* 13, 581–583. doi: 10.1038/nmeth.3869
- Claus, S. P., Guillou, H., and Ellero-Simatos, S. (2016). The gut microbiota: a major player in the toxicity of environmental pollutants? *NPJ Biofilms Microbiomes* 2, 1–11. doi: 10.1038/npjbiofilms.2016.3
- Colston, T. J., and Jackson, C. R. (2016). Microbiome evolution along divergent branches of the vertebrate tree of life: what is known and unknown. *Mol. Ecol.* 25, 3776–3800. doi: 10.1111/mec.13730
- Cornwallis, C. K., Van't Padje, A., Ellers, J., Klein, M., Jackson, R., Kiers, E. T., et al. (2023). Symbioses shape feeding niches and diversification across insects. *Nat. Ecol. Evol.* 7, 1022–1044. doi: 10.1038/s41559-023-02058-0
- Defaveri, J., Shikano, T., Ghani, N. I. A., and Merilä, J. (2012). Contrasting population structures in two sympatric fishes in the Baltic Sea basin. *Mar. Biol.* 159, 1659–1672. doi: 10.1007/s00227-012-1951-4
- Degregori, S., Casey, J. M., and Barber, P. H. (2021). Nutrient pollution alters the gut microbiome of a territorial reef fish. *Mar. Pollut. Bull.* 169:112522. doi: 10.1016/j.marpolbul.2021.112522
- Dulski, T., Kozłowski, K., and Ciesielski, S. (2020). Habitat and seasonality shape the structure of tench (*Tinca tinca* L.) gut microbiome. *Sci. Rep.* 10:4460. doi: 10.1038/s41598-020-61351-1
- Element, G., Engel, K., Neufeld, J. D., Casselman, J. M., Van Coeverden De Groot, P. J., and Walker, V. K. (2020). Distinct intestinal microbial communities of two sympatric anadromous Arctic salmonids and the effects of migration and feeding. *Arct. Sci.* 7, 634–654. doi: 10.1139/as-2020-0011
- Estruch, G., Collado, M., Peñaranda, D., Tomás Vidal, A., Jover Cerdá, M., Pérez Martínez, G., et al. (2015). Impact of fishmeal replacement in diets for gilthead sea bream (*Sparus aurata*) on the gastrointestinal microbiota determined by pyrosequencing the 16S rRNA gene. *PLoS One* 10:e0136389. doi: 10.1371/journal.pone.0136389
- Fang, B., Kemppainen, P., Momigliano, P., and Merilä, J. (2021). Population structure limits parallel evolution in sticklebacks. *Mol. Biol. Evol.* 38, 4205–4221. doi: 10.1093/molbev/msab144
- Feulner, P. G., Chain, F. J., Panchal, M., Eizaguirre, C., Kalbe, M., Lenz, T. L., et al. (2013). Genome-wide patterns of standing genetic variation in a marine population of three-spined sticklebacks. *Mol. Ecol.* 22, 635–649. doi: 10.1111/j.1365-294X.2012.05680.x
- Fietz, K., Rye Hintze, C. O., Skovrind, M., Kjærgaard Nielsen, T., Limborg, M. T., Krag, M. A., et al. (2018). Mind the gut: genomic insights to population divergence and gut microbial composition of two marine keystone species. *Microbiome* 6, 1–16. doi: 10.1186/s40168-018-0467-7
- Fuess, L. E., Den Haan, S., Ling, F., Weber, J. N., Steinel, N. C., and Bolnick, D. I. (2021). Immune gene expression covaries with gut microbiome composition in stickleback. *MBio* 12, e00145–e00121. doi: 10.1128/mBio.00145-21
- Gibson, G. (2005). The synthesis and evolution of a supermodel. *Science* 307, 1890–1891. doi: 10.1126/science.1109835
- Guo, B., Defaveri, J., Sotelo, G., Nair, A., and Merilä, J. (2015). Population genomic evidence for adaptive differentiation in Baltic Sea three-spined sticklebacks. *BMC Biol.* 13, 1–18. doi: 10.1186/s12915-015-0130-8
- Hahn, M. A., Piecyk, A., Jorge, F., Cerrato, R., Kalbe, M., and Dheilly, N. M. (2022). Host phenotype and microbiome vary with infection status, parasite genotype, and parasite microbiome composition. *Mol. Ecol.* 31, 1577–1594. doi: 10.1111/mec.16344
- Hart, P. J. (2003). Habitat use and feeding behaviour in two closely related fish species, the three-spined and nine-spined stickleback: an experimental analysis. *J. Anim. Ecol.* 72, 777–783. doi: 10.1046/j.1365-2656.2003.00747.x
- Hendry, A. P., Bolnick, D. I., Berner, D., and Peichel, C. L. (2009). Along the speciation continuum in sticklebacks. *J. Fish Biol.* 75, 2000–2036. doi: 10.1111/j.1095-8649.2009.02419.x
- Henry, L. P., Bruijning, M., Forsberg, S. K., and Ayroles, J. F. (2021). The microbiome extends host evolutionary potential. *Nat. Commun.* 12, 1–13. doi: 10.1038/s41467-021-25315-x
- Hodžić, A., Dheilly, N. M., Cabezas-Cruz, A., and Berry, D. (2023). The helminth holobiont: a multidimensional host–parasite–microbiota interaction. *Trends Parasitol.* 39, 91–100. doi: 10.1016/j.pt.2022.11.012
- Jackson, R., Monnin, D., Patapiou, P. A., Golding, G., Helantera, H., Oettler, J., et al. (2022). Convergent evolution of a labile nutritional symbiosis in ants. *ISME J.* 16, 2114–2122. doi: 10.1038/s41396-022-01256-1
- Kim, P. S., Shin, N.-R., Lee, J.-B., Kim, M.-S., Whon, T. W., Hyun, D.-W., et al. (2021). Host habitat is the major determinant of the gut microbiome of fish. *Microbiome* 9, 1–16. doi: 10.1186/s40168-021-01113-x
- Kohl, K. D. (2020). Ecological and evolutionary mechanisms underlying patterns of phyllosymbiosis in host-associated microbial communities. *Philos. Trans. R. Soc. B* 375:20190251. doi: 10.1098/rstb.2019.0251
- Kolodny, O., and Schulenburg, H. (2020). Microbiome-mediated plasticity directs host evolution along several distinct time scales. *Philos. Trans. R. Soc. B* 375:20190589. doi: 10.1098/rstb.2019.0589
- Leung, J. M., Graham, A. L., and Knowles, S. C. (2018). Parasite-microbiota interactions with the vertebrate gut: synthesis through an ecological lens. *Front. Microbiol.* 9:843. doi: 10.3389/fmicb.2018.00843
- Lokesh, J., Kiron, V., Sipkema, D., Fernandes, J. M., and Moum, T. (2019). Succession of embryonic and the intestinal bacterial communities of Atlantic salmon (*Salmo salar*) reveals stage-specific microbial signatures. *Microbiologyopen* 8:e00672. doi: 10.1002/mbo3.672
- Lopetus, L. R., Scadaferri, F., Petito, V., and Gasbarrini, A. (2013). Commensal Clostridia: leading players in the maintenance of gut homeostasis. *Gut Pathogens* 5, 23–28. doi: 10.1186/1757-4749-5-23
- Love, M. I., Huber, W., and Anders, S. (2014). Moderated estimation of fold change and dispersion for RNA-seq data with DESeq2. *Genome Biol.* 15:550. doi: 10.1186/s13059-014-0550-8
- Lozupone, C., and Knight, R. (2005). UniFrac: a new phylogenetic method for comparing microbial communities. *Appl. Environ. Microbiol.* 71, 8228–8235. doi: 10.1128/AEM.71.12.8228-8235.2005
- Lozupone, C., Lladser, M. E., Knights, D., Stombaugh, J., and Knight, R. (2011). UniFrac: an effective distance metric for microbial community comparison. *ISME J.* 5, 169–172. doi: 10.1038/ismej.2010.133
- Masłowski, K. M., and Mackay, C. R. (2011). Diet, gut microbiota and immune responses. *Nat. Immunol.* 12, 5–9. doi: 10.1038/ni0111-5
- Mcfall-Ngai, M., Hadfield, M. G., Bosch, T. C., Carey, H. V., Domazet-Lošo, T., Douglas, A. E., et al. (2013). Animals in a bacterial world, a new imperative for the life sciences. *Proc. Natl. Acad. Sci.* 110, 3229–3236. doi: 10.1073/pnas.1218525110
- Mckinnon, J. S., and Rundle, H. D. (2002). Speciation in nature: the threespine stickleback model systems. *Trends Ecol. Evol.* 17, 480–488. doi: 10.1016/S0169-5347(02)02579-X
- McMurdie, P. J., and Holmes, S. (2013). PhyloSeq: an R package for reproducible interactive analysis and graphics of microbiome census data. *PLoS One* 8:e61217. doi: 10.1371/journal.pone.0061217

- Merilä, J. (2013). Nine-spined stickleback (*Pungitius pungitius*): an emerging model for evolutionary biology research. *Ann. N. Y. Acad. Sci.* 1289, 18–35. doi: 10.1111/nyas.12089
- Morales-Rivera, M. F., Valenzuela-Miranda, D., Nuñez-Acuña, G., Benavente, B. P., Gallardo-Escárate, C., and Valenzuela-Muñoz, V. (2022). Atlantic Salmon (*Salmo salar*) transfer to seawater by gradual salinity changes exhibited an increase in the intestinal microbial abundance and richness. *Microorganisms* 11:76. doi: 10.3390/microorganisms11010076
- Oksanen, J., Blanchet, F. G., Kindt, R., Legendre, P., Minchin, P., O'hara, R., et al. (2013). Community ecology package. R package version, 2.0-2. Available at: <https://cran.r-project.org/web/packages/vegan/index.html>
- Quast, C., Pruesse, E., Yilmaz, P., Gerken, J., Schweer, T., Yarza, P., et al. (2012). The SILVA ribosomal RNA gene database project: improved data processing and web-based tools. *Nucleic Acids Res.* 41, D590–D596. doi: 10.1093/nar/gks1219
- Raeymaekers, J. A., Chaturvedi, A., Hablützel, P. I., Verdonck, I., Hellemans, B., Maes, G. E., et al. (2017). Adaptive and non-adaptive divergence in a common landscape. *Nat. Commun.* 8, 1–9. doi: 10.1038/s41467-017-00256-6
- Raeymaekers, J., Huysse, T., Maelfait, H., Hellemans, B., and Volckaert, F. (2008). Community structure, population structure and topographical specialisation of Gyrodactylus (*Monogenea*) ectoparasites living on sympatric stickleback species. *Folia Parasitol.* 55, 187–196. doi: 10.14411/fp.2008.026
- Raeymaekers, J., Maes, G., Audenaert, E., and Volckaert, F. (2005). Detecting Holocene divergence in the anadromous–freshwater three-spined stickleback (*Gasterosteus aculeatus*) system. *Mol. Ecol.* 14, 1001–1014. doi: 10.1111/j.1365-294X.2005.02456.x
- Raeymaekers, J. A., Van Houdt, J. K., Larmuseau, M. H., Geldof, S., and Volckaert, F. A. (2007). Divergent selection as revealed by PST and QTL-based FST in three-spined stickleback (*Gasterosteus aculeatus*) populations along a coastal–inland gradient. *Mol. Ecol.* 16, 891–905. doi: 10.1111/j.1365-294X.2006.03190.x
- Ray, A. K., and Ringø, E. (2014). “The gastrointestinal tract of fish” in *Aquaculture nutrition: gut health, probiotics and prebiotics*. eds. D. Merrifield and E. Ringø (West Sussex: John Wiley & Sons, Ltd.), 1–13.
- R Core Team. (2021). R: A language and environment for statistical computing. R Foundation for Statistical Computing, Vienna, Austria. Available at: <https://www.R-project.org/>
- Rennison, D. J., Rudman, S. M., and Schluter, D. (2019). Parallel changes in gut microbiome composition and function during colonization, local adaptation and ecological speciation. *Proc. R. Soc. B* 286:20191911. doi: 10.1098/rspb.2019.1911
- Robeson, M. S., O'rourke, D. R., Kaehler, B. D., Ziemiński, M., Dillon, M. R., Foster, J. T., et al. (2021). RESCRIPt: Reproducible sequence taxonomy reference database management. *PLoS Comput. Biol.* 17:e1009581. doi: 10.1371/journal.pcbi.1009581
- Roeselers, G., Mittge, E. K., Stephens, W. Z., Parichy, D. M., Cavanaugh, C. M., Guillemin, K., et al. (2011). Evidence for a core gut microbiota in the zebrafish. *ISME J.* 5, 1595–1608. doi: 10.1038/ismej.2011.38
- RStudio Team. (2021). RStudio: Integrated Development for R. RStudio, PBC, Boston, MA. Available at: <http://www.rstudio.com/>
- Schwab, C., Cristescu, B., Northrup, J. M., Stenhouse, G. B., and Gänzle, M. (2011). Diet and environment shape fecal bacterial microbiota composition and enteric pathogen load of grizzly bears. *PLoS One* 6:e27905. doi: 10.1371/journal.pone.0027905
- Sepulveda, J., and Moeller, A. H. (2020). The effects of temperature on animal gut microbiomes. *Front. Microbiol.* 11:384. doi: 10.3389/fmicb.2020.00384
- Sevellec, M., Derome, N., and Bernatchez, L. (2018). Holobionts and ecological speciation: the intestinal microbiota of lake whitefish species pairs. *Microbiome* 6, 1–15. doi: 10.1186/s40168-018-0427-2
- Siriypagoudar, P., Kiron, V., Lokesh, J., Rajeish, M., Kopp, M., and Fernandes, J. (2018). The intestinal mycobiota in wild zebrafish comprises mainly Dithideomycetes while Saccharomycetes predominate in their laboratory-reared counterparts. *Front. Microbiol.* 9:387. doi: 10.3389/fmicb.2018.00387
- Small, C. M., Beck, E. A., Currey, M. C., Tavalire, H. F., Bassham, S., and Cresko, W. A. (2022). Host genomic variation shapes gut microbiome diversity in threespine stickleback fish. *Mbio* e00219–23. doi: 10.1128/mbio.00219-23
- Smith, C. C., Snowberg, L. K., Gregory Caporaso, J., Knight, R., and Bolnick, D. I. (2015). Dietary input of microbes and host genetic variation shape among-population differences in stickleback gut microbiota. *ISME J.* 9, 2515–2526. doi: 10.1038/ismej.2015.64
- Solovyev, M. M., Kashinskaya, E. N., Bochkarev, N. A., Andree, K. B., and Simonov, E. (2019). The effect of diet on the structure of gut bacterial community of sympatric pair of whitefishes (*Coregonus lavaretus*): one story more. *PeerJ* 7:e8005. doi: 10.7717/peerj.8005
- Sommer, F., and Bäckhed, F. (2013). The gut microbiota—masters of host development and physiology. *Nat. Rev. Microbiol.* 11, 227–238. doi: 10.1038/nrmicro2974
- Sullam, K. E., Essinger, S. D., Lozupone, C. A., O'connor, M. P., Rosen, G. L., Knight, R., et al. (2012). Environmental and ecological factors that shape the gut bacterial communities of fish: a meta-analysis. *Mol. Ecol.* 21, 3363–3378. doi: 10.1111/j.1365-294X.2012.05552.x
- Sullam, K. E., Rubin, B. E., Dalton, C. M., Kilham, S. S., Flecker, A. S., and Russell, J. A. (2015). Divergence across diet, time and populations rules out parallel evolution in the gut microbiomes of Trinidadian guppies. *ISME J.* 9, 1508–1522. doi: 10.1038/ismej.2014.231
- Thorburn, D.-M. J., Bal, T. M., Deflem, I. S., Volckaert, F. A., Eizaguirre, C., and Raeymaekers, J. A. (2022). Context-dependent parasite infection affects trophic niche in populations of sympatric stickleback species. *Parasitology* 149, 1164–1172. doi: 10.1017/S0031182022000531
- Varadharajan, S., Rastas, P., Löytynoja, A., Matschiner, M., Calboli, F. C., Guo, B., et al. (2019). A high-quality assembly of the nine-spined stickleback (*Pungitius pungitius*) genome. *Genome Biol. Evol.* 11, 3291–3308. doi: 10.1093/gbe/evz240
- Wang, J., Jaramillo-Torres, A., Li, Y., Kortner, T. M., Gajardo, K., Brevik, Ø. J., et al. (2021). Microbiota in intestinal digesta of Atlantic salmon (*Salmo salar*), observed from late freshwater stage until one year in seawater, and effects of functional ingredients: a case study from a commercial sized research site in the Arctic region. *Anim. Microbiome* 3, 1–16. doi: 10.1186/s42523-021-00075-7
- Wickham, H. (2016). “Data analysis” in *Ggplot2*. ed. H. Wickham (Cham: Springer, Springer International Publishing), 189–201.
- Xu, L., Xiang, P., Zhang, B., Yang, K., Liu, F., Wang, Z., et al. (2022). Host species influence the gut microbiota of endemic cold-water fish in upper Yangtze river. *Front. Microbiol.* 13:906299. doi: 10.3389/fmicb.2022.906299
- Ye, L., Amberg, J., Chapman, D., Gaikowski, M., and Liu, W.-T. (2014). Fish gut microbiota analysis differentiates physiology and behavior of invasive Asian carp and indigenous American fish. *ISME J.* 8, 541–551. doi: 10.1038/ismej.2013.181
- Zander, C. (1990). *RJ Wootton: A functional biology of sticklebacks.*—265 pp. London and Sidney: Croom Helm 1984.£ 17.95.



## OPEN ACCESS

## EDITED BY

Zhiyong Li,  
Shanghai Jiao Tong University, China

## REVIEWED BY

Xiaoshou Liu,  
Ocean University of China, China  
Ola A. Olapade,  
Albion College, United States

## \*CORRESPONDENCE

Cristina Purcarea  
✉ cristina.purcarea@ibiol.ro

RECEIVED 21 August 2023

ACCEPTED 18 December 2023

PUBLISHED 08 January 2024

## CITATION

Menabit S, Lavin P, Begun T, Mureșan M,  
Teacă A and Purcarea C (2024) First  
screening of bacteria assemblages associated  
with the marine polychaete *Melinna palmata*  
Grube, 1870 and adjacent sediments.  
*Front. Mar. Sci.* 10:1279849.  
doi: 10.3389/fmars.2023.1279849

## COPYRIGHT

© 2024 Menabit, Lavin, Begun, Mureșan, Teacă  
and Purcarea. This is an open-access article  
distributed under the terms of the [Creative  
Commons Attribution License \(CC BY\)](#). The  
use, distribution or reproduction in other  
forums is permitted, provided the original  
author(s) and the copyright owner(s) are  
credited and that the original publication in  
this journal is cited, in accordance with  
accepted academic practice. No use,  
distribution or reproduction is permitted  
which does not comply with these terms.

# First screening of bacteria assemblages associated with the marine polychaete *Melinna palmata* Grube, 1870 and adjacent sediments

Selma Menabit<sup>1,2</sup>, Paris Lavin<sup>3</sup>, Tatiana Begun<sup>1</sup>,  
Mihaela Mureșan<sup>1</sup>, Adrian Teacă<sup>1</sup> and Cristina Purcarea<sup>2\*</sup>

<sup>1</sup>Department of Biology and Ecology, National Institute for Research and Development on Marine Geology and Geoecology-GeoEcoMar, Bucharest, Romania, <sup>2</sup>Department of Microbiology, Institute of Biology Bucharest of the Romanian Academy, Bucharest, Romania, <sup>3</sup>Facultad de Ciencias del Mar y Recursos Biológicos, Departamento de Biotecnología, Universidad de Antofagasta, Antofagasta, Chile

Bacteria associated with marine invertebrate play a fundamental role in the biology, ecology, development and evolution of their hosts. Although many studies have been focused on the microbial populations of benthic and pelagic habitats, little is known about bacteria colonizing tube-dwelling polychaete. In this context, the current study provided the first characterization of the *Melinna palmata* Grube, 1870 microbiome based on Illumina sequencing of 16S rRNA gene of the polychaete tissue and proximate sediments collected from the Black Sea, Romania, along a 24.2 m – 45.4 m depth-gradient. The diversity, taxonomic composition and deduced functional profile of the tissue and sediments associated bacterial communities were compared and analyzed in relation with the environmental parameters. This polychaete harbored a distinct bacterial assemblage as compared to their sediments and independent on the depth of their habitat, including 8 phyla in tissues dominated by Proteobacteria, and 12 phyla in sediments majorly represented by Actinobacteriota, respectively. At order level, Synechococcales, Rhodobacterales and Actinomarinales were highly represented in the *M. palmata* microbiome, while Microtrichales, Anaerolineales and Caldilineales were mostly found in sediments. A significant correlation was observed between Cyanobacteria taxa and the dissolved oxygen concentrations in shallow waters impacted by the Danube inputs. Meanwhile, this phylum showed a positive correlation with Planctomycetota colonizing the invertebrate tissues, and a negative one with Actinobacteriota and Chloroflexi found in sediments. The deduced functional profile of these bacterial assemblages suggested the prevalence of the amino acid and carbohydrate metabolism for both analyzed matrices. This pioneering report on the *M. palmata* microbiome highlighted the environment contribution to bacterial species enrichment of the polychaete, and provided a glimpse on the putative role of microbial communities associated with this marine organism.

## KEYWORDS

*Melinna palmata* microbiome, invertebrates bacteria, Black Sea sediments, marine polychaete, illumina sequencing, 16S rRNA gene



# 1 Introduction

Marine benthic organisms are naturally colonized by microorganisms, which play a fundamental role in the biology of their hosts (Kelman et al., 2009; Ketchum et al., 2018). The diversity of bacterial communities associated with marine organisms plays an important role in immunity, metabolism, physiology (Mcfall-Ngai et al., 2013; Bordenstein and Theis, 2015; Theis et al., 2016), as well as in host development, adaptation and evolution (Rosenberg et al., 2007; Zilber-Rosenberg and Rosenberg, 2008) of these invertebrates. The bacterial-host relationship has aroused considerable interest in the field of marine biology (Piel, 2004); some of these microorganisms may be symbionts, pathogens or can create mutualism relations (Kelman et al., 2009). Symbiotic bacteria are found in many biological systems, influencing the host's evolution and suggesting that microorganisms are involved in limiting pathogen colonization through antimicrobial compounds and competition for food resources (Felbeck and Distel, 2004; Desriac et al., 2014). As a result of co-evolving with their specific hosts, microbial symbionts exhibit a diverse array of custom-tailored biochemical traits. This renders them a reservoir of secondary metabolites characterized by distinct bioactivities that hold significant medical and commercial appeal (Zhang et al., 2015). Filtering and deposit feeding invertebrates that can concentrate bacteria from water and sediments also play an important role in aquatic microbiome contribution to the ecosystem, representing biomarkers for the microbial diversity in aquatic environments (Burkhardt et al., 1992; Graczyk et al., 2003; Marino et al., 2005).

Marine ecosystems, among the most complex environments, harbour a significant part of the global microbial population. Certain bacterial species within these ecosystems are essential contributors to many biogeochemical cycles (Muriel-Millán et al., 2021). Many microorganisms, such as taxa belonging to Proteobacteria, engage in symbiotic relationships with various marine invertebrates, influencing processes such as nutrient cycling, digestion, and defence mechanisms (Kunihiro et al., 2011; Summers et al., 2013; Von Borzyskowski et al., 2019). Cyanobacteria are crucial contributors to primary production and often create symbiotic relationships with sponges, corals or molluscs, providing their hosts with fixed carbon through photosynthesis (Erwin and Thacker, 2008; Zhukova et al., 2022). In the broader marine ecosystem, Actinobacteriota's metabolic activities, including the breakdown of complex organic compounds, have a significant impact on the availability of nutrients and the carbon cycling (Goodfellow and William, 1983; Stevens et al., 2007).

Various environmental factors, including salinity, temperature, pH, organic matter content, and oxygen levels, play an important role in shaping the distribution and abundance of microbial communities (Dang and Lovell, 2016; Guo et al., 2022a). These microorganisms' interactions with environmental parameters serve as indicators that reflect the function and structure of marine ecosystems, as highlighted in previous studies (Boucher et al., 2006). For instance, the community structure and dynamics of

bacteria belonging to Proteobacteria, Firmicutes, and Actinobacteriota phyla appeared to be affected by various factors such as salinity, dissolved oxygen, ammonia, phosphate and silicate concentrations (Guo et al., 2022b). Although variations in microbial community can be substantial across different habitat types, primarily due to the impact of environmental gradients (Martiny et al., 2006), some studies suggested consistency in community composition across similar habitats, regardless of geographical distance (Lauber et al., 2009).

Deep screening of free-living bacterial assemblages in the marine environments (Pommier et al., 2010; Costas-Selas et al., 2022; Ruginescu et al., 2022) and of bacteria associated with different organisms (Musella et al., 2020; Li et al., 2023) was successfully carried out based on next-generation sequencing of 16S rRNA genes (Webster and Taylor, 2012), overcoming some of the challenges previously associated with determining microbial diversity (Sogin et al., 2006; Winand et al., 2019).

For the last decades, investigations of bacteria-invertebrate associations from various marine environments became of high interest for the scientific community (Goffredi et al., 2007; Gilbertson et al., 2012; Lo Giudice and Rizzo, 2022). Many studies demonstrated that interactions between these organisms create symbioses leading to production of secondary metabolites with antimicrobial activities by the invertebrates-associated microbiome (Thomas et al., 2010; Graca et al., 2013; Abdelmohsen et al., 2014; Kuo et al., 2019). Also, symbiotic bacteria from bivalves were involved in the host defense mechanisms (Defer et al., 2013), and could contribute to adaptation to environmental stress conditions (Leite et al., 2017). Various methods, such as biochemical, enzymatic, molecular, and transmission electron microscopy techniques confirmed the presence of chemoautotrophic symbiotic bacteria in these organisms, supporting the idea that these bacteria play a crucial role in nutrition (Conway et al., 1992; Eisen et al., 1992). Microbes inhabiting tunicates were able to produce metabolites with anti-tumor effect (Schmidt et al., 2005), and for various biotechnologies and pharmaceutical applications (Paul and Ritson-Williams, 2008; Erwin et al., 2010). Moreover, recent studies have emphasized the potential of symbiotic bacteria found in polychaetes as a novel reservoir for biosurfactant-producing microbes (Rizzo et al., 2013; Markande et al., 2014).

Bacterial communities of tube-building worms could have an important contribution to the biogeochemical processes that occur at the interface between benthic organisms and their habitat. Thus, burrowing organisms appeared to be essential contributors to the biogeochemistry of the benthic environment through excavation, grazing and excretion (Konhauser et al., 2020). Furthermore, polychaetes host symbiotic microorganisms involved in transformation, degradation and detoxification processes, such as *Ophelina* species that are characterized by a high content of metal-resistant bacteria (Neave et al., 2012). Also, *Capitella teleta* was reported to be associated with highly abundant microbes able to degrade polyaromatic hydrocarbons which potentially allows the species to survive in polluted environments or serve as indicators of pollution (Hochstein et al., 2019).

*Melinna palmata* Grube, 1870 is a deposit-feeder tube-dwelling ampharetid polychaeta, with a length of 3–4 cm (Hunt, 1925; Mare, 1942; Fauchald and Jumars, 1979). It builds a mucus-lined tube from which it can emerge to spread its tentacular palate on the sediment surface inhabiting the Black Sea generally at depths ranging from 30 to 40 m (Băcescu et al., 1971). Although this species did not occupy a well-established habitat in the Romanian Black Sea shelf until 1970, its populations started to reach significant densities and biomass a decade later (Gomoiu, 1982). Currently, *M. palmata* and/or *Spisula subtruncata* constitute the engineering species of the Circalittoral mud habitat, reaching an average density of 3,450 specimen  $\text{m}^{-2}$  in the Danube influenced area (Teacă et al., 2020).

Several studies in the Black Sea have been focused on investigating the microbial populations of sediments (Schulz et al., 1999; Thamdrup et al., 2000; Leloup et al., 2007; Schäfer et al., 2007; Coolen and Shtereva, 2009; Schippers et al., 2012) and pelagic habitats (Jørgensen et al., 1991; Sorokin et al., 1995; Glaubitz et al., 2010; Bryukhanov et al., 2015; Ruginescu et al., 2022). In contrast, only one study characterized bacteria associated with the bivalve *Mytilaster lineatus* (Onishchenko and Kiprianova, 2006), while no research has been carried out so far on bacteria colonizing polychaete species in order to untangle the role of these symbionts in the invertebrate marine adaptation and possible microbiome exchanges with the seabed sediments. In this context, the current investigation focused on identifying the bacterial communities associated with the tube-building polychaete *M. palmata* and its surrounding sediments from the Romanian Black Sea shelf based on 16S rRNA gene Illumina sequencing. Comparative analyses of the microbial diversity, community composition and putative functional profile of the polychaete tissue and sediments, and correlation of bacterial taxa with the physicochemical parameters of the sea water were carried out in order to determine if the *M. palmata* bacterial assembly reflects the partial recruitment of surrounding representatives depending on environmental variables. To our knowledge, this study provides the first characterization of the microbiome of the marine polychaete *M. palmata*.

## 2 Materials and methods

### 2.1 Description of the study area

The North-Western part of the Black Sea receives 80% of the basin's total freshwater input originating from the Dnieper, Dniester and Danube, the latter being the major contributor of freshwater and sediment inputs (Mikhailov and Mikhailova, 2008). The Danube River is the second European largest river basin, covering territories of 18 states including EU-Member States, Accession Countries and other countries (ICPDR, 2004). Romanian coastal waters are subject to Danube inputs, which provide significant organic and inorganic matter, the mean annual river flow recorded from all three main branches being of  $6500 \text{ m}^3 \text{ s}^{-1}$ . The direction, range and depth of dispersion of the Danube waters are dependent on the intensity of water flow and wind direction. North and northeast winds are dominant during spring, reaching average speeds of  $5.5 \text{ m s}^{-1}$ , while during autumn, north winds predominate, with an average

speed of  $8.0 \text{ m s}^{-1}$  (Tescari et al., 2006). According to Panin and Jipa (2002), the average sediment discharge from the Danube into the Black Sea is estimated to range between 25 and 35 million tonnes/year, with sandy material accounting 4–6 million tonnes/year. The study area is located within the marine protected area ROSCI0066 (Danube Delta - marine zone), included in Natura 2000 European ecological network (Figure 1A).

The major habitat of the investigated area is represented by Circalittoral muds with *Melinna palmata*. The total benthic communities of this area comprise a diverse assemblage of deposit feeders and suspension filters, such as oligochaetes, polychaetes (*Mellina palmata*, *Heteromastus filiformis*), molluscs (*Mytilus galloprovincialis*, *Spisula subtruncata*, *Abra nitida*, *Pitar rudis*, *Acanthocardia paucicostata*), and bacteriivorous nematodes (*Terschellingia longicaudata*, *Sabatieria pulchra*, *S. abyssalis*, *Neochromadora izhorica*, *Desmolaimus* sp.) (Mureșan and Teacă, 2019; Teacă et al., 2020). Among these, *M. palmata* represented more than 42% of the total average macrozoobenthic density (Mureșan et al., 2019; Mureșan and Teacă, 2019; Teacă et al., 2019; Teacă et al., 2020).

### 2.2 Sample collection

Sediment samples were collected using a Box Corer with a surface of  $0.1 \text{ m}^2$  (Todorova and Konsulova, 2005) from four different sites located in the Romanian northwestern continental shelf of the Black Sea, during June 2020 (Figure 1A). In order to assess the microbial communities from *M. palmata* individuals (Figure 1B) and sediments (Figure 1C), two subsamples were collected from each site. The sedimentary material was collected in sterile containers after discarding the fraction in contact with the sampling equipment, and stored at  $-20^\circ\text{C}$ . For polychaete isolation, sediment particles were removed using  $250 \mu\text{m}$  and  $125 \mu\text{m}$  mesh sieve. Each specimen selected was washed with sterile water and stored in  $200 \mu\text{l}$  Tris-EDTA pH 8 buffer at  $-20^\circ\text{C}$  for genetic analyses (Ross et al., 1990).

### 2.3 Physicochemical parameters

*In situ* measurements of temperature, salinity, dissolved oxygen (DO) and pH of water above the seabed (bottom layer) were performed for each location with an EXO2 multi-parameter probe (YSI Incorporated, Yellow Springs, USA). The salinity was expressed in practical salinity units (PSU) corresponding to parts per thousand (PPT).

### 2.4 DNA Extraction, 16S rRNA gene sequencing and sequence analysis

Total DNA was extracted from two sediment samples and two *Melinna palmata* individuals from each site using DNeasy Blood and Tissue Kit (Qiagen, Hilden, Germany) following an optimized protocol that includes an initial cell disruption step (Iancu et al., 2015). Tissue samples were resuspended into Tris-EDTA buffer pH 8 and homogenized at  $20^\circ\text{C}$  for 12 min in a SpeedMill PLUS cell

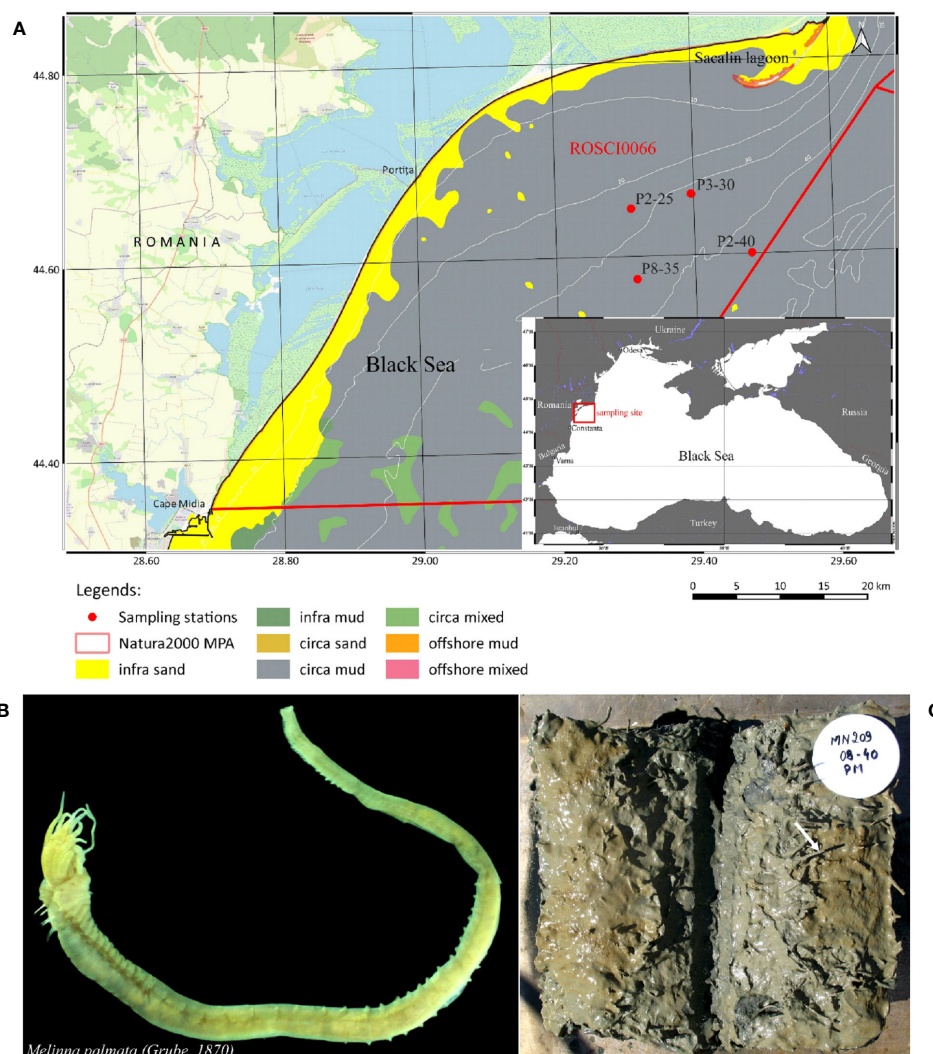


FIGURE 1

Study area and investigated organism. (A) Map of Black Sea sampling locations and detailed sampling sites area (B) *Melinna palmata* specimens collected from the Black Sea (photo by photo by A. Teacă); (C) Sediments collected from the Black Sea studied area containing *M. palmata* (photo by photo by A. Teacă).

homogenizer at 50 Hz (Analytik Jena, Jena, Germany) in the presence of 5 ZR BashingBead 0.2 mm lysis matrix (Zymo Research, Irvine, CA, USA), and further processed according to the manufacturer's protocol. For sediment samples, DNA was isolated using DNeasy PowerSoil Pro Kit (Qiagen, Hilden, Germany) following the manufacturer's instruction.

Sequencing of the amplified V3-V4 region of the 16S rRNA genes was performed using 341F/805R primer pair (Takahashi et al., 2014) and an Illumina MiSeq 300PE platform (Macrogen, Seoul, South Korea).

The resulted DNA sequences were processed using the DADA2 package v1.8) implemented in R (v4.0.2) (Callahan et al., 2016). After removing the forward and reverse primers sequences using cutadapt (v4.2.2) (Martin, 2011), the sequences were trimmed and filtered. Amplicon Sequence Variants (ASVs) were inferred from de-replicated sequences, and chimeras were removed using the "consensus" method. Taxonomic assignment of the ASVs was performed using

the Silva v138 16S rRNA database (silva.nr.v138). Analyses were carried out using MicrobiomeAnalyst 2.0 (Lu et al., 2023).

Pattern Search was used to for sequence assignment to phylum Cyanobacteria. The putative functional profile was obtained by mapping the gene abundance as predicted from Tax4Fun2 according to KEGG metabolism (Lu et al., 2023).

The 16S rRNA gene sequences of the bacteria from *M. palmata* tissues and adjacent sediments of the 16 samples (MP1-MP16) (Table 1) were deposited in the NCBI SRA Sequence Read Archive under the BioProject PRJNA923146.

## 2.5 Statistical analyses

Alpha and Beta diversities were calculated using the pyloseq package (McMurdie and Holmes, 2013). Alpha diversity of ASVs was evaluated based on Chao1, Shannon, Evenness, and Fisher

TABLE 1 Sampling sites and collected samples of *Melinna palmata*.

Sampling site	Coordinates	Water depth (m)	Sample code	Sample type
P2-25	44°38,954'N 29°18,570'E	24.2	MP5	tissue
			MP6	
			MP7	sediment
			MP8	
P3-30	44°39,768'N 29°23,815'E	28.2	MP1	tissue
			MP2	
			MP3	sediment
			MP4	
P8-35	44°34,590'N 29°18,960'E	36.5	MP13	tissue
			MP14	
			MP15	sediment
			MP16	
P2-40	44°36,037'N 29°28,920'E	45.4	MP9	tissue
			MP10	
			MP11	sediment
			MP12	

indices. Bray-Curtis dissimilarity was used to assess the Beta diversity, in order to compare the diversity between samples and microbial communities. Non-metric multidimensional scaling (NMDS) was used to visualize the 2-D matrix where each point represents the entire microbiome of a single sample. The statistical significance ( $p < 0.05$ ) of the clustering pattern in ordination plots was evaluated using Analysis of group Similarities (ANOSIM) and Permutational multivariate analysis of variance (PERMANOVA). Multiple Linear Regression with Covariate Adjustment was used to find associations between the microbial community structure and the physicochemical water parameters using MaAsLin2. All statistical analyses were conducted using MicrobiomeAnalyst 2.0 (Lu et al., 2023).

A correlation analysis based on SECOM (Pearson 1) between abundances in the two matrices was performed (Lin et al., 2022). The principal Component Analysis (PCA) was performed using tidyverse and ggplot2 packages in R v4.2.3. (Wickham, 2016; Wickham et al., 2019; R Core Team, 2023). Student's t-test was used to compare the means of gene abundance between the two types of samples (Wickham, 2016; Mishra et al., 2019; R Core Team, 2023).

### 3 Results

#### 3.1 Characteristics of *Melinna palmata* habitat

Sediment samples containing *M. palmata* Grube, 1870 specimens were collected from 4 sites which formed a perimeter

with an area of about 25 km<sup>2</sup>, with the minimum distance of 6.8 km (between P2-25 and P3-30) and a maximum distance of 14 km (between P8-35 and P2-40) located along the Romanian shore of the Black Sea, where the water depth ranged from 24.2 m to 45.5 m (Figure 1A, Table 1).

The seabed from all sampling locations consisted of mud sediments originating from alluvial deposits made of silt and clay particles.

The physicochemical properties of the sea water showed little variations between the sites (Table 2). Water temperature varied between 9.05°C (P2-40) and 14.80°C (P2-25), with an average of 11.63 ( $\pm 2.40$ ) °C. The average salinity was of 17.97 ( $\pm 0.38$ ) PSU, with a minimum of 17.60 PSU at station P2-25 and a maximum of 18.49 PSU at station P2-40 (Table 2). The dissolved oxygen concentration had a slight increasing trend with the water depth, between 4.40 mg L<sup>-1</sup> and 6.48 mg L<sup>-1</sup> at P3-30 and P2-40, respectively, with an average of 5.32 ( $\pm 0.94$ ) mg L<sup>-1</sup>. A slightly alkaline pH was measured all 4 stations with an average value of 8.05( $\pm 0.12$ ), varying between 7.90 (at P3-30 station) and 8.20 (at P8-35 station) (Table 2).

#### 3.2 Bacterial diversity in *M. palmata* tissues and sediments

The microbial diversity and community structure of *M. palmata* tissues and surrounding sediments were determined from the duplicate samples (Table 1) collected from the Romanian Black Sea coast based on Illumina sequencing of the 16S rRNA gene. The total number of DNA sequences (134975)



TABLE 2 Physicochemical parameters of the seawater collected from the Black Sea sampling sites.

Sampling site	Temperature (°C)	Salinity (PSU)	Dissolved oxygen (mg L <sup>-1</sup> )	pH
P2-25	14.80	17.60	4.75	8.05
P3-30	10.85	17.80	4.40	7.90
P8-35	11.80	18.00	5.65	8.20
P2-40	9.05	18.49	6.48	8.07

corresponded to 1444 unique bacterial amplicon sequence variants (ASVs). Rarefaction curves of both analyzed matrices showed a complete identified bacterial community, thus capturing a representative portion of the microbial diversity present in samples (Supplementary Figure S1).

Alpha diversity analysis of the tissue and sediment associated bacteria based on Chao1 index showed significant differences between the analyzed group (p-value 0.0249; Table 3, Supplementary Figure S2). The microbiome of all sediment samples exhibited higher microbial diversity, with Chao1 index values ranging from 401 to 647.1 and a mean of  $554.8 \pm 27$ . Meanwhile, this diversity index varied within the 295.6 - 628.1 interval, with a mean value of  $425.9 \pm 43.6$  in the case of tissue-associated bacterial communities (Table 3). No major variation was observed between bacterial diversity at different depths

(Supplementary Figure S2B). The corresponding calculated Fisher indices (Table 3) reflected a similar trend (p-value 0.0229), showing a slightly lower diversity for *M. palmata* associated bacteria (average of  $97.37 \pm 11.19$ ) as compared to that of the adjacent sediments (average  $130.3 \pm 6.38$ ). Slight variation of these diversity indices was observed between samples and within the replicate groups (Table 3). The calculated Shannon indices showed higher values for both tissue and sediment associated bacteria with no significant differences. Furthermore, no statistically significant variations between these communities along the depth gradient was observed (Chao1 p-value: 0.61761; [ANOVA] F-value: 0.61619; Shannon p-value: 0.47727; [ANOVA] F-value: 0.88328).

The multidimensional beta diversity analysis of the microbial communities in relation with the type of matrices showed significantly different diversity and relative abundance between

TABLE 3 Number of reads, ASVs and alpha diversity indices of bacterial communities from *M. palmata* tissue and associated sediments with statistical comparison (p-values).

Sample	Sample Type	Number of reads	ASVs	Alpha Diversity index			
				Shanon	Chao1	Fisher	Evenness
MP11	Sediment	111558	10652	$6.14 \pm 0.028$	$608.5 \pm 10.69$	139.9	$0.76 \pm 0.021$
MP12	Sediment	98227	10277	$6.18 \pm 0.031$	$647.1 \pm 8.79$	153.3	$0.74 \pm 0.022$
MP15	Sediment	78852	9764	$5.98 \pm 0.034$	$573.1 \pm 9.7$	132.9	$0.69 \pm 0.023$
MP16	Sediment	76348	9333	$5.94 \pm 0.036$	$544.2 \pm 7.3$	126	$0.7 \pm 0.024$
MP3	Sediment	74447	7030	$5.59 \pm 0.043$	$401 \pm 9.5$	91.96	$0.67 \pm 0.027$
MP4	Sediment	80614	8022	$5.9 \pm 0.036$	$522.5 \pm 10.7$	125	$0.7 \pm 0.025$
MP7	Sediment	79130	7061	$5.94 \pm 0.038$	$526.6 \pm 11.3$	131.1	$0.72 \pm 0.027$
MP8	Sediment	103453	10557	$6.13 \pm 0.03$	$615.3 \pm 9.19$	142.1	$0.75 \pm 0.021$
MP1	Tissue	57849	7305	$5.69 \pm 0.027$	$359.1 \pm 6.89$	79.15	$0.82 \pm 0.022$
MP10	Tissue	60169	4901	$5.57 \pm 0.037$	$323.3 \pm 5.89$	77.63	$0.81 \pm 0.029$
MP13	Tissue	70336	11681	$5.75 \pm 0.027$	$433 \pm 5.6$	88.55	$0.73 \pm 0.019$
MP14	Tissue	85995	10059	$6.09 \pm 0.031$	$594.4 \pm 8.6$	138.1	$0.74 \pm 0.022$
MP2	Tissue	57897	6971	$5.35 \pm 0.037$	$295.6 \pm 7.19$	62.45	$0.71 \pm 0.025$
MP5	Tissue	78262	6948	$5.79 \pm 0.033$	$419.1 \pm 8.1$	98.01	$0.78 \pm 0.024$
MP6	Tissue	71788	6040	$5.56 \pm 0.038$	$354.3 \pm 8.7$	82.1	$0.74 \pm 0.027$
MP9	Tissue	85519	8374	$6.17 \pm 0.028$	$628.1 \pm 21.1$	153	$0.77 \pm 0.021$
Tissue vs Sediment			p=0.1884	p=0.0722	p=0.0249*	p=0.0229 *	p=0.0210*
(t-student two-tailed)			(t=1.383 df=14)	(t=1.944 df=14)	(t=2.512 df=14)	(t=2.555 df=14)	(t=2.599 df=14)

the polychaete tissue and the sediment samples ([ANOSIM] R: 0.77623; p-value < 0.001 [NMDS] Stress = 0.061336) (Figure 2), and [PERMANOVA] F-value: 4.6741; R-squared: 0.2503; p-value: 0.001.

[NMDS] Stress = 0.061336 (Supplementary Figure S3), with higher differences among tissue samples.

### 3.3 Bacterial taxonomic profile in *M. palmata* and associated sediments in relation with environmental factors

Taxonomic assignment of bacterial community from *M. palmata* tissue led to identification of 12 phyla, 14 classes, 26 orders, 26 families and 30 genera, while the adjacent sediments microbiota contained 12 phyla, 19 classes, 34 orders, 29 families and 36 genera. Among these, 14 classes were common to the invertebrate and its habitat, while Fusobacteriia, ABY1, Thermodesulfovibrionia, Parcubacteria and Phycisphaerae were identified only in sediments.

At phylum level, the tissue-colonizing bacteria were dominated by Proteobacteria (16541 ASVs), followed by Actinobacteriota (14171 ASVs), Cyanobacteria (11419 ASVs) and Chloroflexi (6330 ASVs), accounting for a total of 62276 ASVs (Figure 3A). Meanwhile, the sediment communities totaling 72696 ASVs was mostly represented by Actinobacteriota (28581 ASVs) and Chloroflexi (18968 ASVs), with a lower abundance of Proteobacteria (7682 ASVs) and Campylobacterota (6924 ASVs). The relative content of phylum Fimicutes was similar in both tissues and sediments, accounting for 2576 and 2572 ASVs of total reads, respectively, while Planctomycetota taxa were more prominently represented in tissues (5951 ASVs vs. 2887 ASVs, respectively).

Also, low presence of phyla Fusobacteria, Nitrospirota and Patescibacteria (less than 250 ASVs for each group) have been observed in sediments (Figure 3A).

At order level, 24 taxa were found in both polychaete and sediments, with Rhodospirillales and Lachnospirales exclusively identified in tissues, and Christensenellales, SJA\_15, B2M28, Phycisphaerales, Ectothiorhodospirales, Frankiales, Candidatus Kuenenbacteria, Candidatus Moranbacteria, Candidatus Magasanikbacteria and Fusobacteriales only in sediments. At family level, 23 taxa were shared, while Butyricicoccaceae, Lachnospiraceae and Magnetospiraceae representative were specific for tissues and Ectothiorhodospiraceae, Acidothermaceae, Phycisphaeraceae, Hungateiclostridiaceae, Fusobacteriaceae and Christensenellaceae found only in sediments. Among these, Synechococcales (10948 ASVs), Rhodobacterales (10173 ASVs), Actinomarinales (7414 ASVs) were the most prominent representatives in *M. palmata* tissues, while Micotrichales (21239 ASVs), Anaerolineas (9660 ASVs), Caldilineales (8042 ASVs) and Campylobacterales (6924 ASVs) recorded higher relative abundances in sediments (Figure 3B).

From the 36 identified bacterial genera, 28 were common to both types of samples. The tissue-colonizing bacteria were assigned to 30 genera *Butyricoccus* and *Ruminococcus* species were present only in the polychaete tissues, while those associated with sediments belonged to 36 different genera with *Hoeflea*, *Clostridium sensu stricto\_13S*, *M1A02*, *Candidatus Alysiosphaera*, *Psychrilyobacter*, *Levilinea*, *Thiogranum* and *Acidothermus* species exclusively found in these samples (Figure 3C). Among these, species belonging to genera *Ilumatobacter* (163210ASVs) and *Sulfurovum* (6924 ASVs) were dominant in the sediments, while

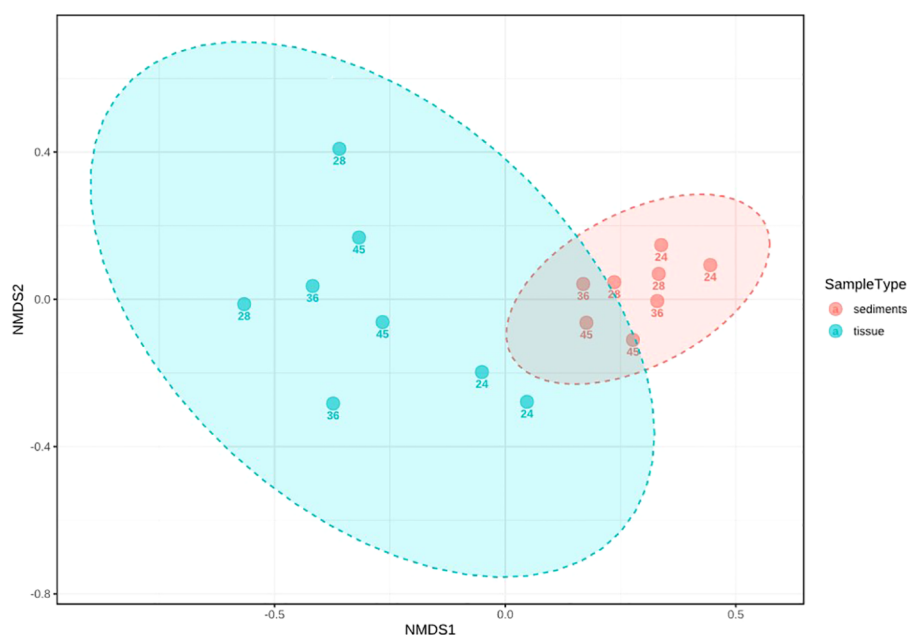


FIGURE 2

Multidimensional analysis (ANOSIM) of the beta diversity of bacterial communities from tissues and sediments, based on ASVs. The sample depth (number) is indicated for each sample.

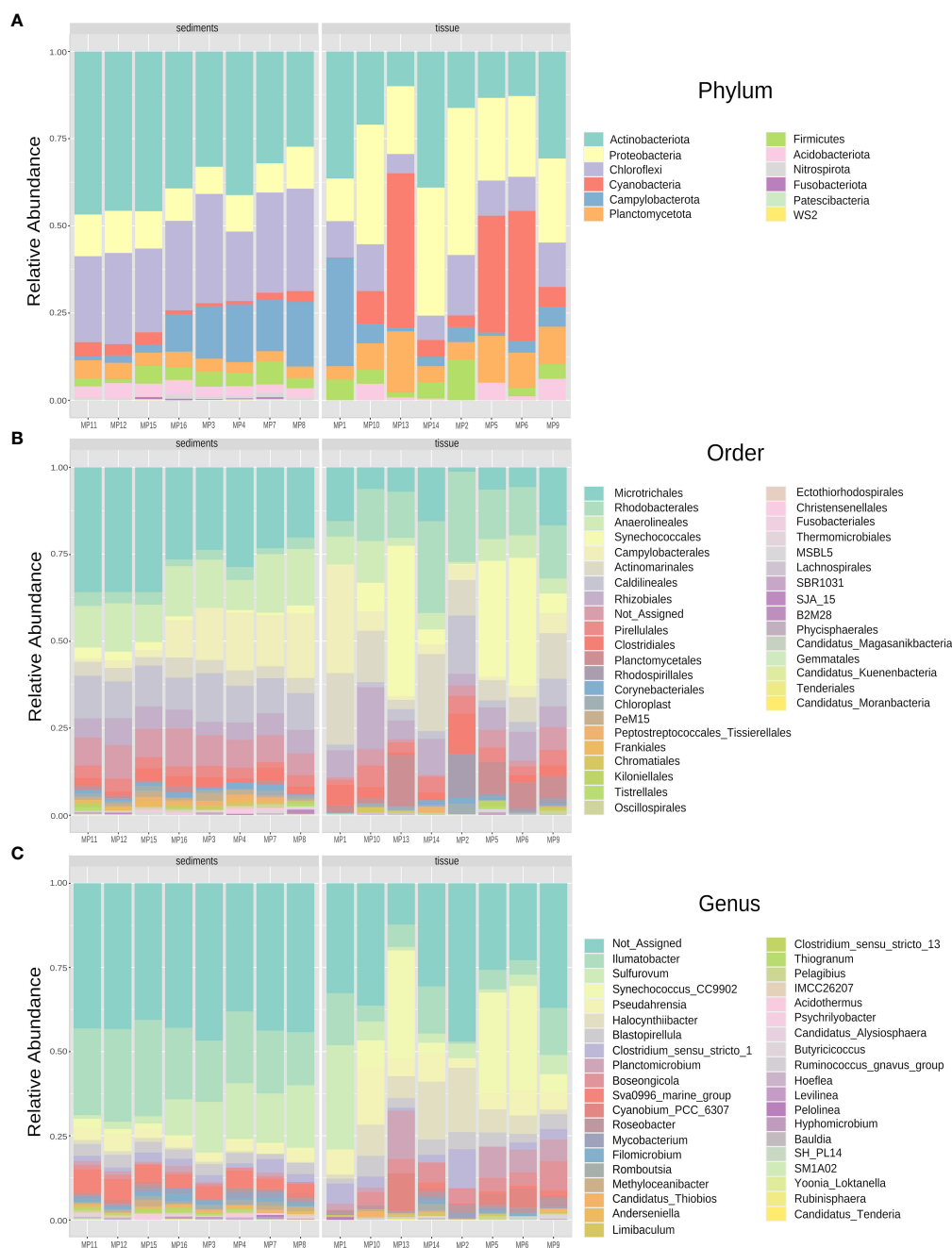


FIGURE 3  
Relative abundance profile of bacterial communities colonizing sediments and tissues of *M. palmata* at Phylum (A), Order (B), and Genus (C) levels.

notable abundance of *Synechococcus-CC9902* (8866 ASVs) was recorded in tissues (Figure 3C).

To assess the effect of the habitat depth on the *M. palmata*-associated bacterial communities and related sediments, the core microbiome of phyla with a higher prevalence than 10% from both tissue and sediments was analyzed for each sampling site (Supplementary Figure S4). No notable differences between the relative abundance of major taxa were observed between communities collected from variable water depth, with the highest

presence in all cases of Actinobacteriota taxa, followed by Chloroflexi, Proteobacteria, and Planctomycetota, and the lowest representation by phylum Nitrospirota (Supplementary Figure S4).

Pearson analysis of phyla abundances from the two types of samples showed the correlation between the top features (bacterial taxa) ranked by their significance according to the cutoff p-value (0.05) and correlation threshold (0.3) (Figure 4). Specifically, Verrucomicrobiota taxa positively correlated with Planctomycetota, both much more abundant in tissues, while

bacteria belonging to phylum Desulfobacterota positively correlated with Nitrospirota and Sumerlaeota taxa highly represented in sediments. Meanwhile, a negative correlation was observed between phyla Nitrospirota and Planctomycetota, as well as between Verrucomicrobiota and Actinobacteriota (Figure 4).

The impact of sea water parameters on the community structure was evaluated by a Multiple Linear Regression analysis showing a significant correlation between Cyanobacteria representatives and DO concentration (p-value 0.0188), with considerable relative abundance of these communities registered at 4.75 mg L<sup>-1</sup> dissolved oxygen in shallow waters (Figure 5). Meanwhile, no significant correlation between other taxa and physicochemical parameters was observed (Supplementary Table S1).

Moreover, a positive pattern correlation between Cyanobacteria phylum and representatives of phylum Planctomycetota colonizing tissues has been identified (Pearson  $r = 0.89083$ ; p-value: 3.6972e-06), while a negative correlation has been observed between the former group and Actinobacteriota (Pearson  $r = 0.76177$ ; p-value: 0.00060532) and with Chroloflexi (Pearson  $r = -0.62317$ ; p-value: 0.0099101) from sediments, respectively (Supplementary Figure S5).

### 3.4 Predicted functional profile of the microbiome of *M. palmata* and sediments

Based on the taxonomic profile and sequence analysis of the ASVs from 16S rRNA metagenomics, an estimated metabolic profile of both *M. palmata* tissue and sediments bacterial communities was generated, in order to evaluate putative contribution of the sediment substrate to the polychaete microbiota (Figure 6).

Analysis of the predicted functional profile of these microbiomes showed no major differences between the distribution of relative abundance of various genes in accordance with the KEGG (Kyoto Encyclopedia of Genes and Genomes) metabolic pathways, with the prevalence of the amino acid and carbohydrate metabolism across all examined samples (Figure 6A).

Nevertheless, the statistical analysis (Student's t-test) indicated a higher content of genes involved in carbohydrates, amino acids, lipid, terpenoids and polyketides metabolism along with the those associated with biodegradation and metabolism of xenobiotics (p-value < 0.05) in the polychaete symbiotic bacteria relative to the prokaryotic community from adjacent sediments. Meanwhile, genes related to biosynthesis and metabolism of lipids, terpenoids,

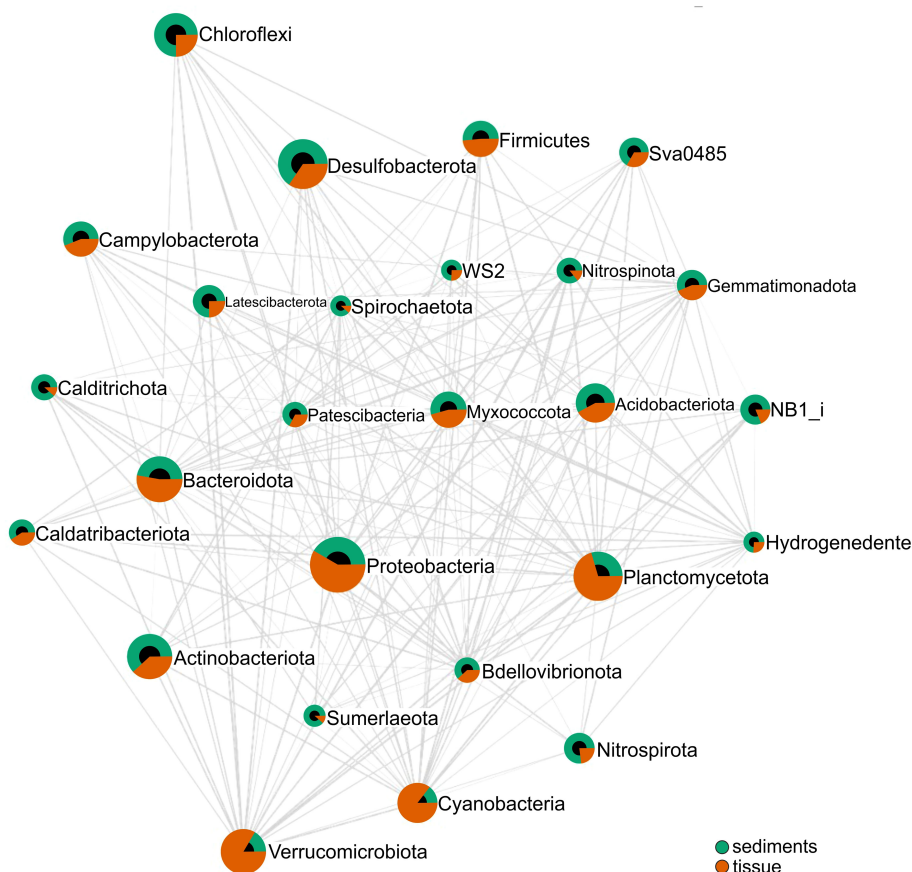


FIGURE 4

Pearson correlation analysis of relative abundance of bacterial phyla associated with sediments and tissues. Phyla connected by an edge (line) correspond to a correlation between them for p-value cutoff (0.05) and correlation threshold (0.3). The connection length reflects the magnitude of the significant correlation (shorter lengths corresponding to stronger correlations), and the diameter corresponds to the relative abundance of each taxon.



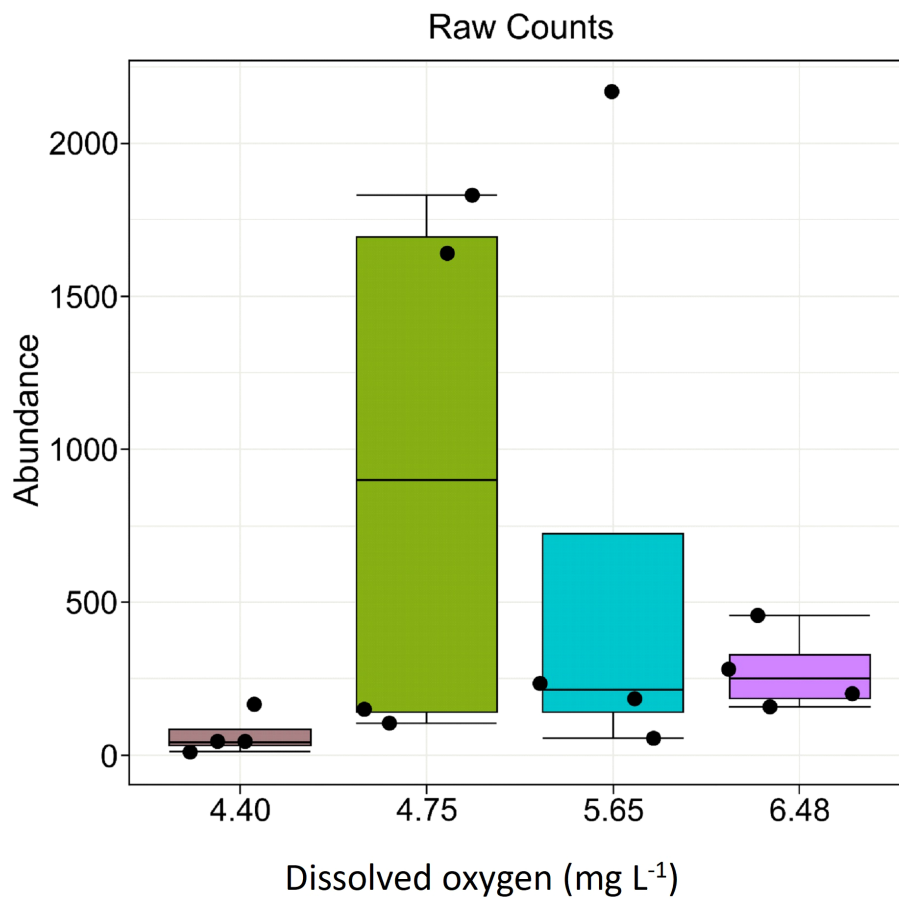


FIGURE 5

Correlation between Cyanobacteria phylum distribution and dissolved oxygen (DO) concentrations of sea water (abundance is expressed in ASVs).

polyketides, nucleotides, cofactors, vitamins, energy, glycans, and other secondary metabolites were evidenced in both the tissue-associated and sediment microbiomes (Figure 6A).

A Principal Component Analysis (PCA) of predicted functional genes indicated differences between the gene functionality diversity of the analyzed matrices (Figure 6B). These findings are in accordance with the outcomes of the NMDS analysis (Figure 2), providing further support for the observed differentiation in genes functionality resulting from the comparison between distinct communities, namely tissues and sediments.

Despite the significant diversity differences between *M. palmata* and sediments-associated bacteria, their predicted metabolic profile based on 16S rRNA taxonomic data could suggest only limited variances between the two communities. Further investigations of these communities by metagenomics and metatranscriptomics are required to highlight the metabolic variability of the polychaete microbiome in relation with that of its substrate, and untangle their putative ecological role.

## 4 Discussion

The current investigation reported original data on the tissue microbiome from the marine polychaete *Melinna palmata* from the

Black Sea, Romania, in relation with the bacterial community of the adjacent sediments. For this invertebrate, a recent study conducted in Arcachon Bay (French Atlantic coast) (Massé et al., 2019) described the aerobic bacterial community composition colonizing the surrounding sediments of this ampharetid polychaete, while so far no investigations have been carried out on the tissue-associated microbiome. In this survey, we applied a culture-independent method based on 16S rRNA gene Illumina sequencing of the bacterial community inhabiting the tissues of *M. palmata* collected from various depths in the Romanian Black Sea sediments in comparison with that of the sediments of collected specimens. The community composition of both analyzed matrices did not show notable changes along the sea depth gradient between 24.2 and 45.8 mm, most likely as a result of similar environmental characteristics in the studied areas (Teacă et al., 2020).

Our findings demonstrated that *M. palmata* harbors a distinct microbiome as compared to that of its habitat, which is consistent with other similar surveys on three sipunculid worms species (*Sipunculus nudus*, *Siphonosoma australe*, *Phascolosoma arcuatum*) from Beibu Gulf, Changhua River and Guangcun that showed a significantly lower microbial diversity as compared to that of their surrounding sediments (Li et al., 2023; Liu et al., 2023). The reported diversity of microorganisms associated with benthic invertebrates, such as worms, was generally lower as compared to its surrounding

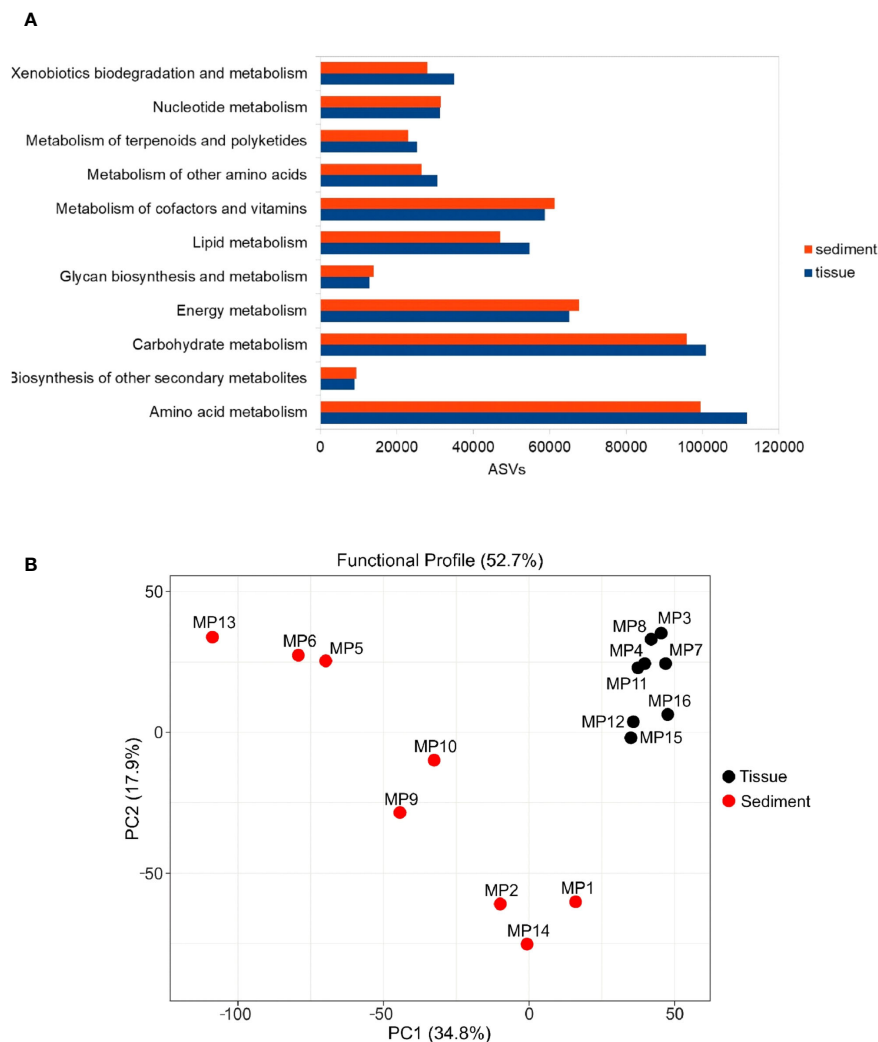


FIGURE 6

Predicted functional profile of bacterial communities from tissues and sediments based on the gene abundance from KEGG metabolic pathways. (A) Number of predicted functional genes based on amplicon sequence variants (ASVs) from the analyzed matrices (B) diversity of functional genes in the analyzed matrices based on PCA analysis.

sediments (Liu et al., 2023). Thus, the tube-dwelling organisms often create microenvironments with particular conditions which might favor the colonization with specific bacterial communities (Furst et al., 2021). Moreover, sediments belong to a more heterogeneous and diverse set of microhabitats, creating a range of niches that can support a wider diversity of bacterial communities (Liu et al., 2023). It has been previously demonstrated that nematodes and macroinvertebrates contributed to the dynamics of bacterial populations (De Mesel et al., 2004; Plante et al., 2022). Free-living nematodes, mainly those inhabiting the rich organic sediments, are non-selective or selective deposit bacterivorous feeders that excrete mineral or readily mineralizable forms that otherwise would have been locked up in the microbial biomass after nutrients ingestion, which exceeds in general the requirements of nematodes (Bonaglia et al., 2014). Moreover, their mucus was shown to stimulate the nitrogen production which, in turn, provided substrate for microorganisms' activity and growth (Moens et al., 2005). In

contrast, macrozoobenthic deposit feeders processed large volumes of sediment. Recent studies showed that the selective and non-selective deposit feeder nematodes and macrozoobenthic species were the dominant species, both as diversity and abundance, of habitats directly impacted by the Danube's inputs (Mureșan and Teacă, 2019; Teacă et al., 2020). Bioturbating organisms, such as *Melinna* sp., were reported to play a substantial role in the nitrogen cycling of sediments and exchanges between sediment and seawater (Laverock et al., 2011). This could be due to their burrow ventilation and particle reworking activities which lead to the redistribution of organic material and increase of sediment–water interface (Kristensen et al., 2012). Recent data indicated that the aerobic bacterial community of *M. palmata* habitats was more diverse as compared to that of the undisturbed sediments (Massé et al., 2019). Moreover, the mucus secreted by invertebrates appeared to stimulate the growth of bacterial and archaeal ammonia oxidizers, fostering a more abundant and distinct microbial community (Dale et al., 2019).

In *M. palmata* tissues, the orders Synechococcales, Rhodobacterales, Actinomarinales, Rhizobiales, Planctomycetales, Pirellulales, and Clostridiales showed a higher relative abundance, while sediments were dominated by Microtrichales, Anaerolineales, Caldilineales and Campylobacterales species. Synechococcales (Cyanobacteria) species that inhabit various ecological habitats are able to perform nitrogen fixation (Foster and O'Mullan, 2008) and create symbiotic relationships with other benthic invertebrates (Kumar and Kumar, 2020) such as sponges (Erwin and Thacker, 2008), ascidians (Tianero et al., 2015), and mollusks (Zhukova et al., 2022). In the current study, high content of Cyanobacteria taxa was found in shallow water sediments strongly influenced by the Danube inputs, at low dissolved oxygen levels. As photoautotrophic primary producers, they contribute to sediment enrichment with organic matter, while reducing the levels of atmospheric and hydrospheric carbon dioxide and bicarbonate (Golubic et al., 2000). In addition, *Synechococcus* species were found associated with sipunculan worms, which might be an important food source for these species (Li et al., 2023; Liu et al., 2023). Therefore, the prevalence of these microorganisms in the *M. palmata* tissues might be also linked to the dietary requirements of this invertebrate. As deposit-feeding organisms, they acquire substantial amounts of sediment, potentially incorporating organic debris and microbes along with it (Lopez and Levinton, 1987). Furthermore, frequent algal blooms in the Danube influence area could affect the sea water microbiome during summer (Raport privind starea mediului in Romania in anul 2019, 2020). Due to this phenomenon, the occurrence of phylum Planctomycetota, represented in tissues by phylotypes belonging to orders Planctomycetales and Pirellulales, was also expected. These bacteria able to use polysaccharides as carbon and energy sources, were also detected in other marine organisms such as sponges (Kallscheuer et al., 2020), fish (Kormas et al., 2022), and other polychaete (Liu et al., 2023).

The presence of Rhodobacterales and Rhizobiales taxa belonging to phylum Proteobacteria could be associated with their involvement in the carbon cycling, being able to assimilate glycolate, one of the most abundant organic carbon sources in the ocean (Von Borzyskowski et al., 2019). Rhodobacterales representatives were identified in different invertebrate species such as *Capitella* sp. and its surrounding organic-enriched sediments (Kunihiro et al., 2011). In the case of *M. palmata*, the prevalence of this group could be associated with its specific habitat represented by rich organic sediments (Buçe et al., 2020; Teacă et al., 2020), suggesting the possible involvement in decomposing and incorporating the organic matter within the organically enriched sediments. Rhodobacterales were positively correlated with some of the most abundant organic pollutants from sediments such as polycyclic aromatic hydrocarbons (PAHs) (Rodríguez et al., 2021). These compounds were detected in high concentrations in benthic fish populating the Romanian Black Sea coast (Damir et al., 2022) that feed also with *Melinna*, which could indicate the functional role of Rhodobacterales within tissues. Moreover, Anaerolineales order (Chloroflexi) that was higher represented in sediments has been reported as highly abundant in polluted sediments (Rodríguez et al., 2021). Therefore, these bacteria may be used as bioindicators of high levels of particular

pollutants. Moreover, some invertebrates (i.e. the marine polychaete *Meganerilla bactericoll*) were reported to obtain bioavailable nitrogen from symbioses with diazotrophs such as Rhizobiales (Summers et al., 2013) by temporary or permanent intracellular interactions with symbionts passed between generations (Fiore et al., 2010). Also, the higher presence of Clostridiales in *Melinna* tissues was in accordance with the previously reported dominance of Firmicutes taxa in the gut microbiome of several marine invertebrates (Priscilla et al., 2022).

A high representation of Actinomarinales in *Melinna* tissue could be due to the adaptation of some of Actinobacteria taxa to colonize marine organisms such as sponges, molluscs, and polychaete tubes, constituting important sources for natural products with pharmaceutical applications (Konig et al., 2006; Fuirst et al., 2021). Meanwhile, the order Microtrichales of Actinobacteria showed a higher relative abundance within sediments. A recent study (Miksch et al., 2021) revealed that members of these heterotroph bacteria, along with Actinomarinales, inhabit muddy bottoms, suggesting their putative involvement in the carbon mineralization processes. The occurrence of Campylobacterales might be related to the low dissolved oxygen concentrations of the study area (Table 2), which is in line with other reports of their presence in marine sediments, usually in habitats characterized by low oxygen/sulfide ratios (Wirsen et al., 2002).

Based on the 16S rRNA gene sequence data obtained, the TAX4FUN tool was used for predicting the functional profiles of bacterial communities associated with the polychaete and sediments, while many questions are raised in the ecology of this ecosystem requiring information on the community function in addition to their taxonomic composition. However, the accuracy of this approach depends on the available genomic information from public databases, which, in many cases, do not represent the microorganisms of the investigated ecosystem (Wemheuer et al., 2020). In addition, the approach used in our survey cannot differentiate the DNA sequences of live and dead organisms, which may impact the accurate inference of the metabolic profile of the analyzed microbial communities, with consequential ecological implications (Wang et al., 2023).

Although the predicted functional profile did not reflect the taxonomic differences found between the communities associated with the polychaete and sediments, the deduced metabolic profile of the *M. palmata* bacterial community was in accordance with previous data demonstrating that several marine bacteria play a significant role in amino acid cycling and utilization (Mudryk et al., 2005; Wünsch et al., 2019). In this context, antimicrobial peptides were isolated from various marine invertebrates such as the worms *Arenicola marina* (Ovchinnikova et al., 2004) and *Nereis diversicolor* (Tasiemski et al., 2007), and from the oyster *Magallana gigas* (Zhang et al., 2018). The current investigation also evidenced the amino acid metabolism as the dominant function among bacteria colonizing both matrices. The dominant species identified in *M. palmata* tissue belonging to Rhodobacterales and Synechococcales are known to be involved in the cofactors metabolism, being capable to synthesize thiamine (vitamin B1), riboflavin (vitamin B2) and cobalamin (vitamin B12) (Cooper et al., 2018; Mills et al., 2020). Moreover, representatives of

Verrucomicrobiota, mainly present in *Melinna* tissues, could play an important role in nutrient cycling, with putative applicative potential in biotechnologies (Cardman et al., 2014), and represent good candidates for production of secondary metabolites and exopolysaccharides (EPS) (Feng et al., 2021).

The higher prevalence of genes involved in carbohydrate, amino acid, and lipid metabolism within tissues could suggest an enhanced capacity for nutrient processing, thereby contributing to the energy metabolism of the polychaete. This metabolic capacity likely plays a crucial role in supporting the organism's growth, reproduction, and other physiological processes. Previous studies indicated that genes associated with terpenoid and polyketide metabolism are frequently linked to the production of secondary metabolites, which serve various ecological functions such as defense against predators or competition with other organisms (Osborn, 2010). Also, microorganisms such as bacteria and fungi have distinct properties that allow them to metabolize xenobiotic substances either partially or entirely in various ecosystems (Migliani et al., 2022). Therefore, the presence of genes involved in xenobiotics biodegradation and metabolism suggests that the polychaete may have evolved a strategy for detoxification and tolerance to potentially harmful substances and expression of these genes could be a response to exposure to pollutants present in sediments.

The current data revealed that *M. palmata* harbors a distinct but significantly lower bacterial diversity as compared with its surrounding sediments, with no prominent differences between the communities along the depth gradient of their habitat. Phylum Proteobacteria dominated the tissue-colonizing bacteria, while Actinobacteriota prevailed in the sediment communities. This investigation showed that bacterial communities colonizing the invertebrate and its surrounding sediments are involved in various metabolic processes, from biosynthesis to degradation of different xenobiotic substances. Overall, this first characterization of the *M. palmata* microbiome can serve as a starting point for revealing the role of associated bacterial communities in the polychaete metabolism and their interchange dynamics within marine habitats.

## Data availability statement

The original contributions presented in the study are publicly available. This data can be found here: <https://www.ncbi.nlm.nih.gov/bioproject/PRJNA923146/>.

## Ethics statement

The manuscript presents research on animals that do not require ethical approval for their study.

## Author contributions

SM: Conceptualization, Formal Analysis, Investigation, Methodology, Writing – original draft. PL: Data curation, Formal

Analysis, Software, Writing – original draft. TB: Funding acquisition, Investigation, Methodology, Resources, Writing – review & editing. MM: Investigation, Resources, Writing – original draft. AT: Investigation, Software, Writing – review & editing. CP: Conceptualization, Funding acquisition, Methodology, Project administration, Supervision, Writing – original draft.

## Funding

The author(s) declare financial support was received for the research, authorship, and/or publication of this article. The study was financially supported by the UEFISCDI ERANET-MARTERA-MOBILTOX-2-224/2021 grant and PNCDI III AMBI AQUA no. 23PFE grant, the Romanian Academy project RO1567-IBB05/2022, the Romanian Ministry of Research CORE Programme project PN 23300202; the European Union Horizon Europe project MARCO-BOLO, grant agreement no. 101082021, the European Union H2020 project DOORS, grant agreement no. 101000518, and the European Commission POIM project SMIS Code 123322, contract no. 253/18.06.201.

## Acknowledgments

The authors thank Lavinia Iancu for technical support.

## Conflict of interest

The authors declare that the research was conducted in the absence of any commercial or financial relationships that could be construed as a potential conflict of interest.

The author(s) declared that they were an editorial board member of Frontiers, at the time of submission. This had no impact on the peer review process and the final decision.

## Publisher's note

All claims expressed in this article are solely those of the authors and do not necessarily represent those of their affiliated organizations, or those of the publisher, the editors and the reviewers. Any product that may be evaluated in this article, or claim that may be made by its manufacturer, is not guaranteed or endorsed by the publisher.

## Supplementary material

The Supplementary Material for this article can be found online at: <https://www.frontiersin.org/articles/10.3389/fmars.2023.1279849/full#supplementary-material>



## References

- Abdelmohsen, U. R., Bayer, K., and Hentschel, U. (2014). Diversity, abundance and natural products of marine sponge-associated actinomycetes. *Nat. Prod. Rep.* 31, 381–399. doi: 10.1039/C3NP70111E
- Băcescu, M., Müller, G., and Gomoiu, M. T. (1971). Cercetări de ecologie bentală în Marea Neagră. *Analiza cantitativă calitativă și comparată faunei bentală pontice. Ecologie marina.* 4, 1–357.
- Bonaglia, S., Nascimento, F. J. A., Bartoli, M., Kiawonn, I., and Bruchert, V. (2014). Meiofauna increases bacterial denitrification in marine sediments. *Nat. Commun.* 5, 5133. doi: 10.1038/ncomms6133
- Bordenstein, S. R., and Theis, K. R. (2015). Host biology in light of the microbiome: ten principles of holobionts and hologenomes. *PLoS Biol.* 13, e1002226. doi: 10.1371/journal.pbio.1002226
- Boucher, D., Jardillier, L., and Debroas, D. (2006). Succession of bacterial community composition over two consecutive years in two aquatic systems: a natural lake and a lake-reservoir. *FEMS Microbiol. Ecology.* 55 (1), 79–97. doi: 10.1111/j.1574-6941.2005.00011.x
- Bryukhanov, A. L., Korneeva, V. A., and Pimenov, N. V. (2015). Detection of anaerobic sulfate reducing bacteria in oxygen containing upper water layers of the black and baltic seas. *Moscow Univ. Biol. Sci. Bull.* 70 (4), 184–188. doi: 10.3103/S0096392515040057
- Bucșe, A., Vasiliu, D., Balan, S., Parvulescu, O. C., and Dobre, T. (2020). Heavy metal spatial distribution and pollution assessment in the surface sediments of the north – western black sea shelf. *Rev. Chim.* 71 (4), 155–170. doi: 10.37358/Rev.Chim.1949
- Burkhardt, W., Watkins, W. D., and Rippey, S. R. (1992). Seasonal effects on accumulation of microbial indicator organisms by *Mercenaria mercenaria*. *Appl. Environ. Microbiol.* 58, 826–831. doi: 10.1128/aem.58.3.826-831.1992
- Callahan, B. J., Mcmurdie, P. J., Rosen, M. J., Han, A. W., Johnson, A. J. A., and Holmes, S. P. (2016). DADA2: High-resolution sample inference from Illumina amplicon data. *Nat. Methods* 13, 581–583. doi: 10.1038/nmeth.3869
- Cardman, Z., Arnosti, C., Durbin, A., Ziervogel, K., Cox, C., Steen, A. D., et al. (2014). *Verrucomicrobia* are candidates for polysaccharide-degrading bacterioplankton in an arctic fjord of Svalbard. *Appl. Environ. Microbiol.* 80 (12), 3749–3756. doi: 10.1128/AEM.00899-14
- Conway, N. M., Howes, B. L., McDowell Capuzzo, J. E., Turner, R. D., and Cavanaugh, C. M. (1992). Characterization and site description of *Solemya borealis* (Bivalvia; Solemyidae), another bivalve-bacteria symbiosis. *Mar. Biol.* 112, 601–613. doi: 10.1007/BF00346178
- Coolen, M. J. L., and Shtereva, G. (2009). Vertical distribution of metabolically active eukaryotes in the water column and sediments of the Black Sea. *FEMS Microbiology Ecology* 70(3):525–39. doi: 10.1111/j.1574-6941.2009.00756.x
- Cooper, M. B., Kazamia, E., Helliwell, K. E., Kudahl, U. J., Sayer, A., Wheeler, G. L., et al. (2018). Cross-exchange of B-vitamins underpins a mutualistic interaction between *Ostreococcus tauri* and *Dinoroseobacter shibae*. *ISME J.* 13 (2), 334–345. doi: 10.1038/s41396-018-0274-y
- Costas-Selas, C., Martínez-García, S., Logares, R., Hernández-Ruiz, M., and Teira, E. (2022). Role of bacterial community composition as a driver of the small-sized phytoplankton community structure in a productive coastal system. *Microb. Ecol.* 86 (2), 777–794. doi: 10.1007/s00248-022-02125-2
- Dale, H., Taylor, J. D., Solan, M., Lam, P., and Cunliffe, M. (2019). Polychaete mucopolysaccharide alters sediment microbial diversity and stimulates ammonia-oxidising functional groups. *FEMS Microbiol. Ecol.* 95 (2), 1. doi: 10.1093/femsec/fiy234
- Damir, N. A., Coatu, V., Pantea, E. D., GalaȚchi, M., Botez, E., and Birghilă, S. (2022). Assessment of polycyclic aromatic hydrocarbons content in marine organisms of commercial interest from the Romanian black sea coast. *Polycyclic Aromatic Compounds.* 42 (10), 7595–7606. doi: 10.1080/10406638.2021.2006243
- Dang, H., and Lovell, C. R. (2016). Microbial surface colonization and biofilm development in marine. *Microbiol. Mol. Biol. Rev.* 80, 91–138. doi: 10.1128/MMBR.00037-15
- Defer, D., Desriac, F., and Henry, J. (2013). Antimicrobial peptides in oyster hemolymph: the bacterial connection. *Fish Shellfish Immunol.* 34 (6), 1439–1447. doi: 10.1016/j.fsi.2013.03.357
- De Mesel, I., Derycke, S., Moens, T., van der Gucht, K., Vincx, M., and Swings, J. (2004). Top-down impact of bacterivorous nematodes on the bacterial community structure: a microcosm study. *Environ. Microbiol.* 6 (7), 733–744. doi: 10.1111/j.1462-2920.2004.00610.x
- Desriac, F., Le Chevalier, P., and Brillet, B. (2014). Exploring the hologenome concept in marine bivalvia: haemolymph microbiota as a pertinent source of probiotics for aquaculture. *FEMS Microbiol. Lett.* 350, 107–116. doi: 10.1111/1574-6968.12308
- Eisen, J. A., Smith, S. W., and Cavanaugh, C. M. (1992). Phylogenetic Relationships of Chemoautotrophic Bacterial Symbionts of *Solemya velum* Say (Mollusca: Bivalvia) determined by 16S rRNA Gene Sequence Analysis. *J. Bacteriol.* 174 (10), 3416–3421. doi: 10.1128/jb.174.10.3416-3421.1992
- Erwin, P. M., López-Legentil, S., and Schuhmann, P. W. (2010). The pharmaceutical value of marine biodiversity for anti-cancer drug discovery. *Ecol. Economics* 70 (2), 445–451. doi: 10.1016/j.ecolecon.2010.09.030
- Erwin, P. M., and Thacker, R. W. (2008). Cryptic diversity of the symbiotic cyanobacterium *Synechococcus spongiarum* among sponge hosts. *Mol. Ecol.* 17 (12), 2937–2947. doi: 10.1111/j.1365-294X.2008.03808.x
- Fauchald, K., and Jumars, P. A. (1979). : The diet of worms: a study of polychaete feeding guilds. *Oceanogr. Mar. Biol. Ann. Rev.* 17, 193–284.
- Felbeck, H., and Distel, L. D. (2004). “Prokaryotic symbionts of marine invertebrates,” in *The prokaryotes: An evolving electronic resource for the microbiological community*. Ed. M. Dworkin (New York: Springer-Verlag).
- Feng, X., Gong, Y., Ye, M. Q., and Du, Z. J. (2021). Antibiotic Modulation of Capsular Exopolysaccharide in *Pelagicoccus enzymogenes* sp. nov. Isolated From Marine Sediment. *Front. Mar. Sci.* 8. doi: 10.3389/fmars.2021.655735
- Fiore, C. L., Jarett, J. K., Olson, N. D., and Lesser, M. P. (2010). Nitrogen fixation and nitrogen transformations in marine symbioses. *Trends Microbiol.* 18 (10), 455–463. doi: 10.1016/j.tim.2010.07.001
- Foster, R. A., and O’Mullan, G. D. (2008). “Nitrogen-fixing and nitrifying symbioses in the marine environment,” in *Nitrogen in the Marine Environment*. Eds. D. G. Capone, D. A. Bronk, M. R. Mulholland and E. J. Carpenter (London: Academic Press Inc.), 1197–1218.
- Fuirst, M., Ward, C. S., Schwaner, C., Diana, Z., Schultz, T., and Rittschof, D. (2021). Compositional and functional microbiome variation between tubes of an intertidal polychaete and surrounding marine sediments. *Front. Mar. Sci.* 8. doi: 10.3389/fmars.2021.656506
- Gilbertson, W. W., Gilbertson Solan, M., and Prosser, J. I. (2012). Differential effects of microorganism–invertebrate interactions on benthic nitrogen cycling. *FEMS Microbiol. Ecol.* 82, 11–22. doi: 10.1111/j.1574-6941.2012.01400.x
- Glaubit, S., Labrenz, M., Jost, G., and Jurgens, K. (2010). Diversity of active chemolithoautotrophic prokaryotes in the sulfidic zone of a Black Sea pelagic redox cline as determined by rRNA-based stable isotope probing. *FEMS Microbiol. Ecol.* 74 (1), 32–41. doi: 10.1111/j.1574-6941.2010.00944.x
- Goffredi, S. K., Johnson, S. B., and Vrijenhoek, R. C. (2007). Genetic diversity and potential function of microbial symbionts associated with newly discovered species of *Osedax* polychaete worms. *Appl. Environ. Microbiol.* 73 (7), 2314–2323. doi: 10.1128/AEM.01986-06
- Golubic, S., Seong-Joo, L., and Browne, K. M. (2000). “Cyanobacteria: Architects of Sedimentary Structures,” in *Microbial Sediments*. Eds. R. E. Riding and S. M. Awramik (Berlin: Springer-Verlag).
- Gomoiu, M. T. (1982). On the populations of *Melinna palmata* Grube at the Romanian littoral of the Black Sea. *Cercetari Marine IRCM.* 15, 115–131.
- Goodfellow, M., and Williams, S. T. (1983). Ecology of Actinomycetes. *Annual Review of Microbiology.* 37, 189–216. doi: 10.1146/annurev.mi.37.100183.001201
- Graca, A. P., Bondoso, J., Gaspar, H., Xavier, J. R., Monteiro, M. C., de la Cruz, M., et al. (2013). Antimicrobial activity of heterotrophic bacterial communities from the Marine Sponge *Erylus discophorus* (Astrophorida, Geodiidae). *PLoS One* 8 (11), e78992. doi: 10.1007/s00436-002-0729-x
- Graczyk, T. K., Conn, D. B., Marcogliese, D. J., Graczyk, H., and DeLaFontaine, Y. (2003). Accumulation of human waterborne parasites by zebra mussels (*Dreissena polymorpha*) and Asian freshwater clams (*Corbicula fluminea*). *Parasitol Res.* 89 (2), 107–112. doi: 10.1007/s00436-002-0729-x
- Guo, R., Ma, X., Zhang, J., Liu, C., Thu, C. A., Win, T. N., et al. (2022a). Microbial community structures and important taxa across oxygen gradients in the Andaman Sea and eastern Bay of Bengal epipelagic waters. *Front. Microbiol.* 13. doi: 10.3389/fmicb.2022.1041521
- Guo, Y., Wu, C., and Sun, J. (2022b). Pathogenic bacteria significantly increased under oxygen depletion in coastal waters: A continuous observation in the central Bohai Sea. *Front. Microbiol.* 13. doi: 10.3389/fmicb.2022.1035904.rft
- Hochstein, R., Zhang, Q., Sadowsky, M. J., and Forbes, V. E. (2019). The deposit feeder *Capitella teleta* has a unique and relatively complex microbiomes likely supporting its ability to degrade pollutants. *Sci. Total Environ.* 670, 547–554. doi: 10.1016/j.scitotenv.2019.03.255
- Hunt, O. (1925). The food of the bottom fauna of the plymouth fishing grounds. *J. Mar. Biol. Assoc. United Kingdom.* 13 (3), 560–599. doi: 10.1017/S0025315400008079
- Iancu, L., Carter, D. O., Junkins, E. N., and Purcarea, C. (2015). Using bacterial and necrophagous insect dynamics for postmortem interval estimation during cold season: Novel case study in Romania. *Forensic Sci. Int.* 254, 106–117. doi: 10.1016/j.forsciint.2015.07.024
- ICPDR (2004). *The Danube River Basin District. River basin characteristics, impact of human activities and economic analysis required under Article 5, Annex II and Annex III, and inventory of protected areas required under Article 6, Annex IV of the EU Water Framework Directive, (2000/60/EC) Part A – Basin-wide overview Short: “Danube Basin*

Analysis (WFD Roof Report 2004). (International Commission for the Protection of the Danube River. Vienna International Centre D0412.)

Jørgensen, B. B., Fossing, H., Wirsén, C. O., and Jannasch, H. W. (1991). Sulfide oxidation in the anoxic Black Sea chemocline. International Commission for the Protection of the Danube River. Vienna International Centre D0412. *Deep-Sea Res.* 38, S1083–S1103. doi: 10.1016/S0198-0149(10)80025-1

Kallscheuer, N., Wiegand, S., Heuer, A., Rensink, S., Boersma, A. S., Jogler, M., et al. (2020). *Blastopirellula retiformator* sp. nov. isolated from the shallow-sea hydrothermal vent system close to Panarea Island. *Antonie Van Leeuwenhoek*. 113 (12), 1811–1822. doi: 10.1007/s10482-019-01377-2

Kelman, D., Kashman, Y., Hill, R., Rosenberg, E., and Loya, Y. (2009). Chemical warfare in the sea: the search for antibiotics from red sea corals and sponges. *Pure Appl. Chem.* 81 (6), 1113–1121. doi: 10.1351/PAC-CON-08-10-07

Ketchum, R. N., Smith, E. G., Vaughan, G. O., Phippen, B. L., McParland, D., Al-Mansoori, N., et al. (2018). DNA extraction method plays a significant role when defining bacterial community composition in the marine invertebrate *echinometra mathaei*. *Front. Mar. Sci.* 5. doi: 10.3389/fmars.2018.00255

Konhäuser, K. O., Hao, W., Li, U., Gunten, K., Bishop, B. A., Alessi, D. S., et al. (2020). *Diopatra cuprea* worm burrow parchment: a cautionary tale of infaunal surface reactivity. *Lethaia*. 53, 47–61. doi: 10.1111/let.12335

König, G. M., Kehraus, S., Seibert, S. F., Abdel-Lateff, A., and Müller, D. (2006). Natural products from marine organisms and their associated microbes. *ChembioChem*. 7 (2), 229–238. doi: 10.1002/cbic.200500087

Kormas, K., Nikouli, E., Kousteni, V., and Damalas, D. (2022). Midgut bacterial microbiota of 12 fish species from a marine protected area in the aegean sea (Greece). *Microb. Ecol.* 86, 1405–1415. doi: 10.1007/s00248-022-02154-x

Kristensen, E., Penha-Lopes, G., Delefosse, M., Valdemarsen, T., Quintana, C. O., and Banta, G. T. (2012). What is bioturbation? The need for a precise definition for fauna in aquatic sciences. *Mar. Ecol. - Prog. Series*. 446, 285–302. doi: 10.3354/meps09506

Kumar, A., and Kumar, P. A. (2020). “Database resources for cyanobacterial research,” in *Advances in Cyanobacterial Biology*. Eds. P. S. Kumar, A. Kumar, V. S. Kumar and A. S. Kumar (London: Academic Press), 47–54. doi: 10.1016/B978-0-12-819311-2.00004-8

Kunihiro, T., Takasu, H., Miyazaki, T., Uramoto, Y., Kinoshita, K., Yodnarasri, S., et al. (2011). Increase in Alphaproteobacteria in association with a polychaete, *Capitella* sp., in the organically enriched sediment. *ISME J.* 5 (11), 1818–1831. doi: 10.1038/ismej.2011.57

Kuo, J., Yang, Y.-T., Lu, M.-C., Wong, T.-Y., Sung, P.-J., and Huang, Y.-S. (2019). Antimicrobial activity and diversity of bacteria associated with Taiwanese marine sponge *Theonella swinhoei*. *Ann. Microbiol.* 69, 253–265. doi: 10.1007/s13213-018-1414-3

Laufer, C., Hamady, M., Knight, R., and Fierer, N. (2009). Pyrosequencing based assessment of soil pH as a predictor of soil bacterial community structure at the continental scale. *Appl Environ Microbiol.* 75 (15), 5111–5120. doi: 10.1128/AEM.00335-09

Laverock, B., Gilbert, J. A., Tait, K., Osborn, A. M., and Widdicombe, S. (2011). Bioturbation: Impact on the marine nitrogen cycle. *Biochem. Soc. Trans.* 39 (1), 315–320. doi: 10.1042/BST0390315

Leite, L., Jude-Lemelleur, F., Raymond, N., Henriques, I., Garabetian, F., and Alves, A. (2017). Phylogenetic diversity and functional characterization of the Manila clam microbiota: a culture-based approach. *Environ. Sci. Pollut. Res.* 24, 21721–21732. doi: 10.1007/s11356-017-9838-z

Leloup, J., Loy, A., Knab, N. J., Borowski, C., Wagner, M., and Jørgensen, B. B. (2007). Diversity and abundance of sulfate-reducing microorganisms in the sulfate and methane zones of a marine sediment, Black Sea. *Environ. Microbiol.* 9 (1), 131–142. doi: 10.1111/j.1462-2920.2006.01122.x

Li, J., Chen, S., Wu, P., Zhu, C., Hu, R., Li, T., et al. (2023). Insights into the relationship between intestinal microbiota of the aquaculture worm *Sipunculus nudus* and surrounding sediments. *Fishes*. 8 (1), 32. doi: 10.3390/fishes8010032

Lin, H., Eggesbo, M., and Peddada, S. D. (2022). Linear and nonlinear correlation estimators unveil undescribed taxa interactions in microbiome data. *Nat. Commun.* 13 (1), 4946. doi: 10.1038/s41467-022-32243-x

Liu, C., Liu, C., Gao, F., Wang, A., Wang, H., Yang, Y., et al. (2023). Composition of Particulate Matter and Bacterial Community in Gut Contents and Surrounding Sediments of Three Sipunculan Species (*Sipuncosoma australe*, *Phascolosoma arcuatum*, and *Sipunculus nudus*). *Int. J. Mol. Sci.* 24 (6), 6001. doi: 10.3390/ijms24066001

Lo Giudice, A., and Rizzo, C. (2022). Bacteria associated with benthic invertebrates from extreme marine environments: promising but underexplored sources of biotechnologically relevant molecules. *Mar. Drugs* 20 (10), 617. doi: 10.3390/md20100617

Lopez, G. R., and Levinton, J. S. (1987). Ecology of deposit-feeding animals in marine sediments. *Q. Rev. Biol.* 62 (3), 235–260. doi: 10.1086/415511

Lu, Y., Zhou, G., Ewald, J., Pang, Z., Shiri, T., and Xia, J. (2023). MicrobiomeAnalyst 2.0: comprehensive statistical, functional and integrative analysis of microbiome data. *Nucleic Acids Res.* 51 (W1), W310–W318. doi: 10.1093/nar/gkad407

Mare, M. F. (1942). A study of a marine benthic community with special reference to the micro-organisms. *J. Mar. Biol. Assoc. UK*. 25 (3), 517–554. doi: 10.1017/S0025315400055132

Marino, A., Lombardo, L., Fiorentino, C., Orlandella, B., Monticelli, L., Nostro, A., et al. (2005). Uptake of *Escherichia coli*, *Vibrio cholerae* non-O1 and *Enterococcus durans* by, and depuration of mussels (*Mytilus galloprovincialis*). *Int. J. Food Microbiol.* 99 (3), 281–286. doi: 10.1016/j.ijfoodmicro.2004.09.003

Markande, A. R., Mikaelyan, A., Bhusan Nayak, B., Patel, K. D., Vachharajani, N. B., Vennila, A., et al. (2014). Analysis of midgut bacterial community structure of *neanthes chilkaensis* from polluted mudflats of Gorai, Mumbai, India. *Adv. Microbiol.* 4, 906–918. doi: 10.4236/aim.2014.413101

Martin, M. (2011). Cutadapt removes adapter sequences from high-throughput sequencing reads. *EMBnet. J.* 17, 10–12. doi: 10.14806/ej.17.1.200

Martiny, J. B. H., Bohannan, B. J. M., Brown, J. H., Colwell, R. K., Fuhrman, J. A., Green, J. L., et al. (2006). Microbial biogeography: putting microorganisms on the map. *Nat. Rev. Microbiol.* 4 (2), 102–112. doi: 10.1038/nrmicro1341

Massé, C., Garabetian, F., Deflandre, B., Maire, O., Costes, L., Mes-mer-Dudons, N., et al. (2019). Feeding ethology and surface sediment reworking by the ampharetid polychaete *Melinna palmata* Grube 1870: Effects on sediment characteristics and aerobic bacterial community composition. *J. Exp. Mar. Biol. Ecology*. 512, 63–77. doi: 10.1016/j.jembe.2018.12.009

Mcfall-Ngai, M., Hadfield, M. G., Bosch, T. C., Carey, H. V., Domazet-Lošo, T., and Douglas, A. E. (2013). Animals in a bacterial world, a new imperative for the life sciences. *Proc. Nat. Acad. Sci. U.S.A.* 110 (9), 3229–3236. doi: 10.1073/pnas.1218525110

McMurdie, P. J., and Holmes, S. (2013). phyloseq: An R package for reproducible interactive analysis and graphics of microbiome census data. *PLoS One* 8 (4), e61217. doi: 10.1371/journal.pone.0061217

Migliani, R., Parveen, N., Kumar, A., Ansari, M. A., Khanna, S., Rawat, G., et al. (2022). Degradation of xenobiotic pollutants: an environmentally sustainable approach. *Metabolites*. 12 (9), 818. doi: 10.3390/metabo12090818

Mikhailov, V. N., and Mikhailova, M. V. (2008). “River mouths,” in *The Black Sea Environment: The Handbook of Environmental Chemistry*, vol. 5. Eds. A. G. Kostianoy and A. N. Kosarev (Berlin: Springer), 91–133.

Miksch, S., Meiners, M., Meyerdieks, A., Probandt, D., Wegener, G., Titschack, J., et al. (2021). Bacterial communities in temperate and polar coastal sands are seasonally stable. *ISME Commun.* 1, 29. doi: 10.1038/s43705-021-00028-w

Mills, L. A., McCormick, A. J., and Lea-Smith, D. J. (2020). Current knowledge and recent advances in understanding metabolism of the model cyanobacterium *Synechocystis* sp. PCC 6803. *Biosci. Rep.* 40 (4), BSR20193325. doi: 10.1042/BSR20193325

Mishra, P., Singh, U., Pandey, C. M., Mishra, P., and Pandey, G. (2019). Application of student's t-test, analysis of variance, and covariance. *Ann. Card Anaesth.* 22 (4), 407–411. doi: 10.4103/aca.ACA\_94\_19

Moens, T., Santos, G. A. P., Thompson, F., Swings, J., Fonsêca-Genevois, V., Vincx, M., et al. (2005). Do nematode mucus secretions affect bacterial growth? *Aquat. Microb. Ecol.* 40, 77–83. doi: 10.3354/ame040077

Mudryk, Z. J., Podgórska, B., and Dwulit, M. (2005). Bacterial utilization of amino acids and carbohydrates in a marine beach. *Baltic Coast. Zone*. 9, 29–41.

Mureșan, M., Teacă, A., Popa, A., and Begun, T. (2019). Free-living marine nematodes community structural changes within a post-dredging site at the Romanian shelf. *J. Environ. Prot. Ecology*. 20 (2), 753–760.

Mureșan, M., and Teacă, A. (2019). The free-living nematode community structure within the Romanian circalittoral habitats. *Geo-Eco-Marina*. 25, 7–13. doi: 10.5281/zenodo.3607208

Muriel-Millán, L. F., Millán-López, S., and Pardo-López, L. (2021). Biotechnological applications of marine bacteria in bioremediation of environments polluted with hydrocarbons and plastics. *Appl. Microbiol. Biotechnol.* 105 (19), 7171–7185. doi: 10.1007/s00253-021-11569-4

Musella, M., Wathsala, R., Tavella, T., Rampelli, S., Barone, M., Palladino, G., et al. (2020). Tissue-scale microbiota of the Mediterranean mussel (*Mytilus galloprovincialis*) and its relationship with the environment. *Sci. Total Environment*. 717, 137209. doi: 10.1016/j.scitotenv.2020.137209

Neave, M. J., Streten-Joyce, C., Glasby, C. J., McGuinness, K. A., Parry, D. L., and Gibb, K. S. (2012). The bacterial community associated with the marine polychaete *Ophelina* sp. (Annelida: Opheliidae) is altered by copper and zinc contamination in sediments. *Microb. Ecol.* 63, 639–650. doi: 10.1007/s00248-011-9966-9

Onishchenko, O. M., and Kiprianova, E. A. (2006). *Shewanella* genus bacteria isolated from the Black Sea water and molluscs. *Mikrobiol. Z.* 68 (2), 12–21.

Osborn, A. (2010). Secondary metabolic gene clusters: evolutionary toolkits for chemical innovation. *Trends Genet.* 26 (10), 449–457. doi: 10.1016/j.tig.2010.07.001

Ovchinnikova, T. V., Aleshina, G. M., Balandin, S. V., Krasnosdembkaya, A. D., Markelov, M. L., Frolova, E. I., et al. (2004). Purification and primary structure of two isoforms of arenicin, a novel antimicrobial peptide from marine polychaeta *Arenicola marina*. *FEBS Lett.* 577 (1–2), 209–214. doi: 10.1016/j.febslet.2004.10.012

Panin, N., and Jipa, D. (2002). Danube river Sediment Input and its Interaction with the North-western Black Sea. *Estuar. Coast. Shelf Sci.* 54 (3), 551–562. doi: 10.1006/ecss.2000.0664

- Paul, V. J., and Ritson-Williams, R. (2008). Marine chemical ecology. *Nat. Prod. Rep.* 25 (4), 662–695. doi: 10.1039/b702742g
- Piel, J. (2004). Metabolites from symbiotic bacteria. *Nat. Prod. Rep.* 21, 519–538. doi: 10.1039/B703499G
- Plante, C. J., Hill-Spanik, K. M., and Emerson, R. (2022). Inputs don't equal outputs: bacterial microbiomes of the ingesta, gut, and feces of the keystone deposit feeder *Ilyanassa obsoleta*. *FEMS Microbiol. Ecol.* 99 (1), fiac152. doi: 10.1093/femsec/fiad010
- Pommier, T., Neal, P. R., Gasol, J. M., Coll, M., Acinas, S. G., and Pedrós-Alí, C. (2010). Spatial patterns of bacterial richness and evenness in the NW Mediterranean Sea explored by pyrosequencing of the 16S rRNA. *Aquat. Microb. Ecol.* 61 (3), 221–233. doi: 10.3354/ame01484
- Priscilla, L., Rajeev, M., Pandian, S. K., and Malathi, E. (2022). Gut associated culturable bacterial community in intertidal polychaete worms (Annelida: Polychaeta), their characterization and implications in captive shrimp aquaculture. *Regional Stud. Mar. Science.* 52, 102274. doi: 10.1016/j.rsma.2022.102274
- Raport privind starea mediului în România în anul 2019 (2020). *Agenția Națională pentru Protecția Mediului* (București: Ministerul Mediului).
- R Core Team (2023). *R: A Language and Environment for Statistical Computing* (Vienna, Austria: R Foundation for Statistical Computing). Available at: <https://www.R-project.org>.
- Rizzo, C., Michaud, L., Hörmann, B., Gerçe, B., Sylatck, C., Hausmann, R., et al. (2013). Bacteria associated with sabellids (Polychaeta: Annelida) as a novel source of surface active compounds. *Mar. pollut. Bulletin.* 70 (1–2), 125–133. doi: 10.1016/j.marpolbul.2013.02.020
- Rodríguez, J., Gallampos, C. M. J., Haglund, P., Timonen, S., and Rowe, O. (2021). Bacterial communities as indicators of environmental pollution by POPs in marine sediments. *Environ. pollut.* 268 (Pt A), 115690. doi: 10.1016/j.envpol.2020.115690
- Rosenberg, E., Koren, O., and Reshef, L. (2007). The role of microorganisms in coral health, disease and evolution. *Nat. Rev. Microbiol.* 5 (5), 355–362. doi: 10.1038/nrmicro1635
- Ross, K. S., Haite, N. E., and Kelly, K. F. (1990). Repeated freezing and thawing of peripheral blood and DNA in suspension: effects on DNA yield and integrity. *J. Med. Genet.* 27 (9), 569–570. doi: 10.1136/jmg.27.9.569
- Ruginescu, R., Lavin, P., Iancu, L., Menabit, S., and Purcarea, C. (2022). Bioprospecting for novel bacterial sources of hydrolytic enzymes and antimicrobials in the Romanian littoral zone of the black sea. *Microorganisms.* 10, 2468. doi: 10.3390/microorganisms10122468
- Schäfer, H., Ferdelman, T. G., Fossing, H., and Muyzer, G. (2007). Microbial diversity in deep sediments of the Benguela Upwelling System. *Aquat. Microb. Ecol.* 50 (1), 1–9. doi: 10.3354/ame01164
- Schippers, A., Kock, D., Höft, C., Köweker, G., and Siegert, M. (2012). Quantification of microbial communities in subsurface marine sediments of the Black Sea and off Namibia. *Frontiers in Microbiology.* 3. doi: 10.3389/fmicb.2012.00016
- Schmidt, E. W., Nelson, J. T., Rasko, D. A., Sudek, S., Eisen, J. A., Haygood, et al. (2005). Patellamide A and C biosynthesis by amicrocin-like pathway in *Prochloron* didemni, the cyanobacterial symbiont of *Lissoclinum patella*. *Proc. Natl. Acad. Sci. U.S.A.* 102, 7315–7320. doi: 10.1073/pnas.0501424102
- Schulz, H. N., Brinkhoff, T., Ferdelman, T. G., Mariné, M. H., Teske, A., and Jørgensen, B. B. (1999). Dense populations of a giant sulfur bacterium in Namibian shelf sediments. *Science.* 284 (5413), 493–495. doi: 10.1126/science.284.5413.493
- Sogin, M. L., Morrison, H. G., Huber, J. A., Welch, D. M., Huse, S. M., Neal, P. R., et al. (2006). Microbial diversity in the deepsea and the underexplored “rare biosphere”. *Proc. Natl. Acad. Sci. U.S.A.* 103 (32), 12115–12120. doi: 10.1073/pnas.0605127103
- Sorokin, Y. I., Sorokin, P. Y., Avdeev, V. A., Sorokin, D. Y., and Ilchenko, S. V. (1995). Biomass, production and activity of bacteria in the Black Sea, with special reference to chemosynthesis and the sulfur cycle. *Hydrobiologia.* 308, 61–76. doi: 10.1007/BF00037788
- Stevens, H., Brinkhoff, T., Rink, B., Vollmers, J., and Simon, M. (2007). Diversity and abundance of Gram positive bacteria in a tidal flat ecosystem. *Environ. Microbiol.* 9 (7), 1810–1822. doi: 10.1111/j.1462-2920.2007.01302.x
- Summers, M. M., Katz, S., Allen, E. E., and Rouse, G. W. (2013). Association of rhizobia with a marine polychaete. *Environ. Microbiol. Rep.* 5 (4), 492–498. doi: 10.1111/1758-2229.12043
- Takahashi, S., Tomita, J., Nishioka, K., Hisada, T., and Nishijima, M. (2014). Development of a prokaryotic universal primer for simultaneous analysis of bacteria and archaea using next-generation sequencing. *PLoS One* 9 (8), e105592. doi: 10.1371/journal.pone.0105592
- Tasiemski, A., Schikorski, D., Le Marrec-Croq, F., Pontoire-Van Camp, C., Boidin-Wichlacz, C., and Sautière, P. E. (2007). Hedistin: a novel antimicrobial peptide containing bromotryptophan constitutively expressed in NK cells-like of the marine annelid, *Nereis diversicolor*. *Dev. Comp. Immunol.* 31, 749–762. doi: 10.1016/j.dci.2006.11.003
- Teacă, A., Mureșan, M., Begun, T., Popa, A., and Ion, G. (2019). Marine benthic habitats within a physical disturbed site from the Romanian Coast of the Black Sea. *J. Environ. Prot. Ecology.* 20 (2), 723–732.
- Teacă, A., Mureșan, M., Menabit, S., Bucse, A., and Begun, T. (2020). Assessment of Romanian circalittoral soft bottom benthic habitats under Danube River influence. *Regional Stud. Mar. Sci.* 40, 101523. doi: 10.1016/j.rsma.2020.101523
- Tescari, S., Umgiesser, G., Ferrarin, C., and Stanica, A. (2006). Current circulation and sediment transport in the coastal zone in front of the Danube Delta. *Geo-Eco-Mar. (Coast. Zones Deltas).* 12, 5–16.
- Thamdrup, B., Rosselló-Mora, R., and Amann, R. (2000). Microbial manganese and sulfate reduction in Black Sea shelf sediments. *Appl. Environ. Microbiol.* 66 (7), 2888–2897. doi: 10.1128/AEM.66.7.2888-2897.2000
- Theis, K. R., Dheilly, N. M., Klassen, J. L., Brucker, R. M., Baines, J. F., and Bosch, T. C. G. (2016). Getting the hologenome concept right: An ecoevolutionary framework for hosts and their microbiomes. *mSystems.* 1 (2), e00028–e00016. doi: 10.1128/mSystems.00028-16
- Thomas, T. R. A., Kavlekar, D. P., and Loka Bharathi, P. A. (2010). Marine drugs from sponge-microbe association—a review. *Mar. Drugs* 8 (4), 1417–1468. doi: 10.3390/md8041417
- Tianero, M. D. B., Kwan, J. C., Wyche, T. P., Presson, A. P., Koch, M., Barrows, L. R., et al. (2015). Species specificity of symbiosis and secondary metabolism in ascidians. *ISME J.* 9 (3), 615–628. doi: 10.1038/ismej.2014.152
- Todorova, V., and Konsulova, T. (2005). *Manual for Quantitative Sampling and Sample Treatment of Marine Soft-Bottom Macrozoobenthos* (PO Box 152, 9000 Varna, Bulgaria: Institute of Oceanology, Bulgarian Academy of Sciences). Available at: [www.blacksea-commission.org](http://www.blacksea-commission.org). 38 pp.
- Von Borzyskowski, L. S., Severi, F., Kruger, K., Hermann, L., Gilardet, A., Sippel, F., et al. (2019). Marine proteobacteria metabolize glycolate via the B-hydroxyaspartate cycle. *Nature* 575, 500–504. doi: 10.1038/s41586-019-1748-4
- Wang, Y., Thompson, K. N., Yan, Y., Short, M. I., Zhang, Y., Franzosa, E. A., et al. (2023). RNA-based amplicon sequencing is ineffective in measuring metabolic activity in environmental microbial communities. *Microbiome.* 11 (1), 1–15. doi: 10.1186/s40168-022-01449-y
- Webster, N. S., and Taylor, M. W. (2012). Marine sponges and their microbial symbionts: love and other relationships. *Environ. Microbiol.* 14 (2), 335–346. doi: 10.1111/j.1462-2920.2011.02460.x
- Wemheuer, F., Taylor, J. A., Daniel, R., Johnston, E., Meinicke, P., Thomas, T., et al. (2020). Tax4Fun2: prediction of habitat-specific functional profiles and functional redundancy based on 16S rRNA gene sequences. *Environ. Microbiome.* 15 (1), 1–12. doi: 10.1186/s40793-020-00358-7
- Wickham, H. (2016). *ggplot2: Elegant Graphics for Data Analysis* (New York, USA: Springer-Verlag), 260.
- Wickham, H., Averick, M., Bryan, J., Chang, W., McGowan, L. D., François, R., et al. (2019). Welcome to the tidyverse. *J. Open Source Software* 4 (43), 1686. doi: 10.21105/joss.01686
- Winand, R., Bogaerts, B., Hoffman, S., Lefevre, L., Delvoe, M., Braekel, J. V., et al. (2019). Targeting the second (Illumina) and third (Oxford Nanopore Technologies) Generation Sequencing Technologies. *Int. J. Mol. Sci.* 21 (1), 298. doi: 10.3390/ijms21010298
- Wirsén, C. O., Sievert, S. M., Cavanaugh, C. M., Molyneux, S. J., Ahmad, A., Taylor, L. T., et al. (2002). Characterization of an autotrophic sulfide-oxidizing marine Arcobacter sp. that produces filamentous sulfur. *Appl. Environ. Microbiol.* 68 (1), 316–325. doi: 10.1128/AEM.68.1.316-325.2002
- Wünsch, D., Trautwein, K., Scheve, S., Hinrichs, C., Feenders, C., Blasius, B., et al. (2019). Amino acid and sugar catabolism in the marine bacterium *phaeobacter inhibens* DSM 17395 from an energetic viewpoint. *Appl. Environ. Microbiol.* 27 (85(24)), e02095–e02019. doi: 10.1128/AEM.02095-19
- Zhang, Y., Cui, P., Wang, Y., and Zhang, S. (2018). Identification and bioactivity analysis of a newly identified defensin from the oyster *Magallana gigas*. *Dev. Comp. Immunol.* 85, 177–187. doi: 10.1016/j.dci.2018.04.014
- Zhang, X., Wei, W., and Tan, R. (2015). Symbionts, a promising source of bioactive natural products. *Sci. China Chem.* 58, 1097–1109. doi: 10.1007/s11426-015-5398-6
- Zhukova, N. V., Eliseikina, M. G., Balakirev, E. S., and Ayala, F. J. (2022). Multiple bacterial partners in symbiosis with the nudibranch mollusk *Rostanga alisae*. *Sci. Rep.* 12, 169. doi: 10.1038/s41598-021-03973-7
- Zilber-Rosenberg, I., and Rosenberg, E. (2008). Role of microorganisms in the evolution of animals and plants: the hologenome theory of evolution. *FEMS Microbiol. Rev.* 32 (5), 723–735. doi: 10.1111/j.1574-6976.2008.00123.x





## OPEN ACCESS

## EDITED BY

Zhiyong Li,  
Shanghai Jiao Tong University, China

## REVIEWED BY

Cara Fiore,  
Appalachian State University, United States  
Kumar Saurav,  
Academy of Sciences of the Czech Republic  
(ASCR), Czechia

## \*CORRESPONDENCE

Maria Costantini  
✉ maria.costantini@szn.it

RECEIVED 02 October 2023

ACCEPTED 20 December 2023

PUBLISHED 11 January 2024

## CITATION

Esposito R, Federico S, Sonnessa M, Reddel S, Bertolino M, Ruocco N, Zagami G, Giovine M, Pozzolini M, Guida M, Zupo V and Costantini M (2024) Characterizing the bacterial communities associated with Mediterranean sponges: a metataxonomic analysis. *Front. Microbiol.* 14:1295459. doi: 10.3389/fmicb.2023.1295459

## COPYRIGHT

© 2024 Esposito, Federico, Sonnessa, Reddel, Bertolino, Ruocco, Zagami, Giovine, Pozzolini, Guida, Zupo and Costantini. This is an open-access article distributed under the terms of the [Creative Commons Attribution License \(CC BY\)](https://creativecommons.org/licenses/by/4.0/). The use, distribution or reproduction in other forums is permitted, provided the original author(s) and the copyright owner(s) are credited and that the original publication in this journal is cited, in accordance with accepted academic practice. No use, distribution or reproduction is permitted which does not comply with these terms.

# Characterizing the bacterial communities associated with Mediterranean sponges: a metataxonomic analysis

Roberta Esposito<sup>1</sup>, Serena Federico<sup>1,2</sup>, Michele Sonnessa<sup>3</sup>, Sofia Reddel<sup>3</sup>, Marco Bertolino<sup>2</sup>, Nadia Ruocco<sup>4</sup>, Giacomo Zagami<sup>5</sup>, Marco Giovine<sup>2</sup>, Marina Pozzolini<sup>2</sup>, Marco Guida<sup>6</sup>, Valerio Zupo<sup>7</sup> and Maria Costantini<sup>1\*</sup>

<sup>1</sup>Department of Ecosustainable Marine Biotechnology, Stazione Zoologica Anton Dohrn, Napoli, Italy,

<sup>2</sup>Department of Earth, Environmental and Life Sciences, University of Genoa, Genoa, Italy, <sup>3</sup>Bio-Fab Research Srl, Rome, Italy, <sup>4</sup>Department of Ecosustainable Marine Biotechnology, Stazione Zoologica Anton Dohrn, Calabria Marine Centre, Amendolara, Italy, <sup>5</sup>Dipartimento Di Scienze Biologiche, Chimiche, Farmaceutiche Ed Ambientali, Università Di Messina, Messina, Italy, <sup>6</sup>Department of Biology, University of Naples Federico II, Complesso Universitario di Monte Sant'Angelo, Naples, Italy,

<sup>7</sup>Department of Ecosustainable Marine Biotechnology, Stazione Zoologica Anton Dohrn, Ischia Marine Centre, Naples, Italy

The oceans cover over 70% of our planet, hosting a biodiversity of tremendous wealth. Sponges are one of the major ecosystem engineers on the seafloor, providing a habitat for a wide variety of species to be considered a good source of bioactive compounds. In this study, a metataxonomic approach was employed to describe the bacterial communities of the sponges collected from Faro Lake (Sicily) and Porto Paone (Gulf of Naples). Morphological analysis and amplification of the conserved molecular markers, including 18S and 28S (RNA ribosomal genes), CO1 (mitochondrial cytochrome oxidase subunit 1), and ITS (internal transcribed spacer), allowed the identification of four sponges. Metataxonomic analysis of sponges revealed a large number of amplicon sequence variants (ASVs) belonging to the phyla Proteobacteria, Chloroflexi, Dadabacteria, and Poribacteria. In particular, *Myxilla* (*Myxilla*) *rosacea* and *Clathria* (*Clathria*) *toxivaria* displayed several classes such as Alphaproteobacteria, Dehalococcoidia, Gammaproteobacteria, Cyanobacteria, and Bacteroidia. On the other hand, the sponges *Ircinia oros* and *Cacospongia mollior* hosted bacteria belonging to the classes Dadabacteriia, Anaerolineae, Acidimicrobiia, Nitrospiria, and Poribacteria. Moreover, for the first time, the presence of Rhizobiaceae bacteria was revealed in the sponge *M. (Myxilla) rosacea*, which was mainly associated with soil and plants and involved in biological nitrogen fixation.

## KEYWORDS

bacteria, metataxonomic analysis, molecular identification, morphological identification, sponges

## 1 Introduction

The Mediterranean Sea is considered very significant in terms of biodiversity, as it hosts 7% of the world's marine biodiversity (with only 0.82% of the oceans' surface), including a large number of endemic species, which are also subject to anthropogenic stress destined to increase in the future (Coll et al., 2010). Among marine organisms, marine sponges emerged on the earth more than 600 million years ago (the Cambrian Age) and represented one of the most important components of benthic fauna.



They are extensively distributed from polar to tropical waters and from intertidal regions to waters thousands of meters deep (Fusetani, 1996), representing dominant taxon in marine communities in terms of species biomass, richness, and spatial coverage (Corriero et al., 2000). A miscellaneous of archaea, heterotrophic bacteria, cyanobacteria, green algae, red algae, cryptophytes, dinoflagellates, and diatoms have been found together with sponges (Larkum et al., 1987; Santavy et al., 1990; Douglas, 1994). Their microbial community is very diverse, with species composition showing temporal and geographical differences (Webster and Hill, 2001). A sponge can be associated with diverse organisms, such as *Theonella swinhoei*, which hosted unicellular bacteria and cyanobacteria at the same time (Bewley et al., 1996). Additionally, a sponge belonging to the *Aplysina* genus included heterogeneous bacteria *Micrococcus* sp., *Bacillus* sp., *Arthrobacter* sp., *Pseudoalteromonas* sp., *Vibrio* sp., and others (Hentschel et al., 2001). The surfaces or internal sides of marine sponges are richer in nutrients than seawater and sediments; therefore, sponges offer both a feeding source and a secure habitat for their microorganisms (Bultel-Poncé et al., 1999). On the other hand, symbiotic microorganisms contribute to the nutritional process through intracellular digestion and/or translocation of metabolites, such as nitrogen fixation, nitrification, and photosynthesis (Wilkinson and Fay, 1979; Wilkinson and Garrone, 1980). Microorganisms also stabilize the skeleton of sponges (Wilkinson et al., 1981) and participate in the host chemical defense system against hunters and biofouling (Bakus et al., 1986; Paul, 1992; Proksch, 1994; Unson et al., 1994). Sponges and associated microorganisms represent very useful organisms as sources of bioactive compounds for marine biotechnology (Cooper and Yao, 2010; Karupiah and Li, 2015; Thompson et al., 2017; Cerrano et al., 2022). In fact, one of the first peptides with antibacterial activity was isolated by the gram-negative bacterium *Vibrio* sp. associated with the sponge *Hyatella* sp. (Oclarit et al., 1994). Starting from this, several studies showed pharmacological applications of natural products from marine sponges and their associated biota (Newman and Cragg, 2020; Zhang et al., 2020; Amelia et al., 2022).

In the present study, we deeply explored the bacterial communities associated with four sponges collected in the Mediterranean Sea. These species were collected in Italy in two different areas: Faro Lake (Sicily) and Porto Paone (Gulf of

Naples). Species were characterized by skeletal morphological observation and amplification of several conserved molecular markers, represented by RNA ribosomal genes (18S and 28S rRNA), mitochondrial cytochrome oxidase subunit 1 (COI), and internal transcribed spacer (ITS). To analyze the biodiversity of symbiotic communities between the two sampling sites, we performed metataxonomic analysis of sponge samples using the Illumina MiSeq platform. More than 1,000 bacterial isolates from four samples were phylogenetically identified to understand if they are host-specific and/or location-specific. Subsequently, the ASV analysis was also applied to reveal the level of variability in the host-specific microbial communities, which were then discussed to assess the biotechnological potential of the sponges under analysis.

## 2 Materials and methods

### 2.1 Sponge sampling

Two sponge samples (indicated as S36 and S39) were collected in the Gulf of Naples by scuba divers from the Stazione Zoologica Anton Dohrn. The sampling site was Porto Paone (40°47'N, 14°9'E), and the specimens were collected at depths between 15 and 17 m. The other two sponges (indicated as S23 and S25) were collected at the Faro Lake in Messina, Sicily (38°16'N, 15°38'E) at depths between 2 and 3 m (Ruocco et al., 2021, see Table 1). This sampling site is located in the Natural Reserve of “Capo Peloro.” The Faro Lake has the shape of a funnel, and due to its maximum depth of 29 m, which more or less coincides with the center of the lake, it is considered the deepest coastal lake in Italy. The Faro Lake is a salty lake connected by two channels to the Strait of Messina and the Tyrrhenian Sea (northern and northeastern side). The abiotic lake parameters of the lake include a salinity range of 26–36 PSU, pH levels ranging from 7.0 to 8.6, and temperature ranging from 10 to 30°C (Saccà et al., 2008; Marra et al., 2016).

### 2.2 Morphological identification of the sponges

The taxonomic analysis was conducted by examining the skeletal architecture and spicule complement of each sponge

TABLE 1 Sample IDs, taxonomy, sampling depth (m), sites, geographical coordinates, and type of substrate of sponge specimens.

Sample IDs	Sponge taxonomy	Sampling depth (m)	Sampling site	Coordinates	Substrate
S23	<i>Clathria (Clathria) toxivaria</i>	2–3	Faro Lake	38°16'N, 15°38'E	Rocks, coralligenous concretions, caves, and epibiotic on other organisms
S25	<i>Myxilla (Myxilla) rosacea</i>	2–3	Faro Lake	38°16'N, 15°38'E	Rocks, coralligenous concretions, caves, and epibiotic on other organisms
S36	<i>Ircinia oros</i>	15–17	Porto Paone	40°47'N, 14°9'E	Sand, mud, rocks, coralligenous concretions, and cave
S39	<i>Cacospongia mollior</i>	15–17	Porto Paone	40°47'N, 14°9'E	Sand, mud, rocks, coralligenous concretions, cave, and epibiotic on other organisms

specimen according to the protocols already published (Núñez-Pons et al., 2022). The taxonomic identification was made at species level as described in the World Porifera Database (WPD; Van Soest et al., 2023).

## 2.3 Molecular identification of sponges

The DNA extraction was performed starting from 10 mg of sponge tissue and employing QIAamp<sup>®</sup> DNA Micro kit (QIAGEN, Germany), according to the manufacturer's protocol. The DNA (ng/μL) was quantified using NanoDrop spectrophotometer. The C1000 Touch Thermal Cycler (Biorad) was used for PCR reaction processes in a 30 μL final volume of master mix with ~50–100 ng of genomic DNA. The reaction mixture was prepared using 6 μL of 5X Buffer GL (GeneSpin Srl, Milan, Italy), 3 μL of dNTPs (2 mM each), 2 μL each of forward and reverse primers (25 pmol/μL), and 0.5 μL of Xtra Taq Polymerase (5 U/μL, GeneSpin Srl, Milan, Italy) as follows:

- i For 18S and 28S, the amplification conditions were 95°C for 2 min followed by 35 cycles of 95°C for 1 min, 60°C (A/B) and 55°C (18S-AF/18S-BR, NL4F/NL4R) for 1 min, and 72°C for 2 min, with a final extension step at 72°C for 10 min (Chombard et al., 1998; Manuel et al., 2003);
- ii ITS primers (RA2/ITS2.2), with initial denaturation at 95°C for 2 min. This was followed by 35 cycles of 95°C for 1 min, 67°C for 1 min, and 72°C for 2 min, with a final extension step at 72°C for 10 min (Worheide et al., 2002; Schmitt et al., 2005);
- iii CO1 primers (dgLCO1490/dgHCO2198), with initial denaturation at 94°C for 3 min, 35 cycles of denaturation at 94°C for 30 s, 45°C for 30 s, and a final step of elongation of 72°C for 1 min (Meyer et al., 2005).

The gel of agarose (1.5% electrophoresis in 40 mM Tris-acetate, 1 mM EDTA, pH 8.0, TAE buffer) was used to separate PCR products; the amplified fragments were identified using a DNA ladder of 100 bp (GeneSpin Srl, Milan, Italy). The QIAquick Gel Extraction Kit (Qiagen) was used to extract the fragments from the gel following the instructions of the manufacturer. The NanoDrop spectrophotometer evaluated the DNA quantity (ng/μL). Applied Biosystems (Life Technologies) 3730 Analyzer (48 capillaries) sequenced both strands of the obtained amplicons. All the sequences from PCR products were then aligned to GeneBank using BLAST (Basic Local Alignment Search Tool) to reach for high similarity sequences. Then, Multialign was used to confirm the alignment with high similarity sequences (<http://multalin.toulouse.inra.fr/multalin/>).

## 2.4 Metagenomic DNA extraction, illumina miseq sequencing, and diversity analysis

The DNeasy<sup>®</sup> PowerSoil<sup>®</sup> Pro Kit (QIAGEN) was used for the extraction of DNA following the protocol described by the

manufacturer. For this extraction, a piece of the tissue weighing about 250 mg was used. Using the NanoDrop spectrophotometer it was possible to evaluate DNA quantity (ng/μL) and quality (A260/280, A260/230). To check for DNA integrity, the samples were loaded on 0.8% agarose gel electrophoresis immersed in TAE buffer. For metataxonomic analysis performed by Bio-Fab Research (Roma, Italy), a final concentration of 30 ng/μL of DNA was used. Illumina adapter overhang nucleotide sequences were added to the gene-specific primer pairs targeting the V3-V4 region (S-DBact-0341-b-S-17/S-D-Bact-0785-a-A-2), according to Klindworth et al. (2013). 16S PCR amplification was performed in a final volume of 25 μL, which was set up using the following quantities: 5 μL of microbial genomic DNA (10 ng/μL in 10 mM Tris pH 8.5), 1x PCR BIO HiFi Buffer (PCR BIOSYSTEMS, USA) composed by 1 mM of dNTPs and 3 mM of MgCl<sub>2</sub>, 0.5 units of PCR BIO HiFi Polymerase (PCR BIOSYSTEMS, USA), and 0.2 μM of each primer. Cycling conditions followed an initial denaturation at 95°C for 3 min, 25 cycles of 95°C for 30 s, 55°C for 30 s, 72°C for 30 s and a final extension step at 72°C for 5 min, hold at 4°C. After the amplification of the 16S, a PCR clean-up was done to purify the V3-V4 amplicon from free primers and primer dimers. After that, a limited-cycle amplification step using Nextera XT Index Kit was carried out to add multiplexing indices and illumine sequencing adapters. In addition, a further clean-up step was performed, followed by a normalization of the libraries and their pooling by denoizing processes. The sequencing on Illumina MiSeq Platform with 2×300 bp paired-end reads took place only after these steps were completed. Taxonomy assignments were done using a “home-made” Naive Bayesian Classifier trained on V3-V4 16S sequences of the SILVA 138.1 release database (Quast et al., 2013). The sample frequencies per feature and per sample are indicated in Supplementary Figures 1, 2. The metataxonomic analysis from raw DNA sequencing data was conducted on the Quantitative Insights Into Microbial Ecology (QIIME 2, Version: 2022.2) platform (Bolyen et al., 2019) by demultiplexing, quality filtering, chimera removal, taxonomic assignment, and both alpha and beta diversity analyses. With the use of R version 4.1.1 (Li, 2021) and Cairo graphics library (Urbanek and Horner, 2020), the taxonomy barplot was generated. To evaluate the species diversity, three different indices were taken into account: Chao 1 index (Chao, 1984) is a qualitative species-based method (species richness in the sample that is the number of ASV) and Shannon (1948), Shannon and Weaver (1949), and Simpson (1949) indexes estimated the quantitative species-based measures, which indicated the community diversity as species richness and evenness. The estimation was made at three taxa levels (Level 5 = Family, Level 6 = Genus, Level 7 = Species). Statistically significant differences for alpha and beta diversities were explored using the Kruskal–Wallis test and pairwise PERMANOVA analysis, respectively. The distance matrix between each pair of sample (independently from environmental variables) was calculated using Bray–Curtis and “un-, weighted” UniFrac metrics.

The data were deposited in the SRA database (submission ID: SUB14019148; BioProject ID: PRJNA1049642).

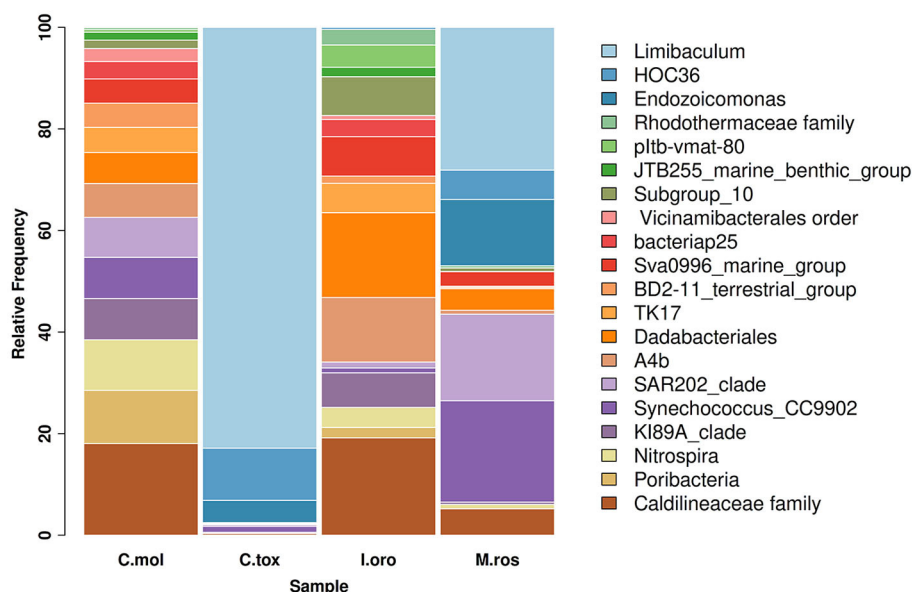


FIGURE 1

Taxonomy barplot comparing the most abundant bacterial phyla at the genus level in sponges *C. mollior*, *C. (C.) toxivaria*, *I. oros*, and *M. (M.) rosacea*. Data were normalized in each sample by median sequencing depth, filtered to low abundance and to sum rows >500.

### 3 Results

#### 3.1 Morphological and molecular characterization

All the sponges were characterized by morphological and molecular approaches. Concerning the morphological analysis, all the analyzed sponges belonged to the class Demospongiae (see Table 1) and usually live in the Mediterranean Sea. Concerning *C. (Clathria) toxivaria*, collected in the Faro Lake (Sicily), molecular tool for characterization of this species identified by morphological analysis was not available in GenBank. The second sponge collected in the Faro Lake was identified by morphological analysis as *M. (Myxilla) rosacea*. In the case of the two sponge samples collected in “Porto Paone” (Gulf of Naples), CO1 was the best molecular marker with 98.5% identity, characterizing the sponge S36 as *Ircinia oros* with 98.5% identity. For Sample S39, this species was identified by ITS as *Cacospongia mollior*, reporting a percentage of sequence similarity of 99%.

#### 3.2 Metataxonomic profile

As indicated by the ASVs analysis, most microbial species had a confidence percentage  $\geq 75\%$ . The complete taxonomy classification of bacterial communities of sponge samples is presented in Supplementary Tables 1–4. In Porto Paone, two sponges (Gulf of Naples) were found: (i) *M. (M.) rosacea* showed the largest number of features (519), especially Alphaproteobacteria, Dehalococcoidia, Gammaproteobacteria, and Cyanobacteria (Figure 1) and (ii) 250 ASVs in *C. (C.) toxivaria*, with a greater abundance of Alphaproteobacteria,

Gammaproteobacteria, and Bacteroidia (Figure 1). In sponges *I. oros* and *C. mollior*, both collected in the Faro Lake (Sicily), 156 and 204 ASVs were detected, respectively. The most abundant bacterial classes in *I. oros* were Dadabacteriia, Anaerolineae, and Acidimicrobiia, while the bacterial community of *C. mollior* was dominated by Nitrospira, Anaerolineae, Dadabacteriia, and Poribacteria (Figure 1). In particular, the taxonomic composition revealed an abundance of Proteobacteria present in *C. toxivaria* (36%) and *M. (M.) rosacea* (35%; Figure 1). In contrast, a low percentage (2%) of Proteobacteria was detected in two sponges collected from the Faro Lake (Sicily). In addition, *C. toxivaria* revealed 1% of Bacteroidia class. The sponge *M. (M.) rosacea* revealed low percentages of Cyanobacteria and Dehalococcoidia (1–0.9%, respectively; Figure 1). Interestingly, this sponge was the only species revealing a certain abundance of Rhizobiaceae, belonging to the phylum Proteobacteria (75.6 %; Figure 1). Concerning the sponges *I. oros* and *C. mollior*, low percentages of Dadabacteria (1%) and Poribacteria (0.9%) were present, respectively (Figure 1). As reported above, the sponges *C. (C.) toxivaria* and *M. (M.) rosacea* revealed a comparable composition in the distribution of microbial species. In fact, a great plethora of Proteobacteria was observed in these species (Figure 1). Similarly, the sponges *I. oros* and *C. mollior* showed the same distribution of bacteria and archaea.

#### 3.3 Principal coordinates analyses (PCoA) of bacterial communities

PCoA based on the relative abundance of genera revealed a significant separation in bacterial community composition

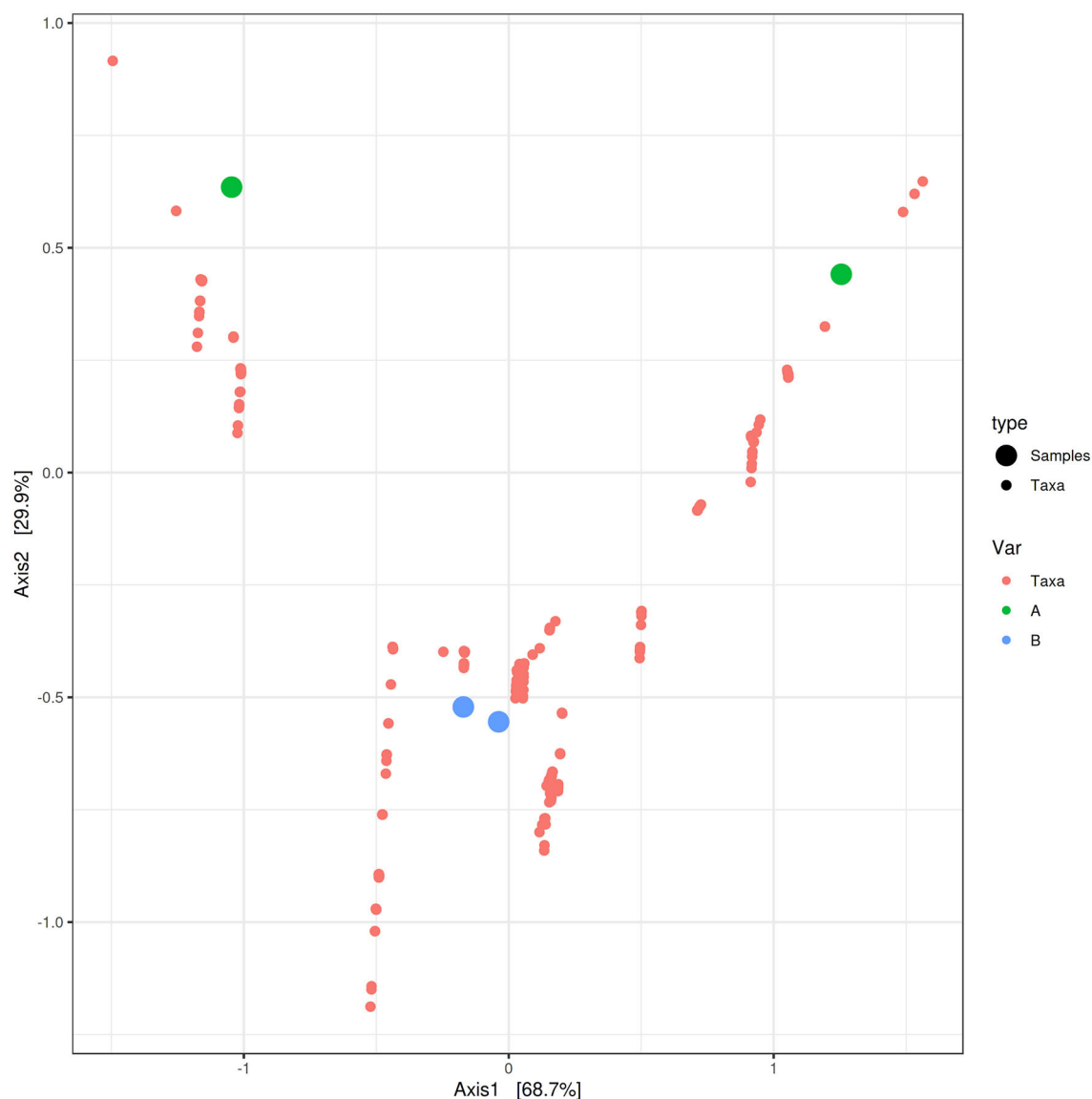


FIGURE 2

Principal coordinates analysis (PCoA) biplot between Group A and Group B for identifying features that contribute the most in terms of separating the samples in a PCoA plot.

between Group A (sponges collected in the Faro Lake) and Group B (sponges collected in Porto Paone), using both principal component scores of PC1 and PC2 (68.7 and 29.9%, respectively; Figure 2 and Table 2). Alpha diversity was used to analyze the samples, and three diversity indices (Chao1, Shannon, and Simpson) were used to determine whether each sample was sequenced at sufficient depth or not. As shown in Figure 3, the Chao index of Group B, including sponges collected in Porto Paone, was lower than that of the sponges collected in the Faro Lake (Group A). The results showed that the species richness of Group B was significantly lower than that of Group A. Moreover, Shannon and Simpson indexes of the Group B were higher than that of the Group A, demonstrating that the two groups had the same trend.

## 4 Discussion

This study builds upon previous investigations where we analyzed the microbial diversity by metataxonomic analysis of eight sponge samples from four sites: *Oceanapia cf. perforate* (Sarà 1960), *Sarcotragus spinosulus* (Schmidt 1862) and *Erylus discophorus* (Schmidt 1862) from Faro Lake in Sicily; *Tethya aurantium* (Pallas 1766) and *Axinella damicornis* (Esper 1794) from “Porto Paone” (Gulf of Naples); *Geodia cydonium* (Jamenson 1811) from “Secca delle fumose” (Gulf of Naples); *Agelas oroides* (Schmidt 1864) and *Acanthella acuta* (Schmidt 1862) from “Punta San Pancrazio” (Gulf of Naples). In fact, here we explored the sponge biodiversity, in terms of microorganisms, in the Mediterranean Sea, analyzing other species from the Strait of Messina and the Gulf of Naples.



TABLE 2 Bacteria clustered with *C. toxivaria*, *M. rosacea*, *I. oros*, and *C. mollior* identified at genus, family, and order levels.

	<i>C. toxivaria</i> (Axis 1 1.25528583537352 and Axis 2 0.441014958183311)	<i>M. rosacea</i> (Axis 1 −1.04618839398916 and Axis 2 0.634895116498213)	<i>I. oros</i> (Axis 1 −0.0380512968287544 and Axis 2 −0.55442518705781)	<i>C. mollior</i> (Axis 1 −0.171355948499607 and Axis 2 −0.521374123467597)
Genus	DEV007	Albidovulu	A4b	AncK6
	Endozoicomonas	AT-s3-44	bacteriap25	Aquimarina
	Entotheonellaceae	Constrictibacter	BD2-11_terrestrial_group	Blastocatella
	Filomicrobium	Cyanobium_PCC-6307	Candidatus_Tenderia	Candidatus_Kaiserbacteria
	JTB255_marine_benthic_group	EF100-94H03	EC94	Candidatus_Nitrosopumilus
	Limibaculum	JG30-KF-CM66	Exiguobacterium	FS142-36B-02
	NS5_marinegroup	Nitrospira	HOC36	Ga0077536
	Pseudohongiella	PAUC43f_marine_benthic_group	NS4_marine_group	NB1-j
	Roseibacillus	Poribacteria	Planctomicrobium	PAUC26f
		Subgroup_11	pltb-vmat-80	Rhodopirellula
Vibrio		Ruegeria	Saccharimonadales	
	Shewanella	Subgroup_9		
Genus			Thalassotalea	Subgroup_21
			Turneriella	TK17
			UBA10353_marine_group	TK30
				Woeseia
Family	Clostridiaceae	Kiloniellaceae	Bacteriovoraceceae	Magnetospiraceae
		Spirochaetacea	Rhizobiaceae	Rhodobacteracea
			Rhodothermacea	Thiotrichaceae
Order				Caldilineales
				Defluviicoccales
				Vicinamibacterales

We first identified four sponges, combining the identification by morphological features with a molecular approach, based on the sequences of 28S and 18S *rDNA*, *ITS*, and *COI*. According to the literature, there is no single marker for all sponge species, and each primer pair displayed its own constraints and strengths (Yang et al., 2017; Ruocco et al., 2021). The difficulty in identifying them is also related to absent or incomplete sequences annotated in the database, thus limiting the phylogenetically based taxonomic methods used for species identification. For this reason, a molecular approach with multi-loci should be employed to ensure reliable sponge identification.

This represents the first record of metataxonomic analysis for the sponges, such as *C. (C.) toxivaria*, *M. (M.) rosacea*, *Ircinia oros*, and *Cacospongia mollior*.

An important finding concerning the species analyzed in this study concerned the fact that the sponges *M. (M.) rosacea* and *C. (C.) toxivaria* collected in the Faro Lake were already recorded in this lake in 2013 suggesting their presence as persistent (Marra et al., 2016). The sponges collected in the Gulf of Naples are typical species in the Mediterranean Sea. In addition, we investigated the bacterial diversity of the Mediterranean sponges by performing the metataxonomic analysis. Our results revealed

that the analyzed sponges hosted various bacterial communities according to the sampling site. Interestingly, as reported in Ruocco et al. (2021), sponges collected in the Faro Lake had a more diverse phyla composition than sponges collected in the Gulf of Naples (Figure 4). In addition, PCA analysis revealed interesting results for the sponges collected in Faro Lake. In fact, *M. (M.) rosacea* is the only sponge with a significant presence of Rhizobiaceae bacteria. The community structure seems to be closely related to the order to which they belong, as demonstrated in the Krona plot and heat map. In fact, *I. oros* and *C. mollior*, belonging to Dictyoceratida order, were recorded as high microbial abundance (HMA) species, while *M. (M.) rosacea* and *C. (C.) toxivaria*, belonging to the Poecilosclerida order, were low microbial abundance (LMA) species. HMA sponges harbor a more diverse symbiotic community than LMA, which were found to be extremely stable at seasonal and interannual scales.

This taxonomic analysis was useful for us, being strongly interested in the biotechnological potential of these sponges. In fact, as reported in the introduction, sponges in general are among the marine organisms richest in bioactive compounds of biotechnological interest. There is a strong debate in the literature whether the bioactive compounds isolated from sponges

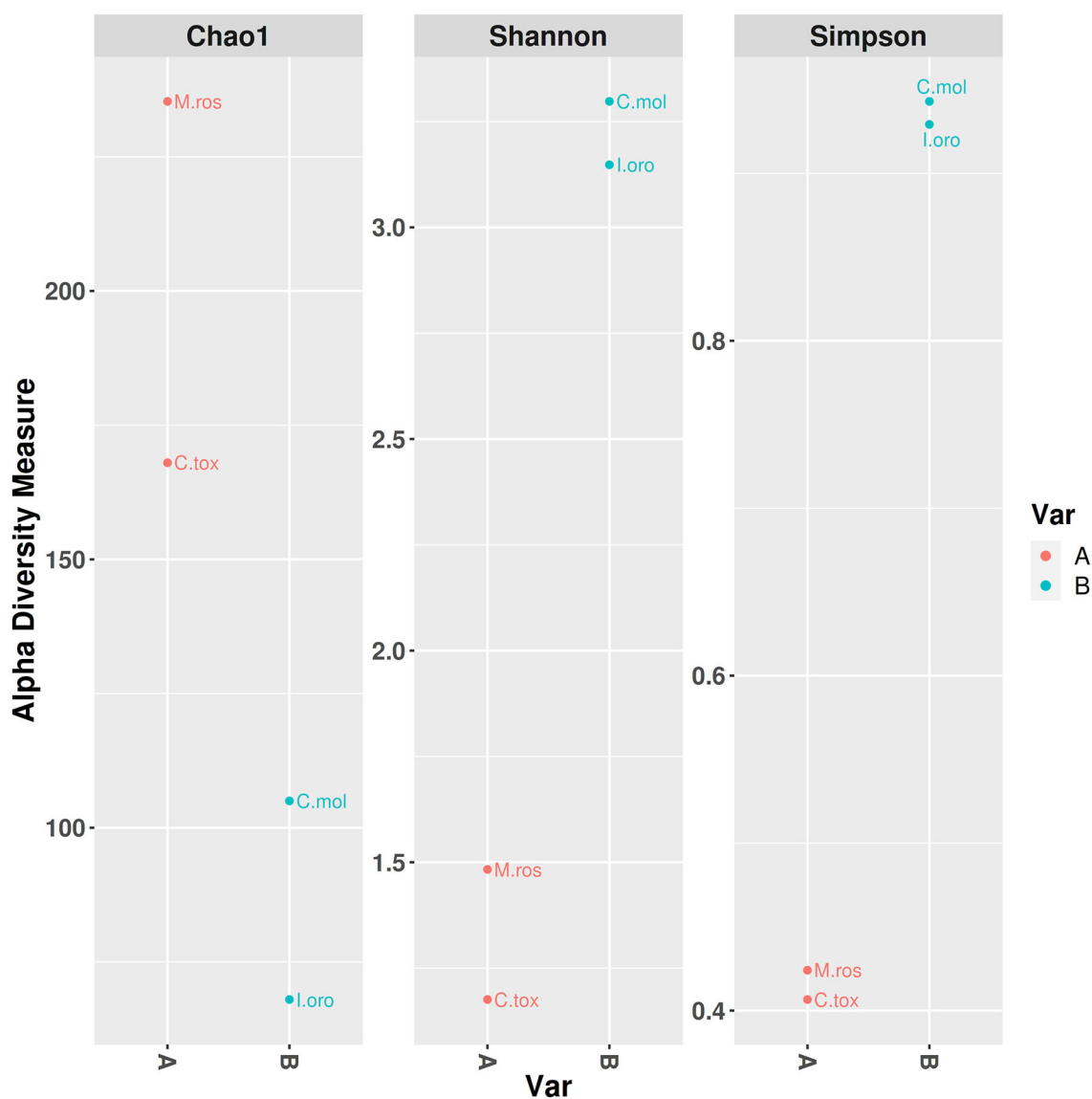


FIGURE 3  
Alpha diversity plot with separate variable A and B.

are produced by the sponges themselves, by the organisms associated with them, or by the interaction between sponges and microorganisms. The fact is that the microorganisms associated with sponges play a fundamental role in their production. Many studies reported that sponge-associated bacteria are good candidates for isolating natural compounds with their application in pharmacological, nutraceutical, and cosmeceutical fields. In this context, our study represents an important step in this field, representing one of the first assessments of the biotechnological potential of mentioned sponge-associated bacteria. In all species of sponges are present Alphaproteobacteria and Gammaproteobacteria, which showed antimicrobial activity making them suitable tools for pharmacological purposes (Thiel and Imhoff, 2003; Thakur et al., 2005; Taylor et al., 2007; Werner, 2010; Haber and Ilan, 2014; Brinkmann et al., 2017; Bibi et al., 2020). The phylum Clostridia (classes Anaerolineae

and Dehalococcidia) is typical of both collection sites, being in all sponge samples. However, no data had been reported so far for marine biotechnology applications for class Anaerolineae. Despite playing an important role in biochemical cycles in various environments, they are manifestly difficult to cultivate due to slow growth (Nakahara et al., 2019; De Castro-Fernández et al., 2023). On the contrary, the anaerobic Dehalococcoides showed an interesting capability to transform various chlorinated organics, which are normally released through industrial and agricultural activities (Bedard et al., 2007; Taş et al., 2010). In the case of the sponge *M. (M.) rosacea*, Rhizobiaceae was the most abundant family (order Alphaproteobacteria) among other bacteria isolated. These bacteria are generally associated with soil and plant hosts and are involved in the process of biological nitrogen fixation (Carrareto-Alves et al., 2015). Therefore, the family Rhizobiaceae, described in this study, was found associated

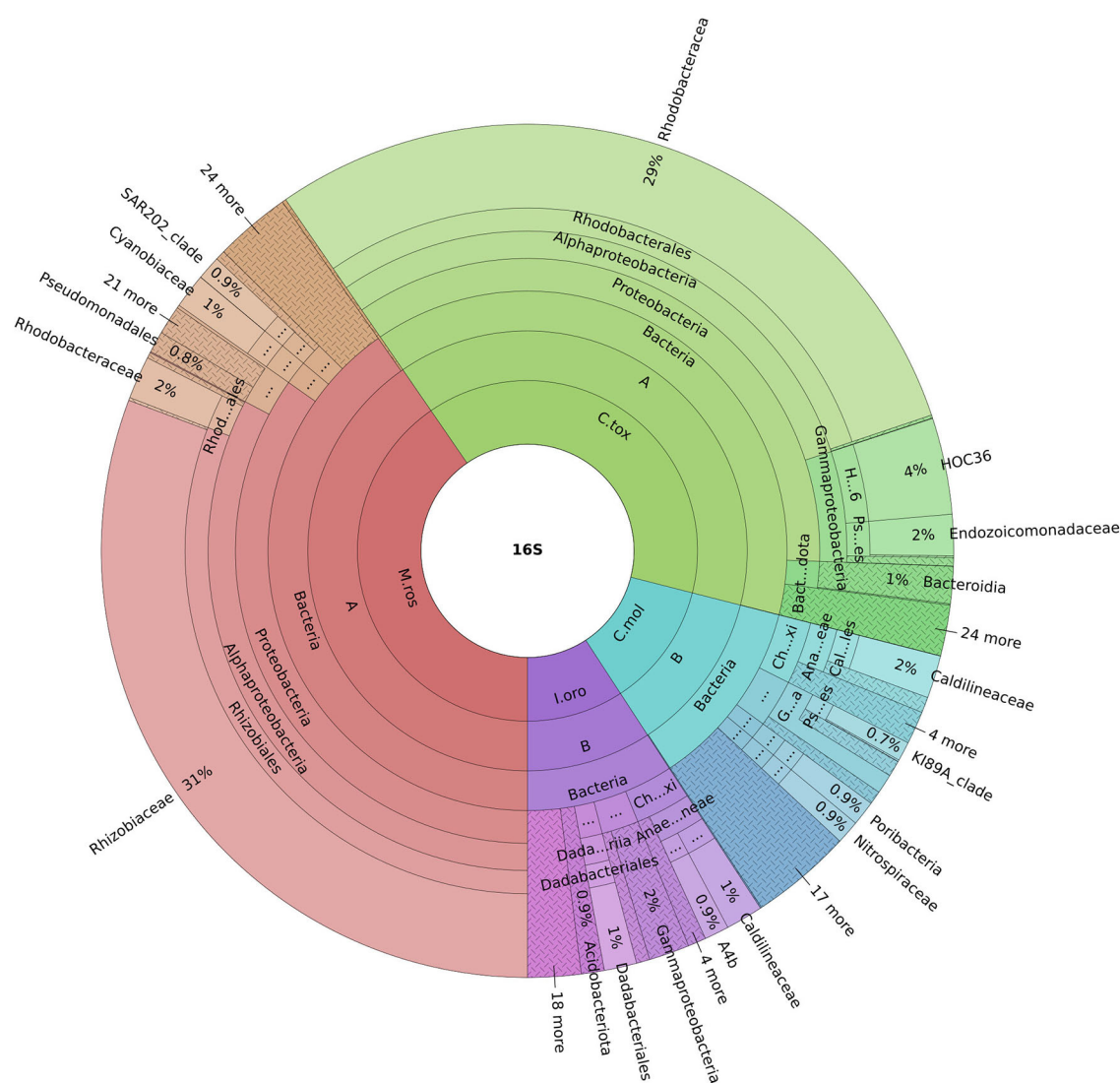


FIGURE 4

Krona plot represents the most abundant phyla for all sponges. Sample code: M.ros, *M. (M.) rosacea*; l.oro, *I. oros*; C.mol., *C. mollior*; C.tox., *C. (C.) toxivaria*.

with the sponge *M. (M.) rosacea* for the first time. Potentially, these bacteria can be used for bioremediation of heavy metals and biodegradation of toxic compounds due to their metabolic capabilities and ecological roles (Aoki et al., 2022). However, their role in marine environments remain unclear because of the limited availability of cultured marine isolates and their sequenced genomes (Kimes et al., 2015). In summary, our data drew attention to the biodiversity of species in the Mediterranean Sea and the 16S rRNA sequence dataset, allowing the detection of several resident microbiomes featured. The sponges and their associated microorganisms revealed good source to identify new compounds for biotechnological applications, and further analyses will be needed to investigate the potential role of the bacteria associated to these sponges. In the meantime, we analyzed the biotechnological potential of these sponges by bioassay-guided fractionation on several human cancer lines, and first results showed specific

antimitotic activity against some cancers. We also tried identifying the chemical structure of the compounds responsible for this activity. We also performed metagenomic and transcriptomic analyses on these sponges, which could help us identify the gene/enzyme responsible for the production of the bioactive compounds. These -omic techniques represent an environmental-friendly approach mainly for organisms, such as the sponges, which cannot be cultivated and are difficult to keep in the laboratory to increase biomass.

## Data availability statement

The original contributions presented in the study are included in the article/Supplementary material, further inquiries can be directed to the corresponding authors.

## Ethics statement

The manuscript presents research on animals that do not require ethical approval for their study.

## Author contributions

RE: Data curation, Investigation, Methodology, Writing – original draft, Writing – review & editing. SF: Data curation, Methodology, Writing – original draft. MS: Data curation, Formal analysis, Methodology, Writing – review & editing. SR: Data curation, Formal analysis, Methodology, Writing – review & editing. MB: Data curation, Formal analysis, Investigation, Methodology, Writing – review & editing. NR: Data curation, Methodology, Writing – review & editing. GZ: Data curation, Methodology, Writing – review & editing. MG: Data curation, Methodology, Supervision, Writing – review & editing. MP: Data curation, Methodology, Supervision, Writing – review & editing. MG: Data curation, Methodology, Writing – review & editing. VZ: Conceptualization, Resources, Writing – original draft, Writing – review & editing. MC: Conceptualization, Funding acquisition, Investigation, Methodology, Resources, Validation, Writing – original draft, Writing – review & editing.

## Funding

The author(s) declare that financial support was received for the research, authorship, and/or publication of this article. SF received support through a Ph.D. fellowship co-funded by the Stazione Zoologica Anton Dohrn (Naples, Italy) and the University of Genoa.

## References

- Amelia, T. S. M., Suaberon, F. A. C., Vad, J., Fahmi, A. D. M., Saludes, J. P., and Bhubalan, K. (2022). Recent advances of marine sponge-associated microorganisms as a source of commercially viable natural products. *Mar. Biotechnol.* 24, 492–512. doi: 10.1007/s10126-022-10130-2
- Aoki, M., Nakahara, N., Kusube, M., and Syutsubo, K. (2022). Metagenome-assembled genome sequence of marine *Rhizobiaceae* sp. strain MnEN-MB40S, obtained from manganese-oxidizing enrichment culture. *Am. Soc. Microbiol.* 11, 16–18. doi: 10.1128/mra.00645-22
- Bakus, G. J., Targett, N. M., and Schulte, B. (1986). Chemical ecology of marine organisms: an overview. *J. Chem. Ecol.* 12, 951–987. doi: 10.1007/BF01638991
- Bedard, D. L., Ritalahti, K. M., and Löffler, F. E. (2007). The Dehalococcoides population in sediment-free mixed cultures metabolically dechlorinates the commercial polychlorinated biphenyl mixture aroclor 1260. *Appl. Environ. Microbiol.* 73, 2513–2521. doi: 10.1128/AEM.02909-06
- Bewley, C. A., Holland, N. D., and Faulkner, D. J. (1996). Two classes of metabolites from *Theonella swinhoei* are localized in distinct populations of bacterial symbionts. *Experientia* 52, 716–722. doi: 10.1007/BF01925581
- Bibi, F., Alvi, S. A., Al-Sofyani, A., Naseere, M. I., Yasir, M., and Azhar, E. I. (2020). Pyrosequencing reveals sponge specific bacterial communities in marine sponges of Red Sea, Saudi Arabia. *Saudi J. Biol. Sci.* 27, 67–73. doi: 10.1016/j.sjbs.2019.05.002
- Bolyen, E., Rideout, J. R., Dillon, M. R., Bokulich, N. A., Abnet, C. C., Al-Ghalith, G. A., et al. (2019). Reproducible, interactive, scalable and extensible microbiome data science using QIIME 2. *Nat. Biotechnol.* 37, 852–857. doi: 10.1038/s41587-019-0209-9
- Brinkmann, C. M., Marker, A., and Kurtböke, D. I. (2017). An overview on marine sponge-symbiotic bacteria as unexploited sources for natural product discovery. *Diversity* 9, 1–31. doi: 10.3390/d9040040
- Bultel-Poncé, V., Berge, J. P., Debitus, C., Nicolas, J. L., and Guvot, M. (1999). Metabolites from the sponge-associated bacterium *Pseudomonas* species. *Mar. Biotechnol.* 1, 384–390. doi: 10.1007/PL00011792
- Carrareto-Alves, L. M., Marcondes de Souza, J. A., de Mello Varani, A., and de Macedo Lemos, E. G. (2015). *The Family Rhizobiaceae*. (Berlin; Heidelberg: Springer-Verlag), 419–437.
- Cerrano, C., Giovine, M., and Steindler, L. (2022). *Petrosia ficiformis* (Poiret, 1789): an excellent model for holobiont and biotechnological studies. *Curr. Opin. Biotechnol.* 74, 61–65. doi: 10.1016/j.copbio.2021.10.022
- Chao, A. (1984). Nonparametric estimation of the number of classes in a population. *Scand. J. Stat.* 1984, 265–270.
- Chombard, C., Boury-Esnault, N., and Tillier, S. (1998). Reassessment of homology of morphological characters in tetractinellid sponges based on molecular data. *Syst. Biol.* 47, 351–366. doi: 10.1080/106351598260761
- Coll, M., Piroddi, C., Steenbeek, J., Kaschner, K., Ben Rais Lasram, F., Aguzzi, J., et al. (2010). The biodiversity of the Mediterranean Sea: estimates, patterns, and threats. *PLoS ONE* 5, e11842. doi: 10.1371/journal.pone.0011842

## Acknowledgments

We thank the scuba diving team of the Stazione Zoologica for their assistance in collecting sponges in the Gulf of Naples. This work was performed in the framework of the PRIN 2022 project “Mediterranean marine organisms as sources of new anti-inflammatory and pro-resolving compounds”.

## Conflict of interest

MS and SR were employed by Bio-Fab Research Srl.

The remaining authors declare that the research was conducted in the absence of any commercial or financial relationships that could be construed as a potential conflict of interest.

The author(s) declared that they were an editorial board member of Frontiers, at the time of submission. This had no impact on the peer review process and the final decision.

## Publisher's note

All claims expressed in this article are solely those of the authors and do not necessarily represent those of their affiliated organizations, or those of the publisher, the editors and the reviewers. Any product that may be evaluated in this article, or claim that may be made by its manufacturer, is not guaranteed or endorsed by the publisher.

## Supplementary material

The Supplementary Material for this article can be found online at: <https://www.frontiersin.org/articles/10.3389/fmicb.2023.1295459/full#supplementary-material>



- Cooper, E. L., and Yao, D. (2010). Diving for drugs: tunicate anticancer compounds. *Drug Discov. Today* 17, 636–648. doi: 10.1016/j.drudis.2012.02.006
- Corriero, G., Liaci, L. S., Ruggiero, D., and Pansini, M. (2000). The sponge community of a semi-submerged Mediterranean cave. *Mar. Ecol.* 21, 85–96. doi: 10.1046/j.1439-0485.2000.00655.x
- De Castro-Fernández, P., Ballesté, E., Angulo-Preckler, C., Biggs, J., Avila, C., and Garcia-Aljaro, C. (2023). How does heat stress affect sponge microbiomes? Structure and resilience of microbial communities of marine sponges from different habitats. *Front. Mar. Sci.* 9, 1–23. doi: 10.3389/fmars.2022.1072696
- Duglas, A. E. (1994). *Symbiotic Interactions*. Oxford: Oxford University Press.
- Fusetani, N. (1996). Bioactive substances from marine sponges. *Tetrahedron* 52, 13837–13866.
- Haber, M., and Ilan, M. (2014). Diversity and antibacterial activity of bacteria cultured from Mediterranean *Axinnella* spp. sponges. *J. Appl. Microbiol.* 116, 519–532. doi: 10.1111/jam.12401
- Hentschel, U., Schmid, M., Wagner, M., Fieseler, L., Gernert, C., and Hacker, J. (2001). Isolation and phylogenetic analysis of bacteria with antimicrobial activities from the Mediterranean sponges *Aplysina aerophoba* and *Aplysina cavernicola*. *FEMS Microbiol. Ecol.* 35, 305–312. doi: 10.1111/j.1574-6941.2001.tb00816.x
- Karuppiyah, V., and Li, Z. (2015). “Marine sponge metagenomics,” in *Handbook of Marine Biotechnology* (Berlin; Heidelberg: Springer Handbooks), 457–473.
- Kimes, N. E., Lopez-Perez, M., Flores-Felix, J. D., Ramirez-Bahena, M. H., Igual, J. M., Peix, A., et al. (2015). *Pseudorhizobium pelagicum* gen. nov., sp. nov. isolated from a pelagic Mediterranean zone. *Syst. Appl. Microbiol.* 38, 293–299. doi: 10.1016/j.syapm.2015.05.003
- Klindworth, A., Pruesse, E., Schweer, T., Peplies, J., Quast, C., Horn, M., et al. (2013). Evaluation of general 16S ribosomal RNA gene PCR primers for classical and next-generation sequencing-based diversity studies. *Nucl. Acids Res.* 41, 1–11. doi: 10.1093/nar/gks088
- Larkum, A. W. D., Cox, G. C., Hiller, R. G., Parry, D. L., and Dibbayawan, T. P. (1987). Filamentous cyanophytes containing phycocouloin and in symbiosis with sponges and an ascidian of coral reefs. *Mar. Biol.* 95, 1–13. doi: 10.1007/BF00447479
- Li, J. (2021). The exploration of the approach to data preparation for Chinese text analysis based on R language. *Open Access Library J.* 8, 1–8. doi: 10.4236/oalib.1107821
- Manuel, M., Borchellini, C., Alivon, E., Le Parco, Y., Vacelet, J., and Boury-Esnault, N. (2003). Phylogeny and evolution of calcareous sponges: monophyly of calcinea and calcarenea, high level of morphological homoplasy, and the primitive nature of axial symmetry. *Syst. Biol.* 52, 311–333. doi: 10.1080/10635150390196966
- Marra, M. V., Bertolino, M., Pansini, M., Giacobbe, S., Manconi, R., and And Pronzato, R. (2016). Long-term turnover of the sponge fauna in Faro Lake (North-East Sicily, Mediterranean Sea). *Ital. J. Zool.* 83, 579–588. doi: 10.1080/11250003.2016.1251981
- Meyer, C. P., Geller, J. B., and Paulay, G. (2005). Fine scale endemism on coral reefs: archipelagic differentiation in turbinid gastropods. *Evolution* 59, 113–125. doi: 10.1111/j.0014-3820.2005.tb00899.x
- Nakahara, N., Nobu, M. K., Takaki, Y., Miyazaki, M., Tasumi, E., Sakai, S., et al. (2019). *Aggregatilinea lenta* gen. nov., sp. nov., a slow-growing, facultatively anaerobic bacterium isolated from seafloor sediment, and proposal of the new order aggregatilineales ord. nov. within the class anaerolineae of the phylum Chloroflexi. *Int. J. Syst. Evol. Microbiol.* 69, 1185–1194. doi: 10.1099/ijsem.0.003291
- Newman, D. J., and Cragg, G. M. (2020). Natural products as sources of new drugs over the nearly four decades from 01/1981 to 09/2019. *J. Nat. Prod.* 83, 770–803. doi: 10.1021/acs.jnatprod.9b01285
- Núñez-Pons, L., Mazzella, V., Rispo, F., Efremova, J., and Calcinai, B. (2022). DNA barcoding procedures of taxonomical and phylogenetic studies in marine animals: porifera as a case study. *Mar. Genomics Methods Protoc.* 10, 195–223. doi: 10.1007/978-1-0716-2313-8\_10
- Oclarit, J. M., Okada, H., Ohta, S., Kaminura, K., Yamaoka, Y., Iizuka, T., et al. (1994). Anti-bacillus substance in the marine sponge, *Hyatella* species, produced by an associated *Vibrio* species bacterium. *Microbios* 78, 7–16.
- Paul, V. J. (1992). *Chemical defenses of benthic marine invertebrates: ecological roles of marine natural products*. Ithaca, NY: Comstock Publishing Associates.
- Proksch, P. (1994). Defensive roles for secondary metabolites from marine sponges and sponge-feeding nudibranchs. *Toxicon* 32, 639–655. doi: 10.1016/0041-0101(94)90334-4
- Quast, C., Pruesse, E., Yilmaz, P., Gerken, J., Schweer, T., Yarza, P., et al. (2013). The SILVA ribosomal RNA gene database project: improved data processing and web-based tools. *Nucl. Acids Res.* 41, 590–596. doi: 10.1093/nar/gk1219
- Ruocco, N., Esposito, R., Zagami, G., Bertolino, M., De Matteo, S., Sonnessa, M., et al. (2021). Microbial diversity in Mediterranean sponges as revealed by metataxonomic analysis. *Sci. Rep.* 11, 1–12. doi: 10.1038/s41598-021-00713-9
- Saccà, A., Guglielmo, L., and Bruni, V. (2008). Vertical and temporal microbial community patterns in a meromictic coastal lake influenced by the Straits of Messina upwelling system. *Hydrobiologia* 600, 89–104. doi: 10.1007/s10750-007-9179-x
- Santavy, D. L., Willenz, P., and Colwell, R. R. (1990). Phenotypic study of bacteria associated with the Caribbean sclerosponge, *Ceratoporella nicholsoni*. *Appl. Environ. Microbiol.* 56, 1750–1762. doi: 10.1128/aem.56.6.1750-1762.1990
- Schmitt, S., Hentschel, U., Zea, S., Dandekar, T., and Wolf, M. (2005). ITS-2 and 18S rRNA gene phylogeny of aplysiniidae (verongida, demospongiae). *J. Mol. Evol.* 60, 327–336. doi: 10.1007/s00239-004-0162-0
- Shannon, C. E. (1948). The Bell system technical journal. *J. Franklin. Inst.* 196, 379–423. doi: 10.1002/j.1538-7305.1948.tb01338.x
- Shannon, C. E., and Weaver, W. (1949). *A Mathematical Model of Communication*. Champaign, IL: University of Illinois Press.
- Simpson, E. (1949). Measurement of diversity. *Nature* 163, 688. doi: 10.1038/163688a0
- Taş, N., Van Eckert, M. H. A., De Vos, W. M., and Smidt, H. (2010). The little bacteria that can diversity, genomics and ecophysiology of “*Dehalococcoides*” spp. in contaminated environments. *Microb. Biotechnol.* 3, 389–402. doi: 10.1111/j.1751-7915.2009.00147.x
- Taylor, M. W., Radax, R., Steger, D., and Wagner, M. (2007). Sponge-associated microorganisms: evolution, ecology, and biotechnological potential. *Microbiol. Mol. Biol. Rev.* 71, 295–347. doi: 10.1128/MMBR.00040-06
- Thakur, A. N., Thakur, N. L., Indap, M. M., Pandit, R. A., Datar, V., and Müller, W. E. (2005). Antiangiogenic, antimicrobial, and cytotoxic potential of sponge-associated bacteria. *Mar. Biotechnol.* 7, 245–252. doi: 10.1007/s10126-004-4085-y
- Thiel, V., and Imhoff, J. F. (2003). Phylogenetic identification of bacteria with antimicrobial activities isolated from Mediterranean sponges. *Biomol. Eng.* 20, 421–423. doi: 10.1016/S1389-0344(03)00069-8
- Thompson, C. C., Kruger, R. H., and Thompson, F. L. (2017). Unlocking marine biotechnology in the developing world. *Trends Biotechnol.* 35, 1119–1121. doi: 10.1016/j.tibtech.2017.08.005
- Unson, M. D., Holland, N. D., and Faulkner, D. J. (1994). A brominated secondary metabolite synthesized by the cyanobacterial symbiont of a marine sponge and accumulation of the crystalline metabolite in the sponge tissue. *Mar. Biol.* 119, 1–11. doi: 10.1007/BF00350100
- Urbanek, S., and Horner, J. (2020). *Cairo: R Graphics Device Using Cairo Graphics Library for Creating High-Quality Bitmap (PNG, JPEG, TIFF), Vector (PDF, SVG, PostScript) and Display (X11 and Win32) Output*. Available online at: <https://cran.r-project.org/> (accessed January 31, 2022).
- Van Soest, R. W. M., Boury-Esnault, N., Hooper, J. N. A., Rützler, K. D., De Voogd, N. J., Alvarez, B., et al. (2023). *World Porifera Database*. Available online at: <https://www.marinespecies.org/porifera> (accessed June 21, 2023).
- Webster, N. S., and Hill, R. T. (2001). The culturable microbial community of the great barrier reef sponge *Rhopileidae odorabile* is dominated by an  $\alpha$ -Proteobacterium. *Mar. Biol.* 138, 843–851. doi: 10.1007/s002270000503
- Werner, T. (2010). Next generation sequencing in functional genomics. *Brief Bioinform.* 2, 499–511. doi: 10.1093/bib/bbq018
- Wilkinson, C., and Garrone, R. (1980). *Nutrition of Marine Sponges. Involvement of Symbiotic Bacteria in the Uptake of Dissolved Carbon*. Oxford: Pergamon Press Ltd.
- Wilkinson, C. R., and Fay, P. (1979). Nitrogen fixation in coral reef sponges with symbiotic cyanobacteria. *Nature* 279, 527–529. doi: 10.1038/279527a0
- Wilkinson, C. R., Nowak, M., Austin, B., and Colwell, R. R. (1981). Specificity of bacterial symbionts in Mediterranean and Great Barrier Reef sponges. *Microb. Ecol.* 7, 13–21. doi: 10.1007/BF02010474
- Worheide, G., Degnan, B., Hooper, J., and Reitner, J. (2002). Phylogeography and taxonomy of the indo-Pacific reef cave dwelling coralline demosponge *Astrosclera willeyana*: new data from nuclear internal transcribed spacer sequences. *Proc. 9th Int. Coral. Reef. Symp.* 1, 339–346.
- Yang, Q., Franco, C. M. M., Sorokin, S. J., and Zhang, W. (2017). Development of a multilocus-based approach for sponge (phylum Porifera) identification: refinement and limitations. *Sci. Rep.* 7, 1–14. doi: 10.1038/srep41422
- Zhang, B., Zhang, T., Xu, J., Lu, J., Qiu, P., Wang, T., et al. (2020). Marine sponge-associated fungi as potential novel bioactive natural product sources for drug discovery: a review. *Mini Rev. Med. Chem.* 20, 1966–2010. doi: 10.2174/138955752066200826123248



## OPEN ACCESS

## EDITED BY

Charles Alan Jacoby,  
University of South Florida St. Petersburg,  
United States

## REVIEWED BY

Dustin Kemp,  
University of Alabama at Birmingham,  
United States  
Karl David Castillo,  
University of North Carolina at Chapel Hill,  
United States

## \*CORRESPONDENCE

Silvia Vimercati  
✉ [silvia.vimercati@kaust.edu.sa](mailto:silvia.vimercati@kaust.edu.sa)

RECEIVED 20 July 2023

ACCEPTED 11 March 2024

PUBLISHED 26 March 2024

## CITATION

Vimercati S, Terraneo TI, Castano CB,  
Barreca F, Hume BCC, Marchese F,  
Ouhssain M, Steckbauer A, Chimienti G,  
Eweida AA, Voolstra CR, Rodrigue M,  
Pieribone V, Purkis SJ, Qurban M, Jones BH,  
Duarte CM and Benzioni F (2024) Consistent  
Symbiodiniaceae community assemblage  
in a mesophotic-specialist coral along  
the Saudi Arabian Red Sea.  
*Front. Mar. Sci.* 11:1264175.  
doi: 10.3389/fmars.2024.1264175

## COPYRIGHT

© 2024 Vimercati, Terraneo, Castano, Barreca,  
Hume, Marchese, Ouhssain, Steckbauer,  
Chimienti, Eweida, Voolstra, Rodrigue,  
Pieribone, Purkis, Qurban, Jones, Duarte and  
Benzioni. This is an open-access article  
distributed under the terms of the [Creative Commons Attribution License \(CC BY\)](https://creativecommons.org/licenses/by/4.0/). The  
use, distribution or reproduction in other  
forums is permitted, provided the original  
author(s) and the copyright owner(s) are  
credited and that the original publication in  
this journal is cited, in accordance with  
accepted academic practice. No use,  
distribution or reproduction is permitted  
which does not comply with these terms.

# Consistent Symbiodiniaceae community assemblage in a mesophotic-specialist coral along the Saudi Arabian Red Sea

Silvia Vimercati<sup>1,2\*</sup>, Tullia I. Terraneo<sup>2</sup>,  
Carolina Bocanegra Castano<sup>2</sup>, Federica Barreca<sup>2</sup>,  
Benjamin C. C. Hume<sup>3</sup>, Fabio Marchese<sup>2</sup>, Mustapha Ouhssain<sup>2</sup>,  
Alexandra Steckbauer<sup>1,2,4</sup>, Giovanni Chimienti<sup>2,5</sup>,  
Ameer A. Eweida<sup>6,7</sup>, Christian R. Voolstra<sup>3</sup>, Mattie Rodrigue<sup>8</sup>,  
Vincent Pieribone<sup>8</sup>, Sam J. Purkis<sup>7,9</sup>, Mohammed Qurban<sup>10</sup>,  
Burt H. Jones<sup>1,2</sup>, Carlos M. Duarte<sup>1,2,4</sup> and Francesca Benzioni<sup>1,2</sup>

<sup>1</sup>Marine Science Program, Biological and Environmental Science and Engineering Division (BESE), King Abdullah University of Science and Technology (KAUST), Thuwal, Saudi Arabia, <sup>2</sup>Red Sea Research Center (RSRC), Division of Biological and Environmental Science and Engineering (BESE), King Abdullah University of Science and Technology, Thuwal, Saudi Arabia, <sup>3</sup>Department of Biology, University of Konstanz, Konstanz, Germany, <sup>4</sup>Computational Bioscience Research Center (CBRC), Division of Biological and Environmental Science and Engineering (BESE), King Abdullah University of Science and Technology, Thuwal, Saudi Arabia, <sup>5</sup>Consorzio Nazionale Interuniversitario per le Scienze del Mare (CoNISMa), Rome, Italy, <sup>6</sup>Marine Conservation Program, NEOM, Saudi Arabia, <sup>7</sup>Center of Carbonate Research, Department of Marine Geosciences, Rosenstiel School of Marine and Atmospheric Science, University of Miami, Miami, FL, United States, <sup>8</sup>OceanX, New York, NY, United States, <sup>9</sup>Khaled bin Sultan Living Oceans Foundation, Annapolis, MD, United States, <sup>10</sup>National Center for Wildlife Development, Riyadh, Saudi Arabia

**Introduction:** The Red Sea is a narrow rift basin characterized by latitudinal environmental gradients which shape the diversity and distribution of reef-dwelling organisms. Studies on Symbiodiniaceae associated with select hard coral taxa present species-specific assemblages and concordant variation patterns from the North to southeast Red Sea coast at depths shallower than 30 m. At mesophotic depths, however, algal diversity studies are rare. Here, we characterize for the first-time host-associated algal communities of a mesophotic specialist coral species, *Leptoseris* cf. *striatus*, along the Saudi Arabian Red Sea coast.

**Methods:** We sampled 56 coral colonies spanning the eastern Red Sea coastline from the Northern Red Sea to the Farasan Banks in the South, and across two sampling periods, Fall 2020 and Spring 2022. We used Next Generation Sequencing of the ITS2 marker region in conjunction with *SymPortal* to denote algal assemblages.

**Results and discussion:** Our results show a relatively stable coral species-specific interaction with algae from the genus *Cladocopium* along the examined latitudinal gradient, with the appearance, in a smaller proportion, of presumed thermally tolerant algal taxa in the genera *Symbiodinium* and *Durusdinium* during the warmer season (Fall 2020). Contrary to shallow water corals, our results do not show a change in Symbiodiniaceae community composition from North to South in this

mesophotic specialist species. However, our study highlights for the first time that symbiont communities are subject to change over time at mesophotic depth, which could represent an important phenomenon to address in future studies.

#### KEYWORDS

MCEs, zooxanthellae, next generation sequencing, ITS2, *SymPortal*

## Introduction

Zooxanthellate scleractinian corals rely on their interaction with photoautotrophic dinoflagellates of the family Symbiodiniaceae Fensome, Taylor, Norris, Sarjeant, Wharton and Williams, 1993 (Muscattine and Porter, 1977). The mutualistic interaction of Symbiodiniaceae with stony corals is essential for the functioning and persistence of tropical and subtropical coral reef ecosystems worldwide (LaJeunesse et al., 2018). Different Symbiodiniaceae can present different physiological responses to environmental stressors, such as photoprotection or thermal tolerance against temperature changes (Rowan, 2004; Sampayo et al., 2008; DeSalvo et al., 2010), which allow them to survive under different environmental conditions (Little et al., 2004; Suwa et al., 2008; Cantin et al., 2009; Jones and Berkemans, 2011). The different physiological requirements of Symbiodiniaceae also influence the coral host distribution range (Rodriguez-Lanetty et al., 2001), their metabolic performance (Cooper et al., 2011a), and stress tolerance (Berkemans and Van Oppen, 2006; Abrego et al., 2008; Howells et al., 2012). Most zooxanthellate corals are consequently restricted in their depth distribution to the photic zone (Dubinsky and Falkowski, 2011; Lesser et al., 2018; Tamir et al., 2019). However, some zooxanthellate coral species can be found in mesophotic conditions commonly associated with greater depths. These contribute to shaping the Mesophotic Coral Ecosystems (MCEs), i.e., tropical and subtropical light-dependent communities between approximately 30 m and 150 m in depth (Lesser et al., 2009; Hinderstein et al., 2010; Baker et al., 2016; Pyle and Copus, 2019).

Among the Scleractinia playing an essential role in MCEs, several species of the genus *Leptoseris* Milne Edwards & Haime, 1849, family Agariciidae Gray, 1847, are important constituents of the MCEs (Fricke et al., 1987; Hinderstein et al., 2010; Rooney et al., 2010; Kahng et al., 2014, 2017; Loya et al., 2019). Different *Leptoseris* species were reported from Indo-Pacific MCEs (see, for example, Fricke and Knauer, 1986; Kahng et al., 2010; Luck et al., 2013; Pochon et al., 2015; Rouzé et al., 2021). In the Red Sea, different authors addressed the physiology and the distribution of *Leptoseris* cf. *striatus* Saville Kent, 1871 (previously referred to as *Leptoseris fragilis* Milne Edwards & Haime, 1849, but see Benzoni, 2022) (Schlichter et al., 1985, 1986, 1994, 1997; Fricke et al., 1987; Schlichter and Fricke, 1991; Kaiser et al., 1993; Ferrier-Pagès et al., 2022). These studies demonstrated

that *L. cf. striatus* is a depth-specialist coral species, living between 70 and 145 m depth (Fricke and Schuhmacher, 1983; Fricke and Knauer, 1986; Kaiser et al., 1993; Tamir et al., 2019). The mesophotic success of this species seems to reside in its morphological and physiological characteristics (Schlichter et al., 1985, 1986, 1988, 1994, 1997; Fricke et al., 1987; Schlichter and Fricke, 1991). Fricke et al. (1987) hypothesized that *L. cf. striatus* conical knobs and plate-light growth forms would act as coral “light traps.” Furthermore, Schlichter et al. (1985, 1986, 1988) and Schlichter and Fricke (1991) reported that in this species, fluorescent proteins beneath zooxanthellae promote photosynthesis by shifting low-wavelength irradiance into long wavelengths within the action spectrum for photosynthesis (i.e., host light-harvesting system). The host light-harvesting system amplifies and increases the zooxanthellae’s photosynthetic efficiency and the coral host’s metabolic efficiency under low-light conditions (Schlichter et al., 1985, 1986, 1988; Schlichter and Fricke, 1991). Moreover, Fricke et al. (1987) demonstrated the inability of this species to grow shallower than 40 meters when transplanted, further reinforcing the idea that *L. cf. striatus* is an obligate mesophotic coral. In particular, the efficient host light-harvesting system mentioned above (Schlichter et al., 1986) is partially destroyed at depths shallower than 40 m, impeding growth (Fricke et al., 1987). Fricke et al. (1987) also reported that the Symbiodiniaceae density associated with *L. cf. striatus* decreases with depth. However, the diversity of the zooxanthellae community associated with the mesophotic specialist *L. cf. striatus* remains unstudied, hence the role of the symbiont’s identity and their variation in space and time, or lack thereof, is unknown.

The Red Sea is a young rift basin characterized by strong latitudinal environmental gradients in water temperature and salinity, which change from the North to the South (Sofianos and Johns, 2003; Raitos et al., 2013; Rowlands et al., 2014, 2016; Chaidez et al., 2017; Manasrah et al., 2019; Berumen et al., 2019a). These conditions influence the diversity, distribution, and evolution of the Red Sea reef-dwelling marine organisms (Berumen et al., 2019a). A total of 331 zooxanthellate coral species are reported from the basin from shallow to mesophotic (see Arrigoni et al., 2019; Berumen et al., 2019b; Terraneo et al., 2019b, 2021), but a few studies focused on the characterization of their Symbiodiniaceae community composition to date (e.g., Winters et al., 2009; Nir et al., 2011, 2014; Byler et al., 2013; Ziegler et al., 2015; Einbinder et al., 2016; Turner et al., 2017; Ben-Zvi

et al., 2020; Ferrier-Pagès et al., 2022; Terraneo et al., 2023). In fact, most studies addressed the Symbiodiniaceae diversity in different coral genera and species from the shallow, euphotic Red Sea water (shallower than 30 m) (Winters et al., 2009; Sawall et al., 2014; Arrigoni et al., 2016; Ezzat et al., 2017; Ziegler et al., 2017; Terraneo et al., 2019a; Hume et al., 2020; Osman et al., 2020; Terraneo et al., 2023). Two reports assessed the Symbiodiniaceae diversity of shallow-water corals along the Red Sea latitudinal gradient, reporting a correlation between the algae diversity and the environmental gradients along the basin, shown as a shift of algae community composition from North to South (Arrigoni et al., 2016; Terraneo et al., 2019a). In particular, the Red Sea species ascribed to the genus *Stylophora* Schweigger, 1820, and the genus *Porites* Link, 1807, presented a shift in algae community from North to South, passing from the genus *Cladocopium* LaJeunesse & H.J. Jeong, 2018 to the genus *Symbiodinium* Freudenthal, 1962, dominance and from the genus *Cladocopium* to the genus *Durudinium* LaJeunesse, 2018 dominance, respectively (Arrigoni et al., 2016; Terraneo et al., 2019a). At mesophotic depths, however, zooxanthellae diversity studies are mostly limited to the Eilat coast of the Gulf of Aqaba (Winters et al., 2009; Nir et al., 2011, 2014; Byler et al., 2013; Einbinder et al., 2016; Turner et al., 2017; Ben-Zvi et al., 2020; Ferrier-Pagès et al., 2022), comprising one study from the NEOM region in the Northern Red Sea (Terraneo et al., 2023), and one study from the central Saudi Arabian Red Sea (Ziegler et al., 2015). Most of these studies focused on a few coral model species. Conversely, the composition and zonation of MCEs Symbiodiniaceae associated with a Red Sea non-model coral species, such as *L. cf. striatus*, and the community variation along the Red Sea latitudinal gradient are still mainly unknown.

With the overall aim to (a) characterize the composition of the Symbiodiniaceae community in the strictly mesophotic *L. cf. striatus* along the Red Sea latitudinal gradient and (b) investigate if symbiont communities are subject to change over time in the Gulf of Aqaba and the North Red Sea (NEOM area), we used Next Generation Sequencing (NGS) of the ITS2 amplicon from 56 colonies of *L. striatus* collected from five distinct regions of the Saudi Arabian Red Sea, spanning from the northern Red Sea (NEOM area) to the South of the Red Sea, as part of an unprecedented sampling effort to characterize the country's marine resources.

## Materials and methods

### Coral sampling

A total of 56 *L. cf. striatus* colonies were collected during the Red Sea Deep Blue Expedition in October and November 2020 (15 colonies), the Red Sea Decade Expedition from February to June 2022 (32 colonies), and the OceanX Relationships Cultivation Expedition in June 2022 (9 colonies) on board the M/V OceanXplorer along the Saudi Arabian Red Sea coast (Appendix S1). Sampling occurred in regions spanning the whole latitudinal range of the Saudi Arabian coast from the Gulf of Aqaba (GoA) (4 sites) and northern Red Sea (NRS) (8 sites) in NEOM waters to the Al Wajh region (AlW) (4 sites), central Red Sea (CRS) (namely

Yanbu and Thuwal) (10 sites) and southern Red Sea (SRS) (4 sites) (Appendix S2). The two distinct sampling regions in NEOM waters were sampled both in Fall 2020 and in Spring 2022, thus allowing us to investigate the Symbiodiniaceae community composition stability across time and between two seasons.

The entire coral colonies, or fragments, were collected between 70 and 127 m water depth using an Argus Mariner XL Remotely Operated Vehicle (ROV) or a Triton 3300/3 submersible with a Schilling T4 hydraulic manipulator. The ROV and the submersible dives were video-recorded, and frame grabs of the colonies were extracted from the videos using the open-source software MPC-HC (Media Player Classic – Home Cinema) and Adobe Premier software PRO™, respectively. The underwater vehicles position was provided by Kongsberg HIPaP 501 USBL (Ultra-Short Baseline), Sonardyne Sprin INS (Inertial Navigation System), and Sonardyne Ranger Pro 2 USBL.

After sampling, a small fragment of each colony, or the whole colony, was preserved in absolute ethanol for molecular analyses. The remaining part of the corallum was bleached in sodium hypochlorite for 48 hours to remove organic tissue parts, rinsed with fresh water, and air-dried for morphological identification. The coral skeletons and tissue samples are deposited at the King Abdullah University of Science and Technology (KAUST, Saudi Arabia).

### Environmental data acquisition

Temperature, salinity, and depth at the sampling localities were recorded using a RBR Maestro CTD mounted on the ROV. Downcast RBR Maestro CTD data were extracted and visualized with Origin Pro 2020 (Origin Lab) software. Standard deviation (SD) was used as an uncertainty metric. RBR Maestro CTD raw data is available in Appendix S3.

### Symbiodiniaceae MiSeq sequencing library preparation

Symbiodiniaceae genomic DNA was extracted from the coral tissues using the DNeasy® Blood and Tissue kit (Qiagen Inc., Hilden, Germany), following the manufacturer's protocol. Symbiodiniaceae genotypes were characterized using PCR amplification of the ITS2 region for the Illumina MiSeq platform in the KAUST Bioscience Core Laboratory. The primer sequences were (overhang adapter sequences underlined): 5' TCGTCGGCAGCGTCAGATGTGTATAAGAGACAGGAATTGCAGAACTCCGTGAACC 3' (SYM\_VAR\_5.8S2) and 5' GTCTCGTGGGCTCGGAGATGTGTATAAGAGACAGCGGGTTCWCTTGTYTGACTTCATGC 3' (SYM\_VAR\_REV) (Hume et al., 2018). PCRs were run with 11 µL of 2X Multiplex PCR kit (Qiagen Inc., Hilden, Germany), 2 µL of 10 µM of each primer, and 5 µL of DNA, in a total volume of 25 µL. The following PCR conditions were used: 15 min at 94°C, followed by 30 cycles of 95°C for 30 s, 56°C for 90 s, 72°C for 30 s, and a final extension step of 10 min at 72°C. PCRs success was tested with QIAxcel Advanced System (Qiagen Inc., Hilden, Germany). Amplified samples were



cleaned with Agencourt AMPure CP magnetic bead system (Beckman Coulter, Brea, CA, USA). Nextera XT indexing and sequencing adapters were added via PCR (8 cycles) following the manufacturer's protocol. Samples were normalized and pooled using SequalPrep™ Normalization Plate Kit 96-well (ThermoFisher Scientific, Waltham, MA, USA). The samples were then checked with Aligen BioAnalyzer 2100 (Agilent Technologies, Santa Clara, CA, USA) and qPCR (ThermoFisher Scientific, Waltham, MA, USA) to check library size and concentration. Libraries were sequenced using the Illumina MiSeq platform (Illumina, San Diego, CA, USA) and kit reagents v3 (2 x 300bp pair-ended reads) at KAUST Bioscience Core Lab, following the manufacturer's protocol.

## Symbiodiniaceae MiSeq data processing

Demultiplexed forward and reverse fastq.gz files were submitted online to the *SymPortal* framework (<https://symportal.org>; Hume et al., 2019). A standardized quality control (QC) of sequences was conducted as part of the submissions using mothur 1.39.5 (Schloss et al., 2009), the BLAST+ suite of executables (Camacho et al., 2009), and Minimum Entropy Decomposition (MED; Eren et al., 2015; Hume et al., 2019). Then, existing sets of ITS2 sequences on the database were used to find and assign ITS2 profiles to samples. The Symbiodiniaceae genotypes are represented as proxies by the ITS2 profile predictions in the *SymPortal* outputs. The online framework was used to download the post-MED ITS2 sequence relative abundances (Appendix S4), the ITS2 profiles relative abundances (Appendix S5), and the corresponding absolute counts between sample distances and between profile distances. We created stacked bar plots to relate the Symbiodiniaceae genotypes to different categorical levels (i.e., body of water, sampling depth) with the R package ggplot2 (Wickham et al., 2016).

## Comparison with *Porites lutea* and *Porites columnaris* in the Red Sea

The Symbiodiniaceae type profiles of *Porites lutea* Milne Edwards & Haime, 1851, and *Porites columnaris* Klunzinger, 1879, from Terraneo et al. (2019a), obtained through *SymPortal* submission, were taken into consideration for this study. In particular, patterns of specificity and generalism and comparison with algal communities of *L. cf. striatus* (this study) and *P. lutea* and *P. columnaris* (Terraneo et al., 2019a) were visualized using Venn Diagrams (Heberle et al., 2015).

## Results

### Coral identification

The scleractinian coral species studied in this work (Figure 1) belongs to the family Agariciidae in the complex clade (Kitahara et al., 2016). To date, it has not been studied from a molecular point

of view and is currently synonymized with *Leptoseris hawaiiensis* Vaughan, 1907 (Hoeksema and Cairns, 2023). However, a morphological study of the type material of both species (illustrated in Dinesen, 1980) has shown consistent differences in corallite shape, size, and number of radial elements. Previous studies in the Red Sea addressing the physiology of this mesophotic specialist have identified it as *Leptoseris fragilis* (Schlichter et al., 1985, 1986, 1994, 1997; Fricke et al., 1987; Schlichter and Fricke, 1991; Kaiser et al., 1993; Ferrier-Pagès et al., 2022). However, Benzoni (2022) recently re-described the type material of *L. fragilis* and provided its first detailed description based on which all diagnostic characters based on skeletal morphology differ from the material we examined.

## Environmental parameters

In Fall 2020, considering this study depth range of 70–130 m, the GoA and the NRS were comparable in terms of water temperature and salinity ( $25.9 \pm 0.7$  °C,  $40.7 \pm 0.05$ , respectively, for the GoA, and  $25.5 \pm 0.6$  °C,  $40.7 \pm 0.04$ , respectively, for the NRS) (Figure 2; Appendix S3). In Spring 2022, the coolest and most saline basin was the GoA ( $22.9 \pm 0.3$  °C,  $40.33 \pm 0.04$ ), followed by the NRS ( $23.05 \pm 0.3$  °C,  $40.3 \pm 0.02$ ), AIW ( $23.1 \pm 0.3$  °C,  $40.2 \pm 0.09$ ), Yanbu ( $23.8 \pm 0.3$  °C,  $39.9 \pm 0.1$ ), Thuwal ( $25.2 \pm 1.4$  °C,  $39.6 \pm 0.5$ ), and finally, SRS ( $25.8 \pm 1.9$  °C,  $39.4 \pm 0.6$ ) (Figure 2; Appendix S3), with the temperature increasing from the North to the South, and the salinity decreasing along the North to South gradient, in agreement with the already known water seasonal and latitudinal gradient previously described from the basin (Sofianos and Johns, 2003; Raitos et al., 2013; Rowlands et al., 2014, 2016; Chaidez et al., 2017; Berumen et al., 2019a; Manasrah et al., 2019).

## Symbiodiniaceae community diversity

A total of 6,876,798 sequences were produced using Illumina MiSeq and then submitted to the *SymPortal*. The post-MED output included 75 different ITS2 sequences associated with *L. cf. striatus*. Of these, 12 belonged to the genus *Symbiodinium*, 60 to the genus *Cladocopium*, and three to the genus *Durusdinium*. *Durusdinium* was only recorded during Spring 2022 in the North and South Red Sea, while *Symbiodinium* and *Cladocopium* were found all along the Saudi Arabian Red Sea coast. Overall, in the 56 coral samples examined, the genus *Symbiodinium* represented 2.6% of the Symbiodiniaceae community, the genus *Cladocopium* 97.1%, and the genus *Durusdinium* 0.02% (Appendices S5, S6).

A total of 17 ITS2 profiles were recovered (Appendix S4). The ITS2 type profile composition per specimen was visualized using stacked bar charts to compare the relative abundance at each locality (Figure 3). Overall, the type profiles were not equally distributed among the samples, with 50/56 specimens interacting with two newly discovered ITS2 profiles (C1-C1cu-C1me-C42dr-C1mf-C1db-C1mg-C1aq and C1-C1cu-C1me-C42dr-C1mf-C1db-C1mg-C89b), and 53/56 specimens associating with the C1 ITS2 majority sequences (Appendix S5). The A1 radiation was found in

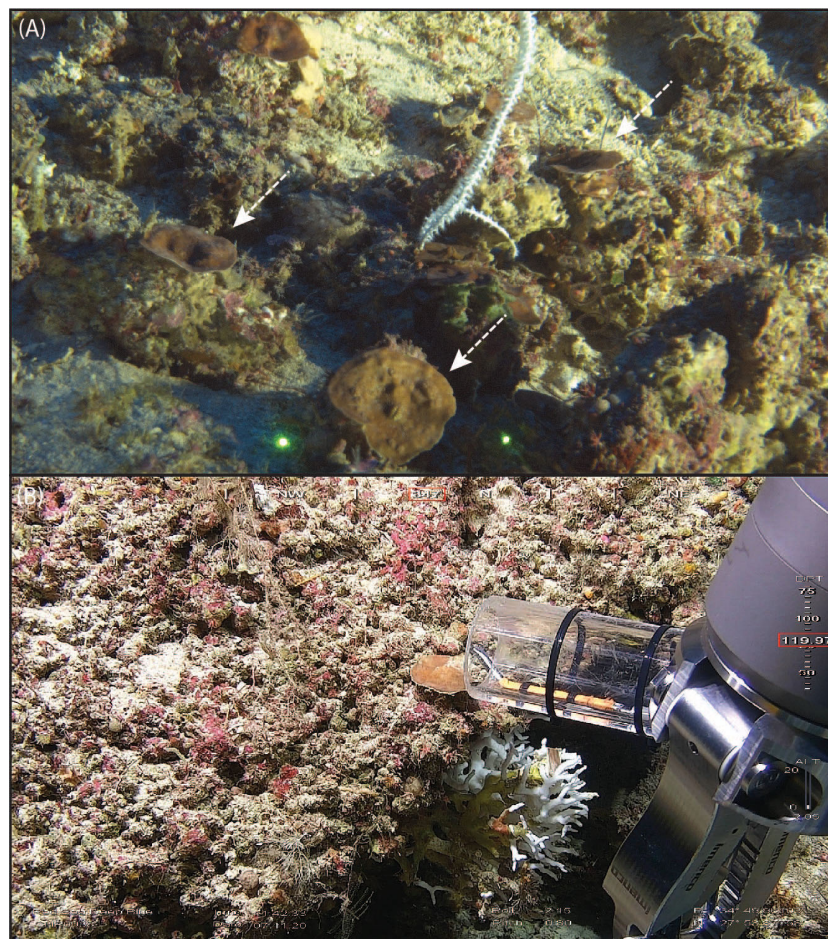


FIGURE 1

In situ pictures of some *Leptoseris* cf. *striatus* specimens analyzed in this study. (A) Different *L. cf. striatus* colonies (pointed with arrows) found during dive NTN0035. (B) Sampling of CHR0038\_17.

14/56 specimens. The remaining profiles, found associated with single specimens, belonged to A11, C3/C3u, C39/C1, C116/C116f, C39, C3/C1, C3, and D4 radiations.

Overall, during Fall 2020, three ITS2 profiles were recorded, specifically C1-C1cu-C1me-C42dr-C1mf-C1db-C1mg-C1aq (9 colonies), C1-C1cu-C1me-C42dr-C1mf-C1db-C1mg-C89b (6 colonies), and A1/A11g (1 colony) (Figure 3). During Spring 2022, the ITS2 profiles C1-C1cu-C1me-C42dr-C1mf-C1db-C1mg-C1aq and C1-C1cu-C1me-C42dr-C1mf-C1db-C1mg-C89b were recovered in association with *L. cf. striatus* at all five examined regions, indicating high levels of specificity (Figure 3). The second most abundant type profile, retrieved from specimens collected in Spring 2022, A1-A1du-A1bw-A1bf, was associated with five colonies at four sampling localities (namely, GoA, NRS, CRS, and SRS) (Figure 3). The ITS2 profiles C116/C116f, C3/C3u/C1-C115, and C3 were found only in the GoA during the spring sampling collection (Figure 3). The type profiles A1-A1mp and A1-A1du-A1bw-A1bf-A1bx were recovered in the NEOM area (GoA and NRS) and only in the GoA, respectively, in Spring 2022 (Figure 3). Finally, the A11 type profile was associated with one Yanbu (CRS) sample in May 2022 (Figure 3). Considering the genus *Durusdinium*, during spring 2022, we recorded only two type

profiles (D4-D4i-4k-D4ak-D6v and D4-D4i) associated with *L. cf. striatus* specimens (Figure 3). The first was associated with two samples in the NRS and SRS, while the latter was associated with one colony in the NRS (Figure 3).

In the different geographical regions that we identified, we also recovered colony-specific profiles, suggesting latitudinal and seasonal signatures (Figure 3). In the GoA, we recovered three specific ITS2 profiles belonging to the A1, C116, and C3 radiations (Figure 3). In the NRS, we found four ITS2 profiles, one found during Fall 2020 (A1/A1g) (Figure 3), and the remaining recovered only during Spring 2022, belonging respectively to A1, D4, C1, and C39 radiations (Figure 3). In the CRS (Yanbu and Thuwal), only one host-specific ITS2 profile was recorded, namely A11 (Figure 3). Finally, in the SRS, we found two ITS2 profiles belonging to the C3 and C39 radiations (Figure 3).

### Unique and shared Symbiodiniaceae ITS2 type profiles of *L. cf. striatus*

Overall, two Symbiodiniaceae type profiles associated with *L. cf. striatus* were the most abundant and found at each analyzed site

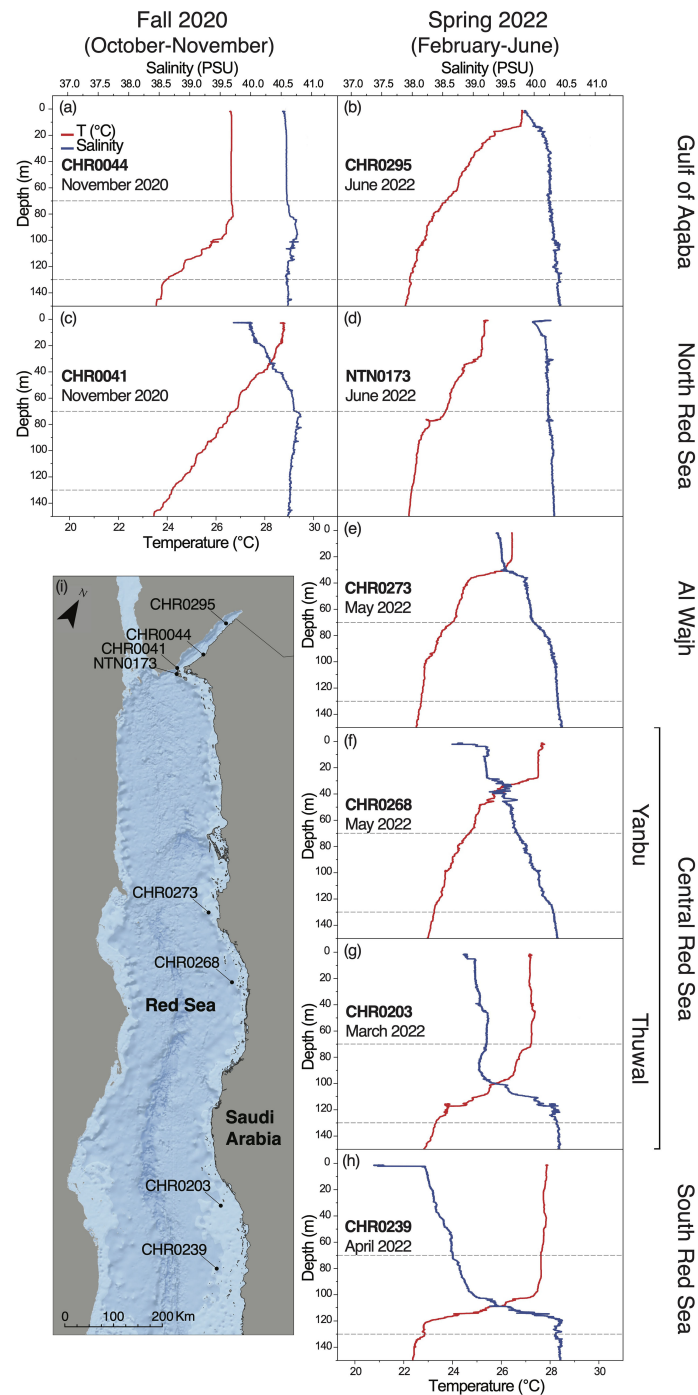


FIGURE 2

Environmental parameters (temperature, and salinity) measured with the RBR CTD along the five regions we investigated during two different seasons, namely (A, B) Gulf of Aqaba, (C, D) North Red Sea, (E) Al Wajh, (F, G) Central Red Sea (Yanbu and Thuwal), (H) South Red Sea. The depth range focused in this study (70–130 m) is highlighted with grey dashed-lines. Temperature profile is in red and salinity profile is in blue. (I) Map of the Saudi Arabian Red Sea showing RBR CTD sampling sites. ESRI World Oceans Basemap, source: Esri, GEBCO, NOAA, National Geographic, DeLorme, HERE, Geonames.org, and other contributors.

(Figures 3, 4). Of the remaining 15 type profiles, four were shared between pairs of regions (in particular, one between CRS and SRS; one between GoA and NRS; one between NRS and SRS; finally, one found in all four regions mentioned before) (Figures 3, 4), while 11 were only found associated at a specific region (Figures 3, 4).

## Discussion

In this work, we characterized for the first time the Symbiodiniaceae community diversity associated with the mesophotic-specialist coral *L. cf. striatus*, occurring from 70 to



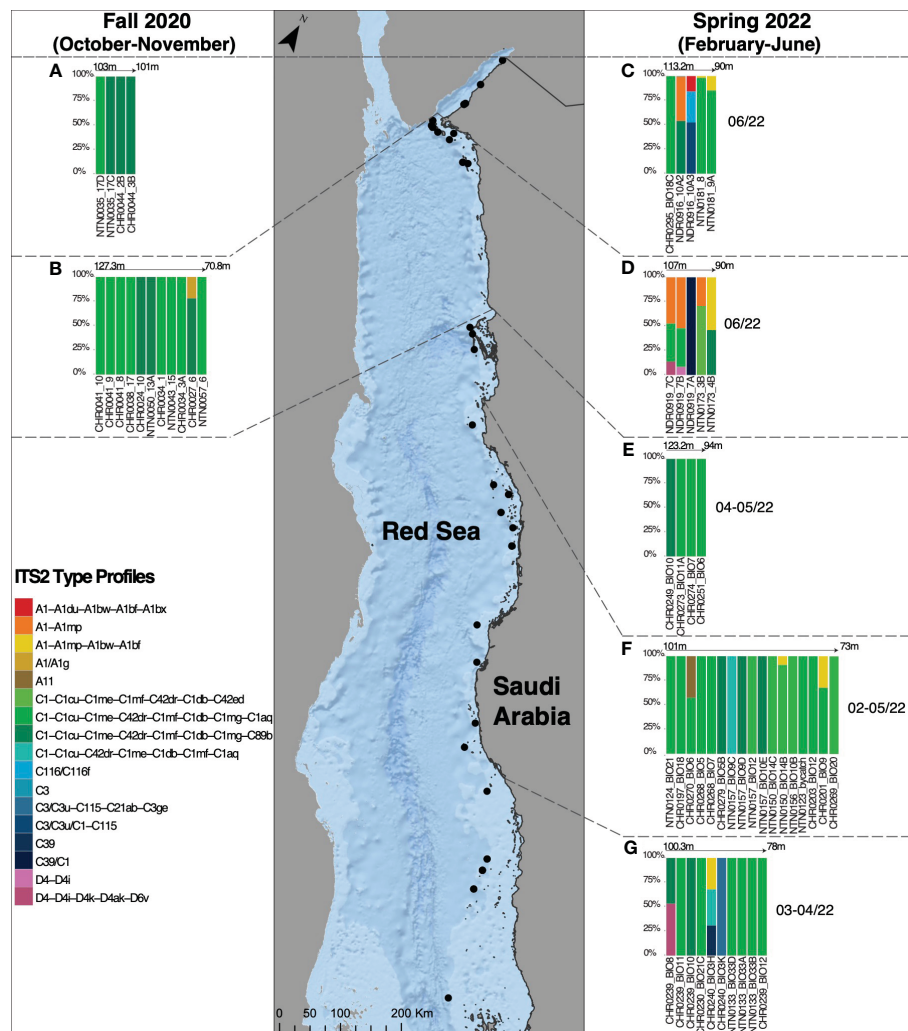


FIGURE 3

Symbiodiniaceae ITS2 type profiles in *Leptoseris cf. striatus* in the Gulf of Aqaba (A, C), in the North Red Sea (B, D), in Al Wajh (E), in the Central Red Sea (Yanbu and Thuwal) (F), and in the South Red Sea (G), found during two different sampling seasons, Fall 2020 (October–November) and Spring 2022 (February–June).

127 m water depth along the Saudi Arabian Red Sea coast. Our measures of temperature and salinity at mesophotic depths showed a decrease in water temperature and an increase in salinity from North to South during Spring 2022. Conversely, in Fall 2020, at upper mesophotic depths, the temperature and the salinity of the Gulf of Aqaba and the Northern Red Sea were comparable ( $25.9 \pm 0.7$  °C and  $40.7 \pm 0.05$ , respectively, for the first and  $25.5 \pm 0.6$  °C and  $40.7 \pm 0.04$ , respectively, for the latter). Then, to identify *L. cf. striatus* dominant zooxanthellae genotypes and compare their diversity throughout the study area, we performed Next Generation Sequencing of the ITS2 marker. Our results showed the presence of 17 Symbiodiniaceae type profiles associated with *L. cf. striatus*, with 2 of them being dominant in each sampling region.

## Symbiodiniaceae genotypes at mesophotic depths

Zooxanthellate corals' growth and survival are influenced by light availability, with consequent limitations on their depth distribution (Done, 2011; Muir et al., 2015). Understanding how zooxanthellate corals can survive in extreme environments, such as mesophotic waters, is still highly debated and is receiving increasing attention as technology improvements allow the exploration of previously inaccessible depths (Armstrong et al., 2019; Turner et al., 2019). Structural adaptation in macro and micro-morphological characters are commonly encountered in mesophotic corals in response to low-light availability, e.g., less self-shading (Ow and Todd, 2010), lower calical relief, or lower





Symbiodiniaceae community associated with different *Porites* species along the entire Saudi Arabian Red Sea. Their data showed a shift from the genus *Cladocopium* to the genus *Durusdinium*, going from the North to the South of the Red Sea, with the central Red Sea *Porites* harboring both genera. Similarly, Sawall et al. (2014) and Arrigoni et al. (2016) reported a shift from *Cladocopium*-dominated to *Symbiodinium*-dominated communities along the same Red Sea latitudinal gradient in the hard coral genus *Pocillopora* Lamarck, 1816 and *Stylophora*, respectively. Together, these results point to a relationship between the Red Sea environmental gradients and the Symbiodiniaceae biogeographical patterns in shallow water taxa.

In this study, when considering zooxanthellae patterns at the genus level, we did not find latitudinal differences in association with the strictly mesophotic *L. cf. striatus*, as the coral species presented *Cladocopium*-dominated communities all along the Saudi Arabian Red Sea coast, despite the presence of modest temperature and salinity gradients in the mesophotic layer, compared to stronger gradients in surface waters. Similar results were found by Terraneo et al. (2023) for the corals *Coscinaraea monile* (Forskål, 1775), *Blastomussa merleti* (Wells, 1961), *Psammocora profundacella* Gardiner, 1898, and *Craterastrea levis* Head, 1983. The authors, however, only compared colonies from the Gulf of Aqaba and the Northern Red Sea, thus a smaller latitudinal gradient than the one examined in this study, and focused on zooxanthellate species commonly mainly occurring at shallow depths with the notable exception of *C. levis*. This species, known to be exclusively living in low-light conditions (Benzoni et al., 2012), showed a lower Symbiodiniaceae diversity at mesophotic depths than the others and was associated with only one profile belonging to the C1 radiation in both the Gulf of Aqaba and the Northern Red Sea (Terraneo et al., 2023). Other studies reported *Cladocopium*-dominated communities in the mesophotic waters of the Gulf of Aqaba (Ezzat et al., 2017; Osman et al., 2020). In fact, there is no evidence of environmental gradients, which we confirm here for temperature and salinity along latitude, shaping symbionts distribution in the Red Sea mesophotic waters.

We compared the variability of *L. cf. striatus* zooxanthellae communities (Figure 4A) to the one previously published from the shallow water *P. lutea* and *P. columnaris* sampled along the Red Sea latitudinal gradient (Terraneo et al., 2019a) (Figures 4B, C). In particular, the previously examined cases of the two shallow water *Porites* species showed a total of 16 different Symbiodiniaceae type profiles (Figure 4) and presented a latitudinal pattern, with only one type profile, C15, shared between the GoA and AIW in *P. columnaris* (Figure 4) (Terraneo et al., 2019a). Hence, the ITS2 type profiles associated with the *Porites* species in the euphotic zone were mostly host-generalist and associated with specific sampling localities. Moreover, both species showed a shift in the Symbiodiniaceae community from *Cladocopium* in the North to *Durusdinium* in the South. As a result, no type profile was shared among the different sampling areas in either species (Figures 4B, C). Conversely, the genotypes recovered in *L. cf. striatus* were mainly represented by the genus *Cladocopium* at all sites. Furthermore, our results show only five genotypes belonging to *Symbiodinium* and

two belonging to *Durusdinium*, both occurring together with *Cladocopium*. As a result, *L. cf. striatus* shared the same two type profiles found in all regions along the Red Sea latitudinal gradient (Figure 4A). This suggests that for this mesophotic specialist coral, the Symbiodiniaceae community variability is not shaped by the same environmental gradients as in the shallow reef dwelling species.

## Site and temporal partitioning of *Leptoseris cf. striatus* Symbiodiniaceae community

The five Saudi Arabian Red Sea regions we investigated were recently identified as four distinct bioregions based on phytoplankton phenology (Kheireddine et al., 2021). The Gulf of Aqaba is commonly considered a coral refuge and resilience area, with the coral communities able to persist through different disturbances and thermal stressors (Fine et al., 2013, 2019). This bioregion (3), together with the Northern and Central Red Sea (4) and the Southern Red Sea (2) bioregions, present a phytoplankton bloom during winter (October to March) and a recurrent summer phytoplankton boom peak (Raitsos et al., 2013; Kheireddine et al., 2021). Conversely, the Southern Red Sea bioregion (1, including the Farasan Banks and the Dahlak Archipelago) is characterized by a summer phytoplankton bloom starting at the end of May (Kheireddine et al., 2021). We sampled the Gulf of Aqaba and the Northern Red Sea in two different years, both supposedly concurrently with the reported phytoplankton bloom (October/November 2020 and June 2022). Our results did not reveal the presence of presumed thermal tolerant genotypes such as *Durusdinium* radiations during fall, when the sea water was warmer and less saline than in June 2022. Conversely, *Symbiodinium* and *Durusdinium* genotypes appeared in June 2022, when the seawater was cooler and more saline sea, indicating that some ecological variables related to temporal environmental changes could shape coral-zooxanthellae association at mesophotic depths. During Spring 2022, we reported a North-South gradient in water temperature and salinity in the mesophotic layer, less pronounced than those reported for surface waters (see Raitsos et al., 2013; Chaidez et al., 2017; Berumen et al., 2019a), in agreement with previous studies (Sofianos and Johns, 2003; Manasrah et al., 2019). In particular, the temperature increases from North to South while the salinity decreases, thus mirroring the shallow water gradient. However, all the remaining regions analyzed during Spring 2022 (namely Al Wajh, Central Red Sea, and Southern Red Sea) presented *Cladocopium*-dominated communities with more presumed thermally tolerant Symbiodiniaceae genotypes in one sample in the southern Red Sea, and not a shift on the Symbiodiniaceae community as shown in other Red Sea shallow water studies (Arrigoni et al., 2016; Terraneo et al., 2019a), indicating that the algal community of this mesophotic coral is consistent across the Red Sea latitudes. Moreover, different studies reported site and seasonal-specific acclimation signatures in corals (e.g., Brown et al., 1999; Fitt et al., 2001; Edmunds, 2009; Anthony et al., 2022; Sawall

et al., 2022). However, processes other than seasonality (e.g., environmental stressors, thermal adaptation, host-symbiont specificity, and anthropogenic disturbances) (see, for example, Silverstein et al., 2012; Cunning et al., 2015; Terraneo et al., 2019a; Howe-Kerr et al., 2020; Claar et al., 2022); could drive the algal community shift in symbiotic corals. It is still unclear which processes made the algal community of *L. cf. striatus* change across 2 sampling time points. Hence, future studies encompassing longer sampling duration and sampling the same individual over time would be required to address whether seasonality or other processes play a role in the Symbiodiniaceae community composition of *L. cf. striatus*.

## Conclusions

This study characterizes the composition and provides evidence for the limited variability of the Symbiodiniaceae community in a depth specialist coral species along a latitudinal gradient spanning approximately 1,300 km of coastline in the Saudi Arabian Red Sea. We found an increase in the mesophotic water temperature and a decrease in the salinity from the North to the South, in agreement with other studies from the basin. Moreover, contrary to shallow water corals, the Symbiodiniaceae communities associated with the strictly mesophotic coral *Leptoseris cf. striatus* were dominated by the same symbiont genus, *Cladocopium*, and type profile radiation, C1, across the entire Red Sea latitudinal gradient and a time span of 1.5 years, with the appearance, in a smaller proportion, of presumed thermally tolerant algal taxa in the genera *Symbiodinium* and *Durusdinium* during the colder water season (Spring 2022). Thus, we conclude the absence of a correlation between Red Sea environmental gradients and the *L. cf. striatus*-associated Symbiodiniaceae community in mesophotic waters of the basin, likely due to strong selection pressures for low-light adaptation. Our results open up questions about drivers of Symbiodiniaceae community changes at mesophotic depth and the need for more in-depth studies addressing the biology and ecology of scleractinian corals occurring in the mesophotic zone.

## Data availability statement

The sequence data supporting this study's findings are openly available in GenBank of NCBI at <https://www.ncbi.nlm.nih.gov/sra>. The associated \*\*BioProject\*\*, and \*\*Bio-Sample\*\* numbers are PRJNA994007, and SAMN36411768 to SAMN36411823 respectively. All the maps were created using ArcGIS® software by Esri. ArcGIS® and ArcMap™ are the intellectual property of Esri and are used herein under license. Copyright © Esri. All rights reserved. For more information about Esri® software, please visit [www.esri.com](http://www.esri.com). All data collected onboard during the Red Sea Decade Expedition (RSDE), including data collected by sensors, acoustic mapping devices, and images collected by ROVs and submersibles, are property of the

National Center for Wildlife (NCW). The videos, images, and audio media obtained during the course of the RSDE are credited to the NCW, Kingdom of Saudi Arabia.

## Author contributions

SV: Conceptualization, Data curation, Formal analysis, Investigation, Methodology, Software, Validation, Visualization, Writing – original draft, Writing – review & editing. TT: Conceptualization, Supervision, Validation, Writing – review & editing. CC: Methodology, Writing – review & editing. FB: Methodology, Writing – review & editing. BH: Methodology, Writing – review & editing. FM: Methodology, Writing – review & editing. MO: Methodology, Writing – review & editing. AS: Writing – review & editing. CG: Writing – review & editing. AA: Data curation, Funding acquisition, Project administration, Resources, Writing – review & editing. CRV: Validation, Writing – review & editing. MR: Data curation, Resources, Writing – review & editing. VP: Data curation, Funding acquisition, Project administration, Resources, Writing – review & editing. MQ: Funding acquisition, Project administration, Resources, Writing – review & editing. SP: Writing – review & editing. BJ: Writing – review & editing. CD: Funding acquisition, Project administration, Resources, Writing – review & editing. FB: Conceptualization, Data curation, Funding acquisition, Resources, Supervision, Validation, Project administration, Writing – review & editing.

## Funding

The author(s) declare financial support was received for the research, authorship, and/or publication of this article. This study was supported by KAUST (FCC/1/1973-49-01 and FCC/1/1973-50-01) and baseline research funds to FBe. The Red Sea Decade Expedition (RSDE) was funded by the National Center for Wildlife (NCW).

## Acknowledgments

We thank NEOM for facilitating and coordinating the Red Sea Deep Blue expedition and, specifically, in addition to AAE, T. Habis, J. Myner, P. Marshall, G. Palavicini, P. Mackelworth, and A. Alghamdi. We thank the National Center for Wildlife (NCW, Saudi Arabia) for the invitation to participate in the Red Sea Decade Expedition. We thank M. Qurban, C. M. Duarte, J. E. Thompson, and N. C. Pluma Guerrero for facilitating and coordinating the Red Sea Decade Expedition. We thank M. Rodrigue and V. Pieribone for facilitating and coordinating the Red Sea Relationship Cultivation expedition. We want to thank OceanX and the crew of OceanXplorer for their operational and logistical support for the duration of this expedition. In particular, we would like to acknowledge the ROV and submersible teams for sample collection and OceanX for support of scientific operations on

board OceanXplorer. We would also like to thank OceanX Media for documenting and communicating this work with the public. We also wish to thank A. Perry, N. Dunn, and S. Bahr for contributing to part of the sampling efforts. Finally, we thank the KAUST Genomics Core Lab for helping with NGS.

## Conflict of interest

The authors declare that the research was conducted in the absence of any commercial or financial relationships that could be construed as a potential conflict of interest.

The author(s) declared that they were an editorial board member of Frontiers, at the time of submission. This had no impact on the peer review process and the final decision.

## References

- Abrego, D., Ulstrup, K. E., Willis, B. L., and van Oppen, M. J. (2008). Species-specific interactions between algal endosymbionts and coral hosts define their bleaching response to heat and light stress. *Proc. R. Soc. B: Biol. Sci.* 275, 2273–2282. doi: 10.1098/rspb.2008.0180
- Anthony, C. J., Lock, C., Taylor, B. M., and Bentlage, B. (2022). Photosystem regulation in coral-associated dinoflagellates (Symbiodiniaceae) is the primary mode for seasonal acclimation. *bioRxiv*, 2022–2012. doi: 10.1101/2022.12.24.520888
- Armstrong, R. A., Pizarro, O., and Roman, C. (2019). “Underwater robotic technology for imaging mesophotic coral ecosystems,” in Mesophotic coral ecosystems. Coral Reefs of the World, vol. 12. Eds. Y. Loya, K. Puglise and T. Bridge (Springer, Cham). doi: 10.1107/978-3-319-92735-0\_51
- Arrigoni, R., Benzoni, F., Terraneo, T. I., Caragnano, A., and Berumen, M. L. (2016). Recent origin and semi-permeable species boundaries in the scleractinian coral genus *Stylophora* from the Red Sea. *Sci. Rep.* 6, 1–13. doi: 10.1038/srep34612
- Arrigoni, R., Berumen, M. L., Stolarski, J., Terraneo, T. I., and Benzoni, F. (2019). Uncovering hidden coral diversity: a new cryptic lobophyllid scleractinian from the Indian Ocean. *Cladistics* 35, 301–328. doi: 10.1111/cla.12346
- Baker, E., Thygesen, K., Harris, P., Andradi-Brown, D., Appeldoorn, R. S., Ballantine, D., et al. (2016). *Mesophotic coral ecosystems: a lifeboat for coral reefs?* (Nairobi and Arendal: The United Nations Environment Programme and GRID-Arendal).
- Benzoni, F. (2022). Re-discovery of the type material of *Leptoseris fragilis* (Cnidaria, Anthozoa, Scleractinia) from the upper mesophotic in La Réunion, a taxonomic puzzle. *Zootaxa* 5178, 596–600. doi: 10.11646/zootaxa.5178.6.8
- Benzoni, F., Arrigoni, R., Stefani, F., and Stolarski, J. (2012). Systematics of the coral genus *Craterastrea* (Cnidaria, Anthozoa, Scleractinia) and description of a new family through combined morphological and molecular analyses. *Syst. Biodivers.* 10 (4), 417–433. doi: 10.1080/14772000.2012.744369
- Ben-Zvi, O., Tamir, R., Keren, N., Tchernov, D., Berman-Frank, I., Kolodny, Y., et al. (2020). Photophysiology of a mesophotic coral 3 years after transplantation to a shallow environment. *Coral Reefs* 39, 903–913. doi: 10.1007/s00338-020-01910-0
- Berkelmans, R., and Van Oppen, M. J. (2006). The role of zooxanthellae in the thermal tolerance of corals: a ‘nugget of hope’ for coral reefs in an era of climate change. *Proc. R. Soc. B: Biol. Sci.* 273, 2305–2312. doi: 10.1098/rspb.2006.3567
- Berumen, M. L., Arrigoni, R., Bouwmeester, J., Terraneo, T. I., and Benzoni, F. (2019b). Corals of the Red Sea. *Coral reefs red sea* (Springer, Cham), 11, 123–155. doi: 10.1007/978-3-030-05802-9\_7
- Berumen, M. L., Voolstra, C. R., Daffonchio, D., Agusti, S., Aranda, M., Irigoien, X., et al. (2019a). “The Red Sea: environmental gradients shape a natural laboratory in a nascent ocean,” in *Coral reefs of the Red Sea* (Springer, Cham), 1–10. doi: 10.1007/978-3-030-05802-9\_1
- Brown, B. E., Dunne, R. P., Ambarsari, I., Le Tissier, M. D. A., and Satapoomin, U. (1999). Seasonal fluctuations in environmental factors and variations in symbiotic algae and chlorophyll pigments in four Indo-Pacific coral species. *Mar. Ecol. Prog. Ser.* 191, 53–69. doi: 10.3354/meps191053
- Byler, K. A., Carmi-Veal, M., Fine, M., and Goulet, T. L. (2013). Multiple symbiont acquisition strategies as an adaptive mechanism in the coral *Stylophora pistillata*. *PLoS One* 8, e59596. doi: 10.1371/journal.pone.0059596
- Camacho, C., Coulouris, G., Avagyan, V., Ma, N., Papadopoulos, J., Bealer, K., et al. (2009). BLAST+: architecture and applications. *BMC Bioinf.* 10, 1–9. doi: 10.1186/1471-2105-10-421
- Cantin, N. E., van Oppen, M. J., Willis, B. L., Mieog, J. C., and Negri, A. P. (2009). Juvenile corals can acquire more carbon from high-performance algal symbionts. *Coral Reefs* 28, 405–414. doi: 10.1007/s00338-009-0478-8
- Carricart-Ganivet, J. P., and Beltrán-Torres, A. U. (1993). Zooxanthellae and chlorophyll a responses in the scleractinian coral *Montastrea cavernosa* at Triángulos-W Reef, Campeche Bank, Mexico. *Rev. biología Trop.*, 491–494.
- Chaidez, V., Dreano, D., Agusti, S., Duarte, C. M., and Hoteit, I. (2017). Decadal trends in Red Sea maximum surface temperature. *Sci. Rep.* 7, 1–8. doi: 10.1038/s41598-017-08146-z
- Chan, Y. L., Pochon, X., Fisher, M. A., Wagner, D., Concepcion, G. T., Kahng, S. E., et al. (2009). Generalist dinoflagellate endosymbionts and host genotype diversity detected from mesophotic (67–100 m depths) coral *Leptoseris*. *BMC Ecol.* 9, 1–7. doi: 10.1186/1472-6785-9-21
- Claar, D. C., McDevitt-Irwin, J. M., Garren, M., Vega Thurber, R., Gates, R. D., and Baum, J. K. (2022). Increased diversity and concordant shifts in community structure of coral-associated Symbiodiniaceae and bacteria subjected to chronic human disturbances. *Mol. Ecol.* 29, 2477–2491. doi: 10.1111/mec.15494
- Cooper, T. F., Lai, M., Ulstrup, K. E., Saunders, S. M., Flematti, G. R., Radford, B., et al. (2011a). *Symbiodinium* genotypic and environmental controls on lipids in reef building corals. *PLoS One* 6, e20434. doi: 10.1371/journal.pone.0020434
- Cooper, T. F., Ulstrup, K. E., Dandan, S. S., Heyward, A. J., Kühl, M., Muirhead, A., et al. (2011b). Niche specialization of reef-building corals in the mesophotic zone: metabolic trade-offs between divergent *Symbiodinium* types. *Proc. R. Soc. B: Biol. Sci.* 278, 1840–1850. doi: 10.1098/rspb.2010.2321
- Cunning, R., Silverstein, R. N., and Baker, A. C. (2015). Investigating the causes and consequences of symbionts shuffling in a multi-partner reef coral symbiosis under environmental changes. *Proc. R. Soc. B: Biol. Sci.* 282, 20141725. doi: 10.1098/rspb.2014.1725
- DeSalvo, M. K., Sunagawa, S., Voolstra, C. R., and Medina, M. (2010). Transcriptomic responses to heat stress and bleaching in the elkhorn coral *Acropora palmata*. *Mar. Ecol. Prog. Ser.* 402, 97–113. doi: 10.3354/meps08372
- Dilworth, J., Caruso, C., Kahkejian, V. A., Baker, A. C., and Drury, C. (2021). Host genotype and stable differences in algal symbiont communities explain patterns of thermal stress response of *Montipora capitata* following thermal pre-exposure and across multiple bleaching events. *Coral Reefs* 40, 151–163. doi: 10.1007/s00338-020-02024-3
- Dinesen, Z. D. (1980). A revision of the coral genus *Leptoseris* (Scleractinia: Fungiina: Agariciidae). *Memoirs Queensland Museum* 20, 181–235.
- Done, T. (2011). “Corals: environmental controls on growth,” in *Encyclopedia of Earth Sciences Series* (Springer, Dordrecht), 281–293. doi: 10.1007/978-90-481-2639-2\_10
- Dubinsky, Z., and Falkowski, P. (2011). “Light as a source of information and energy in zooxanthellate corals,” in *Coral reefs: an ecosystem in transition* (Springer, Dordrecht), 107–118. doi: 10.1007/978-94-007-0114-4\_8
- Edmunds, P. J. (2009). Effect of acclimatization to low temperature and reduced light on the response of reef corals to elevated temperature. *Mar. Biol.* 156, 1797–1808. doi: 10.1007/s00227-009-1213-2
- Einbinder, S., Gruber, D. F., Salomon, E., Liran, O., Keren, N., and Tchernov, D. (2016). Novel adaptive photosynthetic characteristics of mesophotic symbiotic microalgae within the reef-building coral, *Stylophora pistillata*. *Front. Mar. Sci.* 3. doi: 10.3389/fmars.2016.00195

## Publisher’s note

All claims expressed in this article are solely those of the authors and do not necessarily represent those of their affiliated organizations, or those of the publisher, the editors and the reviewers. Any product that may be evaluated in this article, or claim that may be made by its manufacturer, is not guaranteed or endorsed by the publisher.

## Supplementary material

The Supplementary Material for this article can be found online at: <https://www.frontiersin.org/articles/10.3389/fmars.2024.1264175/full#supplementary-material>



- Eren, A. M., Morrison, H. G., Lescault, P. J., Reveillaud, J., Vineis, J. H., and Sogin, M. L. (2015). Minimum entropy decomposition: unsupervised oligotyping for sensitive partitioning of high-throughput marker gene sequences. *ISME J.* 9, 968–979. doi: 10.1038/ismej.2014.195
- Ezzat, L., Fine, M., Maguer, J. F., Grover, R., and Ferrier-Pages, C. (2017). Carbon and nitrogen acquisition in shallow and deep holobionts of the scleractinian coral *S. pistillata*. *Front. Mar. Sci.* 4. doi: 10.3389/fmars.2017.00102
- Ferrier-Pagès, C., Bednarz, V., Grover, R., Benayahu, Y., Maguer, J. F., Rottier, C., et al. (2022). Symbiotic stony and soft corals: Is their host-algae relationship really mutualistic at lower mesophotic reefs? *Limnol. Oceanogr.* 67, 261–271. doi: 10.1002/lno.11990
- Fine, M., Gildor, H., and Genin, A. (2013). A coral reef refuge in the Red Sea. *Global Change Biol.* 19, 3640–3647. doi: 10.1111/gcb.12356
- Fine, M., Gildor, H., Voolstra, C. R., Safa, A., Rinkevich, B., Laffoley, D., et al. (2019). Coral reefs of the Red Sea – Challenges and potential solutions. *Regional Stud. Mar. Sci.* 25, 100498. doi: 10.1016/j.rsma.2018.100498
- Fitt, W. K., Brown, B. E., Warner, M. E., and Dunne, R. P. (2001). Coral bleaching: interpretation of thermal tolerance limits and thermal thresholds in tropical corals. *Coral Reefs* 20, 51–65. doi: 10.1007/s003380100146
- Fricke, H. W., and Knauer, B. (1986). Diversity and spatial pattern of coral communities in the Red Sea upper twilight zone. *Oecologia* 71, 29–37. doi: 10.1007/BF00377316
- Fricke, H. W., and Schuhmacher, H. (1983). The depth limits of Red Sea stony corals: an ecophysiological problem (a deep diving survey by submersible). *Mar. Ecol.* 4, 163–194. doi: 10.1111/j.1439-0485.1983.tb00294.x
- Fricke, H. W., Vareschi, E., and Schlichter, D. (1987). Photoecology of the coral *Leptoseris fragilis* in the Red Sea twilight zone (an experimental study by submersible). *Oecologia* 73, 371–381. doi: 10.1007/BF00385253
- Heberle, H., Meirelles, G. V., da Silva, F. R., Telles, G. P., and Minghim, R. (2015). InteractiVenn: a web-based tool for the analysis of sets through Venn diagrams. *BMC Bioinf.* 16, 169. doi: 10.1186/s12859-015-0611-3
- Hinderstein, L. M., Marr, J. C. A., Martinez, F. A., Dowgiallo, M. J., Puglise, K. A., Pyle, R. L., et al. (2010). Theme section on “Mesophotic coral ecosystems: characterization, ecology, and management”. *Coral reefs* 29, 247–251. doi: 10.1007/s00338-010-0614-5
- Hoeksema, B. W., and Cairns, S. (2023) *World List of Scleractinia*. *Leptoseris hawaiiensis* Vaughan 1907 (World Register of Marine Species). Available online at: <https://www.marinespecies.org/alpha.php?p=taxdetails&id=207291> (Accessed 2023-05-13).
- Howe-Kerr, L. I., Bachelot, B., Wright, R. M., Kenkel, C. D., Bay, L. K., and Correa, A. M. (2020). Symbiont community diversity is more variable in corals that respond poorly to stress. *Glob. Change Biol.* 26, 2220–2234. doi: 10.1111/gcb.14999
- Howells, E. J., Beltran, V. H., Larsen, N. W., Bay, L. K., Willis, B. L., and Van Oppen, M. J. H. (2012). Coral thermal tolerance shaped by local adaptation of photosymbionts. *Nat. Climate Change* 2, 116–120. doi: 10.1038/nclimate1330
- Huang, Y. Y., Carballo-Bolaños, R., Kuo, C. Y., Keshavmurthy, S., and Chen, C. A. (2020). *Leptoseris phrygia* in Southern Taiwan shuffles and switches symbionts to resist thermal-induced bleaching. *Sci. Rep.* 10, 1–11. doi: 10.1038/s41598-020-64749-z
- Hume, B. C., Mejia-Restrepo, A., Voolstra, C. R., and Berumen, M. L. (2020). Fine-scale delineation of Symbiodiniaceae genotypes on a previously bleached central Red Sea reef system demonstrates a prevalence of coral host-specific associations. *Coral Reefs* 39, 583–601. doi: 10.1007/s00338-020-01917-7
- Hume, B. C., Smith, E. G., Ziegler, M., Warrington, H. J., Burt, J. A., LaJeunesse, T. C., et al. (2019). SymPortal: A novel analytical framework and platform for coral algal symbiont next-generation sequencing ITS2 profiling. *Mol. Ecol. Resour.* 19, 1063–1080. doi: 10.1111/1755-0998.13004
- Hume, B. C., Ziegler, M., Poulin, J., Pochon, X., Romic, S., Boissin, E., et al. (2018). An improved primer set and amplification protocol with increased specificity and sensitivity targeting the Symbiodinium ITS2 region. *PeerJ* 6, e4816. doi: 10.7717/peerj.4816
- Jones, A. M., and Berkelmans, R. (2011). Tradeoffs to thermal acclimation: energetics and reproduction of a reef coral with heat tolerant *Symbiodinium* type-D. *J. Mar. Biol.* 2011, 8590. doi: 10.1155/2011/185890
- Kahng, S. E., Copus, J. M., and Wagner, D. (2014). Recent advances in the ecology of mesophotic coral ecosystems (MCEs). *Curr. Opin. Environ. Sustain.* 7, 72–81. doi: 10.1016/j.cosust.2013.11.019
- Kahng, S., Copus, J. M., and Wagner, D. (2017). “Mesophotic coral ecosystems,” in *Marine animal forests*. Eds. S. Rossi, L. Bramanti, A. Gori and C. Orejas (Springer, Cham). doi: 10.1007/978-3-319-21012-4\_4
- Kahng, S. E., Garcia-Sais, J. R., Spalding, H. L., Brokovich, E., Wagner, D., Weil, E., et al. (2010). Community ecology of mesophotic coral reef ecosystems. *Coral Reefs* 29, 255–275. doi: 10.1007/s00338-010-0593-6
- Kaiser, P., Schlichter, D., and Fricke, H. W. (1993). Influence of light on algal symbionts of the deep water coral *Leptoseris fragilis*. *Mar. Biol.* 117, 45–52. doi: 10.1007/BF00346424
- Kheireddine, M., Mayot, N., Ouhssain, M., and Jones, B. H. (2021). Regionalization of the Red Sea based on phytoplankton phenology: a satellite analysis. *J. Geophys. Res.: Oceans* 126, e2021JC017486. doi: 10.1029/2021JC017486
- Kitahara, M. V., Fukami, H., Benzoni, F., and Huang, D. (2016). “The new systematics of Scleractinia: integrating molecular and morphological evidence,” in *The Cnidaria, Past, Present and Future: The world of medusa and her sisters* (Springer, Cham), 41–59. doi: 10.1007/978-3-319-31305-4\_4
- Klaus, J. S., Budd, A. F., Heikoop, J. M., and Fouke, B. W. (2007). Environmental controls on corallite morphology in the reef coral *Montastraea annularis*. *Bull. Mar. Sci.* 80, 233–260.
- LaJeunesse, T. C., Parkinson, J. E., Gabrielson, P. W., Jeong, H. J., Reimer, J. D., Voolstra, C. R., et al. (2018). Systematic revision of Symbiodiniaceae highlights the antiquity and diversity of coral endosymbionts. *Curr. Biol.* 28, 2570–2580. doi: 10.1016/j.cub.2018.07.008
- Lesser, M. P., Slattery, M., and Leichter, J. J. (2009). Ecology of mesophotic coral reefs. *J. Exp. Mar. Biol. Ecol.* 375, 1–8. doi: 10.1016/j.jembe.2009.05.009
- Lesser, M. P., Slattery, M., and Mobley, C. D. (2018). Biodiversity and functional ecology of mesophotic coral reefs. *Annu. Rev. Ecol. Syst.* 49, 49–71. doi: 10.1146/annurev-ecolsys-110617-062423
- Little, A. F., Van Oppen, M. J., and Willis, B. L. (2004). Flexibility in algal endosymbioses shapes growth in reef corals. *Science* 304, 1492–1494. doi: 10.1126/science.1095733
- Loya, Y., Puglise, K. A., and Bridge, T. C. (Eds.) (2019). *Mesophotic coral ecosystems* Vol. 12 (New York: Springer). doi: 10.1007/978-3-319-92735-0
- Luck, D. G., Forsman, Z. H., Toonen, R. J., Leicht, S. J., and Kahng, S. E. (2013). Polyphyly and hidden species among Hawai'i's dominant mesophotic coral genera, *Leptoseris* and *Pavona* (Scleractinia: Agariciidae). *PeerJ* 1, e132. doi: 10.7717/peerj.132
- Manasrah, R., Abu-Hilal, A., and Rasheed, M. (2019). “Physical and chemical properties of seawater in the Gulf of Aqaba and Red Sea,” in *Oceanographic and biological aspects of the Red Sea* (Springer, Cham), 41–73. doi: 10.1007/978-3-319-99417-8\_3
- Muir, P. R., Wallace, C. C., Done, T., and Aguirre, J. D. (2015). Limited scope for latitudinal extension of reef corals. *Science* 348, 1135–1138. doi: 10.1126/science.1259911
- Muko, S., Kawasaki, K., Sakai, K., Takasu, F., and Shigesada, N. (2000). Morphological plasticity in the coral *Porites sillimaniani* and its adaptive significance. *Bull. Mar. Sci.* 66, 225–239.
- Muscantine, L., and Porter, J. W. (1977). Reef corals: mutualistic symbioses adapted to nutrient-poor environments. *Bioscience* 27, 454–460. doi: 10.2307/1297526
- Nir, O., Gruber, D. F., Einbinder, S., Kark, S., and Tchernov, D. (2011). Changes in scleractinian coral *Seriatopora hystrix* morphology and its endocellular *Symbiodinium* characteristics along a bathymetric gradient from shallow to mesophotic reef. *Coral Reefs* 30, 1089–1100. doi: 10.1007/s00338-011-0801-z
- Nir, O., Gruber, D. F., Shemesh, E., Glasser, E., and Tchernov, D. (2014). Seasonal mesophotic coral bleaching of *Stylophora pistillata* in the Northern Red Sea. *PLoS One* 9, e84968. doi: 10.1371/journal.pone.0084968
- Osman, E. O., Suggett, D. J., Voolstra, C. R., Pettay, D. T., Clark, D. R., Pogoreutz, C., et al. (2020). Coral microbiome composition along the northern Red Sea suggests high plasticity of bacterial and specificity of endosymbiotic dinoflagellate communities. *Microbiome* 8, 1–16. doi: 10.1186/s40168-019-0776-5
- Ow, Y. X., and Todd, P. A. (2010). Light-induced morphological plasticity in the scleractinian coral *Goniastrea pectinata* and its functional significance. *Coral Reefs* 29, 797–808. doi: 10.1007/s00338-010-0631-4
- Pochon, X., Forsman, Z. H., Spalding, H. L., Padilla-Gamiño, J. L., Smith, C. M., and Gates, R. D. (2015). Depth specialization in mesophotic corals (*Leptoseris* spp.) and associated algal symbionts in Hawai'i. *R. Soc. Open Sci.* 2, 140351. doi: 10.1098/rsos.140351
- Poquita-Du, R. C., Huang, D., Chou, L. M., and Todd, P. A. (2020). The contribution of stress-tolerant endosymbiotic dinoflagellate *Durussdinium* to *Pocillopora acuta* survival in a highly urbanized reef system. *Coral Reefs* 39, 745–755. doi: 10.1007/s00338-020-01902-0
- Pyle, R. L., and Copus, J. M. (2019). “Mesophotic coral ecosystems: introduction and overview,” in *Mesophotic coral ecosystems*. Coral Reefs of the World, vol. 12. Eds. Y. Loya, K. Puglise and T. Bridge (Springer, Cham). doi: 10.1007/978-3-319-92735-0\_1
- Raitsos, D. E., Pradhan, Y., Brewin, R. J., Stenchikov, G., and Hoteit, I. (2013). Remote sensing the phytoplankton seasonal succession of the Red Sea. *PLoS One* 8, e64909. doi: 10.1371/journal.pone.0064909
- Rodriguez-Lanetty, M., Loh, W., Carter, D., and Hoegh-Guldberg, O. (2001). Latitudinal variability in symbiont specificity within the widespread scleractinian coral *Plesiastrea versipora*. *Mar. Biol.* 138, 1175. doi: 10.1007/s002270100536
- Rooney, J., Donham, E., Montgomery, A., Spalding, H., Parrish, F., Boland, R., et al. (2010). Mesophotic coral ecosystems in the Hawaiian Archipelago. *Coral Reefs* 29, 361–367. doi: 10.1007/s00338-010-0596-3
- Rouze, H., Galand, P. E., Medina, M., Bongaerts, P., Pichon, M., Pérez-Rosales, G., et al. (2021). Symbiotic associations of the deepest recorded photosynthetic scleractinian coral (172 m depth). *ISME J.* 15, 1564–1568. doi: 10.1038/s41396-020-00857-y
- Rouze, H., Lecellier, G., Pochon, X., Torda, G., and Berteaux-Lecellier, V. (2019). Unique quantitative Symbiodiniaceae signature of coral colonies revealed through spatio-temporal survey in Moorea. *Sci. Rep.* 9, 1–11. doi: 10.1038/s41598-019-44017-5

- Rowan, R. (2004). Thermal adaptation in reef coral symbionts. *Nature* 430, 742–742. doi: 10.1038/430742a
- Rowlands, G., Purkis, S., and Bruckner, A. (2014). Diversity in the geomorphology of shallow-water carbonate depositional systems in the Saudi Arabian Red Sea. *Geomorphology* 222, 3–13. doi: 10.1016/j.geomorph.2014.03.014
- Rowlands, G., Purkis, S., and Bruckner, A. (2016). Tight coupling between coral reef morphology and mapped resilience in the Red Sea. *Mar. pollut. Bull.* 105, 575–585. doi: 10.1016/j.marpolbul.2015.11.027
- Sampayo, E. M., Ridgway, T., Bongaerts, P., and Hoegh-Guldberg, O. (2008). Bleaching susceptibility and mortality of corals are determined by fine-scale differences in symbiont type. *Proc. Natl. Acad. Sci.* 105, 10444–10449. doi: 10.1073/pnas.0708049105
- Sawall, Y., Al-Sofyani, A., Banguera-Hinestroza, E., and Voolstra, C. R. (2014). Spatio-temporal analyses of *Symbiodinium* physiology of the coral *Pocillopora verrucosa* along large-scale nutrient and temperature gradients in the Red Sea. *PloS One* 9, e103179. doi: 10.1371/journal.pone.0103179
- Sawall, Y., Nicosia, A. M., McLaughlin, K., and Ito, M. (2022). Physiological responses and adjustments of corals to strong seasonal temperature variations (20–28°C). *J. Exp. Biol.* 225, jeb244196. doi: 10.1242/jeb.244196
- Schlichter, D., and Fricke, H. W. (1991). “Mechanisms of amplification of photosynthetically active radiation in the symbiotic deep-water coral *Leptoseris fragilis*,” in *Hydrobiologia*, vol. 216. (Kluwer Academic Publishers), 389–394. doi: 10.1007/BF00026491
- Schlichter, D., Fricke, H. W., and Weber, W. (1986). Light harvesting by wavelength transformation in a symbiotic coral of the Red Sea twilight zone. *Mar. Biol.* 91, 403–407. doi: 10.1007/BF00428634
- Schlichter, D., Fricke, H. W., and Weber, W. (1988). Evidence for par-enhancement by reflection, scattering and fluorescence in the symbiotic deep-water coral *Leptoseris fragilis* (par= photosynthetically active radiation). *Endocytobiosis Cell Res.* 5, 83–94.
- Schlichter, D., Kampmann, H., and Conrady, S. (1997). Trophic potential and photoecology of endolithic algae living within coral skeletons. *Mar. Ecol.* 18, 299–317. doi: 10.1111/j.1439-0485.1997.tb00444.x
- Schlichter, D., Meier, U., and Fricke, H. W. (1994). Improvement of photosynthesis in zooxanthellate corals by autofluorescent chromatophores. *Oecologia* 99, 124–131. doi: 10.1007/BF00317092
- Schlichter, D., Weber, W. T., and Fricke, H. W. (1985). A chromatophore system in the hermatypic, deep-water coral *Leptoseris fragilis* (Anthozoa: Hexacorallia). *Mar. Biol.* 89, 143–147. doi: 10.1007/BF00392885
- Schloss, P. D., Westcott, S. L., Ryabin, T., Hall, J. R., Hartmann, M., Hollister, E. B., et al. (2009). Introducing mothur: open-source, platform-independent, community-supported software for describing and comparing microbial communities. *Appl. Environ. Microbiol.* 75, 7537–7541. doi: 10.1128/AEM.01541-09
- Silverstein, R. N., Correa, A. M., and Baker, A. C. (2012). Specificity is rarely absolute in coral–algal symbiosis: implications for coral response to climate change. *Proc. R. Soc. B: Biol. Sci.* 279, 2609–2618. doi: 10.1098/rspb.2012.0055
- Silverstein, R. N., Correa, A. M., LaJeunesse, T. C., and Baker, A. C. (2011). Novel algal symbiont (*Symbiodinium* spp.) diversity in reef corals of Western Australia. *Mar. Ecol. Prog. Ser.* 422, 63–75. doi: 10.3354/meps08934
- Sofianos, S. S., and Johns, W. E. (2003). An oceanic general circulation model (OGCM) investigation of the Red Sea circulation: 2. Three-dimensional circulation in the Red Sea. *J. Geophys. Res.: Oceans* 108, 17–1. doi: 10.1029/2001JC001184
- Stat, M., Pochon, X., Franklin, E. C., Bruno, J. F., Casey, K. S., Selig, E. R., et al. (2013). The distribution of the thermally tolerant symbiont lineage (*Symbiodinium* clade D) in corals from Hawaii: correlations with host and the history of ocean thermal stress. *Ecol. Evol.* 3, 1317–1329. doi: 10.1002/ece3.556
- Suwa, R., Hirose, M., and Hidaka, M. (2008). Seasonal fluctuation in zooxanthellae genotype composition and photophysiology in the corals *Pavona divaricata* and *P. decussata*. *Mar. Ecol. Prog. Ser.* 361, 129–137. doi: 10.3354/meps07372
- Tamir, R., Eyal, G., Kramer, N., Laverick, J. H., and Loya, Y. (2019). Light environment drives the shallow-to-mesophotic coral community transition. *Ecosphere* 10, e02839. doi: 10.1002/ecs2.2839
- Terraneo, T. I., Benzoni, F., Arrigoni, R., Baird, A. H., Mariappan, K. G., Forsman, Z. H., et al. (2021). Phylogenomics of *Porites* from the Arabian Peninsula. *Mol. Phylogenet. Evol.* 161, 107173. doi: 10.1016/j.ympev.2021.107173
- Terraneo, T. I., Benzoni, F., Baird, A. H., Arrigoni, R., and Berumen, M. L. (2019b). Morphology and molecules reveal two new species of *Porites* (Scleractinia, Poritidae) from the Red Sea and the Gulf of Aden. *Syst. Biodivers.* 17, 491–508. doi: 10.1080/14772000.2019.1643806
- Terraneo, T. I., Fusi, M., Hume, B. C., Arrigoni, R., Voolstra, C. R., Benzoni, F., et al. (2019a). Environmental latitudinal gradients and host-specificity shape Symbiodiniaceae distribution in Red Sea *Porites* corals. *J. Biogeogr.* 46, 2323–2335. doi: 10.1111/jbi.13672
- Terraneo, T. I., Ouhssain, M., Castano, C. B., Aranda, M., Hume, B. C., Marchese, F., et al. (2023). From the shallow to the mesophotic: a characterization of Symbiodiniaceae diversity in the Red Sea NEOM region. *Front. Mar. Sci.* 10. doi: 10.3389/fmars.2023.1077805
- Turner, J. A., Andradi-Brown, D. A., Gori, A., Bongaerts, P., Burdett, H. L., Ferrier-Pagès, C., et al. (2019). Key questions for research and conservation of mesophotic coral ecosystems and temperate mesophotic ecosystems. *Mesophotic coral Ecosyst.* (Springer, Cham), 12, 989–1003. doi: 10.1007/978-3-319-92735-0\_52
- Turner, J. A., Babcock, R. C., Hovey, R., and Kendrick, G. A. (2017). Deep thinking: a systematic review of mesophotic coral ecosystems. *ICES J. Mar. Sci.* 74, 2309–2320. doi: 10.1093/icesjms/fsx085
- Wickham, H., Chang, W., and Wickham, M. H. (2016). *Package ‘ggplot2’. Create elegant data visualisations using the grammar of graphics*, Vol. 2 (New York: Springer-Verlag), 1–189.
- Wijsman-Best, M. (1974). Habitat-induced modification of reef corals (Faviidae) and its consequences for taxonomy. *Proc. 2nd Int. coral Reef Symp* 2, 217–228.
- Willis, B. L. (1985). “Phenotypic plasticity versus phenotypic stability in the reef corals *Turbinaria mesenterina* and *Pavona cactus*,” in *Proceedings of the Fifth International Coral Reef Symposium*, Vol. 4, 107–112.
- Winters, G., Beer, S., Zvi, B. B., Brickner, I., and Loya, Y. (2009). Spatial and temporal photoacclimation of *Stylophora pistillata*: zooxanthella size, pigmentation, location and clade. *Mar. Ecol. Prog. Ser.* 384, 107–119. doi: 10.3354/meps08036
- Ziegler, M., Arif, C., Burt, J. A., Dobretsov, S., Roder, C., LaJeunesse, T. C., et al. (2017). Biogeography and molecular diversity of coral symbionts in the genus *Symbiodinium* around the Arabian Peninsula. *J. Biogeogr.* 44, 674–686. doi: 10.1111/jbi.12913
- Ziegler, M., Roder, C. M., Büchel, C., and Voolstra, C. R. (2015). Mesophotic coral depth acclimatization is a function of host-specific symbiont physiology. *Front. Mar. Sci.* 2. doi: 10.3389/fmars.2015.00004

# Frontiers in Microbiology

Explores the habitable world and the potential of microbial life

The largest and most cited microbiology journal which advances our understanding of the role microbes play in addressing global challenges such as healthcare, food security, and climate change.

## Discover the latest Research Topics

[See more →](#)

### Frontiers

Avenue du Tribunal-Fédéral 34  
1005 Lausanne, Switzerland  
[frontiersin.org](https://frontiersin.org)

### Contact us

+41 (0)21 510 17 00  
[frontiersin.org/about/contact](https://frontiersin.org/about/contact)

